Archives of Endocrinology and Metabolism

ISSN 2359-4292

OFFICIAL JOURNAL OF THE BRAZILIAN SOCIETY OF ENDOCRINOLOGY AND METABOLISM

Vol. 70 – No. 04 – August 2026

editorial

Goodbye, idiopathic short stature: why "healthy short stature" is a necessary advancement
Ivo J. Prado Arnhold, Berenice B. Mendonca

brief communications

Healthy short stature
Alexander A. L. Jorge, Paulo F. Collett-Solberg, Margaret C. S. Boguszewski

Clinical characteristics, glycemic control & quality of life of patients using Android Artificial Pancreas System (AAPS) in Brazil
Gabriella Lopes Ventura, Laryssa da Silva Messias, Maria Eduarda Pereira Dantas, Milena Oliveira Leite, Débora Souto, Maria de Lourdes Passos Machado, Edson Perrotti, Thiago Mota Soares, Tassia Virginia de Carvalho Oliveira, Lenita Zajdenverg, Joana Dantas, Melanie Rodacki

originals

Dietary pattern and night work: metabolic syndrome in healthcare workers
Francielle Lopes dos Reis, Maria Carlota Borba Brum, Júlio César Ferreira Bertoloto, Maria da Graça Rocha Penha, Sheila de Castro Cardoso Toniasso, Rodrigo Fernandes Soares, Elen Gineste Baccin, Ticiana da Costa Rodrigues

The relationships among nutrition, body composition, muscle strength and physical performance in patients with acromegaly
Natália Nachbar Hupalowski, Claudia Pinheiro Sanches Rocha, Vicente F. C. Andrade, Cesar Luiz Boguszewski, Victoria Zeghbi Cochenski Borba

The essential role of the redox balance in adrenal steroidogenesis
Juliana Lourenço Gebenlian, Aline Faccioli Bodoni, Fernanda Borchers Coeli-Lacchini, Margaret de Castro, Sonir Roberto Rauber Antonini

Genetic alterations of telomere maintenance pathways in paragangliomas
Lucas Batini, Eduardo C. Lobato, Felipe Freitas-Castro, Lucas S. Santana, Gustavo F. C. Fagundes, Ana Caroline F. Afonso, Izabel T. Nakamura, Lucas B. Rossetti, Berenice B. Mendonca, Ana Claudia Latronico, Madson Q. Almeida

Accuracy of portable artificial intelligence-supported fundus camera in the screening of diabetic retinopathy in primary care
Daniela O. Alves, Daniel Lavinsky, Myriam E. B. Strzalkowski, Leila B. Moreira

Type 2 diabetes morbidity, mortality and its associated risk factors across Brazilian regions: findings from the Global Burden of Disease Study 2021
Paula Portal Teixeira, Tatiana Duque-Cartagena, Lucas Scotta Cabral, Bárbara Niegia Garcia de Goulart, Rodrigo dos Reis, Fernando Gerchman, Verônica Colpani, Deborah Carvalho Malta, Yvonne Yiru Xu, Maria Inês Schmidt, Rita Mattiello, Bruce Bartholow Duncan

Diabetic peripheral neuropathy in type 2 diabetes: prevalence and associated factors in Midwest Brazil
Lorrany Campos de Queiroz Melo, Gleyson Souza da Costa, Matheus Eduardo Soares, Adriana Marilia Zanato Teruel, Augusto Baumgart de Liz, Josiane Neves Coelho Marques, Arthur Emílio Leite de Figueiredo, Luiz F. Viola, João Gabriel Guimarães Luz, Adriana Santi

Diagnostic criteria for gestational hyperglycemia in women from a public maternity hospital in Brazil
Thais Mantovani Bernardo, Ênio Luis Damaso, Patrícia Moreira Gomes, Elaine Christine Dantas Moisés

OCT4 and NANOG are involved in adrenocortical tumorigenesis
Marcelo M. Cavalcanti, Mariana P. Halah, Letícia F. Leal, Fernanda B. Coeli-Lacchini, Carlos A. Scrideli, Carlos A. F. Molina, Jose A. Yunes, Silvia Brandalise, Ayrton C. Moreira, Fernando Ramalho, Leandra N. Ramalho, Margaret de Castro, Sonir R. Antonini

Association of handgrip strength and CT-derived body composition with insulin resistance in women with prediabetes and newly diagnosed type 2 diabetes
Elham Yousief, Mona Khozam, Ghada Ayeldeen, Mohamed Hamadna Allah El Ghobashy

The hidden impact of smoking in thyroid eye disease: a link between selenium deficiency, autoimmunity, and retinal microvasculature
Fatma Savur, Serkan Güler, Gülistan Oyur

MicroRNA expression signatures associated with metastatic progression in papillary thyroid carcinoma
Vinicius Ferreira Capelli, Ana Kober Leite, Kelly Cristina Saito, Thérèse Rachell Theodoro, Fátima Solange Pasini, Venâncio Avancini Ferreira Alves, Luiz Paulo Kowalski, Maria Aparecida Silva Pinhal, Edna Teruko Kimura, Leandro Luongo Matos

Age-related changes in METS-IR and HOMA-IR in obese adults and their relationship with cardiometabolic comorbidities
Esra Suay Timurkaan, Gülsüm Altuntaş, Muhammed Fuad Uslu, Hakan Ayyıldız, Mustafa Timurkaan

Associations between peripheral blood whole-genome DNA methylation and obesity in young Chinese males
Meidan Nong, Haiou Lu, Maolin Zhao, Lihong Xiao

Factors associated with lifestyle practices for preventing cardiovascular disease in adults aware of metabolic syndrome
Jong Sun Ok, Kyung-Jin Kim, Kyung-Hee Kim, Do Kyeong Song, Kyung Jin Ahn, Chan Seok Park, Mi-Seung Shin

Relationships between glucose variability with white matter hyperintensity and cerebrovascular abnormalities
Cheng-Chieh Lin, Chia-Ing Li, Chiu-Shong Liu, Chih-Hsueh Lin, Shing-Yu Yang, Tsai-Chung Li

invited review

Reversible congenital hypogonadotropic hypogonadism: keys for clinical management
Chrysoula Archaki, Maria Stamou, Andrew A. Dwyer

case reports

Catheterization of the petrosal sinus: possible advantage of desmopressin stimulation in Cushing disease
Heraldo Mendes Garmes, Sara Calazans de Siqueira, Karla Borges Daniel, Marilia Bortolotto Felippe Trentin, Mariana Tazima Fujiwara, Caroline Schinoll, Mateus Dal Fabbro, Fabio Rogerio, Leonardo Deus-Silva, Fabiano Reis

Pheochromocytoma and multicentric giant cell tumor of bone
João Vicente Silveira, Madson Q. Almeida, Olavo Pires de Camargo, Julio Cesar Carvalho Nardelli, Andre Ferrari de Franca Camargo, Henrique Barbosa Ribeiro, Luiz Aparecido Bortolotto, Heno Ferreira Lopes, Fernanda M. Consolim-Colombo

letters to the editor

Comment on: Evaluation of three inflammation-associated blood indices for predicting malignancy in thyroid nodules
Yusuf Öztürk

Response to the letter to the editor: Evaluation of three inflammation-associated blood indices for predicting malignancy in thyroid nodules
Merve Çatak, Bülent Koca, Zeynep Çetin, Özden Özdemir BAŞER

SBEM Sociedade Brasileira de Endocrinologia e Metabologia

Archives of Endocrinology and Metabolism

OFFICIAL JOURNAL OF THE BRAZILIAN SOCIETY OF ENDOCRINOLOGY AND METABOLISM

Editorial supervisor: Roselaine Monteiro
roselaine@endocrino.org.br

Rua Botucatu, 572 – conjunto 83 – 04023-062 – São Paulo, SP
Telefax: (11) 5575-0311 / 5082-4788

Online submission / Electronic publishing
www.aem-sbem.com • www.scielo.br/abem

SANTANA
Serviços Editoriais
sfsantana3@gmail.com.br

Indexed in Biological Abstracts, Index Medicus, Latindex, Lilacs, MedLine, PubMed, SciELO, Scopus, ISI-Web of Science

BRAZILIAN ARCHIVES OF ENDOCRINOLOGY AND METABOLISM
Brazilian Society of Endocrinology and Metabolism – São Paulo, SP:
Brazilian Society of Endocrinology and Metabolism, volume 5, 1955-
Six issues/year
Continued from: Brazilian Archives of Endocrinology (v. 1-4), 1951-1955
ISSN 2359-4292 (online issues)

1. Endocrinology – journals 2. Metabolism – journals
I. Brazilian Society of Endocrinology and Metabolism II. Brazilian Medical Association

CDU 612.43 Endocrinology
CDU 612.015.3 Metabolism

Archives of Endocrinology and Metabolism

OFFICIAL JOURNAL OF THE BRAZILIAN SOCIETY OF ENDOCRINOLOGY AND METABOLISM

Archives of endocrinology and metabolism Official journal of **SBEM** – Brazilian Society of Endocrinology and Metabolism (Department of the Brazilian Medical Association), **SBD** – Brazilian Diabetes Society, **ABESO** – Brazilian Association for the Study of Obesity and Metabolic Syndrome

2024-2026



EDITOR-IN-CHIEF
Cesar Luiz Boguszewski (PR)

DEPUTY EDITORS
Madson Queiroz de Almeida (SP)
Marcio C. Mancini (SP)

ASSOCIATED EDITORS
Celia Regina Nogueira (SP)
Davi Casale Aragon (SP)
Fernanda Vaisman Balieiro (RJ)
João Roberto de Sá (SP)
Jose A. Sgarbi (SP)
Josivan Gomes de Lima (RN)
Larissa Garcia Gomes (SP)
Leandro Kasuki (RJ)
Letícia F. Gontijo Silveira (MG)
Luiz Claudio Gonçalves de Castro (DF)
Madson Queiroz de Almeida (SP)
Marcelo A. Mori (SP)
Marcio C. Mancini (SP)
Marcio W. Lauria (MG)
Maria Candida Barisson (SP)
Maria Tereza Nunes (SP)
Mario José Abdalla Saad (SP)
Marise Lazaretti-Castro (SP)
Melanie Rodacki (RJ)
Miguel Madeira (RJ)
Rodrigo de Oliveira Moreira (RJ)
Sonir R. Antonini (SP)
Simone van de Sande Lee (SC)
Vania dos Santos Nunes-Nogueira (SP)

EDITORIAL COMMISSION
Alexandre Hohl (SC)
Ana Amélia Hoff (SP)
Andrea Glezer (SP)
Ayrton Custódio Moreira (SP)
Berenice B. Mendonça (SP)
Caroline k Kramer (Toronto)
Catarina Brasil d'Alva (SP)
Dalisbor Marcelo Weber da Silva (PR)
Daisy Crispim Moreira (RS)
Décio Laks Eizirik (Brussels)
Edna Nakandakare (SP)
Edna T. Kimura (SP)
Eduardo Coelho Machado (RS)
Fabio Vasconcellos Comim (MG)
Flávia Amanda Costa Barbosa (SP)
Flavio Hojaij (SP)
Gabriela Heiden Teló (RS)
Gil Guerra-Júnior (SP)
Gisah M. do Amaral (PR)
Hermelinda Cordeiro Pedrosa (DF)
Isabela Judith Benseñor (SP)
Itamar de Souza Santos (SP)
Janice Sepúlveda Reis (MG)
José Augusto Sgarbi (SP)
Julio Z. Abucham (SP)
Luis Henrique Santos Canani (RS)
Luiz Eduardo Armondi Wildemberg (RJ)
Manoel Ricardo Alves Martins (CE)
Marcos Tadashi Kakitani Toyoshima (SP)
Marilia de Brito Gomes (RJ)
Margaret Cristina da Silva Boguszewski (PR)
Melissa Premaor (MG)
Michele Drehmer (RS)
Roberta Cobas (RJ)
Sandra R. G. Ferreira (SP)
Simone Van den Sande Lee (SC)
Sergio Atala Did (SP)
Suemi Marui (SP)
Tânia Aparecida Sanchez Bachega (SP)
Victória Borba (PR)

COORDINATORS OF THE SBEM DEPARTMENTS
ADRENAL AND HYPERTENSION
Flávia Amanda Costa Barbosa (SP)

BASIC ENDOCRINOLOGY
Maria Tereza Nunes (SP)

DIABETES MELLITUS
Ruy Lyra da Silva Filho (PE)

DYSLIPIDEMIA AND ATHEROSCLEROSIS
Márcio Weissheimer Lauria (MG)

ENDOCRINOLOGY OF SPORT AND EXERCISE
Andréa Messias Britto Fioretti (SP)

WOMEN ENDOCRINOLOGY, ANDROLOGY AND TRANSGENERITY
Tayane Muniz Fighera (RS)

PEDIATRIC ENDOCRINOLOGY
Luiz Cláudio Gonçalves de Castro (DF)

BONE AND MINERAL METABOLISM
Francisco José Albuquerque de Paula (SP)

NEUROENDOCRINOLOGY
Andrea Glezer (SP)

OBESITY
Fábio Rogério Trujilho (BA)

THYROID
Rafael Selbach Scheffel (RS)

REPRESENTATIVES OF COLLABORATING SOCIETIES

SBD
Ruy Lyra da Silva Filho (PE)

ABESO
Fábio Rogério Trujilho (BA)

FOUNDER
Waldemar Berardinelli (RJ)

EDITORS-IN-CHIEF, EDITORIAL OFFICE*
1951-1955
Waldemar Berardinelli (RJ)
Thales Martins (RJ)

1957-1972
Clementino Fraga Filho (RJ)

1964-1966*
Luiz Carlos Lobo (RJ)

1966-1968*
Pedro Collett-Solberg (RJ)

1969-1972*
João Gabriel H. Cordeiro (RJ)

1978-1982
Armando de Aguiar Pupo (SP)

1983-1990
Antônio Roberto Chacra (SP)

1991-1994
Rui M. de Barros Maciel (SP)

1995-2006
Claudio Elias Kater (SP)

2007-2010
Edna T. Kimura (SP)

2011-2014
Sergio Atala Dib (SP)

2015-2022
Marcello D. Bronstein (SP)

2022-2023
Beatriz D'Agord Schaan (RS)

SBEM
Sociedade Brasileira de Endocrinologia e Metabologia

Sociedade Brasileira de Endocrinologia e Metabologia

2025-2026



NEUTON DORNELAS GOMES (DF)
President



KAREN FAGGIONI DE MARCA SEIDEL (RJ)
President-Elect



FLÁVIA COIMBRA PONTES MAIA (MG)
Executive Secretary



FÁBIO FERREIRA MOURA (PE)
Treasurer-General



MARISE LAZARETTI CASTRO (SP)
Scientific Director



CLAYTON LUIZ DORNELLES MACEDO (RS)
Director of Communications

SCIENTIFIC DEPARTMENTS – 2025/2026

ACCESS THE WEBSITE

ADRENAL AND HYPERTENSION

Coordinator: Flávia Amanda Costa Barbosa (SP)
Subcoordinator: Adriane Maria Rodrigues (PR)
Directors: Aline Barbosa Moraes (RJ)
Leonardo Vieira Neto (RJ)
Maria Candida Barisson Villares Fragoso (SP)
Rafael Buck Giorgi (SP)
Thaís Castanheira de Freitas Resende (GO)

ACCESS THE WEBSITE

BASIC ENDOCRINOLOGY

Coordinator: Maria Tereza Nunes (SP)
Subcoordinator: Luciani Renata Silveira de Carvalho (SP)
Directors: Carolina Ferraz da Silva (SP)
Lucas Leite Cunha (SP)
Manuela Giuliani Marcondes Rocha Braz (SP)
Milena Gurgel Teles Bezerra (CE)
Rafael Loch Batista (SP)

ACCESS THE WEBSITE

DIABETES MELLITUS

Coordinator: Ruy Lyra da Silva Filho (PE)
Subcoordinator: Saulo Cavalcanti da Silva (MG)
Directors: Fernando Valente (SP)
João Modesto Filho (PB)
Marcello Casaccia Bertoluci (RS)
Rodrigo de Oliveira Moreira (RJ)
Wellington Santana da Silva Junior (PI)

ACCESS THE WEBSITE

DYSLIPIDEMIA AND ATHEROSCLEROSIS

Coordinator: Márcio Weissheimer Lauria (MG)
Subcoordinator: Renan Magalhães Montenegro Junior (CE)
Directors: Joaquim Custódio da Silva Junior (BA)
Joana Rodrigues Dantas Vezzani (RJ)
Lúcia Helena Oliveira Cordeiro (PE)
Marcello Casaccia Bertoluci (RS)
Maria Helane Costa Gurgel Castelo (CE)

ACCESS THE WEBSITE

ENDOCRINOLOGY OF SPORT AND EXERCISE

Coordinator: Andréa Messias Britto Fioretti (SP)
Subcoordinator: Rogério Friedman (RS)
Directors: Alexis Dourado Guedes (BA)
Cristina da Silva Schreiber de Oliveira (SC)
Cristiano Roberto Grimaldi Barcellos (SP)
Fúlvio Clemo Santos Tomaselli (SC)
João Carlos Ramos-Dias (SP)

ACCESS THE WEBSITE

WOMEN ENDOCRINOLOGY, ANDROLOGY AND TRANSGENERITY

Coordinator: Tayane Muniz Fighera (RS)
Subcoordinator: Poli Mara Spritze (RS)
Directors: Alexandre Hohl (SC)
Elaine Maria Frade Costa (SP)
Fábio Vasconcellos Comim (MG)
Marcelo Fernando Ronsoni (SC)
Thyciara Fontenele Marques (CE)

ACCESS THE WEBSITE

PEDIATRIC ENDOCRINOLOGY

Coordinator: Luiz Cláudio Gonçalves de Castro (DF)
Subcoordinator: Sonir Roberto Rauber Antonini (SP)
Directors: Ana Pinheiro Machado Canton (SP)
Gil Guerra Júnior (SP)
Jacqueline Rosângela de Araújo (PE)
Margaret Cristina da Silva Boguszewski (PR)
Nathália Lisboa Rosa Almeida Gomes (MG)

ACCESS THE WEBSITE

BONE AND MINERAL METABOLISM

Coordinator: Francisco José Albuquerque de Paula (SP)
Subcoordinator: Narriane Chaves Pereira de Holanda (PB)
Directors: Bárbara Campolina Carvalho Silva (MG)
Catarina Brasil d'Alva (CE)
Érico Higino Carvalho (PE)
Leonardo Costa Bandeira e Farias (PE)
Victória Zeghbi Cochenski Borba (PR)

ACCESS THE WEBSITE

NEUROENDOCRINOLOGY

Coordinator: Andrea Glezer (SP)
Subcoordinator: Vania dos Santos Nunes Nogueira (SP)
Directors: Beatriz Santana Soares Rocha (MG)
Guilherme Alcides Flôres Soares Rollin (RS)
Leandro Kasuki Jomori de Pinho (RJ)
Manoel Ricardo Alves Martins (CE)
Paula Condé Lamparelli Elias (SP)

ACCESS THE WEBSITE

OBESITY

Coordinator: Fábio Rogério Trujilho (BA)
Subcoordinator: Cynthia Melissa Valério (RJ)
Directors: Bruno Halpern (SP)
Cintia Cercato (SP)
Fernando Gerchman (RS)
Simone Van de Sande Lee (SC)
Thaisa Dourado Guedes Trujilho (BA)

ACCESS THE WEBSITE

THYROID

Coordinator: Rafael Selbach Scheffel (RS)
Subcoordinator: Cléo Otaviano Mesa Júnior (PR)
Directors: Adriano Namo Cury (SP)
Caroline Serrano do Nascimento (SP)
Fernanda Vaisman Balieiro (RJ)
Raquel Andrade de Siqueira (GO)
Susan Chow Lindsey (SP)

PERMANENT COMMISSIONS - 2025/2026

SCIENTIFIC COMMITTEE

Coordinator: Sergio Setsuo Maeda (SP)

Members

Ana Cláudia Latronico (SP)
Caroline Serrano (SP)
Cintia Cercato (SP)
Daniela Espíndola (GO)
Fernanda Vaisman (RJ)
Fernando Giuffrida (BA)
Josivan Lima (RN)
Mônica de Oliveira (PE)
Rodrigo Lamounier (MG)
Sonir Roberto Antonini (SP)
Carolina Garcia Soares Leães (RS)

Members – Local Scientific Committee

Cristiane Leitão (RS)
Fernando Gerchman (RS)
Rafael Selbach Scheffel (RS)
Polimara Spritzer (RS)

COMMITTEE FOR DIVERSITY, EQUITY, AND INCLUSION (CDEI)

Coordinator: Luciana Mattos Barros Oliveira (BA)

Members

Amanda de Araujo Laudier (RJ)
Erik Trovão Diniz (PE)
Flavia Amanda Costa Barbosa (SP)
Lia Lousada (CE)
Andreza Cristina Oliveira Berlink (BA)

COMMITTEE ON THE HISTORY OF ENDOCRINOLOGY AND METABOLISM (CHEM)

Coordinator: Henrique de Lacerda Suplicy (PR)

Members

Cláudio Elias Kater (SP)
Adriana Costa e Forti (CE)
Mauro Antônio Czepielewski (RS)

CAMPAIGN COMMITTEE (CC)

Members

Mateus Dornelles Severo (RS)
Georgia Martina Chichelero (RS)
Rafael Buck Giorgi (SP)
Leonardo Barbi Walter (RS)
Wellington Santana da Silva Junior (MA)
Mariana Guerra Paulino Guerra (ES)
Ximene Antunes (RJ)

PROFESSIONAL ETHICS AND DEFENCE COMMITTEE (CDP)

Coordinator: Ana Karina de Melo Bezerra Sodré (CE)

Members

Adauto Versiani Ramos (MG)
Adriano Namo Cury (SP)
Maria Augusta Karas Zella (PR)

CONTINUING MEDICAL EDUCATION COMMITTEE (CEMC)

Coordinator: Manoel Martins (CE)

Members

Milena Gurgel Teles (CE)
Carolina Castro Porto Silva Janovsky (SP)
André Gonçalves (PI)
Larissa Garcia Gomes (SP)

ENVIRONMENTAL ENDOCRINOLOGY COMMITTEE (CEA)

Coordinator: Elaine Maria Frade Costa (SP)

Members

Eveline Gadelha Pereira Fontenele (CE)
Maria Tereza Nunes (SP)
Caroline Serrano (SP)
Luiz Cláudio Castro (DF)

RARE ENDOCRINE DISEASES COMMITTEE (ENDO-RARAS)

Coordinator: Fernanda Azevedo Correa (Switzerland)

Members

José Viana Lima Junior (SP)
Nathalia Lisboa (MG)
Berenice Bilharinho de Mendonça (SP)
Luiz Cláudio Castro (DF)
Margaret Boguszewski (PR)
Renata Scalco (SP)

BYLAWS AND REGULATORY AFFAIRS COMMITTEE

Coordinator: Rui Monteiro de Barros Maciel (SP)

Members

Paulo Augusto Carvalho Miranda (MG)
Alana Abrantes Nogueira de Pontes (PB)
Rafael Selbach Scheffel (RS)
Paulo Lacativa (RJ)

ETHICS COMMITTEE (CE)

Inspector General: Diana Viegas Martins (BA)
Deputy Coordinator: Luciana Antunes de Almeida Secchi (MS)
1st Board Member: Itairan da Silva Terres (SC)
2nd Board Member: Angela Maria Spinola e Castro (SP)
Member: Marília Gabriela Zanier Gomes (GO)

MEDICAL TRAINING IN ENDOCRINOLOGY AND METABOLISM COMMITTEE

Coordinator: Milena Coelho Fernandes Caldato (PA)

Members

Marcia Helena Soares Costa (RJ)
Luciana Ansaneli Naves (DF)
Rafael Buck Giorgi (SP)

INSTITUTIONAL RELATIONS AND PUBLIC POLICY COMMITTEE

Coordinator: João Lindolfo Cunha Borges (DF)

Members

Maria Edna de Melo (SP)

COMMITTEE FOR THE PROMOTION OF NEW LEADERSHIP (CVNL)

Coordinator: Victoria Rodrigues Granja Alencar (PE)

Members

Leonardo Barbi Walter (RS)
Antonio Bentes de Figueiredo Junior (SP)
Isabella Santiago de Melo Miranda (DF)
Raquel Beatriz Gonçalves Muniz (RJ)

SPECIALIST TITLE IN ENDOCRINOLOGY AND METABOLISM COMMITTEE

Coordinator: Rodrigo de Oliveira Moreira (RJ)
Deputy Coordinator: Maria Edna de Melo (SP)

Members

Margaret de Castro (SP)
Miguel Madeira (RJ)
Monike Lourenço Dias Rodrigues (GO)
Marcelo Fernando Ronsoni (SC)
Cléo Otaviano Mesa Júnior (PR)

INTERNATIONAL COMMITTEE (CI)

Coordinator: Paulo Augusto Carvalho Miranda (MG)

Members

Ana Luiza Maia (RS)
Luciana Ansaneli Naves (DF)
Madson Queiroz de Almeida (SP)
Junia R.O.L Sweizer (Germany)

TEMPORARY COMMITTEE ON ARTIFICIAL INTELLIGENCE AND TECHNOLOGIES IN ENDOCRINOLOGY AND METABOLISM (CIATEM)

Coordinator: Marcio Krakauer (SP)

Members

Walmir Ferreira Coutinho (RJ)
Edson Perrotti Santos (AL)
Felipe Henning Gaia Duarte (SP)
Milena Gurgel Teles Bezerra (CE)

Archives of Endocrinology and Metabolism
ISSN 2359-4292
OFFICIAL JOURNAL OF THE BRAZILIAN SOCIETY OF ENDOCRINOLOGY AND METABOLISM

editorial

Goodbye, idiopathic short stature: why "healthy short stature" is a necessary advancement

Ivo J. Prado Arnhold[1]
https://orcid.org/0000-0003-1739-1354

Berenice B. Mendonca[1]
https://orcid.org/0000-0003-1762-1084

[1] Faculdade de Medicina da Universidade de São Paulo, São Paulo, SP, Brasil

IDIOPATHIC SHORT STATURE – A SHRINKING DIAGNOSIS APPLIED MOSTLY TO HEALTHY CHILDREN

We welcome the term "healthy short stature (HSS)" as it reduces the burden of a diagnosis to most children below the arbitrary definition of normal height (1). It also emphasizes that an individual might be healthy despite a genetic diagnosis (1).

Idiopathic short stature (ISS) has been defined as a condition in which the height of an individual, with normal birthweight and GH sufficient, is more than 2 SD score (SDS) below the corresponding mean height for a given age, sex, and population group, without evidence of systemic, endocrine, nutritional, or chromosomal abnormalities (2).

As technology and our knowledge progresses, we need to adapt and improve nomenclatures and management.

Assuming that height has a Gaussian distribution, 2.3% of the normal population will have a height below -2.0 SD. We consider this threshold (-2 SD) as an indication for investigation to exclude manageable conditions but not as a threshold for treatment (3).

Common sense suggests that the farther the individual is from the mean, or from the parental height, the more likely it is due to a disease, more likely that a genetic abnormality can be found (4), and the more intense the search for a cause should be attempted. Also more likely is the burden of short stature, physically and psychosocially (5). Conversely, the closer to -2.0 SD, the higher the likelihood that a healthy child is a variation of normal.

In the US, according to the FDA, not all children with ISS are granted GH therapy, but only those with a height below -2.25 SD (1.2%). This excludes those between centiles 1.2 to 2.25 (approx. 45%) of patients labelled as ISS. Depending on the availability of rhGH, lower height limits of height may warrant treatment with growth promoting agents (2).

It is important to stress that idiopathic SS as well as healthy SS as suggested by Jorge et al, are diagnoses of exclusion. In fact, the authors expand the list of conditions that should be excluded in order to make the diagnosis of healthy short stature (1).

The authors refer to the lack of standardization for the measurement of body proportions. Interestingly, the sitting height to standing height SDS (SH/H) is a useful parameter which can be applied to different populations independently from the patient's height. For example, the standards developed for the Dutch population can be applied to Brazilian children (6,7). Sitting height can be measured in a specifically designed device, but in practice, it is enough to sit the patient on a removable box (usually 60 cm high) under the same calibrated stadiometer for height measurement and subtracting the height of the box (7).

Genetic testing shows importance of thorough clinical examination, as it is now not infrequent that after the finding of a genetic alteration the patient's phenotype is revisited and minor or previously undetected abnormalities are found.

Received on May/4/2026
Accepted on May/7/2026

DOI: 10.20945/2359-4292-2026-0068

Correspondence to:
Berenice B. Mendonc
beremen@usp.br

Associated editor:
Madson Queiroz de Almeida
https://orcid.org/0000-0002-2957-6148

This is an open-access article distributed under the terms of the Creative Commons Attribution License

Copyright© AE&M all rights reserved.

An important and very frequent condition with an acceptable height prognosis that can be considered as healthy short stature is the constitutional delay in growth and puberty (CDGP) (8). Superimposed to the normal variability in height, there is the variability on the age of development of puberty. Because growth velocity increases significantly during the pubertal growth spurt, differences in the timing of puberty can result in important height differences among peers of the same age. In the 2008 consensus on ISS, CDGP was considered a sub-classification of ISS (2). Before puberty, family history and a delayed bone age are reassuring but CDGP remains a diagnosis of exclusion made after puberty. The genetic basis of delayed puberty is being studied (9-12).

The development and widespread use of genetic testing also imposes new challenges: the discovery of variants classified as of uncertain significance (VUS) necessitate further studies to determine its real participation in the phenotype. The discovery of pathogenic variants in normal individuals indicate the possible variable penetrance and expressivity of these conditions (13).

The authors acknowledge that "Increasing understanding of the monogenic and polygenic architecture of short stature, alongside with genotype-specific treatment responses, will facilitate a transition toward more precise, genetically informed treatment protocols" (1).

The further development and improvement of polygenic scores (PGS) for both height and pubertal timing for all populations will likely help distinguish individuals who have inherited a polygenic variation of height and/or puberty from those in whom another diagnosis should be searched for.

After careful evaluation, we believe that the term healthy short stature is a designation that most short children deserve and includes height among the many individual characteristics.

In conclusion, the article by Jorge and colleagues is highly timely (1). Pediatric endocrinology has a role to play in abandoning terms that do not reflect current knowledge. We recommend the progressive adoption of the term "Healthy Short Stature" in clinical practice, scientific publications, and health systems. Considering that an increase in height represents more a desire than a need, physicians should emphasize the normality and qualities of HSS children, rejecting the concept that being taller means being better.

Disclosure: no potential conflict of interest relevant to this article was reported.

Data availability: datasets related to this article will be available upon request to the corresponding author.

REFERENCES

1. Jorge AAL, Collet-Solberg P, Boguszewski MCS. Healthy short stature: a necessary advancement. Arch Endocrinol Metab. 2026;70(4). doi: 10.20945/2359-4292-2026-0067.
2. Cohen P, Rogol AD, Deal CL, Saenger P, Reiter EO, Ross JL, et al. Consensus statement on the diagnosis and treatment of children with idiopathic short stature: a summary of the Growth Hormone Research Society, the Lawson Wilkins Pediatric Endocrine Society, and the European Society for Paediatric Endocrinology Workshop. J Clin Endocrinol Metab. 2008 Nov;93(11):4210-7. doi: 10.1210/jc.2008- 0509.
3. Mendonca BB, Arnhold IJP. GH Treatment in Children of Normal Height. J Clin Endocrinol Metab. 2024 Sep 16;109(10):e1955-e1958. doi: 10.1210/clinem/dgae457.
4. Scalco RC, Schoones JW, Galetaki D, Santillan-Vasconez AM, Kim GJ, Cellin LP, et al. Diagnostic yield of genetic testing in children with short stature: a systematic review. Eur J Endocrinol. 2026 Feb 4;194(2):S15-S24. doi: 10.1093/ejendo/lvag011.
5. Cianfarani S. Growth Hormone Therapy and Quality of Life: Evidence versus Assumptions. Horm Res Paediatr. 2026;99(3):314-318. doi: 10.1159/000549736.
6. Fredriks AM, van Buuren S, van Heel WJ, Dijkman-Neerincx RH, Verloove-Vanhorick SP, Wit JM. Nationwide age references for sitting height, leg length, and sitting height/height ratio, and their diagnostic value for disproportionate growth disorders. Arch Dis Child. 2005 Aug;90(8):807-12. doi: 10.1136/adc.2004.050799.
7. Malaquias AC, Scalco RC, Fontenele EG, Costalonga EF, Baldin AD, Braz AF, et al. The sitting height/height ratio for age in healthy and short individuals and its potential role in selecting short children for SHOX analysis. Horm Res Paediatr. 2013;80(6):449-56. doi: 10.1159/000355411.
8. Palmert MR, Dunkel L. Delayed puberty. N Engl J Med. 2012;366(5):443-53. doi: 10.1056/NEJMcp1109290.
9. Saengkaew T, Patel HR, Banerjee K, Butler G, Dattani MT, McGuigan M, et al. Genetic evaluation supports differential diagnosis in adolescent patients with delayed puberty. Eur J Endocrinol. 2021 Oct 8;185(5):617-627. doi: 10.1530/EJE-21-0387.
10. Kentistou KA, Kaisinger LR, Stankovic S, Vaudel M, Mendes de Oliveira E, Messina A, et al. Understanding the genetic complexity of puberty timing across the allele frequency spectrum. Nat Genet. 2024 Jul;56(7):1397-1411. doi: 10.1038/s41588-024-01798-4. Epub 2024 Jul 1. Erratum in: Nat Genet. 2024 Aug;56(8):1763-1764. doi: 10.1038/s41588-024-01857-w.
11. Lippincott MF, Schafer EC, Hindman AA, He W, Brauner R, Delaney A, et al.; Delayed Puberty Genetics Consortium. Contributions of Common Genetic Variants to Constitutional Delay of Puberty and Idiopathic Hypogonadotropic Hypogonadism. J Clin Endocrinol Metab. 2024 Dec 18;110(1):e61-e67. doi: 10.1210/clinem/dgae166.
12. Rezende RC, He W, Kaisinger LR, Lerario AM, Schafer EC, Kentistou KA, et al. Deleterious variants in intolerant genes reveal new candidates for self-limited delayed puberty. Eur J Endocrinol. 2025 Mar 27;192(4):481-490. doi: 10.1093/ejendo/lvaf061.
13. Kingdom R, Wright CF. Incomplete Penetrance and Variable Expressivity: From Clinical Studies to Population Cohorts. Front Genet. 2022 Jul 25;13:920390. doi: 10.3389/fgene.2022.920390.

Copyright© AE&M all rights reserved.

Archives of Endocrinology and Metabolism
ISSN 2359-4292
OFFICIAL JOURNAL OF THE BRAZILIAN SOCIETY OF ENDOCRINOLOGY AND METABOLISM

brief communication

Healthy short stature

Alexander A. L. Jorge[1]
https://orcid.org/0000-0003-2567-7360

Paulo F. Collett-Solberg[2]
https://orcid.org/0000-0002-6831-8520

Margaret C. S. Boguszewski[3]
https://orcid.org/0000-0002-5306-0715

[1] Unidade de Endocrinologia Genética (LIM25), Divisão de Endocrinologia, Hospital das Clínicas da Faculdade de Medicina da Universidade de São Paulo, São Paulo, SP, Brasil
[2] Disciplina de Endocrinologia, Departamento de Clínica Médica, Faculdade de Ciências Médicas da Universidade do Estado do Rio de Janeiro, Rio de Janeiro, RJ, Brasil
[3] Departamento de Pediatria, Universidade Federal do Paraná, Curitiba, PR, Brasil

ABSTRACT

Idiopathic short stature (ISS) has been used for more than five decades to label children whose height is below −2 SDS without an identified underlying cause. Although originally conceived as a pragmatic diagnosis of exclusion, ISS has gradually been reified as a disease entity and is now embedded in clinical guidelines, regulatory frameworks and indications for recombinant human growth hormone therapy. In parallel, advances in genomic technologies have uncovered a growing spectrum of monogenic and chromosomal variants among children previously classified as ISS, and highlighted the continuous, polygenic architecture of height in the remainder. These developments render the idiopathic construct increasingly misleading and unstable, as every new etiological discovery shrinks – and conceptually undermines – the ISS category. In this article, we review the historical evolution and current use of ISS, summarize the impact of modern genetic testing on the classification of short stature, and argue that most children currently labeled as having ISS are better described as having "Healthy Short Stature". We define Healthy Short Stature as short stature in otherwise healthy children without systemic, syndromic or endocrine disease, in whom short stature represents the lower extreme of normal growth variation. We discuss how adopting Healthy Short Stature can reduce stigma, remain compatible with ongoing genetic investigation, and provide a more robust framework for aligning clinical practice, research and health policy with contemporary knowledge of human growth biology.

Keywords: Short stature; genetic; idiopathic; height

"Idiopathic

Adjective

An idiopathic disease or medical condition has no known cause"

(https://dictionary.cambridge.org/dictionary/english/idiopathic)

The nomenclature or denomination of a disease or medical condition is a fundamental aspect of medical practice, guiding patient care, research, and health policies with both clinical and economic impact. A disease is generally defined as a structural and/or functional alteration characterized by a distinct set of symptoms and signs with an established etiology. However, in day-to-day practice, the identification of etiology often collides with the limitations of our knowledge of underlying pathophysiological mechanisms. Across virtually all medical specialties, the term idiopathic has been employed to denote conditions with no defined cause (1) and reflects the limits of medical knowledge at a given time. It usually represents a diagnosis of exclusion, established after negative results in a diagnostic workup aimed at identifying known conditions. An idiopathic diagnosis encompasses several different conditions with many pathophysiological mechanisms reflecting our temporary inability to better stratify patient groups. Medical practice and research then follow guidelines developed around an idiopathic diagnosis that represents multiple distinct conditions. Over time, as medical knowledge increases, idiopathic categories are redefined, giving rise to novel disease entities and allowing more precise, mechanism-based approaches.

Received on Feb/24/2026
Accepted on Apr/6/2026

DOI: 10.20945/2359-4292-2026-0067

Correspondence to:
Alexander Augusto de Lima Jorge
Avenida Dr. Arnaldo, 455,
5º andar, sala 5340
01246-903 – São Paulo, SP Brasil
alexj@usp.br

Editor in Chief:
Cesar Luiz Boguszewski
https://orcid.org/0000-0001-7285-7941

This is an open-access article distributed under the terms of the Creative Commons Attribution License

Copyright© AE&M all rights reserved.

Short stature is one of the most common reasons for referral to pediatricians and pediatric endocrinologists. Height below the expected range is a critical warning sign, as it may be the first and only manifestation of diverse underlying conditions. Clinical evaluation, mainly based on history and physical examination, aims to identify children whose short stature is secondary to systemic illness, skeletal dysplasia, or syndromic disorders (2). Complementary laboratory workup, preferably guided by clinical findings or focused on conditions in which short stature may present as the sole initial sign, is also standard practice. Yet, in most children evaluated for short stature, no definitive etiology is identified. In such cases, and in the absence of specific signs or symptoms, children are often labeled as having idiopathic short stature (ISS), a term that has been used for more than 50 years in over 1,200 medical publications (**Figure 1**).

The earliest uses of the term idiopathic in growth disorders date back to the 1960s (e.g., "idiopathic growth failure" (3), "idiopathic growth retardation" (4)). It was only in the 1970s, however, that the term ISS was introduced, designating a heterogeneous group of patients with growth impairment of unknown cause at the time (5,6). For years, ISS was applied in a non-standardized fashion until the first consensus was published in 1996. This consensus restricted ISS to children born appropriate for gestational age, with normal body proportions, adequate nutritional status, and no evidence of chronic systemic disease, psychiatric or severe emotional disorders, or endocrine deficiency (7). The definition was reaffirmed in a joint statement by the Lawson Wilkins Pediatric Endocrine Society and the European Society for Paediatric Endocrinology, which also required exclusion of chromosomal abnormalities and growth hormone deficiency. Importantly, children with dysmorphic features, skeletal dysplasia, or those born small for gestational age were explicitly excluded from ISS (8). This consensus also proposed a minimum diagnostic workup when no clinical findings guided targeted evaluation. At that time — prior to the genomic revolution of the last 15 years — it was recommended that suspected ISS cases undergo bone age radiograph, complete blood count, erythrocyte sedimentation rate, creatinine, electrolytes, bicarbonate, calcium, phosphate, alkaline phosphatase, albumin, TSH, free T4, IGF-1 determination, screening for celiac disease, and karyotyping (all girls, and short boys with associated genital abnormalities) (8).

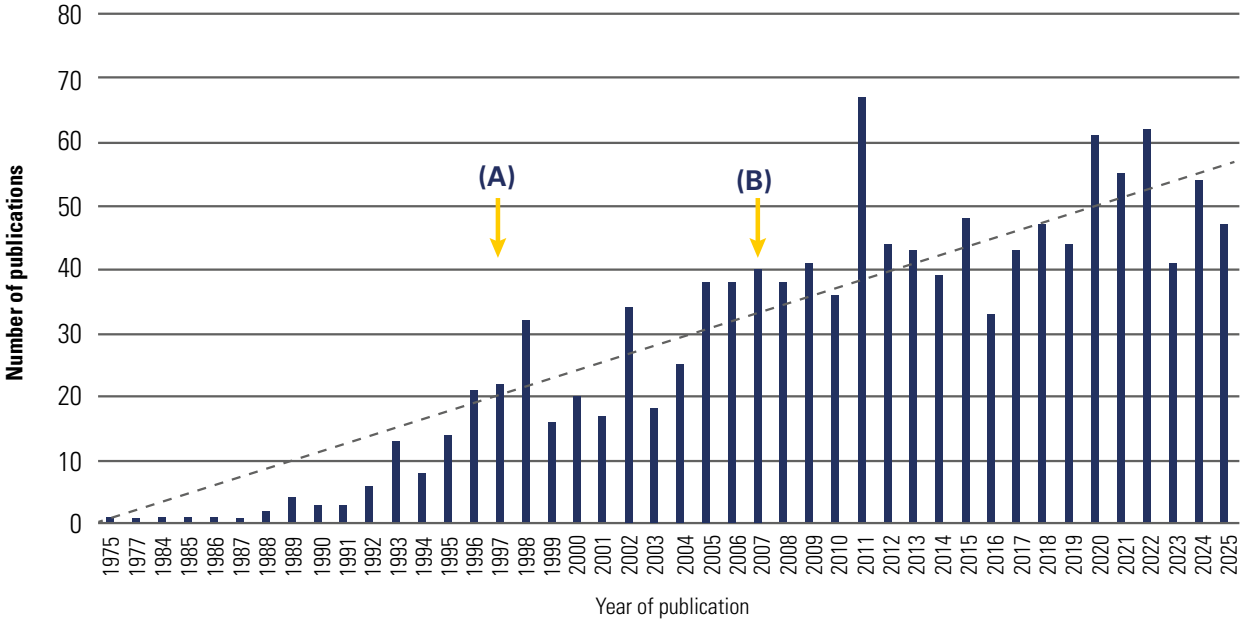


Figure 1. Evolution of the number of publications containing the term "Idiopathic Short Stature" in the title or abstract over the years. Publications referring to the 1996 (**A**) (7) and 2008 (**B**) (8) consensus are highlighted by the arrow. The upward trend is represented by the dotted line.

Copyright© ACEM All rights reserved.

Following these two landmark publications, the use of the term ISS markedly increased in the medical literature (**Figure 1**). Many studies adopted the consensus-based definition of ISS, yet, in practice, the term was often applied more loosely to denote short stature of unknown cause, without strict adherence to the recommended diagnostic framework. Important gaps also emerged, such as the lack of standardized methods for defining normal body proportions. Additionally, when the term ISS was first coined, it was accompanied by the assumption that children with ISS have a polygenic basis of their growth impairment (9,10) — an explanation that, at that time, was beyond the reach of clinical or research evaluation. This view did not anticipate a foreseeable horizon in which genetic testing could uncover the etiology of short stature in children previously labeled as ISS. As a result, ISS came to be used not only as a descriptor of a growth disorder but also, in many instances, as a diagnosis itself.

In parallel with efforts to establish a consensus definition for ISS, studies began to reveal that a subset of children categorized as ISS had monogenic causes for their short stature (11). Each of the genes implicated in phenotypes overlapping with the ISS definition accounted for only a small fraction of affected patients (~2%) (12). Most were associated with autosomal dominant inheritance, frequently observed in families where one of the parents also had short stature (11). Moreover, most of these genes were found to be involved in endochondral bone development, the key biological process underlying longitudinal growth. In the early years of the 21st century, however, genetic testing relied on methodologies that were labor-intensive, costly, and time-consuming, which prevented the widespread incorporation of this analysis into clinical practice outside of research settings.

With the advent of large-scale parallel sequencing — also known as next-generation sequencing (NGS) — the cost of genetic testing decreased dramatically (13), allowing the simultaneous analysis of multiple genes selected for their role in a specific disease (targeted panels), sequencing of almost the entire coding portion of the genome (exome sequencing, ES), and even sequencing of the entire genome (genome sequencing, GS). Broad genetic investigation has thus become the main model for research and, more recently, has permeated clinical practice (13). Over the last 15 years, the methodology has become increasingly automated, with substantial cost reduction and major improvements in bioinformatics pipelines, enabling the identification of variants with accuracy comparable or even superior to that of gold-standard techniques, for both single-nucleotide variants (SNVs) and copy-number variants (CNVs) (14). Commercial laboratories have progressively adopted ES as the main genotyping strategy, applying virtual gene panels tailored to the clinical question at hand (13).

The first study employing NGS to investigate unexplained short stature in children was published in 2013 and reported a diagnostic yield of 2.6% (15). Interestingly, this early report showed that patients harboring pathogenic variants in *PTPN11* — a gene associated with Noonan syndrome — could lack the characteristic clinical phenotype, leading to an initial classification of ISS. Since then, numerous studies have refined both sequencing technology and variant interpretation, progressively increasing diagnostic yield. In patients meeting strict ISS criteria, broad genetic approaches currently yield a molecular diagnosis in approximately 10%–16% of cases (12,16,17). Although there is significant clinical overlap between children with and without an identifiable monogenic cause, severe short stature remains a predictor of a positive genetic finding, as do abnormal body proportions and a family history suggestive of autosomal dominant inheritance (17).

While genetic testing establishes a definitive cause for a relatively small proportion of children initially labeled as ISS, for those in whom a pathogenic variant is identified, the impact is profound — not only by providing an explanation that alleviates parental anxiety, but also by enabling family-based case recognition and guiding individualized clinical management (13,18).

Given this scenario, the use of recombinant human growth hormone (rhGH) in children classified as ISS remains controversial, partly because some short children experience spontaneous catch-up growth during puberty (19), and partly because of the variable treatment response (20,21), likely reflecting the genetic

Copyright© AE&M all rights reserved.

heterogeneity of ISS. A clear proof-of-concept for the relevance of genetic testing is provided by *SHOX* haploinsufficiency, the most frequent monogenic cause of short stature, detected in about 2% of children labeled as ISS (10). Studies have demonstrated that untreated *SHOX*-deficient children tend lose height SDS during the period from the onset of puberty to adulthood (22,23), while rhGH treatment increases final height (23,24) — a benefit that underlies its approved indication in several countries. Thus, identifying a pathogenic *SHOX* variant has direct implications for the management of a child initially classified as ISS.

However, the recognition of a monogenic component in children previously labeled as ISS introduces a semantic and conceptual conflict, as such cases should no longer be considered idiopathic; rather, they should be reclassified based on the genetic finding implicated in the phenotype. Some of the genes identified in these patients are associated with established clinical syndromes, such as *PTPN11* in Noonan syndrome (25). Nevertheless, in the absence of hallmark clinical features besides short stature, it seems inappropriate to extrapolate a syndromic diagnosis based solely on genotype while disregarding the clinical presentation.

In this regard, what terminology should be applied to children with short stature without a genetic diagnosis, whether due to lack of testing or inconclusive results? Persisting to label these children as having idiopathic short stature seems inadequate for several reasons:

1. It is well established that height variation is largely determined by the interplay between numerous common variants with small individual effects and rare variants with moderate or large effects. Thus, in the absence of secondary causes, much of height variation reflects genetic diversity (10).
2. Without broad genetic testing, it is not possible to determine — based solely on clinical findings — whether an individual harbors a pathogenic variant fully or partially explaining their stature.
3. Giving the continuous advances in genomics, even currently negative cases may be elucidated in the near future (13). The incorporation of polygenic scores will likely refine our understanding of what is presently labeled as ISS (26).

Returning to the evaluation and grouping of children with short stature, although it is useful to incorporate descriptive classifications — such as syndromic *vs.* non-syndromic, proportional *vs.* disproportionate, pre- *vs.* postnatal onset, and familial *vs.* non-familial — they offer limited practical meaning to the families. The term "*Isolated Short Stature*" has also been proposed to indicate children for whom short stature is the sole apparent phenotype (11,27), with the semantic convenience of preserving the ISS acronym. However, truly isolated short stature is uncommon; most cases display subtle or non-specific findings — such as fifth finger brachymesophalangia — often present in the general population but also enriched among individuals with pathogenic variants in *IHH* (28).

In light of these considerations, we propose that children whose main clinical manifestation is short stature—without major dysmorphic features, developmental delay, endocrine abnormalities, or systemic disease—should be classified under the term "***Healthy Short Stature***" (HSS) (See **Box 1** for a more detailed definition). This terminology more accurately reflects the upper threshold of diagnostic evaluation currently available through comprehensive clinical and laboratory investigation, while also removing the burden of a "diagnosis" for a characteristic that fundamentally represents a normal variant of human growth diversity. Moreover, the concept of ***Healthy Short Stature*** emphasizes respect for phenotypic variation and may help to mitigate social and psychological biases associated with stature.

Importantly, adopting the term ***Healthy Short Stature*** should not preclude further genetic investigation. Instead, genetic testing should remain contingent on clinical context, accessibility, and informed discussion with families regarding the potential implications of molecular findings (29). An advantage of ***Healthy Short Stature*** is that, if genetic testing identifies an explanation for the short stature, the designation remains applicable, provided the patient does not manifest additional clinical signs and symptoms. This is in the opposite direction of the term ISS, as if the genetic variant responsible for the short stature is identified, the term ISS becomes obsolete. As investigation into the genetics of short stature progresses, we will gain

Copyright© AE&M all rights reserved.

Box 1. Proposed clinical features supporting the designation of Healthy Short Stature

Healthy Short Stature may be considered in a child with short stature when all of the following apply:

- Height SDS < –2
- Short stature as the main clinically relevant finding
- Normal body proportions or only mild disproportion[1]
- No neurodevelopmental disorder
- No major congenital malformations[2]
- No significant minor dysmorphic phenotype on overall physical examination[3]
- No evidence of chronic systemic disease
- No endocrine disorder explaining growth failure
- No nutritional disorder or undernutrition
- No psychiatric disease or severe emotional disturbance affecting growth
- No exposure to medications that can explain impair growth

Additional considerations

- The designation should follow appropriate clinical, laboratory, and imaging evaluation.
- Healthy Short Stature does not preclude genetic testing when clinically indicated.
- Periodic reassessment of clinical findings should be undertaken to ensure that this designation remains appropriate over time.

Footnote: 1. Mild body disproportion may be considered when sitting height-to-height SDS is within approximately ±2.5, in the absence of skeletal abnormalities. **2.** Major congenital malformations are defined as structural abnormalities with significant functional, medical, surgical, or cosmetic consequences. **3.** Minor dysmorphic features are subtle morphological variants with little or no functional impact in isolation; however, a constellation of such findings may be clinically relevant and should prompt consideration of an underlying syndromic diagnosis.

further insights into both physiological and pathological growth. Increasing understanding of the monogenic and polygenic architecture of short stature, alongside with genotype-specific treatment responses, will facilitate a transition toward more precise, genetically informed treatment protocols.

An anticipated resistance to transitioning from ISS to ***Healthy Short Stature*** stems from the established regulatory and reimbursement frameworks for rhGH therapy already in place in numerous countries (30). Renaming the condition could generate administrative barriers to treatment access for eligible children. This incentive structure may also inadvertently discourage physicians from pursuing comprehensive genetic investigation, as maintaining the "idiopathic" label remains a pragmatic strategy for ensuring treatment authorization. Nevertheless, current evidence suggests that the safety and efficacy profiles established for rhGH treatment in short children currently labeled as ISS can be largely extrapolated to those who would instead be designated as having ***Healthy Short Stature***.

In conclusion, ***Healthy Short Stature*** provides a terminology that is more consistent with current genetic knowledge and the lived experience of the majority of short children and their families. This term acknowledges that, in the absence of systemic, syndromic, or endocrine disease, short stature predominantly represents the lower extreme of normal variation rather than a pathological condition. At the same time, this nomenclature preserves and even reinforces the need for careful clinical assessment and judicious application of genetic testing when red flags are identified or when new features emerge over time. By redefining ISS as ***Healthy Short Stature***, we move away from an inherently provisional idiopathic label and toward a resilient, descriptive concept that remains valid alongside future etiological discoveries. This shift may facilitate the alignment of clinical practice, regulatory frameworks, and research agendas with a more nuanced and balanced recognition of human growth diversity.

Authors' contributions: All authors made substantive intellectual contributions to the present study. A.A.L.J., P.F.C-S., and M.C.S.B. also contributed to the conceptualization of the study. A.A.L.J. wrote the first draft, which was edited and revised by P.F.C-S. and M.C.S.B.

Funding: A.A.L.J. is funded by grant 303294/2020-5 from the National Council for Scientific and Technological Development (CNPq).

Disclosure: A.A.L.J. has received consulting fees from Novo Nordisk and Bridgebio and an independent research grant from BioMarin. P.F.C.S. has received consulting fees and support to attend scientific meetings from Pfizer, Novo Nordisk and BioMarin. M.C.S.B has received consulting fees from Novo Nordisk and support to attend scientific meetings from Novo Nordisk, Sandoz and Pfizer.

Data availability: datasets related to this article will be available upon request to the corresponding author.

Copyright© AE&M all rights reserved.

REFERENCES

1. Tirlapur SA, Priest L, Daniels JP, Khan KS, Group MSM. How do we define the term idiopathic? Curr Opin Obstet Gynecol. 2013;25(6):468-73. doi: 10.1097/GCO.0000000000000025.
2. Collett-Solberg PF, Jorge AAL, Boguszewski MCS, Miller BS, Choong CSY, Cohen P, et al. Growth hormone therapy in children; research and practice - A review. Growth Horm IGF Res. 2019;44:20-32. doi: 10.1016/j.ghir.2018.12.004.
3. Soyka LF, Ziskind A, Crawford JD. Treatment of Short Stature in Children and Adolescents with Human Pituitary Growth Hormone (Raben). N Engl J Med. 1964;271:754-64. doi: 10.1056/NEJM196410082711502.
4. Edelmann CM Jr, Houston IB, Rodriguez Soriano J, Boichis H, Stark H. Renal excretion of hydrogen ion in children with idiopathic growth retardation. J Pediatr. 1968;72(4):443-51. doi: 10.1016/s0022-3476(68)80332-4.
5. Spiegel RN, Sather AH, Hayles AB. Cephalometric study of children with various endocrine diseases. Am J Orthod. 1971;59(4):362-75. doi: 10.1016/0002-9416(71)90232-6.
6. Grunt JA, Enriquez AR. Acute and long-term responsiveness to growth hormone in children with short stature. Pediatr Res. 1972;6(8):664-74. doi: 10.1203/00006450-197208000-00004.
7. Ranke MB. Towards a consensus on the definition of idiopathic short stature. Horm Res. 1996;45 Suppl 2:64-6. doi: 10.1159/000184851.
8. Cohen P, Rogol AD, Deal CL, Saenger P, Reiter EO, Ross JL, et al. Consensus statement on the diagnosis and treatment of children with idiopathic short stature: a summary of the Growth Hormone Research Society, the Lawson Wilkins Pediatric Endocrine Society, and the European Society for Paediatric Endocrinology Workshop. J Clin Endocrinol Metab. 2008;93(11):4210-7. doi: 10.1210/jc.2008-0509.
9. Grunauer M, Jorge AAL. Genetic short stature. Growth Horm IGF Res. 2018;38:29-33. doi: 10.1016/j.ghir.2017.12.003.
10. Bicknell LS, Hirschhorn JN, Savarirayan R. The genetic basis of human height. Nat Rev Genet. 2025 Sep;26(9):604-619. doi: 10.1038/s41576-025-00834-1.
11. Vasques GA, Andrade NLM, Jorge AAL. Genetic causes of isolated short stature. Arch Endocrinol Metab. 2019;63(1):70-8. doi: 10.20945/2359-3997000000105.
12. Scalco RC, Schoones JW, Galetaki D, Santillan-Vasconez AM, Kim GJ, Cellin LP, et al. Diagnostic Yield of Genetic Testing in Children with Short Stature: a Systematic Review. Eur J Endocrinol. 2026 Feb 4;194(2):S15-S24. doi: 10.1093/ejendo/lvag011.
13. Dauber A, Jorge AAL, Nilsson O, Dekkers OM, Argente J, Netchine I, et al. International guideline on genetic testing of children with short stature. Eur J Endocrinol. 2026 Feb 4;194(2):R17-R36. doi: 10.1093/ejendo/lvag013.
14. Satam H, Joshi K, Mangrolia U, Waghoo S, Zaidi G, Rawool S, et al. Next-Generation Sequencing Technology: Current Trends and Advancements. Biology (Basel). 2023 Jul 13;12(7):997. doi: 10.3390/biology12070997.
15. Wang SR, Carmichael H, Andrew SF, Miller TC, Moon JE, Derr MA, et al. Large-scale pooled next-generation sequencing of 1077 genes to identify genetic causes of short stature. J Clin Endocrinol Metab. 2013;98(8):E1428-37. doi: 10.1210/jc.2013-1534.
16. Ahn J, Oh J, Suh J, Song K, Kwon A, Chae HW, et al. Next-generation sequencing-based mutational analysis of idiopathic short stature and isolated growth hormone deficiency in Korean pediatric patients. Mol Cell Endocrinol. 2022;544:111489. doi: 10.1016/j.mce.2021.111489.
17. Andrade NLM, Funari MFA, Malaquias AC, Collett-Solberg PF, Gomes N, Scalco R, et al. Diagnostic yield of a multigene sequencing approach in children classified as idiopathic short stature. Endocr Connect. 2022 Nov 14;11(12):e220214. doi: 10.1530/EC-22-0214.
18. Collett-Solberg PF, Ambler G, Backeljauw PF, Bidlingmaier M, Biller BMK, Boguszewski MCS, et al. Diagnosis, Genetics, and Therapy of Short Stature in Children: A Growth Hormone Research Society International Perspective. Horm Res Paediatr. 2019;92(1):1-14. doi: 10.1159/000502231.
19. Greco L, Power C, Peckham C. Adult outcome of normal children who are short or underweight at age 7 years. BMJ. 1995;310(6981):696-700. doi: 10.1136/bmj.310.6981.696.
20. Dauber A, Phillip M, Ferran JM, Kelepouris N, Nedjatian N, Olsen AH, et al. Clinical Predictors of Good/Poor Response to Growth Hormone Treatment in Children with Idiopathic Short Stature. Horm Res Paediatr. 2024:1-12. doi: 10.1159/000542579.
21. Deodati A, Cianfarani S. Impact of growth hormone therapy on adult height of children with idiopathic short stature: systematic review. BMJ. 2011;342:c7157. doi: 10.1136/bmj.c7157.
22. Scalco RC, Melo SS, Pugliese-Pires PN, Funari MF, Nishi MY, Arnhold IJ, et al. Effectiveness of the combined recombinant human growth hormone and gonadotropin-releasing hormone analog therapy in pubertal patients with short stature due to SHOX deficiency. J Clin Endocrinol Metab. 2010;95(1):328-32. doi: 10.1210/jc.2009-1577.
23. Dantas NCB, Funari MFA, Vasques GA, Andrade NLM, Rezende RC, Brito V, et al. Adult Height of Patients with SHOX Haploinsufficiency with or without GH Therapy: A Real-World Single-Center Study. Horm Res Paediatr. 2022;95(3):264-74. doi: 10.1159/000524374.
24. Blum WF, Ross JL, Zimmermann AG, Quigley CA, Child CJ, Kalifa G, et al. GH treatment to final height produces similar height gains in patients with SHOX deficiency and Turner syndrome: results of a multicenter trial. J Clin Endocrinol Metab. 2013;98(8):E1383-92. doi: 10.1210/jc.2013-1222.
25. Jorge AA, Malaquias AC, Arnhold IJ, Mendonca BB. Noonan syndrome and related disorders: a review of clinical features and mutations in genes of the RAS/MAPK pathway. Horm Res. 2009;71(4):185-93. doi: 10.1159/000201106.
26. Lu T, Forgetta V, Wu H, Perry JRB, Ong KK, Greenwood CMT, et al. A Polygenic Risk Score to Predict Future Adult Short Stature Among Children. J Clin Endocrinol Metab. 2021;106(7):1918-28. doi: 10.1210/clinem/dgab215.
27. Fan X, Zhao S, Yu C, Wu D, Yan Z, Fan L, et al. Exome sequencing reveals genetic architecture in patients with isolated or syndromic short stature. J Genet Genomics. 2021;48(5):396-402. doi: 10.1016/j.jgg.2021.02.008.
28. Vasques GA, Funari MFA, Ferreira FM, Aza-Carmona M, Sentchordi-Montane L, Barraza-Garcia J, et al. IHH Gene Mutations Causing Short Stature With Nonspecific Skeletal Abnormalities and Response to Growth Hormone Therapy. J Clin Endocrinol Metab. 2018;103(2):604-14. doi: 10.1210/jc.2017-02026.
29. Dauber A. Genetic Testing for the Child With Short Stature-Has the Time Come To Change Our Diagnostic Paradigm? J Clin Endocrinol Metab. 2019;104(7):2766-9. doi: 10.1210/jc.2019-00019.
30. Danowitz M, Grimberg A. Clinical Indications for Growth Hormone Therapy. Adv Pediatr. 2022;69(1):203-17. doi: 10.1016/j.yapd.2022.03.005.

Copyright© AE&M all rights reserved.

Archives of Endocrinology and Metabolism
ISSN 2359-4292
OFFICIAL JOURNAL OF THE BRAZILIAN SOCIETY OF ENDOCRINOLOGY AND METABOLISM

brief communication

Clinical characteristics, glycemic control & quality of life of patients using Android Artificial Pancreas System (AAPS) in Brazil

Gabriella Lopes Ventura[1]
https://orcid.org/0009-0002-3056-7334
Laryssa da Silva Messias[1]
https://orcid.org/0009-0008-8036-9727
Maria Eduarda Pereira Dantas[2]
https://orcid.org/0000-0003-4704-4492
Milena Oliveira Leite[2]
https://orcid.org/0000-0002-9215-2890
Débora Souto[3]
https://orcid.org/0000-0002-5149-0391
Maria de Lourdes Passos Machado[2]
https://orcid.org/0009-0007-6741-993X
Edson Perrotti[4]
https://orcid.org/0009-0003-9146-4803
Thiago Mota Soares[1]
https://orcid.org/0009-0005-2912-1724
Tassia Virginia de Carvalho Oliveira[2]
https://orcid.org/0000-0003-3265-4239
Lenita Zajdenverg[1]
https://orcid.org/0000-0002-1579-3299
Joana Dantas[1]
https://orcid.org/0000-0002-6088-2813
Melanie Rodacki[1]
https://orcid.org/0000-0002-9007-1325

[1] Universidade Federal do Rio de Janeiro, Rio de Janeiro, RJ, Brasil
[2] Universidade Tiradentes, Aracaju, SE, Brasil
[3] Departamento de Nutrologia e Diabetes, Universidade Federal do Rio de Janeiro, Rio de Janeiro, RJ, Brasil
[4] Universidade Federal de Alagoas, Maceió, AL, Brasil

ABSTRACT

Objective: This study evaluated the safety and efficacy of the Android Artificial Pancreas System (AAPS) in Brazilians with type 1 diabetes mellitus (T1D). **Subjects and methods:** A total of 371 participants were surveyed, including 62 AAPS users and 309 non-users. AAPS configurations included continuous glucose monitoring (CGM), Bluetooth transmitter (MiaoMiao), and a non-automated insulin pump. **Results:** AAPS users had a mean Time in Range (TIR) of 78.5% ± 16.6, with HbA1c levels decreasing from 7.3% ± 1.03 to 6.5% ± 0.7 ($p < 0.001$). Compared to non-AAPS users, AAPS users demonstrated better glycemic control, fewer severe hypoglycemic events ($p = 0.006$), and improved quality of life ($p < 0.0001$). However, 23.08% of AAPS users had a TIR below 70%, and time in level-2 hypoglycemia exceeded recommendations. **Conclusion:** These findings highlight AAPS as a low-cost alternative to commercial systems, with potential to expand access to automated therapy globally, particularly in resource-limited settings.

Keywords: Type 1 diabetes; artificial pancreas; automated insulin delivery systems; quality of life; glycemic control

INTRODUCTION

Type 1 diabetes mellitus (T1D) is a chronic autoimmune disease that leads to hyperglycemia and its potential complications due to the destruction of pancreatic beta cells. Managing T1D typically involves basal-bolus insulin therapy to maintain blood glucose levels near normal and reducing the risk of complications (1). However, this treatment is complex and burdensome, requiring multiple daily insulin injections (MDI) or continuous insulin infusion systems (CIIS), frequent glucose monitoring, carbohydrate counting, and constant attention to insulin adjustments and dietary choices (2,3). Additionally, the risk of hypoglycemia can impact quality of life (4).

Automated insulin delivery systems (AID) can ease the decision-making burden for individuals with T1D, but they are expensive and often inaccessible, particularly in developing countries (5,6). These systems have been shown to improve glycemic control, increase Time in Range (TIR), reduce HbA1c levels and potentially lower the risk of diabetes-related complications (7-13). The AAPS offers a lower-cost alternative for AID, though it has not received regulatory approval in many countries (14,15). AAPS configurations include the First-generation continuous glucose monitoring (CGM), Bluetooth transmitter, and an insulin pump. It is one of the most affordable AID options and is commonly used. The First-generation CGM is an intermittent continuous (is-CGM), while Bluetooth transmitter is a Bluetooth transmitter that converts the CGM into a real-time monitoring

Received on July/10/2025
Accepted on Dec/17/2025
DOI: 10.20945/2359-4292-2026-0066

Correspondence to:
Maria Eduarda Pereira Dantas
maria.epereira@souunit.com.br

Associated editor:
João Roberto de Sá
https://orcid.org/0000-0003-3115-5606

This is an open-access article distributed under the terms of the Creative Commons Attribution License

Copyright© AE&M all rights reserved.

(rtCGM) system with predictive alerts, integrated with AID systems like AAPS. However, the efficacy, safety, and impact on patients' quality of life of this AAPS configuration have not been fully evaluated in individuals with T1D.

The objective of this study was to characterize the profile of AAPS users and compare their clinical characteristics, quality of life (QoL) and glycemic control with patients with T1D using non-automated treatments in the Brazilian population.

SUBJECTS AND METHODS

This observational study surveyed T1D patients using AAPS with First-generation CGM, Bluetooth transmitter Miaomiao), and Roche Accu-Chek Combo or Medtronic Paradigm insulin pump, recruited via social media. Participants using AAPS employed the first-generation CGM with a Bluetooth transmitter, providing continuous glucose readings during sensor wear. However, specific information regarding CGM data coverage (e.g., number of active days or hours) was not available.

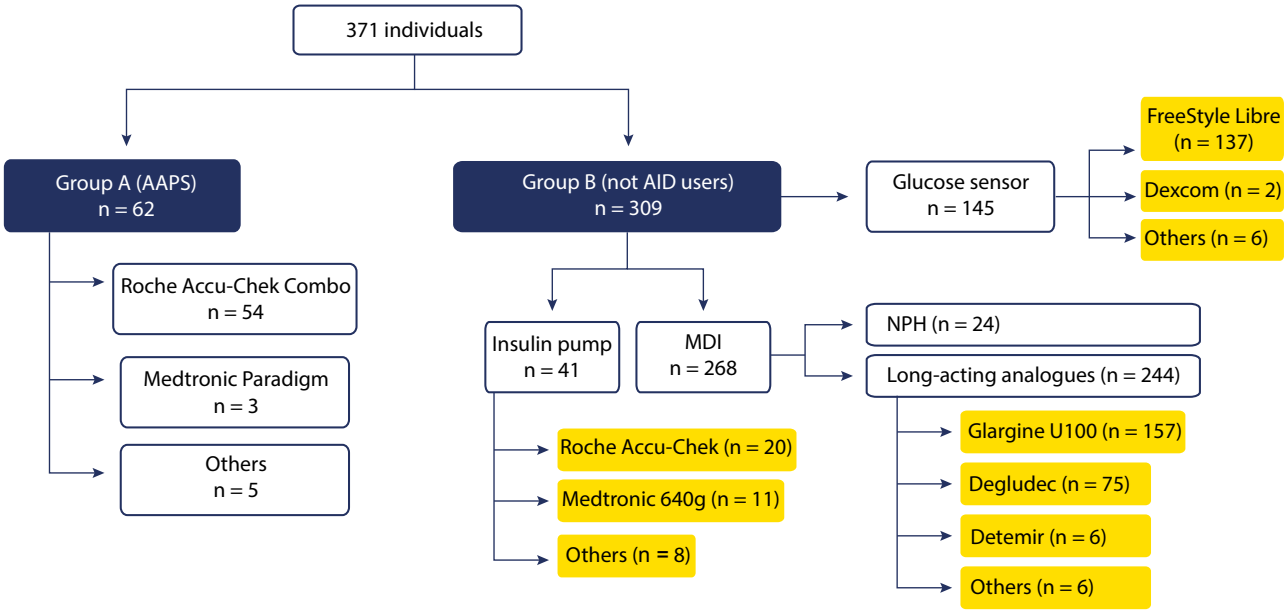
A comparison group of patients not using automated insulin delivery systems was also included. Data was collected remotely through an AirTable form, covering education status, glucose control, hypoglycemia, DKA frequency, and quality of life (DQOL-Brazil). HbA1c levels reported by participants referred to values before and after AAPS use. The "before" value corresponded to the most recent HbA1c prior to initiating AAPS, and the "after" value corresponded to the most recent available measurement during system use. All HbA1c values were self-reported by participants. Data on diabetic ketoacidosis (DKA) episodes were self-reported by participants through the questionnaire. Statistical analysis was conducted using SPSS 21.0, with Mann-Whitney and Chi-square tests to compare groups, considering a significance level of <0.05. Information on whether participants received care through the public (SUS) or private health system was not collected in the questionnaire and therefore percentages for public vs. private care are not available.

This study was approved by the Research Ethics Committee of the Federal University of Rio de Janeiro (CAAE: 71962123.3.0000.5257).

RESULTS

Characteristics of the study group

The study included 371 participants, divided into two groups as detailed in **Figure 1**. Among AAPS users



AAPS: Android Artificial Pancreas System; AID: automated insulin delivery; MDI: multiple daily injections; NPH: Neutral Protamine Hagedorn.

Figure 1. Study population and treatment characteristics of AAPS users and non-AID individuals in Brazil.

Copyright© AE&M all rights reserved.

(group A/n = 62), the mean age and disease duration were 36.4 ± 13.2 and 20.9 ± 12.1 years, respectively. In this group, 75.8% of patients aged 18 years or older and had completed higher education. For those under 18 years, 94.1% of their caregivers had completed higher education. Among AAPS users, 24% of participants had been using the system for less than 6 months, 29.6% for 6 months to 1 year, 27.7% for 1 to 2 years, and 18.5% for more than 2 years. In individuals that did not use AID (Group B/n = 309), the mean age and disease duration were 29.4 ± 11.4 years and 12.6 ± 10.1 years, respectively. Among them, 50.3% of those aged 18 years or older and 56% of the caregivers in those < 18 years old had complete higher education. In group B, 178 (57,6%) participants use glucose sensors (either flash glucose sensors or CGM). Patients' treatments according to groups are described in **Figure 1**.

Glycemic control

HbA1c levels

Among AAPS users, the mean glycated hemoglobin level (HbA1c), before starting AAPS, were 7.3% ± 1.03, which decreased to 6.5 ± 0.7% after treatment ($p < 0.001$).

When comparing groups, Group A demonstrated significantly lower HbA1c levels ($p < 0.001$), a higher proportion of individuals had HbA1c <7% ($p < 0.001$), and fewer severe hypoglycemia events per year ($p = 0.006$) than Group B. The mean weekly rates of reported hypoglycemia were similar between the groups ($p = 0.73$) (**Table 1**).

CGM data

CGM data were collected only in group A and analyzed in 39 users. TIR, time below range (TBR, <70 mg/dL), time in level-2 hypoglycemia (<54 mg/dL), time above range (TAR, >180 mg/dL), time in level-2 hyperglycemia (>250 mg/dL), and the coefficient of variation were 77.9% ± 12.9, 4.4% ± 3.7, 1.7% ± 2.4, 17.5% ± 13.4, 4.12% ± 5.62, and 35.0 ± 7.0, respectively. Notably, 23.08% of users had a TIR below 70%, with 7.69% had a TIR below 60%, and 5.12% had a TIR below 50%.

Treatment satisfaction and quality of life

From those using AAPS who responded, 79.2% reported being very or moderately satisfied with their current treatment, and 64.2% indicated being very or moderately satisfied with the time required for diabetes management.

When comparing quality of life (QoL), Group A had better results in all domains of the questionnaire: satisfaction ($p < 0.0001$), impact ($p < 0.0001$), social/professional concern ($p < 0.0001$) and concern related to T1D ($p < 0.0001$) (**Table 1**).

Diabetic Ketoacidosis (DKA)

Specific data on DKA was collected from 60 patients, including 50 AAPS users (Group A) and 10 non-users (Group B). In Group A, 26% of patients experienced 1 to 2 DKA episodes per year, compared to 40% in Group B. In the group A, 74% of individuals had never had a DKA episode, versus 60% in group B. However, this data was not statistically significant ($p = 0.295$).

Table 1. Characteristics of the study groups

	Group A (AAPS) (n=62)	Group B (n=309)	p-value
QoI Domain Satisfaction	28 ± 11,5	41 ± 9,8	<0,0001
QoI Domain Impact	35 ± 9,3	46 ± 12,9	<0,0001
QoI Domain Social/Professional Concern	10 ± 5,8	15 ± 7,8	<0,0001
QoI Domain Concern related to T1D	8 ± 3,1	10 ± 3,8	<0,0001
A1c before AAPS	7,3% ± 1,03	7,4% ± 2,1	-
A1c after AAPS	6,5% ± 0,7	-	<0,001
A1c < 7%	75,80%	49,20%	<0,001
Hypoglycemia in a week	3,5 ± 2,2	3,3 ± 1,9	p=0,73
Number of severe hypoglycemia	0,5 ± 1,2	1,6 ± 2,1	p=0,006

QoL: quality of life. A1c: glycated hemoglobin.

Copyright© AE&M all rights reserved.

DISCUSSION

This study assessed the safety and efficacy of a lower cost AID system in a real-world setting, with AAPS, IsCGM and Bluetooth transmitter. This analysis is particularly important, as many individuals currently use the system despite the lack of regulatory approval. If demonstrated to be safe and effective, it could provide a more affordable alternative for automated insulin delivery, particularly in developing countries where access to diabetes technology remains limited.

The findings align with previous studies that quantitatively demonstrated the impact of AAPS on glycemic control (15,16). In a study by Braune and cols. (2019), AAPS users showed an improvement in TIR, increasing from 63.8% ± 15.0 before system initiation to 79.5% ± 7.9 after its implementation. Although slightly higher than the 77.9% ± 12.9 observed in this study, this still represents significant glycemic control improvements compared to baseline levels of less than 60%. Similarly, Herzog and cols. (2020) (15) reported that do-it-yourself (DIY) closed loop users in Germany achieved a mean TIR of 79.5% ± 15.3 and reductions in HbA1c of up to 1.0%, consistent with the 0.5% HbA1c reduction observed in this study. However, in this study, the percentage of time spent in level-2 hypoglycemia (<54 mg/dL) was 1.7% ± 2.4%. While no studies have specifically analyzed this metric in AAPS users, data from commercially available artificial pancreas systems, such as the Medtronic MiniMed 780G, report significantly lower values, with TBR2 ranging from 0.5% to 0.6% (13). The slight differences in failure rates to achieve glucose control targets might be related to the various sensors used in the systems (IsCGM, Medtronic Guardian and Dexcom), the DIY nature of AAPS, combined with the absence of regulatory oversight and structured training, as well as differences in patients´ adherence and medical care. Improvements in the algorithm might also be necessary to optimize the results. Further research is needed to determine the impact of these factors on hypoglycemia rates and to improve the safety and consistency of AAPS (11,13,14,16,17).

Quality of life was assessed using the DQOL-Brazil questionnaire, showing better scores for AAPS users than non-users. Similar studies report that DIY AID systems enhance glycemic control, reduce treatment burden, and improve psychosocial outcomes, suggesting AID eases both clinical and emotional aspects of T1D management (15,16).

Better quality of life can improve adherence, reduce distress, and lower the risk of Diabetes Burnout. However, moderate satisfaction (64.2%) with the time required for diabetes management indicates the need for usability improvements. Future AAPS advancements should simplify the interface and reduce the time commitment.

Although widely used, the DQOL-Brazil primarily assesses general diabetes management and may not capture AID-specific benefits. Complementary tools like the Diabetes Distress Scale (DDS) could provide deeper insights, but they have yet to be translated into Portuguese.

Data on DKA occurrence were limited in this study, but the available data suggest that the incidence of DKA was lower among AAPS users compared to those using non-automated systems. The differences could be linked to socioeconomic and educational factors, as AAPS users in this sample had higher socioeconomic and educational levels. This may help to reduce the risk of DKA. Further studies are needed to explore this finding. It is also possible that the low frequency of reported DKA was due to heightened awareness among individuals at risk, although some AAPS users might have developed DKA due to inadequate medical supervision, as the system is DIY. It is important to note that DKA data were self-reported and not verified through medical records, which could lead to recall bias. The questionnaire collected frequency categories (e.g., 0, 1–2 per year) rather than exact counts and we do not have person-time data to calculate incidence per 100 person-years. We acknowledge that incidence rates with 95% CI would be preferable and will include them in future analyses if raw event counts and follow-up time become available.

A potential selection bias should be acknowledged, as participants were recruited through social media. This may have led to a sample composed of individuals more engaged with diabetes management and with greater access to educational and technological

Copyright© AE&M all rights reserved.

resources, potentially contributing to the better glycemic outcomes observed among AAPS users.

This study has limitations. Data were self-reported, and CGM data were unavailable for non-automated users. The non-automated group included individuals on various insulin regimens, introducing variability. Baseline differences between groups (e.g., age, disease duration, educational level) may have influenced the results. We understand that a multivariable analysis could be helpful, but it falls outside the descriptive scope that is the focus of this work. Furthermore, a multivariable analysis does not fit the theoretical model in which this work was conceived. Future analyses with the raw dataset are planned to perform adjusted models. We did not collect data on participants' use of public versus private healthcare services; therefore, we could not analyze the potential influence of healthcare system type on outcomes. Additionally, factors like emotional distress, physical activity, and adherence were not assessed.

Despite this, the data remain relevant given the scarcity of AAPS research. The system is widely used globally, often without regulatory approval, leading to a DIY approach with limited medical oversight. Due to its affordability, AAPS could expand AID access, particularly in developing countries. This real-world study suggests AAPS as a viable alternative for glycemic control in T1D patients. Further randomized studies are needed to validate these findings and support regulatory approval.

In conclusion, in this observational study, individuals using AAPS with First-generation CGM, Bluetooth transmitter, and an insulin pump achieved HbA1c, TIR, TAR, and TBR levels within the targets for good diabetes control, despite a mean time in level-2 hypoglycemia slightly above target. An improvement in HbA1c was observed after initiating the system. Moreover, AAPS users with these devices demonstrated better glycemic control compared to individuals on non-automated insulin therapy, with fewer severe hypoglycemic events and better quality of life. However, some users experienced inadequate glycemic control, which may be associated with the DIY nature of the treatment. Given the significantly lower cost of AAPS compared to commercial automated insulin delivery systems, these findings suggest that this system of AAPS could serve as an alternative to expand access to automated insulin therapy globally. Proper education during system setup and medical guidance during follow-up could further reduce cases of suboptimal glycemic control.

Funding: this research received no external funding.

Acknowledgements: the authors thank all participants and the clinical team involved in data collection.

Disclosure: no potential conflict of interest relevant to this article was reported.

Data availability: datasets related to this article will be available upon request to the corresponding author.

REFERENCES

1. Quattrin T, Mastrandrea LD, Walker LSK. Type 1 diabetes. Lancet. 2023 Jun 24;401(10394):2149-2162. doi: 10.1016/S0140-6736(23)00223-4.
2. Beck RW, Bergenstal RM, Laffel LM, Pickup JC. Advances in technology for management of type 1 diabetes. Lancet. 2019 Oct 5;394(10205):1265-1273. doi: 10.1016/S0140-6736(19)31142-0.
3. American Diabetes Association Professional Practice Committee. 7. Diabetes Technology: Standards of Care in Diabetes-2024. Diabetes Care. 2024 Jan 1;47(Suppl 1):S126-S144. doi: 10.2337/dc24-S007.
4. Roos T, Hermanns N, Groß C, Kulzer B, Haak T, Ehrmann D. Effect of automated insulin delivery systems on person-reported outcomes in people with diabetes: a systematic review and meta-analysis. EClinicalMedicine. 2024 Sep 21;76:102852. doi: 10.1016/j.eclinm.2024.102852.
5. Jennings P, Hussain S. Do-It-Yourself Artificial Pancreas Systems: A Review of the Emerging Evidence and Insights for Healthcare Professionals. J Diabetes Sci Technol. 2020 Sep;14(5):868-877. doi: 10.1177/1932296819894296.
6. Pease A, Lo C, Earnest A, Kiriakova V, Liew D, Zoungas S. The Efficacy of Technology in Type 1 Diabetes: A Systematic Review, Network Meta-analysis, and Narrative Synthesis. Diabetes Technol Ther. 2020 May;22(5):411-421. doi: 10.1089/dia.2019.0417.
7. Garg SK, Weinzimer SA, Tamborlane WV, Buckingham BA, Bode BW, Bailey TS, et al. Glucose Outcomes with the In-Home Use of a Hybrid Closed-Loop Insulin Delivery System in Adolescents and Adults with Type 1 Diabetes. Diabetes Technol Ther. 2017 Mar;19(3):155-163. doi: 10.1089/dia.2016.0421.
8. Tauschmann M, Thabit H, Bally L, Allen JM, Hartnell S, Wilinska ME, et al.; APCam11 Consortium. Closed-loop insulin delivery in suboptimally controlled type 1 diabetes: a multicentre, 12-week randomised trial. Lancet. 2018 Oct 13;392(10155):1321-1329. doi: 10.1016/S0140-6736(18)31947-0.
9. Piccini B, Pessina B, Casalini E, Lenzi L, Toni S. Long-term effectiveness of advanced hybrid closed loop in children and adolescents with type 1 diabetes. Pediatr Diabetes. 2022 Dec;23(8):1647-1655. doi: 10.1111/pedi.13440.
10. Schiaffini R, Deodati A, Nicoletti MC, Carducci C, Ciampalini P, Lorubbio A, et al. Comparison of two advanced hybrid closed loop in a pediatric population with type 1 diabetes: a real-life observational study. Acta Diabetol. 2022 Jul;59(7):959-964. doi: 10.1007/s00592-022-01886-z.
11. Weisman A, Bai JW, Cardinez M, Kramer CK, Perkins BA. Effect of artificial pancreas systems on glycaemic control in patients with type 1 diabetes: a systematic review and meta-analysis of outpatient randomised controlled trials. Lancet Diabetes Endocrinol. 2017 Jul;5(7):501-512. doi: 10.1016/S2213-8587(17)30167-5.

Copyright© AE&M all rights reserved.

12. Fernandes N. A Randomized Trial of Closed-Loop Control in Children with Type 1 Diabetes. N Engl J Med. 2020 Dec 17;383(25):2484. doi: 10.1056/NEJMc2030417.
13. Passanisi S, Lombardo F, Mameli C, Bombaci B, Macedoni M, Zuccotti G, et al. Safety, Metabolic and Psychological Outcomes of Medtronic MiniMed 780G™ in Children, Adolescents and Young Adults: A Systematic Review. Diabetes Ther. 2024 Feb;15(2):343-365. doi: 10.1007/s13300-023-01501-6.
14. Lei M, Lin B, Ling P, Liu Z, Yang D, Deng H, et al. Efficacy and safety of Android artificial pancreas system use at home among adults with type 1 diabetes mellitus in China: protocol of a 26-week, free-living, randomised, open-label, two-arm, two-phase, crossover trial. BMJ Open. 2023 Aug 9;13(8):e073263. doi: 10.1136/bmjopen-2023-073263.
15. Herzog AL, Busch J, Wanner C, von Jouanne-Diedrich HK. Survey about do-it-yourself closed loop systems in the treatment of diabetes in Germany. PLoS One. 2020 Dec 17;15(12):e0243465. doi: 10.1371/journal.pone.0243465.
16. Braune K, O'Donnell S, Cleal B, Lewis D, Tappe A, Willaing I, et al. Real-World Use of Do-It-Yourself Artificial Pancreas Systems in Children and Adolescents With Type 1 Diabetes: Online Survey and Analysis of Self-Reported Clinical Outcomes. JMIR Mhealth Uhealth. 2019 Jul 30;7(7):e14087. doi: 10.2196/14087.
17. Battelino T, Danne T, Bergenstal RM, Amiel SA, Beck R, Biester T, et al. Clinical Targets for Continuous Glucose Monitoring Data Interpretation: Recommendations From the International Consensus on Time in Range. Diabetes Care. 2019 Aug;42(8):1593-1603. doi: 10.2337/dci19-0028.

Copyright© AE&M all rights reserved.

Archives of Endocrinology and Metabolism
ISSN 2359-4292
OFFICIAL JOURNAL OF THE BRAZILIAN SOCIETY OF ENDOCRINOLOGY AND METABOLISM

original

Dietary pattern and night work: metabolic syndrome in healthcare workers

Francielle Lopes dos Reis[1*]
https://orcid.org/0000-0003-2134-1157

Maria da Graça Rocha Penha[4]
https://orcid.org/0009-0008-5723-6408

Elen Gineste Baccin[1]
https://orcid.org/0000-0001-6669-6686

Maria Carlota Borba Brum[2]
https://orcid.org/0000-0001-8124-2527

Sheila de Castro Cardoso Toniasso[4]
https://orcid.org/0000-0001-8692-7330

Ticiana da Costa Rodrigues[6]
https://orcid.org/0000-0001-9254-3712

Júlio César Ferreira Bertoloto[3]
https://orcid.org/0009-0009-5597-5300

Rodrigo Fernandes Soares[5]
https://orcid.org/0009-0004-3887-2645

[1] Serviço de Enfermagem Ambulatorial, Hospital de Clínicas de Porto Alegre, Porto Alegre, RS, Brasil
[2] Departamento de Medicina Social, Universidade Federal do Rio Grande do Sul, Porto Alegre, RS, Brasil
[3] Faculdade de Medicina, Universidade Federal do Rio Grande do Sul, Porto Alegre, RS, Brasil
[4] Serviço de Medicina do Trabalho, Hospital de Clínicas de Porto Alegre, Porto Alegre, RS, Brasil
[5] Escola de Enfermagem, Universidade Federal do Rio Grande do Sul, Porto Alegre, RS, Brasil
[6] Departamento de Medicina Interna, Universidade Federal do Rio Grande do Sul; Serviço de Endocrinologia, Hospital de Clínicas de Porto Alegre, Porto Alegre, RS, Brasil

ABSTRACT

Objective: To assess the relationship between night work, metabolic syndrome (MS) prevalence, and dietary patterns in healthcare workers at a large hospital in southern Brazil. **Subjects and methods:** A cross-sectional study was conducted with 156 healthcare workers (90 day-shift and 66 night-shift) from July 2023 to March 2024. Sociodemographic and occupational, sleep, dietary patterns, meal timing, anthropometric data, blood pressure, and lab test data were collected. **Results:** Night-shift workers had higher blood pressure, lower HDL cholesterol, and 135% greater likelihood of developing MS than those who worked during the day. They consumed more fats and less fiber. Chrononutrition analysis showed night workers had later last meals ($p < 0.001$), longer intervals between first and last meals ($p < 0.001$), and shorter night fasting ($p < 0.001$). Ultra-processed food consumption was similar across shifts. A shorter interval between the first and last meal in night workers was linked to a 7% lower risk of MS. Findings suggest an association between night work and higher MS prevalence, with hypertension, abdominal obesity, unfavorable lipid profile, and disrupted eating timing. Circadian rhythm disruption and misaligned eating patterns, particularly prolonged eating windows and reduced nocturnal fasting, may contribute to the increased metabolic risk. **Conclusion:** Interventions targeting diet and chrononutrition are essential. Occupational health programs should address the specific challenges of night work.

Keywords: Night work; dietary pattern; metabolic risk; chrononutrition; chronotype

INTRODUCTION

Night work is widely associated with various health impacts as it deregulates circadian rhythms, which affect metabolic processes, glucose homeostasis, gastrointestinal motility, and digestive processes; influence changes in eating behavior; increase the risk of metabolic and cardiovascular diseases; and deregulates sleep (1,2). Healthcare workers are exposed to these risks due to the organization of their work, which is characterized by adverse conditions and irregular and prolonged working hours (2).

Current studies link shift work with inadequate dietary patterns (3,4). Their irregularity, sleep deprivation, and a sedentary lifestyle can significantly contribute to chronic diseases and to metabolic syndrome (MS) (4,5). Jung and cols. (5) have reported that the main risk factors for MS in the general adult population include age, higher body mass index (BMI), physical inactivity, and unhealthy eating habits.

In this context, the circadian cycle plays a key role in maintaining physiological and metabolic homeostasis, particularly influenced by exposure to natural light (6,7), regulating various physiological processes such as the sleep-wake cycle, hormone secretion, energy metabolism, insulin sensitivity, gastrointestinal motility, and appetite control (6-8). Night work promotes

Received on Oct/1/2025
Accepted on Jan/22/2026
DOI: 10.20945/2359-4292-2026-0047

Correspondence to:
Francielle Lopes dos Reis
flreis@hcpa.edu.br

Associated editor:
Marcio W. Lauria
https://orcid.org/0000-0001-7558-1231

This is an open-access article distributed under the terms of the Creative Commons Attribution License

Copyright© AE&M all rights reserved.

circadian desynchronization (7,9), with evidence demonstrating that it is associated with metabolic changes, increased systemic inflammation, impaired glycemic control, and increased cardiometabolic risk, in addition to negatively impacting sleep patterns and eating behavior (8-10).

In light of this, it is crucial to consider the contribution of chrononutrition, a field that investigates not only what individuals eat but also when they eat, taking into account the synchronization between food intake and the body's circadian rhythms (8). Consuming food at biologically inappropriate times, such as during the night or during irregular shift schedules, can disrupt peripheral clocks, particularly in metabolic organs such as the liver, leading to weight gain and increased metabolic risk even when overall diet quality is acceptable (9,10). Shift workers often adapt their eating habits to their active hours, frequently consuming energy-dense, nutrient-poor foods during night shifts while reducing intake of fruits, vegetables, and other healthful foods (11,12). Thus, the evaluation of dietary patterns including both the nutritional composition and timing of meals is essential for understanding the risks associated with night work and developing targeted preventive strategies.

As lifestyle changes remain the most effective strategy for preventing MS and aligning biological rhythms, evidence on meal timing and eating window in workers remains limited. Therefore, this study aimed to assess the association between night work, metabolic syndrome, and dietary patterns in healthcare workers at a large hospital in southern Brazil, identifying potential opportunities for prevention and health promotion in this high-risk occupational group.

SUBJECTS AND METHODS

Participants and ethics

This quantitative cross-sectional study analyzed a sample of 156 employees (90 and 66 of whom worked day and night shifts, respectively) from a large hospital in southern Brazil. Participants were recruited by posters, institutional emails, and the online research bulletin board of the institution from July 2023 to March 2024. For the purposes of the study, night-shift workers were considered to work between 7pm and 7am at least 3 times a week, and day-shift workers were considered to work between 7am and 6pm on average 5 times a week.

Healthcare workers included all those who worked in the institution in health promotion and care, including support activities (administrative, hygiene, nutrition, laundry, maintenance, and surveillance). Workers who had worked at the hospital for at least one year on one of the shifts were considered as eligible participants. Exclusion criteria were pregnant women, employees on fixed-term contracts and those in the process of retiring/retired. Face-to-face meetings were held at the Clinical Research Center to collect data. The project was approved by the institution Research Ethics Committee under CAAE nº 67201723.0.0000.5327.

Overall, four self-administered questionnaires were given to participants after they signed an informed consent form (sociodemographic, alcohol consumption, physical activity, and sleep). The sociodemographic questionnaire was applied to gather personal information such as age, gender, marital status, children, schooling, work shift, time working at the institution, working hours and smoking.

The sample size was calculated considering a 95% confidence level, an expected prevalence of 25% for metabolic syndrome (p = 0.25), and a margin of error of 7%, resulting in a minimum sample size of 147 participants. A 10% increase was predicted for possible losses, totaling 162 participants as the total sample size (13). Additionally, chrononutrition variables were consulted to ensure that the planned sample was also adequate for comparing shifts on these variables (14).

Alcohol consumption

Alcohol consumption was assessed using the Alcohol Use Disorders Identification Test questionnaire. Consumption was classified according to the score, with low risk being considered a score from 0 to 7 points; regular risk, one from 8 to 15 points; and high risk, 16 points or above (15).

Physical activity

Individuals' physical activity was assessed using the short International Physical Activity Questionnaire, which

Copyright© AE&M all rights reserved.

classifies physical activity level as sedentary (those who performed no physical activity for at least 10 continuous minutes during the week), irregularly active (those who perform physical activity below active as they fail to meet the recommended frequency or duration), and active/very active (performed vigorous activity: ≥ three days/week and ≥ 20 minutes per session, moderate or walking: ≥ five days/week and ≥ 30 minutes per session, or any activity added together: ≥ five days/week and ≥ 150 minutes/week (walking + moderate + vigorous) based on information in meters/minute/week (16).

Sleep assessment

Daily sleep preferences were assessed using the self-assessment Munich Chronotype Questionnaire. This structured questionnaire regards waking behavior, sleep, and exposure to light on work and non-work days. Sleep duration was calculated as the end of sleep minus the beginning of sleep. Participants reported how many days during the week they had a regular work routine and the times when they go to bed, are ready for bed, fall asleep, how many minutes they need to get up, and how much time they spend outdoors (17).

The following data were calculated based on this information: sleep duration and midpoint for work and rest days, and social jetlag, which is the difference between an individuals' "biological" and "social" clocks, which defines their social commitments throughout the day.

Evaluation of dietary patterns

The Simplified Food Frequency Questionnaire was applied in person by trained researchers (18,19), assessing the consumption scores of fat, fiber, and ultra-processed foods. The frequency of fiber consumption was assessed of fiber consumption: whole grain bread, oats, whole grains, brown rice, beans, peas, lentils, chickpeas, soybeans, oil seeds (peanuts, walnuts, chestnuts, almonds, etc.), fresh fruit or natural juice, raw or cooked leafy greens (lettuce, cabbage, etc.), legumes and vegetables, roots, and tubers (potatoes, sweet potatoes, cassava, etc.). The following foods were included to assess fat consumption: cookies and cakes, whole milk and dairy products (yogurt, cheese, ricotta), olive oil, margarine or vegetable oils (soybean, canola, sunflower), butter or lard, fried snacks, salad with mayonnaise (potato, pasta, *salpicão*), fried foods (potatoes, cassava, polenta, etc.), industrialized snacks (salty snacks), chocolate, ice cream (fatty sweets), industrialized sweets (candies, chewing gum, etc.), eggs, and processed meats (mortadella, ham, salami, sausage, etc.).

The frequency of fat and fiber consumption was evaluated and a weight was established for each frequency. Then, the total values were added up and a score was determined for both fat and fiber consumption (20). Fiber consumption frequency had the following weights: 1× a day or more = 4, from 4 to 6× a week = 3, from 2 to 3× a week = 2, 1× a week = 1, and less than 1× a week = 0; whereas that for the frequency of fats, the following weights: 5 or more times a week = 4, 3 to 4× a week = 3, 1 to 2× a week = 2, 2 to 3× a month = 1, and less than 1× a month = 0.

Fat scores above 22 were considered as high, very high, or relatively high, whereas those below 21, as low or minimal frequency of consumption. Fiber consumption scores equal to or higher than 20 indicated a regular or adequate frequency, whereas those below 19, a low frequency of consumption (18,19).

The following ultra-processed foods were chosen for evaluation according to the classification of the food guide for the Brazilian population and the NOVA classification: margarine, cookies, cakes, industrialized salty snacks, sausages, chocolate, ice cream, industrialized sweets, soft drinks or artificial juices, fast foods, industrialized diet foods, instant noodles, ready-made food, ready-made seasonings, and mayonnaise. Daily consumption scores followed this weight: More than 3×/day = 3; 2 to 3×/day = 2; 1×/day = 1; 5 to 6×/week = 0.79; 2 to 4×/week = 0.43; 1×/week = 0.14; 1 to 3×/month = 0.07; consumes none = 0. In the analysis, a higher score indicates more frequent consumption of ultra-processed foods (20,21). Meal timing variables included the timing of the first and last meals, eating window duration, and nocturnal fasting on working days and days off.

Anthropometric and clinical assessment

Weight and height were measured using a R/1W-200 Welmy anthropometric scale with a capacity of 200 kg

Copyright© AE&M all rights reserved.

and a precision of 0.100 and a Tonelli stadiometer, with a precision of 1 mm. Both measurements were used to calculate body mass index (BMI, kg/m²). The cut-off points adopted for BMI were those suggested by the WHO, i.e.: normal weight (18.5-24.99); overweight (25-29.99), and obese (≥ 30.00) (22).

Blood pressure was measured from participants' left arm as they sat after 10 minutes of rest by a Vital Signs Monitor series 300 Welch Ally digital device in the morning.

The MS outcome variable adopted diagnostic confirmation according to the criteria of the First Brazilian Guideline for the Diagnosis and Treatment of Metabolic Syndrome and the National Cholesterol Education Program Adult Treatment Panel III. Blood samples were taken for tests on free days under a 12-hour fast: fasting glycemia, glycosylated hemoglobin, total cholesterol, HDL, ultrasensitive C-reactive protein, and triglycerides at the time of anthropometric data assessment and application of the Simplified Food Frequency Questionnaire.

Statistical analysis

The normality of continuous variables was analyzed using the Kolmogorov-Smirnov test. Continuous data were shown as means and standard deviations or medians and interquartile ranges, whereas categorical ones as absolute and relative frequencies. The Student's *t*-test for independent samples was used to compare means between day- and night-shift workers. Homogeneity of variance was assessed using Levene's test. In case of asymmetry, the Mann-Whitney non-parametric U test was applied. The chi-squared or Fisher's exact tests were used to compare the proportions between worker groups. Spearman's correlation coefficient was used to assess the association between sleep midpoint and the variables related to the interval between the first and last meal on working and off days. Poisson (categorical) or linear (numerical) regression models were applied to control for confounding factors. In case of asymmetry, the tweedie model with logarithmic transformation was applied. The data were analyzed using SPSS, version 27.0. Statistical significance was set at $p \leq 0.05$.

RESULTS

Night-shift workers had a significantly higher median age and length of service on the shift than day-shift workers, with a higher prevalence of females in both shifts. Alcohol consumption and physical activity did not show significant differences, but night-shift workers had a higher proportion of smokers (**Table 1**).

Regarding clinical assessment, night-shift workers had higher mean/median scores for various parameters such as weight, abdominal circumference; waist-to-hip ratio (WHR), systolic blood pressure and diastolic blood pressure (**Table 2**) when compared to day-shift participants.

The results relating to metabolic syndrome and its components showed that hypertension occurred in 35.9% of workers, 56.1% among night-shift workers. Night-shift workers were 3.48 times more likely to have a change in blood pressure than dayshift workers, when the multivariate model was adjusted for age, gender, and time at work (PR = 3.48; 95% CI: 1.66-7.30) (**Table 3**).

Overall, 41% of the sample had altered HDL cholesterol levels, with 53% of these being night-shift workers. After adjustment, they had 2.20 times lower HDL levels than day-shift workers when adjusted for age, gender, and time at work (PR = 2.20; 95% CI: 1.04-4.66). The result of the regression analysis indicated that every 1 mg/dL increase in HDL levels correlated to a 6% reduction in the probability of MS occurring in night-shift workers. Furthermore, elevated blood glucose levels were observed in 10.9% of workers, with a higher prevalence among night-shift workers. After adjustment, this difference disappeared. MS occurred in 26.3% of the total sample, 39.4% of whom were night-shift workers, who were 135% more likely to develop MS than day workers (PR = 2.35; 95% CI: 1.07-5.15) **(Table 3)**.

After adjustment by the multivariate Poisson Regression model to assess factors independently associated with MS by work shift, men had a significantly higher prevalence of MS, regardless of work shift. During the day, such probability was around 7.76 times higher in men and 2.82 times higher at night.

Copyright© ACE&M all rights reserved.

Table 1. Sociodemographic, behavioral, and occupational characteristics of healthcare workers at a large hospital in southern Brazil, by work shift (n = 156)

Variables	Total (156)	Daytime (90)	Night (66)	*p*
Age (years)	47 (42-56)	45 (40-55)	51 (46- 56)	**< 0.001**
Children Yes	108 (69.2%)	56 (62.2%)	52 (78.8%)	**0.041**
Sex				
Female	115 (73.7%)	74 (82.2%)	41 (62.1%)	**0.006**
Male	41 (26.3%)	16 (17.8%)	25 (37.9%)	
Marital status				
With partner	89 (57%)	46 (51.1%)	43 (65.2%)	0.187
Without partner	67 (43%)	44 (48.9%)	23 (34.8%)	
Schooling				
1st/2nd grade	43 (27.6%)	20 (22.2%)	23 (33.3%)	0.158
Higher education	44 (28.2%)	25 (27.8%)	19 (28.8%)	
Graduate	69 (44.2%)	45 (50%)	24 (36.4%)	
Function				
Care	85 (54.5%)	42 (46.6%)	43 (65.2%)	**<0.001**
Administrative	35 (22.4%)	30 (33.3%)	5 (7.6%)	
Other	36 (23.1%)	18 (20%)	18 (25.2%)	
Length of time working				
1-15 years	91 (58.3%)	68 (75.6%)	23 (34.8%)	**<0.001**
> 15 years	65 (41.7%)	22 (24.4%)	43 (65.2%)	
International Physical Activity Questionnaire				
Sedentary	23 (14.8%)	12 (13.3%)	11 (16.7%)	0.541
Active/Very active	71 (45.5%)	41 (45.6%)	30 (45.4%)	
Irregularly active	62 (39.7%)	37 (41.1%)	25 (37.9%)	
Smoking Yes	17 (10.9%)	5 (5.6%)	12 (18.2%)	**0.018**
Alcohol Use Disorders Identification Test				
Low risk	135 (86.5%)	81 (90%)	54 (81.8%)	0.281
Risk	18 (11.6%)	8 (8.9%)	10 (15.2%)	
High risk	3 (1.9%)	1 (1.1%)	2 (3%)	

Asymmetric variables are represented by medians and interquartile ranges that were assessed using the Mann-Whitney non-parametric U test. The chi-squared or Fisher's exact tests were used for categorical variables. A significance level of $p < 0.05$ was adopted for all tests.

Table 2. Clinical and laboratory parameters of healthcare workers at a large hospital in southern Brazil, according to work shift (n = 156)

Variables	Total (156)	Daytime (90)	Night (66)	*p*
Weight (kg)	74.60 (65.60-87.85)	70 (64.20-85.55)	80.25 (67.35-89.90)	**0.037**
BMI	27.99 (24.59-30.92)	26.55 (24.09-30.49)	28.26 (25.46-31.20)	0.159
AC	93.25 (84.0-102.5)	91 (82-100)	97.75 (89-103)	**0.010**
Female	91 (82-98)	88.8 (81-98)	93 (85.5-99.00)	0.221
Male	101 (93.3-108.5)	93.3 (88.8-111.5)	102 (97.8-106.5)	0.207
WHR	0.84 (±0.09)	0.82 (±0.09)	0.86 (±0.08)	**0.003**
Female	0.81 (±0.08)	0.80 (±0.08)	0.83 (±0.07)	0.072
Male	0.91 (±0.06)	0.91 (±0.06)	0.92 (±0.07)	0.688
Systolic BP	121 (110-134)	116 (109-126)	129.5 (117-140)	**<0.001**
Diastolic BP	75 (67-83)	72.5 (66-81)	78 (68-88)	**0.023**
CRP US	1.35 (0.60-2.80)	1.55 (0.50-3.5)	1.25 (0.60-2.60)	0.383
Total cholesterol	192 (169-222.5)	196 (166-225)	191 (169-211)	0.632
Glycated hemoglobin	5.3 (5.1-5.6)	5.2 (5.1-5.6)	5.4 (5.1-5.7)	0.067
Pre-diabetes	yes 10 (6.4%)	3 (3.3%)	7 (10.6%)	0.097
Diabetes	yes 6 (3.8%)	2 (2.2%)	4 (6.1%)	0.243

AC: abdominal circumference; HDL: high-density lipoprotein; BMI: body mass index; BP: blood pressure; CRP-US: ultrasensitive C-reactive protein; WHR: waist-to-hip ratio.

Variables with a normal distribution are shown as means and standard deviations. The Student's *t*-test was used to analyze them. Asymmetrical variables are shown as medians and interquartile ranges and were assessed using the Mann-Whitney non-parametric U test. The chi-squared or Fisher's exact tests were used for categorical variables. A significance level of $p < 0.05$ was adopted for all tests. RQC calculated mean because it is a symmetrical distribution – Levene's Test for Equality of Variances, other variables are median, asymmetrical distribution – Independent samples Mann-Whitney U test. Pre-diabetes – Fisher's Exact Test.

Copyright© ACE&M all rights reserved.

Sleep duration and social jetlag were similar between the groups, with no statistically significant differences. The midpoint between the start and end of sleep on working days showed a significant difference between night- and day-shift workers, even when adjusted for possible confounding factors (age, gender, children, and time at work) (Table 4), whereas such difference remained insignificant on rest days.

Night workers had greater exposure to natural light on workdays (120 min [60–240] vs. 60 min [30–180]; p < 0.022). On days off, there was no difference between the groups. In adjusted logistic regression models, exposure to natural light was not associated with the presence of metabolic syndrome (OR = 1.01; p < 0.87), low HDL (OR = 1.03; p < 0.62), or high triglycerides (OR = 1.00; p < 0.94). Work shift (night and day) was not independently associated with any of the outcomes after adjustment for other factors.

Chronotype was categorized into three groups based on MSFsc: morning (MSFsc ≤ 3:59 a.m.), intermediate (4:00–4:59 a.m.), and evening (MSFsc ≥ 5:00 a.m.) (23), considering only participants who did not depend on an alarm clock on their days off. In this sample, 56 participants were classified as morning types, 13 as intermediate types, and 37 as evening types. When stratified by work shift, daytime/full-time workers had a higher proportion of morning chronotypes (n = 41), while among night workers there was a more balanced distribution between morning (n = 15) and evening (n = 16) chronotypes, suggesting a tendency toward later sleep phases among those who work night shifts.

Regarding fat consumption, a higher frequency occurred in night-shift workers (62.1%) than in day-shift ones (51.1%). As for fiber consumption, night-shift workers had a higher frequency of low consumption (40.9%) than day-shift ones (26.7%). Despite the evident percentage variations, no statistically significant differences occurred between shifts regarding fat (p < 0.0228; adjusted < 0.242) and fiber frequency intake (p < 0.089; adjusted < 0.147).

Table 3. Diagnosis of metabolic syndrome and its components among healthcare workers at a large hospital in southern Brazil, according to work shift (N = 156)

Variables	Total n (%)	Daytime (n=90) n (%)	Night (n=66) n (%)	*p*	$p^{adjusted*}$	PR (IC 95%)
Hypertension	56 (35.9)	19 (21.1)	37 (56.1)	**< 0.001**	**< 0.001**	**3.48 (1.66-7.30)**
Altered triglycerides	39 (25.0)	17 (18.9)	22 (33.3)	0.061	0.342	1.44 (0.68-3.03)
Altered HDL cholesterol	64 (41.0)	29 (32.2)	35 (53.0)	**0.014**	**0.039**	**2.20 (1.04-4.66)**
Changed AC	82 (52.6)	44 (48.9)	38 (57.6)	0.362	0.636	1.19 (0.57-2.49)
Altered blood glucose	17 (10.9)	5 (5.6)	12 (18.2)	**0.025**	0.198	2.36 (0.64-8.66)
Metabolic syndrome	41 (26.3)	15 (16.7)	26 (39.4)	**0.003**	**0.034**	**2.35 (1.07-5.15)**

*Adjusted for age, gender, and time at work.

Variables with a normal distribution are shown as means and standard deviations. The Student's t-test was used to analyze them. Asymmetrical variables are shown as medians and interquartile ranges. They were assessed using the Mann-Whitney non-parametric U test. The chi-squared or Fisher's exact tests were used for categorical variables. A significance level of p < 0.05 was adopted for all tests. To control for confounding factors, Poisson regression models (categorical) were applied. In case of asymmetry, the tweedie model with logarithmic transformation was applied.

AC: abdominal circumference; HDL: high-density lipoprotein; PR: prevalence ratio.

Table 4. Description of sleep variables by work shift in healthcare workers at a large university hospital in southern Brazil (n = 156)

Variables	Daytime (90)	Night (66)	*p*	$p^{adjusted*}$
Average point of sleep on working days	2:34 (2:01-3:17)	4:48 (3:29 -7:00)	**<0.001**	**<0.001**
Average point of sleep on days off	4:01 (3:27-4:59)	4:25 (3:29-5:45)	0.084	0.098
Sleep duration on working days	6:57 (6:00-7:55)	7:29 (4:55-9:20)	0.184	0.102
Sleep duration on days off	8:00 (7:14-9:00)	8:10 (6:57-9:30)	0.541	0.392
Social jetlag	1:30 (0:44-2:01)	00:44 (00:06-2:37)	0.065	0.220

*Adjusted for age, gender, children, and time at work.

Asymmetrical variables are shown as medians and interquartile ranges. They were assessed using the Mann-Whitney non-parametric U test. The chi-squared or Fisher's exact tests were used for categorical variables. A significance level of p<0.05 was adopted for all tests.

Copyright© AE&M all rights reserved.

Regarding ultra-processed foods, a similar pattern occurred in the frequency of consumption of these foods as both shifts had an estimated consumption closer to 1-2 times a week 0.28 (0.21-0.38). Small differences occurred in the consumption of sausages, with night-shift workers consuming them more frequently — from two to four times a week 0.43 (0.07-0.79), when compared to day workers who consumed them less than once a week 0.14 (0.07-0.43).

Significant differences occurred between groups for the frequency of consumption of industrialized sweets. The regression coefficient (b=-0.65; 95% CI: -1.24 to −0.05) reinforces this difference, indicating an average reduction of 0.65 points in the consumption score for night-shift workers. Both shifts recorded low values — 0.07 (0-0.43) —, but the greater variability between daytime 0.07 (0-0.43) and nighttime workers — 0.07 (0-0.14) — highlights a pattern of reduced consumption frequency in this work shift. The consumption of soft drinks and artificial juices showed a difference close to the limit of significance ($p < 0.052$). Statistical analysis showed no significant differences in most of the food variables when adjusted for age, gender, and time at work.

The first and last meal on working days between shifts and non-working days statically differed (Table 5), suggesting that night-shift workers have a longer eating window on work and off days than day-shift workers. The regression analysis found that reducing the interval between the first and last meal for night-shift workers is associated with a 7% reduction in their risk of MS.

Regarding nocturnal fasting on working days, night-shift workers had a shorter fasting time than day-shift ones [8:00 (6:00-10:00) vs. 11:00 (9:12-12:00) $p < 0.001$], after adjusting for possible confounding factors (age, gender, and time at work). On days off, both groups had a similar duration of overnight fasting [12:00 (10:00-13:00) vs. 12:00 (11:00-13:00) $p < 0.401$] (Table 5). Regarding the number of meals, no differences occurred between the shifts regarding the number of meals on work or off days (Table 5).

When analyzing the correlation between sleep midpoint and variables related to the difference between the first and last meal on work and off days, no significant correlation occurred for either daytime or nighttime individuals. However, on days off, a negative and significant correlation occurred between the difference in meal times and the midpoint of sleep for nocturnal individuals ($rs = −0.250$; $p < 0.043$), suggesting a possible relation between the meal interval and the midpoint of sleep on days off. As for night-time fasting, no significant correlations occurred for daytime ($rs = 0.083$; $p < 0.437$) or nighttime individuals

Table 5. Comparison of dietary pattern and chrononutrition variables between night and day shifts (n = 156)

Variables	total sample n (%)	Daytime (n=90) n (%)	Night (n=66) n (%)	*p*	$p^{adjusted*}$
Fat**					
Low/Minimum	69 (44.2%)	44 (48.9%)	25 (37.9%)	0.228	0.242
High/Very High/Relatively High	87 (55.8%)	46 (51.1%)	41 (62.1%)		
Fiber**					
Adequate Consumption	105 (67.3%)	66 (73.3%)	39 (59.1%)	0.089	0.147
Low consumption	51 (32.7%)	24 (26.7%)	27 (40.9%)		
Median consumption*** of ultra-processed foods	0.28 (0.22-0.38)	0.28 (0.21-0.38)	0.28 (0.21-0.38)	0.971	0.749
Difference in time between first and last meal (hours) on working days	13:52 (12:00-16:00)	13:00 (12:00-14:30)	16:00 (13:00-18:00)	**<0.001**	**<0.001**
Difference in time between first and last meal (hours) on days off work	12:00 (11:00-13:00)	12:00 (11:00-13:00)	12:30 (11:00-14:00)	**0.045**	**0.030**
Night fasting on working days	10:00 (8:00-11:30)	11:00 (9:12-12:00)	8:00 (6:00-10:00)	**<0.001**	**<0.001**
Night fasting on days off	12:00 (11:00-13:00)	12:00 (11:00-13:00)	12:00 (10:00-13:00)	0.401	0.992
Number of meals in the working day	4 (4-5)	4 (4-5)	4 (4-5)	0.489	0.546
Number of meals on days off	4 (4-5)	4 (3-5)	4 (4-5)	0.165	0.149

*Adjusted for age, gender, children, and time at work.
**Fat score greater than 22 – high, very high, relatively high, less than 21 low/minimal consumption; Fiber - equal to or greater than 20 – regular/adequate, less than 19 – low consumption.
***Daily consumption score of ultra-processed foods: More than 3×/day = 3; 2 to 3×/day = 2; 1×/day = 1; 5 to 6×/week = 0.79; 2 to 4×/week = 0.43; 1×/week = 0.14; 1 to 3×/month = 0.07; consumes none = 0.

Copyright© AE&M all rights reserved.

(rs = 0.148; p < 0.235) on working days, indicating that night-time fasting has no statistically relevant association with sleep midpoint in either group.

DISCUSSION

Our results suggest that night work is significantly associated with an increase in the frequency of metabolic syndrome and its individual components (hypertension, increased body measurements such as weight, abdominal circumference and waist-to-hip ratio), which indicate greater accumulation of body fat, similarly to other studies (24). Moreover, an observational study of retired workers suggested that the adverse effects of night shifts on cardiometabolic function may persist after retirement, with differences between men and women (25). Another cross-sectional study highlighted that specific characteristics of night-shift work, such as the frequency and duration of shifts, are associated with high metabolic risk factors, such as increased BMI and waist circumference (25,26).

Research has found significant associations between higher night-shift workload and higher blood pressure levels than lower cumulative night-shift workload (26,27). A systematic review and meta-analysis offers sufficient evidence for a potential link between permanent night-shift work and an increase in blood pressure values, reinforcing the data in (28). The reversal of working hours may be associated with disruption of the circadian cycle and chronic stress. Sleep deprivation and disturbances in rest schedules may configure key factors explaining these changes (29-35).

Social jet lag was greater for daytime workers, but this can be justified by the greater variation between sleep schedules on workdays and days off, as night workers tend to maintain later schedules consistently. These data are consistent with previous studies showing that circadian misalignment is dependent on both chronotype and work shift demands (36).

Despite the circadian difference between shifts, social jet lag and midpoint of sleep were not associated with the metabolic outcomes assessed. Greater exposure to natural light among night-shift workers may also mitigate some of the circadian misalignment, as sunlight is a powerful synchronizer of biological rhythm and improves adaptation to night shifts. This compensatory effect was described (37), and confirmed in working populations (36), who demonstrated that exposure to natural light after the night shift helps realign the circadian rhythm, increasing alertness and reducing the negative effects of dysregulation. Even though night workers have greater exposure to natural light, this did not impact the diagnosis of MS or the lipid profile. Studies show the greater impact of artificial light on HDL and triglyceride levels (38,39).

Night workers have a 12-hour night shift (7:00 p.m. to 7:00 a.m.) with a 60-hour break, which can directly influence both the time of exposure to natural light and the interpretation of circadian patterns. This pattern implies that exposure to natural light on workdays occurs in the morning and during the commute at the end of the night shift, when solar irradiance is already high. In contrast, the rest window (60 hours) means that, on subsequent days, exposure to natural light is similar to that observed among day workers, which may explain the absence of differences between the groups on days off.

Studies suggest that engaging in physical activity at times misaligned with the circadian rhythm may be associated with sleep disturbances and circadian misalignment among shift workers (40). Although it was not possible to assess the timing of physical activity in the present sample, since only the IPAQ was used to measure activity level, it is important to recognize that both the amount and timing of physical activity can influence the metabolic and circadian health of this population.

The later night-shift workers sleep, the shorter the interval between their first and last meal on off days, suggesting that the way they organize their meals may influence when they go to sleep, showing a more regular behavior on days off or a response considered more natural to the biological rhythm outside the pressure of working hours.

Our analysis of eating patterns suggests that these workers often consume more fat and less fiber than daytime workers, suffer a greater impact on the time between the first and last meal and on nighttime fasting, and show disorganized schedules and less fasting

Copyright© AE&M all rights reserved.

on working days. Changes in meal times can negatively impact glucose tolerance and contribute to insulin resistance since eating at night is associated with glycemic peaks and an increased risk of diabetes. This finding suggests that meal timing may represent a modifiable target for metabolic risk reduction among night-shift healthcare workers. Moreover, the higher frequency of fat consumption and lower fiber intake in these workers reinforces the negative effects on glucose metabolism, which can contribute to the development of cardiometabolic dysfunctions. The prevalence of hypertension in these workers may also increase by inadequate dietary patterns, such as the high consumption of sodium in ultra-processed foods (41-43).

A study has explored fasting as an intervention to reduce the impact of simulated night shifts on glucose metabolism. Results showed that overnight fasting can improve insulin sensitivity and glucose tolerance when compared to meals or snacks during the night (44). Moreover, daytime eating at appropriate times can prevent internal circadian dysregulation (45).

In this specific sample, it was impossible to correlate the composition and quantity of the diet with clinical and laboratory variables, but eating times seem to constitute a way of predisposing these workers to a worse quality dietary pattern considering the circadian cycle (14,46). Thus, an increased calorie balance during the 24-hour period of the day due to eating at night could predispose to the risk of obesity and metabolic disorders (47,48).

The influence of environmental factors, such as lack of places to eat, limited healthy food choices, lack of time, easy access to unhealthy foods, and the influence of colleagues' preferences contribute to inadequate food consumption in night-shift workers (49-53), leading to poor food quality and increased calorie intake (54-57).

Lack of knowledge can also contribute to poor choices, making it necessary to consider nutritional education. A well-structured dietary intervention in the workplace that combines nutritional education and environmental dietary modification can help to acquire knowledge and increase consumption of suitable foods (58).

Restricting eating time during the day can also offer an effective strategy for dietary and glycemic control and weight loss, positively affecting insulin resistance and 24-hour glucose levels in people with obesity (59).

The large prospective study Palomar-Cros et al. carried out in France concluded that a late first meal is associated with a higher incidence of type 2 diabetes mellitus. They state that a circadian eating behavior with an early first meal (before 8 a.m.) and an early last meal (before 7 p.m.) may be beneficial in reducing the incidence of type 2 diabetes mellitus (60). Another large study carried out in Spain to analyze eating time patterns associated with body weight found that a later first meal time was associated with a higher BMI, whereas a longer night fast was associated with a lower BMI in cross-sectional and longitudinal analyses (61).

The night-shift workers in the studied sample have a chrononutritional profile with a greater difference between meals and less fasting at night, so it is essential to consider these aspects in the prevention of metabolic diseases. The development of prevention strategies must comprehensively consider biological, behavioral, and social aspects and focus on the factors that can interfere with maintaining health.

This study has some limitations that should be considered. The cross-sectional design prevents establishing causality; data collection at a single center limits the generalizability of the findings; and sleep and dietary patterns were assessed using self-administered questionnaires, which are subject to memory and perception biases. Additionally, voluntary participation may have introduced self-selection bias, as in-person attendance may have favored workers with more flexible routines. Despite these limitations, the study provides clinically relevant insights into modifiable eating behaviors associated with metabolic risk in night-shift healthcare workers. The integration of sleep characteristics, dietary patterns, and metabolic indicators allows the identification of potential targets for workplace-based prevention and intervention strategies, particularly in occupational groups exposed to long-term cardiometabolic risks.

In conclusion, there are significant nutritional challenges for night workers due to factors that may be associated with work organization and/or personal

Copyright© AE&M all rights reserved.

issues. The research results point to the importance of interventions targeted at this group of workers. Implementing strategies that meet nutritional needs and promote healthy habits is essential to reduce risks and improve quality of life. In addition, the creation and/or adaptation of occupational health policies can play a key role in reducing the negative impacts of night work. Measures such as flexible meal times, providing healthier food options in the workplace, and implementing nutrition education programs can contribute to improving the dietary patterns of these professionals. Other strategies could include reducing the workload for those exposed to long shifts, ensuring adequate rest periods, and promoting regular medical follow-up, with the aim of minimizing the effects of circadian cycle reversal and reducing the prevalence of metabolic diseases.

Further studies are needed to gain a deeper understanding of the long-term associations between dietary patterns, daily food consumption time, and their effects on the health of these workers, including other public and private institutions. In particular, it is essential to investigate the role of this dietary pattern in the development of metabolic diseases, such as obesity. Meal timing strategies may represent an additional tool for metabolic risk management in night-shift healthcare workers.

Funding statement: this work is linked to a project approved by the Research Ethics Committee of the *Hospital de Clínicas de Porto Alegre* (HCPA) – CAAE 67201723.0.0000.5327. Financial support was received from the Economic Research Foundation (FIPE/HCPA) and the Rio Grande do Sul State Research Support Foundation (FAPERGS).

Disclosure: no potential conflict of interest relevant to this article was reported.

Data availability: data from the ELSA-Brasil Study is subject to restricted access.

REFERENCES

1. Sooriyaarachchi P, Jayawardena R, Pavey T, King NA. Shift work and the risk for metabolic syndrome among healthcare workers: A systematic review and meta-analysis. Obes Rev. 2022 Oct;23(10):e13489. doi: 10.1111/obr.13489.
2. Wu QJ, Sun H, Wen ZY, Zhang M, Wang HY, He XH, et al. Shift work and health outcomes: an umbrella review of systematic reviews and meta-analyses of epidemiological studies. J Clin Sleep Med. 2022 Feb 1;18(2):653-662. doi: 10.5664/jcsm.9642.
3. Schettini MAS, Passos RFDN, Koike BDV. Shift Work and Metabolic Syndrome Updates: A Systematic Review. Sleep Sci. 2023 Jul 6;16(2):237-247. doi: 10.1055/s-0043-1770798.
4. Hemmer A, Mareschal J, Dibner C, Pralong JA, Dorribo V, Perrig S, et al. The Effects of Shift Work on Cardio-Metabolic Diseases and Eating Patterns. Nutrients. 2021 Nov 22;13(11):4178. doi: 10.3390/nu13114178.
5. Jung H, Dan H, Pang Y, Kim B, Jeong H, Lee JE, et al. Association between Dietary Habits, Shift Work, and the Metabolic Syndrome: The Korea Nurses' Health Study. Int J Environ Res Public Health. 2020 Oct 21;17(20):7697. doi: 10.3390/ijerph17207697.
6. Huang T. Sleep Irregularity, Circadian Disruption, and Cardiometabolic Disease Risk. Circ Res. 2025 Aug 15;137(5):709-726. doi: 10.1161/CIRCRESAHA.125.325613.
7. Nuszkiewicz J, Rzepka W, Markiel J, Porzych M, Woźniak A, Szewczyk-Golec K. Circadian Rhythm Disruptions and Cardiovascular Disease Risk: The Special Role of Melatonin. Current Issues in Molecular Biology. 2025;47(8):664. doi:10.3390/cimb47080664.
8. Xi J, Ma W, Tao Y, Zhang X, Liu L, Wang H. Association between night shift work and cardiovascular disease incidence and mortality: updated systematic review and dose-response meta-analysis. Syst Rev. 2025;14(1):112. doi:10.1186/s13643-025-01806-y.
9. Baek JH, Zhu Y, Jackson CL, Park YM. Artificial Light at Night and Type 2 Diabetes Mellitus. Diabetes Metab J. 2024 Sep;48(5):847-863. doi: 10.4093/dmj.2024.0237.
10. Windred DP, Burns AC, Rutter MK, Lane JM, Saxena R, Scheer FAJL, et al. Light Exposure at Night and Cardiovascular Disease Incidence. JAMA Netw Open. 2025 Oct 1;8(10):e2539031. doi: 10.1001/jamanetworkopen.2025.39031.
11. Johnston JD, Ordovás JM, Scheer FA, Turek FW. Circadian Rhythms, Metabolism, and Chrononutrition in Rodents and Humans. Adv Nutr. 2016 Mar 15;7(2):399-406. doi: 10.3945/an.115.010777.
12. Navruz-Varlı S, Mortaş H. Shift work, shifted diets: an observational follow-up study on diet quality and sustainability among healthcare workers on night shifts. Nutrients. 2024;16(15):2404. doi:10.3390/nu16152404.
13. Ritonja J, Tranmer J, Aronson KJ. The relationship between night work, chronotype, and cardiometabolic risk factors in female hospital employees. Chronobiol Int. 2019 May;36(5):616-628. doi: 10.1080/07420528.2019.1570247.
14. Silva CM, Teixeira BS, Wright KP Jr, Maia YCP, Crispim CA. Time-Related Eating Patterns Are Associated with the Total Daily Intake of Calories and Macronutrients in Day and Night Shift Workers. Nutrients. 2022 May 25;14(11):2202. doi: 10.3390/nu14112202.
15. Santos WS dos, Fernandes DP, Grangeiro AS de M, Lopes GS, Sousa EMP de. Measuring alcohol consumption: confirmatory factor analysis of the Alcohol Use Disorder Identification Test (AUDIT). Psico-USF. [Internet] 2013 [cited 2022 Apr 18] ;18(1):121–30. doi: 10.1590/S1413-82712013000100013.
16. Matsudo S, Araújo T, Marsudo V, Andrade D, Andrade E, Oliveira Luis C, et al. International Physical Activity Questionnaire (IPAQ): validity and reproducibility study in Brazil. Rev Bras Ativ Fís Saúde [Internet]. 2001 [cited 2023 June 22]; 6(2):05-18. doi: 10.12820/rbafs.v.6n2p5-18.
17. Levandovski R, Sasso E, Hidalgo MP. Chronotype: a review of the advances, limits and applicability of the main instruments used in the literature to assess human phenotype. Trends Psychiatry Psychother. 2013;35(1):3-11. doi: 10.1590/s2237-60892013000100002.
18. Block G. Screening questionnaire. In: Dietary assessment resource manual. J Nutr [Internet]. 1994 Nov;124(11 Suppl):2296S-2298S.
19. Rodrigues T, Sônia Tucunduva Philippi. Nutritional assessment and cardiovascular risk in executives undergoing a check-up. Journal of the Brazilian Medical Association. 2008 [Internet] Aug 1;54(4). Available from: https://www.scielo.br/j/ramb/a/PWhwzc8s8kmjmdrtjQYq7bx/abstract/?lang=pt.
20. Monteiro CA, Cannon G, Levy RB, Moubarac JC, Louzada ML, Rauber F, et al. Ultra-processed foods: what they are and how to identify them. Public Health Nutr. 2019 Apr;22(5):936-941. doi: 10.1017/S1368980018003762.
21. Ministry of Health. Food guide for the Brazilian population [Internet]. 2014. Available from: https://bvsms.saude.gov.br/bvs/publicacoes/guia_alimentar_populacao_brasileira_2ed.pdf

Copyright© AE&M all rights reserved.

22. WHO. Obesity: preventing and managing the global epidemic. Report of a WHO consultation. World Health Organization Technical Report Series [Internet] 2000; 894, 1–253. Available from: https://pubmed.ncbi.nlm.nih.gov/11234459/.
23. Juda M, Vetter C, Roenneberg T. Chronotype modulates sleep duration, sleep quality, and social jet lag in shift-workers. J Biol Rhythms. 2013;28(2):141-151. doi: 10.1177/0748730412475042.
24. Cheng WJ, Liu CS, Hu KC, Cheng YF, Karhula K, Härmä M. Night shift work and the risk of metabolic syndrome: Findings from an 8-year hospital cohort. PLoS One. 2021 Dec 13;16(12):e0261349. doi: 10.1371/journal.pone.0261349.
25. Chin BN, Lehrer HM, Tracy EL, Barinas-Mitchell E, Wilckens KA, Carroll LW, et al. Cardiometabolic function in retired night shift workers and retired day workers. Scientific Reports [Internet]. 2023 Mar 30 [cited 2023 Jul 27];13(1):5204. doi: 10.1038/s41598-022-20743-1.
26. Streng AA, Loef B, Dollé MET, van der Horst GTJ, Chaves I, Proper KI, et al. Night shift work characteristics are associated with several elevated metabolic risk factors and immune cell counts in a cross-sectional study. Sci Rep. 2022 Feb 7;12(1):2022. doi: 10.1038/s41598-022-06122-w.
27. Sousa MCP, Cruz JN, Elias CMV, Gonçalves NPC, Sousa ML, Sousa PCC. Vulnerabilities, conceptions and attitudes related to men's health. [internet] 2020; 12:939-945. doi: 10.9789/2175-5361.
28. Moreno CRC, Marqueze EC, Sargent C, Wright Jr KP, Ferguson SA, Tucker P. Working Time Society consensus statements: Evidence-based effects of shift work on physical and mental health. Ind Health. 2019 Apr 1;57(2):139-157. doi: 10.2486/indhealth.SW-1.
29. Souza BB, Monteze NM, de Oliveira FL, de Oliveira JM, de Freitas Nascimento S, Marques do Nascimento Neto R, et al. Lifetime shift work exposure: association with anthropometry, body composition, blood pressure, glucose and heart rate variability. Occup Environ Med. 2015 Mar;72(3):208-15. doi: 10.1136/oemed-2014-102429.
30. Ferguson JM, Costello S, Neophytou AM, Balmes JR, Bradshaw PT, Cullen MR, et al. Night and rotational work exposure within the last 12 months and risk of incident hypertension. Scand J Work Environ Health. 2019 May 1;45(3):256-266. doi: 10.5271/sjweh.3788.
31. Gamboa Madeira S, Fernandes C, Paiva T, Santos Moreira C, Caldeira D. The Impact of Different Types of Shift Work on Blood Pressure and Hypertension: A Systematic Review and Meta-Analysis. Int J Environ Res Public Health. 2021 Jun 23;18(13):6738. doi: 10.3390/ijerph18136738.
32. Bijnens S, Depoortere I. Controlled light exposure and intermittent fasting as treatment strategies for metabolic syndrome and gut microbiome dysregulation in night shift workers. Physiol Behav. 2023 May 1;263:114103. doi: 10.1016/j.physbeh.2023.114103.
33. Ganesan S, Magee M, Stone JE, Mulhall MD, Collins A, Howard ME, et al. The Impact of Shift Work on Sleep, Alertness and Performance in Healthcare Workers. Sci Rep. 2019 Mar 15;9(1):4635. doi: 10.1038/s41598-019-40914-x.
34. de Leeuw PW. Night shifts and hypertension. J Clin Hypertens (Greenwich). 2022 May;24(5):609-610. doi: 10.1111/jch.14459.
35. Lowden A, Öztürk G, Reynolds A, Bjorvatn B. Working Time Society consensus statements: Evidence based interventions using light to improve circadian adaptation to working hours. Ind Health. 2019 Apr 1;57(2):213-227. doi: 10.2486/indhealth.SW-9.
36. Kervezee L, Gonzales-Aste F, Boudreau P, Boivin DB. The relationship between chronotype and sleep behavior during rotating shift work: a field study. Sleep. 2021 Apr 9;44(4):zsaa225. doi: 10.1093/sleep/zsaa225.
37. Boivin DB, Boudreau P. Impacts of shift work on sleep and circadian rhythms. Pathol Biol (Paris). 2014;62(5):292-301. doi: 10.1016/j.patbio.2014.08.001.
38. Gubin D, Kolomeichuk S, Danilenko K, Stefani O, Markov A, Petrov I, et al. Timing and amplitude of light exposure, not photoperiod, predict blood lipids in Arctic residents: a circadian light hypothesis. Biology. 2025;14:799. doi: 10.3390/biology14070799.
39. Nieva-Ramírez DG, Uribe M, Nuño-Lámbarri N. Artificial Light at Night, Sleep Disruption, and Liver Health: Implications for MASLD Pathogenesis. Int J Environ Res Public Health. 2025;22(11):1729. doi: 10.3390/ijerph22111729.
40. Hulsegge G, Gupta N, Proper KI, van Lobenstein N, IJzelenberg W, et al. Shift work, sleep disturbances and social jetlag in rotating shift workers: the Klokwerk+ study. Scand J Work Environ Health. 2019;45(4):396-406. doi: 10.5271/sjweh.3614.
41. Boersma GJ, Mijnster T, Vantyghem P, Kerkhof GA, Lancel M. Shift work is associated with extensively disordered sleep, especially when working nights. Front Psychiatry. 2023 Dec 7;14:1233640. doi: 10.3389/fpsyt.2023.1233640.
42. Cheng WJ, Hang LW, Kubo T, Vanttola P, Huang SC. Impact of sleep timing on attention, sleepiness, and sleep quality among real-life night shift workers with shift work disorder: a cross-over clinical trial. Sleep. 2022 Apr 11;45(4):zsac034. doi: 10.1093/sleep/zsac034.
43. Casjens S, Brenscheidt F, Tisch A, Beermann B, Brüning T, Behrens T, et al. Social jetlag and sleep debts are altered in different rosters of night shift work. PLoS One. 2022 Jan 7;17(1):e0262049. doi: 10.1371/journal.pone.0262049.
44. Díaz-Rizzolo DA, Santos Baez LS, Popp CJ, Borhan R, Sordi-Guth A, Manoogian ENC, et al. Late eating is associated with poor glucose tolerance, independent of body weight, fat mass, energy intake and diet composition in prediabetes or early onset type 2 diabetes. Nutr Diabetes. 2024 Oct 25;14(1):90. doi: 10.1038/s41387-024-00347-6.
45. World Health Organization. Healthy diet. Geneva: WHO; 2020. Available from: https://www.who.int/news-room/fact-sheets/detail/healthy-diet.
46. Centofanti S, Heilbronn LK, Wittert G, Dorrian J, Coates AM, Kennaway D, Gupta C, Stepien JM, Catcheside P, Yates C, Grosser L, Matthews RW, Banks S. Fasting as an intervention to alter the impact of simulated night-shift work on glucose metabolism in healthy adults: a cluster randomised controlled trial. Diabetologia. 2025 Jan;68(1):203-216. doi: 10.1007/s00125-024-06279-1.
47. Chellappa SL, Qian J, Vujovic N, Morris CJ, Nedeltcheva A, Nguyen H, et al. Daytime eating prevents internal circadian misalignment and glucose intolerance in night work. Sci Adv. 2021 Dec 3;7(49):eabg9910. doi: 10.1126/sciadv.abg9910.
48. Tada Y, Kawano Y, Maeda I, Yoshizaki T, Sunami A, Yokoyama Y, et al. Association of body mass index with lifestyle and rotating shift work in Japanese female nurses. Obesity (Silver Spring). 2014 Dec;22(12):2489-93. doi: 10.1002/oby.20908.
49. Balieiro LC, Rossato LT, Waterhouse J, Paim SL, Mota MC, Crispim CA. Nutritional status and eating habits of bus drivers during the day and night. Chronobiol Int. 2014 Dec;31(10):1123-9. doi: 10.3109/07420528.2014.957299.
50. Oussaada SM, van Galen KA, Cooiman MI, Kleinendorst L, Hazebroek EJ, van Haelst MM, et al. The pathogenesis of obesity. Metabolism. 2019 Mar;92:26-36. doi: 10.1016/j.metabol.2018.12.012.
51. Saltiel AR, Olefsky JM. Inflammatory mechanisms linking obesity and metabolic disease. J Clin Invest. 2017 Jan 3;127(1):1-4. doi: 10.1172/JCI92035.
52. Galindo Muñoz JS, Gómez Gallego M, Díaz Soler I, Barberá Ortega MC, Martínez Cáceres CM, Hernández Morante JJ. Effect of a chronotype-adjusted diet on weight loss effectiveness: A randomized clinical trial. Clin Nutr. 2020 Apr;39(4):1041-1048. doi: 10.1016/j.clnu.2019.05.012.
53. Ahluwalia MK. Chrononutrition-When We Eat Is of the Essence in Tackling Obesity. Nutrients. 2022 Nov 29;14(23):5080. doi: 10.3390/nu14235080.
54. Bonnell EK, Huggins CE, Huggins CT, McCaffrey TA, Palermo C, Bonham MP. Influences on Dietary Choices during Day versus Night Shift in Shift Workers: A Mixed Methods Study. Nutrients. 2017 Feb 26;9(3):193. doi: 10.3390/nu9030193.
55. Gupta NJ, Kumar V, Panda S. A camera-phone based study reveals erratic eating pattern and disrupted daily eating-fasting cycle among

Copyright© AE&M all rights reserved.

adults in India. PLoS One. 2017 Mar 6;12(3):e0172852. doi: 10.1371/journal.pone.0172852.

56. McHill AW, Melanson EL, Higgins J, Connick E, Moehlman TM, Stothard ER, et al. Impact of circadian misalignment on energy metabolism during simulated nightshift work. Proc Natl Acad Sci U S A. 2014 Dec 2;111(48):17302-7. doi: 10.1073/pnas.1412021111.
57. Qian J, Morris CJ, Caputo R, Wang W, Garaulet M, Scheer FAJL. Sex differences in the circadian misalignment effects on energy regulation. Proc Natl Acad Sci U S A. 2019 Nov 19;116(47):23806-23812. doi: 10.1073/pnas.1914003116.
58. Geaney F, Kelly C, Di Marrazzo JS, Harrington JM, Fitzgerald AP, Greiner BA, et al. The effect of complex workplace dietary interventions on employees' dietary intakes, nutrition knowledge and health status: a cluster controlled trial. Prev Med. 2016 Aug;89:76-83. doi: 10.1016/j.ypmed.2016.05.005.
59. Sutton EF, Beyl R, Early KS, Cefalu WT, Ravussin E, Peterson CM. Early Time-Restricted Feeding Improves Insulin Sensitivity, Blood Pressure, and Oxidative Stress Even without Weight Loss in Men with Prediabetes. Cell Metab. 2018 Jun 5;27(6):1212-1221.e3. doi: 10.1016/j.cmet.2018.04.010.
60. Palomar-Cros A, Srour B, Andreeva VA, Fezeu LK, Bellicha A, Kesse-Guyot E, et al. Associations of meal timing, number of eating occasions and night-time fasting duration with incidence of type 2 diabetes in the NutriNet-Santé cohort. Int J Epidemiol. 2023 Oct 5;52(5):1486-1497. doi: 10.1093/ije/dyad081.
61. Pons-Muzzo L, de Cid R, Obón-Santacana M, Straif K, Papantoniou K, Santonja I, et al. Sex-specific chrono-nutritional patterns and association with body weight in a general population in Spain (GCAT study). Int J Behav Nutr Phys Act. 2024 Sep 12;21(1):102. doi: 10.1186/s12966-024-01639-x.

Copyright© AE&M all rights reserved.

Archives of Endocrinology and Metabolism
ISSN 2359-4292
OFFICIAL JOURNAL OF THE BRAZILIAN SOCIETY OF ENDOCRINOLOGY AND METABOLISM

original

The relationships among nutrition, body composition, muscle strength and physical performance in patients with acromegaly

Natália Nachbar Hupalowski[1]
https://orcid.org/0000-0002-3396-4418

Claudia Pinheiro Sanches Rocha[1]
https://orcid.org/0000-0003-2713-3543

Vicente F. C. Andrade[1]
https://orcid.org/0000-0001-6101-4359

Cesar Luiz Boguszewski[1]
https://orcid.org/0000-0001-7285-7941

Victoria Zeghbi Cochenski Borba[1]
https://orcid.org/0000-0003-0555-0880

[1] Serviço de Endocrinologia e Metabologia (SEMPR), Hospital de Clínicas, Departamento de Medicina Interna, Universidade Federal do Paraná, Curitiba, PR, Brasil

ABSTRACT

Objective: To investigate the impact of dietary intake profile on body composition, physical performance, and muscle strength in patients with acromegaly. **Subjects and methods:** Observational, cross-sectional study involving patients with acromegaly compared with age and sex-matched controls. Body composition, including total lean mass (TLM) and appendicular lean mass (ALM), was assessed using dual-energy X-ray absorptiometry (DXA). All participants completed a Food Frequency Questionnaire (FFQ) and underwent strength and performance testing. **Results:** A total of 82 patients were included, 41 in the acromegaly group (AG) and 41 in the control group (CG). The AG comprised 23 women and 18 men, mean age 55.9 ± 11.8 years and mean BMI 31.1 ± 5.2 kg/m². Muscle mass was increased in the AG, but strength and physical performance were worse compared to CG. AG exhibited a higher intake of carbohydrates, trans fats, and certain micronutrients, as omega-3, vitamin B9, and beta-carotene, compared to the CG. Niacin (R = -0.316, p = 0.004) and vitamin B6 (R = -0.320, p = 0.042) were associated with performance on the sit to stand test. Beta-carotene (R=-0.429, p=0.005), vitamin E (R = -0.321, p=0.041), and flavone (R = -0.313, p = 0.046) were associated with better time to get up and go (TUG) test performance, whereas caffeine intake (R = 0.344, p = 0.028) was associated with worse time. Additionally, niacin (R = 0.341, p = 0.029) and selenium (R = 0.317, p = 0.046) had a positive impact on the short physical performance battery (SPPB) test. Hand grip strength was positively correlated with monounsaturated fats (R = 0.387, p = 0.012) and selenium (R = 0.316, p = 0.044). Selenium, zinc, omega-6 fatty acids, calcium, and iron, were all positively associated with TLM, while caffeine and isoflavones showed a negative association. **Conclusion:** Patients with acromegaly exhibited increased muscle mass, but their functional capacity were compromised, potentially due to alterations in muscle composition. The intake of nutrients such as selenium, β-carotene, flavonoids, vitamin E and niacin, may improve physical performance and muscle strength.

Keywords: Acromegaly; nutrients intake; body composition; physical performance; muscle mass

INTRODUCTION

Acromegaly is a rare endocrine disorder characterized by excessive secretion of growth hormone (GH) and insulin-like growth factor 1 (IGF-1), typically due to a GH-secreting pituitary adenoma. This hormonal excess leads to a range of clinical features (1), which increase the risk of comorbidities and is accompanied by notable alterations in body composition. Patients with active disease often exhibit a reduction in visceral fat mass and an increase in skeletal muscle mass and extracellular body water (1). Although increased muscle mass may suggest better physical capacity, elevated GH and IGF-I levels can negatively impact peripheral muscle strength, exacerbating musculoskeletal weakness (2).

Muscle health maintenance relies on essential nutrients. Proteins and amino acids play a central role

Received on Ago/12/2025
Accepted on Feb/9/2026
DOI: 10.20945/2359-4292-2026-0048

Correspondence to:
Victoria Zeghbi Cochenski Borba
Serviço de Endocrinologia e Metabologia,
Hospital de Clínicas,
Universidade Federal do Paraná
Avenida Agostinho Leão Jr, 285
80030-110 – Curitiba, PR, Brasil
vzcborba@gmail.com

Associated editor:
Leandro Kasuki
https://orcid.org/0000-0003-1339-3192

This is an open-access article distributed under the terms of the Creative Commons Attribution License

Copyright© AE&M all rights reserved.

in preserving and increasing muscle mass by stimulating muscle protein synthesis. Studies indicate that adequate protein intake combined with resistance training is crucial for promoting muscle anabolism (3). Furthermore, higher intake of proteins and dietary fiber has been associated with lower body fat percentage and body mass index (BMI), demonstrating benefits for body composition and fat control (4). Polyunsaturated fatty acids, such as omega-3, known for their anti-inflammatory properties, also contribute to increased muscle mass and strength by modulating anabolic signaling pathways (5). These lipids are further associated with reduced central adiposity, particularly when combined with strength training (5).

Antioxidant vitamins (C and E) play a crucial role in protecting muscle tissue from oxidative stress, thereby supporting muscle health (6,7). In addition, other nutrients such as iron, niacin (vitamin B3), zinc, vitamin B12, selenium, and proteins are beneficial to lean mass (8). Experimental and observational studies suggest that adequate selenium levels are associated with a lower body fat percentage and a better lean mass profile, whereas both deficiency and excess may impair adipose tissue function (9,10). Monounsaturated fats intake is inversely associated with the risk of sarcopenia, suggesting a protective role in the preservation of muscle mass (11). Additionally, dietary patterns that promote the intake of these fats may improve strength, muscle power, and antioxidant markers (12). While some nutrients demonstrate beneficial effects on body composition and muscle strength, others may exert negative impacts. Trans fats, for instance, are associated with detrimental effects on skeletal muscle mass (13). These lipids impair insulin sensitivity in muscle,interfering with energy metabolism and potentially contributing to a progressive decline in muscle strength and function (14,15). This effect may exacerbate insulin resistance, to which individuals with acromegaly are more susceptible due to the excess of GH and IGF-1 (16).

Chronic alcohol consumption is also linked to a reduction in muscle mass and strength, largely attributed to the inhibition of protein synthesis and the increased rate of muscle degradation (17,18).

Given the limited literature on the nutritional intake of patients with acromegaly and its effects on body composition, physical performance, and muscle strength, this study aims to evaluate the influence of dietary profile on these parameters.

SUBJECTS AND METHODS

This observational, cross-sectional study evaluated patients with acromegaly who were followed at the Neuroendocrine Unit of the Endocrine Division (SEMPR) in our academic research center. The study was approved by the Ethics Committee of our institution under the protocol number 6.293.233 (CAAE: 49629321.7.0000.0096), and all individuals who agreed to participate signed an informed consent form.

Patients with acromegaly of both sexes over the age of 18 were invited to participate by convenience sampling during their routine outpatient medical appointment. The exclusion criteria included uncontrolled metabolic or chronic diseases (e.g., uncontrolled diabetes, uncontrolled hypertension, chronic kidney disease) or active malignant neoplasms; use of medications or drugs that could affect muscle or bone (e.g., hormones, corticosteroids, and GLP-1 agonists); any physical impairment preventing physical function assessment; and patients who were unable to perform the required tests and exams.

The included patients with acromegaly comprised the acromegaly group (AG) and completed a standardized questionnaire about demographic data, disease characteristics, type of treatment, medications in use, lifestyle habits (smoking and alcohol consumption), personal and family history of fractures, and the presence of comorbidities. Data not captured during the interview were collected from medical records. The participants were then referred for nutritional and physical evaluations (weight, height, and body mass index [BMI]), body composition assessment, strength and functional tests.

The diagnosis of acromegaly was based on the 14th Acromegaly Consensus, and the AG was considered to have controlled disease if the IGF-1 levels were within the normal reference range for age and sex (19). A control group (CG), matched by sex and

Copyright© AE&M all rights reserved.

age, was recruited from relatives of patients and individuals from the community.

Body composition

Body composition was assessed using dual-energy X-ray absorptiometry (DXA) with a Hologic Horizon A device – serial number 201383, Bedford, USA. Parameters analyzed included total lean mass in grams (TLM), percentage of total fat mass (%TFM), android/gynoid ratio (A/G), and appendicular lean mass (ALM), measured by the sum of lean mass in the arms and legs. Weight was measured using a calibrated anthropometric scale (Plenna®) with the participant barefoot. Height was measured using a vertical stadiometer (Tonelli Gomes®). Body mass index (BMI) was calculated by dividing weight (in kg) by height squared (in meters). BMI results for participants were classified as underweight (BMI < 18.5 kg/m²), normal weight (18.6 kg/m² < BMI < 24.9 kg/m²), overweight (25.0 kg/m² < BMI < 29.9 kg/m²), obesity grade I (30.0 kg/m² < BMI < 34.9 kg/m²), obesity grade II (35 kg/m² < BMI < 39.9 kg/m²), and grade III obesity (BMI > 40 kg/m²) (20).

Physical performance and muscle strength

Physical performance and strength were evaluated using the short physical performance battery (SPPB), which comprises three tests: strength, performance, and balance. Strength was assessed through the 5-times seat to stand test (STST), where patients were required to rise from and sit back on a chair five consecutive times as quickly as possible without stopping or using their arms. A time below 15 seconds (s) was considered normal (21). Performance was measured using the 4-meter gait speed test (GS), in which patients stood up from a chair, walked 6 meters at a safe speed, the first and last meters were not timed; a speed ≥0.8 m/s was considered normal (22). Balance was evaluated by instructing patients to maintain a standing position without support for 10s with their feet together, followed by another 10s in a semi-tandem position, and then 10s in a tandem position. Each position was scored: maintaining the position for 10s earned 2 points, holding it for 3 to 9.99s earned 1 point, and less than 3s or inability to perform resulted in 0 points (22). Additionally, the time up and go test (TUG) was conducted, requiring patients to stand from a chair without using their arms, walk 3 meters, turn around a cone, return, and sit back down at a comfortable pace. A time of 20s or less was considered normal (22,23). Upper limb strength was assessed using the handgrip strength (HGS) test with a Charder® MG 4800 dynamometer. Patients were instructed to squeeze the dynamometer handle with maximum strength, and an average of three attempts was recorded. Values of ≤ 27 kg for men and ≤ 16 kg for women were considered altered (22).

Food Frequency Questionnaire (FFQ)

To assess dietary patterns and nutrient intake, a validated food frequency questionnaire (FFQ) was used for the adult Brazilian population aged 18 to 60 years, who were overweight, i.e., BMI above 25 kg/m² (24). The FFQ was collected considering the foods consumed over a one-month period and includes 90 foods or preparations, divided into fifteen sections: 1) foods or preparations; 2) pasta; 3) various dishes and snacks; 4) meats; 5) rice, tubers, and vegetables; 6) eggs; 7) dairy products; 8) fats; 9) cereals; 10) green leaves; 11) fruits and juices; 12) miscellaneous; 13) breads, cakes, and cookies; 14) various drinks; and 15) sweets and desserts. During the interview, the participant was asked to indicate whether they consumed the food or preparation, the frequency throughout the month, and the amount consumed in household measures or the approximate value in grams.

During the face-to-face interview in which the food frequency questionnaire was administered, the research team used a standardized photographic manual containing household utensils and portion-size images with corresponding weights (25). Participants were asked to identify the portion size that most closely resembled their usual intake. These standardized images were not photographs of the participants' own meals, but visual aids used to improve accuracy in estimating portion sizes. FFQ data were entered into a pre-designed Excel® spreadsheet, which displayed the quantities of 38 macronutrients, micronutrients, and bioactive compounds per 100 grams of food or preparation. A formula was created, so when the quantity consumed by the patient was entered

Copyright© AE&M all rights reserved.

into the spreadsheet, the calculation was automatic. The calculation of dietary component intake used the Brazilian food composition table (TACO) (26), the USDA food and nutrient database (27), the Brazilian table of carotenoid composition in foods (28), and the Phenol-Explorer 3.0 database (29). The intake pattern was considered inadequate when nutrient intake was below the recommended levels for age and sex, based on Dietary Reference Intakes (DRIs). Thus, the Estimated Average Requirement (EAR) was used, and if EAR values were not available, the Adequate Intake (AI) (30), and the latest WHO guidelines on fat and carbohydrate consumption were applied (31,32).

Statistical analysis

Statistical analyses were performed using the Statistical Package for the Social Sciences (SPSS) software, version 29. A descriptive analysis of the frequency distribution of all variables was conducted. The Kolmogorov-Smirnov test was used to assess the normality of the variables in the study. To evaluate differences between means, Student's t-test was used for parametric data and the Mann-Whitney test for non-parametric data. For the evaluation of categorical data, Fisher's exact test and the chi-square test were used. We employed the Spearman's Rho coefficient to measure the size of the effect of the studied associations, assuming the following cutoff points: at least 0.8 (very strong), 0.6 up to 0.8 (moderately strong), 0.3–0.5 (fair), and < 0.3 (poor) (33). Statistical significances were considered when the p-value was ≤ 0.05.

RESULTS

Fifty-seven patients with acromegaly were invited to participate, eight were excluded either because they lived outside town and could not do the evaluations or had a condition that could impact the test results. Additionally, eight individuals declined to answer the FFQ. Finally, 41 patients were included in the AG (mean age 55.9 ± 11.8 years; 90.2% white and 58.5% women; BMI 31.3 ± 5.2 kg/m²) and were compared to 41 in the CG (mean age 56.8 ± 14.3 years; 82.9% white and 56.1% women; BMI 25.5 ± 3.3 kg/m²). The mean age at diagnosis of acromegaly was 43.7 ± 13.0 years, and the mean disease duration was 12 years. Most of the patients in the AG underwent surgical treatment.

Compared to the CG, the AG group had higher BMI, more fractures, and a higher number of comorbidities, with hypertension, obesity, and hypogonadism being the most prevalent (p < 0.05 for all) (**Table 1**).

Nutritional inadequacies were common in both groups, despite differences in the intake of specific nutrients and bioactive compounds (**Table 2**). The AG had higher intake of carbohydrates (p = 0.019), trans fats (p < 0.001), omega-3 (p = 0.001), folic acid (p = 0.013), thiamine (p = 0.009), and beta-carotene (p 0.001). The mean mineral intake was similar between groups. Both groups showed insufficient daily consumption of fiber, omega-3, omega-6, vitamins A and E, magnesium, potassium, and calcium; only the CG had folic acid intake below the recommended level.

The body composition showed similar %TFM and A/G ratio between groups. In contrast, lean mass were higher in the AG, TLM (male AG 66.7 ± 8.9 kg vs CG 52.3 ± 8.6 kg, p < 0.001 and female AG 47.1 ± 9.1 kg vs CG 38.7 ± 6.0 kg, p = 0.001) and ALM in both men and women (male AG 27.7 ± 4.3 kg vs CG 22.3 ± 3.1 kg, p < 0.001 and female AG 16.9 ± 6.4 kg vs CG 15.0 ± 2.4 kg, p = 0.009) (**Table 3**).

Data on physical performance and muscle strength are presented in **Table 4**. Compared to the CG, the AG showed slower STST (16.6 s ± 5.3 s vs 12.2 s ± 2.5 s; p < 0.001), TUG (12.22 s ± 4.27 s vs 9.4 s ± 2.7 s; p < 0.001) and GS (0.91 m/s ± 0.3 m/s vs 1.16 m/s ± 0.2 m/s; p < 0.001), and lower SPPB scores (9.0 ± 2.6 vs CG 11.8 ± 0.5; p < 0.001).

Correlations between body composition, physical performance tests, muscle strength and the intake of nutrients and bioactive compounds in the AG are detailed in **Figure 1**. The A/G correlated negatively only with isoflavone, while TLM correlated positively with several nutrients, including selenium, omega-6, folic acid, zinc, vitamins B6 and B12, polyunsaturated fats (PUFA), monounsaturated (MUFA), iron, fiber, calcium, proteins, carbohydrates, total fat, and total calories (p < 0.05 for all). Only caffeine showed a negative correlation with TLM (**Figure 1A**).

Copyright© ACE&M all rights reserved.

Table 1. Clinical and nutritional characteristics of the Acromegaly Group (AG) and the Control Group (CG)

Characteristics	AG (n = 41)	CG (n = 41)	P
Age (years)	55.9 ± 11.8	56.8 ± 14.3	0.769
Ethnicity			0.01
White, n (%)	38 (92.7)	34 (82.9)	
Black, n (%)	3 (7.3)	1 (2.4)	
Asian, n (%)	0	6 (14.6)	
Sex, n (%)			
Female	23 (56.1)	23 (56.1)	
Male	18 (43.9)	18 (43.9)	
Smoking, n (%)	7 (17.1)	1 (2.4)	0.02
Height (m)	1.70 ± 0.1	1.64 ± 0.1	0.445
Weight (kg)	87.0 ± 18.6	70.1 ± 11.3	< 0.001
BMI (kg/m²)	31.1 ± 5.2	25.5 ± 3.3	< 0.001
Normal, n (%)	6 (14.6)	25 (61.0)	
Overweight, n (%)	15 (36.6)	11 (26.8)	
Obesity grade I, n (%)	10 (24.4)	5 (12.2)	
Obesity grade II, n (%)	7 (17.1)	0	
Obesity grade III, n (%)	3 (7.3)	0	
Disease data			
Time since diagnosis (years)	12.0 ± 7.8	NA	
Age at diagnosis (years)	43.7 ± 13.0	NA	
Serum IGF-1* (ng/mL)	256.6 ± 164.8	NA	
Surgical treatment, n (%)	35 (85.4)	NA	
Disease control, n (%)			
Controlled	26 (63.4)	NA	
Uncontrolled	15 (36.6)	NA	
Medications, n (%)			
Somatostatin receptor ligands			
Octreotide	26 (63.4)	NA	
Lanreotide	15 (36.6)	NA	
Cabergoline	7 (17.1)	NA	
Pegvisomant	4 (9.7)	NA	
Comorbidities, n (%)			
Hypertension	23 (56.1)	14 (34.1)	0.057
Obesity	20 (48.8)	6 (14.6)	0.001
Dyslipidemia	16 (39.0)	12 (29.3)	0.390
Diabetes	15 (36.6)	3 (7.3)	0.003
Hypothyroidism	9 (21.9)	1 (2.4)	0.01
Hypogonadism	9 (21.9)	0	< 0.001
Men	4 (44.4)	0	
Hormonal replacement	1 (25.0)	0	
Women	5 (55.5)	0	
Hormonal replacement	4 (80.0)	0	
Hypopituitarism	7 (17.1)	0	0.01
Mood disorder	6 (14.6)	0	0.032
Osteoporosis	5 (12.2)	4 (9.7)	1.000
Fracture/patient	0.63 ± 1.11	0.15 ± 0.43	0.01

NA: not applicable; BMI: body mass index; *: value of IGF-1 at the time of evaluation.

Copyright© AE&M all rights reserved.

Table 2. Nutrient intake in the Acromegaly Group (AG) and the Control Group (CG)

Nutrients	EAR	AG (n = 41) Mean ± SD	CG (n = 41) Mean ± SD	*p*
Energy (kcal)		2242.34 ± 929.36	1958.42 ± 784.35	0.059
Macronutrients				
Proteins (g)		104.15 ± 45.13	104.13 ± 48.12	0.893
Carbohydrates (g)	100	267.78 ± 130.47	207.88 ± 96.50	0.019
Fibers (g)	25–38	19.20 ± 7.50	16.78 ± 7.63	0.084
Total fat (g)	ND	71.86 ± 32.73	69.69 ± 33.47	0.640
Saturated (g)	< 10%/day	25.58 ± 12.16	25.13 ± 10.53	0.835
Monounsaturated (g)	ND	23.59 ± 11.12	23.38 ± 12.16	0.738
Poliunsaturated (g)	ND	12.82 ± 5.86	12.26 ± 5.36	0.745
Cholesterol (mg)	<300	383.79 ± 179.79	426.79 ± 212.00	0.325
Trans fat (g)	< 1%/day	2.86 ± 2.55	0.76 ± 0.60	< 0.001
Omega-3 (g)	1.1–1.6	0.36 ± 0.24	0.21 ± 0.18	0.001
Omega-6 (g)	11–17	9.86 ± 5.02	9.15 ± 6.87	0.594
Micronutrients				
Vitamins				
Vitamin A (mg)	500–625	174.07 ± 113.96	174.82 ± 96.15	0.974
Vitamin C (mg)	60–75	188. 73 ± 136.66	145.48 ± 106.18	0.068
Vitamin D (UI)	400UI	182.4 ± 185.2	182 ± 205.6	0.670
Vitamin E (mg)	12	3.86 ± 2.32	4.56 ± 2.66	0.208
B1 (mg)	0.9–1.0	1.58 ± 0.67	1.23 ± 0.51	0.009
B3 (mg)	14–16	25.2 ± 12.2	23.6 ± 11.9	0.530
B6 (mg)	1.1–1.3	1.96 ± 0.97	1.83 ± 0.82	0.503
B9 (mcg)	320	460.42 ± 171.09	371.86 ± 171.96	0.013
B12 (mcg)	2.0	4.44 ± 2.26	4.76 ± 2.42	0.467
Minerals				
Calcium (mg)	800–1000	636.08 ± 380.79	583.27 ± 281.71	0.935
Magnesium (mg)	255–350	280.13 ± 90.54	259.91 ± 98.59	0.336
Potassium (mg)	2600–3400	3056.63 ± 1144.71	2762.02 ± 0.964	0.272
Zinc (mg)	6.8–9.4	12.79 ± 6.57	12.26 ± 5.36	0.802
Trace element				
Selenium (mcg)	45	101.91 ± 43.08	104.02 ± 44.48	0.828
Bioactive compounds				
Betacarotene (mcg)	ND	810.71 ± 592.22	252.65 ± 347.75	0.001
Flavone (mg)	ND	9.33 ± 5.27	5.27 ± 7.70	0.153
Isoflavone (mg)	ND	0.68 ± 0.71	0.66 ± 0.65	0.893
Others				
Alcohol (g)	< 30	1.31 ± 3.66	9.10 ± 11.43	< 0.001
Caffeine (g)	400	84.48 ± 71.85	108.63 ± 107.04	0.323

EAR: estimated average requirement; B12: methylcobalamin; B6: pyridoxine; B9: folic acid; B1: thiamine; B3: niacin.

Copyright© AE&M all rights reserved.

Table 3. Body Composition in the Acromegaly Group (AG) and the Control Group (CG)

	AG (n = 41)	CG (n = 41)	p
Total lean mass (kg)			
Men	66.7 ± 8.9	52.3 ± 8.6	< 0.001
Women	47.1 ± 9.1	38.7 ± 6.0	0.001
Total fat mass (%)			
Men	32.0 ± 3.5	31.2 ± 4.0	0.528
Women	41.3 ± 5.6	42.0 ± 3.7	0.644
ALM (kg)			
Men	27.7 ± 4.3	22.3 ± 3.1	<0.001
Women	16.9 ± 6.4	15.0 ± 2.4	0.009
A/G ratio			
Men	1.11 ± 0.17	1.07 ± 0.14	0.445
Women	0.89 ± 0.11	0.91 ± 0.12	0.543
Elevated A/G ratio, n (%)			
Men	14 (87.5)	17 (89.5)	0.855
Women	13 (59.1)	13 (68.4)	0.536

ALM: appendicular lean mass; A/G: android/gynoid ratio.

Table 4. Physical performance and muscle strength in the Acromegaly Group (AG) and the Control Group (CG)

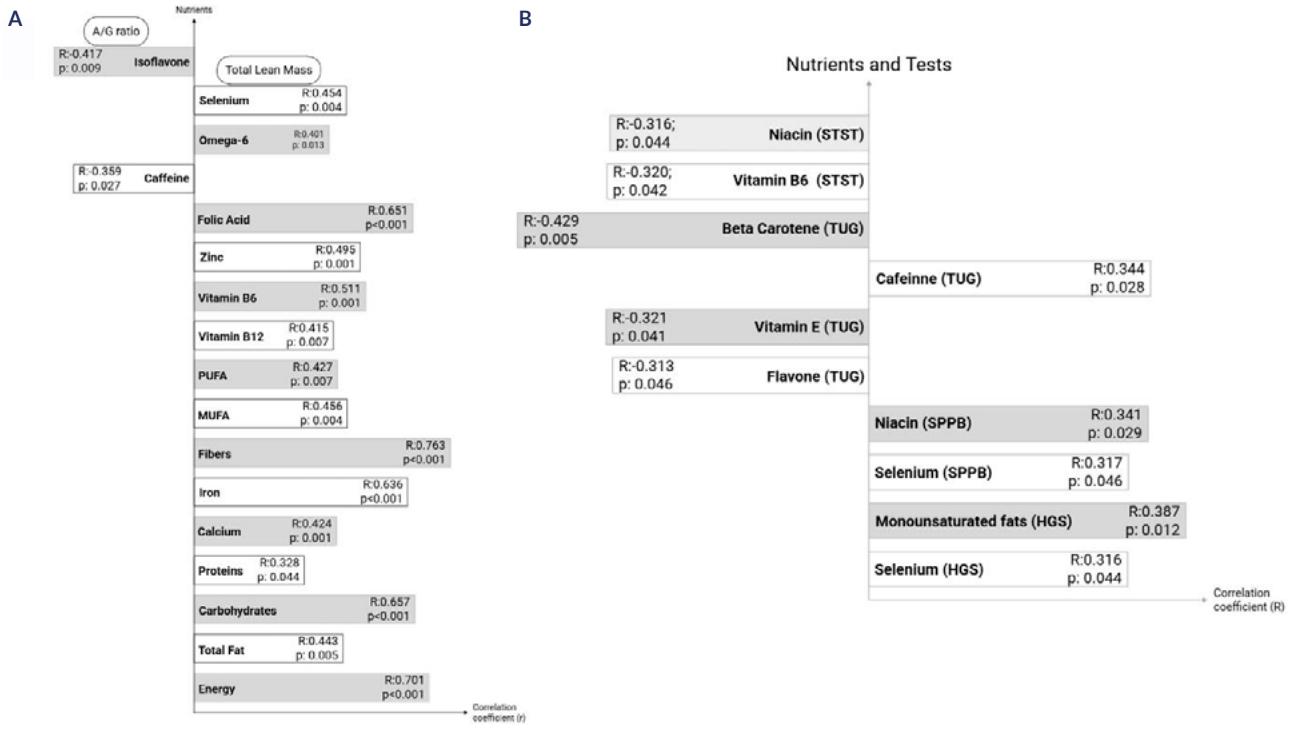
Tests	AG (n = 41)	CG (n = 41)	p
Muscle strength			
STST (s)	16.6 ± 5.3	12.2 ± 2.5	<0.001
Low n (%)	22 (53.6)	2 (4.9)	<0.001
HGS (kg)			
Men	42.1 ± 9.3 (0)	39.4 ± 5.8 (0)	0.293
Low n (%)	0 (0)	0 (0)	
Women	25.7 ± 5.8 (1)	24.6 ± 4.7 (0)	0.488
Low n (%)	1 (2.43)	0 (0)	1.000
Physical performance			
TUG (s)	12.22 ± 4.27	9.4 ± 2.7	0.001
Altered	3 (7.3)	1 (2.4)	0.616
GS (m/s)	0.91 ± 0.3	1.16 ± 0.2	< 0.001
Altered	12 (29.3)	3 (7.3)	0.020
SPPB	9.0 ± 2.6	11.8 ± 0.5	< 0.001
Altered	13 (31.7)	0 (0)	< 0.001

AG: acromegaly group; CG: control group; n: number; %: percentage; s:seconds; kg: kilograms; m/s: meters per second; STST: 5-times seat to stand test; HGS: hand grip strength; TUG: time up and go test; GS: gait speed; SPPB: short physical performance battery test.

Higher intake of beta-carotene, flavonoids, and vitamin E was associated with shorter TUG time, whereas caffeine intake was associated with longer TUG time. Higher intake of monounsaturated fats and selenium was positively correlated with HGS, whereas higher niacin and vitamin B6 intake was inversely correlated with STST time (**Figure 1B**).

Although higher ALM and TLM were observed in patients with uncontrolled disease (ALM 25.16 ± 5.6 kg uncontrolled vs. 19.25 ± 8.0 kg controlled, p = 0.028 and TLM 61.5 ± 12.5 kg uncontrolled vs. 51.3 ± 12.5 kg controlled, p = 0.019). No differences in nutrient intake were observed between patients with controlled versus uncontrolled acromegaly.

Copyright© AE&M all rights reserved.



PUFA: polyunsaturated fats; MUFA: monounsaturated fats; TLM: total lean mass; A/G: android/gynoid ratio; TUG: time up and go test; STST: 5- times sit-to-stand test; HGS: handgrip strength; SPPB: Short Physical Performance Battery.

Figure 1. Correlation between nutrients with body composition (**A**), muscle strength and physical performance (**B**).

DISCUSSION

To our knowledge, this is the first study to evaluate dietary quality in patients with acromegaly and examine its association with body composition, physical performance and muscle strength. Nutritional intake differed between patients and controls and inadequacies in several nutrients and bioactive compounds were common in both groups. Notably, the AG showed higher TLM but poorer strength and physical performance associated with modifications in diet quality, suggesting that increased lean mass does not necessarily translate into better function in this population.

Patients with acromegaly presented significantly higher total body weight compared to the CG largely driven by lean mass. The higher TLM in the AG could be attributed to the anabolic role of GH and IGF-1 in promoting protein synthesis. Previous studies support the altered body composition in acromegaly, characterized by increased skeletal muscle mass and reduced body fat (34,35). However, in our sample, there was no significant difference in body fat percentage or A/G between groups, suggesting that the higher body weight in the AG was predominantly due to increased lean mass, which may also reflect an increase in intramuscular water. TLM was also associated with the intake of various nutrients, including vitamins (B6, B9, and B12), minerals (iron, zinc, calcium, and selenium) and macronutrients (carbohydrates, proteins, and total fats), suggesting that the diet may modulate lean-mass measures in this group.

It was observed that, despite having greater lean mass, patients with acromegaly exhibited a poorer physical function, indicating muscle weakness, as previously reported (36). This deficit was evident in the results of physical performance tests, where individuals with acromegaly performed worse compared to the CG. This altered functionality may be related to increased collagen deposition in muscle tissues, impairing flexibility, and muscle efficiency (37). A study by Martel-Duguech and cols. found that patients with acromegaly had slower gait speed and poorer performance in the STST (36), corroborating our findings. Several nutrients have been positively correlated with better physical performance and body composition,

Copyright© AE&M all rights reserved.

and a balanced, nutrient-rich diet is generally associated with better performance than a nutrient poor diet (38,39).

The positive association between vitamin B6 intake and improved performance has been previously demonstrated (40). However, lower intakes of carbohydrates, omega-3, vitamin D, and saturated fats have been previously observed in individuals with greater frailty (41). Although the AG had higher carbohydrate and omega-3 intakes than the CG, this did not translate into better muscle strength or performance. Saturated fat intake, despite being similar between groups, exceeded recommendations in both groups. In a study involving women, aged 18-79 years, saturated fat intake was inversely associated with lean mass (13), whereas in another study of sedentary men aged 25-45 years, a high-fat diet was associated with reduced whole-body efficiency (42). In our study, mean HGS was similar between the groups, but was better with higher selenium and MUFA intake. A study using data from the National Health and Nutrition Examination Survey (NHANES 2011-2014) higher selenium concentrations were associated with better HGS (43).

TLM was positively associated with several nutrients, including minerals, vitamins, carbohydrates (including fiber), and fat. These findings suggest that a higher intake of these nutrients may be associated with higher lean-mass measures in these individuals. In the study conducted by Borda and cols. (8) with older adults, ALM was positively correlated with PUFAs, zinc, selenium, vitamin B12, niacin, vitamin D, iron, and proteins intake, highlighting the potential role of these nutrients in supporting lean mass (8).

In our study, daily intake of fiber, omega-3, vitamins A, D, and E, magnesium, and calcium, although below the recommended levels for age and sex was positively correlated with body composition and muscle strength. However, because mean intake of these nutrients did not differ significantly between the AG and the CG, we can only hypothesize that meeting recommended daily intakes might be associated with better performance in the AG, potentially mitigating disease-related functional impairment. Alcohol consumption, which is known to negatively impact muscle mass (17,18) was higher in CG, raising the possibility that it may not represent a significant risk factor in this context, or the increased alcohol intake in CG may have impacted a lower lean mass compared to the AG.

Carbohydrates are the primary energy source for exercise, especially high-intensity activities and play an important role in physical performance and muscle strength. Muscle glycogen is the storage form of carbohydrates, and low glycogen availability can impair physical performance (44). We observed higher carbohydrate intake in AG, which is likely due to the higher basal metabolism and total energy expenditure in acromegaly (45,46). Surprisingly, higher carbohydrate intake was not associated with better physical performance, suggesting that other disease related factors may be more important determinants of function.

The folic acid (vitamin B9) is essential for red blood cell production, DNA synthesis, and amino acids (33). In a two-year study of older adults supplemented simultaneously with vitamin B9 and vitamin B12 showed that the supplementation did not improve physical function (47). Similarly, in our study, despite higher folic acid intake in AG, it was not associated with physical performance.

Omega-3, an essential fatty acid, must be obtained through diet. Its anti-inflammatory properties are well established. Omega-3 supplementation (2 g or more per day) has been associated with improvements in GS and TUG performance, and modest increases in muscle mass (48). Omega-3 is a type of PUFA, and in our study, PUFAs were positively correlated with TLM. The intake of omega-3 was assessed from diet rather than supplementation. It remains unclear whether supplementation could potentially improve physical performance and muscle strength in patients with acromegaly (48).

Trans fat was nearly four times higher in the AG than in the CG. This type of fat is associated with increased all-cause mortality and is known to induce inflammation and oxidative stress (49). Evidence on trans fats and physical performance largely comes from animal studies. Liou and cols., 2013 reported reduced grip strength in mice fed with a high trans-fat diet (50). Similarly, Jeyakumar and cols., 2011 reported that trans-fat intake reduced insulin-stimulated glucose uptake in skeletal muscle in female rats, potentially

Copyright© AE&M all rights reserved.

impairing energy production and muscle function (14). These findings suggest that higher trans-fat consumption in the AG contributed to poorer muscle function, although causality cannot be inferred from our design.

Beta-carotene, a precursor of vitamin A, has been associated with strength and performance. In the Framingham Offspring study, higher total carotenoid intake was associated with increased grip strength and a higher walking speed in adults, suggesting a potential role for antioxidants in preserving muscle function (51). In our study, beta carotene intake was approximately three times higher in AG than in CG but was not associated with functionality.

Higher concentrations of selenium have been associated with better mobility and less impairment of limb performance, muscle weakness, and mobility in older adults (52) and with better grip strength in adults without chronic diseases (43). In our study, selenium intake was positively correlated with HGS, SPPB, and TLM. HGS was similar between groups, which raises the possibility that selenium intake may have contributed to comparable HGS despite overall poorer performance of the AG; however, this interpretation is speculative. Although selenium correlated with SPPB within the AG, mean SPPB was still lower in this group than in the CG, highlighting that multiple factors likely contribute to functional impairment.

Although the AG showed a higher consumption of some nutrients compared to the CG, the FFQ indicated that most participants did not meet recommended daily intake for several micronutrients relevant to health and physical performance. The relatively small sample size and the cross-sectional design limit the generalizability and preclude causal inference. In addition, dietary supplements and medication effects on body composition and muscle strength were not assessed and may have influenced the findings. Dietary intake estimation is also subject to measurement bias. Poorer performance in the AG may reflect balance and gait disturbances, reported in acromegaly rather than intrinsic muscle impairment alone. Finally, groups differed in comorbidities and lifestyle factors — particularly the higher prevalence of diabetes and hypertension in the AG — which may have affected muscle health and physical function. A strength of this study is its focuses on dietary intake in acromegaly and its associations with body composition and muscle functionality, areas that remain underexplored.

In conclusion, our findings highlight the complex relationship between nutritional intake, body composition, strength and physical performance in patients with acromegaly. Despite the increased muscle mass, patients with acromegaly showed poorer physical performance and strength. The higher intake of some nutrients, such as selenium, β-carotene, flavonoids, vitamin E, and niacin, may prove to be potentially beneficial, and future studies, ideally prospective, are needed to clarify whether modification in the diet can improve physical function in patients with acromegaly.

Disclosure: no potential conflict of interest relevant to this article was reported.

Data availability: datasets related to this article will be available upon request to the corresponding author.

REFERENCES

1. Guo X, Gao L, Shi X, Li H, Wang Q, Wang Z, et al. Pre- and Postoperative Body Composition and Metabolic Characteristics in Patients with Acromegaly: A Prospective Study. Int J Endocrinol. 2018 Jan 8;2018:4125013. doi: 10.1155/2018/4125013.
2. Lopes AJ, Ferreira AS, Walchan EM, Soares MS, Bunn PS, Guimarães FS. Explanatory models of muscle performance in acromegaly patients evaluated by knee isokinetic dynamometry: Implications for rehabilitation. 2016 Oct;49:160-9. doi: 10.1016/j.humov.2016.07.005.
3. Ganapathy A, Nieves JW. Nutrition and Sarcopenia-What Do We Know? Nutrients. 2020 Jun 11;12(6):1755. doi: 10.3390/nu12061755.
4. Karpińska E, Moskwa J, Puścion-Jakubik A, Naliwajko SK, Soroczyńska J, Markiewicz-Żukowska R, et al. Body Composition of Young Women and The Consumption of Selected Nutrients. Nutrients. 2022 Dec 27;15(1):129. doi: 10.3390/nu15010129.
5. Cruz-Jentoft AJ, Dawson Hughes B, Scott D, Sanders KM, Rizzoli R. Nutritional strategies for maintaining muscle mass and strength from middle age to later life: A narrative review. Maturitas. 2020 Feb;132:57-64. doi: 10.1016/j.maturitas.2019.11.007.
6. Rivera-Paredez B, León-Reyes G, Rangel-Marín D, Salmerón J, Velázquez-Cruz R. Associations between Macronutrients Intake and Bone Mineral Density: A Longitudinal Analysis of the Health Workers Cohort Study Participants. J Nutr Health Aging. 2023;27(12):1196-1205. doi: 10.1007/s12603-023-2038-2.
7. Shen Y, Zhang C, Dai C, Zhang Y, Wang K, Gao Z, et al. Nutritional Strategies for Muscle Atrophy: Current Evidence and Underlying Mechanisms. Mol Nutr Food Res. 2024 May;68(10):e2300347. doi: 10.1002/mnfr.202300347.
8. Borda MG, Samuelsson J, Cederholm T, Baldera JP, Pérez-Zepeda MU, Barreto GE, et al. Nutrient Intake and Its Association with Appendicular Total Lean Mass and Muscle Function and Strength in Older Adults: A Population-Based Study. Nutrients. 2024 Feb 19;16(4):568. doi: 10.3390/nu16040568.
9. Fontenelle LC, Cardoso de Araújo DS, da Cunha Soares T, Clímaco Cruz KJ, Henriques GS, Marreiro DDN. Nutritional status of selenium in overweight and obesity: A systematic review and meta-analysis. Clin Nutr. 2022 Apr;41(4):862-884. doi: 10.1016/j.clnu.2022.02.007.

Copyright© AE&M all rights reserved.

10. Cavedon E, Manso J, Negro I, Censi S, Serra R, Busetto L, et al. Selenium Supplementation, Body Mass Composition, and Leptin Levels in Patients with Obesity on a Balanced Mildly Hypocaloric Diet: A Pilot Study. Int J Endocrinol. 2020 May 28;2020:4802739. doi: 10.1155/2020/4802739.
11. Ali S, Corbi G, Medoro A, Intrieri M, Scapagnini G, Davinelli S. Relationship between monounsaturated fatty acids and sarcopenia: a systematic review and meta-analysis of observational studies. Aging Clin Exp Res. 2023 Sep;35(9):1823-1834. doi: 10.1007/s40520-023-02465-0.
12. Bianchi E, Erbasan H, Riso P, Perna S. Impact of the Mediterranean Diet on Athletic Performance, Muscle Strength, Body Composition, and Antioxidant Markers in Both Athletes and Non-Professional Athletes: A Systematic Review of Intervention Trials. Nutrients. 2024 Oct 11;16(20):3454. doi: 10.3390/nu16203454.
13. Welch AA, MacGregor AJ, Minihane AM, Skinner J, Valdes AA, Spector TD, et al. Dietary fat and fatty acid profile are associated with indices of skeletal muscle mass in women aged 18-79 years. J Nutr. 2014 Mar;144(3):327-34. doi: 10.3945/jn.113.185256.
14. Jeyakumar SM, Prashant A, Rani KS, Laxmi R, Vani A, Kumar PU, et al. Chronic consumption of trans-fat-rich diet increases hepatic cholesterol levels and impairs muscle insulin sensitivity without leading to hepatic steatosis and hypertriglyceridemia in female Fischer rats. Ann Nutr Metab. 2011 Oct;58(4):272-80. doi: 10.1159/000331215.
15. Tardy AL, Giraudet C, Rousset P, Rigaudière JP, Laillet B, Chalancon S, et al. Effects of trans MUFA from dairy and industrial sources on muscle mitochondrial function and insulin sensitivity. J Lipid Res. 2008 Jul;49(7):1445-55. doi: 10.1194/jlr.M700561-JLR200.
16. Vila G, Jørgensen JOL, Luger A, Stalla GK. Insulin Resistance in Patients With Acromegaly. Front Endocrinol (Lausanne). 2019 Jul 30;10:509. doi: 10.3389/fendo.2019.00509.
17. Simon L, Bourgeois BL, Molina PE. Alcohol and Skeletal Muscle in Health and Disease. Alcohol Res. 2023 Nov 2;43(1):04. doi: 10.35946/arcr.v43.1.04.
18. Kimball SR, Lang CH. Mechanisms Underlying Muscle Protein Imbalance Induced by Alcohol. Annu Rev Nutr. 2018 Aug 21;38:197-217. doi: 10.1146/annurev-nutr-071816-064642.
19. Giustina A, Biermasz N, Casanueva FF, Fleseriu M, Mortini P, Strasburger C, et al.; Acromegaly Consensus Group. Consensus on criteria for acromegaly diagnosis and remission. Pituitary. 2024 Feb;27(1):7-22. doi: 10.1007/s11102-023-01360-1.
20. Associação Brasileira para o Estudo da Obesidade e da Síndrome Metabólica (ABESO). Diretrizes brasileiras de obesidade 2016. VI Diretrizes Brasileiras de Obesidade. São Paulo: ABESO; 2016.
21. Vilarinho R, Montes AM, Noites A, Silva F, Melo C. Reference values for the 1-minute sit-to-stand and 5 times sit-to-stand tests to assess functional capacity: a cross-sectional study. Physiotherapy. 2024 Sep;124:85-92. doi: 10.1016/j.physio.2024.01.004.
22. Cruz-Jentoft AJ, Bahat G, Bauer J, Boirie Y, Bruyère O, Cederholm T, et al.; Writing Group for the European Working Group on Sarcopenia in Older People 2 (EWGSOP2), and the Extended Group for EWGSOP2. Sarcopenia: revised European consensus on definition and diagnosis. Age Ageing. 2019 Jan 1;48(1):16-31. doi: 10.1093/ageing/afy169.
23. Podsiadlo D, Richardson S. The timed "Up & Go": a test of basic functional mobility for frail elderly persons. J Am Geriatr Soc. 1991 Feb;39(2):142-8. doi: 10.1111/j.1532-5415.1991.tb01616.x.
24. Salvo VLMA de, Gimeno SGA. Reprodutibilidade e validade do questionário de frequência de consumo de alimentos. Rev Saude Publica. 2002;36(4):505-512. doi:10.1590/S0034-89102002000400015.
25. Crispim SP, Fisberg RM, Almeida CCB, Nicolas G, Knaze V, Pereira RA. Manual fotográfico de quantificação alimentar. Curitiba: Universidade Federal do Paraná; 2017.
26. Giuntini EB, Lajolo FM, Menezes EW. Tabela Brasileira de Composição de Alimentos TBCA-USP (versões 3 e 4) no contexto internacional. Arch Latinoam Nutr. 2006;56(4).
27. Montville JB, Ahuja JKC, Martin CL, Heendeniya KY, Omolewa-Tomobi G, Steinfeldt LC, et al. USDA Food and Nutrient Database for Dietary Studies (FNDDS), 5.0. Procedia Food Sci. 2013;2:99-112.
28. Rodrigues-Amaya DB. Tabela brasileira de composição de carotenoides em alimentos. Brasília: Ministério do Meio Ambiente; 2008.
29. Rothwell JA, Perez-Jimenez J, Neveu V, Medina-Remón A, M'hiri N, García-Lobato P, et al. Phenol-Explorer 3.0: a major update of the Phenol-Explorer database to incorporate data on the effects of food processing on polyphenol content. Database (Oxford). 2013 Oct 7;2013:bat070. doi: 10.1093/database/bat070.
30. Padovani RM, Amaya-Farfán J, Colugnati FAB, Domene SMÁ. Dietary reference intakes: application of tables in nutritional studies. Rev Nutr. 2006;19(6):741-760.
31. World Health Organization. Saturated fatty acid and trans-fatty acid intake for adults and children. Geneva: World Health Organization; 2023.
32. World Health Organization. Carbohydrate intake for adults and children: WHO guideline. Geneva: World Health Organization; 2023.
33. Chan YH. Biostatistics 104: correlational analysis. Singapore Med J. 2003;44(12):614-619. PMID: 14770254.
34. Reid TJ, Jin Z, Shen W, Reyes-Vidal CM, Fernandez JC, Bruce JN, et al. IGF-1 levels across the spectrum of normal to elevated in acromegaly: relationship to insulin sensitivity, markers of cardiovascular risk and body composition. Pituitary. 2015 Dec;18(6):808-19. doi: 10.1007/s11102-015-0657-2.
35. Bredella MA, Schorr M, Dichtel LE, Gerweck AV, Young BJ, Woodmansee WW, et al. Body Composition and Ectopic Lipid Changes With Biochemical Control of Acromegaly. J Clin Endocrinol Metab. 2017 Nov 1;102(11):4218-4225. doi: 10.1210/jc.2017-01210.
36. Martel-Duguech L, Alonso-Pérez J, Bascuñana H, Díaz-Manera J, Llauger J, Nuñez-Peralta C, et al. Intramuscular fatty infiltration and physical function in controlled acromegaly. Eur J Endocrinol. 2021 Jun 5;185(1):167-177. doi: 10.1530/EJE-21-0209.
37. Hansen TB, Gram J, Bjerre P, Hagen C, Bollerslev J. Body composition in active acromegaly during treatment with octreotide: a double-blind, placebo-controlled cross-over study. Clin Endocrinol (Oxf). 1994 Sep;41(3):323-9. doi: 10.1111/j.1365-2265.1994.tb02552.x.
38. Lukaski HC. Vitamin and mineral status: effects on physical performance. Nutrition. 2004 Jul-Aug;20(7-8):632-44. doi: 10.1016/j.nut.2004.04.001.
39. Beck KL, von Hurst PR, O'Brien WJ, Badenhorst CE. Micronutrients and athletic performance: A review. Food Chem Toxicol. 2021 Dec;158:112618. doi: 10.1016/j.fct.2021.112618.
40. Grootswagers P, Mensink M, Berendsen AAM, Deen CPJ, Kema IP, Bakker SJL, et al. Vitamin B-6 intake is related to physical performance in European older adults: results of the New Dietary Strategies Addressing the Specific Needs of the Elderly Population for Healthy Aging in Europe (NU-AGE) study. Am J Clin Nutr. 2021 Apr 6;113(4):781-789. doi: 10.1093/ajcn/nqaa368.
41. Moradell A, Fernández-García ÁI, Navarrete-Villanueva D, Sagarra-Romero L, Gesteiro E, Pérez-Gómez J, et al. Functional Frailty, Dietary Intake, and Risk of Malnutrition. Are Nutrients Involved in Muscle Synthesis the Key for Frailty Prevention? Nutrients. 2021 Apr 8;13(4):1231. doi: 10.3390/nu13041231.
42. Edwards LM, Murray AJ, Holloway CJ, Carter EE, Kemp GJ, Codreanu I, et al. Short-term consumption of a high-fat diet impairs whole-body efficiency and cognitive function in sedentary men. FASEB J. 2011 Mar;25(3):1088-96. doi: 10.1096/fj.10-171983.
43. Pei J, Yan L, Wu Y, Zhang X, Jia H, Li H. Association between low blood selenium concentrations and poor hand grip strength in United States adults participating in NHANES (2011-2014). Appl Physiol Nutr Metab. 2023 Jul 1;48(7):526-534. doi: 10.1139/apnm-2022-0228.
44. Vigh-Larsen JF, Ørtenblad N, Nielsen J, Emil Andersen O, Overgaard K, Mohr M. The Role of Muscle Glycogen Content and Localization in High-Intensity Exercise Performance: A Placebo-Controlled Trial.

Copyright© AE&M all rights reserved.

Med Sci Sports Exerc. 2022 Dec 1;54(12):2073-2086. doi: 10.1249/MSS.0000000000003002.

45. Møller N, Schmitz O, Jøorgensen JO, Astrup J, Bak JF, Christensen SE, Alberti KG, Weeke J. Basal- and insulin-stimulated substrate metabolism in patients with active acromegaly before and after adenomectomy. J Clin Endocrinol Metab. 1992 May;74(5):1012-9. doi: 10.1210/jcem.74.5.1569148.
46. O'Sullivan AJ, Kelly JJ, Hoffman DM, Freund J, Ho KK. Body composition and energy expenditure in acromegaly. J Clin Endocrinol Metab. 1994 Feb;78(2):381-6. doi: 10.1210/jcem.78.2.8106626.
47. Nasser C, Nobre C, Mesquita S, Ruiz JG, Carlos HR, Prouvot L, et al. Semana da conscientização sobre a importância do ácido fólico. J Epilepsy Clin Neurophysiol. 2005;11(4). doi 10.1590/S1676-26492005000400009.
48. Huang YH, Chiu WC, Hsu YP, Lo YL, Wang YH. Effects of Omega-3 Fatty Acids on Muscle Mass, Muscle Strength and Muscle Performance among the Elderly: A Meta-Analysis. Nutrients. 2020 Dec 4;12(12):3739. doi: 10.3390/nu12123739.
49. de Souza RJ, Mente A, Maroleanu A, Cozma AI, Ha V, Kishibe T, et al. Intake of saturated and trans unsaturated fatty acids and risk of all cause mortality, cardiovascular disease, and type 2 diabetes: systematic review and meta-analysis of observational studies. BMJ. 2015 Aug 11;351:h3978. doi: 10.1136/bmj.h3978.
50. Liou J, Tuazon MA, Burdzy A, Henderson GC. Moderate compared to low dietary intake of trans-fatty acids impairs strength of old and aerobic capacity of young SAMP8 mice in both sexes. Lipids. 2013 Nov;48(11):1135-43. doi: 10.1007/s11745-013-3831-1.
51. Sahni S, Dufour AB, Fielding RA, Newman AB, Kiel DP, Hannan MT, et al. Total carotenoid intake is associated with reduced loss of grip strength and gait speed over time in adults: The Framingham Offspring Study. Am J Clin Nutr. 2021 Feb 2;113(2):437-445. doi: 10.1093/ajcn/nqaa288.
52. García-Esquinas E, Carrasco-Rios M, Ortolá R, Sotos Prieto M, Pérez-Gómez B, Gutiérrez-González E, et al. Selenium and impaired physical function in US and Spanish older adults. Redox Biol. 2021 Jan;38:101819. doi: 10.1016/j.redox.2020.101819.

Copyright© AE&M all rights reserved.

Archives of Endocrinology and Metabolism
ISSN 2359-4292
OFFICIAL JOURNAL OF THE BRAZILIAN SOCIETY OF ENDOCRINOLOGY AND METABOLISM

original

The essential role of the redox balance in adrenal steroidogenesis

Juliana Lourenço Gebenlian[1]
https://orcid.org/0000-0002-9724-3783

Aline Faccioli Bodoni[2]
https://orcid.org/0000-0001-8827-5882

Fernanda Borchers Coeli-Lacchini[2]
https://orcid.org/0000-0001-6568-7497

Margaret de Castro[2]
https://orcid.org/0000-0003-4932-4623

Sonir Roberto Rauber Antonini[1]
https://orcid.org/0000-0003-4778-8803

[1] Departamento de Pediatria, Faculdade de Medicina de Ribeirão Preto, Universidade de São Paulo, Ribeirão Preto, SP, Brasil
[2] Departamento de Clínica Médica, Faculdade de Medicina de Ribeirão Preto, Universidade de São Paulo, Ribeirão Preto, SP, Brasil

ABSTRACT

Objective: To analyze the impact of nicotinamide nucleotide transidrogenase (NNT) enzyme impairment on cortisol production, reactive oxygen species (ROS) formation, mitochondrial activity, and mitogen-activated protein kinase 8 (MAPK8) expression in the adrenocortical cell line. **Materials and methods**: siRNA NNT knockdown was performed in H295R adrenocortical cells to evaluate the effects on cortisol secretion (RIA) and reactive oxygen species (ROS) intracellular production (DCFDA) in basal conditions and after stimulation with 10 uM forskolin. MAPK8 mRNA relative expression and protein localization were evaluated using quantitative PCR (qPCR) and immunofluorescence, respectively. **Results:** NNT knockdown in the H295R adrenal cells specifically reduced NNT RNA and protein levels. Under basal conditions, no changes in ROS intracellular production or cortisol secretion were seen in NNT-depleted H295R cells. However, under forskolin (10 μM), a potent steroidogenesis agent, we observed a marked reduction in cortisol production ($p < 0.0001$) at the expense of normal ROS intracellular production and increased MAPK8 expression ($p = 0.008$). **Conclusion**: NNT-deficient adrenocortical cells can maintain mitochondrial homeostasis and cortisol secretion in basal conditions. However, under stress, these cells seem to maintain the redox balance at the expense of impaired steroidogenesis. MAPK8 pathway activation appears to compensate for NNT deficiency.

Keywords: Adrenal steroidogeneses; oxidative stress; *NNT* gene

INTRODUCTION

Cortisol production occurs partially within mitochondria, resulting in the release of reactive oxygen species (ROS). ROS must be actively eliminated to maintain homeostasis in the intramitochondrial environment. For this reason, adrenal cortex cells are supplied with high levels of enzymatic and non-enzymatic antioxidants to maintain redox homeostasis. Disturbances in the redox homeostasis in the intramitochondrial environment of adrenal cells may have a deleterious effect on steroidogenesis (1).

Received on Nov/22/2025
Accepted on Feb/25/2026
DOI: 10.20945/2359-4292-2026-0049

Correspondence to:
Sonir R. Antonini
Departamento de Pediatria,
Faculdade de Medicina de Ribeirão Preto,
Universidade de São Paulo,
Avenida Bandeirantes, 3900
14049-900 – Ribeirão Preto, SP, Brasil
antonini@fmrp.usp.br

Associated editor:
Madson Queiroz de Almeida
https://orcid.org/0000-0002-2957-6148

This is an open-access article distributed under the terms of the Creative Commons Attribution License

The maintenance of redox homeostasis, which reflects the delicate balance between ROS and antioxidant systems, plays a crucial role in hormonal regulation and cellular function. Some hormones, such as melatonin, estrogens, insulin, and glucagon, possess antioxidant properties, protecting cells from oxidative damage and modulating essential physiological processes, including development, growth, and aging. Conversely, hormones such as catecholamines, thyroid hormones, and corticosteroids can increase ROS production, contributing to oxidative stress. Alterations in hormonal balance or endocrine system function can modify redox states in vertebrates, leading to pathological conditions associated with oxidative stress (2).

Abnormal oxidative stress is related to a multitude of pathological conditions, including neurodegenerative disorders, diabetes mellitus, cardiovascular disease, aging, and changes in hormone synthesis by the adrenal glands. The effects of oxidative stress or ROS

Copyright© AE&M all rights reserved.

accumulation on steroidogenesis are partially understood. However, the mechanisms involved have not yet been determined (3,4).

The antioxidant defense system has complex and specific mechanisms for each cell type. Tissues with greater energy consumption, such as the liver, brain, and steroidogenic tissues, are supplied with high levels of enzymatic and non-enzymatic antioxidants, such as superoxide dismutase (SODs), glutathione reductase, glutathione peroxidase (GPX), and catalase. These antioxidant components are essential for the detoxification of ROS (1). The glutathione cycle detoxification system depends on nicotinamide adenine dinucleotide phosphate (NADPH), which is synthesized in the intramitochondrial environment through the enzyme Nicotinamide Nucleotide Transhydrogenase (NNT) (5).

The NNT protein is crucial for the elimination of ROS and the maintenance of cellular homeostasis. NNT requires the energy of the mitochondrial proton gradient to produce high concentrations of NADPH, which is responsible for regenerating reduced glutathione (GSH) into oxidized glutathione (GSSG), thereby maintaining a high GSH/GSSG ratio (5).

Loss-of-function mutations in the NNT gene have been described in patients with primary adrenal insufficiency, most of which are associated with the familial glucocorticoid deficiency (FGD) phenotype (6,7).

In the human adrenocortical carcinoma cell line (H295R), silencing the NNT gene through small interfering RNA (siRNA) reduced the GSH/GSSG ratio and promoted an increase in O2- concentrations. Such effects demonstrate the dysregulation of redox potential promoted by decreased NNT activity (6).

In a previous study, we developed a knockout model for NNT using H295R cells and CRISPR/Cas9 technology. In that study, we observed that NNT impairment resulted in increased ROS production, decreased mitochondrial labeling, and a decrease in the size and density of cholesterol droplets. A reduction in the secretion of cortisol and aldosterone was also observed. These data indicate that the abolition of NNT generates a state of increased oxidative stress, in addition to inhibiting steroidogenesis in affected cells (8).

In the C57BL6/J mouse lineage, which is naturally deficient in NNT, a lack of organization in the zona fasciculata of the adrenal gland is observed during embryological development. A reduction in corticosterone secretion and expression of the CYP11A1 gene, which participates in the mitochondrial stage of adrenal steroidogenesis (6,9), was also noted. Additionally, knockout mice for the NNT gene, when subjected to stress, exhibited impairment in the stimulated increase in corticosterone secretion and greater ACTH secretion compared to control animals. An increase in plasma concentrations of neurotransmitters such as norepinephrine and dopamine was also noted (10).

Decreased activity of NNT, in adrenal pheochromocytoma cells (PC12 cell line), reduced intracellular NADPH levels, reduced the GSH/GSSG ratio, and increased H2O2 levels, culminating in an increase in the oxidative state, as also observed in H295R cell line. The reduction in NNT expression in these cells also resulted in an increased expression of phosphorylated mitogen-activated protein kinase 8 (MAPK8) (11). These studies demonstrate the important role of MAPK8 and raise the question about its role in maintaining the adrenal cells' redox state and a possible crosstalk with the NNT enzyme.

In the present study, our objective was to evaluate the effects on steroidogenesis in the case of changes in antioxidant defense mechanisms. In H295R human adrenocortical tumor cells, we investigated the effects of reducing NNT expression on steroidogenesis under basal conditions and in response to induced stress. In addition, considering the established role of MAPK signaling in cellular stress responses, we investigated MAPK8 as a potential compensatory mechanism contributing to mitochondrial homeostasis and redox balance. These studies provide a better understanding of the oxidative stress affected by adrenal function.

MATERIALS AND METHODS

H295R cell culture

H295R adrenocortical carcinoma cell line (RRID: CVCL_0458) was grown in DMEM F12 Medium supplemented with 5% NuSerum, 1% penicillin/streptomycin solution, and insulin-transferrin-selenium in a humidified incubator at 37 °C in a 5% CO_2 atmosphere.

Copyright© AE&M all rights reserved.

The H295R cell line was obtained from the American Type Culture Collection (ATCC).

The medium was replaced with fresh medium containing either vehicle or test drugs such as forskolin (FSK; Merck-Aldrich) (final concentration = 10 μM) and hydrogen peroxide (H_2O_2; Merck-Aldrich) (final concentration = 1 mM). Forskolin treatment was performed for 24 h, and H_2O_2 treatment for 3 h. Cells were maintained in complete medium and were not subjected to serum starvation. All the stock solutions of the test drugs were prepared in DMSO (Merck-Aldrich) or water, respectively. Within the experiment, the total final concentration of DMSO (less than 0.1%) was maintained constant across conditions.

siRNA transfection - *NNT* silencing

The cells were seeded in 96-well culture plates, for evaluation of viability, 24 for mRNA relative expression, and immunofluorescence or 6-well culture plates for protein expression analysis. After 24 hours, the medium was replaced by antibiotic-free complete medium, and the cells were transfected with 40 nM of either small-interfering RNA (siNNT – L-009809-00-0005) or silencer negative control (NT – siNonTargeting D-001206-13-05) (SMARTpool ON-TARGET plus SiRNA, Horizon) using DharmaFECT 1 transfection reagent (Horizon). After 24 hours of incubation, the medium was replaced, and the cells were harvested after 48 hours for gene expression. Two independent experiments were performed in triplicate.

Viability

Cells (3 x 10^4 per well) were seeded in 96-well plates. After 96 h, Cell Titer 96 Aqueous One Solution (Promega) was added to each well, which was followed by incubation for 1 h. Absorbance at 490 nm was read with a microplate reader (Bio-Rad).

RNA isolation and RT-qPCR

Cells (3 x 10^5 per well) were seeded in 24-well plates. Total RNA was extracted by using the TRIzol Reagent (Thermo Scientific), and mRNA was subjected to reverse transcription from 500 ng of total RNA by using the High-Capacity cDNA Reverse 260 Transcription kit and MultiScribe enzyme (Thermo Scientific). To assess gene expression using TaqMan assays (Thermo Scientific), quantitative Real-Time PCR (qPCR) of the following genes was performed: NNT (Hs00966097_m1), *CYP11B1* (HS01596404), *CYP11A1* (HS00897320_M1), and *GUSB* (4326320E), *ACTB* (4352935) were used as an endogenous control. We performed two independent experiments in triplicate for the final analyses. For all the analyses , mRNA relative expression value was determined by the $2^{-\Delta\Delta Ct}$ method. Results were normalized to the Ct values of the endogenous controls *GUSB* and *ACTB*.

Western blot analysis

Cells (1 x 10^6 per well) were seeded in 6-well plates. Cells were lysed with the CelLytic M (Merck-Aldrich), and Protease and Phosphatase Inhibitor Cocktails (P8340 and P5726, both Merck-Aldrich) were added.

Protein concentration was measured by the Pierce™ BCA Protein Assay Kits (Thermo Scientific). Equal amounts (30 μg) of protein were subjected to SDS-PAGE, transferred to nitrocellulose membranes, blocked in TBST-T containing 5% Blotting-Grade Blocker (Bio-Rad), and probed with the aforementioned anti-NNT antibody (dilution: 1:200; RRID: AB1079495). Anti-GAPDH antibody (dilution: 1:1,000; RRID: AB_627678) was used as a loading control. Immunocomplexes were visualized with horseradish peroxidase (HRP) conjugated anti-mouse (dilution: 1:4,000, RRID: AB_631736) and anti-rabbit (dilution: 1:3000; RRID: AB_628497) antibody and developed with enhanced chemiluminescence Kit ECL Western Blotting Detection Reagents (GE Healthcare) on a ChemiDoc XRS+ System (Bio-Rad, Hercules, CA, USA). Acquired bands were analyzed using the Image Lab™ software (Bio-Rad).

Mitochondrial function analysis

A parameter of mitochondrial function was described previously (12). Intracellular reactive oxygen species (ROS) levels; 20,70-dichlorodihydrofluorescein diacetate (H2DCFDA - (Thermo Scientific) was used. Cells were incubated with 5 μM H2DCFDA at 37 °C for 30 min, washed, and analyzed by using the BD-FACS

Copyright© AE&M all rights reserved.

Canto flow cytometer (Becton Dickinson); 495-nm excitation and 527-nm emission wavelengths were used. Mean fluorescence intensities were analyzed with the BD – FACS-Diva Version 6.1.3 software (Becton Dickinson). At least 10,000 cells were analyzed.

MitoTracker Deep Red FM (Thermo Fisher Scientific), a dye that stains mitochondria in live cells, was used to measure mitochondrial intensity. Cells were incubated with MitoTracker Deep Red (250nM) or DAPI (0.5 µg/mL) at 37 °C for 30 min. The cells were fixed, and mounting medium (Thermo Fisher Scientific, MA, USA) was added. Digital images were acquired with the Confocal Microscope Leica SP5 (Leica Microsystems). The different fluorophores were excited using the 644-nm, 665-nm, 365-nm, and 405 nm wavelengths. LAS AF version 2.7.3.9723 software (Leica Microsystems) was used for acquisition. Mean fluorescence intensities were analyzed with the BD – FACS-Diva Version 6.1.3 software (Becton Dickinson) using 644-nm excitation and 665-nm emission wavelengths. Two independent experiments were carried out in triplicate.

Intracellular reactive oxygen species (ROS) levels were analyzed using the 20,70-dichlorodihydrofluorescein diacetate (H2DCFDA; Thermo Scientific). Cells were incubated with 5 µM H2DCFDA at 37 °C for 30 min and analyzed in the BD-FACS Canto flow cytometer (Becton Dickinson), using 495-nm excitation and 527-nm emission wavelengths. Mean fluorescence intensities were analyzed with the BD – FACS-Diva Version 6.1.3 software (Becton Dickinson). Two independent experiments were carried out in triplicate.

Cortisol assay

Cortisol was measured by using an in-house developed radioimmunoassay (RIA) as described previously (13).

Immunofluorescence

Cells (3 x 10^5 per well) were seeded on coverslips in 24-well plates. After 24 hours, the cells were fixed in 4% formaldehyde and blocked with 1% BSA. MAPK8 was detected using primary antibody for MAPK8 protein ((dilution: 1:200) AB18680), and Donkey anti-Rabbit IgG (H+L) Highly Cross-Adsorbed Secondary Antibody, Alexa Fluor™ 488 as secondary antibody (RRID:AB_2535792) Nuclear staining was accomplished using DAPI (dilution: 1:25000 #4083, Cell Signaling Technology), and the slides were set with ProLong™ Diamond (Thermo Fisher Scientific). Fluorescence was acquired with the Confocal Microscope Leica SP5 (Leica Microsystems). The different fluorophores were excited at 644-nm, 665-nm, 365-nm, and 405-nm.

Statistical analysis

Data are presented as the mean ± SD or the mean ± SEM. Statistical significance was determined by using a Student's t-test or one-way ANOVA followed by Tukey's. The GraphPad Prism 8.0® software was used for these analyses (GraphPad, San Diego, CA, USA), and the level of significance was set at $p \leq 0.05$.

RESULTS

Relationship between oxidative stress and cortisol production

We observed that the induction of oxidative stress, with H_2O_2, in H295R adrenal cells caused an increase in ROS production ($p < 0.0001$) (**Figure 1A**). In response, the mitochondrial activity also was increased under these conditions ($p < 0.0001$) (**Figure 1B**). This dysregulation of redox homeostasis, caused by oxidative stress, impairs cortisol secretion in adrenal cells ($p = 0.0004$) (**Figure 1C**).

We also observed the impact of steroidogenesis induction on redox homeostasis. Cortisol increase ($p < 0.0001$) (**Figure 1F**), by FSK stimulus, resulted in an increase in ROS production ($p = 0.002$) (**Figure 1D**) and mitochondrial activity ($p = 0.006$) (**Figure 1E**).

NNT knockdown in H295R adrenocortical cells

Through the application of the RNAi system commercially available, targeting regions of exons 2 to 22 in the NNT gene, we achieved NNT knockdown. Greater than 78% NNT knockdown was established in H295R cells, quantified by real-time quantitative PCR (**Figure 2A**), resulting in a mRNA expression of thereabout 22% in comparison with control H295R. A reduction in NNT protein expression was confirmed by immunoblotting (**Figure 2B**).

Copyright© AE&M all rights reserved.

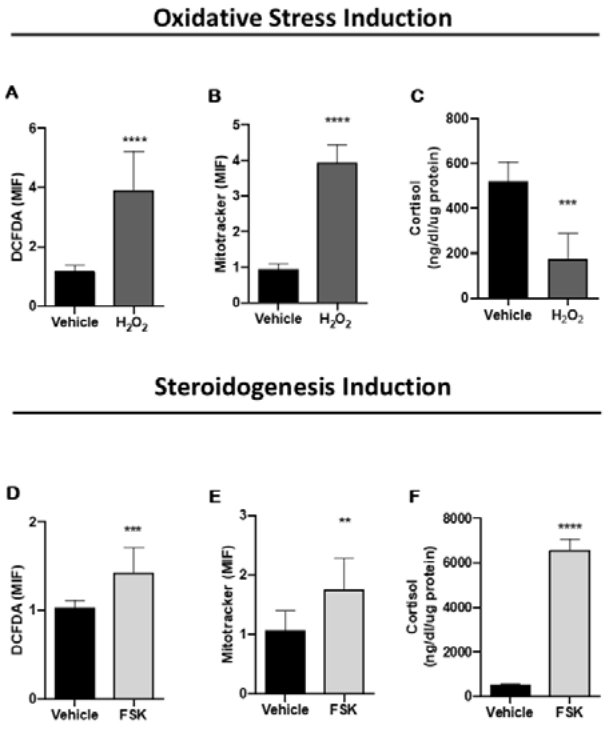


Figure 1. Relationship between oxidative stress and cortisol production. (A) Reactive oxygen species (ROS) production, quantified with 20,70-dichlorodihydrofluorescein diacetate (DCFDA, Merck-Aldrich), cells treated with hydrogen peroxide (H_2O_2) show an increase in ROS production when compared to the vehicle (n=6; p≤ 0.0001). (B) Cells labeled with Mitotracker Red show an increase in mitochondrial activity after treatment with H_2O_2 (n=6; p≤ 0.0001). (C) Reduction in cortisol production after induction of oxidative stress (n=6; p=0.0004). (D) Increase in ROS production after steroidogenesis induction with forskolin (FSK) treatment (n=6; p= 0.0002). (E) Important increase of the mitochondrial activity in H295R cells after steroidogenesis induction (n=6; p=0.006). (F) Increased cortisol production after FSK treatment (n=6; p≤ 0.0001). Data represents the mean ± SD Student´s test.

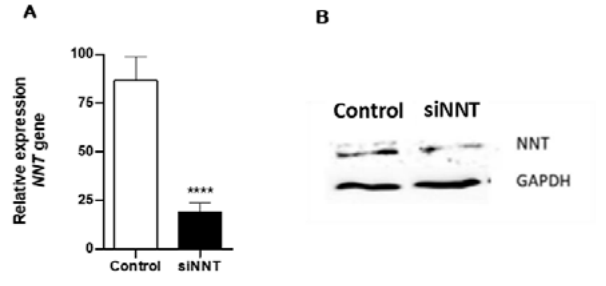


Figure 2. siRNA knock-in of the NNT gene in H295R cells. (A) NNT mRNA expression was quantified using real-time qPCR and normalized to GUSB (n=6; p≤ 0.0001). (B) Reduced expression of the protein NNT is seen in siNNT after Western blot analysis. Data represents the mean ± SD Student´s test.

The NNT knockdown in H295R enhances mitochondrial activity while maintaining redox homeostasis

The number of cells verified after 72 hours of culture, via cell titer assay, showed an increase in control H295R cell proliferation under FSK stimulus (p < 0.002). Despite that, NNT knockdown H295R cells didn't reveal an increase in proliferation (Figure 3A).

Under the same conditions, the oxidative stress profile was verified through DCFDA stain. Control cells showed an enhancement in ROS formation, under steroidogenesis induction conditions (p < 0.02). H295R NNT knockdown cells didn't reveal ROS increase under the same condition (Figure 3B).

Mitochondrial activity was evaluated with the color stain MitoTracker Deep Red FM. Control H295R cells presented a higher absorption of MitoTracker signaling for an increase in mitochondrial activity under FSK stimulus condition (p < 0.003). NNT knockdown cells have shown a greater increase in mitochondrial activity when submitted to steroidogenesis induction (p = 0.006) (Figure 3C).

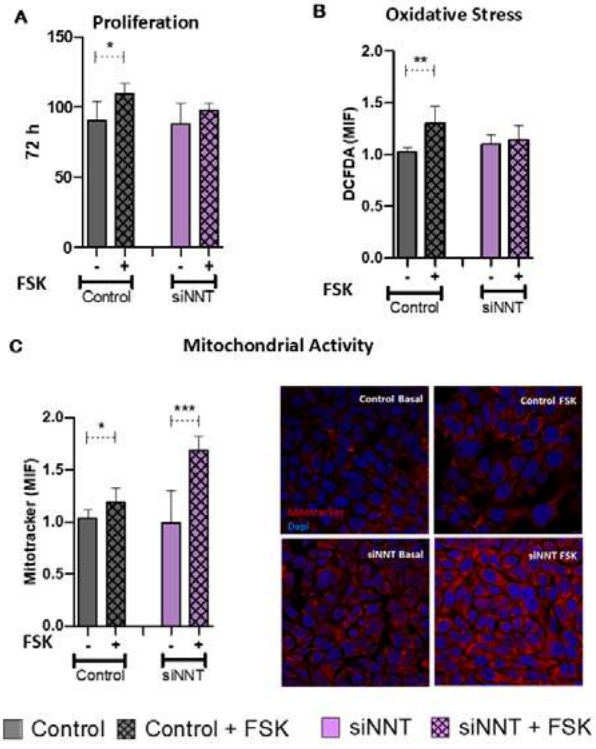


Figure 3. Evaluation of proliferation and mitochondrial function after stimulation of steroidogenesis. (A) Cell proliferation analysis indicates an increase in proliferation in control cells (n=6; p≤ 0.02). (B) ROS production, quantified with 20,70-dichlorodihydrofluorescein diacetate (DCFDA), in the control cells, who presented increased ROS production after steroidogenesis induced with forskolin (FSK) (n=6; p≤=0.02). (C) Quantitative staining with MitoTracker Red showing increased mitochondrial activity in control (n=6; p≤ 0.03) and siNNT cells (n=6; p= 0.0006). Representative image of mitochondrial activity increase in control and siNNT cells.

Copyright© ACE&M all rights reserved.

NNT knockdown in H295R affects cortisol levels without compromising key steroidogenic components

After real-time quantitative PCR, we observed that NNT knockdown didn't alter P450c11α (*CYP11A1*) or P450c11β (*CYP11B1*) transcription pattern under plain medium or steroidogenesis stimulus conditions. The induction of steroidogenesis, through FSK treatment, showed an increase in *CYP11A1* and *CYP11B1* mRNA expression in control ($p = 0.001$; $p < 0.0001$) and NNT knockdown ($p = 0.03$; $p = 0.0006$) H295R cells (**Figures 4A and 4B**).

FSK treatment in control H295R cells significantly increased the cortisol secretion ($p < 0.0001$). Nevertheless, NNT knockdown deeply impaired the cortisol secretion in H295R cells under steroidogenic challenge (**Figure 4C**).

NNT knockdown in H295R alters MAPK8 expression

NNT knockdown increases *MAPK8* relative gene expression, when compared with control cells, under basal ($p = 0.008$) and steroidogenesis stimulus ($p = 0.03$) (**Figures 5B and 5C**). We also observed MAPK8 protein expression via immunofluorescence. The green fluorescence is intensified in H295R NNT knockdown cells (**Figure 5**).

DISCUSSION

Changes in antioxidant defense mechanisms can lead to the accumulation of ROS. Disruption of the balance of these species leads to a process known as oxidative stress, which can compromise cellular functions and result in damage and death (14).

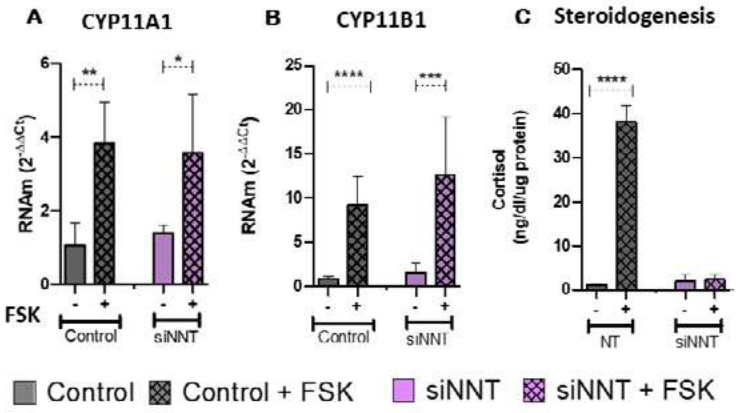


Figure 4. Evaluation of adrenal steroidogenesis. (**A**) Control cells and cells with reduced NNT show increased expression of the CYP11A1 gene (n=6; p=0.001 and p=0.03). (**B**) Control cells and cells with reduced NNT show increased expression of the CYP11B1 gene (n=6; p≤ 0.0001 and p=0.0006). (**C**) Control cells show an increase in cortisol production after stimulation with forskolin (FSK) (n=6; p≤ 0.0001).

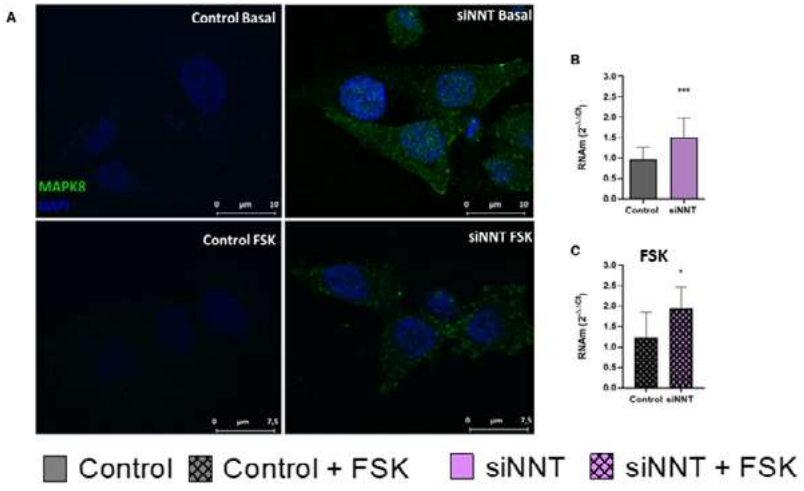


Figure 5. NNT knockdown alters MAPK8 expression. (**A**) Representative figure of MAPK8 protein expression, through immunofluorescence. (**B**) NNT knockdown increases MAPK8 relative gene expression under regular condition (n=6; p=0.008) (**C**) and steroidogenesis stimulus with forskolin (FSK) (n=6; p=0.03).

Copyright© ACE&M all rights reserved.

Steroidogenesis significantly contributes to mitochondrial ROS production. These species are generated in the process of electron transfers by the P450 system. To prevent the formation of oxidative stress, steroidogenic tissues are supplied with high levels of enzymatic and non-enzymatic antioxidants. Changes in antioxidant defense mechanisms may compromise steroidogenesis (15).

Studies of oxidative stress induction, on steroidogenic Leydig cell line (MA-10) have shown inhibition in progesterone production (3,16). In accordance with the literature, we observed that adrenal cells challenged by hydrogen peroxide stimulus showed an increase in ROS production as well as in mitochondrial activity. The creation of a stressor environment triggered an important decrease in cortisol production, resulting in a compromise of steroidogenesis in this cell line. The oxidative stress impact on steroidogenesis, in adrenal cells, goes both ways. Our data showed that the increase on steroidogenesis via forskolin stimulus leads to an increase in mitochondrial activity and ROS production in response to the stressor challenge.

NNT protein plays a massive role in ROS elimination and the maintenance of cellular homeostasis. Its primary function is to maintain high concentrations of NADPH in the intramitochondrial environment, responsible for GSH to GSSG regeneration and increasing the GSH/GSSG ratio during the ROS degradation process (6).

Although the importance of NNT protein in adrenal steroidogenesis has been widely known (6,10), there is still a lack of knowledge to be enlightened here. This study analyzed the in vitro adrenocortical cell line H295R to evaluate the impact of NNT knockdown on adrenal steroidogenesis, ROS production, and mitochondrial activity.

Through silencing with siRNA, our experiments were able to transiently reduce the expression of the NNT protein in the H295R cell line. Under these conditions, the cells were able to maintain the normal functioning of antioxidant defense mechanisms, as we can observe in the analysis of ROS formation and mitochondrial function.

Studies of chronic reduction in NNT expression, made with CRISPR-Cas9 or Short hairpin permanent depletion of expression models, showed impairment in mitochondrial functions leading to oxidative stress (8,9). In contrast, our work evaluated the acute effects of NNT knockdown induced by iRNA, which results in a transient reduction in expression. Thus, the impairment of mitochondrial function appears to be related to the duration of exposure to this stressful situation. Furthermore, the introduction of a new stressor, induced by FSK to stimulate steroidogenesis, showed that cells deficient in NNT must increase mitochondrial demand to maintain cellular homeostasis.

As expected, we found that FSK in control cells stimulates steroidogenesis, resulting in increased cortisol secretion and expression of CYP11A1 and CYP11B1 genes. When evaluating the response to this stimulus in cells with NNT knockdown, we noticed a distinct response. Although the expression of the CYP11A1 and CYP11B1 genes is maintained, they do not result in increased cortisol secretion. This observation indicates that damage to the NNT protein impacts cortisol secretion. These data show that, faced with a partial and temporary decrease in the function of the NNT protein, cells activate a predilection mechanism, blocking steroidogenesis to moderate the increase in ROS and maintain cellular homeostasis.

Oxidative stress stimulates the activation of several intracellular pathways, including the stress-activated protein kinase signaling pathway, c-Jun-N-terminal (SAP/JNK). In this pathway, two dual-specificity kinases, MAP2K4 and MAP2K7, phosphorylate and activate the MAPK8 protein. MAPK8 promotes cell apoptosis, decreased gap junctions (GAP) between cells, fibrosis, increased expression of genes for hypertrophy, and mitochondrial dysfunction. During this process, there is an increase in the activation of the MAPK8 protein located in the cytosol and its translocation to the inner mitochondrial membrane, which suggests an interconnection between the cytosol and mitochondria for the maintenance of redox balance (11,17).

In a study using adrenal pheochromocytoma cells from PC12 rats, silenced NNT gene promoted a reduction in intracellular NADPH levels, the GSH/GSSG ratio, and an increase in H_2O_2 levels, culminating in an increase in the oxidative state. The reduction of

Copyright© AE&M all rights reserved.

NNT expression in these cells also resulted in an increase in the expression of phosphorylated MAPK8 (11). This fact was also observed in the present study; as we reduced NNT expression in H295R cell line, an increase in gene and protein expression of MAPK8 was observed. In our study, the cells did not show dysregulation in redox balance, which suggests that the activation of the MAPK8 pathway may be serving as a compensatory pathway in these cells, allowing them to maintain redox balance at the expense of cortisol secretion.

Several studies using animal models have demonstrated the relationship between oxidative stress, autophagy, and multiple signaling pathways in maintaining cellular homeostasis. ROS generation has been associated with the activation of MAPK pathways, which can influence mitochondrial integrity, as well as the PI3K/AKT/mTOR signaling cascade, which regulates autophagy and cell survival. These findings support our observations, in which oxidative stress induced by NNT deficiency may trigger compensatory activation of MAPK8, helping to preserve mitochondrial homeostasis and partially sustain steroidogenic function. Overall, these results reinforce the idea that redox imbalance engages multiple signaling pathways to maintain cell survival and function, and they highlight potential targets for future investigation (18,19).

These findings regarding the impairment of steroidogenesis with the protein knockdown of NNT are consistent with what is observed in the clinic in patients with adrenal insufficiency. In recent years, mutations in the NNT gene have been associated with type 4 glucocorticoid deficiency with or without mineralocorticoid deficiency phenotype (6,8,20,21).

The relationship between NNT and oxidative stress is well established in the literature; however, our study provides important contributions by demonstrating how stress conditions can further compromise adrenal redox homeostasis and reveal compensatory mechanisms, such as MAPK8 activation, that help partially preserve mitochondrial and steroidogenic function. Despite the new insights provided by this study, some limitations should be acknowledged. Notably, the reduction of NNT was partial, which may not fully reproduce complete enzyme deficiency. Furthermore, the analysis was restricted to total MAPK8 protein expression, without evaluating its phosphorylated or activated forms, limiting conclusions regarding MAPK8 functional regulation and compensatory mechanisms. Future investigations could address these gaps by including analyses of MAPK8 phosphorylation, direct assessment of the activity of tricarboxylic acid (TCA) cycle enzymes, or evaluation of mitochondrial complex subunit expression, which could offer a broader view of cellular energy metabolism. These observations highlight important directions for future research and reinforce the relevance of this study in elucidating the role of NNT and compensatory mechanisms in adrenal redox homeostasis and steroidogenesis.

The NNT protein is localized to the inner mitochondrial membrane and plays a crucial role in maintaining cellular redox balance. Under physiological conditions, ATP production by the mitochondrial respiratory chain partially reduces molecular oxygen, generating reactive oxygen species (ROS). In adrenal cells, steroidogenesis further contributes to mitochondrial ROS production, particularly during the conversion of pregnenolone to 11-deoxycortisol, thereby increasing the oxidative burden within the mitochondrial matrix. In this context, NNT is essential for preserving mitochondrial function and cellular homeostasis by sustaining NADPH availability. In NNT-deficient cells, ROS generated by both oxidative phosphorylation and steroidogenic activity accumulate over time due to impaired NADPH production. Consequently, steroidogenesis is attenuated, likely as a compensatory mechanism to limit oxidative stress and prioritize ATP generation through mitochondrial respiration (**Figure 6**) (1,14).

The genotype–phenotype relationship in NNT deficiency remains poorly defined, reflecting the marked clinical heterogeneity observed in affected individuals. Although initially described as a cause of familial isolated glucocorticoid deficiency, clinical evidence has shown that patients harboring pathogenic variants in NNT may present a broader spectrum of adrenal impairment, including mineralocorticoid deficiency. In addition, in recent years, alterations in gonadal steroidogenesis and even disorders of sex development have been reported, indicating that multiple steroidogenic axes may be affected (22). Our experimental data

Copyright© AE&M all rights reserved.

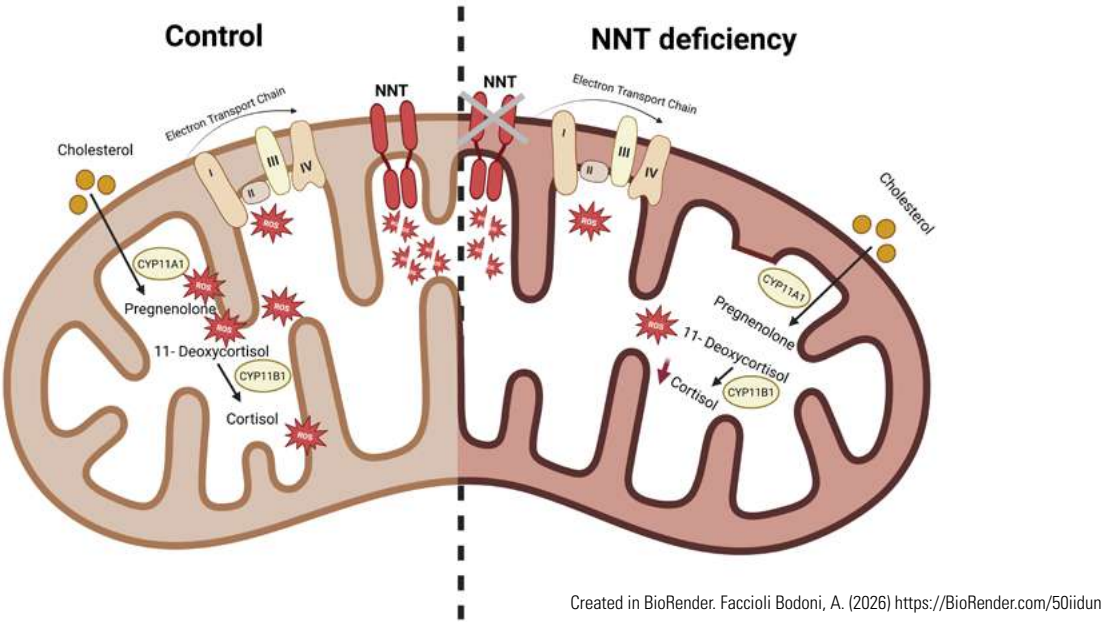


Figure 6. Representative figure of mitochondrial activity. In control cells, we observe that electron transport through the mitochondrial chain and the release of ROS during steroidogenesis are depleted via the NNT intermediate. In NNT deficiency, our data suggest a decrease in cortisol production to maintain cellular homeostasis.

suggest a possible mechanism underlying this clinical variability by demonstrating that NNT-deficient cells can maintain steroidogenesis and cellular homeostasis for a period, with functional impairment becoming evident only after chronic exposure to NNT deficiency. This delayed phenotypic manifestation suggests the involvement of compensatory mechanisms, such as the activation of oxidative stress–responsive pathways, including MAPK8, which may transiently sustain steroidogenic function. Consistently, patients with NNT deficiency typically do not present with clinical manifestations in the first days of life, with diagnosis often established after the first year of life or at later ages, reinforcing the concept that progressive failure of these adaptive mechanisms contributes to the observed phenotypic variability (22).

In summary, NNT-deficient adrenocortical cells can maintain mitochondrial homeostasis and cortisol secretion in basal conditions. However, under stress, these cells seem to maintain the redox balance at the expense of impaired steroidogenesis. MAPK8 pathway activation appears to compensate for NNT deficiency.

Authors' contributions: Juliana Lourenço Gebenlian: conceptualization, methodology, investigation, formal analysis, writing, writing – original draft. Aline Faccioli Bodoni: methodology, investigation, formal analysis, writing – original draft. Fernanda Borchers Coeli-Lacchini: methodology, writing, writing – original draft Margaret de Castro: resources, writing, writing – original draft, Funding acquisition. Sonir Roberto R. Antonini: conceptualization, formal analysis, supervision, resources, writing, writing – original draft, funding acquisition.

Acknowledgments: we thank Jose Roberto Silva, Renata S. Pugliesi, and Wendy Turatti (Laboratory of Endocrinology-Neuroendocrinology, FMRP-USP), Prof. Dr. Vânia Luiza Deperon Bonato and Denise Brufato Ferraz (Flow Citometry Laboratory, Department of Biochemistry and Immunology, FMRP-USP), and Prof. Dr. Munira Muhammad Abdel Baqui and Elizabete Rosa Milani (Confocal Microscopy Multiuser Laboratory, FMRP-USP) for their competent technical support.

Funding: this work was funded by the Coordination for the Improvement of Higher Education Personnel (CAPES) (JLG), and by the Sao Paulo State Research Foundation (FAPESP) grant 14/03989-6 (SRA). SRA also received support from CNPq-Brazil and FAEPA-HCFMRP-USP.

Disclosure: no potential conflict of interest relevant to this article was reported.

Data availability: datasets related to this article will be available upon request to the corresponding author.

REFERENCES

1. Prasad R, Kowalczyk JC, Meimaridou E, Storr HL, Metherell LA. Oxidative stress and adrenocortical insufficiency. J Endocrinol. 2014 Jun;221(3):R63-73. doi: 10.1530/JOE-13-0346.
2. Sahoo DK, Chainy GBN. Hormone-linked redox status and its modulation by antioxidants. Vitam Horm. 2023;121:197-246. doi: 10.1016/bs.vh.2022.10.007.
3. Diemer T, Allen JA, Hales KH, Hales DB. Reactive oxygen disrupts mitochondria in MA-10 tumor Leydig cells and inhibits steroidogenic

Copyright© AE&M all rights reserved.

acute regulatory (StAR) protein and steroidogenesis. Endocrinology. 2003 Jul;144(7):2882-91. doi: 10.1210/en.2002-0090.

4. Patani A, Balram D, Yadav VK, Lian KY, Patel A, Sahoo DK. Harnessing the power of nutritional antioxidants against adrenal hormone imbalance-associated oxidative stress. Front Endocrinol (Lausanne). 2023 Nov 30;14:1271521. doi: 10.3389/fendo.2023.1271521.
5. Haddad JJ. Oxygen sensing and oxidant/redox-related pathways. Biochem Biophys Res Commun. 2004 Apr 16;316(4):969-77. doi: 10.1016/j.bbrc.2004.02.162.
6. Meimaridou E, Kowalczyk J, Guasti L, Hughes CR, Wagner F, Frommolt P, et al. Mutations in NNT encoding nicotinamide nucleotide transhydrogenase cause familial glucocorticoid deficiency. Nat Genet. 2012 May 27;44(7):740-2. doi: 10.1038/ng.2299.
7. Francisco A, Goler AMY, Navarro CDC, Onder A, Yildiz M, Kendir Demirkol Y, et al. Lack of NAD(P)+ transhydrogenase activity in patients with primary adrenal insufficiency due to NNT variants. Eur J Endocrinol. 2024 Feb 1;190(2):130-138. doi: 10.1093/ejendo/lvae011.
8. Bodoni AF, Coeli-Lacchini FB, Gebenlian JL, Sobral LM, Garcia CB, Silva WA, et al. Nicotinamide Nucleotide Transhydrogenase Is Essential for Adrenal Steroidogenesis: Clinical and In Vitro Lessons. J Clin Endocrinol Metab. 2023 May 17;108(6):1464-1474. doi: 10.1210/clinem/dgac705.
9. Chortis V, Taylor AE, Doig CL, Walsh MD, Meimaridou E, Jenkinson C, et al. Nicotinamide Nucleotide Transhydrogenase as a Novel Treatment Target in Adrenocortical Carcinoma. Endocrinology. 2018 Aug 1;159(8):2836-2849. doi: 10.1210/en.2018-00014.
10. Picard M, McManus MJ, Gray JD, Nasca C, Moffat C, Kopinski PK, et al. Mitochondrial functions modulate neuroendocrine, metabolic, inflammatory, and transcriptional responses to acute psychological stress. Proc Natl Acad Sci U S A. 2015 Dec 1;112(48):E6614-23. doi: 10.1073/pnas.1515733112.
11. Yin F, Sancheti H, Cadenas E. Silencing of nicotinamide nucleotide transhydrogenase impairs cellular redox homeostasis and energy metabolism in PC12 cells. Biochim Biophys Acta. 2012 Mar;1817(3):401-9. doi: 10.1016/j.bbabio.2011.12.004.
12. Sobral LM, Coletta RD, Alberici LC, Curti C, Leopoldino AM. SET/I2PP2A overexpression induces phenotypic, molecular, and metabolic alterations in an oral keratinocyte cell line. FEBS J. 2017 Sep;284(17):2774-2785. doi: 10.1111/febs.14148.
13. Castro M, Moreira AC. Beta-lipotropin/adrenocorticotropic hormone responses to corticotropin releasing hormone, hypoglycemia, metyrapone and dexamethasone in normal human subjects. Braz J Med Biol Res. 1990;23(11):1107-15. PMID: 1966779.
14. Nelson DL, Cox MM. Princípios de bioquímica de Lehninger. Porto Alegre: Artmed; 2011.
15. Haddad JJ. Antioxidant and prooxidant mechanisms in the regulation of redox(y)-sensitive transcription factors. Cell Signal. 2002 Nov;14(11):879-97. doi: 10.1016/s0898-6568(02)00053-0.
16. Hales DB, Allen JA, Shankara T, Janus P, Buck S, Diemer T, Hales KH. Mitochondrial function in Leydig cell steroidogenesis. Ann N Y Acad Sci. 2005 Dec;1061:120-34. doi: 10.1196/annals.1336.014.
17. Zhou Q, Lam PY, Han D, Cadenas E. c-Jun N-terminal kinase regulates mitochondrial bioenergetics by modulating pyruvate dehydrogenase activity in primary cortical neurons. J Neurochem. 2008 Jan;104(2):325-35. doi: 10.1111/j.1471-4159.2007.04957.x.
18. Sahoo DK, Stewart T, Lindgreen EM, Patel B, Patel A, Trivedi JN, et al. Restorative Effects of Synbiotics on Colonic Ultrastructure and Oxidative Stress in Dogs with Chronic Enteropathy. Antioxidants (Basel). 2025 Jun 13;14(6):727. doi: 10.3390/antiox14060727.
19. Sahoo DK, Wong D, Paital B, Ruby RE, Patel A. Role of Endoplasmic Reticulum Stress-Associated Genes in Septic Neonatal Foals. Antioxidants (Basel). 2025 Aug 21;14(8):1024. doi: 10.3390/antiox14081024..
20. Francisco A, Goler AMY, Navarro CDC, Onder A, Yildiz M, Kendir Demirkol Y, et al. Lack of NAD(P)+ transhydrogenase activity in patients with primary adrenal insufficiency due to NNT variants. Eur J Endocrinol. 2024 Feb 1;190(2):130-138. doi: 10.1093/ejendo/lvae011.
21. Roucher-boulez F, Mallet-motak D, Samara-boustani D, Jilani H, Ladjouze A, Souchon P françois. NNT mutations : a cause of primary adrenal insufficiency , oxidative stress and extra- adrenal defects. 2016;73–84.
22. Roucher-Boulez F, Mallet-Motak D, Samara-Boustani D, Jilani H, Ladjouze A, Souchon PF, et al. NNT mutations: a cause of primary adrenal insufficiency, oxidative stress and extra-adrenal defects. Eur J Endocrinol. 2016 Jul;175(1):73-84. doi: 10.1530/EJE-16-0056.

Copyright© AE&M all rights reserved.

Archives of Endocrinology and Metabolism
ISSN 2359-4292
OFFICIAL JOURNAL OF THE BRAZILIAN SOCIETY OF ENDOCRINOLOGY AND METABOLISM

original

Genetic alterations of telomere maintenance pathways in paragangliomas

Lucas Batini[1]
https://orcid.org/0009-0005-3858-531X
Gustavo F. C. Fagundes[1]
https://orcid.org/0000-0003-4097-3029
Berenice B. Mendonca[2]
https://orcid.org/0000-0003-1762-1084
Eduardo C. Lobato[1]
https://orcid.org/0000-0003-1830-2587
Ana Caroline F. Afonso[2]
https://orcid.org/0009-0002-6179-0854
Ana Claudia Latronico[1]
https://orcid.org/0000-0001-6782-693X
Felipe Freitas-Castro[1]
https://orcid.org/0000-0002-5340-432X
Izabel T. Nakamura[1]
https://orcid.org/0009-0002-2474-8411
Madson Q. Almeida[1,3]
https://orcid.org/0000-0002-2957-6148
Lucas S. Santana[1]
https://orcid.org/0000-0003-0428-2386
Lucas B. Rossetti[1]
https://orcid.org/0000-0001-6993-9903

[1] Unidade de Adrenal, Laboratório de Endocrinologia Molecular e Celular LIM25, Divisão de Endocrinologia e Metabologia, Hospital das Clínicas, Faculdade de Medicina da Universidade de São Paulo, São Paulo, SP, Brasil
[2] Laboratório de Hormônios e Genética Molecular LIM42 e Laboratório de Sequenciamento em Larga Escala (SELA), Divisão de Endocrinologia e Metabologia, Hospital das Clínicas, Faculdade de Medicina da Universidade de São Paulo, São Paulo, SP, Brasil
[3] Unidade de Oncologia Endócrina, Instituto do Câncer do Estado de São Paulo (ICESP), Faculdade de Medicina da Universidade de São Paulo, São Paulo, SP, Brasil

ABSTRACT

Objective: To investigate somatic pathogenic variants (PVs) in the *TERT* promoter region and variants in the *ATRX* gene, both related to telomere maintenance in cancer, in a Brazilian cohort of adrenal and extra-adrenal paragangliomas (PPGLs), and to correlate these with metastatic disease as well as with clinical, radiological, and pathological characteristics. **Materials and methods:** The *TERT* promoter was analyzed by automated Sanger sequencing or whole-exome somatic sequencing in a cohort of 79 patients with PPGLs (53 non-metastatic and 26 metastatic), encompassing a total of 81 tumors. *ATRX* was assessed through whole-exome somatic sequencing in 26 patients from this cohort. **Results:** Germline PVs in Cluster 1A genes were identified in 28 of 79 patients (35.4%), including 20 patients harboring PVs in the *Succinate Dehydrogenase Complex Iron Sulfur Subunit B gene* (*SDHB*) (25.3%) and 8 patients (10.1%) with PVs in other Cluster 1A genes. Somatic PVs in the *TERT* promoter (c.-124C>T/C228T) were detected in two metastatic PPGLs (2.5% of the total cohort). Three PPGLs (two metastatic), among the 26 patients studied, harbored somatic *ATRX* variants classified as likely benign (11.5%). Somatic PVs in the *TERT* promoter were identified in patients with germline *SDHB* PVs. Among metastatic patients with germline *SDHB* PVs, the frequency of somatic PVs in the *TERT* promoter was 16.7%. **Conclusion:** This study expands the understanding of telomere maintenance mechanisms in PPGLs in a Brazilian cohort enriched for *SDHB* alterations. Somatic variants in the *TERT* promoter were associated with aggressive tumor features, such as extra-adrenal location, germline *SDHB* PVs, and metastatic disease.

Keywords: Adrenal paraganglioma; paraganglioma; telomerase; genetics; exome sequencing

INTRODUCTION

Adrenal and extra-adrenal paragangliomas (PPGLs) are neuroendocrine neoplasms derived from chromaffin cells of the adrenal medulla (adrenal PPGLs, formerly named pheochromocytomas) or from sympathetic and parasympathetic ganglia (PPGLs) (1,2). These tumors have marked clinical heterogeneity and a high association with hereditary syndromes, with germline pathogenic or likely pathogenic variants (PVs) detected in up to 40% of cases (3). Although most PPGLs are non-metastatic, approximately 15–20% are metastatic, as defined by the presence of metastases in non-chromaffin tissues. Metastatic PPGLs are more prevalent in patients with genetic alterations in the pseudohypoxic cluster, larger tumors (≥ 5 cm), extra-adrenal PPGLs, and those with a noradrenergic or dopaminergic biochemical profile (4,5).

The classification of PPGLs has recently changed with the 2022 WHO Classification, which designates all PPGLs as paragangliomas: adrenal and extra-adrenal PPGLs referring to the tumors traditionally known as pheochromocytomas and PPGLs, respectively (6). PPGLs are closely associated with germline

Received on Dec/26/2025
Accepted on Mar/9/2026
DOI: 10.20945/2359-4292-2026-0050

Correspondence to:
Madson Q. Almeida
Unidade de Adrenal, Laboratório de Endocrinologia Molecular e Celular LIM25
Divisão de Endocrinologia e Metabologia, Hospital das Clínicas,
Faculdade de Medicina da Universidade de São Paulo,
01246-903 – São Paulo, SP, Brasil
madson.a@hc.fm.usp.br

Editor in chief:
César Boguszewski
https://orcid.org/0000-0001-7285-7941

This is an open-access article distributed under the terms of the Creative Commons Attribution License

Copyright© AE&M all rights reserved.

PVs, present in approximately 30–40% of cases, and with somatic PVs, identified in up to 30% of tumors (7). More than 20 susceptibility genes are implicated, broadly categorized into three major molecular clusters: Cluster 1, comprising genes involved in cellular pseudohypoxia signaling, particularly the *Succinate Dehydrogenase Complex Iron Sulfur Subunit B* gene (*SDHB*); Cluster 2, involving genes related to tyrosine kinase–driven signaling pathways; and Cluster 3, involving alterations in the WNT/β-catenin pathway (7,8). At our institution, genetic testing was performed in 182 patients with PPGLs, the largest Brazilian cohort to date, revealing *SDHB* as the most frequently altered gene (16.5%), a prevalence higher than that reported in other international cohorts (7,9,10). In addition, a germline *SDHB* exon 1 deletion was responsible for approximately half of these cases, consistent with a Brazilian founder effect, as we have previously demonstrated (11). In another Brazilian cohort of 115 PPGL patients from a separate institution, 67 had a germline variant identified; the frequency of *SDHB* PVs in this group was roughly 7% (8 patients) (12).

Pathological mechanisms of telomere elongation can be activated in various cancer types. The two principal mechanisms are *telomerase reverse transcriptase* gene (*TERT*) activation and alternative lengthening of telomeres (ALT) (13). Most human cancers display some degree of *TERT* hyperactivity, which is the primary mechanism underlying replicative immortality (13,14). The predominant genetic mechanism for pathological *TERT* activation involves somatic PVs at hotspot sites in the *TERT* promoter (C228T and C250T), which lead to increased gene transcription and are associated with metastatic behavior in PPGLs (15). Additionally, the ALT mechanism has been strongly linked to somatic variants in the *ATRX chromatin remodeler* gene (*ATRX*). A previous study involving PPGL 200 patients demonstrated that the ALT phenotype correlates with *ATRX* variants and metastatic disease, highlighting *ATRX* alterations as significant prognostic markers in this tumor type (15). Interestingly, somatic PVs in the *TERT* promoter and *ATRX* are more frequently observed in *SDHB*-related PPGLs (15,16).

In a multi-omics study, *ATRX* and *TERT* alterations were also associated with metastatic PPGLs, together with high tumor mutational burden, high microsatellite instability, and Cluster 1A PVs (17). Nevertheless, genetic alterations in telomere maintenance pathways have not yet been investigated in a Brazilian PPGL cohort. Given the distinct genetic landscape of PPGLs among different ethnicities, including the high prevalence of *SDHB* PVs in our Brazilian cohort, we aimed to investigate somatic PVs in the *TERT* promoter and *ATRX* in PPGLs from Brazilian patients.

MATERIALS AND METHODS

Ethical aspects and inclusion criteria

This study was conducted in accordance with the ethical principles outlined in the Declaration of Helsinki (18). The project was approved by the Research Ethics Committee of Hospital das Clínicas da Faculdade de Medicina da Universidade de São Paulo (approval no. 5.156.162) and the Instituto do Câncer de São Paulo Octavio Frias de Oliveira (approval no. 1448/19). Written informed consent was obtained from all participants or their legal guardians.

In this study, 81 tumors from 79 patients with PPGLs were evaluated, including one case of a metastasis paired with its primary tumor and one patient with two primary tumors. Among these, 53 patients had non-metastatic PPGL, and 26 had metastatic PPGL. The biochemical and imaging diagnosis of PPGLs followed the recommendations of the Endocrine Society (1). Metastatic disease was defined as the presence of a neuroendocrine tumor in non-chromaffin tissue, confirmed by biopsy or functional imaging (^{131}I-MIBG, PET-CT with ^{68}Ga-DOTATE, or octreoscan) (6,19). Staging was performed using the TNM system for PPGLs developed by the American Joint Committee on Cancer (19). The main inclusion criterion was the availability of blood and tumor DNA for prior genetic investigation. All PPGL cases included had a confirmed histopathological diagnosis. Cases without a genetic diagnosis were defined as those lacking PVs in genes previously associated with PPGL pathogenesis, according to the criteria of the American College of Medical Genetics and Genomics (ACMG) and the Association for Molecular Pathology (AMP) (20).

Copyright© ABE&M all rights reserved.

Study cohort and sample collection

The cohort of 79 PPGL patients had previously undergone Sanger sequencing, targeted gene panel sequencing, and/or whole-exome sequencing (WES) (10). Germline DNA was extracted from peripheral blood using the salting-out method. Tumor tissue samples obtained during routine surgery were stored in liquid nitrogen prior to nucleic acid extraction, totaling 68 cases. In 13 cases where only formalin-fixed, paraffin-embedded (FFPE) tumor tissue blocks were available, blocks containing more than 90% tumor content were selected by an experienced adrenal tumor pathologist based on hematoxylin and eosin-stained slides. Two 20 µm sections were obtained from each selected FFPE block for DNA extraction.

DNA extraction and quality assessments

DNA was extracted from fresh tissue samples using the AllPrep DNA/RNA/miRNA Mini Kit (Qiagen, Germany). DNA from FFPE tissues was extracted using the QIAamp DNA FFPE Advanced kit (Qiagen, Hilden, Germany). For FFPE samples, a protocol optimized for next-generation sequencing was employed, treating DNA with uracil-N-glycosylase to minimize artifactual nucleotide changes due to cytosine deamination. The quality and concentration of extracted DNA were assessed using a NanoDrop spectrophotometer.

PCR Amplification and Sanger sequencing of the *TERT* promoter

The *TERT* promoter region (chr5: 1295151-1295313) was amplified with previously described oligonucleotides (15) (Primer F: GTCCTGCCCCTTCACCTT; Primer R: CAGCGCTGCCTGAAACTC), generating a 163 bp amplified fragment for sequencing. PCR reactions were performed using 10–15 pmol/µL of each oligonucleotide and 200 µM deoxynucleotide triphosphate in a final volume of 25 µL. The PCR protocol consisted of 35 cycles with an annealing temperature of 59 °C (15).

TERT promoter was performed with the KAPA HiFi Hot Start ReadyMix kit (Kapa Biosystems). The concentration of cDNA or DNA in the PCR products was estimated by comparison to molecular weight markers of known concentrations (ΦX) on agarose gel. The resulting amplicons underwent enzymatic purification using ExoSap-it (Life Technologies, Carlsbad, CA, USA), incubated at 37 °C for 15 min, followed by enzyme inactivation at 80 °C for 15 min.

Sequencing reactions were performed using the ABI PrismTMBigDyeTerminator kit (Applied Biosystems, USA), with 10–100 ng of PCR product, adjusted according to fragment size. Sequencing was performed on an ABI Prism Genetic Analyzer 3130xl (Applied Biosystems, USA). Electropherograms were read using the Sequencher v. 4.10.1 software (GeneCodes Corporation, USA), always in comparison with the reference gene sequence and an electropherogram from a normal individual.

Whole-exome sequencing and bioinformatics analysis

In addition to Sanger sequencing, analysis of the *TERT* promoter region and *ATRX* somatic variants was performed in 26 samples previously investigated by WES (10). The WES was conducted using the DNA nanoball sequencing platform (DNBSEQ, BGI Genomics Europe, Denmark) after somatic exome enrichment with KAPA HyperExome Probes (USA), ensuring high-quality sequencing characterized by a low duplicate rate and deep coverage. Raw FASTQ files were demultiplexed and processed through a pre-mapping pipeline to assess integrity and quality and to clean sequencing artifacts and barcodes. Grommer1 was used to verify FASTQ file integrity (ASCII encoding offset, Phred score calculation, read pair identification, etc.) while FastQC assessed sequencing quality (number of reads, read length distribution, read quality, etc.). Sequence filtering and trimming were performed using BBDuk (BBTools package). Processed FASTQ files were submitted to a reference-based (GRCh37/hg19) mapping approach using BWA-MEM alignment algorithm, and duplicate reads were marked or removed using Picard2. Mapping quality and coverage of target regions were assessed with Qualimap3 (Qiagen, Germany) (10). Across the 26 DNA samples, ≥89.56% (mean: 95.17%) of the reference achieved a minimum depth of 20× coverage.

Variant identification and validation

The *TERT* promoter region (chr5: 1295151–1295313) was manually inspected for hotspot variants using

Copyright© AE&M all rights reserved.

the Integrative Genomics Viewer software (21). The two main *TERT* hotspots, chr5: 1295228 and chr5: 1295250, had mean coverage depths of 111.17× and 96.88×, respectively. *TERT* promoter variants selected for further analysis had coverage >20×, allelic balance >10%, no significant strand bias, and adequate base and mapping quality. Visualization filters were applied to ensure that detected variants were not artificial due to strand bias or poor read quality. All WES-identified *TERT* promoter variants were confirmed by Sanger sequencing. *ATRX* single nucleotide variants and copy number variants were analyzed using the Franklin platform (Qiagen, Germany). Variants were included if they showed at least 20× coverage, allelic balance >10%, and were located within the available WES coverage region.

Statistical analysis

Descriptive statistics were reported as absolute and relative frequencies for qualitative variables and as means with standard deviations or medians with interquartile ranges, for quantitative variables. Quantitative variables were compared between two groups using the t-test if the assumption of normality was met, otherwise, the Mann-Whitney U test was applied. Normality was assessed with the Shapiro-Wilk test and equality of variances with the Brown-Forsythe test. Categorical variables were compared using Pearson's chi-square test or Fisher's exact test, as appropriate. Statistical analyses were performed using the JASP software v. 19.0 (University of Amsterdam, Netherlands). All hypothesis tests were two-tailed, with a significance level set at 0.05.

RESULTS

Cohort characteristics

In the cohort of 79 patients, the median age at diagnosis was 33 years (range: 10–72 years). The cohort comprised 50 females (63.3%). Adrenal PPGL was diagnosed in 45 patients, whereas 28 patients developed extra-adrenal PPGL. Multiple PPGLs were observed in 23 patients (29.1%). Metastases were diagnosed in 26 patients (32.9%). TNM staging distribution was: 18 patients at stage I (22.7%), 27 at stage II (34.2%), 12 at stage III (15.2%), and 15 at stage IV (19.0%). TNM staging could not be assessed in seven patients. The mean maximum tumor diameter by imaging measured 5.9 cm for adrenal PPGLs and 6.2 cm for extra-adrenal PPGLs (**Table 1**).

Table 1. Clinical, biochemical, and evolutive characteristics of patients with adrenal paragangliomas and paragangliomas who underwent genetic testing

Patients	n = 79
Age at diagnosis (years)[a]	33 (10–72)
Female sex, n (%)	50 (63.3)
Adrenal paragangliomas, n (%)	45 (57.0)
Bilateral	13 (28.9)
Paragangliomas, n (%)	28 (35.4)
Abdominal	22 (64.7)
Thoracic	1 (3.0)
Genitourinary	1 (3.0)
Head and neck	6 (17.6)
Multiple paragangliomas[b]	23 (29.1)
Hormone profile, n (%)	
Non-functioning	10 (12.7)
Adrenergic	3 (3.8)
Noradrenergic	28 (35.4)
Mixed	16 (20.2)
Unknown	15 (17.8)
Unavailable	8 (10.1)
Largest diameter at imaging (cm)[c]	
Adrenal paraganglioma	5.9 ± 3.1
Paraganglioma	6.2 ± 3.0
Metastatic patient, n (%)	26 (32.9)
TNM staging, n (%)	
1	18 (22.7)
2	27 (34.2)
3	12 (15.2)
4	15 (19.0)
Unavailable	7 (8.9)

[a]Median (range).
[b]Bilateral adrenal paraganglioma or adrenal paraganglioma with paraganglioma or multiple paragangliomas.
[c]Mean ± standard error.

Genetic findings

Germline PVs in Cluster 1A genes were identified in 28 patients (35.4%), including 20 harboring *SDHB* PVs (25.3%) and 8 (10.1%) harboring PVs in other Cluster 1A genes (including additional *SDHx* genes, *FH*, *SLC25A11*, and *DSLT*). PVs in Cluster 1B genes (*VHL* and *EPAS1*) were identified in 7 patients (8.9%), and PVs in Cluster 2 genes (e.g., *NF1*, *MAX*, *RET*, *HRAS*,

Copyright© AE&M all rights reserved.

and *TMEM127*) were identified in 27 patients (34.2%). Seventeen patients (21.5%) had negative genetic testing. The distributions, as well as the percentage of metastatic cases within each cluster, are presented in **Figure 1.**

The somatic *TERT* promoter PV C228T was detected in two PPGLs, representing 2.5% of total cases in the cohort. Both patients harbored germline *SDHB* PVs and had metastatic behavior. *TERT* promoter PVs were detected by automated Sanger sequencing and somatic exome analysis (**Figure 2**). The somatic *TERT* promoter PV C250T was not identified in any patient.

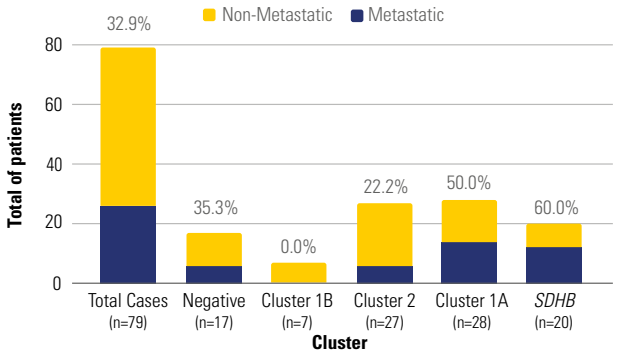


Figure 1. Total of patients and proportion of metastatic tumors by genetic cluster. Note the higher proportion of metastases in patients in Cluster 1A, especially those with *SDHB* pathogenic variants.

The *ATRX* gene was evaluated by WES in 26 PPGLs, 21 of which belonged to Cluster 1A. *ATRX* variants were identified in three tumors (11.5%), all classified as likely benign (LB). The corresponding cases are briefly reported below, although these variants are not likely related to pathogenic alterations in telomere maintenance pathways. Notably, in a case in which both the primary tumor and the corresponding metastatic lesion were simultaneously analyzed, no variants were identified in either the *TERT* promoter or *ATRX*.

Clinical, biochemical, and radiological characteristics

Clinical, biochemical, and radiological characteristics of tumors harboring genetic alterations in the *TERT* promoter or *ATRX* are described below and summarized in **Table 2**. The first patient whose tumor harbored a C228T PV in *TERT* (*TERT:c.-124C>T*) was a male with a germline *SDHB* PV (*SDHB*:c.591delC; p.Ser198Alafs*22), a frameshift variant resulting in a truncated protein. At age 18, he presented with resistant hypertension despite clinical management. Although he exhibited symptoms and an abdominal mass identified by ultrasound at that time, definitive diagnosis and treatment were only established at age 33.

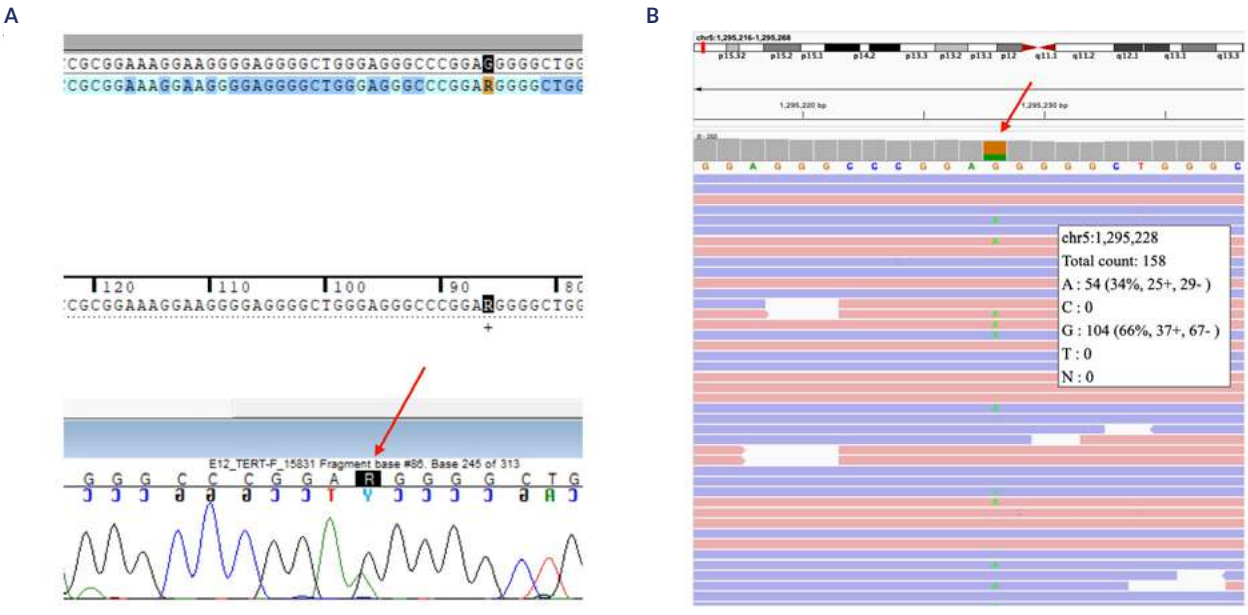


Figure 2. Identification of the somatic *TERT* promoter variant. (**A**) Sanger sequencing chromatogram of the *TERT* promoter region in a somatic PPGL sample displaying the c.-124C>T variant detected in DNA as G>A (arrow). (**B**) Integrative Genomics Viewer visualization of aligned Whole Exome Sequencing data from the same tumor. The variant (chr5:1,295,228 G>A) is present at a 34% variant allele frequency with a total read depth of 158× (arrow). Reads are color-coded by strand to demonstrate a balanced distribution, supporting the technical reliability of the call and the absence of strand bias.

Copyright© AE&M all rights reserved.

Table 2. Clinical, histopathological, and genetic characteristics of tumors with somatic findings in *TERT* promoter or *ATRX*

Germline driver	Somatic variant	ACMG	Hormone profile	Age at diagnosis (years)	Local	Size (cm)[a]	Metastasis
SDHB (C.591delC / p.Ser198Alafs*22)	*TERT:c.-124C>T*	P	NE	33	PGL Abd	13.5	Yes
SDHB (c.293G>A/ p.Cys98Tyr)	*TERT:c.-124C>T*	P	NE	57	PGL GU	8	Yes
SDHB (c.exon 1 del / p.?)	*ATRX:* c.20+22T>C	LB	NF	25	PGL HN	Unknown	Yes
SDHB (c.688C>T / p.Arg230Cys)	*ATRX:* c.1633C>G	LB	NE	29	PGL Abd	14.7	Yes
Unknown	*ATRX:* c.-88C>T	LB	NE	34	Ad	9.5	No

SDHB: succinate dehydrogenase complex iron sulfur subunit B; FH: fumarate hydratase gene; P: pathogenic; VUS: variant of uncertain significance; LB: likely benign; NE: norepinephrine; NF: non-functioning; Abd: abdominal; GU: genitourinary; HN: head/neck; Ad: adrenal paraganglioma; PGL, paraganglioma; ACMG: American College of Medical Genetics and Genomics Classification.

[a]The largest diameter at imaging.

He was diagnosed with an abdominal PPGL exhibiting a noradrenergic secretion profile, consistent with the clinical symptoms he manifested. Surgical resection revealed a 13.5 cm PPGL, staged as T3NxM0 (stage III), with a Pheochromocytoma of the Adrenal Gland Scaled Score (PASS) of 2. The patient remains under follow-up and treatment.

The second patient, who harbored the same *TERT* PV, was a male with a germline *SDHB* PV (*SDHB*:c.293G>A; p.Cys98Tyr), a missense variant with strong familial segregation, as several relatives with the same PV had also been diagnosed with PPGLs. His tumor was an 8 cm bladder PPGL, characterized by paroxysmal hypertension triggered by bladder distension, and a noradrenergic secretion profile consistent with his clinical history and symptoms. He had been followed by the cardiology service for nearly 12 years due to heart failure with reduced ejection fraction before being diagnosed with PPGL at age 57. At diagnosis and treatment, the tumor was staged as T2NxM1a (stage IV) with bone metastases and a PASS score of 5. Two months later, he was hospitalized for an ischemic stroke and died shortly thereafter. Notably, both the *TERT* somatic PV and *SDHB* germline PV co-occurred with a heterozygous germline *TP53* PV (*TP53*:c.1010G>A; p.Arg337His), which may have contributed to the aggressive phenotype and poor prognosis.

Somatic *ATRX* variants were identified in three tumors, all classified as LB. The first patient, diagnosed at age 25 with a nonfunctioning cervical PPGL, subsequently developed bone and lung metastases and was staged as T2NxM1c (stage IV). Genetic analysis revealed a germline *SDHB* PV (exon 1 deletion; seq[GRCh37/hg19] 1p36.13(17375250_17390928) x1) and a somatic LB *ATRX* variant (*ATRX*:c.20+22T>C).

The second patient was a male who presented with a 14.7 cm abdominal PPGL with a noradrenergic secretion profile and distant metastases to bone and lymph nodes. He was staged as T2N1M1a (stage IV) and remains under follow-up with the endocrinology service. Genetic testing identified a germline *SDHB* PV (*SDHB*:c.688C>T; p.Arg230Cys) and a somatic LB *ATRX* variant (*ATRX*:c.1633C>G).

The third patient had a 9.5 cm left adrenal PPGL with a noradrenergic secretion profile, diagnosed and treated at age 34. The tumor was staged as T2NxM0 (stage II), with a PASS score of 5. No germline PVs were previously detected, and the somatic *ATRX* variant was classified as LB (*ATRX*:c.-88C>T).

Correlation of genetic data with clinical and histopathological findings

A significant association was observed between the presence of PVs in Cluster 1A genes and metastases, with a higher rate of metastasis in this cluster than others (50% vs. 23.5%, respectively; $p = 0.017$) (**Figure 1**). Similarly, tumors harboring germline *SDHB* PVs showed a higher prevalence of metastatic disease than tumors without *SDHB* PVs (60% vs. 23.7%, respectively; $p = 0.003$). Among metastatic cases, somatic *TERT* promoter alterations were detected in 2 out of 26 cases (7.7%). When only considering metastatic tumors harboring germline *SDHB* PVs, *TERT* promoter alterations were observed in 2 of 12 cases (16.7%). *ATRX* variants were detected in 2 of the 13 metastatic tumors subjected to WES (15.4%), two LB variants. When restricting the analysis to metastatic

Copyright© AE&M all rights reserved.

tumors with germline *SDHB* PVs, *ATRX* variants were identified in 2 of 12 cases (16.7%).

DISCUSSION

This study presents the first systematic evaluation of genetic alterations in telomere maintenance pathways in a Brazilian cohort of PPGLs, characterized by a high prevalence of *SDHB* PVs. Consistent with previous reports, we confirmed a strong association between Cluster 1A alterations, particularly germline *SDHB* PVs, and aggressive disease features, including metastatic presentation (7,17). The high frequency of *SDHB* alterations observed in our cohort, largely driven by a recurrent exon 1 deletion, reinforces the relevance of population-specific genetic backgrounds and founder effects in shaping the molecular epidemiology of PPGLs (9–11,22).

In PPGLs, PVs in the *TERT* promoter and in *ATRX* represent key markers of pathological telomere-elongation mechanisms that promote replicative immortality (14). Telomeres are repetitive nucleoprotein structures at chromosome ends whose integrity is essential for chromosomal stability and proper regulation of cell division. Progressive telomere shortening, resulting from the incomplete replication of linear DNA molecules by DNA polymerase, is evolutionarily counteracted by telomerase, a ribonucleoprotein complex whose catalytic core adds telomeric repeats to chromosome ends (23).

Our findings further suggest that somatic alterations in the *TERT* promoter, although infrequent, occur preferentially in *SDHB*-related PPGLs and are associated with metastatic behavior. Both tumors harboring *TERT* promoter C228T variants in our cohort were PPGLs, displayed a noradrenergic biochemical phenotype, and developed metastatic disease. These observations are consistent with prior studies linking *TERT* promoter PVs to telomerase activation, replicative immortality, and poor prognosis in PPGLs and other solid tumors (15). Notably, the absence of the C250T variant in our cohort reflects its lower prevalence reported in PPGLs compared with other malignancies (24,25).

In addition to *TERT* alterations, *ATRX* variants were identified in a subset of tumors, predominantly within Cluster 1A. Most patients harboring *TERT* or *ATRX* variants had tumors larger than the cohort's mean diameter (5.9 cm for adrenal PPGLs and 6.2 cm for extra-adrenal PPGLs) and had a predominantly noradrenergic profile. These two characteristics are associated with metastatic disease, as described herein. Furthermore, these patients had worse outcomes than others in the cohort, with most developing metastatic disease (4 out of 5), further supporting the possible relationship between these variants and prognostic markers.

Although *ATRX* variants were classified as LB according to current ACMG criteria, their presence was associated with larger tumor size and a higher prevalence of metastatic disease. This observation supports previous evidence linking *ATRX* dysfunction to the ALT phenotype and tumor aggressiveness in PPGLs (15–17,26). Importantly, variant classification frameworks are largely optimized for germline variants, and their applicability to somatic alterations, particularly in genes involved in chromatin remodeling and telomere biology, remains limited. Thus, the biological impact of somatic *ATRX* variants may be underestimated when relying solely on conventional pathogenicity categories. Nevertheless, we acknowledge that further investigation (including functional studies and additional gene expression assays) is necessary to validate these specific *ATRX* variants and their possible association with the ALT phenotype.

The association between telomere-related genetic alterations and adverse clinical features was further supported by our imaging and clinical analyses. Paragangliomas harboring *TERT* promoter or *ATRX* variants exhibited larger diameters on imaging and a higher prevalence of metastatic disease compared with tumors lacking these alterations. These findings suggest that telomere maintenance dysregulation, especially through *TERT* promoter PVs, may contribute not only to metastatic potential but also to enhanced tumor growth. Although germline *SDHB* PVs represent the strongest genetic predictor of metastatic disease, approximately 50% of patients with *SDHB*-mutated PPGLs do not develop metastases (27–29). From a clinical perspective, identifying additional molecular alterations may help refine risk stratification, especially in patients with *SDHB*-related disease, for whom predicting malignant behavior remains challenging.

Copyright© AE&M all rights reserved.

A study evaluating 79 individuals with germline *SDHB* PVs, including 34 with metastatic disease, found *TERT* promoter PVs in 14 patients (41.2% of metastatic cases) (16). These findings were not replicated in a larger French cohort of 200 PPGLs, which reported a 3.5% prevalence for somatic *TERT* promoter PVs (15). Among 11 patients with both germline *SDHB* PVs and metastatic disease, 5 (41.7%) harbored *TERT* promoter variants, compared with 18% in our cohort (15). Although limited by sample size, this discrepancy warrants further investigation in larger and independent cohorts.

This study has several strengths. It represents the first dedicated analysis of telomere maintenance–related genetic alterations in a Brazilian PPGL cohort, a population with a distinct genetic background and a high prevalence of *SDHB* PVs. Comprehensive molecular characterization, combining germline testing, somatic *TERT* promoter sequencing, and WES for *ATRX*, enabled an integrated evaluation of telomere-related pathways in relation to clinical, biochemical, and radiological features. In addition, the use of standardized diagnostic criteria, centralized pathological review, and detailed phenotypic annotation strengthened the robustness of genotype–phenotype correlations. Nevertheless, some limitations must be acknowledged. The retrospective design and the relatively small number of tumors harboring *TERT* promoter or *ATRX* alterations limited statistical power and precluded multivariable analyses. Furthermore, functional validation of *ATRX* variants and direct assessment of telomere length or ALT phenotype were not performed, preventing definitive conclusions regarding causality. Lastly, although our cohort is enriched for *SDHB*-related disease, this may limit the generalizability of the findings to populations with different genetic architectures.

In conclusion, our study expands the understanding of telomere maintenance mechanisms in PPGLs within a Brazilian population enriched for *SDHB* alterations. Somatic variants in the *TERT* promoter were associated with aggressive tumor features, such as extra-adrenal location, germline *SDHB* PVs, and metastatic disease. These findings underscore the importance of integrating telomere-related genetic alterations into the molecular characterization of PPGLs and support their potential role as prognostic markers.

Funding: This work was supported by the São Paulo Research Foundation – FAPESP (grant no. 2019/15873-6 for M.Q.A.; grant no. 2025/00196-0 for E.C.L.) and FAPESP undergraduate research (grant no. 2024/16730-2 for L.B.A.). M.Q.A. also received funding from the National Council for Scientific and Technological Development – CNPq (grant no. 304091/2021-9).

Disclosure: no potential conflict of interest relevant to this article was reported.

Data availability: datasets related to this article will be available upon request to the corresponding author.

REFERENCES

1. Lenders JW, Duh QY, Eisenhofer G, Gimenez-Roqueplo AP, Grebe SK, Murad MH, et al.; Endocrine Society. Pheochromocytoma and paraganglioma: an endocrine society clinical practice guideline. J Clin Endocrinol Metab. 2014 Jun;99(6):1915-42. doi: 10.1210/jc.2014-1498.
2. Lenders JWM, Kerstens MN, Amar L, Prejbisz A, Robledo M, Taieb D, et al. Genetics, diagnosis, management and future directions of research of phaeochromocytoma and paraganglioma: a position statement and consensus of the Working Group on Endocrine Hypertension of the European Society of Hypertension. J Hypertens. 2020 Aug;38(8):1443-1456. doi: 10.1097/HJH.0000000000002438.
3. Nölting S, Bechmann N, Taieb D, Beuschlein F, Fassnacht M, Kroiss M, et al. Personalized Management of Pheochromocytoma and Paraganglioma. Endocr Rev. 2022 Mar 9;43(2):199-239. doi: 10.1210/endrev/bnab019.
4. Wachtel H, Hutchens T, Baraban E, Schwartz LE, Montone K, Baloch Z, et al. Predicting Metastatic Potential in Pheochromocytoma and Paraganglioma: A Comparison of PASS and GAPP Scoring Systems. J Clin Endocrinol Metab. 2020 Dec 1;105(12):e4661–70. doi: 10.1210/clinem/dgaa608.
5. Li M, Prodanov T, Meuter L, Kerstens MN, Bechmann N, Prejbisz A, et al. Recurrent Disease in Patients With Sporadic Pheochromocytoma and Paraganglioma. J Clin Endocrinol Metab. 2023 Jan 17;108(2):397-404. doi: 10.1210/clinem/dgac563.
6. Mete O, Asa SL, Gill AJ, Kimura N, de Krijger RR, Tischler A. Overview of the 2022 WHO Classification of Paragangliomas and Pheochromocytomas. Endocr Pathol. 2022;33(1):90-114. doi: 10.1007/s12022-022-09704-6.
7. Fishbein L, Leshchiner I, Walter V, Danilova L, Robertson AG, Johnson AR, et al.; Cancer Genome Atlas Research Network; Pacak K, Nathanson KL, Wilkerson MD. Comprehensive Molecular Characterization of Pheochromocytoma and Paraganglioma. Cancer Cell. 2017 Feb 13;31(2):181-193. doi: 10.1016/j.ccell.2017.01.001.
8. Monteagudo M, Calsina B, Salazar-Hidalgo ME, Martínez-Montes ÁM, Piñeiro-Yáñez E, Caleiras E, et al. MAML3-fusions modulate vascular and immune tumour microenvironment and confer high metastatic risk in pheochromocytoma and paraganglioma. Best Pract Res Clin Endocrinol Metab. 2024 Dec;38(6):101931. doi: 10.1016/j.beem.2024.101931.
9. Jiang J, Zhang J, Pang Y, Bechmann N, Li M, Monteagudo M, et al. Sino-European Differences in the Genetic Landscape and Clinical Presentation of Pheochromocytoma and Paraganglioma. J Clin Endocrinol Metab. 2020 Oct 1;105(10):dgaa502. doi: 10.1210/clinem/dgaa502.
10. Fagundes GFC, Freitas-Castro F, Santana LS, Ledesma FL, Petenuci J, Afonso ACF, et al. Insights into the genetic landscape of

Copyright© AE&M all rights reserved.

pheochromocytomas and paragangliomas in a Brazilian cohort. Eur J Endocrinol. 2025 Jan 6;192(1):1-14. doi: 10.1093/ejendo/lvae160.

11. Fagundes GFC, Freitas-Castro F, Santana LS, Afonso ACF, Petenuci J, Funari MFA, et al. Evidence for a Founder Effect of SDHB Exon 1 Deletion in Brazilian Patients With Paraganglioma. J Clin Endocrinol Metab. 2023 Jul 14;108(8):2105-2114. doi: 10.1210/clinem/dgad028.
12. Lima JV Jr, Scalissi NM, de Oliveira KC, Lindsey SC, Olivati C, Ferreira EN, et al. Germline genetic variants in pheochromocytoma/paraganglioma: single-center experience. Endocr Oncol. 2023 May 10;3(1):e220091. doi: 10.1530/EO-22-0091.
13. Roake CM, Artandi SE. Regulation of human telomerase in homeostasis and disease. Nat Rev Mol Cell Biol. 2020;21(7):384-397. doi:10.1038/s41580-020-0234-z.
14. Boltze C, Mundschenk J, Unger N, Schneider-Stock R, Peters B, Mawrin C, et al. Expression profile of the telomeric complex discriminates between benign and malignant pheochromocytoma. J Clin Endocrinol Metab. 2003 Sep;88(9):4280-6. doi: 10.1210/jc.2002-021299.
15. Job S, Draskovic I, Burnichon N, Buffet A, Cros J, Lépine C, et al. Telomerase Activation and ATRX Mutations Are Independent Risk Factors for Metastatic Pheochromocytoma and Paraganglioma. Clin Cancer Res. 2019 Jan 15;25(2):760-770. doi: 10.1158/1078-0432.CCR-18-0139.
16. Flynn A, Pattison AD, Balachander S, Boehm E, Bowen B, Dwight T, et al. Multi-omic analysis of SDHB-deficient pheochromocytomas and paragangliomas identifies metastasis and treatment-related molecular profiles. Nature Communications. 2025;16(1). doi:10.1038/s41467-025-57595-y.
17. Calsina B, Piñeiro-Yáñez E, Martínez-Montes ÁM, Caleiras E, Fernández-Sanromán Á, Monteagudo M, et al. Genomic and immune landscape Of metastatic pheochromocytoma and paraganglioma. Nat Commun. 2023 Feb 28;14(1):1122. doi: 10.1038/s41467-023-36769-6.
18. World Medical Association. World Medical Association Declaration of Helsinki: ethical principles for medical research involving human subjects. JAMA. 2013 Nov 27;310(20):2191-4. doi: 10.1001/jama.2013.281053.
19. Fishbein L, Del Rivero J, Else T, Howe JR, Asa SL, Cohen DL, et al. The North American Neuroendocrine Tumor Society Consensus Guidelines for Surveillance and Management of Metastatic and/or Unresectable Pheochromocytoma and Paraganglioma. Pancreas. 2021 Apr 1;50(4):469-493. doi: 10.1097/MPA.0000000000001792.
20. Richards S, Aziz N, Bale S, Bick D, Das S, Gastier-Foster J, et al.; ACMG Laboratory Quality Assurance Committee. Standards and guidelines for the interpretation of sequence variants: a joint consensus recommendation of the American College of Medical Genetics and Genomics and the Association for Molecular Pathology. Genet Med. 2015 May;17(5):405-24. doi: 10.1038/gim.2015.30.
21. Robinson JT, Thorvaldsdóttir H, Wenger AM, Zehir A, Mesirov JP. Variant Review with the Integrative Genomics Viewer. Cancer Res. 2017;77(21):e31-e34. doi: 10.1158/0008-5472.CAN-17-0337.
22. Freitas-Castro F, Almeida MQ. Personalized management for phaeochromocytomas and paragangliomas in Latin America: A genetic perspective. Best Pract Res Clin Endocrinol Metab. 2025;39(1):101922. doi: 10.1016/j.beem.2024.101922.
23. Liu M, Zhang Y, Jian Y, Gu L, Zhang D, Zhou H, et al. The regulations of telomerase reverse transcriptase (TERT) in cancer. Cell Death Dis. 2024;15(1):90. doi: 10.1038/s41419-024-06454-7.
24. Yuwanati M, Sarode S, Sarode G, Gadbail A, Gondivkar S, Chaurasia A, et al. Association of TERT promoter mutation with oral squamous cell carcinoma: a systematic review and meta-analysis. Sci Rep. 2025 Apr 30;15(1):15257. doi: 10.1038/s41598-025-98133-6.
25. Marczyk VR, Maia AL, Goemann IM. Distinct transcriptional and prognostic impacts of TERT promoter mutations C228T and C250T in papillary thyroid carcinoma. Endocr Relat Cancer. 2024;31(9). doi: 10.1530/ERC-24-0058.
26. Toledo RA, Qin Y, Cheng ZM, Gao Q, Iwata S, Silva GM, et al. Recurrent Mutations of Chromatin-Remodeling Genes and Kinase Receptors in Pheochromocytomas and Paragangliomas. Clin Cancer Res. 2016 May 1;22(9):2301-10. doi: 10.1158/1078-0432.CCR-15-1841.
27. Amar L, Baudin E, Burnichon N, Peyrard S, Silvera S, Bertherat J, et al. Succinate dehydrogenase B gene mutations predict survival in patients with malignant pheochromocytomas or paragangliomas. J Clin Endocrinol Metab. 2007 Oct;92(10):3822-8. doi: 10.1210/jc.2007-0709.
28. Hescot S, Curras-Freixes M, Deutschbein T, van Berkel A, Vezzosi D, Amar L, et al.; European Network for the Study of Adrenal Tumors (ENS@T). Prognosis of Malignant Pheochromocytoma and Paraganglioma (MAPP-Prono Study): A European Network for the Study of Adrenal Tumors Retrospective Study. J Clin Endocrinol Metab. 2019 Jun 1;104(6):2367-2374. doi: 10.1210/jc.2018-01968.
29. Petenuci J, Fagundes GFC, Benedetti AFF, Guimaraes AG, Afonso ACF, Mota FT, et al. SDHB large deletions are associated with absence of MIBG uptake in metastatic lesions of malignant paragangliomas. Endocrine. 2021 May;72(2):586-590. doi: 10.1007/s12020-020-02594-w.

Copyright© AE&M all rights reserved.

Archives of Endocrinology and Metabolism
ISSN 2359-4292
OFFICIAL JOURNAL OF THE BRAZILIAN SOCIETY OF ENDOCRINOLOGY AND METABOLISM

original

Accuracy of portable artificial intelligence-supported fundus camera in the screening of diabetic retinopathy in primary care

Daniela O. Alves[1]
https://orcid.org/0000-0002-9058-725X

Daniel Lavinsky[2]
https://orcid.org/0000-0001-7197-1259

Myriam E. B. Strzalkowski[3]
https://orcid.org/0009-0007-8647-1952

Leila B. Moreira[1]
https://orcid.org/0000-0002-4730-7988

[1] Programa de Pós-graduação, Departamento de Educação, Hospital de Clínicas de Porto Alegre, Porto Alegre, RS, Brasil
[2] Departamento de Oftalmologia, Hospital de Clínicas de Porto Alegre, Porto Alegre, RS, Brasil
[3] Escola de Enfermagem, Universidade Federal do Rio Grande do Sul, Porto Alegre, RS, Brasil

ABSTRACT

Objective: Research on the use of portable fundus cameras utilizing artificial intelligence (AI) for diabetic retinopathy (DR) screening in primary care remains limited. We aimed to evaluate the accuracy and reliability of DR screening in primary care using a smartphone-based, AI-assisted device in a small municipality in southern Brazil. **Materials and methods:** The reference standard was classification of fundus images by a retina specialist. Patients with diabetes enrolled in the Brazilian Family Health Program were recruited for the study. A general ophthalmologist obtained fundus images from 134 patients, and a retina specialist validated the DR diagnosis by AI. **Results:** The sample was predominantly female, with most patients having type 2 diabetes mellitus (T2DM). The age ranged from 17 to 81 years. Blood pressure was controlled in 34.9% of the sample. HbA1c levels ranged from 5.4% to 13.9%, and 35.3% of participants had levels below 7.0%. After excluding eight participants due to low image quality, the DR prevalence was 24.6%. The AI-based screening test for DR in primary care demonstrated a sensitivity of 100% (95% CI 88.8–100) and a specificity of 66.3% (95% CI 55.9–75.7). The negative predictive value (NPV) was 100% (95% CI 94.3–100), and the positive predictive value (PPV) was 49.2% (95% CI 36.4–62.1). **Conclusion:** The smartphone-based, AI-assisted device showed good accuracy and excellent performance for DR screening in primary care. It can avoid unnecessary medical referrals and help prioritize patients with advanced disease who require early treatment to prevent severe complications.

Keywords: Diabetes mellitus; diabetic retinopathy; artificial intelligence; screening; primary health care

INTRODUCTION

In 2021, type 2 diabetes mellitus (T2DM) accounted for 75.3 million (95% UI 63.5–90.2) global disability-adjusted life years (DALYs) (1), representing 2.6% (2.3–2.9) of total global DALYs. T2DM contributed to 95.4% of the total diabetes-related burden. Since 2010, the percentage increase in DALYs attributable to T2DM was 52.2%. The International Diabetic Federation (2) estimated that 996 billion U.S. dollars were spent on diabetes care, and that three of every four adults with diabetes live in low-income countries.

Diabetic retinopathy (DR) is one of the leading chronic complications of diabetes mellitus (DM), affecting about one-third of patients. Among them, 10% are at risk of irreversible vision loss, and some may progress to blindness (3). DR is the leading cause of vision loss among working-age adults and a threat to the quality of life for millions worldwide (3-5), mainly because it is asymptomatic in early stages. Many studies (6-8) have demonstrated that DR screening is cost-effective in preventing irreversible vision loss and morbidity. However, implementing screening programs remains challenging in large countries with unequal access to healthcare services, especially in low-income

Received on Apr/3/2025
Accepted on Jan/28/2026
DOI: 10.20945/2359-4292-2026-0051

Correspondence to:
Leila B. Moreira
lbmoreira@hcpa.edu.br (LBM)

Associated editor:
Melanie Rodacki
https://orcid.org/0000-0002-9007-1325

This is an open-access article distributed under the terms of the Creative Commons Attribution License

Copyright© AE&M all rights reserved.

regions (9). Therefore, cost-effective alternatives to in-person ophthalmologist evaluations or seven-field color fundus imaging have been explored (10). These methods include portable fundus cameras, artificial intelligence (AI), and telemedicine.

Studies have demonstrated positive results for both AI-only models and portable retinal cameras (11-14). However, research on the use of portable fundus imaging combined with AI for DR screening in primary care remains limited. In India, two studies (15,16) validated the reliability of a portable retinal camera equipped with offline AI software, operated by non-physician healthcare professionals. Our study aims to evaluate the accuracy and reliability of an AI-assisted, smartphone-based device for DR screening in primary care in a small municipality in southern Brazil.

MATERIALS AND METHODS

This cross-sectional observational study, prospectively designed, was conducted to screen for retina changes in individuals with diabetes using a smartphone-based portable retinal camera combined with AI software in a primary care center in the city of Glorinha – State of Rio Grande do Sul – in southern Brazil. The municipality has about 8,000 inhabitants and 733 patients with diabetes registered in the municipal pharmacy. It has broad coverage by the Brazilian Unified Health System (*Sistema Único de Saude* – SUS) via family health services and a large percentage of rural residents.

Patients with diabetes enrolled in the Family Health Program were recruited via various methods: direct contact during routine visits to healthcare units, active outreach by health agents and scheduled medical appointments, direct engagement during *HIPERDIA* group activities (a Ministry of Health program for patients with arterial hypertension and diabetes), and advertisements via social media platforms (Instagram and Facebook) or posters displayed in local health units. All participants received detailed information about the study and provided written informed consent. The study adhered to the principles of the Declaration of Helsinki. The Institutional Ethics and Research Committee approved the project (CAAE 67676323.0.000.5327).

We used a smartphone-based handheld device (Eyer®, Phelcom Technologies – São Carlos, Brazil) connected to EyerCloud®, a cloud storage system. Mydriasis is not mandatory when using this camera. Images were analyzed in real-time by a general ophthalmologist and by EyerMaps®, an AI software that detects retinal changes and classifies the images by displaying a color-coded indicator in the upper right corner: green (low probability of alteration), yellow (medium probability of alteration), and orange or red (high probability of alteration). If the image quality is insufficient for AI analysis, no color indicator is displayed. Fundus imaging examples are shown in the supporting file (**Figures S1-S7**). The reference standard was the analyses and classification of fundus images by a retina specialist, as patients with diabetes in primary care in Brazil are typically referred to specialists for DR screening. The AI software is a direct resource of the fundus camera and does its analysis automatically when the image is taken. It does not use any information other than the image captured to make the analysis. The fundus camera device and the AI model were developed in Brazil using local data mostly (some contribution from North America and European countries), and are approved by ANVISA, the Brazilian regulatory agency. Both were validated in the Brazilian population (14,17).

Color fundus imaging was performed by a general ophthalmologist. Fundus images obtained were registered in medical records at the health unit and informed to patients. The diagnosis and classification of DR were posteriorly made by a retina specialist, according to the International Classification of Diabetic Retinopathy criteria (18): 1 – no DR, 2 – mild non-proliferative DR (NPDR), 3 – moderate NPDR, 4 – severe NPDR, 5 – proliferative DR (PDR), 6 – post-laser treatment, 7 – inconclusive. When images were of insufficient quality for AI analysis, no color indicator appeared in the upper right corner; these cases were categorized as negative AI results for the purpose of evaluating test performance. The retina specialist was blinded to the patients' demographic and clinical data, having access only to images stored as PDF files identified by a numeric code attributed to each patient at the time of evaluation. The images in those PDF files included the AI-attributed color code. The retina specialist

Copyright© ALE&M all rights reserved.

was clearly instructed to evaluate images only for DR changes. The fundus classification was registered in a spreadsheet, and results were transcribed and verified using Research Electronic Data Capture (REDCap) (19). We followed established clinical guidelines (20) to classify patients as either "non-referral" or "referral" cases for DR: patients with no DR or mild NPDR (non-referral) were advised to continue monitoring clinical parameters in primary care with a follow-up fundus exam in 12 months, while those with moderate NPDR or more severe DR (referral) were referred to a specialist in secondary or tertiary level. Additionally, the general ophthalmologist performing the fundus imagens could identify abnormalities corresponding to DR or other conditions, as well as referring patients when necessary. We defined metabolic control as glycated hemoglobin (HbA1c) below 7.0% (21), and controlled blood pressure was defined as below 130/80 mmHg (22), according to current recommendations.

Participants were consecutively included according to the inclusion criterion, which was having a diagnosis of DM. The exclusion criterion was having any condition that prevented fundus imaging, such as lack of patient cooperation or severe media opacities. To perform the exam, 1% tropicamide could be instilled in both eyes to optimize data collection, provided there were no contraindications. While waiting for mydriasis, demographic and clinic data were obtained via interviews and health unit's records and inserted into the database. Subsequently, each patient was registered in the EyerCloud® system, and at least two images were captured — one centered on the macula and another on the optic nerve. If necessary, new images were taken to obtain two good quality images. When possible, a retina map was obtained using five or more images to include the mid-peripheral retina.

A sample size of 139 subjects was calculated to estimate the proportion of DR cases, with a 10% confidence interval width. Accounting for a 10% potential loss, the target sample size was increased to 155. The calculation (Wald method) considered a 95% confidence level and an expected DR prevalence of 10%, and was calculated using the online PSS Health tool (23).

Descriptive statistics (means and proportions) were used to characterize the sample. DR prevalence was presented as a rate with a 95% confidence interval. The association between DR and potential risk factors or outcomes was analyzed using the chi-squared test. Agreement between the retina specialist and the AI system was evaluated using Cohen's kappa coefficient. Test sensitivity, specificity, and positive and negative predictive values with a 95% confidence interval were calculated.

RESULTS

We collected data from May 17, 2023, to November 25, 2023, from 130 participants and from another 26 participants from July 05, 2025, to August 02, 2025. We excluded 4 participants as they failed to confirm a DM diagnosis in their medical records, 22 pre-DM, and one participant was excluded due to an inability to cooperate during the exam. To perform the exam, 36 patients did not receive mydriatic eye drops because they had to leave the health facility by driving a vehicle after the exam, or there was no need for mydriasis. Fifty two percent of participants evaluated had their first recommended fundus examination after being diagnosed DM. Of the 134 subjects evaluated, 126 were included in the accuracy analysis (**Figure 1**).

Table 1 shows the characteristics of the total sample (n = 134) and of the subgroup analyzed for DR presence or absence (n = 126), according to the retina specialist's interpretation. The sample was predominantly composed of women and individuals with T2DM, and most participants had not undergone a fundus examination since their diagnosis. Age ranged from 17 to 81 years, and time since diagnosis varied from less than one year to 42 years. From all sample (n = 134), 54 participants (40,1%) had a body mass index greater than 30 kg/m². Blood pressure was controlled in 34.9% of the sample. Among the 134 participants, 77 reported symptoms in the lower limbs (e.g., pain or discomfort), with the most common (55%) being fatigue, cramps, or itching. These were most frequently located in the calves and tended to be more intense at night. HbA1c values ranged from 5.4% to 13.9% (available for 116 participants), and 35.3% had HbA1c levels < 7.0 mg/dL. Participants with DR had higher systolic blood pressure, longer duration of illness, and a higher prevalence of current or previous diabetic ulcers and presumed peripheral neuropathy.

Copyright© AE&M all rights reserved.

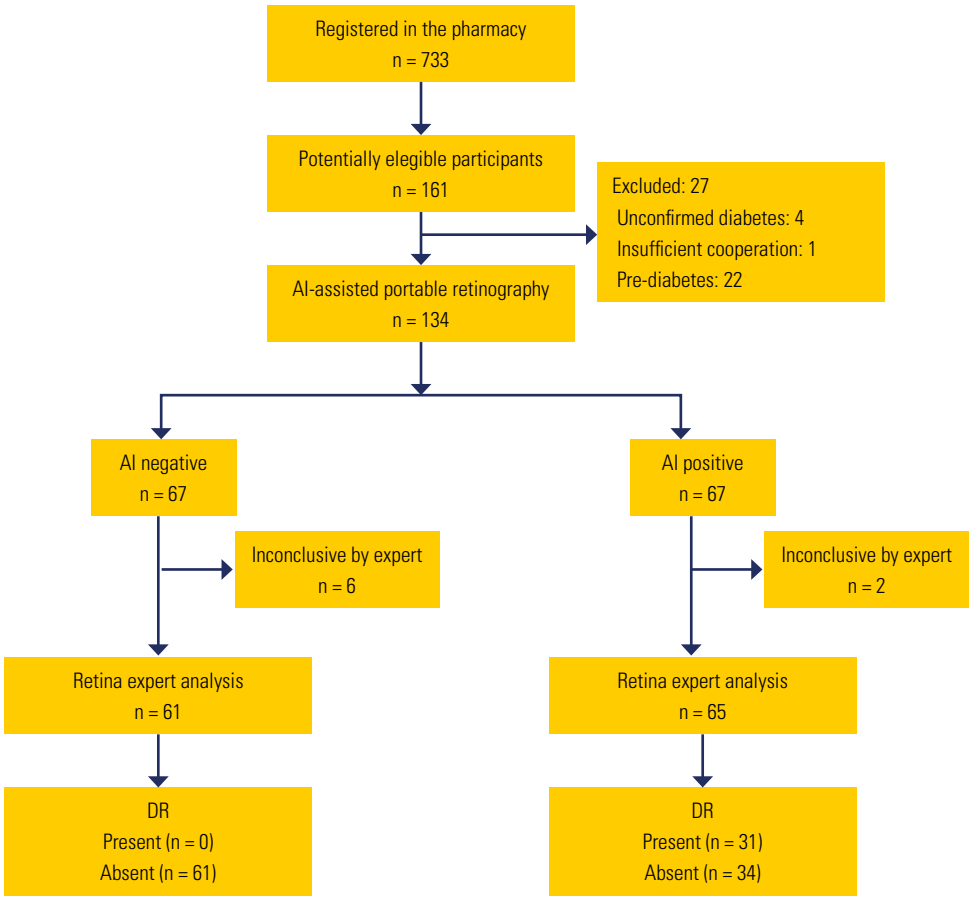


Figure 1. Study flowchart

Table 1. Demographic description and clinical characteristics in the sample by the presence of DR (average and SD or n and %)

	Sample (n = 134)	DR positive (n=31)	DR negative (n=95)	p
Female	73 (54.5)	18 (58.1)	51 (53.7)	0.67
Age, years	62.5 (±13)	61.4 (±11.1)	63.1 (±13.0)	0.51
HbA1c (%)	8.3 (±2.1)	9.1 (±2.23)	8.0 (1.9)	0.01
Systolic BP (mmHg)	131.9 (±17.1)	138.9 (±18.5)	129.7 (±16.4)	0.01
DiastolicBP (mmHg)	77.3 (±10.6)	79.5 (±12.5)	76.6 (±10.1)	0.02
BMI (kg/m^2)	29.5 (±5.2)	29.9 (±5.2)	29.0 (±4.8)	0.379
DM type				0.64*
DM1	6 (4.5)	2 (6.5)	4 (4.2)	
DM2	128 (95.5)	29 (93.5)	91 (95.8)	
Hypertension	111 (82.8)	27 (87.1)	77 (81.1)	0.44
Dyslipidemia	96 (71.6)	21 (67.7)	68 (71.6)	0.68
Previous stroke	10 (7.5)	4 (13.3)	6 (6.3)	0.25*
Previous heart attack	22 (16.5)	4 (13.3)	17 (17.9)	0.56
Hypothyroidism	32 (23.9)	4 (12.9)	27 (28.4)	0.08
Diabetic ulcer	30 (22.4)	9 (29.0)	20 (21.1)	0.36
Renal dysfunction	21 (15.7)	3 (9.7)	17 (17.9)	0.40*
NSS≥3	66 (49.3)	19 (61.3)	43 (45.3)	0.12

BMI: body mass index; NSS: Neuropathy Symptom Score; DR: diabetic retinopathy
*Fisher exact test

Copyright© AE&M all rights reserved.

The sensitivity of portable retinography with AI as a screening tool for DR in primary care was 100% (95% CI 88.8–100), while specificity was 66.3% (95% CI 55.9–75.7) (Table 2). The negative predictive value (NPV) was 100% (95% CI 94.3–100), and the positive predictive value (PPV) was 49.2% (95% CI 36.4–62.1). The agreement between AI and the retina specialist, measured by the Kappa coefficient, was 0.492 (p-value < 0.001).

Table 2. Accuracy of portable retinography using artificial intelligence (AI) versus retina specialist assessment for diagnosing diabetic retinopathy (n=126)

	Retina specialist positive	Retina specialist negative	TOTAL
AI positive	31	32	63
AI negative	0	63	63
TOTAL	31	95	126

p <0.001; kappa = 0.492.

Excluding the eight participants whose images were deemed inconclusive by the retina expert, the prevalence of DR diagnosed by the specialist was 24,6% (CI 95% 17.4-33.1). Among the 31 participants with DR, 45.2% (n = 14) had mild NPDR, 45.2% (n = 14) had moderate NPDR, 3,2% (n = 1) had PDR and 6.4% (n = 2) had undergone laser treatment. No cases of severe NPDR were identified.

An exploratory analysis excluding all three patients hose images had no sufficient quality for IA classification showed Sensitivity 100%, Specificity 63%, PPV 48%, NPV 100%.

The results of the AI-based test and the reference standard (retina specialist evaluation) are presented in Table 3. The AI algorithm indicated abnormal findings in the presence of moderate NPDR or worse, choroidal nevus, optic nerve changes suggestive of glaucoma, drusen, and other nonspecific or non-pathological alterations. Out of the 67 patients (Figure 1) AI had not indicated funduscopic changes, six were inconclusive by retina specialist and 61 showed no signs of DR by retina specialist evaluation (resulting in no false negatives). In the group of ungradable images — for both AI and specialist — cataracts were the main reason for the inability to classify the images. All patients with significant media opacity were referred to further evaluation. The researcher, however, could not classify the cataracts.

Among the 126 participants whose fundus images could be graded by the retina specialist, and according to the dichotomous classification based on clinical referral, 109 (86.5%) were classified as "non-referrable" DR — meaning they could remain under primary care follow-up, with a new exam recommended in 12 months. In contrast, 17 participants (13.5%) presented "referrable" DR, requiring evaluation and treatment at a higher level of care. In this subgroup, the EyerMaps® software did not fail to detect changes in any of the cases. In this context, the sensitivity and negative predictive value remained at 100%, while the specificity was 57.8% and the positive predictive value was 27.0%. Ten individuals were classified as "inconclusive" by the specialist, being eight negative and two positive for any alteration by AI, and were excluded from the test attributes analysis.

Table 3. Results of the artificial intelligence (AI) test by the results of the reference standard (N = 134)

Reference standard	AI + n (%)	AI - n (%)	Total
Inconclusive	2 (3.1)	6 (8.7)	8 (6.0)
No apparent DR	32(49.2)	63 (91.3)	95 (70.9)
Mild NPDR	14 (21.5)	0	14 (10.4)
Moderate NPDR	14 (21.5)	0	14 (11.2)
PRD	1(1.5)	0	1 (0.7)
Post-laser	2 (3.1)	0	2 (1.5)
Total	65 (48.5)	69 (51.5)	134

DR: diabetic retinopathy; NPDR: non-proliferative DR; PDR: proliferative DR.

Copyright© AE&M all rights reserved.

DISCUSSION

In this cross-sectional study with 126 patients with DM, we aimed to evaluate the performance of an AI-supported portable fundus camera for DR screening in primary care. According to the specialist's classification of fundus imaging, the prevalence of DR was 24.6%. The AI-supported portable fundus camera demonstrated a sensitivity of 100% and a specificity of 66.3% for DR detection. The NPV was 100%, while the PPV was 49.2%. These findings corroborate the impression already obtained by other studies that AI-assisted portable retinography is an excellent screening tool (13,14,16), as it has high specificity and high NPV. This feature means the test is effective and safe to be implemented as a screening test in primary care.

The prevalence of microvascular complications — such as any form of DR — found in the primary care diabetic patient sample is among the lowest reported in studies included in a brazilian meta-analysis (24). The summarized prevalence in the meta-analysis was 33% and prevalence ranged between studies from 5.3% to 85.7%. A study (13) aiming DR screening conducted in a Brazilian urban primary care setting with a handheld smartphone-based retinal camera recorded DR prevalence of 24.1% in a sample of 439 individuals with DM. The rate is included in the CI95% of our study. The prevalence rates vary widely across studies due to differences in study design, populations, sample characteristics, including age and DM duration. The most prevalent risk factors for DR observed in this study align with previous findings: DM duration, age over 50 years, comorbidities such as hypertension, overweight or obesity, heart attack and stroke history, and insufficient metabolic control (3,13,25).

Even in countries with established national protocols for screening DM complications, coverage remains challenging (26-28). Notably, about 50% of patients evaluated had their first recommended fundus examination after being diagnosed with DM in this study. In Brazil, most of the population is assisted by SUS (29), and according to the Ministry of Health recommendations (30), patients diagnosed with DM in primary care should be referred to an ophthalmologist for fundoscopy every 12 months. Specialists are typically available only at secondary or tertiary care levels, resulting in several months of waiting for ophthalmologist consultation. AI-supported smartphone-based portable retinography may be a solution to improve DM assistance.

AI programs have been developed and validated for ocular disease screening, including DR (11–13,15,16,31). Most algorithms are programmed to detect significant changes in DR, such as hard exudates, flame-shaped hemorrhages, and significant vascular abnormalities. Some algorithms can identify patients with DR who require referral to a retina specialist ("referrable DR"). Others can differentiate between normal fundus imaging and those showing possible pathologic changes, as well as indicate when image quality is insufficient for analysis.

In Mumbai, India, between 2018 and 2019, a study (16) involving 1,378 primary care patients evaluated the reliability of an offline AI in a smartphone-based fundus camera for community screening of DR by healthcare workers. Like us, they included rural population, although ethnically different from that of Brazil. Images were captured using the smartphone-based portable fundus camera Remidio Non-Mydriatic Fundus on Phone (Remidio Innovative Solutions Pvt. Ltd.). Patients were diagnosed as referable DR and non-referable DR by the algorithm based on characteristic DR images. Differences between algorithms may explain the higher specificity than our study. The sensitivity was 100%, with specificity close to 90%. For any DR, sensitivity was 89.13% and specificity was 94.43%, based on assessments by two blinded retina specialists. Our study showed high sensitivity to identify any abnormalities in the fundus image — not limited to DR — which explains the higher number of false positives when considering only DR. The high NPV indicates that if no abnormalities are detected, the patient is unlikely to have DR. Therefore, this AI-supported camera enables effective screening to identify patients who require additional evaluation and intervention at specialized centers. To enhance specificity in the method used in our study regarding RD, telemedicine consultation can be associated.

Furthermore, AI software is highly effective in selecting patients who can safely continue follow-up in primary care with another exam scheduled after one

Copyright© AE&M all rights reserved.

year. Consequently, AI-supported portable retinography may be a cost-effective method for DR screening in primary care. Souza and cols. (32) assessed applicability and economic viability of fundus photography-based teleophthalmology screening for DR in two referral health centers from different cities in the state of Minas Gerais-BR comparing its cost with that of an ordinary ophthalmology visit. They concluded that the method was a viable, effective, and significantly cheaper strategy for the screening of DR, with cost reduction of 28.76 US$ per patient.

A study conducted in China (33) assessed the cost-effectiveness of AI-based and ophthalmologist-led DR screening in rural populations using a Markov model for health economic assessments. From the health system perspective, compared to no screening, AI-based screening incurred an incremental cost was approximately USD 5,211.31 with an incremental utility of 0.33. Compared to AI-based screening, ophthalmologist-led screening had an incremental cost of approximately USD 2,070.19 but resulted in a negative incremental utility of -0.31. Compared to no screening, the incremental cost-effectiveness ratio (ICER) for AI-based DR screening was USD 15,595.47 per quality-adjusted life year (QALY), which is less than the ICER threshold in China of USD 30,224.03. A study (34) conducted in Ontario suggests that a portable retinal camera is a more cost-effective means of screening for DR than a retina specialist in isolated First Nations communities. It is possible that the RD screening method with portable retinography and AI will also be cost-effective for the Brazilian public health system to prevent blindness.

The AI algorithm integrated with the smartphone-based portable fundus camera used in our study can identify and grade several retinal alterations. It cannot diagnose the underlying disease or condition leading to false positive results regarding DR, but it is effective in providing proper health care for those individuals needing specialist evaluation. Due to the method's low specificity, patients with false-positive DR results will be referred to specialists for other, not necessarily pathological, changes, which may increase the demand for ophthalmological appointments. On the other hand, the high NPV prevents unnecessary referrals for DR screening. The next step to perform with Brazilian data is assessing cost-effectiveness of AI-assisted portable retinography and the financial impacts of wide implementing this tool to the primary care assistance.

Our study has some limitations. The sample size was calculated for a prevalence of DR lower than that recorded in the study, resulting in wide confidence interval for the estimated DR prevalence. Some clinical data were collected retrospectively from patients' records, with missing data in some variables. On the other hand, the missing data do not bias the main results of the study. The retina specialist received subjects' images containing the color code provided by the AI software. Although the specialist was aware of how the EyerMaps® software works and was instructed to analyse the fundus images only for DR, the color code might unconsciously have influenced the specialist analysis. It can be a potential bias that may have increased the DR prevalence, and influenced sensitivity and specificity rates. Although the rates should be seen with caution, they are in consonance with similar studies (13,32). Finally, the study was conducted at a single center, limiting the generalization of the results to the general population of diabetics assisted in the primary care of SUS in Brazil.

The portable AI-based fundus camera used in our study is user-friendly and efficient, enabling image capture and AI-based diagnosis. It can be operated by non-medical professionals or generalist practitioners in primary care units, provided they receive adequate training in fundus photography (35). Equipped with wireless internet connectivity, the device can synchronize all data to the cloud, enabling telemedicine applications. This image storage facilitates continued data updates and patient follow-up, data sharing between primary care teams and other centers, and supports retrospective research. It is essential to highlight ethical issues that must be evaluated and managed cautiously.

In conclusion, AI-supported portable fundus cameras have emerged as a disruptive tool for DR screening, diabetes management and optimizing medical referral processes. This technology can reduce unnecessary medical referrals while ensuring timely and

Copyright© AE&M all rights reserved.

precise identification of severe cases at risk of significant complications if left untreated. Furthermore, AI-assisted portable retinography can offer improved DR screening worldwide, reducing costs, waiting time, and DM-related morbidity.

Authos' contributions: all authors contributed equally to this work.

Funding: this study was supported by the Foundation for the Coordination of Improvement of Higher Education Personnel – CAPES (88887.800657/2022); National Council for Scientific and Technological Development – CNPq [21/2022] and Research Financing and Incentive Program of the Hospital de Clínicas de Porto Alegre – FIPE-HCPA (0052-2023). The funding agencies had no role in the design of the study, data collection, analysis, interpretation, and manuscript preparation. The authors received no specific funding for this work.

Acknowledgments: we would like to thank Ophthalmologic Leandro Alves LTDA Clinic for providing the portable fundus camera used in this study, and Phelcom Technologies for granting a free license to access the AI software.

Disclosure: no potential conflict of interest relevant to this article was reported.

Data availability: datasets related to this article will be available upon request to the corresponding author.

REFERENCES

1. Institute for Health Metrics and Evaluation. Diabetes mellitus type 2 - Level 4 cause [Internet]. Seattle (WA): IHME; 2021 [cited 2024 Jul 20]. Available from: https://www.healthdata.org/research-analysis/diseases-injuries-risks/factsheets/2021-diabetes-mellitus-type-2-level-4-disease.
2. International Diabetes Federation. IDF Diabetes Atlas. 10th ed. Brussels: International Diabetes Federation; 2021 [cited 2024 Jul 20]. Available from: https://www.diabetesatlas.org.
3. Kropp M, Golubnitschaja O, Mazurakova A, Koklesova L, Sargheini N, Vo TKS, et al. Diabetic retinopathy as the leading cause of blindness and early predictor of cascading complications-risks and mitigation. EPMA J. 2023 Feb 13;14(1):21-42. doi: 10.1007/s13167-023-00314-8.
4. Zayed MG, Karsan W, Peto T, Saravanan P, Virgili G, Preiss D. Diabetic Retinopathy and Quality of Life: A Systematic Review and Meta-Analysis. JAMA Ophthalmol. 2024 Mar 1;142(3):199-207. doi: 10.1001/jamaophthalmol.2023.6435. Erratum in: JAMA Ophthalmol. 2024 May 1;142(5):494. doi: 10.1001/jamaophthalmol.2024.0765.
5. Leasher JL, Bourne RR, Flaxman SR, Jonas JB, Keeffe J, Naidoo K, et al.; Vision Loss Expert Group of the Global Burden of Disease Study. Global Estimates on the Number of People Blind or Visually Impaired by Diabetic Retinopathy: A Meta-analysis From 1990 to 2010. Diabetes Care. 2016 Sep;39(9):1643-9. doi: 10.2337/dc15-2171. Erratum in: Diabetes Care. 2016 Nov;39(11):2096. doi: 10.2337/dc16-er11.
6. Rodriguez-Acuña R, Mayoral E, Aguilar-Diosdado M, Rave R, Oyarzabal B, Lama C, et al. Andalusian program for early detection of diabetic retinopathy: implementation and 15-year follow-up of a population-based screening program in Andalusia, Southern Spain. BMJ Open Diabetes Res Care. 2020 Oct;8(1):e001622. doi: 10.1136/bmjdrc-2020-001622.
7. Pasquel FJ, Hendrick AM, Ryan M, Cason E, Ali MK, Narayan KM. Cost-effectiveness of Different Diabetic Retinopathy Screening Modalities. J Diabetes Sci Technol. 2015 Dec 29;10(2):301-7. doi: 10.1177/1932296815624109.
8. Broadbent DM, Wang A, Cheyne CP, James M, Lathe J, Stratton IM, et al. Safety and cost-effectiveness of individualised screening for diabetic retinopathy: the ISDR open-label, equivalence RCT. Diabetologia. 2021;64. doi: 10.1007/s00125-020-05313-2
9. Das T, Takkar B, Sivaprasad S, Thanksphon T, Taylor H, Wiedemann P, et al. Recently updated global diabetic retinopathy screening guidelines: commonalities, differences, and future possibilities. Eye (Basingstoke). 2021. doi: 10.1038/s41433-021-01572-4
10. Abou Taha A, Dinesen S, Vergmann AS, Grauslund J. Present and future screening programs for diabetic retinopathy: a narrative review. Int J Retina Vitreous. 2024 Feb 3;10(1):14. doi: 10.1186/s40942-024-00534-8.
11. Oliveira JAE, Nakayama LF, Zago Ribeiro L, de Oliveira TVF, Choi SNJH, Neto EM, et al. Clinical validation of a smartphone-based retinal camera for diabetic retinopathy screening. Acta Diabetol. 2023 Aug;60(8):1075-1081. doi: 10.1007/s00592-023-02105-z.
12. Titoneli CC, Filho MS, Lencione D, Vieira FP, Stuchi JA, Paula JS. Clinical validation of a smartphone-based handheld fundus camera for the evaluation of optic nerve head. Arq Bras Oftalmol. 2021;84. doi: 10.5935/0004-2749.20210080.
13. Queiroz MS, de Carvalho JX, Bortoto SF, de Matos MR, das Graças Dias Cavalcante C, Andrade EAS, et al. Diabetic retinopathy screening in urban primary care setting with a handheld smartphone-based retinal camera. Acta Diabetol. 2020;57. doi: 10.1007/s00592-020-01585-7.
14. Korn Malerbi F, Lelis Dal Fabbro A, Botelho Vieira Filho JP, Franco LJ. The feasibility of smartphone based retinal photography for diabetic retinopathy screening among Brazilian Xavante Indians. Diabetes Res Clin Pract. 2020;168. doi: 10.1016/j.diabres.2020.108380.
15. Natarajan S, Jain A, Krishnan R, Rogye A, Sivaprasad S. Diagnostic Accuracy of Community-Based Diabetic Retinopathy Screening with an Offline Artificial Intelligence System on a Smartphone. JAMA Ophthalmol. 2019;137. doi: 10.1001/jamaophthalmol.2019.2923.
16. Jain A, Krishnan R, Rogye A, Natarajan S. Use of offline artificial intelligence in a smartphone-based fundus camera for community screening of diabetic retinopathy. Indian J Ophthalmol. 2021 Nov;69(11):3150-3154. doi: 10.4103/ijo.IJO_3808_20.
17. Malerbi FK, Andrade RE, Morales PH, Stuchi JA, Lencione D, de Paulo JV, et al. Diabetic Retinopathy Screening Using Artificial Intelligence and Handheld Smartphone-Based Retinal Camera. J Diabetes Sci Technol. 2022 May;16(3):716-723. doi: 10.1177/1932296820985567.
18. Wilkinson CP, Ferris FL 3rd, Klein RE, Lee PP, Agardh CD, Davis M, et al.; Global Diabetic Retinopathy Project Group. Proposed international clinical diabetic retinopathy and diabetic macular edema disease severity scales. Ophthalmology. 2003 Sep;110(9):1677-82. doi: 10.1016/S0161-6420(03)00475-5.
19. Harris PA, Taylor R, Minor BL, Elliott V, Fernandez M, O'Neal L, et al.; REDCap Consortium. The REDCap consortium: Building an international community of software platform partners. J Biomed Inform. 2019 Jul;95:103208. doi: 10.1016/j.jbi.2019.103208.
20. The Royal Australian and New Zealand College of Ophthalmologists. RANZCO screening and referral pathway for diabetic retinopathy: clinical assessment [Internet]. Sydney: RANZCO; [cited 2024 Jul 20]. Available from: https://doi.org/10.1111/dme.12957.
21. American Diabetes Association. American Diabetes Association releases 2023 Standards of Care in Diabetes to guide prevention, diagnosis, and treatment for people living with diabetes [Internet]. Arlington (VA): American Diabetes Association; 2022 [cited 2024 Jul 20]. Available from: https://diabetes.org/newsroom/press-releases/2022/american-diabetes-association-releases-2023-standards-of-care-in-diabetes.
22. Whelton PK, Carey RM, Aronow WS, Casey DE Jr, Collins KJ, Dennison Himmelfarb C, et al. 2017 ACC/AHA/AAPA/ABC/ACPM/AGS/APhA/ASH/ASPC/NMA/PCNA Guideline for the Prevention,

Copyright© AE&M all rights reserved.

Detection, Evaluation, and Management of High Blood Pressure in Adults: Executive Summary: A Report of the American College of Cardiology/American Heart Association Task Force on Clinical Practice Guidelines. Hypertension. 2018 Jun;71(6):1269-1324. doi: 10.1161/HYP.0000000000000066. Epub 2017 Nov 13. Erratum in: Hypertension. 2018 Jun;71(6):e136-e139. doi: 10.1161/HYP.0000000000000075.

23. Borges RB, Mancuso ACB, Camey SA, Leotti VB, Hirakata VN, Azambuja GS, et al. Power and Sample Size for Health Researchers: uma ferramenta para cálculo de tamanho amostral e poder do teste voltado a pesquisadores da área da saúde. Clin Biomed Res. 2021;41(4). doi: 10.22491/2357-9730.109542.
24. Chagas TA, Dos Reis MA, Leivas G, Santos LP, Gossenheimer AN, Melo GB, et al. Prevalence of diabetic retinopathy in Brazil: a systematic review with meta-analysis. Diabetol Metab Syndr. 2023 Mar 2;15(1):34. doi: 10.1186/s13098-023-01003-2.
25. Scanlon PH, Aldington SJ, Stratton IM. Epidemiological issues in diabetic retinopathy. Middle East Afr J Ophthalmol. 2013 Oct-Dec;20(4):293-300. doi: 10.4103/0974-9233.120007.
26. Pereira AMP, da Silva Laureano RM, de Lima Neto FB. Five regions, five retinopathy screening programmes: a systematic review of how Portugal addresses the challenge. BMC Health Serv Res. 2021 Jul 30;21(1):756. doi: 10.1186/s12913-021-06776-8.
27. Chabba N, Silwal PR, Bascaran C, McCormick I, Goodman L, Gordon I, et al. What is the coverage of retina screening services for people with diabetes? Protocol for a systematic review and meta-analysis. BMJ Open. 2024;14. doi: 10.1136/bmjopen-2023-081123.
28. Carrillo-Larco RM, Guzman-Vilca WC, Varghese JS, Pasquel FJ, Caixeta R, Antini C, et al. Compliance with eye and foot preventive care in people with self-reported diabetes in Latin America and the Caribbean: Pooled, cross-sectional analysis of nine national surveys. Prim Care Diabetes. 2024;18. doi: 10.1016/j.pcd.2024.03.001.
29. Instituto Brasileiro de Geografia e Estatística (IBGE). PNS 2019: seven of ten persons who search for same health service go to public network [Internet]. Rio de Janeiro: IBGE; 2020 [cited 2024 Jul 20]. Available from: https://agenciadenoticias.ibge.gov.br/en/agencia-press-room/2185-news-agency/releases-en/28796-pns-2019-seven-of-ten-persons-who-search-for-same-health-service-go-to-public-network.
30. Protocolo Clínico de Diretrizes Terapêuticas (PCDT) para diabetes Mellitus Tipo II — Ministério da Saúde. [cited 20 Jul 2024]. Available: https://www.gov.br/saude/pt-br/composicao/saps/ecv/publicacoes/protocolo-clinico-de-diretrizes-terapeuticas-pcdt-para-diabetes-mellitus-tipo-ii/view.
31. Malerbi FK, Mendes G, Barboza N, Morales PH, Montargil R, Andrade RE. Diabetic Macular Edema Screened by Handheld Smartphone-based Retinal Camera and Artificial Intelligence. J Med Syst. 2022;46. doi: 10.1007/s10916-021-01795-8.
32. Souza GF, Figueira RM, Alkmim MB, Sousa LAP, Bonisson L, Ribeiro ALP, et al. Teleophthalmology Screening for Diabetic Retinopathy in Brazil: Applicability and Economic Assessment. Telemed J E Health. 2020 Mar;26(3):341-346. doi: 10.1089/tmj.2018.0241.
33. Li H, Li G, Li N, Liu C, Yuan Z, Gao Q, et al. Cost-effectiveness analysis of artificial intelligence-based diabetic retinopathy screening in rural China based on the Markov model. PLoS One. 2023 Nov 16;18(11):e0291390. doi: 10.1371/journal.pone.0291390.
34. Maberley D, Walker H, Koushik A, Cruess A. Screening for diabetic retinopathy in James Bay, Ontario: a cost-effectiveness analysis. CMAJ. 2003 Jan 21;168(2):160-4. PMID: 12538543.
35. Wong TY, Sun J, Kawasaki R, Ruamviboonsuk P, Gupta N, Lansingh VC, et al. Guidelines on Diabetic Eye Care: The International Council of Ophthalmology Recommendations for Screening, Follow-up, Referral, and Treatment Based on Resource Settings. Ophthalmology. 2018 Oct;125(10):1608-1622. doi: 10.1016/j.ophtha.2018.04.007.

Copyright© AE&M all rights reserved.

SUPPLEMENTARY MATERIALS

Images examples of retinography captured in the study.

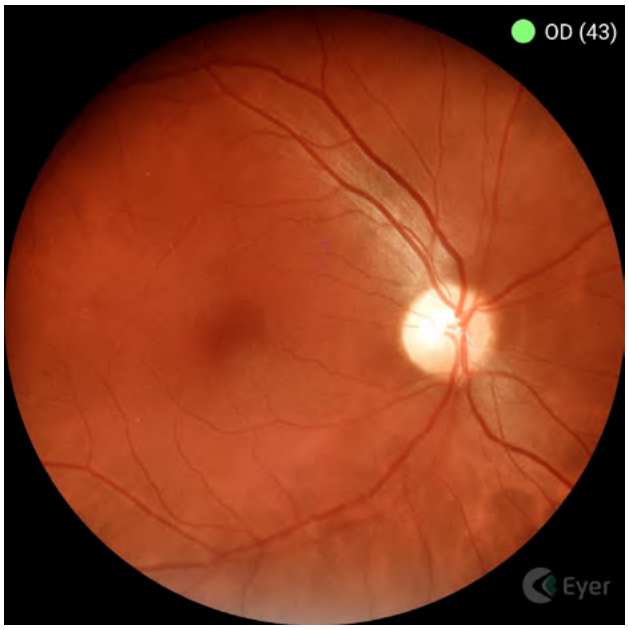


Figure S1. Absence of DR (AI shows green circle).

Healthy optic nerve, blood vessels without changes, no hemorrhages of exudates, good macula visualization.



Figure S3. Moderate NPDR (the same **Figure S2**) with AI markings.

Same image as above with AI markings in the anterior "heat map," highlighting the areas where abnormalities were identified.



Figure S2. Moderate NPDR; AI shows a red circle, indicating the presence of a change.

Optic nerve with normal appearance. Presence of microaneurysms and microhemorrhages (small red dots) in at least three quadrants, as well as the presence of some hard exudates (round yellow lesions near vessels).

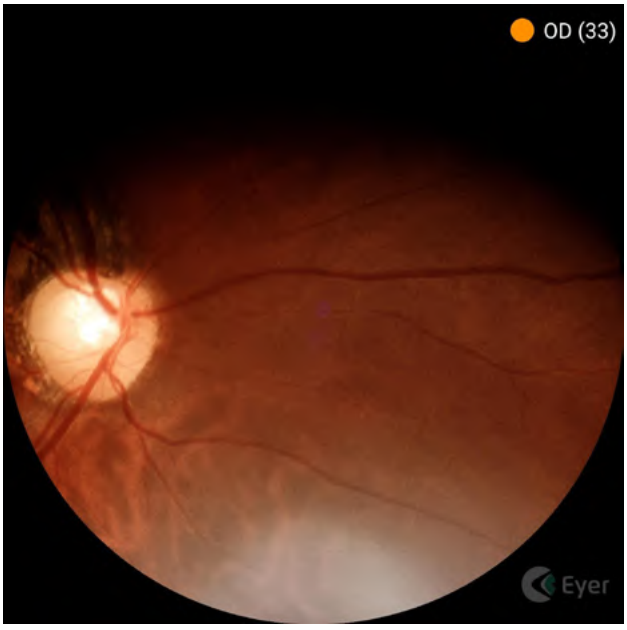


Figure S4. Fundoscopy change that is not DR, identified by AI (orange circle). Optic nerve with suspected glaucoma, and need further evaluation.

Enlargement of the optic nerve cupping and peripapillary atrophy.

Copyright© AE&M all rights reserved.

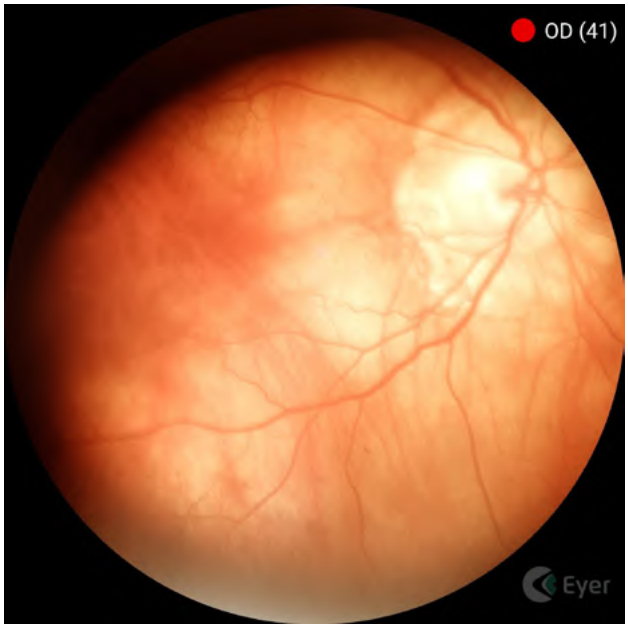


Figure S5. Fundus change detected by AI, but not DR.

Myoptic choroidopathy, a condition present in subjects with high grade myopia (at least 6 spherical diopters). This patient has low vision and risk of retinal detachment.



Figure S7. Fundus image impossible to classification; AI does not show any color.

Image without quality to evaluate presence or absence of DR changes.



Figure S6. Non-pathological retinal change; AI does not identify a problem.

White stretch marks represents atrophy of the retinal pigment epithelium: variation of the normality and does not need additional evaluation.

Copyright© AE&M all rights reserved.

Archives of Endocrinology and Metabolism
ISSN 2359-4292
OFFICIAL JOURNAL OF THE BRAZILIAN SOCIETY OF ENDOCRINOLOGY AND METABOLISM

original

Type 2 diabetes morbidity, mortality and its associated risk factors across Brazilian regions: findings from the Global Burden of Disease Study 2021

Paula Portal Teixeira[1]
https://orcid.org/0000-0001-7109-7661

Rodrigo dos Reis[2]
https://orcid.org/0000-0003-1766-0964

Yvonne Yiru Xu[6]
https://orcid.org/0000-0001-5078-0111

Tatiana Duque-Cartagena[2]
https://orcid.org/0000-0003-0881-1441

Fernando Gerchman[1]
https://orcid.org/0000-0001-5873-9498

Maria Inês Schmidt[2]
https://orcid.org/0000-0002-3837-0731

Lucas Scotta Cabral[3]
https://orcid.org/0000-0001-8820-2181

Verônica Colpani[4]
https://orcid.org/0000-0002-7908-4213

Rita Mattiello[2]
https://orcid.org/0000-0002-0548-3342

Bárbara Niegia Garcia de Goulart[2]
https://orcid.org/0000-0002-2502-5883

Deborah Carvalho Malta[5]
https://orcid.org/0000-0002-8214-5734

Bruce Bartholow Duncan[2]
https://orcid.org/0000-0002-7491-2630

[1] Programa de Pós-graduação em Ciências Médicas: Endocrinologia, Universidade Federal do Rio Grande do Sul, Porto Alegre, RS, Brasil
[2] Programa de Pós-graduação em Epidemiologia, Faculdade de Medicina, Universidade Federal do Rio Grande do Sul, Porto Alegre, RS, Brasil
[3] Programa de Pós-graduação em Cardiologia e Ciências Cardiovasculares, Universidade Federal do Rio Grande do Sul, Porto Alegre, RS, Brasil
[4] Centro de Avaliação de Tecnologias em Saúde, Hospital Sírio-Libanês, São Paulo, SP, Brasil.
[5] Programa de Pós-graduação em Saúde Pública, Universidade Federal de Minas Gerais, Belo Horizonte, MG, Brasil
[6] Institute for Health Metrics and Evaluation, University of Washington, Seattle, USA

ABSTRACT

Objective: To describe Brazilian national and regional trends in type 2 diabetes mellitus (T2DM) prevalence, incidence, burden, and exposure to T2DM risk factors. **Materials and methods:** We sourced the Global Burden of Diseases Study (GBD) 2021 to obtain estimates and trends of T2DM deaths, incidence, prevalence, Years of Life Lost (YLLs), Years Lived with Disability (YLDs), and Disability Adjusted Life Year (DALYs) in Brazil and its regions. We present crude and age-standardized metrics, as well as the exposure to T2DM risk factors between 1990 and 2021. **Results:** The national age-standardized prevalence of T2DM increased by 37.4% (95% UI 32.7 to 42.6) and the incidence by 32.3% (95% UI 27.6 to 37.7) from 1990 to 2021. Age-standardized deaths by T2DM decreased by 18.0% (95% UI -21.4 to -15.3), and the accompanying YLLs by 22.8% (95% UI -25.8 to -20.2). YLDs increased by 35.4% (95% UI 29.1 to 41.3), while DALYs' rates reduced by 3.1% (95% UI -8.2 to 1.7) since 1990. The Northeast region showed higher age-standardized prevalence, incidence, YLLs, and YLDs in 2021, while the North region had the most pronounced increases. T2DM prevalence increased consistently, alongside rises in exposure to sugar-sweetened beverage consumption and high BMI. While smoking exposure declined in all regions, low physical activity and diets high in red and processed meat increased over time. **Conclusion:** T2DM burden in Brazil is growing due to the increasing exposure to T2DM risk factors. Greater emphasis on prevention and public policies focusing on reducing risk factors and inequalities can reduce T2DM burden in Brazil.

Keywords: Diabetes mellitus; global burden of disease study; risk factors; Brazil

INTRODUCTION

Type 2 diabetes mellitus (T2DM) is a non-communicable disease that affects mainly adults and is characterized by insulin resistance and reduced pancreatic insulin secretion (1). The condition is a major cause of blindness, kidney failure, heart attacks, stroke, and lower limb amputation, especially in those with poor glycemic control (2). According to the NCD Risk Factor Collaboration (NCD-RisC), in 2022, age-standardized diabetes prevalence in the world was 13.9% for women and 14.3% for men, representing around 828 million adults living with diabetes worldwide (3). Projections from the Global Burden of Diseases, Injuries and Risk Factors Study (GBD) show that, despite significant improvements envisioned in its treatment, T2DM can become Brazil´s leading cause of disease burden, represented by disability-adjusted life year (DALYs), in 2050 (4).

Received on Aug/19/2025
Accepted on Jan/28/2026
DOI: 10.20945/2359-4292-2026-0052

Correspondence to:
Paula Portal Teixeira
Universidade Federal do Rio Grande do Sul
Programa de Pós-graduação em
Ciências Médicas: Endocrinologia
90035003 – Porto Alegre, RS, Brasil
papteixeira@hcpa.edu.br

Associated editor:
Melanie Rodacki
https://orcid.org/0000-0002-9007-1325

This is an open-access article distributed under the terms of the Creative Commons Attribution License

Copyright© ACE&M all rights reserved.

Previous studies evaluating the burden of T2DM in Brazil have focused exclusively on prevalence (5-7), incidence (8), mortality (9-11), risk factors (12), or hospitalizations (10), while some, based on GBD data, focused on DALYs (13) or economic outcomes (14). However, comprehensive assessments of the aggregate burden of non-fatal and fatal outcomes and risk factors of T2DM across the country are scarce. Additionally, some studies that relied only on self-reported T2DM data (5,6,11,12) underestimated the total prevalence of the condition and considered only those aged 18 and over (8,11), overlooking the increasing incidence of T2DM in younger populations. Finally, none of these studies have gone beyond 2019, making it pertinent to incorporate the available and more current data.

To help inform Brazilian stakeholders in confronting the country's diabetes epidemic, we aimed to provide a comprehensive picture of the T2DM burden in Brazil and its macro-regions. We describe national and regional trends in prevalence, incidence, and burden, and trends in exposure to underlying potentially modifiable behavioral, environmental, and metabolic diabetes risk factors from 1990 to 2021.

MATERIALS AND METHODS

Overview and definitions

This study adheres to the Guidelines for Accurate and Transparent Health Estimates Reporting (GATHER) statement, ensuring quality reporting and transparency in assessing health estimates (15). The GBD is a multinational collaboration that synthesizes primary and secondary epidemiological data to comprehensively evaluate the health impact of diseases, injuries, and risk factors within diverse populations and geographical contexts worldwide. All steps related to the GBD 2021 estimation process, from compiling data sources through data identification and extraction, data adjustment, case definitions, and metric estimations, have been previously described in greater detail (16-18). This manuscript was produced as part of the GBD Brazil Network (19) following the GBD Protocol.

For this analysis, we downloaded data directly from the GBD Results Tool (http://ghdx.healthdata.org/gbd-results-tool). We focused on estimates of T2DM deaths, prevalence, incidence, Years of Life Lost due to premature mortality (YLLs), Years Lived with Disability (YLDs), and Disability-adjusted Life Years (DALYs) in Brazil and its regions (North, Northeast, Central-West, Southeast, and South), presenting the overall percent change of each estimate from 1990 to 2021. We also described the percentage change in age-standardized death rates disaggregated by sex to assess whether the estimates apply uniformly across male and females. All estimates are shown in rate per 100,000 habitants as age-standardized and in crude form (encompassing all age groups) and accompanied by 95% uncertainty intervals (UIs). We also present estimates on the percent change in population exposure to several major T2DM risk factors for Brazil overall and by region between 1990 and 2021. All graphs presented in this manuscript were generated using The R Foundation for Statistical Computing Platform, version 4.1.2 (2021).

Diabetes definition

The GBD study categorizes causes of death and disability into four hierarchical levels, from a broader to a more detailed level, and diabetes mellitus is considered a level 3 cause. Its burden is the combination of type 1 (T1DM) and type 2 (T2DM) diabetes mellitus. The reference case definition for overall diabetes is the presence of a fasting plasma glucose (FPG) ≥126 mg/dL (7 mmol/L) or the report of drug treatment for diabetes (insulin or anti-diabetic drugs) (20). In order to standardize data with different definitions of diabetes, when data on an oral glucose tolerance test (OGTT) and glycated hemoglobin are also reported, these values are transformed into FPG equivalents.

Diabetes data sources and estimation

To estimate T2DM mortality in Brazil, GBD 2021 gathered data on deaths from 40 sources, including vital registration in ICD-10 codes, which are all provided through the Global Health Data Exchange (GHDx) (https://ghdx.healthdata.org/). To do so, GBD conducts systematic literature reviews of published studies, which it aggregates to data from government and international organization websites, primary data sources, and contributions by country GBD collaborators and

Copyright© AE&M all rights reserved.

the World Health Organization (WHO). Deaths from diabetes, identified by the International Classification of Diseases (ICD) version 10 (E10–E14 and P70.2), were modelled to generate diabetes mortality estimates using a Bayesian geospatial regression analysis called Cause of Death Ensemble model (CODEm) (16). Estimates were obtained by age, sex, year, and geography. Additionally, whenever deaths obtained from GBD sources were coded to an implausible underlying cause of death or unspecified diabetes types, corrections and redistributions by manual and statistical methods were performed to redistribute these deaths to probable underlying causes, including T2DM (16).

Type-specific diabetes deaths were estimated using vital registration data. It was assumed that all deaths under age 15 were due to T1DM. Once the data had been gathered and cleaned, estimates were modeled over the years and across regions (16). To estimate premature mortality, the GBD employed the metric Years of Life Lost (YLLs), multiplying the number of deaths from T2DM in each age group by the reference life expectancy at the average age of death for those who die in that age group.

For non-fatal estimation, GBD obtained data from 17 sources in Brazil, including systematic reviews that only consider population representative surveys obtained directly or through publications. After data compiling and initial adjustments, prevalence data were summarized across Brazil's regions using a hierarchical Bayesian meta-regression modeling tool (DisMod-MR 2.1), which integrated the various metrics to provide consistent prevalence, incidence, and mortality estimates (18). The model considers covariates and the location hierarchy to inform locations, years, ages, and sex where data is missing. For non-fatal outcomes, GBD derived estimates of T2DM by deducting the estimated prevalence of T1DM from the overall estimated diabetes mellitus prevalence. Estimates of prevalence and incidence were split between T1DM and T2DM, with all cases <15 years of age assumed to be T1DM, and are not the focus of this manuscript (20).

The GBD estimated the burden due to disability (morbidity) through the metric Years Lived with Disability (YLDs), obtained by the product of the prevalence of each sequelae of T2DM (neuropathy, diabetic foot, lower limb amputation, vision loss due to retinopathy, as well as living with diabetes) and its corresponding disability (18,21). The disability weights, on a scale from 0 to 1, represent the magnitude of health loss in the presence of these complications and were calculated separately for each sequelae. The sum of YLDs across sequelae and age/sex strata produced the total YLDs for T2DM for a given year and location. Finally, Disability-Adjusted Life Years (DALYs) were obtained through the sum of YLLs and YLDs and represent total health loss due to premature mortality or morbidity from T2DM (18).

Risk factors estimation

The GBD identified risk factors associated with T2DM through systematic reviews and meta-analyses using meta-regression procedures. Based on the exposure levels to each risk factor, a Bayesian meta-regression model (DisMod-MR 2.1) and spatiotemporal Gaussian process regression model (ST-GPR) were used to estimate the exposure levels for the entire population over time. The relative risk for each risk factor was then used to calculate the excess disability and death that occurred above the theoretical minimum exposure level (TMREL), representing the level of risk exposure that minimizes the risk of T2DM at the population level. The level of exposure to risk factors was estimated by their Summary Exposure Value (SEV). For continuously measured risk factors, the SEV weighs the prevalence of different levels of the risk factor by the severity of the burden caused at each level. GBD 2021 reported SEVs on a scale from 0 to 100%. Though the comparison of the absolute values of SEVs across risk factors is of limited value, tendencies in SEVs across time and space facilitate comparisons of risk factor exposures (17).

RESULTS

In 2021, Brazil presented an age-standardized diabetes prevalence of 5095.8 per 100,000 habitants (95% UI 4578.5 to 5678.2) and an age-standardized diabetes incidence of 279.1 (95% UI 251.6 to 309.3) per 100,000. From 1990 to 2021, these frequencies increased by 37.4% (95% UI 32.7 to 42.6) and 32.3%

Copyright© AE&M all rights reserved.

(95% UI 27.6 to 37.7), respectively. However, when considering all age groups, the changes from 1990 to 2021 were notably higher, 135.5% (95% UI 127.5 to 145.0) and 113% (95% UI 102.8 to 123.5), respectively (**Table 1**).

Regionally, the Northeast stood out with the highest age-standardized prevalence of T2DM in 2021, 5816.3 per 100,000 habitats (95% UI 5261.1 to 6430.2), as well as the highest incidence, at 317.9 (95% UI 288.1 to 350.0), 14% greater than that for Brazil overall. In contrast, the Southeast region had the lowest age-standardized prevalence, at 4638.6 (95% UI 4132.9 to 5225.9), and incidence, at 252.5 (95% UI 225.6 to 283.0). The North region showed the most pronounced increase in the age-standardized prevalence of T2DM from 1990 to 2021, 57.1% (95% UI 50.9 to 63.4), 53% greater than that for Brazil overall and contrasting with the Southeast region, which experienced the smallest increase, 20.3% (95% UI 14.9 to 26.2). Considering all age estimates, the South region showed the highest prevalence and incidence, and the North region was the lowest for both estimates **(Table 1)**.

The age-standardized mortality rate in Brazil in 2021 was 25.8 (95% UI 23.5 to 27.3) per 100,000 habitants by 2021, reflecting an 18% decrease (95% UI -21.4 to -15.3) since 1990. YLLs were 536.7 (95% UI 501.5 to 558.5) per 100,000 inhabitants, a 22.8% decrease (95% UI -25.8 to -20.2) compared to 1990. When age-standardized mortality was disaggregated by sex, females experienced a 28% reduction in age-standardized deaths (-28.0%; 95% UI -32.1 to -24.7), whereas males exhibited only a 3% reduction (-3.0%; 95% UI -7.8 to 1.9) (**Supplementary Figure 1**). Age-standardized YLDs reached 486.9 (95% UI 337.6 to 664.1) per 100,000, a 35.4% increase (95% UI 29.1 – 41.3), and DALYs summed to 1023.6 (95% UI 870.9 to 1203.7) per 100,000, representing a minimal 3.1% (95% UI -8.2 to 1.7) decrease from 1990. Estimates of change in metrics for all ages, as shown in **Table 1**, were notably higher than those adjusted for age. Considering all disease causes, the GBD ranked T2DM as Brazil's 3rd leading cause of disease burden in 2021, up from the 12th leading cause in 1990 (data not shown).

The Northeast region displayed the highest age-standardized mortality rate (32.2, 95% UI 29.3 to 34.3) per 100,000 habitants, 25% greater than that for Brazil overall, while the Central-West (22.2; 95% UI 19.9 to 23.8) and Southeast (22.1; 95% UI 19.7 to 23.6) presented the lowest mortality rates. The North region had a 26.1% increase, while deaths in Brazil overall decreased, especially in the Southeast region (-35%; 95% UI -38.9% to -31.2). As seen in **Table 1** and in **Supplementary Figure 2**, the same discordant trends occurred for YLLs. As shown by age-standardized YLDs, morbidity has consistently increased in all regions since 1990, with a tendency of slight decrease after 2020 observed in **Supplementary Figure 2**. The North region with a 53.4% (95% UI 46.3 to 60.7) increase, 50% greater than for Brazil overall. The North region also presented the most pronounced increase in DALYs, 34.8% (95% UI 27.2 to 41.4), compared to virtually no change for Brazil overall, and a 20.3% (95% UI -25.6 to -15.0) reduction in the Southeast region. In 2021, the Northeast region had the highest YLD (557.1; 95% UI 384.7 to 757.1) and DALY (1228.0; 95% UI 1051.5 to 1431.9) rates **(Table 1)**.

Figure 1 graphically displays the change in age-standardized T2DM prevalence and DALYs in Brazil and its macro-regions between 1990 and 2021. The consistent increase in prevalence contrasts with the relatively stable course of DALYs over the study period. Slightly higher prevalences of DALYs are present in the North and Northeast regions, and lower ones are in the South and Southeast regions.

Figure 2 shows Brazil's DALY rates per 100,000 habitants and macro-regions, stratified by age group. Overall, DALY rates increased with age for all regions but with notable regional disparities. The North and Northeast consistently showed somewhat higher DALYs for all age groups, whereas the Central-West and Southeast regions had lower rates in almost all age groups.

Figure 3 illustrates the change in age-standardized measures (1990–2021) for the prevalence of T2DM and its associated risk factors, with 1990 as the reference year for Brazil, disaggregated by region. A consistent increase in T2DM prevalence was observed across all regions, accompanied by varied

Copyright© ACE&M all rights reserved.

Table 1. Burden of T2DM in Brazil and its regions from 1990 to 2021

	All ages		Age-standardized	
	Rate per 100,000, 2021 (95% UI)	Change 1990–2021 (%)	Rate per 100,000, 2021 (95% UI)	Change 1990–2021 (%)
Prevalence				
Brazil	5895.9 (5290.8 to 6575.9)	135.5 (127.5 to 145)	5095.8 (4578.5 to 5678.2)	37.4 (32.7 to 42.6)
North	4783.0 (4312.9 to 5324.6)	176.1 (164.7 to 188.5)	5566.9 (5020.0 to 6173.2)	57.1 (50.9 to 63.4)
Northeast	5982.3 (5414.4 to 6628.3)	153.6 (144.7 to 163)	5816.3 (5261.1 to 6430.2)	55.5 (49.9 to 61)
Central-West	5869.7 (5277.5 to 6518.9)	180.5 (167.7 to 193.6)	5335.0 (4806.3 to 5888.8)	44 (38.4 to 50.0)
Southeast	5910.6 (5267.4 to 6666.4)	107.9 (98.3 to 119)	4638.6 (4132.9 to 5225.9)	20.3 (14.9 to 26.2)
South	6414.3 (5731.9 to 7192.9)	174.6 (161.6 to 189.1)	4916.2 (4403.0 to 5498.6)	50.4 (43.9 to 58)
Incidence				
Brazil	326.1 (293.3 to 362.6)	113.0 (102.8 to 123.5)	279.1 (251.6 to 309.3)	32.3 (27.6 to 37.7)
North	292.9 (263.9 to 324.4)	170.1 (156.7 to 185)	303.4 (273.3 to 334.0)	55.9 (49.3 to 63)
Northeast	336.2 (304.7 to 371.1)	147.3 (137 to 159.1)	317.9 (288.1 to 350.0)	51.4 (45.4 to 57.8)
Central-West	338.9 (304.1 to 376.8)	145.1 (130.6 to 162.9)	288.4 (260.0 to 319.9)	36.6 (29.9 to 43.9)
Southeast	316.6 (281.8 to 355.5)	79.6 (68.9 to 91.6)	252.5 (225.6 to 283.0)	14.3 (8.3 to 20.7)
South	347.4 (309.2 to 388.3)	134.5 (121.2 to 150.5)	271.4 (242.6 to 302.4)	41.3 (35.1 to 48.7)
Deaths				
Brazil	28.7 (26.2 to 30.2)	20.5 (14.2 to 25.8)	25.8 (23.5 to 27.3)	-18.0 (-21.4 to -15.3)
North	22.7 (20.6 to 24.6)	88.2 (71.6 to 106.3)	31.7 (28.5 to 34.4)	26.1 (16.2 to 36.3)
Northeast	32.0 (29.1 to 34.1)	51.7 (41.8 to 61.3)	32.2 (29.3 to 34.3)	-2.8 (-8.0 to 1.8)
Central-West	21.1 (19.1 to 22.6)	30.5 (20.8 to 39.5)	22.2 (19.9 to 23.8)	-7.0 (-13.1 to -0.9)
Southeast	27.7 (24.8 to 29.5)	-3.6 (-10.2 to 2.3)	22.1 (19.7 to 23.6)	-35.0 (-38.9 to -31.2)
South	32.8 (29.7 to 35.0)	36.9 (26.5 to 45.3)	25.9 (23.3 to 27.7)	1.9 (-4.8 to 8.3)
Years of Life Lost (YLL)				
Brazil	612.5 (574.0 to 636.7)	61.3 (51.9 to 70.3)	536.7 (501.5 to 558.5)	-22.8 (-25.8 to -20.2)
North	521.1 (479.9 to 561.8)	161.2 (133.9 to 192.2)	665.2 (610.1 to 717.7)	22.4 (12.5 to 32.5)
Northeast	676.3 (632.0 to 712.8)	146.0 (125.4 to 169.8)	670.9 (626.1 to 707.4)	-6.3 (-11.1 to -1.6)
Central-West	478.6 (444.1 to 509.7)	66.7 (53.4 to 81.3)	460.6 (423.5 to 491.0)	-12.8 (-18.5 to –7.0)
Southeast	592.0 (548.4 to 628.9)	17.6 (9.9 to 25.2)	463.8 (428.9 to 492.8)	-39.3 (-42.6 to -35.6)
South	673.0 (621.6 to 715.0)	55.5 (44.0 to 66.0)	515.9 (475.7 to 548.1)	-6.7 (-12.8 to -0.5)
Years Lives with Disability (YLDs)				
Brazil	564.5 (391.3 to 771.9)	95.2 (86.0 to 105.1)	486.9 (337.6 to 664.1)	35.4 (29.1 to 41.3)
North	449.9 (316.3 to 616.1)	129.1 (116.7 to 141.5)	533.4 (374.3 to 728.1)	53.4 (46.3 to 60.7)
Northeast	571.0 (393.8 to 778.6)	110.3 (99.4 to 120.5)	557.1 (384.7 to 757.1)	52.8 (45.4 to 59.2)
Central-West	556.3 (383.8 to 751.8)	128.0 (113.4 to 143.1)	508.0 (349.8 to 683.2)	41.3 (33.2 to 48.6)
Southeast	568.9 (392.7 – 780.1)	73.5 (63.1 to 84.2)	443.4 (306.3 to 607.7)	19.6 (12.5 to 26.6)
South	617.2 (426.0 to 841.9)	120.0 (106.4 to 134.1)	469.0 (325.3 to 638.4)	45.6 (37.1 to 54.1)
Disability Adjusted Life Years (DALYs)				
Brazil	1177.0 (999.4 to 1387.0)	79.2 (69.8 to 87.8)	1023.6 (870.9 to 1203.7)	-3.1 (-8.2 to 1.7)
North	971.0 (824.8 to 1146.3)	155.8 (139.8 to 175.4)	1198.7 (1022.4 to 1410.5)	34.8 (27.2 to 41.4)
Northeast	1247.4 (1068.0 to 1456.4)	143.0 (128.4 to 160.2)	1228.0 (1051.5 to 1431.9)	13.5 (6.9 to 19.6)
Central-West	1034.9 (867.4 to 1241.5)	97.6 (85.4 to 109.5)	968.6 (815.0 to 1155.7)	9.2 (3.0 to 14.8)
Southeast	1160.9 (980.3 – 1385.4)	40.5 (31.7 to 48.6)	907.2 (766.2 to 1082.3)	-20.3 (-25.6 to –15.0)
South	1290.2 (1096.4 to 1524.5)	81.1 (71.3 to 90.7)	984.9 (835.9 – 1161.5)	13.2 (7.3 to 19.1)

UI: Uncertainty intervals.

Copyright© ACE&M all rights reserved.

but usually parallel changes in most diabetes risk factors. Consumption of sugar-sweetened beverages had the most pronounced increases in the Central-West, Southeast and South regions, followed by high BMI with a sharp and uniform increase nationwide. Increases in both these, high red meat and processed meat consumption were usually equal to or greater than those of prevalent diabetes. On the other hand, the exposure to smoking has decreased in all regions, and the more recently recognized risk factor, air pollution, increased in Central-West and Southeast, and reduced in other regions. Finally, low physical activity experienced smaller increases in all regions.

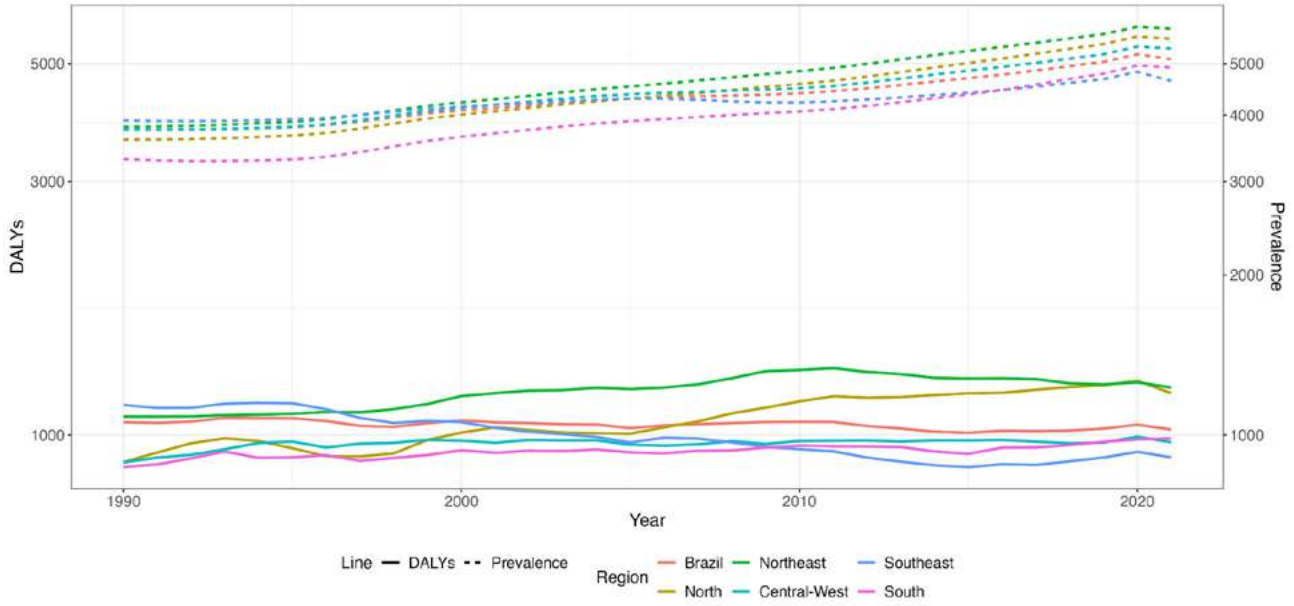


Figure 1. Prevalence and Disability-Adjusted Life Years (DALYs) lost to T2DM in Brazil and its macro-regions.
Dashed lines represent age-standardized prevalence rates, and the solid lines represent age-standardized DALYs rates per 100,000 habitants from 1990 to 2021.

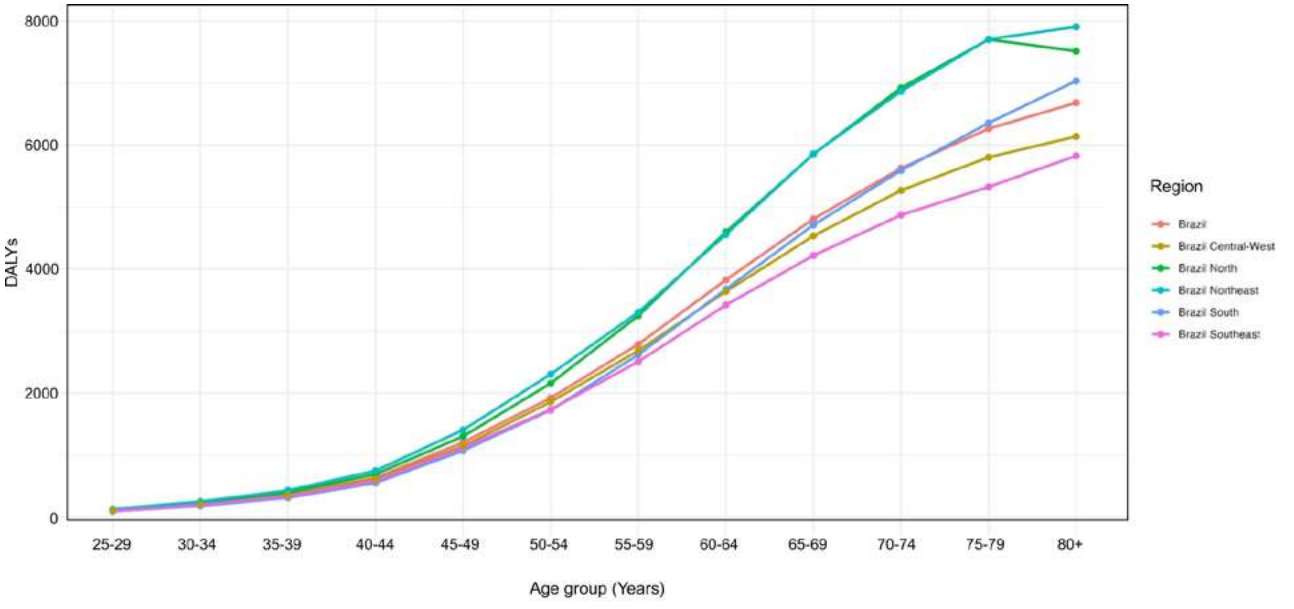


Figure 2. Disability-Adjusted Life Years (DALYs) of T2DM in Brazil and macro-regions in 2021, by age and region.
The Y axis represents age-standardized DALYs, in rates per 100.000 habitants.

Copyright© AE&M all rights reserved.

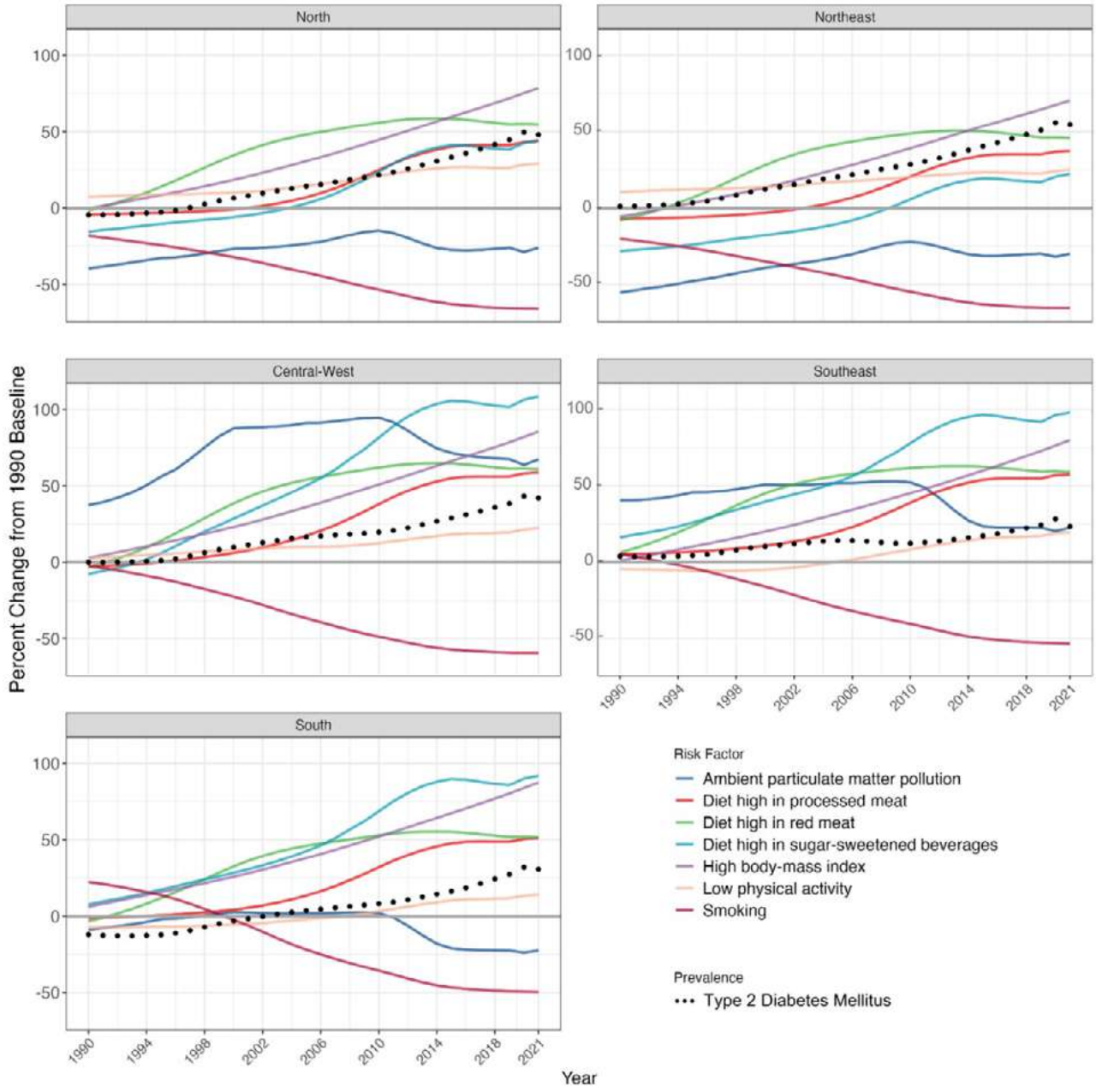


Figure 3. Change in age-standardized prevalence and risk factors' exposure for T2DM in macro-regions.

Data are presented as age-standardized percent change, from 1990 to 2021. The baseline for each risk factor is its SEV in 1990 for Brazil overall.

DISCUSSION

In this study, we showed a large fatal and non-fatal burden of T2DM in Brazil in 2021. Between 1990 and 2021, the national age-standardized prevalence of T2DM increased by 37% and its incidence by 32%. Despite this surge in cases, age-standardized deaths decreased by 18% and YLLs by almost 23%, reflecting improved outcomes and advances in diabetes care; notably, this mortality reduction was more pronounced in females than in males. Conversely, age-standardized YLDs increased substantially by 35%, leading to only a modest 3% reduction in DALYs, suggesting that gains in preventing premature deaths are increasingly offset by a growing burden of living with the disease. Furthermore, while age-standardized rates showed declines in mortality, crude diabetes mortality, YLLs, and DALYs actually increased across Brazil over these three decades, primarily driven by

Copyright© ACE&M all rights reserved.

population aging. Regionally, the Northeast presented slightly greater age-standardized frequency and burden in 2021, and the North experienced considerably larger increases in these metrics since 1990. Exposure to most diabetes risk factors, when age-standardized, also showed marked increases in all regions over the period, with sugar-sweetened beverage consumption, high BMI and red and processed meat consumption outstripping the increases in diabetes prevalence in most regions.

Increases in both crude and age-standardized prevalence and incidence related to T2DM in Brazil between 1990 and 2021 are by global trends, as age-standardized diabetes prevalence increased by more than 100% in almost half of the 204 countries and territories included in the GBD, and more than 90% of these diabetes cases were T2DM (20). This pattern has been observed in most low- and middle-income countries (LMICs) in a more rapid way compared to high-income countries, gradually shifting from environments leading infectious, childhood, and maternal diseases to be the principal public health concerns to ones with a higher burden from non-communicable diseases (22). For example, International Diabetes Federation (IDF) estimated that 94% of the increase in the number of people with diabetes by 2045 will occur in low and middle-income countries (23).

In contrast, significant reductions in age-standardized mortality rates for T2DM and YLL were observed in Brazil, with more pronounced declines in the Southeast and Central-West. Alongside regional disparities, clear sex-specific patterns were observed, with females experiencing a more favorable trend in T2DM mortality with greater reductions over time than males. These findings indicate that the improvements have not occurred uniformly across geographic regions or between sexes, highlighting differences in behavioral susceptibility to health risks (24) and heterogeneous impact of health system advances across the country. These trends likely reflect not only global advances in evidence-based care of diabetes and the management of complications, notably the cardiovascular ones, but also, specifically in Brazil, the expansion of primary care and improvement across all levels of the health system following the creation and consolidation of the Unified Health System (25,26). These actions have blunted the rise in morbimortality accompanying the rapid increase in diabetes cases. Since 2007, the right to receive free anti-diabetic medications and related treatment supplies (e.g., syringes) has been guaranteed to people living with diabetes in Brazil, with a major increase in access to free diabetes medications starting in 2011 (27). In 2019, the Brazilian Congress enacted the National Policy for Diabetes Prevention and Comprehensive Assistance to Diabetic Persons was established, aiming to increase population awareness about diabetes detection and treatment.

Besides some advances in the Brazilian health system and treatment policies, increases in both crude and age-standardized fatal and non-fatal burden of T2DM were observed in the Northeast and North, in contrast to the Southeast region, exacerbating regional Brazilian health disparities. The North and Northeast regions suffer from poorer health outcomes due to historical, socioeconomic, and structural factors, with key challenges such as elevated poverty levels, restricted access to quality healthcare services, and lower levels of educational attainment (28). These challenges within specific settings should be addressed to reduce regional health inequalities and improve public health outcomes (29-31).

Additionally, deferred care-seeking during the COVID-19 pandemic may have affected T2DM morbidity and mortality across Brazilian regions, as poorer health-care infrastructures were less equipped to manage infections and the increased demand for health services. Although GBD 2021 estimates were adjusted for the impact of COVID-19, it is not possible to fully evaluate the pandemic's specific contribution to T2DM-related burden. In our study, annual trends in prevalence, DALYs, and YLLs after 2019 remained consistent with those observed in previous years across all regions. However, age-standardized YLDs showed a reduction trend after 2019-2020 in all regions, which may be reflecting an under-identification of T2DM complications due to the pandemics' impact on medical appointments (32). These trends should be monitored in future GBD iterations, and targeted efforts within health-care services are needed to

Copyright© AE&M all rights reserved.

recover delayed services resulting from the pandemic period.

Finally, we showed that diabetes risk factor control, except for tobacco, has, in large part, worsened over the last three decades in Brazil, contributing to its increasing incidence and prevalence. Over the past three decades, Brazil's socioeconomic and urban development has been accompanied by significant societal changes. Notably, there has been an increase in the consumption of ultra-processed foods and a rise in dense urbanization that offers limited recreational space (33-35). This urban growth is coupled with challenges such as inadequate sidewalks, poor lighting, and crime, hindering regular physical activity, exacerbating many risk factors, and impeding substantial improvements in others, such as promoting physical activity (35). These changes appear to be the motor of the current diabetes epidemic. However, other less well-described factors related to environmental pollution resulting from societal change may also play a significant role (36), as well as the increased exposure to endocrine-disrupting chemicals in ultra-processed products or their packaging (37,38).

The World Health Organization (WHO) provided a list of interventions, including population-based ones, considered to be the most cost-effective means of preventing chronic diseases such as diabetes, including 1) increasing prices and taxes on tobacco and alcohol products, 2) promoting awareness through mass media on the importance of healthy diets and physical activity, 3) Reducing salt consumption and salt content in food and replacing trans fats by polyunsaturated fats, and/or restrict the marketing of food and beverage of these products, especially for children (39). Despite the attractiveness of these multisectoral and population-based approaches, implementation in Brazil, like in most countries, has been partial. Recent analyses suggest that, despite improvements in clinical care, the goals set by the United Nations for the year 2030 concerning chronic diseases, including diabetes, will not be reached (40). The inability of the Brazilian government and society, either unaware of the impact of these underlying actors or unable to direct social development in a healthy direction, has produced this major public health failure. The Strategic Action Plans to Tackle Non-Communicable Diseases (NCDs) in Brazil (2011-2022 and 2021-2030) were created to cope with and restrain NCD risk factors in the next 10 years (41,42). However, evidence regarding the effectiveness of its policies remains limited.

This study acknowledges several limitations that are inherent to dealing with modelled and secondary data. First, while Brazilian mortality data is generally reliable, deficiencies in the Brazilian national mortality information system in earlier years of the GBD series add uncertainty to the trends in the mortality and burden metrics we report, especially for the North and Northeast. Second, we were unable to assess trends in specific causes of death among individuals with T2DM because the GBD relies on the underlying cause recorded on death certificates. This means that when T2DM is listed as the cause of death, it is not possible to determine whether it resulted, for example, from cardiovascular disease or other conditions. Third, estimating diabetes prevalence also poses challenges due to its reliance on laboratory data as required by the GBD framework. Being based on only 17 Brazilian studies into models initially oriented by global data, our estimates of prevalence, incidence, and YLDs are especially subject to error. Finally, the assumption that all deaths under the age of 15 are related to T1DM can produce a misclassification bias, and under- or overestimations in T1DM metrics can influence our results, as the non-fatal burden of T2DM is obtained by removing that of T1DM from the total diabetes mellitus.

Nonetheless, a significant strength of our study is the use of up-to-date, internationally comparable disease metrics derived from rigorous and sophisticated GBD analyses to assess the burden and trends of T2DM. By considering the best available epidemiological evidence and controlling for different sources of bias, the wide 95% uncertainty intervals presented in the tables indicate the large degree of uncertainty present. However, it provides a straightforward synthesis of the current T2DM scenario in Brazil, instrumental in guiding the planning, implementation, and evaluation of public policies to mitigate the burden of this condition.

In conclusion, the burden of T2DM in Brazil has significantly increased from 1990 to 2021, most notably

Copyright© AE&M all rights reserved.

in the North and Northeast regions. Addressing disparities requires targeted interventions that improve healthcare access, enhance care integration, and expand educational programs. Unless prevention strategies that address key risk factors such as excessive weight, sedentary behavior and an unhealthy diet are implemented, the burden of T2DM will likely continue to grow at an accelerated pace.

Ethics approval and consent to participate: not applicable.

Consent for publication: not applicable.

Funding: this study used data from IHME, funded by the Gates Foundation. PP Teixeira received a research scholarship from the Brazilian National Council for Scientific and Technological Development (CNPq). BB Duncan and MI Schmidt are investigators of the *Instituto de Avaliação de Tecnologia em Saúde* (IATS), and BB Duncan, MI Schmidt, R Mattiello, F Gerchman, and BNG Goulart received research fellowships from the Brazilian National Council for Scientific and Technological Development (CNPq). T Duque-Cartagena received funding from the Coordination for the Improvement of Higher Education Personnel (CAPES – Financial Code 001). Funders had no role in manuscript design, data collection, data analysis and interpretation, and writing.

Authors' contributions: PPT, LSC, RM, and BBD were responsible for the manuscript's concept, design, and drafting. PPT, TDC, RR, and RM were involved in data acquisition and analysis. All authors were involved in data interpretation and critical review of the manuscript for important intellectual content. RM and BBD were the supervisors and took responsibility for the integrity and accuracy of the data.

Disclosure: no potential conflict of interest relevant to this article was reported.

Availability of data and materials: the data supporting this study's findings are publicly available online for download from the GBD Results Tool (http://ghdx.healthdata.org/gbd-results-tool).

REFERENCES

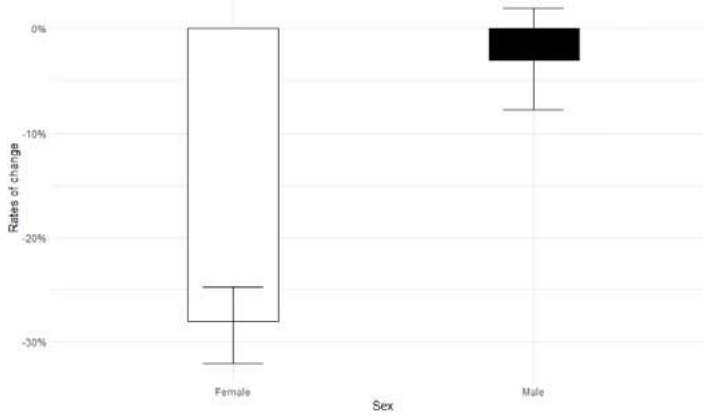
1. Lu X, Xie Q, Pan X, Zhang R, Zhang X, Peng G, et al. Type 2 diabetes mellitus in adults: pathogenesis, prevention and therapy. Signal Transduct Target Ther. 2024;9(1):262. doi: 10.1038/s41392-024-01951-9.
2. Stratton IM, Adler AI, Neil HA, Matthews DR, Manley SE, Cull CA, et al. Association of glycaemia with macrovascular and microvascular complications of type 2 diabetes (UKPDS 35): prospective observational study. Bmj. 2000;321(7258):405-12. doi: 10.1136/bmj.321.7258.405.
3. Worldwide trends in diabetes prevalence and treatment from 1990 to 2022: a pooled analysis of 1108 population-representative studies with 141 million participants. Lancet. 2024;404(10467):2077-93. doi: 10.1016/s0140-6736(24)02317-1.
4. Institute for Health Metrics and Evaluation (IHME). GBD Foresight Visualization Available from: https://vizhub.healthdata.org/gbd-foresight/2024 [cited by May, 2025].
5. Reis R, Duncan BB, Malta DC, Iser BPM, Schmidt MI. Evolution of diabetes in Brazil: prevalence data from the 2013 and 2019 Brazilian National Health Survey. Cad Saude Publica. 2022;38Suppl 1(Suppl 1):e00149321. doi: 10.1590/0102-311x00149321.
6. Malta DC, Bernal RTI, Iser BPM, Szwarcwald CL, Duncan BB, Schmidt MI. Factors associated with self-reported diabetes according to the 2013 National Health Survey. Rev Saude Publica. 2017;51(suppl 1):12s. doi: 10.1590/s1518-8787.2017051000011
7. Telo GH, Cureau FV, Szklo M, Bloch KV, Schaan BD. Prevalence of type 2 diabetes among adolescents in Brazil: Findings from Study of Cardiovascular Risk in Adolescents (ERICA). Pediatr Diabetes. 2019;20(4):389-96. doi: 10.1111/pedi.12828. PubMed PMID: 30737879.
8. Sun P, Wen H, Liu X, Ma Y, Jang J, Yu C. Time trends in type 2 diabetes mellitus incidence across the BRICS from 1990 to 2019: an age-period-cohort analysis. BMC Public Health. 2022;22(1):65. doi: 10.1186/s12889-021-12485-y.
9. Schmidt MI, Duncan BB, Ishitani L, da Conceição Franco G, de Abreu DM, Lana GC, et al. Trends in mortality due to diabetes in Brazil, 1996-2011. Diabetol Metab Syndr. 2015;7:109. doi: 10.1186/s13098-015-0105-5.
10. Florêncio RB, de Araújo Fonseca LG, da Silva VFD, Lima I NDF, Gualdi LP. Diabetes mellitus hospitalization and mortality rate according to a national database in Brazil: a longitudinal study. BMC Public Health. 2021;21(1):403. doi: 10.1186/s12889-021-10438-z.
11. Bracco PA, Gregg EW, Rolka DB, Schmidt MI, Barreto SM, Lotufo PA, et al. A nationwide analysis of the excess death attributable to diabetes in Brazil. J Glob Health. 2020;10(1):010401. doi: 10.7189/jogh.10.010401.
12. Miranda C, Sousa TM, Caldeira TCM, Claro RM. Health risk factors among adult individuals with and without diabetes in Brazil: Vigitel (2020-2023). Public Health. 2024;234:120-5. doi: 10.1016/j.puhe.2024.06.009.
13. Duncan BB, França EB, Passos VMA, Cousin E, Ishitani LH, Malta DC, et al. The burden of diabetes and hyperglycemia in Brazil and its states: findings from the Global Burden of Disease Study 2015. Rev Bras Epidemiol. 2017;20Suppl 01(Suppl 01):90-101. doi: 10.1590/1980-5497201700050008.
14. Bahia LR, da Rosa MQM, Araujo DV, Correia MG, Dos Rosa RDS, Duncan BB, et al. Economic burden of diabetes in Brazil in 2014. Diabetol Metab Syndr. 2019;11:54. doi: 10.1186/s13098-019-0448-4.
15. Stevens GA, Alkema L, Black RE, Boerma JT, Collins GS, Ezzati M, et al. Guidelines for Accurate and Transparent Health Estimates Reporting: the GATHER statement. Lancet. 2016;388(10062):e19-e23. doi: 10.1016/s0140-6736(16)30388-9.
16. Global burden of 288 causes of death and life expectancy decomposition in 204 countries and territories and 811 subnational locations, 1990-2021: a systematic analysis for the Global Burden of Disease Study 2021. Lancet. 2024;403(10440):2100-32. doi: 10.1016/s0140-6736(24)00367-2.
17. Global burden and strength of evidence for 88 risk factors in 204 countries and 811 subnational locations, 1990-2021: a systematic analysis for the Global Burden of Disease Study 2021. Lancet. 2024;403(10440):2162-203. doi: 10.1016/s0140-6736(24)00933-4.
18. Global incidence, prevalence, years lived with disability (YLDs), disability-adjusted life-years (DALYs), and healthy life expectancy (HALE) for 371 diseases and injuries in 204 countries and territories and 811 subnational locations, 1990-2021: a systematic analysis for the Global Burden of Disease Study 2021. Lancet. 2024;403(10440):2133-61. doi: 10.1016/s0140-6736(24)00757-8.
19. Malta DC, de Azeredo Passos VM, Machado IE, Marinho Souza MF, Ribeiro ALP. The GBD Brazil network: better information for health policy decision-making in Brazil. Popul Health Metr. 2020;18(Suppl 1):23. doi: 10.1186/s12963-020-00224-1.
20. Global, regional, and national burden of diabetes from 1990 to 2021, with projections of prevalence to 2050: a systematic analysis for the Global Burden of Disease Study 2021. Lancet. 2023;402(10397):203-34. doi: 10.1016/s0140-6736(23)01301-6.

Copyright© AE&M all rights reserved.

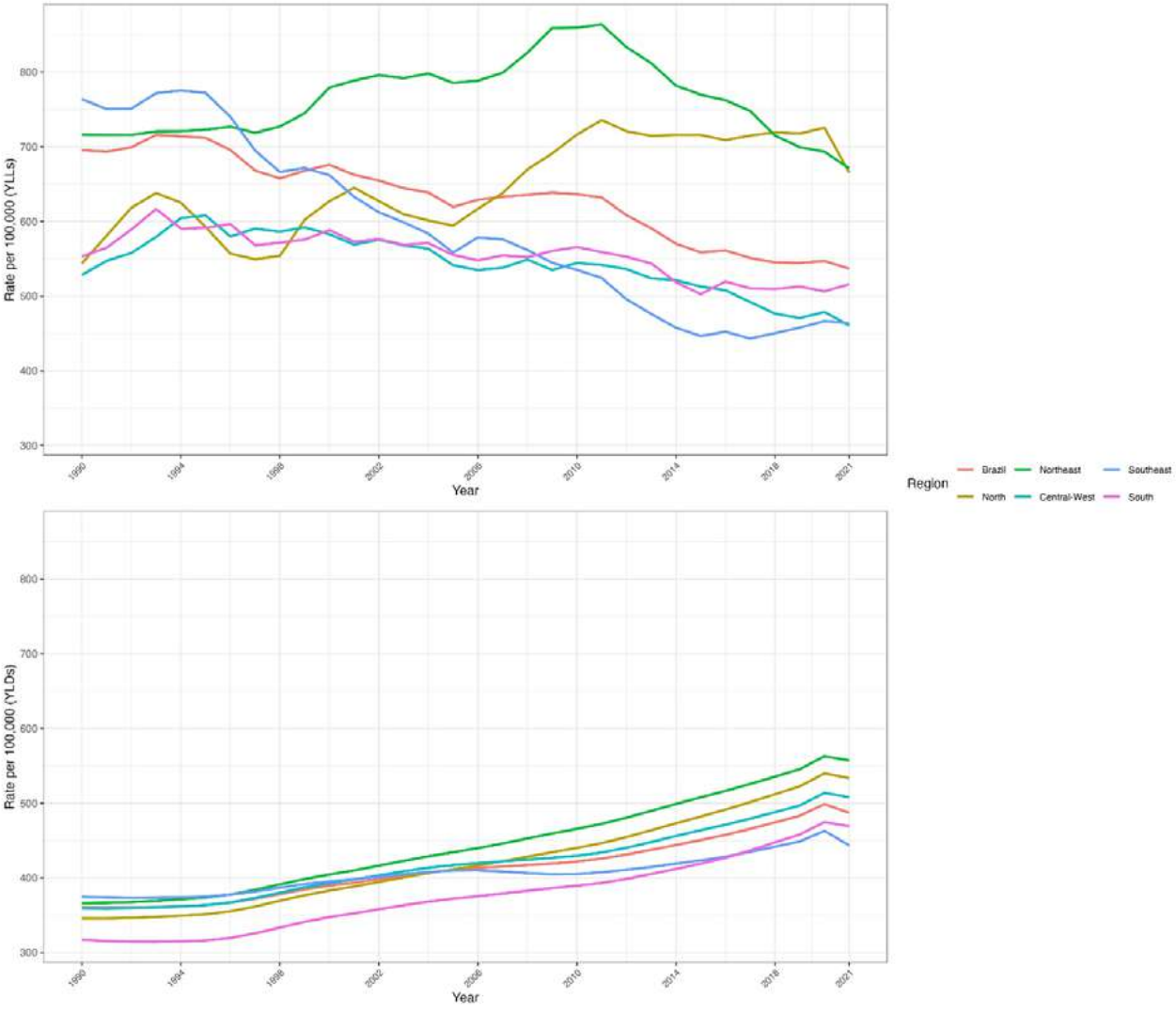
21. Salomon JA, Haagsma JA, Davis A, de Noordhout CM, Polinder S, Havelaar AH, et al. Disability weights for the Global Burden of Disease 2013 study. Lancet Glob Health. 2015;3(11):e712-23. doi: 10.1016/s2214-109x(15)00069-8.
22. Pan American Health Organization (PAHO). The burden of diabetes mellitus in the Region of the Americas, 2000–2019. Washington (DC): Pan American Health Organization; 2021.
23. International Diabetes Federation (IDF). IDF Diabetes Atlas. 10th ed. Brussels: International Diabetes Federation; 2021. Available from: www.diabetesatlas.org.
24. Global age-sex-specific mortality, life expectancy, and population estimates in 204 countries and territories and 811 subnational locations, 1950-2021, and the impact of the COVID-19 pandemic: a comprehensive demographic analysis for the Global Burden of Disease Study 2021. Lancet. 2024;403(10440):1989-2056. doi: 10.1016/s0140-6736(24)00476-8.
25. Hone T, Saraceni V, Medina Coeli C, Trajman A, Rasella D, Millett C, et al. Primary healthcare expansion and mortality in Brazil's urban poor: A cohort analysis of 1.2 million adults. PLoS Med. 2020;17(10):e1003357. doi: 10.1371/journal.pmed.1003357.
26. Pimenta L, Dutra VGP, de Castro ALB, Guimarães RM. Analysis of conditions sensitive to primary care in a successful experience of primary healthcare expansion in Brazil, 1998-2015. Public Health. 2018;162:32-40. doi: 10.1016/j.puhe.2018.05.011.
27. Silva RM, Caetano R. "Farmácia Popular do Brasil" Program: characterization and evolution between 2004 and 2012. Cien Saude Colet. 2015;20(10):2943-56. doi: 10.1590/1413-812320152010.17352014.
28. Instituto Brasileiro de Geografia e Estatística (IBGE). Síntese de indicadores sociais: uma análise das condições de vida da população brasileira: 2021. Rio de Janeiro: IBGE; 2021.
29. Gaspar RS, Rossi L, Hone T, Dornelles AZ. Income inequality and non-communicable disease mortality and morbidity in Brazil States: a longitudinal analysis 2002-2017. Lancet Reg Health Am. 2021;2:100042. doi: 10.1016/j.lana.2021.100042.
30. Neves RG, Saes MO, Duro SMS, Flores TR, Tomasi E. Inequalities in care for the people with diabetes in Brazil: A nationwide study, 2019. PLoS One. 2022;17(6):e0270027. doi: 10.1371/journal.pone.0270027.
31. Leitão VBG, Andrade LG, Bacurau AGM, Assumpção D, Francisco P. [Diabetes mellitus: complications associated with time since diagnosis, health insurance, use of health services, and medication use, Brazilian National Health Survey 2019]. Cad Saude Publica. 2025;41(5):e00106624. doi: 10.1590/0102-311xpt106624.
32. Barone MTU, Harnik SB, de Luca PV, Lima BLS, Wieselberg RJP, Ngongo B, et al. The impact of COVID-19 on people with diabetes in Brazil. Diabetes Res Clin Pract. 2020;166:108304. doi: 10.1016/j.diabres.2020.108304.
33. Louzada M, Cruz GLD, Silva K, Grassi AGF, Andrade GC, Rauber F, et al. Consumption of ultra-processed foods in Brazil: distribution and temporal evolution 2008-2018. Rev Saude Publica. 2023;57:12. doi: 10.11606/s1518-8787.2023057004744.
34. Touvier M, da Costa Louzada ML, Mozaffarian D, Baker P, Juul F, Srour B. Ultra-processed foods and cardiometabolic health: public health policies to reduce consumption cannot wait. Bmj. 2023;383:e075294. doi: 10.1136/bmj-2023-075294.
35. Carlin A, Perchoux C, Puggina A, Aleksovska K, Buck C, Burns C, et al. A life course examination of the physical environmental determinants of physical activity behaviour: A "Determinants of Diet and Physical Activity" (DEDIPAC) umbrella systematic literature review. PLoS One. 2017;12(8):e0182083. doi: 10.1371/journal.pone.0182083.
36. Bowe B, Xie Y, Li T, Yan Y, Xian H, Al-Aly Z. The 2016 global and national burden of diabetes mellitus attributable to PM(2·5) air pollution. Lancet Planet Health. 2018;2(7):e301-e12. doi: 10.1016/s2542-5196(18)30140-2.
37. Trasande L, Zoeller RT, Hass U, Kortenkamp A, Grandjean P, Myers JP, et al. Estimating burden and disease costs of exposure to endocrine-disrupting chemicals in the European union. J Clin Endocrinol Metab. 2015;100(4):1245-55. doi: 10.1210/jc.2014-4324.
38. de Paula LCP, Alves C. Food packaging and endocrine disruptors. J Pediatr (Rio J). 2024;100 Suppl 1(Suppl 1):S40-s7. doi: 10.1016/j.jped.2023.09.010.
39. World Health Organization (WHO). Global report on diabetes [Internet]. Geneva: World Health Organization; 2016 [cited 2024 Nov 22]. 83 p. Available from: https://iris.who.int/handle/10665/204871.
40. Malta DC, Gomes CS, Veloso GA, Teixeira RA, Felisbino Mendes MS, Brant LCC, et al. Noncommunicable disease burden in Brazil and its states from 1990 to 2021, with projections for 2030. Public Health. 2024;236:422-9. doi: 10.1016/j.puhe.2024.09.006.
41. Ministério da Saúde. Plano de ações estratégicas para o enfrentamento das doenças crônicas não transmissíveis (DCNT) no Brasil 2011-2022. Brasília, DF: Secretaria de Vigilância em Saúde. Ministério da Saúde, 2011.
42. Ministério da Saúde. Plano de Ações Estratégicas para o enfrentamento das doenças crônicas não transmissíveis no Brasil (2021-2030). Brasília, DF: Secretaria de Vigilância em Saúde. Ministério da Saúde, 2021.

Copyright© AE&M all rights reserved.

SUPPLEMENTARY MATERIALS



Supplementary Figure 1. Rate of change in age-standardized mortality attributed to T2DM in Brazil, according to sex, from 1990 to 2021.



Supplementary Figure 2. Years of life lost (YLL) and Years Lived with Disability (YLD) due to T2DM in Brazil and its macro-regions. The lines represent age-standardized YLL and YLDs rates per 100,000 habitants from 1990 to 2021.

Copyright© ACE&M all rights reserved.

Archives of Endocrinology and Metabolism
ISSN 2359-4292
OFFICIAL JOURNAL OF THE BRAZILIAN SOCIETY OF ENDOCRINOLOGY AND METABOLISM

original

Diabetic peripheral neuropathy in type 2 diabetes: prevalence and associated factors in Midwest Brazil

Lorrany Campos de Queiroz Melo[1]
https://orcid.org/0009-0003-7880-9117

Augusto Baumgart de Liz[2]
https://orcid.org/0009-0006-1398-5883

João Gabriel Guimarães Luz[1]
https://orcid.org/0000-0003-0274-732X

Gleyson Souza da Costa[2]
https://orcid.org/0000-0003-2488-6910

Josiane Neves Coelho Marques[2,3]
https://orcid.org/0009-0005-7330-7171

Adriana Santi[1]
https://orcid.org/0000-0002-3681-5899

Matheus Eduardo Soares[2]
https://orcid.org/0000-0002-4683-0646

Arthur Emílio Leite de Figueiredo[3]
https://orcid.org/0009-0008-0586-1471

Adriana Marilia Zanato Teruel[2]
https://orcid.org/0000-0001-8869-9853

Luiz F. Viola[3]
https://orcid.org/0000-0003-1167-7933

[1] Programa de Pós-graduação em Biociências e Saúde, Universidade Federal de Rondonópolis, Rondonópolis, MT, Brasil
[2] Curso de Medicina, Universidade Federal de Rondonópolis, Rondonópolis, MT, Brasil
[3] Centro de Diabetes e Endocrinologia de Rondonópolis, Rondonópolis, MT, Brasil

ABSTRACT

Objective: This study investigated the prevalence and factors associated with diabetic peripheral neuropathy (DPN) among adults with type 2 diabetes mellitus (T2DM) attending a referral center in Midwest Brazil. **Subjects and methods:** This cross-sectional study included 276 patients with T2DM, categorized into DPN and non-DPN groups. DPN was assessed using the Neuropathy Disability Score. Sociodemographic and lifestyle data were collected via structured interviews, whereas clinical and laboratory data were obtained from medical records. **Results:** DPN prevalence was 64.5% (95% CI: 58.9%–70.1%). Among those affected, most were female (59.0%), aged over 67 years old (37.7%), living with diabetes for more than 10 years (52.3%). Poor glycemic control and a sedentary lifestyle were observed in 78.9% and 85.4% of participants, respectively. In multivariable analysis, male sex (PR = 1.32; 95% CI: 1.12–1.56), retirement/inactivity (PR = 1.43; 95% CI: 1.11–1.85), T2DM duration >10 years (PR = 1.22; 95% CI: 1.03–1.44), sedentary lifestyle (PR = 1.34; 95% CI: 1.02–1.76), peripheral arterial disease (PR = 1.25; 95% CI: 1.08–1.46), and prior acute myocardial infarction (PR = 1.21; 95% CI: 1.01–1.45) were independently associated with higher DPN prevalence. **Conclusion:** DPN was highly prevalent among patients with T2DM. Particular attention should be directed toward men, older adults, individuals with long-standing diabetes, and those with cardiovascular comorbidities. Promoting regular physical activity and comprehensive management of cardiovascular risk factors may help prevent disease progression and related complications.

Keywords: Type 2 diabetes mellitus; peripheral neuropathy; prevalence; risk factors; cardiovascular disease

INTRODUCTION

Type 2 diabetes mellitus (T2DM) is a chronic disease of high global prevalence, affecting approximately 828 million people in 2022, with a diagnostic frequency of 10.2% in the Brazilian population (1). Diabetic neuropathy is the most prevalent microvascular complications, affecting more than 50% of patients over the course of the disease, commonly presenting as diabetic peripheral neuropathy (DPN) (2).

Received on Oct/27/2025
Accepted on Mar/9/2026

DOI: 10.20945/2359-4292-2026-0053

Correspondence to:
Adriana Santi
Programa de Pós-graduação
em Biociências e Saúde,
Universidade Federal de Rondonópolis.
Av. dos Estudantes, 5055, Cidade Universitária
78736-900 – Rondonópolis, MT, Brasil
santi@ufr.edu.br

Associated editor:
Simone van de Sande Lee
https://orcid.org/0000-0002-5592-1603

This is an open-access article distributed under the terms of the Creative Commons Attribution License

Progressive degeneration of sensory neurons predisposes individuals to multiple adverse outcomes that negatively impact their quality of life, including pain-related physical disability, ulcers, infections, and lower-limb amputations. These complications can also lead to mood disorders, sleep impairment, and reduced work performance, resulting in a significant psychological, social, and physical burden (3,4).

DPN prevalence vary widely, from 1% to 80% across countries, reflecting differences in diagnostic criteria, assessment methods, patient age, diabetes duration, and presence of comorbidities (3-6). Studies show that Africa and South and Central America have some of the highest DPN prevalence. Associated risk factors include advanced age (> 70 years), longer duration of diabetes, poor glycemic control, metabolic syndrome (obesity, hypertension, low HDL-c, hypertriglyceridemia), sedentary lifestyle, smoking, and alcohol

Copyright© AE&M all rights reserved.

consumption (4-8). Importantly, DPN can be prevented or delayed by adequate glycemic control and lifestyle changes targeting modifiable risk factors (2,9).

In Midwest Brazil, few studies have evaluated the prevalence and factors associated with this complication at secondary care settings. Dutra and cols. (10) investigated risk factors for foot ulceration among 117 patients with diabetes treated in outpatient units of three public hospitals in the Federal District; however, foot ulcers represent a DPN progression. Similarly, Reis and cols. (11) evaluated predictive factors for DPN in a small sample of 111 older patients followed at a primary health unit in the same state.

Muzy and cols. (12) conducted a comprehensive analysis to assess the prevalence of diabetes and its complications, and the characteristics of diabetes care in Brazil, using data from three national surveys: the National Survey of Health, the Primary Care Access and Quality Improvement Program, and the Popular Pharmacy Program. The authors found that neuropathy was the most prevalent diabetes-related complication nationwide, that only 30% of patients underwent foot examinations, and that the Midwest had the second-highest neuropathy incidence (3,114.7 cases per 100,000 inhabitants), second only to the Southeast (3,496.0 per 100,000).

Despite these findings, none of these studies directly examined the factors associated with DPN, even though identifying such determinants is crucial to improve preventive strategies and optimize disease management within public health systems (13). Accordingly, this study investigated the prevalence and associated factors of DPN among individuals with T2DM treated at a referral center in Midwest Brazil.

SUBJECTS AND METHODS

This cross-sectional study involved a sample of patients receiving care at a referral health service in the municipality of Rondonópolis, Mato Grosso, Midwestern Brazil, between August 2021 and December 2023. Sample size was estimated with Epi Info software, version 7.2.6.0 (Centers for Disease Control and Prevention, Atlanta, GA, USA), considering a population size of 1,464 individuals, corresponding to the annual number of patients with T2DM assisted at the studied referral health service. A 5% significance level, a 95% confidence interval (95% CI), and an expected 31.5% DPN prevalence were adopted, based on a meta-analysis by Sun and cols. (14) conducted with individuals with T2DM. These parameters resulted in a minimum required sample size of 270 participants.

Participants were invited to join the study while in the waiting room prior to their appointments. Adult patients (≥ 18 years), both males and females, with a diagnosis of T2DM confirmed in their medical records were eligible. Participants who agreed to participate in the study voluntarily signed the informed consent form. Exclusion criteria included presence of lower-limb amputations (at any level), active ulcers, and neurological or psychiatric disordersDPN presence was assessed using the Brazilian version of the Neuropathy Disability Score (NDS), validated by Moreira and cols. (15) and recommended by the Brazilian Diabetes Society (16), after excluding other potential neuropathy causes. NDS shows high sensitivity (89%) and specificity (100%) for evaluating both small and large nerve fibers based on tests of vibratory sensation, thermal sensitivity, superficial pain, and the Achilles reflex. Based on the score, DPN severity was classified as follows: absent (< 3 points), mild (3–5 points), moderate (6–8 points), and severe (≥ 9 points). Individuals with NDS ≥ 3 were considered to have DPN (15). Accordingly, participants were divided into two groups: DPN and non-DPN.

Additionally, the Neuropathic Symptom Score (NSS), Visual Analogue Scale (VAS), and Plantar Protective Sensitivity Test (PPS) were applied to further characterize DPN. NSS evaluated the presence and severity of neuropathic symptoms, classified as absent (0–2 points), mild (3–4 points), moderate (5–6 points), or severe (≥ 7 points) [14]. VAS assessed self-reported pain intensity, categorized as absent (0), mild (1–2 points), moderate (3–7 points), or severe (≥ 8 points) (17). PPS was assessed using the Semmes–Weinstein 10 g monofilament and categorized according to Feng, Schlosser, and Sumpio (18) as follows: present (preserved sensitivity), reduced (partial sensitivity at some points), or absent (no perception of the tactile stimulus). All neurological tests and foot examinations were performed bilaterally, in a private setting, by a previously trained research team.

Copyright© AE&M all rights reserved.

Sociodemographic and lifestyle data were collected using a semi-structured questionnaire administered individually and in a private setting by trained members of the research team. Variables included sex (male or female); age group (≤ 59 years, 60–67 years, or > 67 years); self-reported race/skin color (white/yellow or black/mixed-race/indigenous); marital status (with a partner — married or in a stable union — or without a partner — single, widowed, or divorced); schooling level (0–7 years: illiterate or incomplete middle school; ≥ 8 years: complete middle school, incomplete or complete high school, or higher education); work status (active or retired/inactive); current smoking; nutritional therapy adherence and sedentary lifestyle.

To assess nutritional status, body mass index (BMI) was calculated as weight (kg) divided by height squared (kg/m²). Weight and height data were obtained from medical records. Based on BMI values, patients were classified as underweight/eutrophic (BMI < 25 kg/m²), overweight (BMI ≥ 25 and < 30 kg/m²), or obese (BMI ≥ 30 kg/m²), according to the World Health Organization (19).

Clinical variables were obtained from medical records, including diabetes duration (≤ 10 or > 10 years), glycemic control, and treatment regimen (use of oral antidiabetic drugs and/or insulin therapy). Glycemic control was considered adequate when HbA1c < 7.0%, according to the American Diabetes Association (20). Presence of comorbidities and complications was investigated, including systemic arterial hypertension, dyslipidemia, myocardial infarction (MI), ischemic stroke, peripheral arterial disease (PAD), retinopathy, and diabetic kidney disease (DKD).

Statistical analyses were conducted using Stata 16.1 (StataCorp LLC, College Station, TX, USA) and RStudio 2024.04.2 (R Foundation for Statistical Computing, Vienna, Austria). First, a univariate analysis was conducted to describe the absolute and relative frequencies of the explanatory variables in relation to the outcome (DPN presence). Chi-squared tests assessed differences in distributions. For laboratory parameters, data non-normality was verified by Shapiro–Wilk test. As the variables did not follow a normal distribution, results were expressed as medians and minimum–maximum values, and comparisons between groups were performed using the Mann–Whitney U test.

Next, a Poisson's multiple generalized linear model (GLM) with a logarithmic link function and robust variance was fitted to model DPN occurrence as a function of potential predictors. The multivariate analysis only included variables with a $p < 0.20$ in the univariate analysis. Notably, laboratory parameters were excluded from the model due to vast missing information. Variable selection followed the stepwise forward method, and the Akaike Information Criterion (AIC) evaluated the impact of including each predictor on the final model. Variables with p-value < 0.05 were considered significantly associated with the outcome.

Magnitude of associations was estimated using prevalence ratio (PR) and its corresponding 95% CI in both univariate and multivariate analyses. This measure was adopted to avoid overestimating associations in conditions of high outcome prevalence, as recommended by Tamhane and cols. (21) for cross-sectional studies.

This study was approved by the Human Research Ethics Committee of the Federal University of Rondonópolis, Mato Grosso, Brazil (CAAE no. 47720421.6.0000.0126). All participants provided written informed consent prior to participation.

RESULTS

Of the 285 patients initially evaluated, nine were excluded: seven due to recent or previous amputation, one due to cognitive impairment, and one due to a neurodegenerative disorder. Our final sample therefore comprised 276 patients.

Of these, 178 were diagnosed with DPN corresponding to a 64.5% prevalence (95% CI, 58.9%–70.1%). **Table 1** presents the distribution of participants according to DPN status, sociodemographic variables, nutritional status, and lifestyle habits. Most DPN patients were female (59.0%), aged over 67 years (37.7%), and those who self-identified as Black, Mixed-race, or Indigenous (71.9%). Most participants reported having a partner (59.6%), tertiary education (61.2%), and being retired or unemployed (81.5%). A total of 77 patients (43.3%) had obesity, and most reported adherence to nutritional guidance (78.1%).

Copyright© ALE&M all rights reserved.

Sedentary lifestyle exhibited high frequency (85.4%) and 8.4% reported smoking.

Compared with non-DPN individuals, DPN patients differed significantly by sex (p = 0.006), age group (p = 0.009), schooling level (p = 0.033), employment status (p = 0.002), and sedentary lifestyle (p = 0.026) (**Table 1**).

Regarding neuropathy characteristics, 158 patients (88.7%) reported experiencing symptoms, and 151 (84.8%) self-reported pain. As shown in **Figure 1**, the study sample exhibited a moderate degree of neuropathy, with moderately intense symptoms and neuropathic pain. Protective plantar sensitivity was absent in over one-third of DPN patients (n = 65; 36.5%).

Table 1. Participants distribution according to DPN and sociodemographic variables, nutritional status, and lifestyle habits

Variable	DPN				p	PR	95% CI
	No		Yes				
	n	%	n	%			
Sex							
Female	74	75.5	105	59.0	0.006*	Ref.	-
Male	24	24.5	73	41.0		1.28	1.08 - 1.52
Age category (years)[a]							
≤ 59	47	48.0	54	30.3	0.009*	Ref.	-
59 -| 67	28	28.6	57	32.0		1.25	0.99 - 1.59
> 67	23	23.4	67	37.7		1.39	1.12 - 1.73
Race/color							
White/yellow	35	35.7	50	28.1	0.189	Ref.	-
Black/mixed-race/indigenous	63	64.3	128	71.9		1.14	0.93 - 1.40
Marital status							
Without partner	48	49.0	72	40.4		1.13	0.94 - 1.36
With partner	50	51.0	106	59.6	0.171	Ref.	-
Schooling years							
0-7	51	52.0	69	38.8	0.033*	1.21	1.01 - 1.46
≥8	47	48.0	109	61.2		Ref.	-
Employment status							
Retired or inactive	63	64.3	145	81.5	0.002*	1.44	1.11 - 1.87
Active	35	35.7	33	18.5		Ref.	-
Nutritional status[b]							
Underweight or normal weight	16	16.3	35	19.6	0.791	Ref.	-
Overweight	38	38.8	66	37.1		0.92	0.73 - 1.17
Obesity	44	44.9	77	43.3		0.93	0.74 - 1.17
Nutritional therapy							
No	25	25.5	39	21.9	0.498	0.93	0.75 - 1.16
Yes	73	74.5	139	78.1		Ref.	-
Sedentary lifestyle							
No	25	25.5	26	14.6	0.026*	Ref.	-
Yes	73	74.5	152	85.4		1.33	1.00 - 1.76
Smoking							
No	85	89.5	163	91.6	0.567	Ref.	-
Yes	10	10.5	15	8.4		0.92	0.65 - 1.27
Don't know/didn't answer	3	-	-	-		-	-

DPN: diabetic peripheral neuropathy; PR: prevalence ratio; 95% CI: 95% confidence interval.
*Significant at p < 0.05. Chi-squared test.
[a] Defined according to tertile distribution.
[b] Defined from Body Mass Index calculation.

Copyright© AE&M all rights reserved.

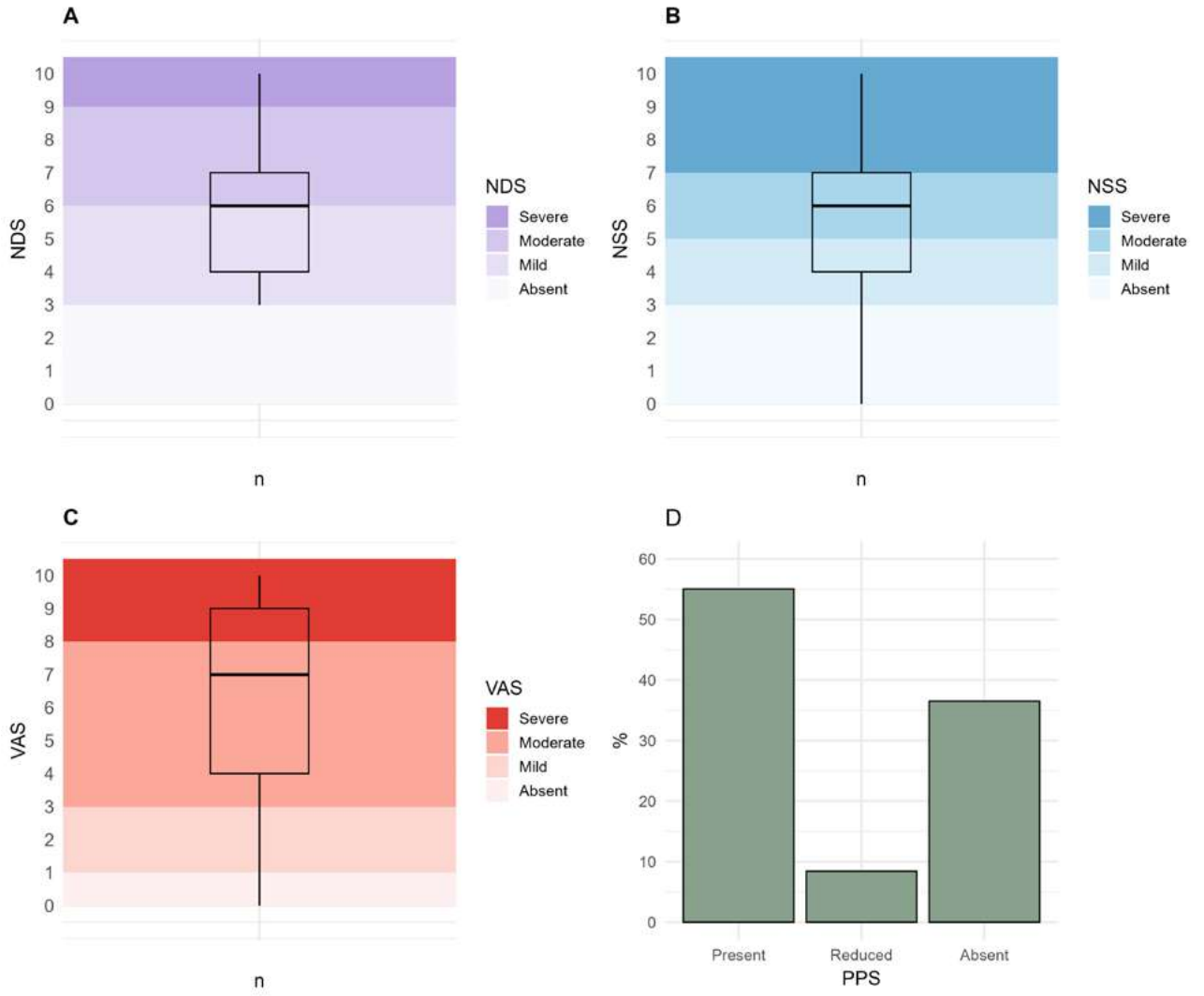


Figure 1. Participants distribution according to DPN characteristics. (**A**) Neuropathy Disability Score (NDS); (**B**) Neuropathy Symptom Score (NSS); (**C**) Visual Analogue Scale (VAS); and (**D**) Plantar Protective Sensation (PPS). Panels A, B, and C are expressed as median values.

Table 2 presents the distribution of participants according to DPN status and clinical variables. Most DPN patients had a diabetes duration longer than 10 years (52.3%), were using insulin (54.5%), and exhibited poor glycemic control (78.9%). Comorbidities presented high prevalence, particularly systemic arterial hypertension (81.5%) and dyslipidemia (82.0%). Among microvascular complications, 73 patients (41.0%) exhibited retinopathy, whereas MI was the most frequent macrovascular complication, occurring in 29 DPN patients (16.3%).

In comparing patients with and without DPN, statistically significant differences were observed for MI (p = 0.007), PAD (p = 0.012), and DKD (p = 0.035). Regarding laboratory parameters, DPN patients presented higher serum creatinine levels (**Table 3**).

Table 4 presents the variables that remained significantly associated with DPN after adjusting the final multivariate model. DPN prevalence was 32% higher among male than among female patients (PR = 1.32; 95% CI, 1.12–1.56) and 43% higher among retired or inactive participants compared with those active in the labor market (PR = 1.43; 95% CI, 1.11–1.85).

Moreover, sedentary individuals had a 34% higher DPN prevalence than physically active ones (PR = 1.34; 95% CI, 1.02–1.76). Additional factors associated with DPN included a diabetes duration longer than 10 years (PR = 1.22; 95% CI, 1.03–1.44), presence of PAD (PR = 1.25; 95% CI, 1.08–1.46), and a history of MI (PR = 1.21; 95% CI, 1.01–1.45).

Copyright© ACE&M all rights reserved.

Table 2. Participants distribution according to DPN and clinical variables

Variable	NPD				p	PR	95% CI
	No		Yes				
	n	%	n	%			
DM duration (years)							
< 10	58	59.2	85	47.7	0.069	Ref.	
> 10	40	40.8	93	52.3		1.18	0.99 - 1.40
Glicemic control[a]							
No	73	77.7	135	78.9	0.807	1.03	0.82 - 1.28
Yes	21	22.3	36	21.1		Ref.	
Missing data	4	-	7				
Insulin therapy							
No	47	48.0	81	45.5	0.696	Ref.	
Yes	51	52.0	97	54.5		1.03	0.87 - 1.23
Oral antidiabetic drug							
No	4	4.1	12	6.7	0.366	1.17	0.87 - 1.58
Yes	94	95.9	166	93.3		Ref.	
Systemic arterial hypertension							
No	28	28.6	33	18.5	0.055	Ref.	
Yes	70	71.4	145	81.5		1.25	0.97 - 1.60
Dyslipidemia							
No	17	17.3	32	18.0	0.896	Ref.	
Yes	81	82.7	146	82.0		0.98	0.79 - 1.23
Myocardial infarction							
No	93	94.9	149	83.7	0.007*	Ref.	
Yes	5	5.1	29	16.3		1.39	1.17 - 1.64
Ischemic stroke							
No	93	94.9	162	91.0	0.244	Ref.	
Yes	5	5.1	16	9.0		1.20	0.93 - 1.55
Peripheral arterial disease							
No	97	99.0	163	91.6	0.012*	Ref.	
Yes	1	1.0	15	8.4		1.49	1.28-1.75
Retinopathy							
No	69	70.4	105	59.0	0.060	Ref.	
Yes	29	29.6	73	41.0		1.19	1.00 - 1.41
Diabetic kidney disease							
No	87	88.8	140	78.7	0.035*	Ref.	
Yes	11	11.2	38	21.3		1.26	1.05 - 1.51

DPN: diabetic peripheral neuropathy; PR: prevalence ratio; 95% CI: 95% confidence interval.
*Significant at $p < 0.05$. Chi-squared test.
[a] Adequate glycemic control defined as HbA1c <7%.

Table 3. Comparison of laboratory parameters between non-DPN and DPN participants

Parameter	DPN		p
	No	Yes	
FBG (mg/dL) (n=258)	148 (127–196)	159 (120.5–218.5)	0.498
HbA1c (%) (n=265)	8.4 (7.3–10.2)	8.4 (7.2–10.2)	0.953
TC (mg/dL) (n=243)	169.5 (140.5–198.7)	174.0 (139.5–206.9)	0.391
LDL (mg/dL) (n=259)	88.5 (64.59–117.4)	86.2 (60.75–123.0)	0.842
Creatinine (mg/dL) (n=263)	0.8 (0.7–0.99)	0.97 (0.79–1.3)	0.001*
Vitamin B12 (pg/mL) (n=182)	399.0 (336.0–515.0)	456.4 (292.0–658.3)	0.460

DPN: diabetic peripheral neuropathy; FBG: fasting blood glucose; HbA1c: glycated hemoglobin; TC: total cholesterol; LDL: low-density lipoprotein. Results expressed as median (25th–75th percentiles).
*Significant at $p < 0.05$. Mann–Whitney U test.

Copyright© AE&M all rights reserved.

Table 4. DPN-associated factors among individuals treated at a reference center. Midwest, Brazil

Variable	p	Adjusted[a] PR	95% CI
Male sex	0.001*	1.32	1.12 - 1.56
Retired or inactive	0.006*	1.43	1.11 - 1.85
Sedentary lifestyle	0.034*	1.34	1.02 - 1.76
DM duration > 10 years	0.021*	1.22	1.03 - 1.44
Peripheral arterial disease	0.003*	1.25	1.08 - 1.46
Myocardial infarction	0.037*	1.21	1.01 - 1.45

DPN: Diabetic Peripheral Neuropathy. PR: Prevalence ratio. 95% CI: 95% confidence interval.
*Significant at $p < 0.05$. Poisson Regression.
[a]Adjusted for: sex, employment status, sedentary lifestyle, duration of diabetes, peripheral arterial disease, and history of myocardial infarction.

DISCUSSION

Diabetic Peripheral neuropathy (DPN) is a serious diabetes complication, contributing to lower-limb amputations, disabling neuropathic pain, and increased mortality (22-24). Herein, were identified several independent factors associated with this condition, including male sex, retirement or inactivity, longer duration of diabetes, sedentary lifestyle, PAD, and a history of MI. These findings highlight the multifactorial nature of DPN in T2DM patients treated at a referral center in Midwest Brazil.

DPN prevalence was 64.5% (95% CI, 58.9%–70.1%), higher than the prevalence reported in a recent systematic review and meta-analysis which estimated a 46.5% rate (95% CI, 38.0%–55.0%) in Latin America and the Caribbean (25). Referral bias may partially explain this higher rate, as patients with more severe or complex complications are more likely to receive care at referral centers. Additional contributing factors may include the older age and longer diabetes duration observed among the study participants.

Regarding disease characteristics, 88.7% of patients reported DPN symptoms, indicating a moderate degree of neuropathy. Of the total sample, 84.8% reported pain (**Figure 1**), a frequency higher than that reported by Li and cols. (26) who found that 57.2% of patients experience painful DPN. In literature, painful DPN is associated with depression (27), reduced quality of life (28,29), a greater number of comorbidities, and increased healthcare costs (30).

In the present study, male sex was significantly associated with a higher DPN prevalence (PR = 1.32; 95% CI, 1.12–1.56), a finding consistent with previous reports (31-33). Similarly, Aaberg and cols. (34) observed that men with diabetes developed neuropathic complications at an earlier age (approximately 63 years) than their female counterparts (around 67 years). This finding is further supported by Abraham and cols. (35), who reported more severe electrophysiological abnormalities in men with diabetes, regardless of the degree of polyneuropathy.

As for sex-related differences, women tend to experience more intense neuropathic symptoms, particularly pain (35), which is also the most common reason for seeking medical care (36). Taken together, these findings underscore the importance of considering sex-specific factors in DPN evaluation and management. Targeted screening and preventive strategies should prioritize older male patients with diabetes to delay the onset of neuropathic complications and reduce associated morbidity.

In our study, DPN patients were older (> 67 years) and had a longer diabetes duration (>10 years). Longer T2DM duration is associated with prolonged exposure to chronic hyperglycemia, which intensifies its deleterious effects on multiple organ systems (37). Consistent with previous studies (2,8,11,38-40), were observed a significant association between longer diabetes duration and DPN (PR = 1.22; 95% CI, 1.03–1.44). Although a nonmodifiable risk factor, diabetes duration remains an essential indicator for early detection and timely management of DPN (41).

No significant association was observed between insulin therapy or glycemic control and DPN presence. Nonetheless, 54.5% of patients were using insulin, despite 78.9% achieving inadequate glycemic control. Insulin therapy is often regarded as a marker of long-standing or difficult-to-control T2DM (40).

Copyright© AE&M all rights reserved.

Conversely, maintaining optimal glycemic control may help delay DPN progression in T2DM patients, although the evidence supporting this association is stronger in T1DM patients (42).

DPN prevalence was 43% higher among retired or inactive participants compared with those who were economically active (PR = 1.43; 95% CI, 1.11–1.85). Despite limited evidence regarding the association between DPN and employment or retirement status in literature, this finding may reflect the combined effects of advanced age and longer disease duration. According to the Brazilian social security legislation, retirement typically occurs around the age of 60 years or older (43), reinforcing the plausibility of this observation (8,44).

Salih and cols. (45) reported that patients aged ≥ 60 years were 4.47 times more likely to present DPN than those aged 40 (95% CI, 2.40–8.35). The authors attributed this multifactorial association to the combined effects of prolonged diabetes duration such as chronic hyperglycemia, comorbidities, vascular and physiological changes that come with the aging process.

Sedentary lifestyle remained significantly and independently associated with DPN after multivariate analysis (**Table 4**). Similarly, Abdissa and cols. (40), in a study conducted at a university hospital in Ethiopia, reported that physically inactive patients with diabetes were 2.02 times more likely to develop DPN than those who were physically active (OR, 2.02; 95% CI, 1.14–3.55). Likewise, Salih and cols. (45) found that physically inactive individuals with T2DM were 1.69 times more likely to develop DPN compared with physically active (95% CI, 1.14–2.49).

Data from the Vigitel survey (1) indicated a 32.2% (95% CI: 29.5–34.9) prevalence of physical activity among individuals aged 65 years and older. In contrast, 85.4% of patients with DPN reported a sedentary lifestyle, revealing a markedly higher prevalence in this sample. Similarly, Nolan and cols. (46), who investigated self-reported physical activity levels in T2DM patients aged 33 to 88 years, also observed that individuals with DPN were less physically active than those without DPN.

Positive impacts have been reported from lifestyles that include physical activities and moderate intensity exercise, as well as those focused on flexibility, balance, and range of motion. Such practices have shown beneficial effects for individuals living with T2DM and DPN, including improvements in metabolic profile and microvascular circulation. These effects are associated with the release of neuroprotective factors that attenuate oxidative stress and promote the increase or regeneration of cutaneous nerve fibers, contributing to the reduce neuropathic pain symptoms and, consequently, to improved quality of life (2,3, 47-51).

Diabetes alone significantly increases the cardiovascular risk (CVR) of patients by approximately two- to fourfold when compared with individuals without the disease (52). Moreover, recent evidence suggests that DPN presence is associated with an additional CVR elevation (53). High frequencies of CVR factors were identified: systemic arterial hypertension (81.5%), dyslipidemia (82.0%), and obesity (43.3%). Despite no direct association between these risk factors and DPN, results revealed significant associations with two cardiovascular complications: PAD and previous MI. DPN prevalence was 25% higher among patients with PAD and 21% higher among those with a history of MI compared with individuals without these complications (PR = 1.25; 95% CI: 1.08–1.46 and PR = 1.21; 95% CI: 1.01–1.45, respectively).

Consistent with our findings, Pfannkuche and cols. (8) revealed an independent association between PAD and DPN (OR = 1.81; 95% CI: 1.07–3.08). This coexistence exacerbates vascular dysfunction, thereby increasing the risk of complications like foot ulcers and amputations (54). Conversely, a previous nonfatal MI, a major adverse cardiovascular event, represents an additional warning sign regarding the clinical condition of these patients and highlights the need for rigorous management of lipid, blood pressure, and glycemic parameters through both pharmacological therapy and lifestyle changes (19,54,55).

A previous study conducted in London involving 13,043 patients recorded 399 nonfatal cardiovascular events. After adjusting for confounding factors, DPN was associated with a higher incidence of these events among patients with diabetes, with a hazard ratio (HR) of 1.33 (95% CI: 1.02–1.75) (56). Similarly, in a systematic review focused on patients newly diagnosed with

Copyright© AE&M all rights reserved.

T2DM, Aikaeli and cols. (57) reported a prevalence of 7% for MI and rates ranging from 1% to 27% for ischemic heart disease among macrovascular complications. These findings underscore the importance of an early diagnosis of T2DM and its complications, given the often silent progression of the disease and the detrimental impact of delayed diagnosis and treatment on patients' quality of life.

Study limitations include its cross-sectional design, which precludes causal inference, and the use of convenience sampling, which may limit generalizing our findings to the broader population with diabetes. Additionally, data on lifestyle habits were self-reported, which may have led participants to provide socially desirable answers. The high DPN prevalence observed in the study sample may be partially explained by referral bias, as a greater number of patients with complications are typically referred to specialized services. Another important limitation concerns the considerable missing information in medical records regarding laboratory parameters, which prevented a more detailed analysis of their association with DPN and underscored the need for improved documentation of patient clinical data.

As for strengths, we highlight its contribution to expanding knowledge on factors associated with DPN in a municipality in Midwest Brazil, where few investigations on this topic have been conducted. Moreover, the present results may enhance national understanding of diabetic peripheral neuropathy, contributing to public policies and health education in the comprehensive care of Brazilian patients.

CONCLUSION

DPN was highly prevalent in the study sample, highlighting the urgent need for systematic screening programs focused on early detection and timely initiation of appropriate treatment, as recommended by international reference institutes. Investing in diagnostic equipment and professional training for implementing screening tests, particularly in primary care settings where most patients with T2DM are initially diagnosed, could substantially improve early DPN identification.

Regarding risk factors, greater attention should be directed toward male and older individuals, those with long-standing diabetes, and patients with a history of cardiovascular disease. Lifestyle modification and strict control of cardiovascular risk factors should be strongly encouraged among DPN patients. In this regard, educational initiatives focusing on T2DM management and foot care can help minimize the risk of major complications. Moreover, conducting longitudinal studies can help guide more effective prevention and management strategies of diabetic peripheral neuropathy.

Acknowledgments: to the Municipal Health Department of Rondonópolis–MT and the CEDERO team for enabling data collection. To the patients who consented to participate in this research. To UFR, CNPq, and FAPEMAT undergraduate research scholarships.

Funding: the authors declare that no financial support was received.

Author's contributions: conception and design: AS, AELF. Analysis and interpretation: AS, LCQM, JGGL. Data collection: LCQM, GSC, MES, AMZT, ABL, JNCM. Writing the article: AS, LCQM. Critical revision of the article: AS, LFCV. Final approval of the article: AS, LFCV. Statistical analysis: JGGL. Overall responsibility: AS.

Disclosure: no potential conflict of interest relevant to this article was reported.

Data availability: datasets related to this article will be available upon request to the corresponding author.

REFERENCES

1. Brasil. Ministério da Saúde. Secretaria de Vigilância em Saúde e Ambiente. Departamento de Análise Epidemiológica e Vigilância de Doenças Não Transmissíveis. Vigitel Brasil 2023: vigilância de fatores de risco e proteção para doenças crônicas nas capitais dos 26 estados brasileiros e no Distrito Federal em 2023 [recurso eletrônico]. Brasília: Ministério da Saúde; 2023. Disponível em: http://bvsms.saude.gov.br/bvs/publicacoes/vigitel_brasil_2023.pdf.
2. Pop-Busui R, Boulton AJM, Feldman EL, Bril V, Freeman R, Malik RA, et al. Diabetic neuropathy: a position statement by the American Diabetes Association. Diabetes Care. 2017 Jan;40(1):136-54. doi: 10.2337/dc16-2042.
3. Elafros MA, Kellen C, Nix LM, Callaghan BC. Towards prevention of diabetic peripheral neuropathy: clinical presentation, pathogenesis, and new treatments. Lancet Neurol. 2022 Oct;21(10):922-36. doi: 10.1016/S1474-4422(22)00188-0.
4. Feldman EL, Callaghan BC, Pop-Busui R, Zochodne DW, Wright DE, Bennett DL, et al. Diabetic neuropathy. Nat Rev Dis Primers. 2019 Jun;5(1):41. doi: 10.1038/s41572-019-0092-1.
5. Lu B, Hu J, Wen J, Zhang Z, Zhou L, Li Y, et al. Determination of peripheral neuropathy prevalence and associated factors in Chinese subjects with diabetes and pre-diabetes – Shanghai diabetic neuropathy epidemiology and molecular genetics study (SH-DREAMS). PLoS One. 2013 Apr;8(4):e61053. doi: 10.1371/journal.pone.0061053.
6. Monteiro-Soares M, Santos JV. Diabetes foot-related complications. Brussels (BE): International Diabetes Federation – IDF Atlas Reports; 2022. Disponível em: https://diabetesatlas.org/atlas/diabetic-foot-2022/

Copyright© AE&M all rights reserved.

7. Lu Y, Xing P, Cai X, Luo D, Xu G, Zhang L, et al. Prevalence and risk factors for diabetic peripheral neuropathy in type 2 diabetic patients from 14 countries: estimates of the INTERPRET-DD study. Front Public Health. 2020;8:534372. doi: 10.3389/fpubh.2020.534372.
8. Pfannkuche A, Alhajjar A, Moghadam S, Hamel J, Strom A, Ziegler D. Prevalence and risk factors of diabetic peripheral neuropathy in a diabetics cohort: register initiative "Diabetes and Nerves." Endocr Metab Sci. 2020 Jul;1(1–2):100053. doi: 10.1016/j.endmts.2020.100053.
9. ElSayed NA, Aleppo G, Aroda VR, Bannuru RR, Brown FM, Bruemmer D, et al. Retinopathy, neuropathy, and foot care: Standards of Care in Diabetes – 2023. Diabetes Care. 2023 Jan;46(Suppl 1):S203-S215. doi: 10.2337/dc23-S012.
10. Dutra LMA, Araújo LMS, Ferreira C, de Carvalho RBN, Santos ICRV. Assessment of ulceration risk in diabetic individuals. Rev Bras Enferm. 2018;78(Suppl 2):733-9. doi: 10.1590/0034-7167-2017-0337.
11. Reis IFA, Rocha FC, Lima AEO, Pereira LMC, Oliveira GF, Fernandes BKC. Fatores preditivos da neuropatia diabética em idosos atendidos na atenção primária. Rev Enferm Refer. 2021 Nov;5(7):e20148. doi: 10.12707/rv20148.
12. Muzy J, Campos MR, Emmerick ICM, Silva RS, Schramm JMA. Prevalência de diabetes mellitus e suas complicações e caracterização das lacunas na atenção à saúde a partir da triangulação de pesquisas. Cad Saude Publica. 2021;37(5):e00076120. doi: 10.1590/0102-311X00076120
13. Cheng Y, Cao W, Zhang J, Wang J, Liu X, Wu Q, Lin Q. Determinants of diabetic peripheral neuropathy and their clinical significance: a retrospective cohort study. Front Endocrinol (Lausanne). 2022 Jul 26;13:934020.doi:10.3389/fendo.2022.934020.
14. Sun J, Wang Y, Zhang X, Zhu S, He H. Prevalence of peripheral neuropathy in patients with diabetes: A systematic review and meta-analysis. Prim Care Diabetes. 2020 Oct;14(5):435-444. doi: 10.1016/j.pcd.2019.12.005.
15. Moreira RO, Castro AP, Papelbaum M, Appolinário JC, Ellinger VC, Coutinho WF, et al. Tradução para o português e avaliação da confiabilidade de uma escala para diagnóstico da polineuropatia distal diabética. Arq Bras Endocrinol Metab. 2005 Dec;49(6):944-50. doi: 10.1590/S0004-27302005000600014.
16. Rolim L, Santos AL, Oliveira JEP, Milech A. Diagnóstico e tratamento da neuropatia periférica diabética. Diretriz Oficial da Sociedade Brasileira de Diabetes 2023. doi: 10.29327/557753.2022-14.
17. Cruccu G, Anand P, Attal N, Garcia-Larrea L, Haanpää M, Jørum E, et al. EFNS guidelines on neuropathic pain assessment. Eur J Neurol. 2004 Mar;11(3):153-62. doi: 10.1111/j.1468-1331.2004.00791.x.
18. Feng Y, Schlösser FJ, Sumpio BE. The Semmes Weinstein monofilament examination as a screening tool for diabetic peripheral neuropathy. J Vasc Surg. 2009 Sep;50(3):675-82. doi: 10.1016/j.jvs.2009.05.017.
19. World Health Organization (WHO). *Obesity: preventing and managing the global epidemic: report of a WHO consultation*. Geneva: World Health Organization; 2000 [cited 2025 Oct 17]. Available from: https://iris.who.int/handle/10665/42330.
20. American Diabetes Association. Standards of care in diabetes—2025. Diabetes Care. 2025;48(Suppl 1):S1–S188. doi:10.2337/dc25-SINT.
21. Tamhane AR, Westfall AO, Burkholder GA, Cutter GR. Prevalence odds ratio versus prevalence ratio: choice comes with consequences. Stat Med. 2016 Jul;35(30):5730-5. doi: 10.1002/sim.7059.
22. Sloan G, Selvarajah D, Tesfaye S. Pathogenesis, diagnosis and clinical management of diabetic sensorimotor peripheral neuropathy. Nat Rev Endocrinol. 2021 May;17:400-20. doi: 10.1038/s41574-021-00496-z.
23. Ezzatvar Y, García-Hermoso A. Global estimates of diabetes-related amputations incidence in 2010–2020: a systematic review and meta-analysis. Diabetes Res Clin Pract. 2023 Jan;195:110194. doi: 10.1016/j.diabres.2022.110194.
24. Vági OE, Kolossváry E, Zsóri KS, Fekete BC, Kempler P, Lengyel C, et al. The association between distal symmetric polyneuropathy in diabetes with all-cause mortality: a meta-analysis. Front Endocrinol. 2023;14:1079009. doi: 10.3389/fendo.2023.1079009.
25. Yovera-Aldana M, Velásquez-Rimachi V, Huerta-Rosario A, Palomino R, Maticorena-Quevedo J, Diez-Canseco F, et al. Prevalence and incidence of diabetic peripheral neuropathy in Latin America and the Caribbean: a systematic review and meta-analysis. PLoS One. 2021 May;16(5):e0251642. doi: 10.1371/journal.pone.0251642.
26. Li C, Yang G, Feng Z, Wan L, Wang Z, Wang Y, et al. Prevalence of painful diabetic peripheral neuropathy in type 2 diabetes mellitus and diabetic peripheral neuropathy: a nationwide cross-sectional study in mainland China. Diabetes Res Clin Pract. 2023 Apr;198:110602. doi: 10.1016/j.diabres.2023.110602.
27. D'Amato C, Morganti R, Greco C, Di Gennaro F, Marfia GA, Giacomelli A, et al. Diabetic peripheral neuropathic pain is a stronger predictor of depression than other diabetic complications and comorbidities. Diabetes Vasc Dis Res. 2016 Nov;13(6):418-28. doi: 10.1177/1479164116653240.
28. Ernandes RDC, Tavares DMS, Rodrigues RCM, Nogueira GS, Pimenta CJL. Impact of diabetic neuropathy on quality of life and postural balance in Brazilian older adults. Acta Ortop Bras. 2020 Nov;28(6):275-9. doi: 10.1590/1413-785220202806234529.
29. Borbjerg MK, Dalsgaard EM, Andersen ST, Andersen H, Jørgensen ME, Nielsen JS, et al. Understanding the impact of diabetic peripheral neuropathy and neuropathic pain on quality of life and mental health in 6,960 people with diabetes. Diabetes Care. 2025 Mar;48(4):588-95. doi: 10.2337/dc24-2287.
30. Ebata-Kogure N, Kubo T, Masuda H, Matsushita K, Onishi Y, Takeuchi M, et al. Clinical and economic burdens experienced by patients with painful diabetic peripheral neuropathy: an observational study using a Japanese claims database. PLoS One. 2017 Oct;12(10):e0187250. doi: 10.1371/journal.pone.0187250.
31. Booya F, Bandarian F, Larijani B, Pajouhi M, Nooraei M, Lotfi J. Potential risk factors for diabetic neuropathy: a case control study. BMC Neurol. 2005 Dec 10;5:24. doi: 10.1186/1471-2377-5-24.
32. Gogia S, Rao CR. Prevalence and risk factors for peripheral neuropathy among type 2 diabetes mellitus patients at a tertiary care hospital in coastal Karnataka. Indian J Endocrinol Metab. 2017;21(5):665-669. doi: 10.4103/ijem.IJEM_43_17.
33. Jaiswal M, Divers J, Dabelea D, Isom S, Bell RA, Martin CL, et al. Prevalence of and risk factors for diabetic peripheral neuropathy in youth with type 1 and type 2 diabetes: SEARCH for Diabetes in Youth Study. Diabetes Care. 2017 Sep;40(9):1226-32. doi:10.2337/dc17-0179.
34. Aaberg ML, Burch DM, Hud ZR, Zacharias MP. Gender differences in the onset of diabetic neuropathy. J Diabetes Complications. 2008 Mar-Apr;22(2):83-7. doi: 10.1016/j.jdiacomp.2007.06.009.
35. Abraham A, Barnett C, Katzberg HD, Lovblom LE, Perkins BA, Bril V. Sex differences in neuropathic pain intensity in diabetes. J Neurol Sci. 2018 May;388:103-6. doi: 10.1016/j.jns.2018.03.008.
36. Tesfaye S, Boulton AJM, Dyck PJ, Freeman R, Horowitz M, Kempler P, et al. Painful diabetic peripheral neuropathy: consensus recommendations on diagnosis, assessment and management. Diabetes Metab Res Rev. 2011 Jun;27(7):629-38. doi: 10.1002/dmrr.1225.
37. Vitale M, Gualdani E, Morieri ML, Bianchi C, Bonora E, Cavalot F, et al. Association between age at diagnosis and all-cause mortality in type 2 diabetes: the renal insufficiency and cardiovascular events (RIACE) Italian multicenter study. Acta Diabetol. 2024 May;61:1107-16. doi: 10.1007/s00592-024-02294-1.
38. Cardoso CRL, Salles GF. Predictors of development and progression of microvascular complications in a cohort of Brazilian type 2 diabetic patients. J Diabetes Complications. 2008 May-Jun;22(3):164-70. doi: 10.1016/j.jdiacomp.2007.02.004.
39. Reis de Matos M, Zanella MT, Brandão AP, Campana EMG, Gomes MB. Distal symmetric and cardiovascular autonomic neuropathies in Brazilian individuals with type 2 diabetes followed in a primary health care unit: a cross-sectional study. Int J Environ Res Public Health. 2020 May;17(9):3232. doi: 10.3390/ijerph17093232.

Copyright© AE&M all rights reserved.

40. Abdissa D, Hamba N, Nigussie D, Adema S. Prevalence and determinants of peripheral neuropathy among type 2 adult diabetes patients attending Jimma University Medical Center, southwest Ethiopia, 2019: an institutional-based cross-sectional study. J Diabetes Res. 2020 Jun;2020:9562920. doi: 10.1155/2020/9562920.
41. Wang DD, Bakhotmah BA, Hu FB, Alzahrani HA. Prevalence and correlates of diabetic peripheral neuropathy in a Saudi Arabic population: a cross-sectional study. PLoS One. 2014 Sep 3;9(9):e106935. doi:10.1371/journal.pone.0106935.
42. Callaghan BC, Price RS, Feldman EL. Enhanced glucose control for preventing and treating diabetic neuropathy. Cochrane Database Syst Rev. 2012 Jun;2012(6):CD007543. doi: 10.1002/14651858.CD007543.pub2.
43. Brasil. Ministério da Previdência Social. Instituto Nacional do Seguro Social. Regras de Aposentadorias. Brasília: Ministério da Previdência Social; 2024. Available from: https://www.gov.br/inss/pt-br/direitos-e-deveres/aposentadoria/regras-de-aposentadorias.
44. Andersen ST, Witte DR, Dalsgaard EM, Andersen H, Nawroth P, Fleming T, et al. Risk factors for incident diabetic polyneuropathy in a cohort with screen-detected type 2 diabetes followed for 13 years: ADDITION-Denmark. Diabetes Care. 2018 Feb;41(5):1068-75. doi: 10.2337/dc17-2062.
45. Salih MH, Woredekal AT, Tadesse F, Abate A, Yimam B, Mohammed S, et al. Peripheral neuropathy and associated factors among type 2 diabetic patients attending referral hospitals in the Amhara region: a multi-center cross-sectional study in Ethiopia. Sci Rep. 2024 Aug;14:19662. doi: 10.1038/s41598-024-70314-9.
46. Nolan RC, Dwyer T, Eser P, Kingwell BA, Jones G, Green DJ. Self-reported physical activity using the International Physical Activity Questionnaire (IPAQ) in Australian adults with type 2 diabetes, with and without peripheral neuropathy. Can J Diabetes. 2016 Dec;40(6):576-9. doi: 10.1016/j.jcjd.2016.05.013.
47. Callaghan BC, Gao L, Li Y, Zhou X, Reynolds E, Banerjee M, et al. Dietary weight loss in people with severe obesity stabilizes neuropathy and improves symptomatology. Obesity (Silver Spring). 2021 Dec;29(12):2108-18. doi: 10.1002/oby.23246.
48. Kluding PM, Pasnoor M, Singh R, Jernigan S, Farmer K, Rucker J, et al. The effect of exercise on neuropathic symptoms, nerve function, and cutaneous innervation in people with diabetic peripheral neuropathy. J Diabetes Complications. 2012 Sep;26(5):424-9. doi: 10.1016/j.jdiacomp.2012.05.007.
49. The Look-AHEAD Research Group. Effects of a long-term lifestyle modification programme on peripheral neuropathy in overweight or obese adults with type 2 diabetes: the Look-AHEAD study. Diabetologia. 2017;60:980-8. doi: 10.1007/s00125-017-4253-z.
50. O'Brien PD, Hinder LM, Callaghan BC, Feldman EL. Neurological consequences of obesity. Lancet Neurol. 2017 Jun;16(6):465-77. doi: 10.1016/S1474-4422(17)30084-4.
51. Silva Júnior WS, Foss-Freitas MC, Tannus LRM, Oliveira JEP, Gomes MB. Atividade física e exercício no pré-diabetes e DM2. Diretriz Oficial da Sociedade Brasileira de Diabetes 2023. doi: 10.29327/557753.2022-8.
52. Dal Canto E, Ceriello A, Rydén L, Ferrini M, Hansen TB, Schnell O, et al. Diabetes as a cardiovascular risk factor: an overview of global trends of macro and microvascular complications. Eur J Prev Cardiol. 2019 Dec;26(Suppl 2):25-32. doi: 10.1177/2047487319878371.
53. Schmidt AM. Diabetes mellitus and cardiovascular disease: emerging therapeutic approaches. Arterioscler Thromb Vasc Biol. 2019 Apr;39(4):558-68. doi: 10.1161/ATVBAHA.119.310961.
54. Fitridge R, Hinchliffe RJ, Forsythe RO, Apelqvist J, Boyko EJ, Mills JL, et al. The intersocietal IWGDF, ESVS, SVS guidelines on peripheral artery disease in people with diabetes and a foot ulcer. Diabetes Metab Res Rev. 2024 Mar;40(3):e3686. doi: 10.1002/dmrr.3686.
55. Izar M, Lottenberg AM, Fonseca FAH, Sposito AC, Bertoluci MC, Schaan BD, et al. Manejo do risco cardiovascular: dislipidemia. Diretriz Oficial da Sociedade Brasileira de Diabetes 2023. doi: 10.29327/557753.2022-19.
56. Brownrigg JR, de Lusignan S, McGovern A, Hughes C, Thompson MM, Ray KK, et al. Peripheral neuropathy and the risk of cardiovascular events in type 2 diabetes mellitus. Heart. 2014 Dec;100(23):1837-43. doi: 10.1136/heartjnl-2014-305657.
57. Aikaeli F, Njim T, Gissing S, Moyo F, Alam U, Mfinanga SG, et al. Prevalence of microvascular and macrovascular complications of diabetes in newly diagnosed type 2 diabetes in low-and-middle-income countries: A systematic review and meta-analysis. PLOS Glob Public Health. 2022 Jun 15;2(6):e0000599. doi: 10.1371/journal.pgph.0000599.

Copyright© AE&M all rights reserved.

Archives of Endocrinology and Metabolism
ISSN 2359-4292
OFFICIAL JOURNAL OF THE BRAZILIAN SOCIETY OF ENDOCRINOLOGY AND METABOLISM

original

Diagnostic criteria for gestational hyperglycemia in women from a public maternity hospital in Brazil

Thais Mantovani Bernardo[1]
https://orcid.org/0000-0002-4549-3836

Ênio Luis Damaso[2]
https://orcid.org/0000-0002-0498-1411

Patrícia Moreira Gomes[3]
https://orcid.org/0000-0003-3981-8961

Elaine Christine Dantas Moisés[1]
https://orcid.org/0000-0001-9099-4544

[1] Departamento de Ginecologia e Obstetrícia, Faculdade de Medicina de Ribeirão Preto, Universidade de São Paulo, Ribeirão Preto, SP, Brasil
[2] Departamento de Medicina, Faculdade de Medicina de Bauru, Universidade de São Paulo, Bauru, SP, Brasil
[3] Departamento de Clínica Médica, Divisão de Endocrinologia e Metabolismo, Faculdade de Medicina de Ribeirão Preto, Universidade de São Paulo, Ribeirão Preto, SP, Brasil

ABSTRACT

Objective: This study aimed to determine the prevalence of hyperglycemia using different diagnostic criteria for gestational diabetes mellitus. **Subjects and methods:** This cross-sectional study evaluated parturients attending a hospital complex from January to December 2017. Data were obtained retrospectively from medical records. Fasting glucose and 75-g oral glucose tolerance test results were used to assess the prevalence of hyperglycemia during pregnancy. The diagnostic criteria evaluated were: 1998 World Health Organization (WHO98), 2003 American Diabetes Association (ADA03), 2015 National Institute for Health and Care Excellence (NICE15), and 2015 International Federation of Gynecology and Obstetrics (FIGO15). The overall kappa coefficient was used to analyze agreement among the four sets of diagnostic criteria. All analyses were performed using SAS 9.2, and a significance level of 5% was adopted for all tests. **Results:** Data from 2,262 women were analyzed. The prevalence of hyperglycemia differed depending on the diagnostic criteria: 10.3% (FIGO15), 7.34% (NICE15), 3.1% (ADA03), and 5.7% (WHO98). The overall kappa coefficient of agreement was 0.61. Individual analysis of each set of diagnostic criteria showed a kappa coefficient indicating moderate agreement, with FIGO15 used as the gold standard. **Conclusion:** In this population of pregnant women, the prevalence of hyperglycemia varied according to the diagnostic criteria used, with the prevalence of the disease being lower as the criteria became stricter. Lastly, the criteria showed moderate agreement when compared collectively and individually to FIGO15.

Keywords: Pregnancy; gestational diabetes mellitus; prevalence; diagnostic criteria

INTRODUCTION

Gestational diabetes mellitus (GDM) is defined as any degree of glucose intolerance first recognized during pregnancy (1). It is a significant public health concern due to its association with maternal and fetal complications during pregnancy, as well as its potential long-term consequences. GDM increases the risk of preterm birth, fetal macrosomia, preeclampsia, and neonatal complications (1,2).

The first diagnostic criteria for GDM were proposed by O'Sullivan and Mahan in 1964 (3). In 1998, the World Health Organization (WHO98) recommended using diagnostic thresholds for non-pregnant individuals: fasting glucose ≥126 mg/dL or 2-hour glucose ≥140 mg/dL following a 75-gram oral glucose tolerance test (75-g OGTT) (4). Subsequently, the American Diabetes Association (ADA03) suggested fasting glucose ≥95 mg/dL, 1-hour ≥180 mg/dL, and 2-hour ≥155 mg/dL, requiring at least two abnormal results (5). The Latin American Diabetes Association (ALAD08) and the National Institute for Health and Care Excellence (NICE15) later recommended fasting glucose ≥100 mg/dL and 2-hour glucose ≥140 mg/dL (6,7).

Received on Jun/22/2025
Accepted on Jan/28/2026
DOI: 10.20945/2359-4292-2026-0054

Correspondence to:
Ênio Luis Damaso
Departamento de Ginecologia e Obstetrícia,
Faculdade de Medicina de Ribeirão Preto,
Universidade de São Paulo
Av. Bandeirantes, 3900
14049-900 – Ribeirão Preto, SP, Brasil
eniodamaso@usp.br

Associated editor:
João Roberto de Sá
https://orcid.org/0000-0003-3115-5606

This is an open-access article distributed under the terms of the Creative Commons Attribution License

Copyright© AE&M all rights reserved.

A significant advancement occurred with the Hyperglycemia and Adverse Pregnancy Outcome study in 2008, which included 25,505 pregnant women undergoing 75-g OGTT between 24 and 32 weeks of gestation. The study demonstrated that increases in maternal glucose levels, even below diabetic thresholds, were independently associated with adverse perinatal outcomes (8). Based on these findings, the International Association of Diabetes and Pregnancy Study Groups (IADPSG) recommended universal screening with fasting glucose at the first prenatal visit and a 75-g OGTT between 24 and 28 weeks of gestation (9).

Currently, diagnostic criteria for GDM proposed by the American Diabetes Association (5), the World Health Organization (4), the International Federation of Gynecology and Obstetrics (FIGO15) (10), and the Endocrine Society Clinical Practice Guidelines (11) are based on the results of the Hyperglycemia and Adverse Pregnancy Outcome study, with values corresponding to those recommended by IADPSG: one or more values equal to or above 92–125 mg/dL (fasting), 180 mg/dL (1 hour), and 153–199 mg/dL (2 hours) after anhydrous 75-g glucose load (9). The diagnosis of overt diabetes in pregnancy includes fasting glucose (≥126 mg/dL), 2-hour glucose (≥200 mg/dL), random glucose (≥200 mg/dL), or glycated hemoglobin (≥6.5%) (9). In Brazil, the Brazilian Federation of Gynecology and Obstetrics Associations, the Brazilian Diabetes Society, the Pan American Health Organization, and the Brazilian Ministry of Health have adopted the same IADPSG diagnostic recommendations in 2017 (12).

It is estimated that approximately 16% of live births occur in women who experienced hyperglycemia during pregnancy, with about 8% of these cases involving pre-existing diabetes (13). Therefore, given the limited data and ongoing debate regarding optimal diagnostic thresholds, this study aimed to determine the prevalence of hyperglycemia using different diagnostic criteria and to assess the agreement among them in a population of pregnant women.

SUBJECTS AND METHODS

Study design and period

This observational, cross-sectional study analyzed data from the hospital complex of Ribeirão Preto (São Paulo State, Brazil). The complex, managed by the University of São Paulo, comprises two units: the medium-complexity Referral Center for Women's Health of Ribeirão Preto (CRSMRP-MATER) and the high-complexity University Hospital of the Ribeirão Preto Medical School (HCFMRP-USP). Both provide pregnancy and postpartum care through the Brazilian public health system, serving a population of approximately 1.4 million people. Ribeirão Preto is located in northeastern São Paulo State, having a human development index of 0.800 in 2010 and ranking 40th in Brazil (14). This study analyzed data from pregnant women attended between January and December 2017, coinciding with the adoption of Brazil's updated diagnostic criteria. It was conducted as outlined by STROBE guidelines for reporting observational studies and adhered to the Declaration of Helsinki. Additionally, it was approved by the Research Ethics Committee of HCFMRP-USP and CRSMRP-MATER (CAAE no. 62213416.9.0000.5440).

Participants

The study included pregnant women residing in Ribeirão Preto who delivered at CRSMRP-MATER or HCFMRP-USP in 2017. Only those who completed prenatal care and gave birth at these institutions were included, ensuring adherence to national diagnostic guidelines. Exclusion criteria included multiple pregnancies, previous diagnosis of type 1 or type 2 diabetes mellitus, and absence of prenatal care in Ribeirão Preto. For GDM prevalence analyses, women without fasting glucose or 75-g OGTT results were excluded. For the analysis of adverse outcomes, women with missing data on delivery, maternal, or perinatal outcomes were also excluded.

Data collection

Data were collected retrospectively from medical records. Clinical and sociodemographic variables were retrieved, including maternal age, self-reported skin color, comorbidities, lifestyle habits, parity, previous cesarean sections, prenatal care, gestational age at delivery, and type of delivery. Fasting blood glucose in early pregnancy (up to 20 weeks) and the 75-g OGTT performed between 24 and 28 weeks were analyzed

Copyright© AE&M all rights reserved.

to assess the prevalence of hyperglycemia and diagnostic agreement. Four diagnostic criteria were applied: WHO98 (4), ADA03 (5), NICE15 (7), and FIGO15 (10). According to WHO98 criteria (4), gestational diabetes is diagnosed with fasting plasma glucose ≥126 mg/dL or 2-hour plasma glucose ≥140 mg/dL after a 75-g OGTT. ADA03 criteria (5) define GDM as two or more values meeting or exceeding the following thresholds during a 75-g OGTT: fasting ≥95 mg/dL, 1-hour ≥180 mg/dL, and 2-hour ≥155 mg/dL. NICE15 criteria (7) recommend diagnosing GDM when fasting plasma glucose is ≥100 mg/dL or 2-hour plasma glucose is ≥140 mg/dL after 75-g OGTT. The FIGO15 criteria (10), based on IADPSG recommendations (9), establish GDM diagnosis via a fasting plasma glucose ≥92 mg/dL, or one or more of the following OGTT thresholds: ≥92 mg/dL (fasting), ≥180 mg/dL (1 hour), or ≥153 mg/dL (2 hour). For clarity, the FIGO15 diagnostic criteria applied are fully equivalent to the IADPSG recommendations and have been the official diagnostic standard in Brazil since 2017 (9,10,12).

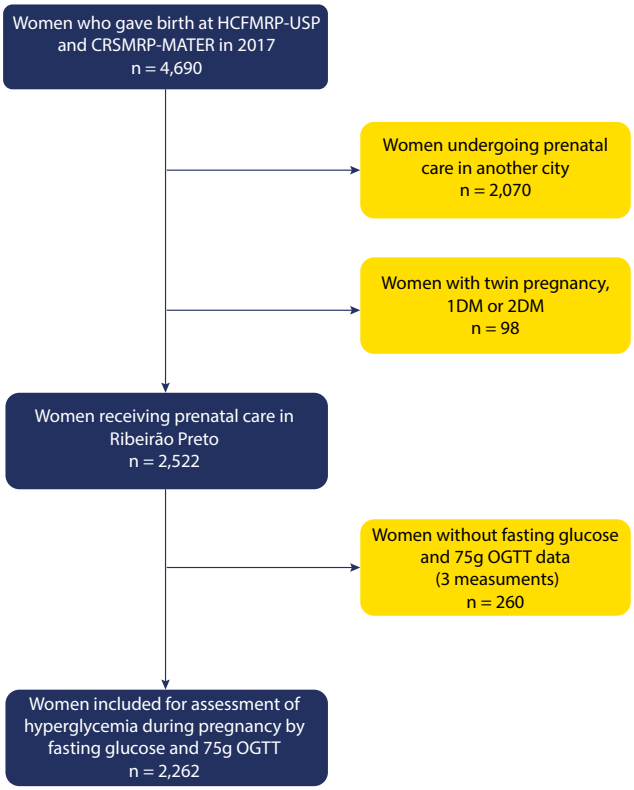


Figure 1. Flowchart depicting the study design.

Statistical analysis

Exploratory analyses were conducted to characterize the sample. Quantitative variables are summarized using measures of central tendency and dispersion, while qualitative variables are presented as absolute and relative frequencies. Agreement among the four diagnostic criteria was assessed using the kappa coefficient, as described by Cohen (15). A kappa value of 1 indicates perfect agreement, 0 indicates chance agreement, and negative values represent agreement below chance. Interpretation of kappa values followed the Landis and Koch (16) classification: poor (<0), negligible (0.00–0.20), weak (0.21–0.40), moderate (0.41–0.60), strong (0.61–0.80), and almost perfect (0.81–1.00). All statistical analyses were performed using SAS version 9.2 (SAS Institute, USA) using a significance level of 5%.

RESULTS

From an initial 4,690 records, the final sample of 2,262 pregnant women was selected based on the availability of fasting plasma glucose and/or 75-g OGTT results. The sample selection process is summarized in **Figure 1**.

Table 1 presents the clinical and sociodemographic characteristics of the study population. The mean maternal age was 26.4 years (SD ±5.7), with 70.2% aged 20–34 years. Regarding self-reported race, 65.2% identified as white and 34.3% as black. Educational attainment was high, with 65% having completed at least secondary education. Most women (93.9%) initiated prenatal care before 20 weeks, and 93.4% attended at least six prenatal consultations. The mean pregestational body mass index was 26.2 kg/m^2, with 41.5% classified as being overweight or obese.

To evaluate potential selection bias, we compared the baseline characteristics of women who underwent screening with those who did not. Non-screened women were more likely to be older than 34 years, report higher rates of drug use, and have fewer than six prenatal visits. These differences suggest that the excluded population may have had a higher underlying risk for GDM. The detailed analysis is presented in **Supplementary Table 1**.

The prevalence of hyperglycemia during pregnancy was calculated for the full cohort (n = 2,262) using fasting glucose and/or OGTT data according to

Copyright© AE&M all rights reserved.

Table 1. Clinical and sociodemographic characteristics of women assessed for the prevalence of gestational hyperglycemia (n = 2,262)

Variable	n	%	Variable	n	%
Maternal age (years)			Prenatal (≥ 6 visits)		
Mean (SD)	26.41	(6.60)	No	83	3.67
Median (min–max)	26	(13-47)	Yes	2,112	93.37
Maternal age (years)			Not reported	67	2.96
< 20	372	16.44	Total number of pregnancies		
20–34	1589	70.25	1	777	34.35
> 34	301	13.31	2	642	28.38
Skin color			3	420	18.57
White	1,474	65.16	4	237	10.48
Black	776	34.31	≥ 5	86	8.22
Brown	7	0.31	Parity		
Yellow	2	0.09	0	885	39.12
Not reported	3	0.13	1	703	31.08
Drug use			2	393	17.37
Yes	254	11.23	3	175	7.74
No	2,008	88.77	4	58	2.56
Maternal diseases			≥ 5	48	2.12
None	1,371	60.6	Previous cesarean section		
Hypertensive disorders of pregnancy	244	10.78	0	1,742	77.01
			1	370	16.36
HIV	14	0.62	2	115	5.08
Others	632	27.93	3	32	1.41
Not reported	1	4	≥ 4	3	0.13

FIGO15, NICE15, WHO98, and ADA03 criteria. Of these, 1,772 women had complete three-point OGTT results, allowing for the application of all four criteria. For the remaining 490 women with only fasting glucose data, only the FIGO15, NICE15, and WHO98 criteria could be applied, as ADA03 requires complete OGTT data. **Table 2** lists the prevalence rates obtained with each diagnostic criterion. Among women with any available glucose data, the prevalence ranged from 3.1% (ADA03) to 10.3% (FIGO15). NICE15 and WHO98 criteria yielded intermediate rates of 7.3% and 5.7%, respectively. In the subgroup with complete OGTT data, prevalence was highest with FIGO15 (11.6%), followed by NICE15 (8.8%), WHO98 (6.3%), and ADA03 (3.9%).

The prevalence of these variations across diagnostic criteria are illustrated in **Figure 2**.

Table 3 presents the absolute margin of error for prevalence estimates, considering both the total sample and the subgroup with complete OGTTs. The margins ranged from 0.71 to 1.32 percentage points, depending on criterion and sample size. Agreement between diagnostic sets was evaluated using kappa statistics. The overall kappa among the four criteria was 0.61, indicating moderate agreement. When compared individually to FIGO15 as the reference, kappa values were 0.65 for NICE15, 0.51 for WHO98, and 0.44 for ADA03.

DISCUSSION

This study evaluated the medical records of women who received prenatal care through the Brazilian public health system and gave birth at HCFMRP-USP and CRSM-MATER. In 2017, the FIGO15 criteria were already recommended in Ribeirão Preto.

Prevalence of hyperglycemia varied across diagnostic criteria: 10.3% (FIGO15), 7.3% (NICE15), 3.1% (ADA03), and 5.7% (WHO98). This highlights the direct impact of the diagnostic strategy on the proportion of women identified with GDM and its

Copyright© AE&M all rights reserved.

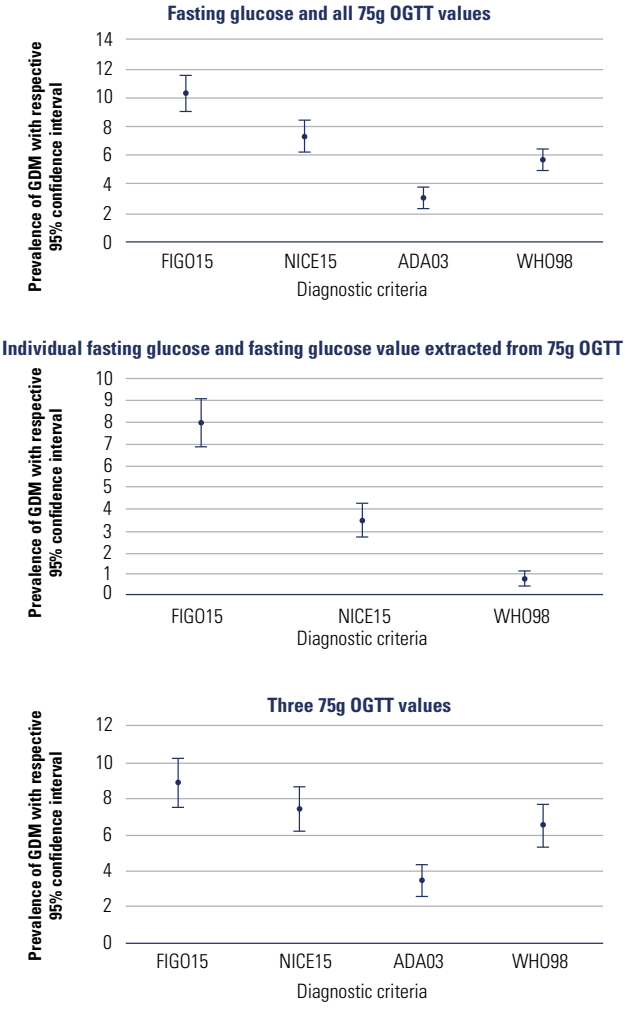


Figure 2. Prevalence of gestational hyperglycemia in women with fasting glucose and 75-g OGTT values according to each set of diagnostic criteria

implications for clinical practice, public health policy, and international comparability of data. Since the initial recognition of hyperglycemia in pregnancy, the absence of a universal diagnostic standard has hindered accurate estimates of GDM prevalence (9). Broad early definitions, encompassing any degree of hyperglycemia first recognized during pregnancy, contributed to discrepancies across studies.

Globally, GDM prevalence estimates vary widely from 1% to 37.7%, with a mean prevalence of 16.2% (10,17). The International Diabetes Federation reports a pooled global standardized prevalence of 14.0%. By region, standardized GDM prevalence is 7.1% in North America and the Caribbean, 7.8% in Europe, 10.4% in South and Central America, 14.2% in Africa, 14.7% in the Western Pacific, 20.8% in South-East Asia, and 27.6% in the Middle East and North Africa. According to economic status, the standardized prevalence is 12.7% in low-income countries, 9.2% in middle-income countries, and 14.2% in high-income countries (18). A meta-analysis indicated an overall pooled prevalence of 4.4%, while specifically applying FIGO15 criteria resulted in 10.6% (19), consistent with our findings.

An investigation comparing various diagnostic criteria found that GDM prevalence ranged from 9.2% to 45.3%, depending on the thresholds used (20).

Table 2. Prevalence of gestational hyperglycemia in women with fasting glucose and 75-g OGTT values according to each set of diagnostic criteria

Criteria	Fasting glucose and all 75g OGTT values		Individual fasting glucose and fasting glucose value extracted from 75-g OGTT		Three 75g OGTT values	
	n (%)	95% CI (%)	n (%)	95% CI (%)	n (%)	95% CI (%)
FIGO15						
No	2,029 (89.70)	88.45; 90.95	2,082 (92.04)	90.93; 93.16	1,615 (91.14)	89.82; 92.46
Yes	233 (10.30)	9.05; 11.55	180 (7.96)	6.84; 9.07	157 (8.86)	7.54; 10.18
NICE15						
No	2,096 (92.66)	91.59; 93.74	2,184 (96.55)	95.8; 97.3	1,641 (92.61)	91.39; 93.83
Yes	166 (7.34)	6.26; 8.41	78 (3.45)	2.7; 4.2	131 (7.39)	6.17; 8.61
ADA03						
No	2,191 (96.90)	96.19; 97.62	-	-	1,711 (96.56)	95.71; 97.41
Yes	71 (3.10)	2.38; 3.81	-	-	61 (3.44)	2.59; 4.29
WHO98						
No	2,133 (94.30)	93.34; 95.25	2,245 (99.25)	98.89; 99.6	1,657 (93.51)	92.36; 94.66
Yes	129 (5.70)	4.75; 6.66	17 (0.75)	0.4; 1.11	115 (6.49)	5.34; 7.64
GDM diagnosis by some of the criteria						
No	1,998 (88.33)	87.01; 89.65	2,082 (92.04)	90.93; 93.16	1,586 (89.50)	88.08; 90.93
Yes	264 (11.67)	10.35; 12.99	180 (7.96)	6.84; 9.07	186 (10.50)	9.07; 11.92

Copyright© AE&M all rights reserved.

Table 3. Estimation of the margin of error based on the sample

Variable	Diagnostic criteria	Prevalence of hyperglycemia	n	Absolute error (pp)
Fasting glucose and all 75-g OGTT values	FIGO15	233 (10.3%)	2,262	1.25
	NICE15	166 (7.34%)	2,262	1.07
	ADA03	70 (3.1%)	2,261	0.71
	WHO98	129 (5.7%)	2,262	0.96
	S-GDM	264 (11.67%)	2,262	1.32
Individual fasting glucose and fasting glucose value extracted from 75-g OGTT	FIGO15	180 (7.96%)	2,262	1.12
	NICE15	78 (3.45%)	2,262	0.75
	WHO98	17 (0.75%)	2,262	0.36
	S-GDM	180 (7.96%)	2,262	1.12
Three 75-g OGTT values	FIGO15	157 (8.86%)	1,772	1.32
	NICE15	131 (7.39%)	1,772	1.22
	ADA03	61 (3.44%)	1,772	0.85
	WHO98	115 (6.49%)	1,772	1.15
	S-GDM	186 (10.5%)	1,772	1.43

Adoption of the IADPSG criteria significantly increased GDM detection, and prevalence rates can vary by a factor of 1.5 to 4.9. In Brazil, data are limited and divergent. A reanalysis of a cohort from 1991 to 1995 showed a GDM prevalence of 18% when using IADPSG criteria, which decreased to 2.7% under stricter definitions (21). A 2024 systematic review reported a pooled prevalence of 14% (95% CI: 11.0–16.0) for GDM in Brazil (22). Although more sensitive criteria (i.e., IADPSG) identify additional cases, this increase does not necessarily result in more adverse outcomes.

Among the evaluated criteria, FIGO15 consistently showed the highest prevalence, as expected due to its broader diagnostic thresholds. Conversely, ADA03 was the most restrictive, requiring two abnormal glucose values and thus producing lower prevalence rates, aligning with findings from other studies, such as that by Çelik and cols. (23), which confirmed that broader thresholds akin to those of FIGO15 significantly increase detection rates. Although IADPSG and FIGO15 criteria increase GDM diagnosis rates, they improve maternal and neonatal outcomes and reduce healthcare costs. A Spanish study demonstrated that use of IADPSG criteria led to increased detection, improved pregnancy outcomes, and cost savings (24).

Agreement analyses showed moderate concordance among diagnostic sets, supporting the systematic differences found. Notably, agreement between FIGO15 and WHO98 was low when only fasting glucose was available. The FIGO15 criteria are notable for being the first to base diagnosis on perinatal outcomes, facilitating early intervention and influencing maternal and neonatal morbidity and mortality. Early diagnosis of overt diabetes also enables more intensive management; for example, maintaining glycated hemoglobin below 6% reduces risks of large-for-gestational-age infants, preterm delivery, and preeclampsia (17).

Despite our promising findings, this study's limitations include its retrospective, observational design, possible selection bias, and potential confounding factors. The use of a convenience sample also limited the generalizability of findings, highlighting the need for multicenter studies to better characterize GDM prevalence across Brazil's diverse population.

In conclusion, the prevalence of gestational hyperglycemia varied according on the diagnostic criteria, with ADA03 yielding the lowest and FIGO15 the highest prevalence. Broader criteria such as FIGO15 enhance early identification and allow for timely intervention, potentially improving maternal and neonatal outcomes. These findings support public health priorities in low- and middle-income countries.

Author contributions: TMB: conception and design, data collection, analysis and interpretation of data. ELD: drafting the manuscript and critical revision of intellectual content. PMG: critical revision of intellectual content and final approval of the version to be published. ECDM: study conception, inter-

Copyright© AE&M all rights reserved.

pretation of data, critical revision, and final approval of the version to be published.

Disclosure: there are no potential conflict of interest to declare.

Data availability: data related to this article will be available upon request to the corresponding author.

REFERENCES

1. Sweeting A, Wong J, Murphy HR, Ross GP. A Clinical Update on Gestational Diabetes Mellitus. Endocr Rev. 2022 Sep 26;43(5):763-793. doi: 10.1210/endrev/bnac003.
2. Li T, Ma X, Ma L. Effects of gestational diabetes mellitus on offspring: A literature review. Int J Gynaecol Obstet. 2025 Oct;171(1):82-93. doi: 10.1002/ijgo.70185.
3. O'Sullivan JB, Mahan CM. Criteria for the oral glucose tolerance test in pregnancy. Diabetes. 1964 Jun;13:278-85. PMID: 14166677.
4. Alberti KG, Zimmet PZ. Definition, diagnosis and classification of diabetes mellitus and its complications. Part 1: diagnosis and classification of diabetes mellitus provisional report of a WHO consultation. Diabet Med. 1998 Jul;15(7):539-53. doi: 10.1002/(SICI)1096-9136(199807)15:7<539::AID-DIA668>3.0.CO;2-S.
5. American Diabetes Association. Gestational diabetes mellitus. Diabetes Care. 2003 Jan;26 Suppl 1:S103-5. doi: 10.2337/diacare.26.2007.s103.
6. Asociación Latinoamericana de Diabetes (ALAD). Consenso Latinoamericano de Diabetes y Embarazo. Rev ALAD. 2008;16(2):55-69.
7. National Collaborating Centre for Women's and Children's Health (UK). Diabetes in pregnancy: management of diabetes and its complications from preconception to the postnatal period. London: National Institute for Health and Care Excellence (UK); 2015 Feb. PMID: 25950069.
8. HAPO Study Cooperative Research Group; Metzger BE, Lowe LP, Dyer AR, Trimble ER, Chaovarindr U, Coustan DR, et al. Hyperglycemia and adverse pregnancy outcomes. N Engl J Med. 2008 May 8;358(19):1991-2002. doi: 10.1056/NEJMoa0707943.
9. International Association of Diabetes and Pregnancy Study Groups Consensus Panel; Metzger BE, Gabbe SG, Persson B, Buchanan TA, Catalano PA, Damm P, et al. International association of diabetes and pregnancy study groups recommendations on the diagnosis and classification of hyperglycemia in pregnancy. Diabetes Care. 2010 Mar;33(3):676-82. doi: 10.2337/dc09-1848.
10. Hod M, Kapur A, Sacks DA, Hadar E, Agarwal M, Di Renzo GC, et al. The International Federation of Gynecology and Obstetrics (FIGO) Initiative on gestational diabetes mellitus: A pragmatic guide for diagnosis, management, and care. Int J Gynaecol Obstet. 2015 Oct;131 Suppl 3:S173-211. doi: 10.1016/S0020-7292(15)30033-3.
11. Blumer I, Hadar E, Hadden DR, Jovanović L, Mestman JH, Murad MH, Yogev Y. Diabetes and pregnancy: an endocrine society clinical practice guideline. J Clin Endocrinol Metab. 2013 Nov;98(11):4227-49. doi: 10.1210/jc.2013-2465.
12. Zajdenverg L, Façanha C, Dualib P, Golbert A, Moisés E, Calderon I, et al. Rastreamento e diagnóstico da hiperglicemia na gestação: Diretriz oficial da Sociedade Brasileira de Diabetes – 2023. São Paulo: Sociedade Brasileira de Diabetes; 2023. doi: 10.29327/557753.2022-11.
13. International Diabetes Federation. IDF Diabetes Atlas, 9th ed. Brussels: International Diabetes Federation; 2019.
14. Instituto Brasileiro de Geografia e Estatística (IBGE). Estimativa populacional 2020. Rio de Janeiro: IBGE; 2020.
15. Cohen J. A coefficient of agreement for nominal scales. Educ Psychol Meas. 1960 Apr;20(1):37-46. doi: 10.1177/001316446002000104.
16. Landis JR, Koch GG. The measurement of observer agreement for categorical data. Biometrics. 1977 Mar;33(1):159-74. PMID: 843571.
17. McIntyre HD, Catalano P, Zhang C, Desoye G, Mathiesen ER, Damm P. Gestational diabetes mellitus. Nat Rev Dis Primers. 2019 Jul 11;5(1):47. doi: 10.1038/s41572-019-0098-8.
18. Wang H, Li N, Chivese T, Werfalli M, Sun H, Yuen L, et al. IDF Diabetes Atlas: estimation of global and regional gestational diabetes mellitus prevalence for 2021 by International Association of Diabetes in Pregnancy Study Groups criteria. Diabetes Res Clin Pract. 2022 Jan;183:109050.
19. Behboudi-Gandevani S, Amiri M, Bidhendi Yarandi R, Ramezani Tehrani F. The impact of diagnostic criteria for gestational diabetes on its prevalence: a systematic review and meta-analysis. Diabetol Metab Syndr. 2019 Dec;11(1):11. doi: 10.1186/s13098-019-0406-1.
20. Agarwal MM, Dhatt GS, Othman Y. Gestational diabetes: differences between the current international diagnostic criteria and implications of switching to IADPSG. J Diabetes Complications. 2015 May-Jun;29(4):544-9. doi: 10.1016/j.jdiacomp.2015.03.006.
21. Trujillo J, Vigo A, Duncan BB, Falavigna M, Wendland EM, Campos MA, et al. Impact of the International Association of Diabetes and Pregnancy Study Groups criteria for gestational diabetes. Diabetes Res Clin Pract. 2015 May;108(2):288-95. doi: 10.1016/j.diabres.2015.02.007.
22. Mocellin LP, Gomes HA, Sona L, Giacomini GM, Pizzuti EP, Nunes GB, et al. Gestational diabetes mellitus prevalence in Brazil: a systematic review and meta-analysis. Cad Saude Publica. 2024;40(8):e00064919. doi: 10.1590/0102-311XEN064919.
23. Çelik C, Oral E, Özdo□an E, Atak M, Kumbak B, Karslı MF, et al. Comparison of different diagnostic criteria for gestational diabetes mellitus in Turkish pregnant women: prevalence, maternal and neonatal outcomes. J Obstet Gynaecol Res. 2021 Jan;47(1):219-27. doi: 10.1111/jog.14550.
24. Duran A, Sáenz S, Torrejón MJ, Bordiú E, Del Valle L, Galindo M, et al. Introduction of IADPSG criteria for the screening and diagnosis of gestational diabetes mellitus results in improved pregnancy outcomes at a lower cost in a large cohort of pregnant women: the St. Carlos Gestational Diabetes Study. Diabetes Care. 2014 Sep;37(9):2442-50. doi: 10.2337/dc14-0179.

Copyright© AE&M all rights reserved.

SUPPLEMENTARY MATERIAL

Supplementary Table 1. Clinical and sociodemographic characteristics of screened vs. non-screened women who gave birth at HCFMRP-USP and CRSM-MATER in 2017

Variable	Not screened (n = 260)	Screened (n = 2,262)	p*
Maternal age (years)			
< 20	25 (9.62%)	314 (13.88%)	<0.01
20–34	166 (63.85%)	1,600 (70.73%)	
> 34	69 (26.54%)	348 (15.38%)	
Skin color‡			
White	191 (73.46%)	1,474 (65.25%)	0.05
Black	69 (26.54%)	776 (34.35%)	
Brown	0 (0%)	7 (0.31%)	
Yellow	0 (0%)	2 (0.09%)	
Drug use			
No	44 (16.92%)	2,008 (88.77%)	<0.01
Yes	216 (83.08%)	254 (11.23%)	
Maternal diseases			
None	157 (60.38%)	1,371 (60.64%)	0.45
Hypertensive disorders of pregnancy	24 (9.23%)	244 (10.79%)	
HIV	0 (0%)	14 (0.62%)	
Others	79 (30.38%)	632 (27.95%)	
Prenatal (≥ 6 visits)			
No	37 (14.23%)	83 (3.78%)	<0.01
Yes	223 (85.77%)	2,112 (96.22%)	
Total number of pregnancies			
1	85 (32.69%)	777 (34.35%)	0.04
2	75 (28.85%)	642 (28.38%)	
3	35 (13.46%)	420 (18.57%)	
4	32 (12.31%)	237 (10.48%)	
≥ 5	33 (12.69%)	186 (8.22%)	
Parity			
0	107 (41.15%)	885 (39.12%)	0.01
1	74 (28.46%)	703 (31.08%)	
2	34 (13.08%)	393 (17.37%)	
3	20 (7.69%)	175 (7.74%)	
4	14 (5.38%)	58 (2.56%)	
≥ 5	11 (4.23%)	48 (2.12%)	
Previous cesarean section			
0	200 (76.92%)	1,742 (77.01%)	<0.01
1	36 (13.85%)	370 (16.36%)	
2	14 (5.38%)	115 (5.08%)	
3	6 (2.31%)	32 (1.41%)	
≥ 4	4 (1.54%)	3 (0.13%)	

*Chi-square test; ‡Fisher's exact test.

Copyright© AE&M all rights reserved.

Archives of Endocrinology and Metabolism
ISSN 2359-4292
OFFICIAL JOURNAL OF THE BRAZILIAN SOCIETY OF ENDOCRINOLOGY AND METABOLISM

original

OCT4 and NANOG are involved in adrenocortical tumorigenesis

Marcelo M. Cavalcanti[1#] https://orcid.org/0009-0004-5530-9395
Mariana P. Halah[1#] https://orcid.org/0000-0002-9411-6105
Letícia F. Leal[1] https://orcid.org/0000-0003-2200-3985
Fernanda B. Coeli-Lacchini[2] https://orcid.org/0000-0001-6568-7497
Carlos A. Scrideli[1] https://orcid.org/0000-0001-6618-789X
Carlos A. F. Molina[3] https://orcid.org/0000-0002-5118-778X
Jose A. Yunes[4] https://orcid.org/0000-0002-1316-3525
Silvia Brandalise[4] https://orcid.org/0000-0003-3696-9852
Ayrton C. Moreira[5] https://orcid.org/0000-0002-8096-6803
Fernando Ramalho[6] https://orcid.org/0000-0002-7529-466X
Leandra N. Ramalho[6] https://orcid.org/0000-0002-3486-5294
Margaret de Castro[5] https://orcid.org/0000-0003-4932-4623
Sonir R. Antonini[1] https://orcid.org/0000-0003-4778-8803

[1] Departamento de Pediatria, Faculdade de Medicina de Ribeirão Preto, Universidade de São Paulo, Ribeirão Preto, SP, Brasil
[2] Hemocentro de Ribeirão Preto, Faculdade de Medicina de Ribeirão Preto, Universidade de São Paulo, Ribeirão Preto, SP, Brasil
[3] Departamento de Cirurgia, Faculdade de Medicina de Ribeirão Preto, Universidade de São Paulo, Ribeirão Preto, SP, Brasil
[4] Centro Infantil Boldrini, Universidade Estadual de Campinas, Campinas, SP, Brasil
[5] Departamento de Clínica Médica, Faculdade de Medicina de Ribeirão Preto, Universidade de São Paulo, Ribeirão Preto, SP, Brasil
[6] Departamento de Patologia, Faculdade de Medicina de Ribeirão Preto, Universidade de São Paulo, Ribeirão Preto, SP, Brasil

[#]These authors contributed equally to this manuscript.

ABSTRACT

Objective: To investigate the involvement of regulators of pluripotency and self-renewal of embryonic stem cells in adrenocortical tumors (ACT). **Subjects and methods:** Clinicopathological data and tissues from 114 ACT patients (96 pediatric-pACT; 18 adults) were analyzed. Normal fetal (n = 33) and postnatal adrenals (n = 26) were used as controls. STAT3, NANOG, SOX2, and OCT4 expression was evaluated by qPCR and IHC. We evaluated intracellular NANOG localization by immunofluorescence and its interaction with beta-catenin after inhibiting the Wnt pathway in a beta-catenin-mutated ACT cell line (NCI-H295). **Results:** IHC showed NANOG, OCT4, SOX2, and STAT3 expression in fetal adrenals until mid-pregnancy, disappearing thereafter. Positive OCT4 nuclear staining was found in 32% of pACT samples and was associated with metastasis (OR = 2.28; 95% CI:1.13-4.59; P < 0.05). ACTs presented lower SOX2 mRNA expression (P < 0.01). STAT3 mRNA levels were higher in cortisol-secreting ACT (P = 0.01) and in adult adenomas (P < 0.01). NANOG mRNA was higher in p.S45P CTNNB1 mutated ACT (P < 0.01). NCI-H295 cells exhibit nuclear NANOG expression, which was decreased by inhibiting the Wnt/beta-catenin pathway (P < 0.01). **Conclusion:** Markers of pluripotency and self-renewal of embryonic stem cells are expressed until mid-pregnancy, contributing to the adult adrenal stem cell niche. They are absent postnatally but are expressed in a subset of ACT. Specifically, pS45P beta-catenin-mutated ACTs express more NANOG. Increased OCT4 expression in pACT is associated with worse prognosis, and inhibiting the Wnt/beta-catenin pathway in these cells impairs NANOG expression.

Keywords: Adrenal cortex neoplasms; pathogenesis; adrenocortical carcinoma, pediatric

INTRODUCTION

Deregulation of important signaling pathways that play significant roles in orchestrating early embryonic development and morphogenesis has been previously described in adrenocortical tumorigenesis (1-5). They include wingless-type (Wnt), Hedgehog (HH), and Notch, all of which are involved in the balance between stem cell self-renewal and differentiation (6,7).

The canonical Wnt/β-catenin pathway is involved in stem cell proliferation, differentiation, and migration within their niche (8,9). Activation of the Wnt pathway has been consistently observed in adrenocortical tumorigenesis, either through activating mutations in *CTNNB1* in pediatric (1) and adult adrenocortical tumors (ACT) (5), or through *ZNRF3* mutations and deletions in adult tumors (10,11). Additionally, our previous data have shown that abnormal beta-catenin accumulation was present in most pediatric

Received on Ago/26/2025
Accepted on Dec/26/2025
DOI: 10.20945/2359-4292-2026-0055

Correspondence to:
Sonir R. Antonini
Faculdade de Medicina de Ribeirão Preto,
Universidade de São Paulo
Avenida Bandeirantes, 3900
14049-900, Ribeirão Preto, SP, Brasil
antonini@fmrp.usp.br

Associated editor:
Madson Queiroz de Almeida
https://orcid.org/0000-0002-2957-6148

This is an open-access article distributed under the terms of the Creative Commons Attribution License

Copyright© ACE&M all rights reserved.

ACTs (pACT), even those without *CTNNB1* mutations, suggesting other mechanisms might be involved (1).

HH signaling regulates stem cell proliferation and differentiation in the central nervous system (7), skin (7), intestine (12), mammary gland (13), pancreas (14), and adrenal cortex (4). In adrenocortical tumorigenesis, we previously showed that adult adrenocortical carcinomas (ACC) exhibit higher expression of Sonic Hedgehog (SHH) pathway components, including *PTCH1*, *SMO*, *GLI3*, and *SUFU*, compared with normal adult adrenal cortices (4). Conversely, pACT showed lower mRNA expression of *SHH*, *PTCH1*, *SMO*, *GLI1*, and *GLI3* than control pediatric adrenal cortices (4).

Notch signaling acts through intercellular interactions in several tissues, maintaining stem cell proliferation and determining stem cell fate (15). The activation of Notch signaling through the upregulation of *JAG1* has been reported in a variety of cancers, including ACC (2,16). Moreover, in ACC, *JAG1* seems to be overexpressed in a subgroup of patients with better clinical outcomes (17).

Octamer-binding transcription factor 4 (OCT4), signal transducer and activator of transcription 3 (STAT3), SRY-box transcription factor 2 (SOX2), and NANOG are key transcription factors implicated in cancer biology (18-21). They are master regulators of pluripotency and self-renewal in embryonic stem cells, either by interacting with each other or by regulating pathways involved in stem cell proliferation, such as the LIF/STAT3 pathway (18-21). They have central roles in maintaining cancer stem cell (CSC) properties and promoting aggressive tumor behavior. In the adrenals, NANOG, OCT4, and STAT3 are expressed only during early embryonic stages in murine embryos (prior to E9), before steroidogenic function begins, suggesting that these proteins maintain adrenal cortex cells in an undifferentiated state (22-25). There is little data on the expression pattern of NANOG, OCT4, SOX2, and STAT3 during human adrenal development.

Together or separately, increased NANOG, OCT4, and SOX2 expression has been associated with tumorigenesis, metastasis, and/or recurrence in poorly differentiated breast cancer, glioblastomas, bladder carcinomas, squamous cell carcinoma of the skin, prostate cancer, and head and neck squamous carcinoma (26-29). One previous study reported that STAT3 positive staining was more frequent in ACC than in adrenocortical adenomas ACA (30). There is likely a link between the mechanisms that maintain stem cells and the abnormal molecular pathways involved in adrenocortical tumorigenesis. Nevertheless, the potential involvement of the stem cell markers NANOG, OCT4, SOX2, and STAT3 in ACT has not been thoroughly investigated in these tumors.

OCT4 is aberrantly expressed in numerous malignancies and is enriched in CSC populations, regulating self-renewal, pluripotency, epithelial–mesenchymal transition, and therapy resistance (31,32). In addition to its cell-intrinsic effects, OCT4 contributes to tumor progression by shaping the tumor microenvironment through enhanced angiogenesis, immune evasion, and metabolic reprogramming (31,32). Co-expression of OCT4 and Nanog has been linked to more aggressive clinicopathological features and poorer outcomes in some cancers (33,34).

STAT3 is essential for CSC maintenance and is activated in many cancer types, acting as a major oncogenic driver by regulating proliferation, survival, angiogenesis, immune suppression, and resistance to therapy (35). Its activation correlates with an unfavorable prognosis, and it cooperates with other stemness-associated transcription factors, including Nanog and SOX2, to sustain CSC properties (35-37).

SOX2 is frequently overexpressed across solid tumors and supports CSC maintenance and is associated with poor prognosis, lymph node metastasis, and disease recurrence (38). It interacts with multiple oncogenic signaling pathways, including STAT3 and Wnt/β-catenin, to drive tumor progression and cellular plasticity (38).

NANOG is a master regulator of pluripotency and self-renewal in CSCs (33,34). High NANOG expression is linked to advanced tumor stage, metastatic spread, chemo resistance, and poor clinical outcomes in a wide range of malignancies (39). Nanog promotes tumorigenesis through activation of pathways such as JAK/STAT, Wnt/β-catenin, and TGF-β, and its co-expression with OCT4 further strengthens CSC traits (39).

Together, these transcription factors orchestrate the stemness, plasticity, and aggressive phenotype

Copyright© AE&M all rights reserved.

of cancer cells. By sustaining CSC survival and therapy resistance, they represent promising targets for therapeutic strategies to eliminate CSCs and improve long-term treatment outcomes. There is limited research directly utilizing the markers OCT4, STAT3, SOX2, and NANOG to study adrenocortical tumors.

Therefore, we performed a study to assess the expression of these markers in ACT. First, we evaluated the expression patterns of NANOG, OCT4, SOX2, and STAT3 in normal adrenal cortex across different developmental stages, including fetal and postnatal adrenal cortices. Then, we evaluated mRNA and protein expression of *NANOG*, *OCT4*, *SOX2*, and *STAT3* genes in pediatric and adult ACTs and their association with clinical features. In addition, we analyzed the in vitro interaction between Wnt/β-catenin signaling and *NANOG*.

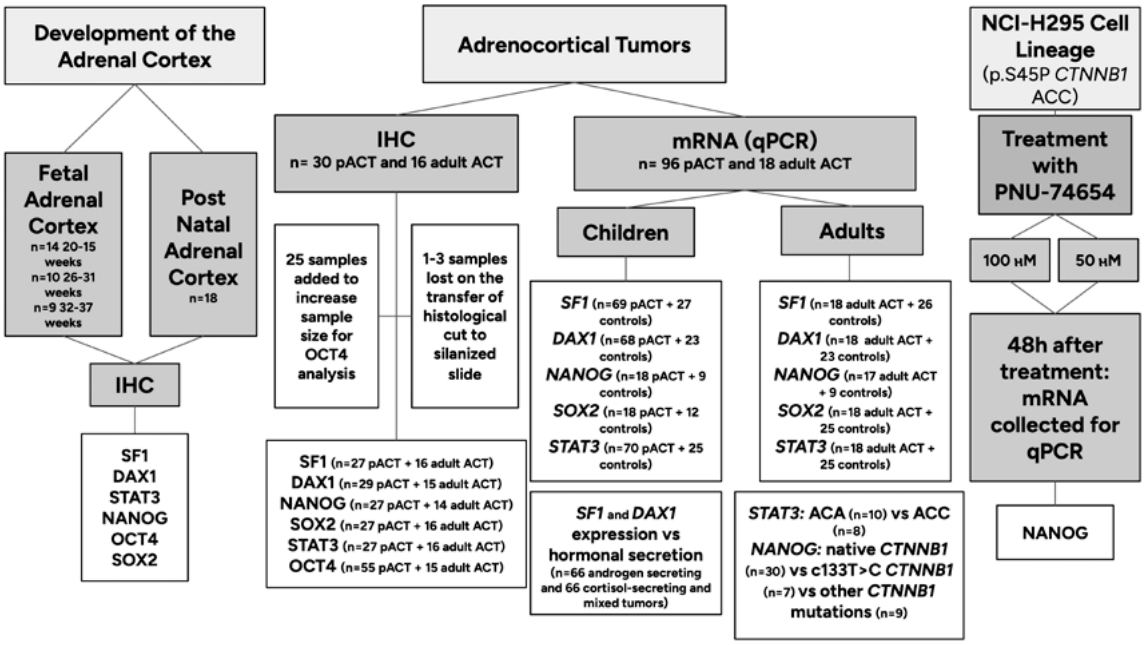
MATERIALS AND METHODS

Experimental design

Experimental design is detailed in **Figure 1**. Different sample sizes were used for each experiment due to limitations on the number of samples and the quantity of material available. Protein expression of SF1, DAX1, NANOG, OCT4, SOX2 and STAT3 was evaluated. Due to the availability of biological material, it was performed in a subset of pACT samples. In each analysis, in the results section, the exact number of samples is specified.

Controls – Fetal and postnatal normal adrenal cortices

For the immunohistochemistry (IHC) study, we evaluated a group of 33 normal prenatal adrenal paraffin-embedded tissues obtained from spontaneously miscarried fetuses grouped according to gestation age: 20–25 weeks (n = 14), 26–31 weeks (n = 10), 32–37 weeks (n = 9). As postnatal controls, we evaluated 18 adrenals from children between birth and 10 years old who underwent routine autopsy examination in our Department of Pathology; fetuses or children with multiple malformations or children with known endocrine diseases, or previous use of glucocorticoids were excluded. Also, 26 specimens of normal adrenal cortices were analyzed as controls in quantitative polymerase chain reaction (qPCR) experiments: 12 pediatric specimens obtained after surgical treatment of Wilms' tumor and 14 from adult subjects with sudden death who underwent routine autopsy.



IHC: immunohistochemistry; qPCR: quantitative polymerase chain reaction; pACT: pediatric adrenocortical tumors; ACT: adrenocortical tumors, ACA: adrenocortical adenoma; ACC: adrenocortical carcinoma.

Figure 1. Experimental design.

Copyright© AE&M all rights reserved.

The surgical tissues were collected at the time of surgery. The autopsy specimens and the fetal tissues from miscarriages were collected at the moment of the evaluation by the Pathology Department, which occurred a couple of hours after death or miscarriage or at a maximum period of 12 hours after the patient's death or the occurrence of miscarriage if the event was during the night shift to minimize degradation and variability in both IHC and PCR analyses.

Information regarding the origin of each pediatric control and fetal tissue is on **Supplementary Table 1**, and the adult control tissue information is on **Supplementary Table 2**. Fetal tissues originated from spontaneous miscarriages; autopsy-derived tissues were obtained from individuals without clinical or pathological evidence of endocrine or neoplastic disease processes, and who did not use glucocorticoids; surgical control specimens were collected from patients undergoing procedures for non-inflammatory, non-neoplastic indications.

Patients

We evaluated 114 patients with ACT (96 Pediatric and 18 adults) who were diagnosed and followed at two reference centers in southeastern Brazil (**Tables 1 and 2**). According to the experiment, the entire cohort or a subset of it was analyzed. Routine diagnostic tests and imaging evaluations were performed before surgical treatment, and the patients were followed up after surgery, as previously reported (1,4,5).

Table 1. Clinicopathological data of pACTs

Gender		Male		18	19%
		Female		78	81%
Deaths		Alive		74	77%
		Dead		15	16%
		Unknown due to loss of follow up		7	7%
Age at diagnosis (years)		Median		1.6	
		Minimum; maximum		0.4; 15.6	
Weiss score		0		2	2.1%
		1		3	3.1%
		2		1	1.0%
		3		4	4.2%
		4		15	15.6%
		5		10	10.4%
		6		25	26.0%
		7		15	15.6%
		8		11	11.5%
		9		8	8.3%
		Unknown		2	2.1%
		Deaths	>5 year survival		
Tumor Stage	I	4 (6.7%)	35 (58.3%)	60	62.5%
	II	3 (21.4%)	9 (64.3%)	14	14.6%
	III	1 (7.7%)	5 (38.5%)	13	13.5%
	IV	7 (77.8%)	2 (22.2%)	9	9.4%
Relapse and/or Metastasis		Yes		18	18.8%
		No		52	54.2%
		Unknown		26	27.1%
Chemotherapy	Yes			19	19.8%
	No			48	50.0%
	Unknown			29	30.2%
Surgery	Yes			96	100%
		Female	Male		
Hormone Secretion	Virilizing	43	8	51	53.1%
	Mixed (Virilizing + Cushing)*	32	9	41	42.7%
	Non secreting	3	1	4	4.2%

* Clinical or subclinical Cushing syndrome.

Copyright© AE&M all rights reserved.

Table 2. Clinicopathological data of adult ACTs

Gender		Male		2	11%
		Female		16	89%
Deaths		Alive		14	78%
		Dead		3	16%
		Unknown due to loss of follow up		1	6%
Age at diagnosis (years)		Median		42.5	
		Minimum; Maximum		21; 66	
Weiss score		0		1	5.5%
		1		7	38.9%
		2		2	11.1%
		3		2	11.1%
		4		3	16.7%
		5		0	0%
		6		3	16.7%
		Deaths	>5 year survival		
Tumor Stage	I	0	3 (42.8%)	7	38.9%
	II	1 (16.7%)	4 (66.7%)	6	33.3%
	III	0	0	1	5.6%
	IV	2 (50%)	1 (25%)	4	22.2%
Relapse and/or Metastasis		Yes		5	2.,8%
		No		13	72.2%
Chemotherapy	Yes			6	33.3%
	No			12	66.7%
Surgery	Yes			18	100%
			Female	Male	
Hormone Secretion		Virilizing	2	0	2	11.1%
		Cushing	7	0	7	38.9%
		Mixed (Virilizing + Cushing*)	5	2	7	38.9%
		Non functioning	2	0	2	11.1%

* Clinical or subclinical Cushing syndrome.

Tumor stages were classified according to the International Pediatric Adrenocortical Tumor Registry for children and Macfarlane modified by Sullivan (40) for adults. In adult ACT, a Weiss score of less than three was used to classify the tumors as ACA, and a score of three or greater was used to classify them as ACC (41). In the pediatric group, we also assessed the Weiss score but did not categorize ACT as ACA or ACC according to this criterion because it is not entirely applicable and does not accurately predict clinical outcomes in this age group (41). This study was approved by the Ethics Committee (HCRP Process 3019/2013). Informed written consent was obtained from patients and controls or their parents.

Sample size

Owing to the rarity of the condition, we employed a convenience sampling approach for the pediatric and the adult cohort. We included all consecutive eligible patients identified during the study period. This sample size reflects the maximum feasible recruitment for this population in our University Hospital during the study period. For each experiment, either qPCR or IHC, the number of samples of pACT, adult tumors and controls is specified in the results and was selected according to tissue availability.

IHC analyses

Standardization of IHC analyses

Paraffin blocks containing tissues known to express the target proteins (identified from manufacturer information or the Human Protein Atlas) were sectioned at 5 µm onto poly-L-lysine–coated slides. Sections were deparaffinized overnight, cleared in xylene, and rehydrated through graded alcohols. Heat-induced antigen retrieval was performed in Diva Decloaker 10X® buffer (Biomedical Care, CA, USA) at 90 °C for 40 min, followed by cooling in distilled water. IHC staining was carried out using the REVEAL Polyvalent HRP-DAB Detection System® (Spring Bioscience, CA,

Copyright© AE&M all rights reserved.

USA). Endogenous peroxidase was blocked for 15 min, followed by protein blocking for 10 min. Primary antibodies were tested in serial dilutions (1:25–1:300) and incubated overnight at 4 °C. After washing, slides were incubated with the rabbit anti-mouse complement for 10 min, HRP conjugate for 15 min, and DAB for 5 min. Hematoxylin counterstaining was performed for 15 s, followed by bluing, dehydration, clearing, and mounting. Optimal antibody dilutions were determined from the positive control slides (**Table 3**), with representative images shown in **Supplementary Figure 1**.

Fetal and postnatal adrenal cortices

The adrenal morphology was evaluated by routine hematoxylin-eosin staining. We performed the IHC studies using the primary antibodies described previously (**Table 3**). Labeling was developed with 3,3-diaminobenzidine (DAB; Vector Laboratories Inc.), and the nuclei were stained with Harris hematoxylin. For the analyses, we subcategorized our samples into gestational and postnatal age groups: 20–25 weeks (n = 14), 26–31 weeks (n = 10), 32–37 weeks (n = 9), and postnatal (n = 18). These samples were analyzed by M.M.C. and confirmed by an experienced pathologist (L.Z.R.). We present a descriptive analysis of each developmental stage.

Tumors

Depending on the availability of paraffin-embedded samples, IHC studies to analyze STAT3, NANOG, SOX2, and OCT4 proteins were initially performed in a subset of 46 ACT samples (30 pediatric and 16 adult samples) from the University Hospital of the Ribeirao Preto Medical School. During the transfer of the histological cut to the silanized slide, some samples were lost. Therefore, the number of samples differs between analyses. In each analysis, in the results section, the exact number of samples is specified.

Preliminary analysis of our group's data showed that increased OCT4 expression was associated with recurrence and/or metastasis. Therefore, we decided to improve our sample size and added 25 pACT samples from Centro Infantil Boldrini in the analysis. The use of these samples was approved by this collaborative center's ethic committee (07/12). As negative controls, all specimens were incubated with an isotope-matched control antibody under identical conditions. Preparations for each marker were evaluated randomly in at least ten representative high-power fields (x400) by an experienced pathologist (L.N.R.). Two samples stained for STAT3 and three stained for NANOG had to be excluded due to the bending of the material during preparation.

The nuclear staining of the tumor samples was evaluated using the H score. The intensity score of this staining was classified on a scale ranging from 0 (absent) to 3 (strong). In addition, the percentage of positive staining tumor cells observed in each sample was categorized into a positivity score as follows: 0% - score 0; 1 to 9%, score 0.1; 10-49%, score 0.5, and ≥ 50% score 1.0. Then, we multiplied this positivity score (0, 0.1, 0.5, or 1) by the intensity score (0, 1, 2, or 3) to obtain a final semi-quantitative score (H score), ranging from 0 to 3. Although a formal inter-observer reliability analysis was not conducted, all immunohistochemical evaluations were performed by the pathology team of our University Hospital and reviewed by a pathologist who is an expert in adrenal diseases (L.Z.R.) and the first author of this study (M.M.C.). This process helped ensure a shared interpretive framework.

Table 3. List of antibodies used in immunohistochemistry experiments, tissues used as positive controls, and dilutions

Antibodies (Manufacturer)	Positive-Control	Dilution
Anti human SF-1 mouse monoclonal antibody PP-N1665-00 (Perseus Proteomics®)	Testicle	1:25
Anti-NR0B1/DAX1 antibody ab60144 (Abcam®)	Lung	1:25
Anti-STAT3 (phospho Y705) antibody [EP2147Y] ab76315 (Abcam®)	Colon	1:25
Anti-SOX-2 (Y-17) sc-17320 (Santa Cruz Biotechnology®)	Colon	1:25
Anti-NANOG antibody - ChIP Grade ab21624 (Abcam®)	Testicle	1:25
Anti-OCT-3/4 (C-10) sc-5279 (Santa Cruz Biotechnology®)	Testicle	1:50

Copyright© AE&M all rights reserved.

RNA extraction, DNAse digestion, and cDNA synthesis

Total RNA was extracted using Trizol Reagent (Invitrogen®, Karlsruhe, Germany) according to the manufacturer's protocol. RNA integrity was checked according to the 28S/18S rate, with an acceptable range of 1.6 to 2.0, and confirmed by 1.2% agarose gel. RNA concentrations were quantified by spectrometry (Nanodrop2000, Thermo Fisher Scientific Inc., Waltham, MA, USA).

To guarantee a pure RNA without DNA contamination, RNA samples (1 µg) were exposed to DNase (1 µL) for 15 min at room temperature, and then it was inactivated with 1 µL EDTA 25mM for 10 min at 65°C. mRNA was reverse-transcribed using MultiScribe™ enzyme and the High-Capacity cDNA Reverse Transcription Kit (Life Technologies). cDNA was diluted (1:5) for qPCR.

mRNA Quantification by qPCR

The mRNA expression levels were measured in duplicate using TaqMan assay (Life Technologies, Foster City, CA, USA) according to the manufacturer's recommendation. The target genes evaluated were *STAT3* (Hs01047580_m1), *NANOG* (Hs04260366_g1), *SOX2* (Hs01053049_s1), and *OCT4* (Hs01654807_s1). The 2-ΔΔCt method was used to determine the relative expression of mRNA. The results were normalized with *GUSB* (Hs99999908_m1) as endogenous control. In the present study, *GUSB* was chosen as the reference gene because it follows the same standardization that was previously published by our group in gene expression analyses in adrenocortical tumors (4). In this previous study, we evaluated three extensively used endogenous controls (*TBP*, *GUSB* e *GAPDH*), and we observed that *GUSB* presented with the most stable expression in all adrenocortical human tissues. Considering this previously stablished and published validation, we have chosen *GUSB* and an endogenous control, keeping methodological consistency with the work already published by our group. The median obtained from the 2-ΔΔCt adrenal tumor tissue value was compared with the median value obtained from 2-ΔΔCt of normal adrenal tissue, obtaining the value which shows the number of times (fold) that this gene is hyper- or hypo-expressed in tumor tissue compared to control tissue (42).

Immunofluorescence (IF)

Cells were cultured on coverslips placed in 24-well plates for the immunofluorescence (IF) assays. The NCI-H295 medium was collected, and cells were fixed in methanol for 3 minutes, washed 3 times with 0.01 M PBS, and incubated with 10% normal horse serum for one hour for blocking. Sections were then incubated overnight at room temperature with anti-NANOG primary antibody (dilution: 1:100, #610154, BD Biosciences). Next, cells were washed 3 times with 0.01 M PBS, incubated with secondary antibody CyTM5-conjugated AffiniPure donkey anti-mouse antibody (Jackson Immuno Research, #715-175-150, dilution: 1:250; red color) for four hours, and washed 3 times with 0.01 M PBS. For nuclear counterstaining, cells were incubated with 4', 6-diamidino-2-phenylindole (DAPi; Cell Signaling Technology, #4083, dilution: 1:25,000) for 2 minutes, washed in 1X PBS, and slides were set with Fluoromount (Sigma-Aldrich). Expression and localization of NANOG were observed with a Leica TCS SP5 laser scanning confocal microscope (Leica Microsystems, Wetzlar, Germany) with fixed exposure time for all samples.

PNU-74654 treatment of H295 cells

The NCI-H295 adrenocortical cell line was kindly provided by Professor Claudimara Lofti (University of Sao Paulo) and was cultured in RPMI 1640 medium (GIBCO, Life Technologies, Foster City, CA) supplemented with 2% fetal bovine serum (Sigma Aldrich, St. Louis, MO, USA), 1% ITS Premix (BD Biosciences) and 1% penicillin/streptomycin (100 mg/mL; GIBCO Life Technologies) and harvested weekly. Cells were cultured in a monolayer and maintained under standard conditions at 37°C in a humidified atmosphere (5% CO2 – 95% air). The NCI-H295 carries the p.S45P CTNNB1 mutation, which constitutively activates the Wnt pathway signaling.

To assess the potential interaction between the Wnt/β-catenin pathway and *NANOG* mRNA expression, we analyzed *NANOG* mRNA levels in NCI-H295 cells under basal conditions and after the treatment of these cells with different doses of PNU-7654 over standard periods. PNU-7654 inhibits the Wnt signaling by preventing the interaction of Tcf and beta-catenin. PNU-74654 compound (Sigma Aldrich) was

Copyright© AE&M all rights reserved.

resuspended in Dimethyl Sulfoxide (DMSO; Sigma Aldrich) at stock concentrations of 31.2 mM, and cells were treated with vehicle (0.1%-0.4%) DMSO as a control. PNU-4654 was diluted 100X in a growth medium for working solutions and then diluted to 10 µM, 50 µM, and 100µM. Total RNA from NCI-H295 cells was isolated using TRIzol® according to the manufacturer's protocol (Life Technologies). RNA extraction and cDNA synthesis were performed as described above. For qPCR, TaqMan® assay *NANOG* (Hs04260366_g1) was used according to the manufacturer's recommendation using cDNA (diluted 1:5) as a template. TaqMan® assay for NCI-H295 cells: Relative expression values were determined by the 2-ΔΔCt method using *GUSB* (ID: 4326320E) as endogenous control.

Our primary objective in this study was to explore the functional relevance of *NANOG* expression and the Wnt/β-catenin pathway inhibition in the context of adrenocortical carcinoma. We have not described dose-response curves or time-course studies because we employed a targeted experimental design based on concentrations and NCI-H295 cell viability in different times after PNU-74654 reported in prior literature (43). This previous study from our group demonstrated that this treatment in both concentrations significantly decreased viability of adrenocortical tumor cells. NCI-H295 cells were treated with PNU-74654, a beta-catenin inhibitor, with a range of concentrations: 5, 10, 50, 100 and 200 µM, and the effects were measured at different time points: after 24, 48, 72, and 96 hours. Higher concentrations (100 and 200 µM) caused a significant decrease in viability by 24–48 h. For lower concentrations, a reduction in viability became evident at later times (72–96 h). At 48 h, there was a clear dose-dependent increase in early and late apoptosis and reduced nuclear and cytoplasmic β-catenin accumulation versus vehicle. The highest concentrations used in these previous study (100–200 µM) could be questioned for cytotoxicity, but these doses did not affect Y1 mouse adrenal and HeLa non-adrenal cell lines under similar conditions, supporting specificity in blocking Wnt/β-catenin signaling.

Statistical analysis

The Mann-Whitney test was used to compare mRNA expression levels between ACT samples and controls. The Kruskal-Wallis test was used for comparisons between mRNA expression and different tumor stages. Spearman's test was used to analyze the correlations between the expression of evaluated genes. Log-rank test and Kaplan-Meier plot were used to analyze the association between gene expression and overall survival. In the analysis of the association between survival outcomes with mRNA expression levels, the ACT samples were categorized as increased (hyper-expressed) or decreased (hypo-expressed), based on whether it is higher or lower than the median gene expression 2-ΔΔCt of the control samples, and Kaplan-Meier curves and Log-rank analysis were performed. One-way ANOVA followed by Holm-Sidak's multiple comparisons post-test was used to evaluate the differences between before and after treatment with all concentrations of PNU-74654. Non-continuous variables were expressed in the plots as median and interquartile range, and continuous variables were expressed as median and standard error (SEM). The significant limit for all the tests was established at 95% (p-value ≤ 0.05). Statistical analysis was performed using GraphPad Prism 6 (GraphPad, San Diego, CA).

RESULTS

NANOG, OCT4, SOX2 And STAT3 protein expression during the adrenal development

We showed that all of the studied stem cell maintenance proteins (NANOG, OCT4, SOX2, and STAT3) were expressed between 20 and 25 weeks of gestational period (**Figures 2A, 2B, 2C and 2F**). After that, only OCT4 and STAT3 kept staining between 26 and 30 weeks (**Figures 2H and 2L**). However, none of these proteins were detected after 31 weeks of gestation and in the postnatal adrenal cortices **(Figures 2M, 2N, 2O and 2R**).

At 20-25 weeks of gestational age, the expression of the four proteins was located at the same adrenal layers but with different intensities. SOX2 stained strongly through the capsule and cortical regions (**Figure 2C**); OCT4 staining was stronger at the capsular region when compared with the rest of the cortex (**Figure 2B**); STAT3 staining was also observed in the capsule and cortex but in moderate intensity (**Figure 2F**); NANOG was expressed only in the

Copyright© AE&M all rights reserved.

capsular region and with weak intensity (**Figure 2A**). Between 26 and 30 weeks of gestational age, OCT4 and STAT3 kept the same pattern of expression as those between 20 and 25 weeks (**Figure 2H and 2L**), while NANOG and SOX2 were no longer expressed (**Figures 2G and 2I**). From 31 weeks till the end of gestation and in the postnatal life, OCT4 and STAT3 were also no longer expressed (**Figures 2N and 2O**).

Clinical and pathological results

Pediatric patients

We evaluated 96 children (81% female) with a median age at the diagnosis of 1.6 years (0.4-15.6 years). Seventy-six patients (79%) were diagnosed in the first five years of life, including 19 (20%) diagnosed in the first year. Virilization due to androgen excess was the most common clinical finding in this group, and it was present in 92 patients (96%), including 51 patients with androgen-secreting tumors and 41 patients with both cortisol and androgen-secreting tumors (mixed tumors). Only four patients presented with non-secreting adrenal tumors, which were incidentally discovered (**Table 1**).

The germline p.R337H *P53* mutation was detected in 82 out of 96 pediatric patients (85%), and somatic exon 3 *CTNNB1* mutations were found in 10 out of 70 pediatric samples analyzed (14%).

Complete clinical and pathological features, including sex, age, clinical presentation, tumor stage, treatments, and death as an outcome, are described in **Table 1**. Part of these clinical data had been previously reported (1,4).

Adult patients

We evaluated 18 adults (89% female) with a median age at the diagnosis of 42.5 years (21-66 years). Cortisol-secreting tumors were found in 14 patients (77%), 50% of them being mixed cortisol and androgen-secreting tumors. Two patients presented with androgen-secreting tumors, and the other two patients had non-secreting tumors. According to the Weiss score tumor system, 44% of these tumors were carcinomas. The germline p.R337H *P53* mutation was detected in 4 patients (22%), and somatic *CTNNB1* mutations were detected in 7 patients (39%).

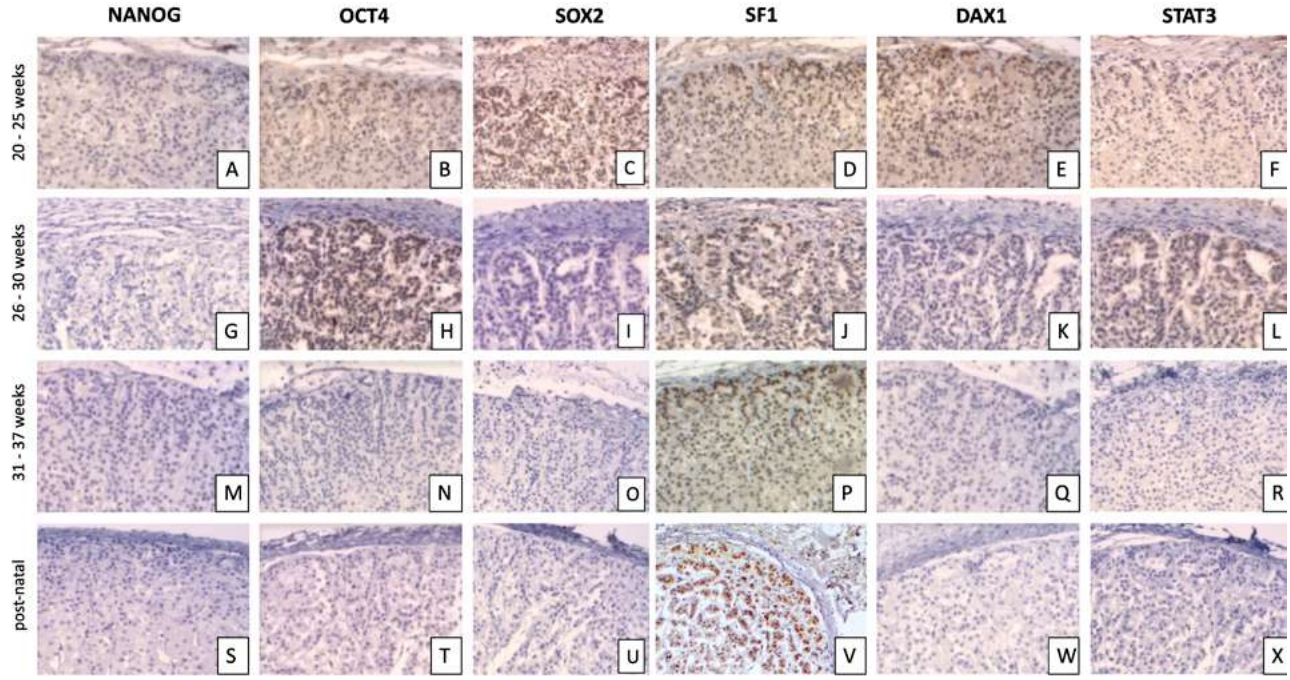


Figure 2. Immunohistochemistry (IHC) of NANOG, OCT4, SOX2, SF1, DAX1 and STAT3 protein expression during the adrenal development. IHC expression of NANOG at 20-25 weeks (**A**), 26-30 weeks (**G**), 31-37 weeks (**M**) of gestational period and postnatal (**S**). IHC expression of OCT4 at 20-25 weeks (**B**), 26-30 weeks (**H**), 31-37 weeks (**N**) of gestational period and postnatal (**T**). IHQ expression of SOX2 at 20-25 weeks (**C**), 26-30 weeks (**I**), 31-37 weeks (**O**) of gestational period and postnatal (**U**). IHQ expression of SF1 at 20-25 weeks (**D**), 26-30 weeks (**J**), 31-37 weeks (**P**) of gestational period and postnatal (**V**). IHQ expression of DAX1 at 20-25 weeks (**E**), 26-30 weeks (**K**), 31-37 weeks (**Q**) of gestational period and postnatal (**W**). IHQ expression of STAT3 at 20-25 weeks (**F**), 26-30 weeks (**L**), 31-37 weeks (**R**) of gestational period and postnatal (**X**).

Copyright© AE&M all rights reserved.

Clinical and pathological features, including sex, age, clinical presentation, tumor stage, treatment, and death, are described in Table 2.

The stem cell marker proteins expression in ACT

pACT

IHC for NANOG, OCT4, SOX2, and STAT3 was evaluated in a subset of pACT. We also evaluated a second tier of pACT samples to confirm the findings on OCT4 in the first cohort as described previously in the Methods section. Positive OCT4 nuclear staining was found in 18 out of 55 samples (32%) (Figure 3H). Interestingly, positive OCT4 was positively associated with metastatic pACT (odds ratio, 2.28; 95% confidence interval [CI]: 1.13 to 4.59; Fisher's test: p-value < 0.05 – Figure 3I). Only three out of 27 samples (11%) presented with positive nuclear staining of NANOG (Figure 3F). All of the samples were negative for STAT3 and SOX2 staining (Figures 3J and 3L).

Adult ACT

IHC for NANOG, OCT4, SOX2, and STAT3 was evaluated in a subset of adult ACT (10 ACA, 6 ACC) samples (Figures 3F and 3H, Figures 3K and 3M). As in the pediatric samples, all adult samples were negative for STAT3 and SOX2 staining (Figures 3K and 3M). Only 1 out of 16 (7%) samples presented with positive nuclear staining of NANOG (Figure 3F). Positive OCT4 nuclear staining was also found in 1 sample (distinct from the one staining for NANOG) (Figure 3H).

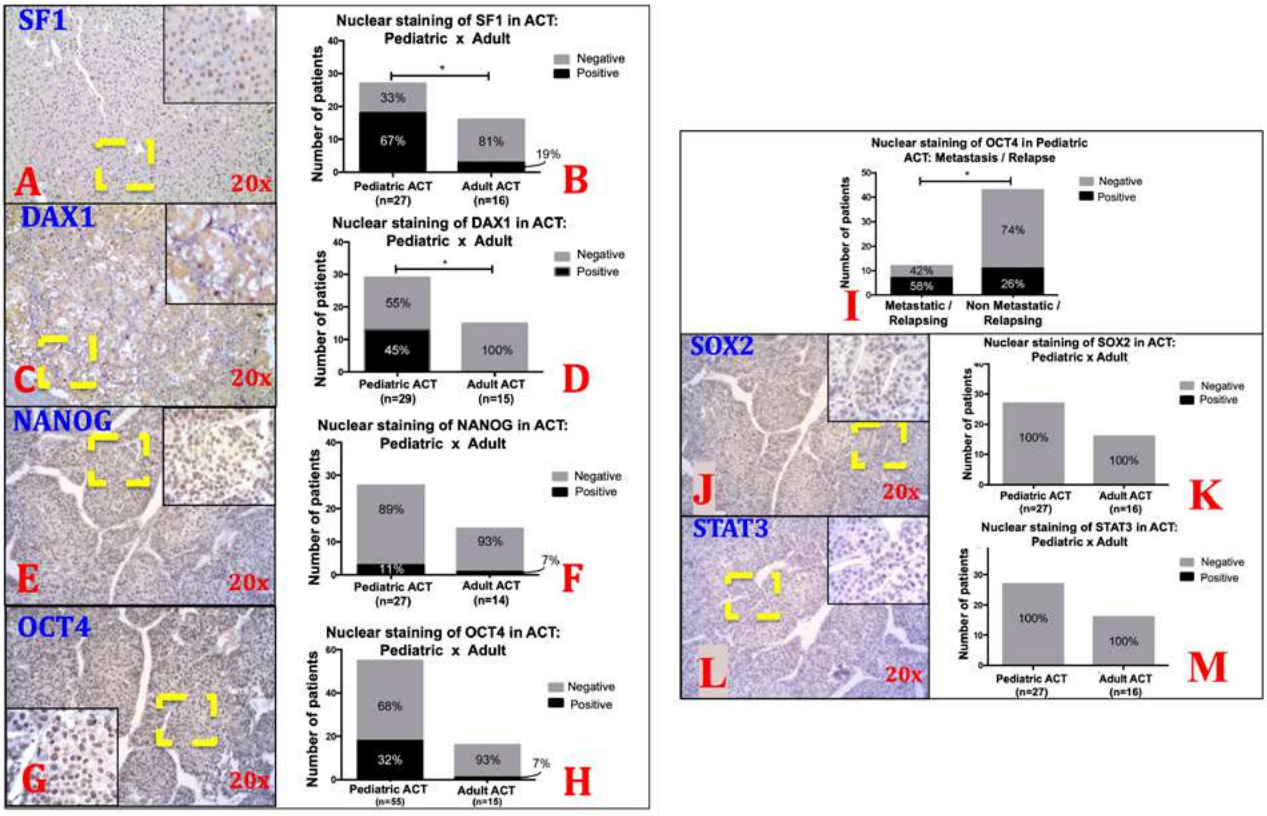


Figure 3. Immunohistochemistry in ACT: Pediatric vs Adult patients. (**A**) Positive nuclear staining for SF1. (**B**) Graphic depiction of the percentage of pediatric and adult ACT patients with positive nuclear staining for SF1 (*p<0.05). (**C**) Positive nuclear staining for DAX1. (**D**) Graphic depiction of the percentage of pediatric and adult ACT patients with positive nuclear staining for DAX1 (*p<0.05). (**E**) Positive nuclear staining for NANOG. (**F**) Graphic depiction of the percentage of pediatric and adult ACT patients with positive nuclear staining for NANOG. (**G**) Positive nuclear staining for OCT4. (**H**) Graphic depiction of the percentage of pediatric and adult ACT patients with positive nuclear staining for OCT4. (**I**) Percentage of OCT4 positive samples in metastatic/relapsing versus non-metastatic/non-relapsing ACTs (*p<0.05). (**J**) Nuclear staining for SOX2. (**K**) Graphic depiction of the percentage of pediatric and adult ACT patients with positive nuclear staining for SOX2. (**L**) Nuclear staining for STAT3. (**M**) Graphic depiction of the percentage of pediatric and adult ACT patients with positive nuclear staining for STAT3.

Copyright© AE&M all rights reserved.

The Stem Cell Marker mRNA Expression

pACT

Concerning the mRNA expression of stem cell maintenance transcription factors, pediatric patients presented with no difference in *STAT3* and *NANOG* expression between pACT and controls (p-value=0.31 and p-value=0.48, respectively – **Figures 4D and 4C**). pACT presented with lower *SOX2* mRNA expression when compared with controls (**Figure 4E** – p-value < 0.01). The mRNA expression of *OCT4* could not be analyzed because the cycle threshold (CT) of almost all the samples was undetermined.

Adult ACT

As in the pediatric group, adult ACTs presented with lower mRNA expression levels of *SOX2* (p-value < 0.01; **Figure 5E**) when compared to normal adrenal cortices. *STAT3* and *NANOG* expression did not differ (p-value = 0.15 and p-value = 0.85, respectively; **Figures 5D and 5C**) between adult ACT and control adrenal cortices. Curiously, cortisol-secreting tumors showed higher *STAT3* mRNA expression levels than other secreting tumors (p-value = 0.01). Among the adult ACT group, *STAT3* mRNA expression levels were higher in ACAs than in ACCs (p-value < 0.01; **Figure 5F**). However, neither the ACA nor the ACC groups had *STAT3* mRNA expression levels distinguished from control adult adrenal cortices (p-value = 0.13 and p-value = 0.77, respectively). Furthermore, survival was not different regarding *STAT3* mRNA expression levels (log-rank test, p-value = 0.87).

mRNA expression levels of *NANOG* were higher among patients carrying the p.S45P *CTNNB1* mutation (p-value < 0.01), in both adults and children (**Figure 5H**). No differential mRNA expression was observed in association with p.R337H *P53*. No association was observed among patterns of mRNA expression of any gene in this study, tumor stage, or overall survival in the adult or pACT groups.

In vitro data

NANOG expression pattern in NCI-H295 cells

Considering the finding of higher *NANOG* mRNA expression in p.S45P *CTNNB1* mutated tumors, we performed in vitro tests using the NCI-H295 lineage, which carries this mutation, to evaluate where and if NANOG protein was expressed and its cellular location. On immunofluorescence, a bright green light was observed in the nucleus of some NCI-H295 cells (**Figure 6**), confirming that this protein is expressed in this lineage. As it was expressed in only a few cells, it seems that these may constitute a subgroup of cells with different characteristics.

Effect of the Wnt/beta-catenin signaling inhibition by PNU-7654 on NANOG mRNA expression levels in H295 cells

NANOG mRNA expression in NCI-H295 cells was detected under basal conditions. After 48h under PNU-74654 treatment at 50 and 100μM, a significant decrease in *NANOG* mRNA expression levels was observed (25% and 46% reduction, respectively; ANOVA: p-value < 0.01; **Figure 6**).

DISCUSSION

The expression pattern of the stem cell maintenance genes NANOG, OCT4, SOX2, and STAT3 during the development of healthy human adrenal cortex in different stages of development or in ACT has not been further explored to date. In the present study, we analyzed the expression pattern of these stem cell maintenance genes in control adrenal cortices from the second half of gestation, the postnatal period, and in ACT from children and adults. Furthermore, we also performed an in vitro experiment to demonstrate that the Wnt/β-catenin pathway signaling regulates the *NANOG* expression in p.S45P β-catenin mutated ACT.

We observed that the human adrenal cortex cells still maintain the expression of NANOG, OCT4, and STAT3 after steroidogenesis begins, which occurs around week 7 of gestation in humans. It is different from what is observed in murine embryonic stem cells, in which the expression of these proteins ceases when adrenal steroidogenesis starts (23,44,45). These discrepancies likely reflect fundamental species differences in adrenal development, which were also previously described in mouse and primate gene-expression studies throughout embryological development (46,47). Therefore, while murine models provide valuable mechanistic insights, direct extrapolation to

Copyright© AE&M all rights reserved.

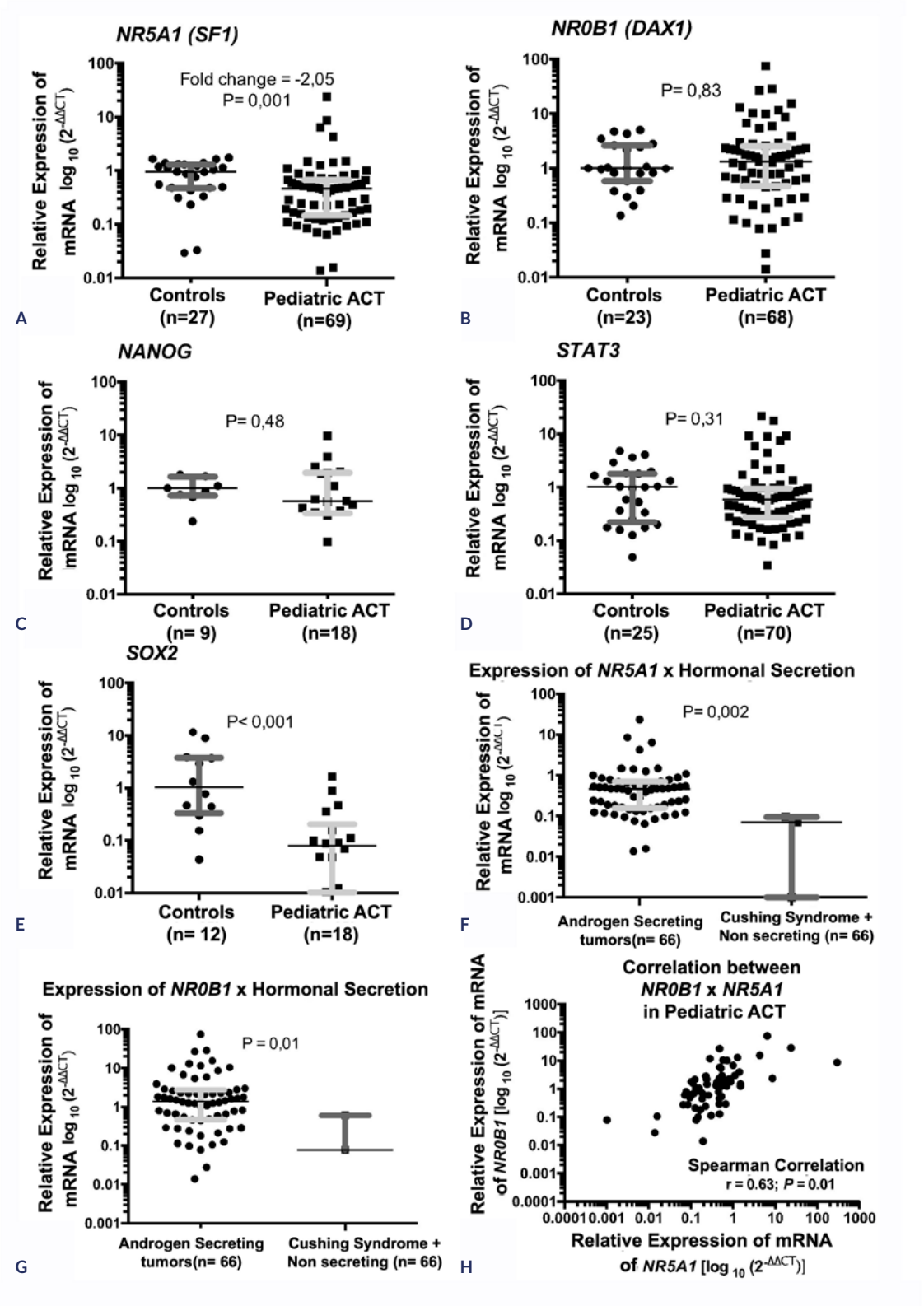


Figure 4. Gene expression in pACT. (**A**) *SF1* mRNA expression in control tissues and pACT tissues (p=0.001). (**B**) *DAX1* mRNA expression in control tissues and pACT tissues (p=0.83). (**C**) *NANOG* mRNA expression in control tissues and pACT tissues (p=0.48). (**D**) *STAT3* mRNA expression in control tissues and pACT tissues (p=0.31). (**E**) *SOX2* mRNA expression in control tissues and pACT tissues (p=0.001). (**F**) *SF1* mRNA expression in patients with androgen-secreting tumors and in patients with Cushing syndrome or non-secreting tumors. (**G**) *DAX1* mRNA expression in patients with androgen-secreting tumors and in patients with Cushing syndrome or non-secreting tumors. (**H**) Correlation between *DAX1* and *SF1* expression in pACT (r=0.63 and p=0.01).

Copyright© AE&M all rights reserved.

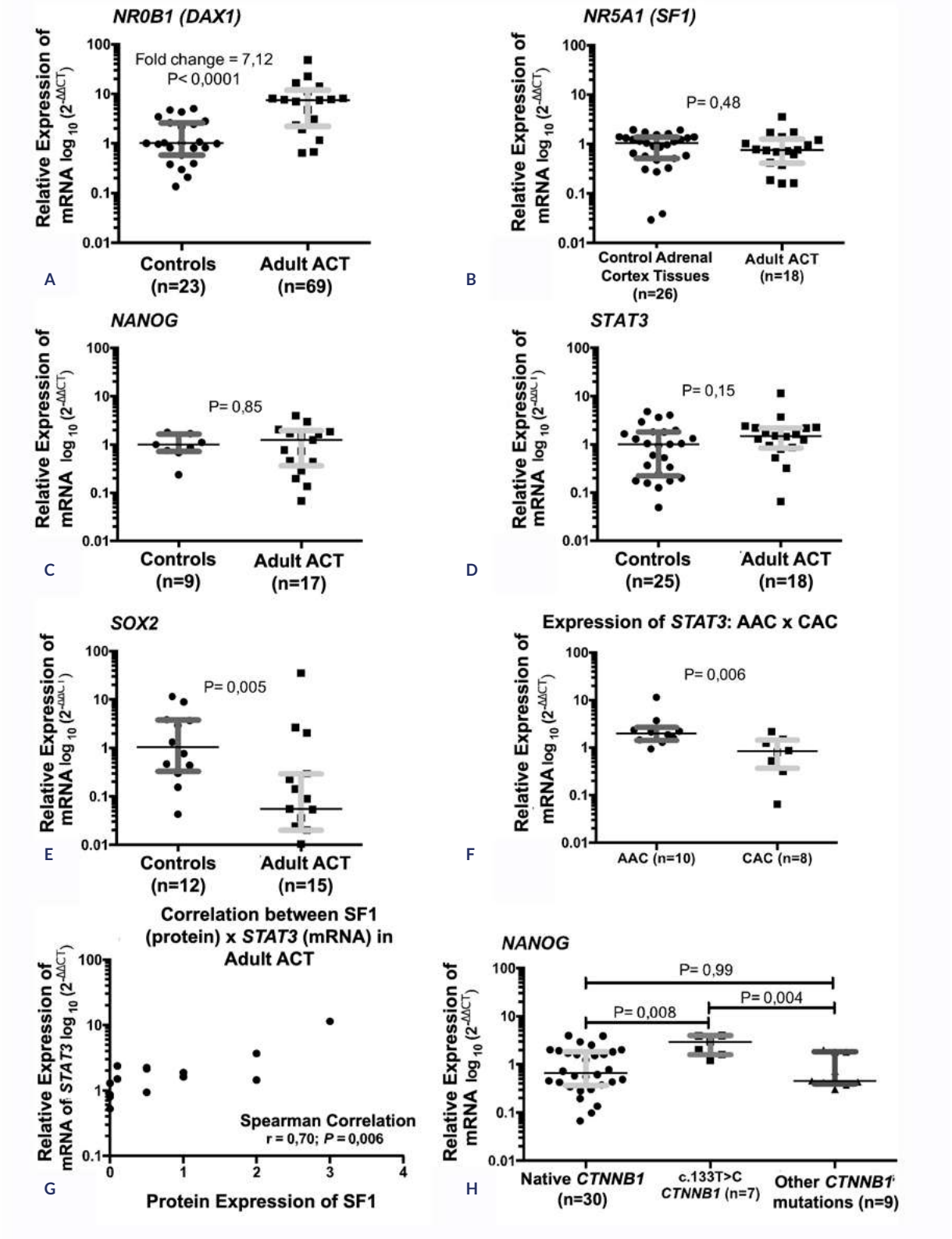


Figure 5. Gene expression in Adult ACT. (**A**) *DAX* mRNA expression in control tissues and adult ACT tissues (p=0.0001). (**B**) *SF1* mRNA expression in control tissues and adult ACT tissues (p=0.48). (**C**) *NANOG* mRNA expression in control tissues and adult ACT tissues (p=0.85). (**D**) *STAT3* mRNA expression in control tissues and adult ACT tissues (p=0.15). (**E**) *SOX2* mRNA expression in control tissues and adult ACT tissues (p=0.005). (**F**) *STAT3* mRNA expression in adenomas and in carcinomas. (**G**) Correlation between *STAT3* and *SF1* expression in pACT (r= 0.7 and p=0.006) (**H**) *NANOG* expression in patients with native *CTNNB1*, in patients with c.133T>C *CTNNB1* mutation, and inpatients with other *CTNNB1* mutations.

Copyright© AE&M all rights reserved.

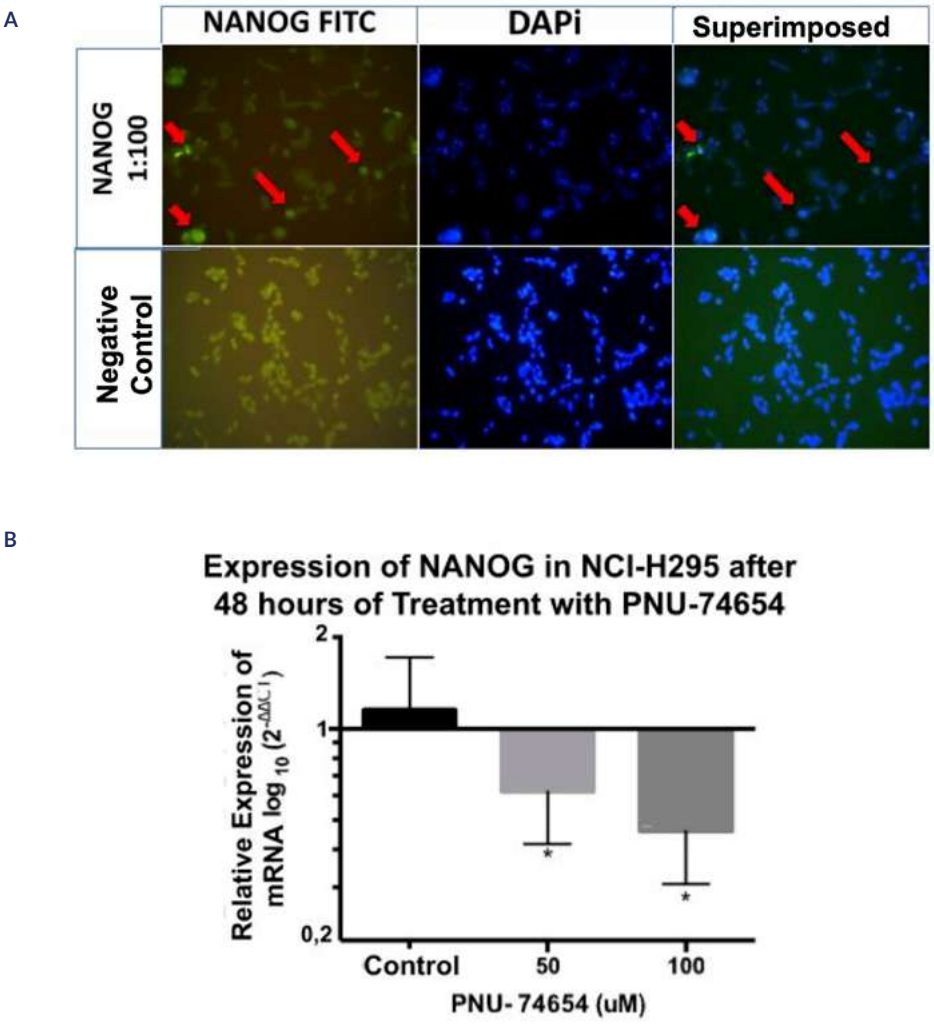


Figure 6. *NANOG* mRNA expression. (**A**) *NANOG* mRNA expression after inhibiting the Wnt/β-catenin signaling in NCI-H295 cells after 48hs treatment with PNU-74654 at 50 and 100 µM. (**B**) ICF shows NANOG staining in some NCI-H295 cells under basal conditions..

human development must be made with caution. In this context, our findings suggest that the human adrenal cortex may retain stemness-related transcriptional programs longer than the murine cortex. Our data also implies that the adult stem cell niche does not need *NANOG*, *OCT4*, *SOX2*, and *STAT3* activity to maintain itself, as the expression of these proteins was not observed in the postnatal adrenal cortices.

It is well known that almost all tissues possess adult stem cell niches, which serve to replace worn-out tissues (48). The adult stem cell niche in the adrenal cortex is located within and/or underneath the capsular region. A more intense expression of OCT4, SOX2, and STAT3 in the subcapsular region of the adrenal cortex between 20 and 31 weeks of gestation suggests that these markers may contribute to the establishment of the adult stem cell niche but not maintain it.

Increased OCT4 expression was found in one-third of the pACTs and was associated with metastatic disease. However, this finding was not observed in adult ACT. Previous data in the literature showed increased OCT4 expression associated with worse prognosis and chemotherapy resistance in several types of cancer. This data is consistent with our findings in metastatic tumors (49).

Both pediatric and adult ACTs presented with lower levels of SOX2 expression when compared to control tissues. Therefore, this marker might not be associated with the pathogenesis of adrenocortical tumors as it is in other types of cancer, such as breast and colorectal cancer (50,51).

Copyright© AE&M all rights reserved.

STAT3 expression was higher in cortisol-secreting ACAs compared to other tumors, but no difference was observed compared to control tissues. STAT3 is crucial to the control of the anti-tumor immune response, and its hyperactivation is found in several types of cancer and is associated with a worse prognosis (52). Whether or not STAT3 has a role in the pathogenesis of cortisol-secreting pACT warrants further investigation.

mRNA expression levels of *NANOG* were higher among patients carrying the p.S45P *CTNNB1* mutation in adults and children, as confirmed in in vitro experiments. *NANOG* mRNA expression was decreased by inhibition of Wnt/beta-catenin signaling. Data in the literature have shown that *NANOG* can induce stemness, self-renewal, and invasive and metastatic behavior in some types of cancers through JAK/STAT and Wnt/beta-catenin (53), which is consistent with our findings in pACT and adult ACT. Wnt/β-catenin signaling has been shown to regulate *NANOG* expression via β-catenin/TCF complexes directly, and through interaction with OCT4, contributing to the maintenance of stemness and tumor-initiating capacity (54). Takao and cols. demonstrated that β-catenin up-regulates Nanog expression by directly interacting with Oct-3/4 in embryonic stem cells (54). In our study, we have observed a dose-dependent decrease in *NANOG* mRNA expression in the NCI-H295 cell line 48 hours after blocking the Wnt/β-catenin pathway with PNU 74654. Similar findings have been reported previously in lung cell lines (55) and small-cell lung cancer (56). In the latter, coexpression of *OCT4* and *NANOG* increased the self-renewal potential of cancer cells, increased drug resistance, and tumorigenic capacity through Wnt/β-catenin signaling activation. Our findings indicate an association between *NANOG* and *OCT4* expression and the activation of the Wnt/β-catenin pathway, which is linked with the pathogenesis of adrenocortical tumors.

This study has some limitations that should be acknowledged. First, because ACTs are rare, the adult cohort was necessarily small and based on a convenience sample, which limits statistical power and reduces the ability to detect subtle differences between groups. Second, acquiring control pediatric and adult tissues is challenging. We only obtained fetal tissue after 20 weeks of gestational age, and earlier gestational periods were not analyzed, and conclusions should not be drawn concerning early developmental periods. We had a heterogeneous control group that can influence the results. However, we applied exclusion criteria to minimize bias. Third, although *GUSB* was selected as the endogenous control for qPCR based on prior reports of its stability in similar tissues, we did not perform a formal reference gene stability assessment across all sample types, which might affect normalization accuracy. Fourth, we did not conduct an inter-observer reliability analysis for the IHC evaluations. Finally, the descriptive comparison of fetal and postnatal adrenal cortex IHC did not include statistical testing, limiting the strength of conclusions regarding developmental expression patterns. Despite these limitations, our study provides original and valuable data on a rare disease and suggests that stem cell–associated markers may contribute to the pathogenesis and prognosis of ACTs.

In conclusion, we found increased expression of OCT4, SOX2, and STAT3 in the subcapsular region of the adrenal cortex between 20 and 31 weeks of gestation, suggesting that these markers may contribute to the establishment of the adult stem cells niche but appear not to be essential to maintain it. OCT4 expression was increased in pACTs and was associated with a worse prognosis. Expression of *NANOG* was higher in both adult and pediatric patients with ACTs carrying p.S45P *CTNNB1* mutation, and its expression was decreased after Wnt/β-catenin signaling inhibition in an adrenocortical cell line harboring this mutation. *STAT3* expression was increased in cortisol-secreting ACTs, but whether or not it plays a role in pathogenesis or prognosis is unclear since there was no difference in gene expression when compared with controls. *SOX2* seems to not play a role in ACT pathogenesis.

Financial support: this work was funded by FAPESP (Sao Paulo State Research Foundation; grant 14/03989), CNPq (Brazilian National Council for Research), CAPES (Coordination for the Improvement of Higher Education Personnel, and FAEPA (HCRP-FMRP Support Foundation for Research, Teaching and Assistance).

Disclosure: no potential conflict of interest relevant to this article was reported.

Copyright© AE&M all rights reserved.

Data availability: the data sets analysed in this study are included in the manuscript.

REFERENCES

1. Leal LF, Mermejo LM, Ramalho LZ, Martinelli CE, Yunes JA, Seidinger AL, et al. Wnt/β-Catenin Pathway Deregulation in Childhood Adrenocortical Tumors. J Clin Endocrinol Metab. 2011 Oct 1;96(10):3106–14. doi: 10.1210/jc.2011-0363
2. Simon DP, Giordano TJ, Hammer GD. Upregulated JAG1 Enhances Cell Proliferation in Adrenocortical Carcinoma. Clin Cancer Res. 2012 Mar 17;18(9):2452–64. doi: 10.1158/1078-0432.ccr-11-2371
3. Simon DP, Hammer GD. Adrenocortical stem and progenitor cells: Implications for adrenocortical carcinoma. Mol Cell Endocrinol. 2012 Mar;351(1):2–11. doi: 10.1016/j.mce.2011.12.006
4. Gomes DC, Leal LF, Mermejo LM, Scrideli CA, Martinelli CE, Fragoso MCBV, et al. Sonic Hedgehog Signaling Is Active in Human Adrenal Cortex Development and Deregulated in Adrenocortical Tumors. J Clin Endocrinol Metab. 2014 Jul 1;99(7):E1209–16. doi: 10.1210/jc.2013-4098
5. Mermejo LM, Leal LF, Colli LM, Fragoso MCBV, Latronico AC, Tone LG, et al. Altered expression of noncanonical Wnt pathway genes in paediatric and adult adrenocortical tumours. Clin Endocrinol (Oxf). 2014 Apr 10;81(4):503–10. doi: 10.1111/cen.12462
6. Duncan AW, Rattis FM, DiMascio LN, Congdon KL, Pazianos G, Zhao C, et al. Integration of Notch and Wnt signaling in hematopoietic stem cell maintenance. Nat Immunol. 2005 Jan 23;6(3):314–22. doi: 10.1038/ni1164
7. Palma V. Hedgehog-GLI signaling regulates the behavior of cells with stem cell properties in the developing neocortex. Development. 2003 Dec 10;131(2):337–45. doi: 10.1242/dev.00930
8. Reya T, Clevers H. Wnt signalling in stem cells and cancer. Nature. 2005 Apr;434(7035):843–50. doi: 10.1038/nature03319
9. Rizvi AZ, Wong MH. Epithelial Stem Cells and Their Niche: There's No Place Like Home. Stem Cells. 2005 Feb;23(2):150–65. doi: 10.1634/stemcells.2004-0096
10. Assié G, Letouzé E, Fassnacht M, Jouinot A, Luscap W, Barreau O, et al. Integrated genomic characterization of adrenocortical carcinoma. Nat Genet. 2014 Jun 1;46(6):607–12. doi: 10.1038/ng.2953
11. Juhlin CC, Goh G, Healy J, Fonseca AL, Scholl UI, Stenman A, et al. Whole-Exome Sequencing Characterizes the Landscape of Somatic Mutations and Copy Number Alterations in Adrenocortical Carcinoma. J Clin Endocrinol Metab. 2015 Mar 1;100(3):E493–502. doi: 10.1210/jc.2014-3282
12. Ramalho-Santos M, Melton DA, McMahon AP. Hedgehog signals regulate multiple aspects of gastrointestinal development. Development. 2000 Jun 15;127(12):2763–72. doi: 10.1242/dev.127.12.2763
13. Liu S, Dontu G, Wicha MS. Mammary stem cells, self-renewal pathways, and carcinogenesis. Breast Cancer Res [Internet]. 2005 Mar 30;7(3). doi: 10.1186/bcr1021
14. Kawahira H, Scheel DW, Smith SB, German MS, Hebrok M. Hedgehog signaling regulates expansion of pancreatic epithelial cells. Dev Biol. 2005 Apr;280(1):111–21. doi: 10.1016/j.ydbio.2005.01.008
15. Chiba S. Concise Review: Notch Signaling in Stem Cell Systems. Stem Cells. 2006 Nov;24(11):2437–47. doi: 10.1634/stemcells.2005-0661
16. Gao J, Chen C, Hong L, Wang J, Du Y, Song J, et al. Expression of Jagged1 and its association with hepatitis B virus X protein in hepatocellular carcinoma. Biochem Biophys Res Commun. 2007 May;356(2):341–7. doi: 10.1016/j.bbrc.2007.02.130
17. Ronchi CL, Sbiera S, Altieri B, Steinhauer S, Wild V, Bekteshi M, et al. Notch1 pathway in adrenocortical carcinomas: correlations with clinical outcome. Endocr Relat Cancer. 2015 May 15;22(4):531–43. doi: 10.1530/erc-15-0163
18. Pera MF. Defining pluripotency. Nat Methods. 2010 Oct 28;7(11):885–7. doi: 10.1038/nmeth1110-885
19. Torres-Padilla ME ., Chambers I. Transcription factor heterogeneity in pluripotent stem cells: a stochastic advantage. Development. 2014 May 27;141(11):2173–81. doi: 10.1242/dev.102624
20. Wagner RT, Cooney AJ. Minireview: The Diverse Roles of Nuclear Receptors in the Regulation of Embryonic Stem Cell Pluripotency. Mol Endocrinol. 2013 Jun 1;27(6):864–78. doi: 10.1210/me.2012-1383
21. Zeineddine D, Hammoud AA, Mortada M, Boeuf H. The Oct4 protein: more than a magic stemness marker. Am J Stem Cells [Internet]. 2014 Sep 5;3(2):74. Available from: https://pmc.ncbi.nlm.nih.gov/articles/PMC4163606/
22. Chambers I, Colby D, Robertson M, Nichols J, Lee S, Tweedie S, et al. Functional Expression Cloning of Nanog, a Pluripotency Sustaining Factor in Embryonic Stem Cells. Cell. 2003 May;113(5):643–55. doi: 10.1016/s0092-8674(03)00392-1
23. Niakan KK, McCabe ERB. DAX1 origin, function, and novel role. Mol Genet Metab. 2005 Sep;86(1-2):70–83. doi: 10.1016/j.ymgme.2005.07.019
24. Pan GJ, Chang ZY, Schöler HR, Pei D. Stem cell pluripotency and transcription factor Oct4. Cell Res. 2002 Dec;12(5-6):321–9. doi: 10.1038/sj.cr.7290134
25. Raz R, Lee CK, Cannizzaro LA, D'Eustachio P, Levy DE. Essential role of STAT3 for embryonic stem cell pluripotency. Proc Natl Acad Sci U S A. 1999 Mar 16;96(6):2846–51. doi: 10.1073/pnas.96.6.2846
26. Ben-Porath I, Thomson MW, Carey VJ, Ge R, Bell GW, Regev A, et al. An embryonic stem cell-like gene expression signature in poorly differentiated aggressive human tumors. Nat Gen. 2008;40(5):499–507. doi: 10.1038/ng.127
27. Boumahdi S, Driessens G, Lapouge G, Rorive S, Nassar D, Le Mercier M, et al. SOX2 controls tumour initiation and cancer stem-cell functions in squamous-cell carcinoma. Nature [Internet]. 2014 Jul 1;511(7508):246–50. doi: 10.1038/nature13305
28. Jeter CR, Badeaux M, Choy G, Chandra D, Patrawala L, Liu C, et al. Functional evidence that the self-renewal gene NANOG regulates human tumor development. Stem Cells. 2009 May;27(5):993–1005. doi: 10.1002/stem.29
29. Koo BS, Lee SH, Kim JM, Huang S, Kim SH, Rho YS, et al. Oct4 is a critical regulator of stemness in head and neck squamous carcinoma cells. Oncogene [Internet]. 2015 Apr 1;34(18):2317–24. doi: 10.1038/onc.2014.174
30. Zhu Y, Xu Y, Chen D, Zhang C, Rui W, Zhao J, et al. Expression of STAT3 and IGF2 in adrenocortical carcinoma and its relationship with angiogenesis. Clin Transl Oncol. 2013 Oct 31;16(7):644–9. doi: 10.1007/s12094-013-1130-1
31. Chen W, Wang YJ. Multifaceted roles of OCT4 in tumor microenvironment: biology and therapeutic implications. Oncogene. 2025 Apr 14;44(18):1213–29. doi: 10.1038/s41388-025-03408-x
32. Wang YJ, Herlyn M. The emerging roles of Oct4 in tumor-initiating cells. Am J Physiol Cell Physiol. 2015 Dec 1;309(11):C709–18. doi: 10.1152/ajpcell.00212.2015
33. Wang D, Lu P, Zhang H, Luo M, Zhang X, Wei X, et al. Oct-4 and nanog promote the epithelial-mesenchymal transition of breast cancer stem cells and are associated with poor prognosis in breast cancer patients. Oncotarget. 2014 Sep 30;5(21). doi: 10.1152/ajpcell.00212.2015
34. Rasti A, Mehrazma M, Madjd Z, Abolhasani M, Saeednejad Zanjani L, Asgari M. Co-expression of Cancer Stem Cell Markers OCT4 and NANOG Predicts Poor Prognosis in Renal Cell Carcinomas. Sci Rep. 2018 Aug 6;8(1). doi: 10.1038/s41598-018-30168-4
35. Godugu D, Chilamakuri R, Agarwal S. STAT3 axis in cancer and cancer stem cells: From oncogenesis to targeted therapies. Biochim Biophys Acta Rev Cancer. 2025 Sep 30;1880(6):189461–1. doi: 10.1016/j.bbcan.2025.189461
36. El-Tanani M, Al Khatib AO, Aladwan SM, Abuelhana A, McCarron PA, Tambuwala MM. Importance of STAT3 signalling in cancer, metastasis and therapeutic interventions. Cell Signal. 2022 Apr;92:110275. doi: 10.1016/j.cellsig.2022.110275

Copyright© ACE&M all rights reserved.

37. Tolomeo M, Cascio A. The Multifaced Role of STAT3 in Cancer and Its Implication for Anticancer Therapy. Int J Mol Sci. 2021 Jan 9;22(2):603. doi: 10.3390/ijms22020603
38. Ding LN, Yu YY, Ma CJ, Lei CJ, Zhang HB. SOX2-associated signaling pathways regulate biological phenotypes of cancers. Biomed Pharmacother [Internet]. 2023 Apr 1;160:114336. doi: 10.1016/j.biopha.2023.114336
39. Gawlik-Rzemieniewska N, Bednarek I. The role of NANOG transcriptional factor in the development of malignant phenotype of cancer cells. Cancer Biol Ther. 2015 Nov 30;17(1):1–10. doi: 10.1080/15384047.2015.1121348
40. Sullan M, Boileau M, Hodges CV. Adrenal Cortical Carcinoma. J Urol. 1978 Dec 1;120(6):660-5. doi: 10.1016/s0022-5347(17)57317-6.
41. Lau SK, Weiss LM. The Weiss system for evaluating adrenocortical neoplasms: 25 years later. Hum Pathol. 2009 Jun;40(6):757-68. doi: 10.1016/j.humpath.2009.03.010.
42. Livak KJ, Schmittgen TD. Analysis of Relative Gene Expression Data Using Real-Time Quantitative PCR and the 2−ΔΔCT Method. Methods. 2001 Dec;25(4):402-8. doi: https://doi.org/10.1006/meth.2001.1262.
43. Leal LF, Bueno AC, Gomes DC, Abduch R, Castro M de, Antonini SR. Inhibition of the Tcf/beta-catenin complex increases apoptosis and impairs adrenocortical tumor cell proliferation and adrenal steroidogenesis. Oncotarget [Internet]. 2015 Oct 16;6(40):43016-32. doi: 10.18632/oncotarget.5513.
44. Goto M. In humans, early cortisol biosynthesis provides a mechanism to safeguard female sexual development. J Clin Invest. 2006 Mar 23;116(4):953-60. doi: 10.1172/jci25091.
45. Hart AH, Hartley L, Ibrahim M, Robb L. Identification, cloning and expression analysis of the pluripotency promoting Nanog genes in mouse and human. Dev Dyn. 2004;230(1):187-98. doi: 10.1002/dvdy.20034.
46. Del Valle I, Young MD, Kildisiute G, Ogunbiyi OK, Buonocore F, Simcock IC, et al. An integrated single-cell analysis of human adrenal cortex development. JCI insight [Internet]. 2023 Jul 24;8(14). doi: 10.1172/jci.insight.168177.
47. Cheng K, Seita Y, Moriwaki T, Noshiro K, Sakata Y, Hwang YS, et al. The developmental origin and the specification of the adrenal cortex in humans and cynomolgus monkeys. Sci Adv [Internet]. 2022 Apr 22;8(16):eabn8485. doi: 10.1126/sciadv.abn8485.
48. Natarajan TG, Ganesan N, FitzGerald KT. Cancer stem cells and markers: New model of tumorigenesis with therapeutic implications. Cancer Biomark. 2011 Oct 26;9(1-6):65-99. doi: 10.3233/cbm-2011-0173.
49. Mohiuddin IS, Wei SJ, Kang MH. Role of OCT4 in cancer stem-like cells and chemotherapy resistance. Biochim Biophys Acta Mol Basis Dis. 2020 Apr;1866(4):165432. doi: 10.1016/j.bbadis.2019.03.005.
50. Dey A, Kundu M, Das S, Jena BC, Mandal M. Understanding the function and regulation of Sox2 for its therapeutic potential in breast cancer. Biochim Biophys Acta Rev Cancer [Internet]. 2022 Mar 1;1877(2):188692. doi: 10.1016/j.bbcan.2022.188692.
51. Takeda K, Mizushima T, Yokoyama Y, Hirose H, Wu X, Qian Y, et al. Sox2 is associated with cancer stem-like properties in colorectal cancer. Sci Rep. 2018 Dec;8(1). doi: 10.1038/s41598-018-36251-0.
52. Zou S, Tong Q, Liu B, Huang W, Tian Y, Fu X. Targeting STAT3 in Cancer Immunotherapy. Mol Cancer. 2020 Sep 24;19(1). doi: 10.1186/s12943-020-01258-7.
53. Vasefifar P, Motafakkerazad R, Maleki LA, Najafi S, Ghrobaninezhad F, Najafzadeh B, et al. Nanog, as a key cancer stem cell marker in tumor progression. Gene. 2022 Jun;827:146448. doi: 10.1016/j.gene.2022.146448.
54. Takao Y, Yokota T, Koide H. β-Catenin up-regulates Nanog expression through interaction with Oct-3/4 in embryonic stem cells. Biochem Biophys Res Commun. 2006 Dec 21;353(3):699–705. doi: 10.1016/j.bbrc.2006.12.072.
55. Han B, Zhang X, Lou Y, Zheng X, Wang H, Su J, et al. Wnt blockers inhibit the proliferation of lung cancer stem cells. Drug Des Devel Ther. 2015 Apr 1;9:2399–9. doi: 10.2147/dddt.s76602.
56. Liu L, Zhu H, Liao Y, Wu W, Liu L, Liu L, et al. Inhibition of Wnt/β-catenin pathway reverses multi-drug resistance and EMT in Oct4+/Nanog+ NSCLC cells. Biomed Pharmacother. 2020 Jul 1;127:110225–5. doi: 10.1016/j.biopha.2020.110225.

Copyright© AE&M all rights reserved.

SUPPLEMENTARY MATERIALS

Supplementary table 1. Characteristics of fetal and post-natal control samples

Sex	Gestational Age	Chronological Age	Cause of Death
M	22 weeks 5 days	-	Chorioamnionitis
F	22 weeks	-	Prematurity
M	22weeks 2 days	-	Prematurity/anoxia
F	25 weeks	-	Hyaline membrane syndrome
M	21 weeks	-	Anoxia
F	25 weeks	-	Anoxia/pre-eclampsia
M	22 weeks	-	Anoxia/chorioamnionitis
M	22 weeks	-	Anoxia
M	24 weeks	-	Prematurity/patent foramen ovale
M	21 weeks 4 days	-	Anoxia
M	21 weeks 4 days	-	Anoxia
M	21 weeks	-	Anoxia
F	24 weeks 4 days	-	Fetal distress
M	21 weeks 2 days	-	Prematurity
M	29 weeks	-	Diaphragmatic hernia
F	28 weeks 1 day	-	Pneumonia/anoxia
F	30 weeks 1 day	-	Anoxia
M	27 weeks	-	Anoxia/twin pregnancy
F	29 weeks	-	
F	26 weeks	-	Prematurity/amniorrhexis
F	26 weeks 1 day	-	Prematurity
M	29 weeks 6 days	-	Shock/pneumonia
F	35 weeks	-	Anoxia
M	35 weeks	-	Premature placental abruption
M	35 weeks 1 day	-	Sepsis/amniorrhexis
M	37 weeks	-	Diaphragmatic hernia/pulmonary hypoplasia
M	36 weeks 3 days	-	Anoxia
F	37 weeks	-	Premature placental abruption
F	37 weeks	-	Anoxia/pneumonia
M	34 weeks	-	Anoxia
F	-	4 days	Cardiopathy/anoxia
F	-	57 days	Cardiopathy
M	-	38 days	Cardiopathy
M	-	1 year	Septic shock
F	-	5 months	Sepsis
M	-	3.5 years	Encephalitis
M	-	3 months	Septic shock
M	-	5 months	Cardiopathy/shock
M	-	4 months	Post-operative following cardiac surgery
F	-	11 days	Cardiopathy/meningitis
M	-	2 years	Post-operative following cardiac surgery
M	-	8 days	Cardiac insuficiency/cardiopathy
F	-	1 month	Jejunual atresia/pneumonia
F	-	10 years	Post-operative following cardiac surgery

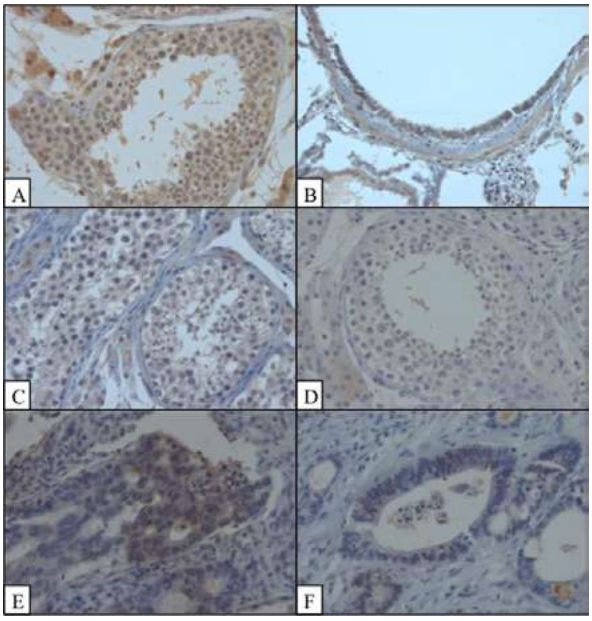
F: female; M: male.

Copyright© AE&M all rights reserved.

Supplementary table 2. Characteristics of adult and pediatric control samples

Sex	Gestational Age	Chronological Age
F	51	Pulmonary embolism
M	41	Accute pancreatitis
M	54	Accute myocardial infarction
M	49	Acute pulmonary edema
M	48	Acute pulmonary edema
M	54	Accute myocardial infarction
M	44	Accute pancreatitis
M	36	Acute pulmonary edema
F	48	Pneumonia
M	45	Sudden Death
ND		
ND		
ND		
ND		
ND	75	Cardiac arrest
ND	0.01	
ND	0.04	
F	0.1	Wilms' tumor surgical procedure
F	2.0	Wilms' tumor surgical procedure
F	3.6	Wilms' tumor surgical procedure
F	0.4	Wilms' tumor surgical procedure
M	5.3	Wilms' tumor surgical procedure
F	2.3	Wilms' tumor surgical procedure
F	4.2	Wilms' tumor surgical procedure
M	2.2	Wilms' tumor surgical procedure
F	4.7	Wilms' tumor surgical procedure

F: female; M: male; ND: no data.



Supplementary Figure 1. IHC photos of positive controls used to standardize the antibodies. Testicular tissue marked with anti-SF1 (**A**), anti-OCT4 (**C**), and anti-NANOG (**D**). Lung tissue marked with anti-DAX1 (**B**). Colon tissue marked with anti-SOX2 (**E**) and anti-STAT3 (**F**).

Copyright© AE&M all rights reserved.

Archives of Endocrinology and Metabolism
ISSN 2359-4292
OFFICIAL JOURNAL OF THE BRAZILIAN SOCIETY OF ENDOCRINOLOGY AND METABOLISM

original

Association of handgrip strength and CT-derived body composition with insulin resistance in women with prediabetes and newly diagnosed type 2 diabetes

Elham Yousief[1]
https://orcid.org/0000-0001-8346-3825

Ghada Ayeldeen[1]
https://orcid.org/0000-0001-6319-7830

Mona Khozam[1]
https://orcid.org/0009-0008-4912-895X

Mohamed Hamadna Allah El Ghobashy[1]
https://orcid.org/0000-0002-5830-9022

[1] Department of Internal Medicine, Faculty of Medicine, Cairo University, Cairo, Egypt

ABSTRACT

Objective: To examine the associations of handgrip strength and CT-derived muscle and visceral fat indices with insulin resistance in middle-aged women with prediabetes and newly diagnosed type 2 diabetes. **Subjects and methods:** This cross-sectional study included 44 women aged 40–60 years attending a tertiary endocrinology clinic. Participants were classified according to the American Diabetes Association (ADA, 2022) criteria as having prediabetes (n = 29) or newly diagnosed type 2 diabetes (n = 15). All participants underwent anthropometric assessment, biochemical testing, L3-level CT imaging for visceral adipose tissue (VAT) and psoas muscle measurements, and handgrip strength evaluation using a digital dynamometer. Insulin resistance was assessed using the homeostatic model assessment for insulin resistance (HOMA-IR). Multivariable linear regression analysis was performed to identify independent factors associated with HOMA-IR. **Results:** Dominant-hand grip strength demonstrated an inverse association with HOMA-IR (β = −0.297, p = 0.033). VAT volume and BMI were not significantly associated with HOMA-IR after adjustment (p > 0.75). The overall model explained 28% of the variance in HOMA-IR (R^2 = 0.28; adjusted R^2 = 0.14). Psoas muscle thickness showed a borderline inverse relationship with HOMA-IR (p = 0.079). **Conclusion:** In this cohort of women with early glucose dysregulation, handgrip strength was independently associated with insulin resistance, whereas visceral adiposity was not. These findings suggest that muscle performance may represent a clinically relevant correlation of early metabolic impairment. Longitudinal studies are needed to clarify the temporal relationships.

Keywords: Handgrip strength; insulin resistance; HOMA-IR; visceral adiposity; CT imaging; prediabetes; type 2 diabetes; women

INTRODUCTION

Prediabetes and type 2 diabetes mellitus (T2DM) are increasingly prevalent among middle-aged women and are strongly influenced by alterations in body composition. The accumulation of visceral adipose tissue has traditionally been considered a principal contributor to insulin resistance because of its endocrine activity and inflammatory signaling properties (1-3). However, skeletal muscle is the primary site of insulin-mediated glucose disposal, accounting for about 70%–80% of postprandial glucose uptake. Consequently, changes in muscle quantity or functional capacity may significantly influence insulin sensitivity independently of adiposity (4,5).

Recent studies suggest that muscle strength may provide clinically relevant information beyond measures of muscle mass alone. Functional decline can precede measurable reductions in cross-sectional muscle area, reflecting early impairments in contractile efficiency and metabolic flexibility (6-8). In women, particularly during midlife, shifts in fat distribution and muscle quality may further modify metabolic risk profiles (9,10). Prospective data from Asian populations demonstrate that lower muscle strength is independently associated with an increased incidence of prediabetes and T2DM after adjustment for visceral adiposity (1). Similarly, cross-sectional analyses have reported that reduced muscle performance correlates with markers of insulin resistance across diverse cohorts (11,12).

Received on Nov/22/2025
Accepted on Mar/9/2026

DOI: 10.20945/2359-4292-2026-0056

Correspondence to:
Elham Yousief
drelhamyousief@gmail.com

Associated editor:
Marcio W. Lauria
https://orcid.org/0000-0001-7558-1231

This is an open-access article distributed under the terms of the Creative Commons Attribution License

Copyright© AE&M all rights reserved.

Although visceral adiposity is consistently associated with cardiometabolic disease, its independent contribution to insulin resistance seems to vary according to disease stage and population characteristics (13-15). Some investigations suggest that combined muscle–fat indices may better reflect metabolic health than fat measures alone (2,16,17). Furthermore, interventional studies demonstrate that resistance training improves insulin sensitivity even in the absence of significant reductions in fat mass, underscoring the metabolic importance of muscle performance (18-20).

Despite growing interest in this field, the relative associations of functional muscle strength and CT-derived visceral adiposity with insulin resistance remain insufficiently characterized in women with early glucose abnormalities. Therefore, this study aims to evaluate the relationships between handgrip strength, CT-based body composition parameters, and insulin resistance measured by HOMA-IR in women with prediabetes and newly diagnosed T2DM.

SUBJECTS AND METHODS

Study design and setting

A cross-sectional observational study was conducted at the Kasr El Ainy Centre for Endocrinology and Diabetes, Faculty of Medicine, Cairo University, from August 2022 to December 2023. The objective is to examine the associations between skeletal muscle performance, CT-derived body composition parameters, and insulin resistance among women with early disturbances in glucose metabolism.

Given the cross-sectional design, analyses were restricted to evaluating statistical associations without inferring temporal direction or causality.

Participants

Women aged 40–60 years attending the outpatient endocrinology clinic were consecutively screened for eligibility. Participants were included if they met the American Diabetes Association (ADA, 2022) criteria for either prediabetes or newly diagnosed type 2 diabetes mellitus (T2DM).

Prediabetes was defined as: Fasting plasma glucose between 100–125 mg/dL and/or; HbA1c between 5.7%–6.4%.

Newly diagnosed T2DM was defined as: fasting plasma glucose ≥ 126 mg/dL and/or; HbA1c ≥ 6.5%, in individuals who had not initiated glucose-lowering therapy.

Exclusion criteria included any medical condition or pharmacologic treatment known to significantly influence muscle mass, fat distribution, or insulin sensitivity. These included thyroid dysfunction, Cushing's syndrome, chronic liver disease, chronic kidney disease, malignancy, polycystic ovary syndrome, and current use of corticosteroids, insulin sensitizers, or anabolic agents.

A total of 44 eligible participants were enrolled. Sample size estimation was based on detecting moderate correlations ($r \geq 0.35$) with 80% statistical power at a 5% significance level.

Ethical approval

The study protocol was reviewed and approved by the Research Ethics Committee of the Faculty of Medicine, Cairo University (Approval No. MD-322-2022). All participants provided written informed consent prior to enrollment. The study adhered to the principles of the Declaration of Helsinki.

Clinical and anthropometric assessment

Standardized anthropometric measurements were obtained. Body weight and height were measured with participants wearing light clothing and no footwear. Body mass index (BMI) was calculated as weight (kg) divided by height squared (m^2). Waist circumference was measured at the midpoint between the lower costal margin and the iliac crest.

These conventional indices were included to enable comparison between anthropometric markers of adiposity and imaging-derived measurements.

Laboratory evaluation

Venous blood samples were collected following an overnight fast of at least eight hours. Laboratory analyses included: fasting plasma glucose; fasting insulin; HbA1c; lipid profile (total cholesterol, triglycerides, HDL-C, LDL-C); alanine aminotransferase (ALT); aspartate aminotransferase (AST).

Insulin resistance was estimated using the homeostasis model assessment formula:

HOMA-IR = (Fasting glucose × Fasting insulin) / 405.

Copyright© ACE&M all rights reserved.

HOMA-IR was analyzed as a continuous variable and served as the primary metabolic outcome.

CT-Based body composition assessment

Non-contrast computed tomography imaging was performed at the level of the third lumbar vertebra (L3) using a 64-slice multidetector scanner. The L3 region was selected due to its established correlation with total-body skeletal muscle and visceral fat compartments.

Using dedicated image-analysis software, the following parameters were quantified: visceral adipose tissue (VAT) volume (cm^3); Psoas muscle index (PMI), calculated as total psoas cross-sectional area normalized to height (cm^2/m^2); Psoas muscle thickness (PMTH), calculated as the mean of bilateral measurements.

These imaging-derived metrics were used to characterize structural muscle and fat compartments.

Muscle strength measurement

Muscle performance was assessed using a calibrated digital hand dynamometer. Participants were positioned according to standardized procedures and instructed to perform three maximal voluntary contractions with each hand, with one-minute rest intervals between attempts.

Hand dominance was self-reported. The mean value of the dominant hand was used for statistical analysis to ensure methodological consistency across participants.

Reduced muscle strength was defined according to the European Working Group on Sarcopenia in Older People (EWGSOP2) criteria.

Statistical analysis

Statistical analyses were performed using SPSS version 28.0 (IBM Corp., Armonk, NY, USA).

Continuous variables were assessed for normality using the D'Agostino–Pearson test. Normally distributed variables are shown as mean ± standard deviation, while skewed data are expressed as median with interquartile range.

Associations between HOMA-IR and body composition variables were evaluated using Pearson or Spearman correlation coefficients, as appropriate.

To identify variables independently associated with insulin resistance, multivariable linear regression analysis was conducted with HOMA-IR as the dependent variable. Independent variables entered into the model included: dominant-hand grip strength; visceral adipose tissue volume; Psoas muscle index; Psoas muscle thickness; BMI; age.

Model assumptions, including linearity and absence of multicollinearity, were verified prior to interpretation. Results are reported as standardized beta coefficients (β) with corresponding p-values. A two-sided p-value < 0.05 was considered statistically significant.

Methodological considerations

The cross-sectional design limits interpretation to associations. Menopausal status, physical activity level, dietary intake, and inflammatory biomarkers were not systematically assessed and may represent potential confounders. These factors are acknowledged as limitations and should be addressed in future longitudinal studies.

RESULTS

Participant characteristics

The study included 44 women aged between 40 and 60 years, with a mean age of 45.5 ± 5.9 years. According to the American Diabetes Association (ADA, 2022) criteria, 29 participants (65.9%) met the definition of prediabetes, while 15 (34.1%) were classified as having newly diagnosed type 2 diabetes. **Table 1** one summarizes the baseline demographic, metabolic, and body composition parameters.

The cohort demonstrated elevated adiposity overall, with a mean BMI of 34.6 ± 6.8 kg/m^2 and a median visceral adipose tissue (VAT) volume of 295.5 cm^3 (interquartile range: 150.3–436.8). Mean dominant-hand grip strength was 17.5 ± 5.4 kg. Structural muscle parameters showed a mean psoas muscle index (PMI) of 7.45 ± 2.74 cm^2/m^2 and a mean psoas muscle thickness (PMTH) of 6.23 ± 0.71 cm. The mean HOMA-IR value was 3.72 ± 2.25, reflecting variability in insulin resistance across participants.

Copyright© AE&M all rights reserved.

Table 1. Baseline characteristics of participants

Parameter	Mean ± SD/Median (IQR)
Age (years)	45.5 ± 5.9
BMI (kg/m²)	34.6 ± 6.8
Waist circumference (cm)	98.2 ± 10.3
Fasting glucose (mg/dL)	112.4 ± 41.5
Fasting insulin (μIU/mL)	13.3 ± 6.6
HOMA-IR	3.72 ± 2.25
QUICKI	0.32 ± 0.03
Triglycerides (mg/dL)	125.0 (86.5–188.5)
Visceral adipose tissue (cm³)	295.5 (150.3–436.8)
Handgrip strength (right, kg)	17.5 ± 5.4
Handgrip strength (left, kg)	16.8 ± 5.2
PMI (cm²/m²)	7.45 ± 2.74
PMTH (cm)	6.23 ± 0.71

Bivariate associations

Correlation analyses were conducted to explore the relationships between insulin resistance and body composition measures (Table 2).

Table 2. Correlation coefficients between muscle and metabolic parameters

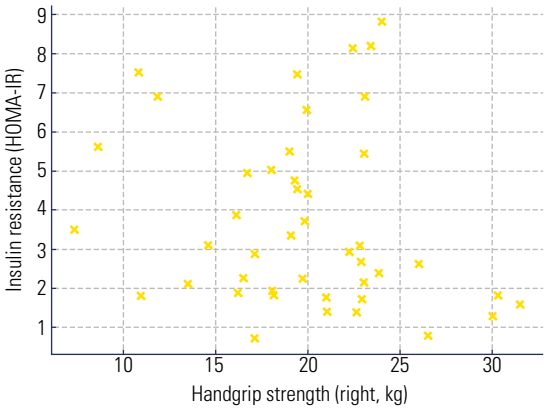
Parameter	HOMA-IR (r)	p-value
Fasting insulin	0.78	< 0.001
Fasting glucose	0.64	< 0.001
Handgrip strength (right)	–0.29	0.033
Handgrip strength (left)	–0.19	0.07
Visceral adipose tissue volume	0.04	0.81
PMTH	–0.18	0.08
BMI	0.02	0.75

HOMA-IR showed strong positive correlations with fasting insulin (r = 0.78, p < 0.001) and fasting plasma glucose (r = 0.64, p < 0.001), supporting the internal consistency of metabolic measurements.

An inverse correlation was observed between dominant-hand grip strength and HOMA-IR (r = −0.29, p = 0.033). Participants with lower grip strength tended to exhibit higher levels of insulin resistance. Figure 1 illustrates this relationship, where the fitted regression line shows a negative slope.

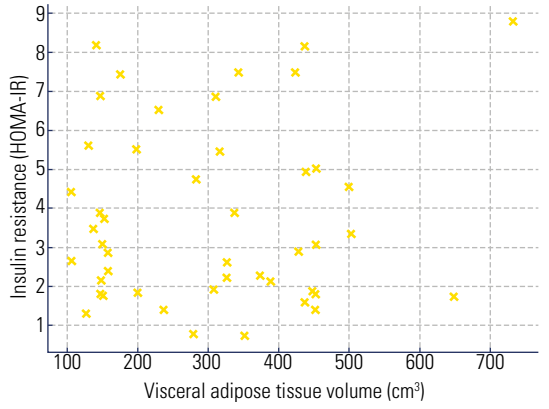
In contrast, VAT volume did not demonstrate a statistically significant correlation with HOMA-IR (r = 0.04, p = 0.81). Figure 2 shows the absence of a clear linear pattern. Similarly, BMI showed no meaningful association with insulin resistance (r = 0.02, p = 0.75).

PMTH displayed a weak inverse relationship with HOMA-IR (r = −0.18, p = 0.08), while PMI was not significantly correlated.



Scatter plot illustrating the inverse relationship between dominant-hand grip strength and insulin resistance (HOMA-IR). The regression line demonstrates a modest negative association (r = –0.29, p = 0.033).

Figure 1. Inverse association between handgrip strength and insulin resistance (HOMA-IR).



Scatter plot showing the relationship between visceral adipose tissue (VAT) volume and insulin resistance (HOMA-IR). No significant linear association was observed (r = 0.04, p = 0.81).

Figure 2. Relationship between visceral fat volume and insulin resistance.

Multivariable regression analysis

To examine independent associations, multivariable linear regression analysis was performed with HOMA-IR as the dependent variable (Table 3).

After adjustment for age, BMI, VAT volume, PMI, and PMTH, dominant-hand grip strength remained independently associated with HOMA-IR (β = −0.297, p = 0.033). The negative beta coefficient indicates that lower muscle strength corresponded to higher levels of insulin resistance.

Copyright© AE&M all rights reserved.

Table 3. Multiple linear regression predicting HOMA-IR

Predictor	β Coefficient	p-value	Interpretation
Handgrip strength (right)	–0.297	0.033	Significant inverse predictor
Handgrip strength (left)	0.251	0.067	Trend toward significance
PMTH	–0.784	0.079	Suggestive inverse relationship
PMI	0.259	0.163	Not significant
Visceral adipose tissue volume	0.0006	0.815	No predictive effect
BMI	0.018	0.754	No predictive effect
Age	–0.027	0.687	No predictive effect

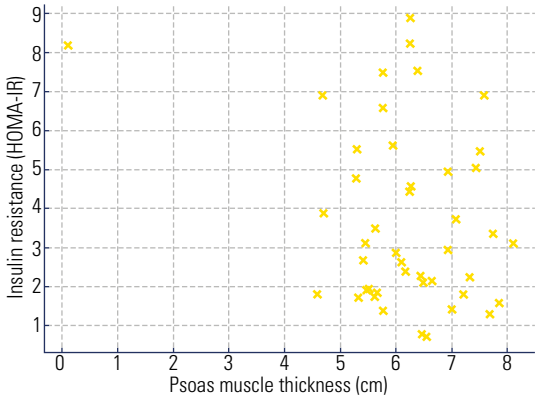
Neither VAT volume (β = 0.0006, p = 0.815) nor BMI (p = 0.754) retained statistical significance in the adjusted model. PMI also did not demonstrate an independent association (p = 0.163).

PMTH showed a borderline inverse association (β = −0.784, p = 0.079), suggesting a possible relationship that warrants further investigation. **Figure 3** shows the distribution of PMTH in relation to HOMA-IR.

The final regression model explained 28% of the observed variability in HOMA-IR (R^2 = 0.28; adjusted R^2 = 0.14), indicating that additional unmeasured factors likely contribute to insulin resistance in this population.

Summary of observed associations

Within this cohort of women with early glucose abnormalities: Dominant-hand grip strength was independently associated with insulin resistance. Visceral adipose tissue volume was not independently associated with HOMA-IR. Structural muscle thickness demonstrated a borderline inverse relationship.



Scatter plot depicting the relationship between psoas muscle thickness (PMTH) and insulin resistance (HOMA-IR). A modest inverse trend was observed (β = –0.784, p = 0.079).

Figure 3. Relationship between muscle thickness and metabolic risk

These findings describe cross-sectional associations and should not be interpreted as indicating temporal or causal relationships.

DISCUSSION

This study examined the relationships between muscle performance, imaging-derived body composition parameters, and insulin resistance in women with prediabetes and newly diagnosed type 2 diabetes. The primary observation was that dominant-hand grip strength was independently associated with HOMA-IR, whereas visceral adipose tissue volume was not statistically significant after adjustment for covariates. These findings describe associative patterns within this cohort and should be interpreted accordingly.

Interpretation in the context of previous research

Skeletal muscle plays a central role in glucose disposal under insulin-stimulated conditions. Functional impairment of muscle may therefore influence systemic glucose regulation even in the absence of marked structural atrophy. Several observational studies have reported inverse relationships between muscle strength and markers of glucose dysregulation. For example, longitudinal analyses in Asian populations have demonstrated that individuals with lower baseline muscle strength were more likely to develop prediabetes or type 2 diabetes during follow-up (1). Similarly, cross-sectional investigations have linked reduced muscle performance with higher insulin resistance indices across diverse adult populations (11,18).

Importantly, growing evidence suggests that muscle strength and muscle mass may not convey identical metabolic information. Some studies have indicated

Copyright© AE&M all rights reserved.

that functional measures such as handgrip strength show stronger correlations with metabolic outcomes than imaging-based muscle area alone (6,17). This distinction aligns with the current findings, in which dominant-hand grip strength remained associated with HOMA-IR, while psoas muscle index did not demonstrate independent significance.

With respect to adiposity, visceral fat has traditionally been considered a principal contributor to insulin resistance because of its pro-inflammatory and endocrine properties (2,3). However, imaging-based studies have reported variable associations between visceral fat volume and insulin resistance once muscle-related parameters are included in multivariable models (13,15). In this analysis, visceral adipose tissue volume was not independently associated with HOMA-IR after adjustment. This does not negate the metabolic relevance of adiposity but suggests that, within this sample, muscle performance demonstrated a stronger statistical relationship with insulin resistance than VAT volume.

The borderline association observed between psoas muscle thickness and HOMA-IR further supports the notion that muscle characteristics may relate to metabolic function. Although this finding did not reach conventional statistical significance, the direction of association was consistent with prior reports describing inverse relationships between muscle quality markers and insulin resistance (5,14). Larger studies would be necessary to clarify this relationship.

Clinical considerations

Handgrip strength is a simple and reproducible measure that can be obtained in routine clinical settings without specialized imaging. While CT-derived metrics provide precise quantification of body compartments, they are less feasible for broad metabolic screening. The association between grip strength and HOMA-IR suggests that functional muscle assessment may contribute additional information when evaluating metabolic status among women with early glucose abnormalities. However, these findings should be interpreted as exploratory and hypothesis-generating.

Limitations

Several limitations warrant consideration.

First, the cross-sectional design precludes inference regarding temporal sequence or causality. It cannot be determined whether reduced muscle strength contributes to insulin resistance or reflects metabolic impairment.

Second, the sample size was modest, which may have limited statistical power to detect smaller associations, particularly for structural muscle measures.

Third, menopausal status was not systematically documented. Given the age range of participants, hormonal transitions may have influenced both body composition and insulin sensitivity. This variable should be incorporated into future investigations.

Fourth, physical activity level, dietary intake, and inflammatory markers were not assessed and may represent unmeasured confounders.

Finally, CT analysis was based on a single L3 slice, which, although validated, may not fully capture whole-body fat and muscle distribution.

In conclusion, in this cohort of women with prediabetes and newly diagnosed type 2 diabetes, dominant-hand grip strength was independently associated with insulin resistance as measured by HOMA-IR, whereas visceral adipose tissue volume was not statistically significant in adjusted analyses. These findings highlight the potential relevance of muscle performance as a correlate of metabolic dysfunction in early-stage glucose abnormalities.

Given the observational nature of the study, prospective research is required to determine whether changes in muscle strength precede, accompany, or follow alterations in insulin sensitivity. Future studies incorporating larger samples and longitudinal designs will be essential to clarify the clinical implications of these associations.

Ethics approval and consent to participate: this study was conducted in accordance with the ethical standards of the institutional research committee and the 1964 Declaration of Helsinki and its later amendments. Ethical approval was obtained from the Research Ethics Committee of the Faculty of Medicine, Cairo University (Approval No. MD-322-2022). Written informed consent was obtained from all participants prior to inclusion in the study. Participants were informed of the study objectives, assured of the confidentiality of their information, and notified of their right to withdraw from the study at any time without consequence.

Consent for publication: all authors have reviewed the manuscript and provided consent for its publication. Informed consent for the publication of anonymized data was obtained from all participants.

Copyright© AE&M all rights reserved.

Availability of data and materials: the datasets used and/or analyzed during this study are available from the corresponding author upon reasonable request. Raw CT imaging data were handled in accordance with institutional privacy and ethical guidelines.

Competing interests: the authors declare that they have no competing interests related to this work.

Funding: this research received no external funding. The study was self-supported by the research team

Authors' contributions: Elham Yousief: conceptualization, study design, supervision, data interpretation, and manuscript drafting. Mona Khozam: data collection and patient recruitment, and revision of the manuscript. Ghada Ayeldeen: laboratory investigations and biochemical analysis. Mohamed Hamadna Allah El Ghobashy: data analysis, statistical interpretation, and manuscript editing. All authors contributed to the critical revision of the manuscript, approved the final version, and agree to be accountable for all aspects of the work

Ethical statement: the authors affirm that this article is original work and that all ethical and professional standards were maintained throughout the research process.

Acknowledgements: the authors would like to express their gratitude to the staff of the Kasr El Ainy Centre for Endocrinology and Diabetes for their technical assistance and support during data collection.

Disclosure: no potential conflict of interest relevant to this article was reported.

Data availability: datasets related to this article will be available upon request to the corresponding author.

REFERENCES

1. Wong BWX, Tan CY, Ho JH, Lim XY, Lee SY, Ng CH, et al. Individual and combined effects of muscle strength and visceral adiposity on incident prediabetes and type 2 diabetes in Asian women. Diabetes Obes Metab. 2025;27(1):1-12. doi:10.1111/dom.15642.
2. Tang S, Wu H, Liu M, Li J, Lu GQ, Li XH. Association between skeletal muscle mass-to-visceral fat area ratio and insulin resistance in type 2 diabetes. J Diabetes Metab Disord 2025;24(3):103–114. doi:10.1007/s40200-025-01644-2.
3. Hernández-Flandes RN, Tapia-González MA. Decrease in visceral adipose tissue in obesity and diabetes treated with liraglutide. Diabetology 2025;6(7):67. doi:10.3390/diabetology6070067.
4. Guo C, Dai T, Zhang H, Li Y, Wang X, Chen L. Effect of resistance training on body composition and physical function in older females with sarcopenic obesity. Front Aging Neurosci. 2025;17:1495218. doi:10.3389/fnagi.2025.1495218.
5. Ortez Toro JJ. Diabetes and sarcopenia: unraveling the metabolic crossroads of muscle loss and glycemic dysregulation. Endocrines. 2025;6(3):47. doi:10.3390/endocrines6030047.
6. Tang T, Hao J, Yang Q, Li X, Zhang Y, Wang L. Lipoprotein profile as a predictor of type 2 diabetes with sarcopenia: a cross-sectional study. Endocrine. 2025;85(4):912–921. doi:10.1007/s12020-025-04226-7.
7. Li M, Liu Y, Gao L, Zhang H, Wang X, Chen Y, et al. Triglyceride-glucose index and body mass index interactions protect against sarcopenia in non-diabetic middle-aged women. Front Public Health. 2025;13:1475330. doi:10.3389/fpubh.2024.1475330.
8. Sun YL, Zhang L, Cao YH, Liu X, Wang Q, Li H, et al. Impact of high body fat and low muscle mass on bone mineral density in postmenopausal women with diabetes. Aging Clin Exp Res. 2025;37(2):413-423. doi:10.1007/s40520-025-03163-9.
9. Dulloo AG, Ramessur V, Hunma S, Jeewon R, Soobrayen T, Goorah S, et al. Visceral-to-peripheral adiposity ratio and low muscle strength in young women: association with sarcopenic obesity. Int J Obes. 2025;49(3):1934–1946. doi:10.1038/s41366-025-01934-y.
10. Kılınç GE, Vergi Y. Nutritional approach to diabetic sarcopenia: a comprehensive review. Curr Nutr Rep. 2025;14(1):55-68. doi:10.1007/s13668-025-00637-0.
11. Dubey U, Kalia A, Rijhwani P, Sharma R, Gupta S, Verma A, et al. A cross-sectional study on prevalence of sarcopenia in patients with type 2 diabetes mellitus. J Clin Community Pract. 2025;12(2):1084. Available from: https://www.jccpractice.com/article/a-cross-sectional-study-on-prevalence-of-sarcopenia.
12. Rondanelli M, Gasparri C, Moroni A, Perna S, Faliva MA, Naso M, et al. Residential program for sarcopenic obesity management in adults with obesity: an open-label trial. Nutrients. 2025;17(9):1511. doi: 10.3390/nu17091511.
13. De Lorenzo A, Itani L, El Ghoch M, Di Renzo L, Calabrese V, Marsella LT, et al. Association between sarcopenic obesity and DXA-derived visceral adipose tissue in adults. Nutrients. 2024;16(11):1645. doi:10.3390/nu16111645.
14. Danciu AA, Bala C, Inceu G, Roman G, Popa A, Vlad A, et al. Metabolomic signature of sarcopenia and diabetes: implications for targeted therapies. Int J Mol Sci. 2025;26(15):7574. doi:10.3390/ijms26157574.
15. Xiang Y, Wang Z, Xu J, Liu H, Zhang Y, Chen X, et al. Association between sarcopenia and weight-adjusted waist index in men with type 2 diabetes. BMC Endocr Disord. 2025;25:1846. doi:10.1186/s12902-025-01846-y.
16. Wendra W, Tanuwidjaja T. Sarcopenic obesity in postmenopausal women: relationship between fat, muscle, and strength. Contagion J. 2025;9(1):87-96. doi:10.32627/contagion.2025.24341.
17. Yogesh M, Patel M, Gandhi R, Shah K, Mehta P, Desai H, et al. Sarcopenia in type 2 diabetes among Asian populations: a systematic review and meta-analysis. BMC Endocr Disord. 2025;25(6):1935. doi:10.1186/s12902-025-01935-y.
18. Seko T, Himuro N, Koyama M, Tanaka S, Yamamoto H, Ito K, et al. Low skeletal muscle mass is associated with progression of insulin resistance in older adults. Diabetol Int. 2025;16(2):843–852. doi:10.1007/s13340-025-00843-9.
19. Abad-González AL, Veses S, Argente Pla M, Navarro JF, Martínez R, López A, et al. Medical nutrition therapy and physical exercise for hyperglycemic patients with sarcopenia. Nutrients. 2025;17(3):499. doi: 10.3390/nu17030499.
20. Mukhtar D, Hafsari H, Syahrowadi Q. The impact of resistance training on metabolic health and disease prevention in aging populations. Am J Clin Pract. 2025;7(2):68-78. Available from: https://americanjournal.us/index.php/american/article/view/68.

Copyright© AE&M all rights reserved.

Archives of Endocrinology and Metabolism
ISSN 2359-4292
OFFICIAL JOURNAL OF THE BRAZILIAN SOCIETY OF ENDOCRINOLOGY AND METABOLISM

original

The hidden impact of smoking in thyroid eye disease: a link between selenium deficiency, autoimmunity, and retinal microvasculature

Fatma Savur[1]
https://orcid.org/0000-0001-5769-5876

Serkan Güler[1]
https://orcid.org/0000-0001-7142-4220

Gülistan Oyur[1]
https://orcid.org/0000-0002-6941-8240

[1] Istanbul Health Sciences University, Basaksehir Cam and Sakura City Hospital, Ophthalmology Department, Istanbul, Turkey

ABSTRACT

Objective: To investigate the impact of smoking on serum selenium levels, autoimmune activity, and macular microvascular density in patients with clinically inactive thyroid-associated orbitopathy (TAO), using optical coherence tomography angiography (OCTA). **Subjects and methods:** This retrospective cross-sectional study included 44 patients with inactive TAO (24 smokers, 20 non-smokers) and 32 age- and sex-matched healthy controls. All participants underwent ophthalmologic evaluation and laboratory testing for thyroid hormones, selenium, and thyroid-stimulating immunoglobulin (TSI). Macular vessel density was measured using spectral-domain OCTA at the superficial capillary plexus, deep capillary plexus, outer retinal layer, and choriocapillaris. Clinical activity score (CAS) was used to assess disease activity. The collected data were analyzed statistically. **Results:** Smokers with TAO exhibited significantly higher CAS ($p = 0.016$) and TSI levels ($p = 0.027$), and lower serum selenium concentrations ($p = 0.042$) compared to non-smokers. Central superficial and deep capillary plexus densities were significantly reduced in smokers versus healthy controls ($p = 0.029$ and $p = 0.017$, respectively). No significant differences were observed between smokers and non-smokers within the TAO group, or in the outer retinal layer and choriocapillaris layers among all groups. **Conclusion:** Smoking status was associated with lower selenium levels, higher TSI levels, and increased CAS. Furthermore, retinal microvascular attenuation detected by OCTA, even in the absence of clinical activity in TAO, may serve as a significant indicator of persistent vascular deterioration.

Keywords: Optical coherence tomography angiography; retinal microvasculature; selenium; smoking; thyroid-associated orbitopathy

INTRODUCTION

Thyroid-associated orbitopathy (TAO) is an autoimmune inflammatory disease that can occur in all thyroid conditions, but is most prevalent in patients with Graves' disease (1). Although the orbital disease generally follows a mild course, it can lead to severe complications in 3–5% of cases. During the course of TAO, numerous individual risk factors have been identified, including phenotype, thyroid hormone dysfunction, and smoking (2-4). Multiple studies have investigated the relationship between TAO and smoking (4,5), and evidence has shown that smoking is the most significant modifiable risk factor for TAO, increasing the risk of severe disease forms and reducing treatment responsiveness in active TAO (6). *In vitro* studies have indicated that increased production of reactive oxygen species contributes to the pathogenesis of thyroid-related orbitopathy (7-9). Selenium is an antioxidant mineral required for selenocysteine synthesis (10); it is one of the agents that can potentially inhibit pathogenic mechanisms implicated in TAO. Deficiency has been shown to affect free radical formation in TAO, conversion of thyroxine (T4) to triiodothyronine (T3), and the autoimmune thyroid process (11). Nonetheless, there is limited research examining the effects of smoking on macular microvascular changes in inactive TAO (12).

Received on Oct/25/2025
Accepted on Feb/27/2026
DOI: 10.20945/2359-4292-2026-0057

Correspondence to:
Fatma Savur
Basaksehir Cam and Sakura City Hospital,
Ophthalmology Department,
P.O. Box 34200, Basaksehir, Istanbul, Turkey
drfatmagezer@hotmail.com

Associated editor:
Celia Regina Nogueira
https://orcid.org/0000-0002-4014-0660

This is an open-access article distributed under the terms of the Creative Commons Attribution License

Copyright© AE&M all rights reserved.

Although previous studies have individually examined the roles of smoking, selenium, and retinal vascular changes in TAO, there remains a lack of comprehensive research exploring the interplay among these factors, particularly in patients with clinically inactive disease. Notably, the combined impact of smoking and selenium deficiency on both immunological activity and retinal microvascular integrity is largely unexplored. Given the critical role of oxidative stress and vascular compromise in TAO pathogenesis, it is essential to determine whether modifiable lifestyle factors such as smoking contribute to ongoing subclinical inflammation and ocular perfusion abnormalities, even during periods of clinical inactivity. Therefore, this study aims to comprehensively evaluate the effect of smoking on serum selenium levels, clinical activity score (CAS), thyroid autoantibodies, and macular microvascular parameters measured by optical coherence tomography angiography (OCTA) in patients with inactive TAO. By integrating biochemical, immunological, and imaging data, this study seeks to provide novel insights into the systemic and ocular consequences of smoking in TAO and to identify potential clinical targets for early risk stratification and therapeutic intervention.

SUBJECTS AND METHODS

Study population

This single-center, cross-sectional observational study was conducted at a tertiary eye care center. The retrospective study included the right eyes of 44 patients with inactive TAO (smoking group, n = 24) and 32 healthy participants (control group; age- and gender-matched). Informed consent was obtained from all participants, and the study was conducted in accordance with the principles of the Declaration of Helsinki. The protocol was reviewed and approved by the local ethics committee. All participants underwent comprehensive ophthalmologic examinations, including biomicroscopy, Hertel exophthalmometry, and indirect ophthalmoscopy. Demographic data, including age, gender, smoking status, and duration of TAO, were collected. Following thorough ophthalmological examination, CAS, thyroid-stimulating hormone (TSH), free thyroxine (fT4), free triiodothyronine (fT3), selenium (Se), and thyroid-stimulating immunoglobulin (TSI) levels were recorded for patients with TAO. The CAS system was used to assess disease activity. Patient and severity classification were performed using the European Group for Graves' Ophthalmopathy criteria (13,14). Patients with CAS < 3 and no previous history of active TAO treatment were included.

Patients with active TAO or previous TAO treatment (e.g., orbital radiotherapy, systemic steroids, or other immunomodulators) were excluded. To prevent confounding effects on choroidal and retinal vasculature, participants with refractive errors greater than ±2 diopters, corneal opacities, cataracts, retinal vascular pathologies (e.g., diabetes, hypertension, systemic vasculitic diseases), and choroidal disease were excluded.

Intervention and observation procedures

Vascular density measurements were performed using spectral-domain OCTA (DRI OCT Tritron, Topcon, Japan). The instrument acquires 6 × 6 mm macular volumetric scans with a sample density of 320 × 320 A-scans at a rate of 100,000 A-scans/second. The device employs an OCTA algorithm to generate angiograms (15). The algorithm uses blood flow as contrast and provides vessel density (VD) and flow field data based on the split-spectrum amplitude-correlation angiography algorithm. Participants fixated on the target following pupil dilation. Four measurements were obtained per participant, and images with a signal strength index >60 were evaluated by an experienced ophthalmologist (F.S.). Macular vessel density was analyzed at four levels: the superficial retinal capillary plexus (SCP), the deep retinal capillary plexus (DCP), the outer retinal layer (ORL), and the choroidal capillaris (CC) (16). It is acknowledged that differences in wavelength and light source can lead to variable detection of choroidal vasculature across devices (17). The density map was displayed in five regions (foveal, nasal, temporal, superior, and inferior), and the vessel density of each region was automatically calculated as a percentage. To minimize daily fluctuations, all scans were performed within a standardized window (13:00–14:00) for all participants. The primary outcome measures were smoking status, serum selenium

Copyright© AE&M all rights reserved.

level, and retinal vascular density measurements by OCTA.

Statistical analysis

The statistical analyses were performed using the SPSS software (IBM SPSS Statistics for Windows, IBM Corp., v. 28.0, Armonk, NY) analyses. Mean, standard deviation, median, minimum and maximum values, frequencies, and percentages. Normality was assessed via the Kolmogorov-Smirnov test. Mann-Whitney U test was used to compare quantitative variables between groups. The Chi-square test was used for comparisons of qualitative variables. Statistical significance was set at $p < 0.05$.

RESULTS

The mean age of smokers (female: n = 19; male: n = 5) was 39.7 ± 12.7 years; non-smokers (female: n = 12; male: n = 8) had a mean age of 42.3 ± 13.3 years; the control group (female: n = 18; male: n = 14) had a mean age of 37.3 ± 11.1 years. No statistically significant differences were observed between groups in terms of age or gender distribution ($p > 0.05$ for all). TAO patients who smoked had significantly higher CAS and TSI levels, and significantly lower selenium levels than non-smokers ($p = 0.016$, $p = 0.027$, and $p = 0.042$, respectively). There were no significant differences in thyroid-stimulating hormone, free triiodothyronine, and free thyroxine laboratory values between smokers and non-smokers in the TAO group ($p = 0.521$, $p = 0.359$, and $p = 0.497$, respectively) (Table 1).

Central SCP and central DCP vascular densities were significantly lower in both smoking and non-smoking TAO patients than in the control group ($p = 0.029$, $p = 0.017$, $p = 0.011$, $p = 0.004$, respectively). No significant differences were observed in ORL-VD and CC-VD parameters by OCTA among groups ($p > 0.05$ for all). Among inactive TAO patients, OCTA-derived macular vessel density parameters did not differ significantly between smokers and non-smokers ($p > 0.05$ for all) (Table 2).

DISCUSSION

TAO is a debilitating autoimmune disorder of the orbit, predominantly affecting patients with Graves' disease. Among various modifiable risk factors, smoking has been consistently identified as the most significant environmental contributor to TAO development, severity, and treatment resistance (18-20). The pathogenic mechanisms in TAO include oxidative stress, fibroblast activation, immune dysregulation, and increased production of inflammatory cytokines—processes exacerbated by smoking (21,22).

Table 1. Demographic and clinical data of all subjects

Variables		Group			p^*	p^{**}	p^{***}
		Control (n = 32)	Smoker TAO (n = 24)	Non-smoker TAO (n = 20)			
Age (years) Mean ± SD (median)		37.3 ± 11.1 (1.5)	39.6 ± 12.1 (39.5)	42.3±13.3 (44.0)	0.872[m]	0.258[m]	0.453[m]
Sex, n (%)	Female	18 (56.3%)	19 (79.2%)	12 (60%)	0.073[X²]	0.790[X²]	0.165[X²]
	Male	14 (43.7%)	5 (20.8%)	8 (40%)			
Proptosis, mm		N/A	21.6 ± 3.3 (20.5)	21.7 ± 3.2 (22.0)			0.7410.936
Axial length, mm		23.1 ± 1.2 (23.0)	22.9 ± 1.1 (23.0)	23.1 ± 1.2 (23.0)			
CAS (range: 0–7)		N/A	1.0 ± 0.9 (1.0)	0.4 ± 0.7 (0.0)			0.016[m]
TSI (IU/L)		N/A	14.1 ± 16.1 (5.7)	4.88 ± 6.11 (3.2)			0.027[m]
Se (µg/L)		N/A	82.4 ± 21.9 (86.1)	102.1 ± 18.9 (102.7)			0.042[m]
TSH (µIU/mL)		N/A	1.3 ± 1.8 (0.6)	0.8 ± 1.0 (0.6)			0.521[m]
fT3 (pg/mL)		N/A	5.4 ± 5.3 (3.5)	3.8 ± 2.7 (3.3)			0.359[m]
fT4 (ng/dL)		N/A	2.0 ± 1.9 (1.4)	2.0 ± 2.3 (1.3)			0.497[m]

TAO: Thyroid-associated orbitopathy; N/A: not applicable; TSH: thyroid stimulating hormone; fT3: free triiodothyronine; fT4: free thyroxine; TSI: thyroid stimulating immune globulin; CAS: clinical activity score; Se: selenium.

X^2: Chi-Square test, m: Mann-Whitney U test, $p \leq 0.05$ indicates a significant difference.

*p: for control group vs smoker TAO group, **p: for control group vs non-smoker TAO group, ***p: for smoker TAO group vs non-smoker TAO group.

Copyright© AES&M all rights reserved.

Table 2. Comparisons OCTA parameters between groups

OCTA parameters	Group						*p**	*p***	*p****
	Control (n = 32)		Smoker TAO (n = 24)		Non-Smoker TAO (n = 20)				
	Mean ± SD (median)		Mean ± SD (median)		Mean ± SD (median)				
VD of SCP (%)									
Central	22.6 ± 3.1	22.9	21.2 ± 6.0	20.2	20.3 ± 3.3	20.3	**0.029**[m]	**0.017**[m]	0.872[m]
Superior	48.7 ± 3.4	49.5	47.5 ± 4.2	48.5	48.3 ± 4.3	49.6	0.131[m]	0.802[m]	0.412[m]
Nasal	46.8 ± 2.0	46.7	46.3 ± 2.4	46.9	46.1 ± 2.5	46.7	0.718[m]	0.429[m]	0.896[m]
Inferior	47.9 ± 2.4	48.1	47.4 ± 3.9	47.2	46.1 ± 3.6	47.0	0.435[m]	0.561[m]	0.332[m]
Temporal	47.9 ± 1.8	47.8	47.3 ± 2.2	47.6	47.6 ± 2.2	47.8	0.638[m]	0.803[m]	0.968[m]
VD of DCP (%)									
Central	20.1 ± 3.6	20.1	17.0 ± 6.3	15.4	16.1 ± 5.1	16.1	**0.011**[m]	**0.004**[m]	0.825[m]
Superior	49.9 ± 3.3	50.3	49.0 ± 4.6	50.0	48.8 ± 5.0	49.1	0.357[m]	0.362[m]	0.849[m]
Nasal	48.3 ± 1.9	48.6	47.4 ± 2.6	48.2	46.8 ± 2.7	47.4	0.183[m]	**0.013**[m]	0.352[m]
Inferior	49.2 ± 2.4	49.5	48.4 ± 3.0	48.2	46.2 ± 5.9	47.7	0.322[m]	0.073[m]	0.332[m]
Temporal	47.0 ± 2.5	47.2	46.5 ± 3.1	46.8	46.0 ± 3.5	45.4	0.617[m]	0.230[m]	0.459[m]
VD of ORL (%)									
Central	41.2 ± 3.5	41.2	42.7 ± 2.9	42.0	40.8 ± 3.2	41.3	0.118[m]	0.904[m]	0.204[m]
Superior	48.9 ± 2.0	48.9	49.2 ± 2.0	49.5	50.1 ± 1.6	49.5	0.412[m]	0.076[m]	0.362[m]
Nasal	49.0 ± 1.8	49.5	49.3 ± 1.3	49.4	50.5 ± 3.0	50.6	0.810[m]	0.062[m]	0.126[m]
Inferior	48.9 ± 1.7	49.0	49.5 ± 2.0	49.9	50.0 ± 1.7	49.7	0.057[m]	0.085[m]	0.764[m]
Temporal	48.8 ± 1.8	48.7	49.4 ± 2.2	48.9	50.3 ± 2.9	49.2	0.555[m]	0.149[m]	0.280[m]
VD of CC (%)									
Central	52.5 ± 2.0	52.2	52.6 ± 2.6	52.3	52.2 ± 2.6	52.2	0.960[m]	0.741[m]	0.904[m]
Superior	53.0 ± 1.7	53.0	52.5 ± 2.3	51.9	52.5 ± 2.6	52.7	0.177[m]	0.561[m]	0.741[m]
Nasal	52.5 ± 1.6	52.1	52.5 ± 2.0	52.7	52.5 ± 2.8	52.7	0.857[m]	0.936[m]	0.849[m]
Inferior	52.9 ± 1.7	53.1	53.5 ± 1.6	53.3	52.4 ± 2.7	52.7	0.406[m]	0.429[m]	0.218[m]
Temporal	52.7 ± 1.2	52.6	53.1 ± 2.2	53.5	52.2 ± 2.6	52.2	0.258[m]	0.976[m]	0.718[m]

TAO: thyroid-associated orbitopathy; OCTA: optical coherence tomography angiography; VD: vessel density; SCP: superficial retinal capillary plexus; DCP: deep retinal capillary plexus; ORL: outer retinal layer; CC: choriocapillaris.

Data are presented asmean ± standard deviation, X^2: for Chi-Square test, m: mann-Whitney U test, $p \leq 0.05$ indicates a significant difference.

*p: for control group vs smoker TAO group, **p: for control group vs non-smoker TAO group, ***p: for smoker TAO group vs non-smoker TAO group.

This study demonstrated that smoking is associated with significantly increased CAS and TSI levels, and significantly decreased serum selenium levels, in patients with inactive TAO. These results support prior reports suggesting that smoking alters selenium status and contributes to systemic oxidative imbalance (23,24). Our findings provide substantial evidence that smoking contributes to TAO pathogenesis and may prolong low-grade autoimmune activity during clinically inactive stages.

This study addresses a significant gap in the current literature. While previous studies have assessed retinal microvascular changes in TAO using OCTA, few have investigated such changes in the inactive phase, and none have simultaneously assessed serum selenium status, autoimmune markers (TSI), and smoking exposure. Some studies have reported vascular dropout in active TAO, while others have identified reduced macular perfusion in inactive TAO without considering modifiable systemic factors such as selenium or smoking (25-27). In one study comparing TAO patients who smoked and those who did not, Ceyhanoğlu and cols. (12) found no significant difference in macular vascular parameters compared to controls, but peripapillary vascular parameters were significantly lower only in TAO patients who smoked versus controls.

It is noteworthy that while both central superficial and deep capillary plexus vascular densities were reduced in both smoker and non-smoker TAO groups

Copyright© AE&M all rights reserved.

compared to healthy controls, no significant difference was observed between TAO subgroups. This suggests that chronic TAO-associated inflammation, independent of smoking effects, may lead to subclinical retinal microvascular impairment, consistent with previous OCTA studies (25,26). Previous work has shown that smoking reduces vascular density in deep retinal capillary plexus independently of systemic disease (28,29). In our study, the absence of a smoker control group limited the ability to evaluate the additive effects of smoking on retinal microvascular structure in TAO.

This study provides evidence that smoking status is associated with serum selenium levels, clinical severity, autoimmunity, and retinal microvascular changes in inactive TAO. This multidimensional perspective offers novel insights into the intersection of systemic oxidative and inflammatory factors with localized orbital pathology and establishes a new framework for risk stratification in apparently quiescent disease stages.

In this cohort, smoking was associated with lower serum selenium levels and increased immune activation in TAO patients. Selenium is a well-established antioxidant that modulates thyroid hormone metabolism and limits free radical-mediated tissue damage (30,31). Randomized controlled trials have shown that selenium supplementation in mild TAO yields improved clinical outcomes, delayed progression, and enhanced quality of life (31). However, there is limited literature evaluating this association in the context of smoking.

The authors propose a hypothesis of significant relevance: that smoking may exacerbate selenium deficiency, thereby increasing oxidative stress and prolonging immune activation in TAO. This hypothesis is reinforced by previous research linking smoking with reduced selenium bioavailability and elevated systemic oxidative stress markers (22-24). Our findings indicated an association between smoking and lower selenium levels in TAO, highlighting the further prospective studies to determine whether selenium monitoring or supplementation in smokers with TAO provides clinical benefit, especially given the narrow therapeutic range of selenium.

The findings of this study also have important clinical implications. Central SCP and DCP vascular densities were diminished in all TAO patients, regardless of smoking status, compared to controls. These results are consistent with reports of early macular and peripapillary vascular dropout in both active and inactive TAO (25-27). The results of this study indicate the presence of persistent subclinical microvascular changes, most likely attributable to long-term orbital inflammation, tissue remodeling, or ischemia associated with orbital volume expansion. In contrast to previous studies that focused exclusively on the active phase, our findings demonstrate that vascular impairments may persist into the inactive phase. This underscores the value of OCTA as a noninvasive biomarker for identifying early or residual orbital dysfunction.

It is important to acknowledge the limitations of this study. The OCTA device utilized provides a limited 6 × 6 mm scan area, which restricts the generalizability of microvascular observations to the entire retinal or orbital vasculature. Additionally, OCTA is unable to measure flow velocity or directionality, both of which are essential for a comprehensive understanding of retrobulbar hemodynamics. Variability among OCTA devices and segmentation algorithms may also negatively impact the reproducibility of results across centers. Each device relies on a unique algorithm to detect flow, and clinicians should be aware that these differences can influence imaging results and lead to discrepancies in follow-up assessments. To mitigate these issues, ensure consistency, and enable accurate comparisons of OCTA measurements, patients should be imaged with the same device and scan size whenever possible across visits.

Other limitations include the retrospective design, small sample size, absence of a smoker control group, and lack of selenium level data in the control group. The retrospective design and small sample size may have limited the statistical power to detect more subtle subgroup differences. These limitations prevent a clear assessment of the relationships among smoking status, serum selenium levels, clinical severity, autoimmunity, and retinal microvascular changes in TAO, and also limit the generalizability of our findings to all TAO patients. Despite these constraints, our results

Copyright© AE&M all rights reserved.

provide preliminary data supporting the need for future prospective and longitudinal studies. We believe that such studies, particularly with larger sample groups, will clarify the need for selenium supplementation in TAO smokers and elucidate whether the microvascular changes detected by OCTA are meaningfully related to clinical outcomes.

In conclusion, the OCTA findings revealed a reduction in macular microvascular density among patients with TAO, particularly within the SCP and DCP layers, regardless of smoking status. Therefore, OCTA may serve as a valuable adjunct tool for detecting persistent vascular changes in TAO patients and for guiding therapeutic interventions. Additionally, the study observed that, among patients with inactive TAO, smoking was associated with increased autoimmune activity (as evidenced by elevated CAS and TSI levels) and decreased serum selenium levels, which may indicate ongoing subclinical inflammation and heightened oxidative stress. These results support the assertion that smoking cessation is an essential component of TAO management, even during periods of disease inactivity. Although patients with TAO who smoke exhibited lower selenium levels, prospective studies with larger sample sizes are necessary to clarify the clinical significance of selenium monitoring and to determine whether these findings can be generalized to the broader TAO population.

Acknowledgments: not applicable.

Funding: the author(s) received no financial support for the research, authorship, and/or publication of this article.

Ethics approval and consent to participate: the study adhered to the tenets of the Declaration of Helsinki. Ethics committee approval was received from the Basaksehir Cam and Sakura City Hospital ethics committee (grant no. 10.07.2024.49).

Artificial intelligence (AI) disclosure: no AI applications or assistive technologies were used in the preparation of this manuscript.

Author contributions statement: FS, SG, GO members collected data. FS interpreted the data and performed statistical analysis. FS was the major contributor in writing the manuscript. All authors read and approved the final manuscript.

Disclosure: no potential conflict of interest relevant to this article was reported.

Availability of data and materials: the datasets used and/or analyzed are available from the corresponding author upon request.

REFERENCES

1. Mourits MP, Koornneef L, Wiersinga WM, Prummel MF, Berghout A, van der Gaag R. Clinical criteria for the assessment of disease activity in Graves' ophthalmopathy: a novel approach. Br J Ophthalmol. 1989 Aug;73(8):639-44. doi: 10.1136/bjo.73.8.639.
2. Prummel MF, Wiersinga WM, Mourits MP, Koornneef L, Berghout A, van der Gaag R. Effect of abnormal thyroid function on the severity of Graves' ophthalmopathy. Arch Intern Med. 1990 May;150(5):1098-101. PMID: 1691908.
3. Perros P, Kendall-Taylor P, Neoh C, Frewin S, Dickinson J. A prospective study of the effects of radioiodine therapy for hyperthyroidism in patients with minimally active graves' ophthalmopathy. J Clin Endocrinol Metab. 2005 Sep;90(9):5321-3. doi: 10.1210/jc.2005-0507.
4. Wiersinga WM. Smoking and thyroid. Clin Endocrinol (Oxf). 2013 Aug;79(2):145-51. doi: 10.1111/cen.12222.
5. Bartalena L, Piantanida E, Gallo D, Lai A, Tanda ML. Epidemiology, Natural History, Risk Factors, and Prevention of Graves' Orbitopathy. Front Endocrinol (Lausanne). 2020 Nov 30;11:615993. doi: 10.3389/fendo.2020.615993.
6. Winsa B, Mandahl A, Karlsson FA. Graves' disease, endocrine ophthalmopathy and smoking. Acta Endocrinol (Copenh). 1993 Feb;128(2):156-60. doi: 10.1530/acta.0.1280156.
7. Burch HB, Lahiri S, Bahn RS, Barnes S. Superoxide radical production stimulates retroocular fibroblast proliferation in Graves' ophthalmopathy. Exp Eye Res. 1997 Aug;65(2):311-6. doi: 10.1006/exer.1997.0353.
8. Heufelder AE, Wenzel BE, Bahn RS. Methimazole and propylthiouracil inhibit the oxygen free radical-induced expression of a 72 kilodalton heat shock protein in Graves' retroocular fibroblasts. J Clin Endocrinol Metab. 1992 Apr;74(4):737-42. doi: 10.1210/jcem.74.4.1532179.
9. Lu R, Wang P, Wartofsky L, Sutton BD, Zweier JL, Bahn RS, Garrity J, Burman KD. Oxygen free radicals in interleukin-1beta-induced glycosaminoglycan production by retro-ocular fibroblasts from normal subjects and Graves' ophthalmopathy patients. Thyroid. 1999 Mar;9(3):297-303. doi: 10.1089/thy.1999.9.297.
10. Rayman MP. The importance of selenium to human health. Lancet. 2000 Jul 15;356(9225):233-41. doi: 10.1016/S0140-6736(00)02490-9.
11. Khong JJ, Goldstein RF, Sanders KM, Schneider H, Pope J, Burdon KP, et al. Serum selenium status in Graves' disease with and without orbitopathy: a case-control study. Clin Endocrinol (Oxf). 2014 Jun;80(6):905-10. doi: 10.1111/cen.12392.
12. Ceylanoglu KS, Sen EM, Doguizi S, Hondur G. Smoking effect on peripapillary and macular microvascular structure in inactive Graves' ophthalmopathy. Int Ophthalmol. 2021 Oct;41(10):3411-3417. doi: 10.1007/s10792-021-01904-z.
13. Mourits MP, Prummel MF, Wiersinga WM, Koornneef L. Clinical activity score as a guide in the management of patients with Graves' ophthalmopathy. Clin Endocrinol (Oxf). 1997 Jul;47(1):9-14. doi: 10.1046/j.1365-2265.1997.2331047.x.
14. Bartalena L, Baldeschi L, Dickinson A, Eckstein A, Kendall-Taylor P, Marcocci C, et al, Wiersinga WM; European Group on Graves' Orbitopathy (EUGOGO). Consensus statement of the European Group on Graves' orbitopathy (EUGOGO) on management of GO. Eur J Endocrinol. 2008 Mar;158(3):273-85. doi: 10.1530/EJE-07-0666.
15. Lu Y, Wang JC, Zeng R, Katz R, Vavvas DG, Miller JW, et al. Quantitative Comparison Of Microvascular Metrics On Three Optical Coherence Tomography Angiography Devices In Chorioretinal Disease. Clin Ophthalmol. 2019 Oct 22;13:2063-2069. doi: 10.2147/OPTH.S215322.
16. Gokmen O, Ozgur G. The effect of religious fasting and dehydration at Ramadan on choroidal thickness and Retinal vessel densities, measured with optical coherence tomography angiography. Eur J Ophthalmol. 2021 Mar;31(2):497-504. doi: 10.1177/1120672120958297.

Copyright© AEM All rights reserved.

17. Miller AR, Roisman L, Zhang Q, Zheng F, Rafael de Oliveira Dias J, Yehoshua Z, et al. Comparison Between Spectral-Domain and Swept-Source Optical Coherence Tomography Angiographic Imaging of Choroidal Neovascularization. Invest Ophthalmol Vis Sci. 2017 Mar 1;58(3):1499-1505. doi: 10.1167/iovs.16-20969. Erratum in: Invest Ophthalmol Vis Sci. 2017 Apr 1;58(4):2166. doi: 10.1167/iovs.16-20969a.
18. Bartalena L, Marcocci C, Tanda ML, Manetti L, Dell'Unto E, Bartolomei MP, et al. Cigarette smoking and treatment outcomes in Graves ophthalmopathy. Ann Intern Med. 1998 Oct 15;129(8):632-5. doi: 10.7326/0003-4819-129-8-199810150-00010.
19. Eckstein A, Quadbeck B, Mueller G, Rettenmeier AW, Hoermann R, Mann K, et al. Impact of smoking on the response to treatment of thyroid associated ophthalmopathy. Br J Ophthalmol. 2003 Jun;87(6):773-6. doi: 10.1136/bjo.87.6.773.
20. Pfeilschifter J, Ziegler R. Smoking and endocrine ophthalmopathy: impact of smoking severity and current vs lifetime cigarette consumption. Clin Endocrinol (Oxf). 1996 Oct;45(4):477-81. doi: 10.1046/j.1365-2265.1996.8220832.x.
21. Matheis N, Lantz M, Grus FH, Ponto KA, Wolters D, Brorson H, et al. Proteomics of Orbital Tissue in Thyroid-Associated Orbitopathy. J Clin Endocrinol Metab. 2015 Dec;100(12):E1523-30. doi: 10.1210/jc.2015-2976.
22. Morrow JD, Frei B, Longmire AW, Gaziano JM, Lynch SM, Shyr Y, et al. Increase in circulating products of lipid peroxidation (F2-isoprostanes) in smokers. Smoking as a cause of oxidative damage. N Engl J Med. 1995 May 4;332(18):1198-203. doi: 10.1056/NEJM199505043321804.
23. Park K, Rimm E, Siscovick D, Spiegelman D, Morris JS, Mozaffarian D. Demographic and lifestyle factors and selenium levels in men and women in the U.S. Nutr Res Pract. 2011 Aug;5(4):357-64. doi: 10.4162/nrp.2011.5.4.357.
24. Swanson CA, Longnecker MP, Veillon C, Howe M, Levander OA, Taylor PR, et al. Selenium intake, age, gender, and smoking in relation to indices of selenium status of adults residing in a seleniferous area. Am J Clin Nutr. 1990 Nov;52(5):858-62. doi: 10.1093/ajcn/52.5.858.
25. Akpolat C, Kurt MM, Yılmaz M, Ordulu F, Evliyaoglu F. Analysis of Foveal and Parafoveal Microvascular Density and Retinal Vessel Caliber Alteration in Inactive Graves' Ophthalmopathy. J Ophthalmol. 2020 Mar 19;2020:7643737. doi: 10.1155/2020/7643737.
26. Wu Y, Tu Y, Bao L, Wu C, Zheng J, Wang J, et al. Reduced Retinal Microvascular Density Related to Activity Status and Serum Antibodies in Patients with Graves' Ophthalmopathy. Curr Eye Res. 2020 May;45(5):576-584. doi: 10.1080/02713683.2019.1675177.
27. Jamshidian Tehrani M, Mahdizad Z, Kasaei A, Fard MA. Early macular and peripapillary vasculature dropout in active thyroid eye disease. Graefes Arch Clin Exp Ophthalmol. 2019 Nov;257(11):2533-2540. doi: 10.1007/s00417-019-04442-8.
28. Zhu X, Yang K, Xiao Y, Ye C, Zheng J, Su B, et al. Association of cigarette smoking with retinal capillary plexus: an optical coherence tomography angiography study. Acta Ophthalmol. 2022 Nov;100(7):e1479-e1488. doi: 10.1111/aos.15157.
29. Dogan M, Akdogan M, Gulyesil FF, Sabaner MC, Gobeka HH. Cigarette smoking reduces deep retinal vascular density. Clin Exp Optom. 2020 Nov;103(6):838-842. doi: 10.1111/cxo.13070.
30. Bartalena L, Kahaly GJ, Baldeschi L, Dayan CM, Eckstein A, Marcocci C, et al. The 2021 European Group on Graves' orbitopathy (EUGOGO) clinical practice guidelines for the medical management of Graves' orbitopathy. Eur J Endocrinol. 2021 Aug 27;185(4):G43-G67. doi: 10.1530/EJE-21-0479.
31. Marcocci C, Kahaly GJ, Krassas GE, Bartalena L, Prummel M, Stahl M, et al.; European Group on Graves' Orbitopathy. Selenium and the course of mild Graves' orbitopathy. N Engl J Med. 2011 May 19;364(20):1920-31. doi: 10.1056/NEJMoa1012985.

Copyright© AE&M all rights reserved.

Archives of Endocrinology and Metabolism
ISSN 2359-4292
OFFICIAL JOURNAL OF THE BRAZILIAN SOCIETY OF ENDOCRINOLOGY AND METABOLISM

original

MicroRNA expression signatures associated with metastatic progression in papillary thyroid carcinoma

Vinicius Ferreira Capelli[1]
https://orcid.org/0000-0001-7097-5936

Ana Kober Leite[2,3]
https://orcid.org/0000-0001-7814-757X

Kelly Cristina Saito[4]
https://orcid.org/0000-0001-6397-6754

Thérèse Rachell Theodoro[5]
https://orcid.org/0000-0003-0498-2622

Fátima Solange Pasini[6]
https://orcid.org/0000-0002-0361-7781

Venâncio Avancini Ferreira Alves[7]
https://orcid.org/0000-0001-5285-4460

Luiz Paulo Kowalski[2]
https://orcid.org/0000-0002-0481-156X

Maria Aparecida Silva Pinhal[8]
https://orcid.org/0000-0003-4001-1663

Edna Teruko Kimura[4]
https://orcid.org/0000-0001-8403-4459

Leandro Luongo Matos[2,3]
https://orcid.org/0000-0002-5068-8208

[1] Faculdade de Medicina Santa Marcelina, São Paulo, SP, Brasil
[2] Departamento de Cirurgia de Cabeça e Pescoço, Instituto do Câncer do Estado de São Paulo, Hospital das Clínicas da Faculdade de Medicina da Universidade de São Paulo, São Paulo, SP, Brasil
[3] Faculdade Israelita de Ciências da Saúde Albert Einstein, Hospital Albert Einstein, São Paulo, SP, Brasil
[4] Departamento de Biologia Celular e do Desenvolvimento, Instituto de Ciências Biomédicas, Universidade de São Paulo, São Paulo, SP, Brasil
[5] Departamento de Saúde Pública, Faculdade de Medicina do ABC, São Paulo, SP, Brasil
[6] Centro de Investigação Translacional em Oncologia, Instituto do Câncer do Estado de São Paulo Paulo (ICESP), Hospital das Clínicas (HCFMUSP), Faculdade de Medicina da Universidade de São Paulo, São Paulo, SP, Brasil
[7] Departamento de Patologia, Instituto do Câncer do Estado de São Paulo, Laboratório de Investigação Médica 14 (LIM14), Faculdade de Medicina da Universidade de São Paulo, São Paulo, SP, Brasil
[8] Departamento de Bioquímica, Faculdade de Medicina do ABC, São Paulo, SP, Brasil

ABSTRACT

Objective: The objective of this study is to compare the miRNA expression profiles of primary tumors and matched metastatic lesions from patients who died due to progression of metastatic PTC. **Subjects and methods:** We conducted an exploratory study of patients with PTC who died from disease progression and had tissue samples available from both primary tumors and distant metastases. Total RNA was extracted and analyzed to assess the expression of 64 preselected miRNAs. Expression data were normalized using endogenous controls (let-7g-5p and miR-181a-5p), and differential expression was calculated using the $2^{-\Delta Ct}$ method. Those miRNAs detected in < 70% of samples or with cycle threshold (Ct) > 36 were excluded. Univariate analyses were performed using paired tests, and multivariate results were adjusted for multiple comparisons using the Benjamini–Hochberg false discovery rate (FDR) method. **Results:** Out of 3,555 patients treated for PTC between 1986 and 2015, eight patients were included. Univariate analysis identified five miRNAs differentially expressed in metastatic lesions: let-7e-5p, miR-10b-5p, miR-30e-3p, miR-423-5p, and miR-483-3p. After multivariate adjustment, miR-10b-5p and miR-30e-3p remained independently overexpressed in metastatic tissues. **Conclusion:** This study is one of the first to demonstrate distinct miRNA expression profiles in metastatic versus primary tumors in fatal PTC cases. The identified miRNAs are known to regulate processes such as cell migration, invasion, and apoptosis in other cancers, suggesting their potential contribution to PTC metastasis.

Keywords: Papillary thyroid carcinoma; microRNAs; metastasis; death

INTRODUCTION

Papillary thyroid carcinoma (PTC) is the most prevalent form of thyroid cancer and is typically associated with excellent prognosis and indolent clinical behavior. However, a small subset of cases develops distant metastases, which account for most disease-related mortality (1). Despite advances in the understanding of common genetic alterations (2), the molecular mechanisms that differentiate indolent from aggressive PTC, particularly in cases that progress to distant metastasis, remain insufficiently understood (3).

Although genetic mutations have been extensively studied, the role of microRNAs (miRNAs) in the progression of PTC is an area of emerging research. These small non-coding RNAs play critical roles in gene regulation and have been implicated in various stages of tumor development, invasion, and metastasis across several cancer types (4). While dysregulated miRNA

Received on Sep/9/2025
Accepted on Mar/9/2026
DOI: 10.20945/2359-4292-2026-0058

Correspondence to:
Leandro Luongo Matos
Departamento de Cirurgia de Cabeça e Pescoço,
Instituto do Câncer do Estado de São Paulo,
Hospital das Clínicas da Faculdade,
Medicina da Universidade de São Paulo
Av. Dr. Enéas de Carvalho Aguiar, 255
8º andar – sala 8174
05403-000 – São Paulo, SP, Brasil
l.matos@fm.usp.br

Associated editor:
Jose A. Sgarbi
https://orcid.org/0000-0001-7187-984X

This is an open-access article distributed under the terms of the Creative Commons Attribution License

Copyright© AE&M all rights reserved.

expression in thyroid tumors compared to normal tissue has been reported (3), few studies have specifically investigated their involvement in metastatic dissemination and poor clinical outcomes in solid malignancies, and none have addressed this question directly in PTC.

The objective of this study was to compare the miRNA expression profiles of primary tumors and matched metastatic lesions from patients who died due to progression of metastatic PTC. By identifying differentially expressed miRNAs associated with distant disease, we aim to provide insights into the biological processes underlying metastatic progression and contributing to mortality in this typically indolent malignancy. This study was conducted using paired formalin-fixed paraffin-embedded (FFPE) samples from a cohort of patients with PTC evaluated and treated at the Head and Neck Surgery Service of the Instituto do Câncer do Estado de São Paulo (ICESP) and Hospital das Clínicas, Faculdade de Medicina da USP (HC-FMUSP).

SUBJECTS AND METHODS

This study was approved by the Institutional Ethics Committee (CAAE: 44997215.1.0000.0065). Patients included had available samples from both the primary tumor and any metastatic tissues. The tissue samples used for molecular analysis consisted of a small portion of tumor remnants, selected by microdissection and embedded in FFPE blocks, which were originally collected for histopathological examination; this procedure ensured that only tumor tissue fragments were analyzed.

Sequencing for *BRAF* and *TERT* mutations and *NTRK* fusion

Genomic DNA was extracted from the FFPE samples using a standardized protocol. Nested PCR was used to amplify the *BRAF* and *TERT* promoter gene regions. Specific primers were designed using the Primer-BLAST tool. The PCR products were visualized by gel electrophoresis, purified, and then subjected to capillary sequencing using the Sanger method. Sequence analysis and mutation identification were performed using Sequence Scanner software (Applied Biosystems, Thermo Fisher Scientific, Waltham, MA, USA) and BLAT database alignment. Additionally, all samples underwent next-generation sequencing using the Ion Torrent platform (Thermo Fisher Scientific). Data were processed on the Ion Torrent Server and annotated via the Oncomine Knowledge Base (Thermo Fisher Scientific). The sequencing panel was designed to detect gene fusions involving *NTRK1*, *NTRK2*, and *NTRK3*, including known fusion partners for each gene. These techniques have been employed in previously published studies of our group (2,3).

MicroRNA detection technique

A total of 64 miRNAs were preselected for analysis based on a comprehensive literature review, as previously described (3). These miRNAs were selected because they have been previously associated with tumor aggressiveness, epithelial–mesenchymal transition (EMT), metastatic spread, or prognosis in different cancer types, including thyroid cancer pathogenesis and metastatic behavior. Total RNA was extracted from ten 5-µm sections of FFPE tissue using the MagMAX FFPE RNA Ultra Kit (Thermo Fisher Scientific). Expression levels of selected miRNAs were quantified using reverse transcription followed by quantitative PCR (RT-qPCR), employing the TaqMan Low Density Array (TLDA) platform (Applied Biosystems). The sequences of all 64 selected miRNAs are demonstrated in **Supplementary Table 1**.

Each sample was analyzed in triplicate to ensure consistency. Cycle threshold (Ct) values greater than 36 were excluded as unreliable, and only miRNAs expressed in at least 70% of the samples were included for downstream analysis, following the validated pipeline from our previous study (3). This filtering step led to the exclusion of 18 miRNAs from the original panel (miR-129-5p, miR-130b-3p, miR-137-3p, miR-138-2-3p, miR-146b-3p, miR-155-3p, miR-17-3p, miR-187-3p, miR-302c-3p, miR-30e-5p, miR-34b-3p, miR-34c-5p, miR-455-3p, miR-4788, miR-506-3p, miR-654-3p, miR-9-5p, and miR-98-5p).

For normalization, the quantile method was applied using Expander software, selecting the most stable endogenous miRNAs as references. Specifically, the average expression of let-7g-5p and miR-181a-5p

Copyright© AE&M all rights reserved.

was used as an internal control, selected based on their stability after quantile normalization. The relative expression of each miRNA was calculated using the $2^{-\Delta Ct}$ method, enabling the identification of differentially expressed miRNAs between the two patient groups.

Statistical analysis

Categorical data were described as frequencies. Continuous variables were reported as means (standard deviations [SD] or standard errors [SE]). The ranking of paired tissues in the miRNA profile analysis was evaluated using the Wilcoxon test. Variables with p-values < 0.10 in univariate analysis were further assessed using multivariate linear regression to identify independently associated miRNAs, given the very small sample size (8 pairs), which does not support stable estimation in mixed-effects frameworks. To correct for multiple comparisons, p-values were adjusted using the Benjamini–Hochberg false discovery rate (FDR) method. An FDR-adjusted p-value (q-value) < 0.05 was considered statistically significant. All analyses were conducted using SPSS v29.0 (IBM Corp., Armonk, NY, USA). A graphical representation of differential miRNA expression was produced with assistance from ChatGPT (OpenAI) using Python, with code generated and refined by the authors. In this visualization, bubble size reflected statistical significance using the -log10 (FDR) transformation, and bubble color encoded the β coefficients from the multivariate model.

RESULTS

Out of a total of 3,555 patients diagnosed with PTC and treated from 1986 to 2015, 108 (3%) were identified as having distant metastasis, either at the initial PTC diagnosis or during follow-up. From this cohort, we selected eight patients who died due to disease progression and had available tissue from both the primary tumor and metastatic sites, with a mean time from diagnosis to death of 44 months (SD 12.6 months). The majority were women (75%) with a mean age of 55.2 years (SD 9.6 years). All patients underwent R0 surgery, and 87.5% received radioiodine therapy. Half of the patients developed radioiodine-refractory disease, and 75% had evidence of vascular invasion. All patients exhibited distant metastases—most commonly to the lung (7; 87.5%), bone (7; 87.5%), or multiple sites (7; 87.5%). Three patients (37.5%) had *BRAF* mutation detected at the primary tumor and also at the metastatic tissue. Four patients (50%) exhibited *TERT* mutations, including the same three patients with *BRAF* mutations, in both primary and metastatic specimens. One patient had an exclusive *TERT* mutation detected only on metastatic tissue, while no samples displayed *NTRK* fusions. The complete descriptive data are available in **Table 1**.

Remarkably, miRNAs let-7e-5p, miR-10b-5p, miR-30e-3p, miR-423-5p, and miR-483-3p were overexpressed in metastatic tissues compared to primary tumor tissues, as shown in **Table 2**.

The five differentially expressed miRNAs identified in univariate analysis were subsequently subjected to multivariate linear regression analysis. The resulting p-values were adjusted for multiple comparisons using the FDR method. After adjustment, three miRNAs remained independently and significantly associated with metastatic tissue in the multivariate model. Specifically, miR-10b-5p (β: +1.376; 95% confidence interval [CI]: 0.260 to 0.953; p = 0.006) and miR-30e-3p (β: +1.017; 95% CI: 0.593 to 1.775; p = 0.004) showed positive independent coefficients, indicating an association with metastatic tissue. In contrast, miR-483-3p exhibited a negative independent coefficient (β: -1.078; 95% CI: -2.830 to -0.226; p = 0.030), despite its higher expression in metastatic tissue in univariate analysis, suggesting that the apparent upregulation of miR-483-3p reflects shared variance with other metastasis-associated miRNAs, rather than an independent metastatic signal. Notably, let-7e-5p (β: −0.173; p = 0.887) and miR-423-5p (β: +0.054; p = 0.916) did not retain statistical significance after adjustment. These results are summarized in a bubble plot demonstrated in **Figure 1**.

DISCUSSION

The molecular mechanisms that differentiate indolent from aggressive PTC, particularly at the metastatic stage, are still poorly understood. Although miRNAs may contribute to the metastatic cascade,

Copyright© AE&M all rights reserved.

Table 1. Descriptive data of patients with metastatic papillary thyroid carcinoma who died due to disease progression and were included in the study

Categorical variables	Frequency (n)	Valid %
Sex		
Male	2	25
Female	6	75
R0 Surgery*	8	100
Reoperation	2	25
Radioiodine Therapy (RAI)	7	87.5
Stimulated Thyroglobulin (> 4 ng/mL)	8	100
Radioiodine Refractoriness	4	50
Lymph Node Recurrence	2	25
Site of Distant Metastasis		
Lung	7	87.5
Liver	2	25
Bone	7	87.5
Multiple Sites	7	87.5
Cause of Death		
Airway Obstruction	3	37.5
Metastatic Tumor Progression	5	72.5
Aggressive Histological Variant	1	12.5
TNM 8th Edition – pT		
pT1	3	37.5
pT2	2	25
pT3	1	12.5
pT4a	2	25
TNM 8th Edition – pN		
pN0	4	50
pN1a	2	25
pN1b	2	25
Vascular Invasion	6	75
Extrathyroidal Extension	4	50
Microscopic	1	12.5
Macroscopic	3	37.5
Multifocality	5	62.5
Dedifferentiation	5	62.5
Mutation Profile		
BRAF (Primary Tumor)	3	37.5
BRAF (Metastatic Tissue)	3	37.5
TERT (Primary Tumor)	4	50
TERT (Metastatic Tissue)	5	62.5
NTRK Fusion (Primary Tumor)	0	0
NTRK Fusion (Metastatic Tissue)	0	0

Continuous variables	Minimum	Maximum	Mean	SD
Age (years)	42	72	55.2	9.6
Cumulative Radioiodine Dose (mCi)	200	720	349	169.4
Tumor Size (cm)	0.4	13.5	3.6	4.5
Time from Diagnosis to Death (months)	30	67	44	12.6
Time from Diagnosis to Metastasis (months)	0	13	1.9	4.6
Time from Diagnosis to Disease Progression (months)	13	61	27	16.4
Time from Metastasis to Death (months)	22	67	42.1	14.7
Time from Disease Progression to Death (months)	3	41	17	11.7

*R0 surgery: complete resection with negative margins.
SD: standard deviation.

Copyright© AE&M all rights reserved.

Table 2. Comparison of microRNA expression between primary tumor and metastatic tissue

miR-10b-5p	Primary tumor		Metastatic tissue		*P*-value (Wilcoxon test)
	Mean	SE	Mean	SE	
let-7b-5p	0.02886	0.011184	0.33854	0.174389	0.093
let-7c-5p	0.02886	0.276381	2.07338	0.88759	0.465
let-7d-5p	0.02886	0.039087	0.76483	0.260128	0.249
let-7e-5p	*0.02886*	*0.215269*	*3.77295*	*0.735996*	*0.036*
let-7f-5p	0.02886	0.562676	4.28175	1.142207	0.753
let-7i-5p	0.02886	4.832131	15.96943	7.14814	0.600
miR-1-3p	0.02886	1.212567	19.44099	9.018971	0.063
miR-101-3p	4.23332	0.810301	3.19856	0.649048	0.398
miR-10b-5p	*0.37133*	*0.069863*	*2.23117*	*0.807449*	*0.018*
miR-125a-5p	6.30632	1.241309	8.45051	2.054138	0.208
miR-138-5p	3.44566	1.271794	4.09477	2.284513	1.000
miR-141-3p	14.46202	3.71996	20.58323	6.642364	0.893
miR-16-5p	5.6556	0.747569	8.40206	3.212635	0.398
miR-17-5p	2.2212	0.73003	1.96044	0.701114	1.000
miR-181b-5p	0.25988	0.062959	0.44196	0.088307	0.345
miR-18a-5p	0.05851	0.03011	0.18816	0.098839	1.000
miR-191-5p	1.02326	0.247608	1.34079	0.2897	0.735
miR-199a-3p	1.02775	0.346961	0.40159	0.183531	0.310
miR-19a-3p	0.76139	0.382344	0.46611	0.126985	0.753
miR-19b-3p	1.45986	0.687182	1.70509	0.574711	0.500
miR-200a-3p	2.52547	0.654323	3.09188	0.916931	0.889
miR-200b-3p	30.90601	10.271064	23.8411	9.510103	0.327
miR-200c-3p	13.44791	4.665669	27.43071	8.587642	0.123
miR-203a-3p	0.09001	0.048652	0.03674	0.021409	0.109
miR-205-5p	1.64797	1.369495	3.41519	2.121461	1.000
miR-20a-5p	0.63947	0.212446	0.66561	0.129087	0.735
miR-21-5p	45.36348	12.57295	42.09528	11.896246	0.866
miR-214-3p	0.32772	0.142964	0.22648	0.116418	0.310
miR-221-3p	18.86526	6.648546	20.11025	6.30474	0.575
miR-222-3p	1.04256	0.350446	1.43419	0.354886	0.327
miR-29a-3p	6.23873	0.48776	6.73183	1.380566	0.674
miR-30a-5p	4.96206	0.592394	5.99355	0.875202	0.345
miR-30b-5p	17.94068	3.919451	13.94327	4.067131	0.612
miR-30c-5p	33.66616	6.438056	31.07315	17.379167	0.463
miR-30d-5p	2.20432	0.455019	1.52911	0.534786	0.398
miR-30e-3p	*0.58264*	*0.092873*	*1.43238*	*0.276001*	*0.028*
miR-31-5p	0.06265	0.042879	0.41265	0.205599	0.273
miR-34a-5p	3.09104	0.778726	6.54144	2.432161	0.063
miR-423-5p	*0.3717*	*0.080369*	*1.48887*	*0.337737*	*0.046*
miR-429	0.12836	0.040788	0.22871	0.08896	0.225
miR-483-3p	*0.13068*	*0.04256*	*0.59526*	*0.152839*	*0.043*
miR-92a-3p	11.7837	4.260977	12.08097	4.242697	0.866
miR-146b-5p	1.40705	0.553416	1.91032	1.169727	0.345

SE: standard error.

Copyright© AE&M all rights reserved.

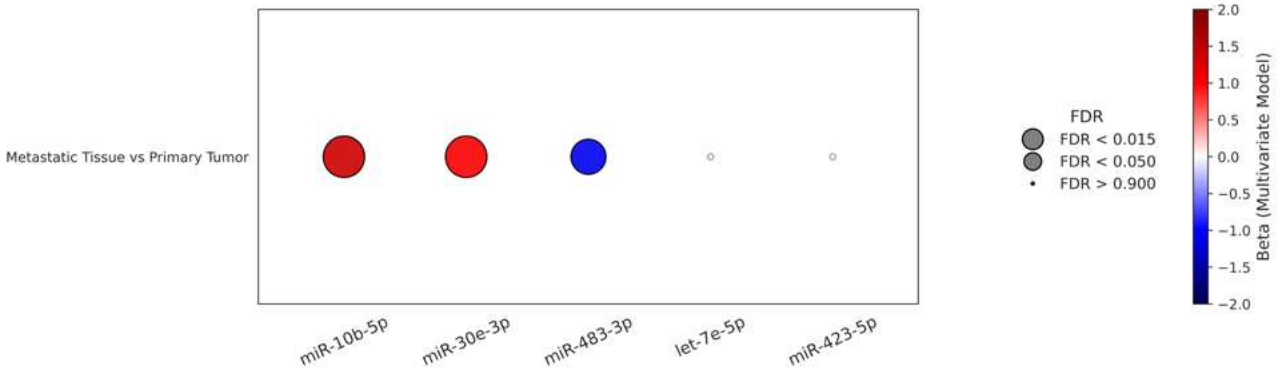


Figure 1. Multivariate association of selected microRNAs in metastatic tissue compared with primary tumors of patients with papillary thyroid carcinoma. Bubble color represents the direction and magnitude of the association based on regression coefficients (β) from the multivariate linear regression model, with positive coefficients shown in red and negative coefficients in blue. Bubble size is proportional to statistical significance and reflects -log10(FDR). While miR-10b-5p and miR-30e-3p showed positive independent coefficients, indicating an association with metastatic tissue, miR-483-3p exhibited a negative independent coefficient after multivariate adjustment. Notably, let-7e-5p and miR-423-5p did not retain statistical significance after FDR correction and are displayed with reduced opacity.

comparative analyses between primary tumors and matched metastatic lesions in lethal cases are notably lacking. The present study is part of a broader investigation previously published by our group (3), which aimed to identify miRNAs associated with disease-specific mortality in patients with metastatic PTC. In that study, we analyzed samples from 24 patients and demonstrated that the overexpression of miR-101-3p, miR-17-5p, and miR-191-5p was significantly associated with death due to disease progression. From that original cohort, we specifically selected eight patients with available paired samples from both the primary tumor and metastatic sites, which constituted the final study population of the present analysis. The current analysis builds upon those findings by further exploring the functional relevance of selected miRNAs within the context of aggressive PTC biology, reinforcing their potential role in metastatic progression.

In this exploratory study, we found that miR-10b-5p and miR-30e-3p were significantly overexpressed in metastatic tissues compared to their matched primary tumors. Moreover, the divergence between univariate and multivariate results for miR-483-3p likely reflects shared variance with other metastasis-associated miRNAs, particularly given the small sample size, and should therefore be interpreted as a context-dependent rather than an independent effect. Each of these miRNAs has been previously linked to metastatic behavior in other tumor types.

For instance, miR-10b-5p has been linked to the promotion of migration and invasion, with consistent associations with metastasis in breast, gastric, and hepatocellular carcinomas, reinforcing its potential relevance in PTC dissemination (5-7). Additionally, miR-10b-5p has been consistently implicated in the enhancement of tumor invasiveness and metastatic potential across several malignancies, providing mechanistic clues that may be relevant to metastatic dissemination in PTC. In gastric cancers, miR-10b promotes cellular migration and invasion largely through suppression of tumor-suppressive transcription factors such as HOXD10, thereby releasing downstream prometastatic effectors, including RhoC and matrix-remodeling enzymes that facilitate EMT and tissue invasion (6). In hepatocellular carcinoma, esophageal cancer, and low-grade gliomas, miR-10b-5p has been shown to modulate cell-cycle progression and apoptosis through targeting *KLF4*, contributing to an aggressive phenotype characterized by increased proliferation and migratory capacity (7). Evidence from non-small cell lung cancer further supports its role in metastasis: circulating exosomal miR-10b-5p is independently associated with worse survival and is proposed to promote metastatic spread by transferring proinvasive signals to recipient cells and modifying the tumor microenvironment (5). Together, these converging findings across tumor types indicate that miR-10b-5p acts as a regulator of pathways involved

Copyright© AE&M all rights reserved.

in cytoskeletal remodeling, EMT induction, apoptosis suppression, and extracellular matrix degradation — biological functions that may plausibly contribute to the metastatic behavior observed in advanced PTC.

Similarly, miR-30e-3p demonstrates a context-dependent dual role in cancer biology, acting either as a tumor suppressor or an oncogenic mediator depending on the molecular background and the signaling pathways engaged. In head and neck squamous cell carcinoma, miR-30e-3p suppresses TGF-β pathway mediators—notably TGFβR1 and BMPR2 — leading to reduced migration, invasion, and enhanced antitumoral immune activation through M1 macrophage polarization (8). Additional mechanistic data from gastric cancer indicate that miR-30e-3p can inhibit Snail1, thereby attenuating EMT and metastatic potential (9). Taken together, these findings show that miR-30e-3p intersects with multiple pathways relevant to tumor progression—including TP53/MDM2 regulation, PTEN/AKT signaling, TGF-β signaling, and EMT — supporting the possibility that its overexpression in metastatic PTC reflects engagement of similar invasion- and survival-related mechanisms.

Furthermore, miR-483-3p, located within the *IGF2* gene locus, has been consistently associated with oncogenesis through antiapoptotic and proliferative mechanisms in several malignancies (10-15). In colorectal cancer, miR-483-3p has been shown to promote proliferation and migration through the suppression of *DLC-1*, thereby enhancing metastatic potential (10) In pancreatic cancer, this miRNA directly inhibits DPC4/Smad4, disrupting TGF-β signaling and facilitating tumor growth and invasion (11). Coordinated regulation of *IGF2* and miR-483 family members further contributes to oncogenic signaling and cell-cycle progression in multiple solid tumors (13). In pancreatic ductal carcinoma, miR-483-3p has been associated with aggressive clinical behavior through modulation of apoptotic pathways and enhancement of proliferative signaling (14). Additionally, miR-483-3p has been reported to be upregulated in treatment-resistant breast cancer models, where its increased expression has been associated with modulation of metastasis-related genes (15). Taken together, these mechanisms highlight miR-483-3p as a regulator of apoptosis inhibition, TGF-β pathway disruption, proliferative capacity, and cytoskeletal and migratory remodeling across several cancer types.

In contrast, a previous study suggested a tumor-suppressive role for miR-483-3p, including the regulation of cyclin E1 signaling in breast cancer (12). In our cohort, miR-483-3p displayed higher expression in metastatic tissue in univariate paired analysis; however, this signal did not persist as an independent association after multivariate adjustment. Specifically, miR-483-3p exhibited a negative coefficient in the multivariate model, indicating that its apparent upregulation in metastatic lesions was not independent of other miRNAs included in the analysis. This divergence between univariate and multivariate results is most plausibly explained by shared variance among metastasis-associated miRNAs and by coefficient instability inherent to multivariate modeling in very small samples, like ours. Given the expected coexpression and biological interdependence of miRNAs involved in metastatic progression, multivariate adjustment in this context likely partitioned overlapping biological signals across correlated predictors rather than revealing true biological downregulation. Accordingly, the role of miR-483-3p in metastatic PTC should be interpreted as context-dependent rather than as an independent suppressive or promotive marker. These findings underscore the regulatory complexity of miR-483-3p and highlight the need for functional and larger-scale studies to clarify whether its expression reflects adaptive responses within the metastatic microenvironment or indirect modulation of metastatic programs.

The process of metastasis in epithelial tumors, including PTC, involves multiple steps such as EMT, invasion, and extravasation, all of which can be regulated by miRNAs. While some miRNAs have been identified as prometastatic in PTC, others act as metastasis suppressors (16).

This study is limited by its small sample size, which reduces statistical power, reflecting the challenge of acquiring high-quality, matched pathological specimens for molecular analysis in advanced PTC. Moreover, because seven of the eight patients received radioactive iodine, three were treated with targeted therapies,

Copyright© AE&M all rights reserved.

and six underwent additional systemic treatments, we cannot exclude the possibility that some of the observed miRNA differences reflect treatment-related molecular alterations rather than metastatic progression alone. Another limitation is that, by prioritizing selected biologically plausible miRNAs, the panel did not include all well-known miRNAs previously associated with PTC. Nonetheless, it represents a pioneering effort to explore miRNA expression directly in metastatic tissues from patients with lethal disease.

Our findings expand this body of knowledge by identifying novel miRNAs — overexpressed miR-10b-5p and miR-30e-3p — specifically in metastatic tissues from patients with lethal disease, underscoring their potential role in the metastatic process. These initial findings suggest that miRNA profiling could enhance our understanding of metastatic progression in PTC and may ultimately support the development of prognostic biomarkers or therapeutic targets. Further large-scale, multicenter studies and functional validations are needed to further elucidate the precise roles of these miRNAs in thyroid cancer metastasis.

Author contributions: conceptualization: A.K.L., L.L.M. Data curation: V.F.C., A.K.L. Formal analysis: V.F.C., A.K.L., K.C.S., T.R.T., F.S.P., L.L.M. Funding acquisition: E.T.K., L.L.M. Methodology: A.K.L., K.C.S., T.R.T., F.S.P., V.A.F.A., M.A.S.P., E.T.K., L.L.M. Supervision: L.P.K., M.A.S.P., E.T.K. Writing – original draft: V.F.C., L.L.M. Writing – review & editing: A.K.L., K.C.S., T.R.T., F.S.P., V.A.F.A., L.P.K., M.A.S.P., E.T.K.

Funding: Edna Teruko Kimura received grants for this study by the *Fundação de Amparo à Pesquisa do Estado de São Paulo* (FAPESP), Public Brazilian Agency (grants number: 2020/12459-1 and 2019/25116-8), and Leandro Luongo Matos received grants for this study by the *Conselho Nacional de Desenvolvimento Científico e Tecnológico*— CNPq, Public Brazilian Agency, (grants number: 407520/2018-0, 311210/2021-0, 409443/2021-2, 304044/2021-0, and 124395/2023-6).

Acknowledgements: none

Disclosure: no potential conflict of interest relevant to this article was reported.

Data availability: datasets related to this article will be available upon request to the corresponding author.

REFERENCES

1. Nunes KS, Matos LL, Cavalheiro BG, Magnabosco FF, Tavares MR, Kulcsar MA, et al. Risk factors associated with disease-specific mortality in papillary thyroid cancer patients with distant metastases. Endocrine. 2022 Mar;75(3):814-822. doi: 10.1007/s12020-021-02901-z.
2. K Kimura ET, Nikiforova MN, Zhu Z, Knauf JA, Nikiforov YE, Fagin JA. High prevalence of BRAF mutations in thyroid cancer: genetic evidence for constitutive activation of the RET/PTC-RAS-BRAF signaling pathway in papillary thyroid carcinoma. Cancer Res. 2003 Apr 1;63(7):1454-7. PMID: 12670889.
3. Leite AK, Saito KC, Theodoro TR, Pasini FS, Camilo LP, Rossetti CA, Cavalheiro BG, Alves VAF, Kowalski LP, Pinhal MAS, Kimura ET, Matos LL. Profile of MicroRNAs Associated with Death Due to Disease Progression in Metastatic Papillary Thyroid Carcinoma Patients. Cancers (Basel). 2023 Jan 31;15(3):869. doi: 10.3390/cancers15030869.
4. Menderico Junior GM, Theodoro TR, Pasini FS, de Menezes Ishikawa M, Santos NSS, de Mello ES, da Silva Pinhal MA, Moyses RA, Kulcsar MAV, Dedivitis RA, Cernea CR, Kowalski LP, de Matos LL. MicroRNA-mediated extracellular matrix remodeling in squamous cell carcinoma of the oral cavity. Head Neck. 2021 Aug;43(8):2364-2376. doi: 10.1002/hed.26686.
5. Liu Q, Yu Z, Yuan S, Xie W, Li C, Hu Z, Xiang Y, Wu N, Wu L, Bai L, Li Y. Circulating exosomal microRNAs as prognostic biomarkers for non-small-cell lung cancer. Oncotarget. 2017 Feb 21;8(8):13048-13058. doi: 10.18632/oncotarget.14369.
6. Mei L, Lu Z, Shen Z, Xu S. The prognostic and diagnostic values of MicroRNA-10b in gastric cancer: A comprehensive study based on meta-analysis and TCGA database. Medicine (Baltimore). 2020 Jun 5;99(23):e20508. doi: 10.1097/MD.0000000000020508.
7. Xiao H, Bai J, Yan M, Ji K, Tian W, Liu D, et al. Discovery of 5-Signature Predicting Survival of Patients with Lower-Grade Glioma. World Neurosurg. 2019 Jun;126:e765-e772. doi: 10.1016/j.wneu.2019.02.147.
8. Conrad O, Burgy M, Foppolo S, Jehl A, Thiéry A, Guihard S, et al. Tumor-Suppressive and Immunomodulating Activity of miR-30a-3p and miR-30e-3p in HNSCC Cells and Tumoroids. Int J Mol Sci. 2023 Jul 6;24(13):11178. doi: 10.3390/ijms241311178.
9. Gu XJ, Li YJ, Wang F, Ye T. MiR-30e-3p inhibits gastric cancer development by negatively regulating THO complex 2 and PI3K/AKT/mTOR signaling. World J Gastrointest Oncol. 2022 Nov 15;14(11):2170-2182. doi: 10.4251/wjgo.v14.i11.2170.
10. Cui H, Liu Y, Jiang J, Liu Y, Yang Z, Wu S, et al. IGF2-derived miR-483 mediated oncofunction by suppressing DLC-1 and associated with colorectal cancer. Oncotarget. 2016 Jul 26;7(30):48456-48466. doi: 10.18632/oncotarget.10309.
11. Hao J, Zhang S, Zhou Y, Hu X, Shao C. MicroRNA 483-3p suppresses the expression of DPC4/Smad4 in pancreatic cancer. FEBS Lett. 2011 Jan 3;585(1):207-13. doi: 10.1016/j.febslet.2010.11.039.
12. Huang X, Lyu J. Tumor suppressor function of miR-483-3p on breast cancer via targeting of the cyclin E1 gene. Exp Ther Med. 2018 Sep;16(3):2615-2620. doi: 10.3892/etm.2018.6504.
13. Veronese A, Lupini L, Consiglio J, Visone R, Ferracin M, Fornari F, et al. Oncogenic role of miR-483-3p at the IGF2/483 locus. Cancer Res. 2010 Apr 15;70(8):3140-9. doi: 10.1158/0008-5472.CAN-09-4456.
14. Wang C, Sun Y, Wu H, Yu S, Zhang L, Meng Y, Liu M, Yang H, Liu P, Mao X, Lu Z, Chen J. Elevated miR-483-3p expression is an early event and indicates poor prognosis in pancreatic ductal adenocarcinoma. Tumour Biol. 2015 Dec;36(12):9447-56. doi: 10.1007/s13277-015-3690-x.
15. Kim OH, Jeon TJ, Kang H, Chang ES, Hong SA, Kim MK, Lee HJ. hsa-mir-483-3p modulates delayed breast cancer recurrence. Sci Rep. 2025 Jan 3;15(1):693. doi: 10.1038/s41598-024-84437-6.
16. Borrelli N, Denaro M, Ugolini C, Poma AM, Miccoli M, Vitti P, et al. miRNA expression profiling of 'noninvasive follicular thyroid neoplasms with papillary-like nuclear features' compared with adenomas and infiltrative follicular variants of papillary thyroid carcinomas. Mod Pathol. 2017 Jan;30(1):39-51. doi: 10.1038/modpathol.2016.157.

Copyright© AE&M all rights reserved.

Supplementary Table 1. Primer sequences for the studied microRNAs

microRNA	Sequence
let-7b-5p	UGAGGUAGUAGGUUGUGGUU
let-7c-5p	UGAGGUAGUAGGUUGUAUGGUU
let-7d-5p	AGAGGUAGUAGGUUGCAUAGUU
let-7e-5p	UGAGGUAGGAGGUUGUAUAGUU
let-7f-5p	UGAGGUAGUAGAUUGUAUAGUU
let-7g-5p	UGAGGUAGUAGUUUGUACAGUU
let-7i-5p	UGAGGUAGUAGUUUGUGCUGUU
miR-1-3p	UGGAAUGUAAAGAAGUAUGUAU
miR-101-3p	UACAGUACUGUGAUAACUGAA
miR-10b-5p	UACCCUGUAGAACCGAAUUUGUG
miR-125a-5p	UCCUGAGACCCUUUAACCUGUGA
miR-129-5p	CUUUUUGCGGUCUGGGGCUUGC
miR-130b-3p	CAGUGCAAUGAUGAAAGGGCAU
miR-137-3p	UUAUUGCUUAAGAAUACGCGUAG
miR-138-2-3p	GCUAUUUCACGACACCAGGGUU
miR-138-5p	AGCUGGUGUUGUGAAUCAGGCCG
miR-141-3p	UAACACUGUCUGGGUAAAGAUGG
miR-146b-3p	UGCCCUGUGGACUCAGUUCUGG
miR-146b-5p	UGAGAACUGAAUUCCAUAGGCU
miR-155-3p	CUCCUACAUAUUAGCAUUAACA
miR-16-5p	UAGCAGCACGUAAAUAUUGGCG
miR-17-3p	ACUGCAGUGAAGCACUUGUAG
miR-17-5p	CAAAGUGCUUACAGUGCAGGUAG
miR-181a-5p	AACAUUCAACGCUGUCGGUGAGU
miR-181b-5p	AACAUUCAUUGCUGUCGGUGGGU
miR-187-3p	UCGUGUCUUGUGUGCAGCCGG
miR-18a-5p	UAAGGUGCAUCUAGUGCAGAUAG
miR-191-5p	CAACGGAAAUCCCAAAAGCAGCUG
miR-199a-3p	ACAGUAGUCUGCACAUUGGUUA
miR-19a-3p	UGUGCAAAUCUAUGCAAAACUGA
miR-19b-3p	UGUGCAAAUCCAUGCAAAACUGA
miR-200a-3p	UAACACUGUCUGGGUAACGAUGU

microRNA	Sequence
miR-200b-3p	UAAUACUGCCUGGUAAUGAUGA
miR-200c-3p	UAAUACUGCCGGGUAAUGAUGGA
miR-203a-3p	GUGAAAUGUUUAGGACCACUAG
miR-205-5p	UCCUUCAUUCCACCGGAGUCUG
miR-20a-5p	UAAAGUGCUUAUAAGUGCAGGUAG
miR-21-5p	UAGCUUAUCAGACUGAUGUUGA
miR-214-3p	ACAGCAGGCACAGACAGGCAGU
miR-221-3p	AGCUACAUUGUCUGCUGGGUUUC
miR-222-3p	AGCUACAUCUGGCUACUGGGU
miR-29a-3p	UAGCACCAUCUGAAAUCGGUUA
miR-302c-3p	UAAGUGCUUCCAUGUUUCAGUGG
miR-30a-5p	UGUAAACAUCCUCGACUGGAAG
miR-30b-5p	UGUAAAACAUCCUACACUCAGCU
miR-30c-5p	UGUAAACAUCCUACACUCUCAGC
miR-30d-5p	UGUAAACAUCCCCGACUGGAAG
miR-30e-3p	CUUUCAGUCGGAUGUUUACAGC
miR-30e-5p	UGUAAAACAUCCUUGACUGGAAG
miR-31-5p	AGGCAAGAUGCUGGCAUAGCU
miR-34a-5p	UGGCAGUGUCUUAGCUGGUUGU
miR-34b-3p	CAAUCACUAACUCCACUGCCAU
miR-34c-5p	AGGCAGUGUAGUAGCUGAUUGC
miR-423-5p	UGAGGGGCAGAGAGCGAGACUUU
miR-429	UAAUACUGUCUGGUAAAACCGU
miR-455-3p	GCAGUCCAUGGGCAUAUACAC
miR-4788	UUACGGACCAGCUAAGGGAGGC
miR-483-3p	UCACUCCUCUCCUCCCGUCUU
miR-506-3p	UAAGGCACCCUUCUGAGUAGA
miR-654-3p	UAUGUCUGCUGACCAUCACCUU
miR-9-5p	UCUUUGGUUAUCUAGCUGUAUGA
miR-92a-3p	UAUUGCACUUGUCCCGGCCUGU
miR-98-5p	UGAGGUAGUAAGUUGUAUUGUU

Copyright© AE&M all rights reserved.

Archives of Endocrinology and Metabolism
ISSN 2359-4292
OFFICIAL JOURNAL OF THE BRAZILIAN SOCIETY OF ENDOCRINOLOGY AND METABOLISM

original

Age-related changes in METS-IR and HOMA-IR in obese adults and their relationship with cardiometabolic comorbidities

Esra Suay Timurkaan[1]
https://orcid.org/0000-0001-5654-7070

Gülsüm Altuntaş[2]
https://orcid.org/0000-0002-2673-8594

Muhammed Fuad Uslu[1]
https://orcid.org/0000-0001-6300-5130

Hakan Ayyıldız[1]
https://orcid.org/0000-0002-3133-9862

Mustafa Timurkaan[1]
https://orcid.org/0000-0003-1950-0489

[1] Department of Internal Medicine Clinic, Fethi Sekin City Hospital, Elazig, Turkey
[2] Department of Intensive Care Clinic, Fırat University, Elazig, Turkey

ABSTRACT

Objective: Insulin resistance (IR) is central to cardiometabolic risk in obesity, but the clinical utility of IR indices may vary by age. We compared homeostasis model assessment for insulin resistance (HOMA-IR) and metabolic score for insulin resistance (METS-IR) across age groups in obese adults and examined comorbidity burden and discriminatory performance for type 2 diabetes mellitus (T2DM) and hypertension (HT). **Subjects and methods:** This retrospective, single-center study included adults with a BMI ≥ 30 kg/m^2 (n = 481) across four age strata (18–40, 40–65, 65–75, and ≥75 years). Spearman correlation assessed the association between HOMA-IR and METS-IR. Comorbidity burden (0–3 chronic conditions) was modeled using ordinal logistic regression per 1-SD increase in z-scores, adjusted for age, sex, and BMI. Receiver operating characteristic analysis and multivariable logistic regression assessed T2DM and HT. **Results:** HOMA-IR and METS-IR were moderately correlated (ρ = 0.342 and $p < 0.001$, respectively). METS-IR was associated with comorbidity burden (adjusted odds ratio [OR] 1.84; 95% confidence interval [CI] 1.26–2.69; $p < 0.01$), whereas HOMA-IR was not (OR 1.12; 95% CI 0.92–1.36; $p = 0.256$). Discriminatory performance was limited for T2DM (area under curve [AUC] 0.500 vs. 0.537) and HT (AUC 0.471 vs. 0.519). METS-IR remained associated with T2DM (OR 2.51; 95% CI 1.60–3.93; $p < 0.001$) and HT (OR 1.81; 95% CI 1.13–2.91; $p < 0.05$). **Conclusion:** In obese adults, METS-IR demonstrated a stronger association with comorbidity burden than HOMA-IR. However, because both indices showed limited discriminatory performance for T2DM and HT, they should not be used as standalone tools for treatment guidance or diagnostic classification. Rather, they should be interpreted alongside age, clinical, and biochemical findings, as isolated use may be misleading and fail to identify disease in specific patient subgroups.

Keywords: HOMA-IR; METS-IR; obesity; insulin resistance; comorbidity burden.

INTRODUCTION

Obesity involves more than excess adipose tissue; it affects metabolic, hormonal, and inflammatory processes, predisposing individuals to insulin resistance (IR). Insulin resistance plays a central role in the pathogenesis of metabolic syndrome components such as type 2 diabetes mellitus (T2DM), dyslipidemia, hypertension (HT), and cardiovascular disease (1,2). The hyperinsulinemic-euglycemic clamp test, accepted as the gold standard for evaluating IR, is impractical for routine practice as it requires specialized equipment, trained personnel, and significant time (3). Consequently, indirect indices based on fasting glucose and insulin values, such as the homeostasis model assessment for insulin resistance (HOMA-IR), are preferred in clinical and epidemiological studies. Although HOMA-IR provides a practical measurement, its values vary by age, sex, body mass index (BMI), and population (4).

Received on Jan/22/2026
Accepted on Mar/24/2026

DOI: 10.20945/2359-4292-2026-0059

Correspondence to:
Muhammed Fuad USLU
Department of Internal Medicine Clinic,
Fethi Sekin City Hospital
23280 Elazig, Turkey
dr.fuslu@gmail.com

Associated editor:
Marcio W. Lauria
https://orcid.org/0000-0001-7558-1231

This is an open-access article distributed under the terms of the Creative Commons Attribution License

Copyright© AE&M all rights reserved.

These limitations have driven the development of alternative indices that do not require insulin measurement. The metabolic score for insulin resistance (METS-IR) estimates IR by combining fasting glucose, triglycerides, HDL cholesterol, and BMI using a logarithmic formula (5). The fact that it does not require insulin levels, is based on commonly used biochemical parameters, and is less costly makes it an attractive option for routine practice. In addition, METS-IR is a strong predictor of metabolic syndrome and cardiovascular disease risk (6).

Age-related metabolic changes complicate the assessment of IR. Declining pancreatic β-cell reserve, loss of muscle mass, and altered adipose tissue distribution influence age-related insulin sensitivity. Based on this, it is plausible that HOMA-IR changes with age (7). Duan and cols. (8) analyzed NHANES 2001–2018 data and demonstrated a positive association between METS-IR and all-cause mortality. This association was particularly pronounced in individuals under 65 years of age and was stronger than that of HOMA-IR (8). This finding suggests that METS-IR varies by age and may have different predictive utility across age groups. In obese individuals, comparing HOMA-IR and METS-IR scores is important not only in terms of how accurately they reflect IR, but also in terms of how stable they are according to age and to what extent they provide benefit in predicting comorbidities. In the current literature, few large-scale studies have directly compared these indices across age groups in obese populations.

This study compared HOMA-IR and METS-IR in obese individuals across age strata to examine the effect of age on these scores. We also evaluated the performance of both indices in distinguishing accompanying diseases, primarily T2DM and HT. Thus, we aimed to determine the age-related stability, sensitivity, and clinical utility of these insulin-based and non-insulin-based formulas.

SUBJECTS AND METHODS

Study design and patient selection

This retrospective, observational, single-center study reviewed the records of adult patients who presented to the Internal Medicine outpatient clinics of Elazig Fethi Sekin City Hospital between January 1, 2020, and January 1, 2025. The inclusion criteria comprised patients with a BMI ≥30 kg/m^2 and complete demographic, clinical, and laboratory data available in the hospital's electronic information management system. Patients with missing, incomplete or unreliable data were excluded. In order to ensure the reliability of the results, we used strict criteria to minimize common confounding conditions and ensure that IR indices were evaluated within a more homogeneous obese population. Hence, we excluded patients if they were using insulin for diabetes, receiving immunosuppressive or chronic steroid therapy, had known chronic inflammatory disease or thyroid dysfunction, were in the early postoperative follow-up period, had advanced heart failure or advanced hepatic or renal dysfunction, had active psychiatric disease requiring treatment, had a history of malignancy, or were pregnant. After all data were obtained, the cohort was categorized into four age groups: Group 1 (18–40 years; young adult), Group 2 (40–65 years; middle-aged), Group 3 (65–75 years; older), and Group 4 (≥75 years; advanced age). This classification served as the primary grouping variable.

Data collection and measurements

We extracted age, sex, height, body weight, fasting plasma glucose (mg/dL), triglycerides (mg/dL), LDL cholesterol (LDL-C, mg/dL), HDL cholesterol (HDL-C, mg/dL), total cholesterol (mg/dL), hemoglobin A1c (HbA1c, %), and fasting insulin (mIU/L) from the laboratory system. The BMI was calculated as weight (kg) divided by height (m^2).

Calculation of insulin resistance indices

Two indices were used to evaluate IR in obese individuals. The HOMA-IR was calculated using fasting insulin and fasting glucose levels using **Equation 1** (9):

HOMA-IR = (fasting insulin [μU/mL] × fasting glucose [mg/dL]) / 405 (1)

The METS-IR is a composite score derived from glucose, triglycerides, HDL-C, and BMI values; it was calculated using **Equation 2** (5):

METS-IR = ln[2 × glucose (mg/dL) + triglycerides (mg/dL)] × BMI / ln[HDL-C (mg/dL)] (2)

Copyright© AEM All rights reserved.

Both scores were analyzed as continuous variables and standardized into z-scores for modeling to ensure comparability.

Variable definitions and comorbidity coding

T2DM and HT were defined as binary variables according to definitive ICD codes and active treatment records. In the raw table, the T2DM and HT variables were coded as 1 (diagnosis present) and 2 (diagnosis absent); in the analyses, these variables were recoded as 1 (present) and 0 (absent). Comorbidity burden was created by counting the number of predefined chronic diseases in the patient files. Comorbidity burden was calculated based on the presence of HT, T2DM, dyslipidemia, coronary artery disease, cerebrovascular disease, chronic kidney disease, chronic liver disease, and chronic lung disease. Each diagnosis was coded as 0 (absent) and 1 (present) and summed. In the analyses, this variable was used both for descriptive purposes and as an ordinal outcome variable. Sex was coded as a binary variable (1 = female, 2 = male). Age was analyzed as both a continuous variable and a categorical variable based on the four predefined strata.

Statistical analyses

Statistical analyses were performed using R software (version 4.5.1; RStudio). Continuous variables were summarized as medians with interquartile ranges [IQR], and categorical variables as counts and percentages.

Correlation analyses

Spearman's rank correlation coefficient (ρ) assessed the relationship between HOMA-IR and METS-IR in the overall cohort and within each age group. Correlations between age and both indices were similarly evaluated.

Ordinal logistic regression

Ordinal logistic regression models examined the association between comorbidity burden (range: 0–3) and the HOMA-IR and METS-IR scores. In these models, the number of comorbidities was the dependent variable, with HOMA-IR or METS-IR z-scores as the primary independent variables. Age (continuous), sex, and BMI were included in the models as covariates, and the results were reported as odds ratios (OR) with 95% confidence intervals (CI) per 1 standard deviation (SD) increase in the score.

Receiver operating characteristic analyses

The receiver operating characteristic curves were generated to assess the performance of HOMA-IR and METS-IR for T2DM and HT. Area under the curve (AUC) values and 95% CIs were calculated using the pROC package and compared via the DeLong method. The positive class was defined as the presence of T2DM or HT in the relevant analysis.

Logistic regression models

Multivariable logistic regression evaluated the independent effects of HOMA-IR and METS-IR z-scores for T2DM and HT, with the dependent variables being T2DM and HT, respectively, the main independent variable was the HOMA-IR z-score or METS-IR z-score, and the covariates were age (continuous), sex, and BMI. Results were presented as ORs, 95% CIs, and *p*-values.

Linear regression analyses

To evaluate the linear relationship between age and IR scores in more detail, multivariable linear regression models were constructed with HOMA-IR and METS-IR separately as dependent variables. In these models, age was the main independent variable, and sex and BMI were included as covariates. In addition, age×HOMA-IR and age×METS-IR interaction terms were added to supplementary models for T2DM to test whether the associations of the scores with T2DM changed significantly by age.

Missing data management

Because records with missing data were excluded during patient selection, a complete-case approach was used for all models.

Visualization

The ggplot2 package generated scatter plots, box plots by age group, and distribution plots by comorbidity burden. Trend lines for continuous variables were fitted using locally estimated scatterplot smoothing with 95% CIs.

Copyright© AE&M all rights reserved.

Statistical significance

All tests were two-sided, with $p < 0.05$ considered statistically significant. No adjustments were made for multiple comparisons; thus, findings are considered exploratory.

RESULTS

Clinical and demographic characteristics

Participants were distributed relatively evenly across the four age groups (Table 1). Females predominated in all age groups. Median BMI ranged from 34.6 to 35.6 kg/m^2 and showed no clear trend with advancing age. Glucose and triglyceride levels were higher in the 40–65 and 65–75 age groups, although these differences remained within expected limits for the participants' BMI and metabolic status. In the overall cohort, T2DM prevalence was 25.8% (n = 124). By age group, T2DM prevalence was 5.3% (7/132) in the 18–40 group, 32.5% (41/126) in the 40–65 group, 33.1% (41/124) in the 65–75 group, and 35.4% (35/99) in the ≥75 group. Similarly, HT was present in 16.2% (n = 78) of the cohort. Across age groups, HT prevalence was 3.0% (4/132) in the 18–40 group, 23.0% (29/126) in the 40–65 group, 18.5% (23/124) in the 65–75 group, and 22.2% (22/99) in the ≥75 group (Table 1).

HOMA-IR and METS-IR levels and their relationship

A moderate positive correlation between HOMA-IR and METS-IR emerged in the overall cohort (Spearman $p = 0.34$; $p < 0.001$). In age-stratified analyses, this correlation remained significant across all groups ($p = 0.32$, 0.37, 0.39, and 0.29 for the 18–40, 40–65, 65–75, and ≥75 age groups, respectively; all $p < 0.01$) (Table 2). A scatter plot demonstrated an upward trend between HOMA-IR and METS-IR across the obese cohort (Figure 1A). Box plots by age group revealed no marked shift in HOMA-IR or METS-IR distributions from young adulthood to advanced age, although the distributions became more heterogeneous in older groups (Figure 1B).

Table 2. Spearman correlations between HOMA-IR and METS-IR overall and by age group

Age group (years)	Spearman rho	*p*-value
Overall	0.342	<0.001
18–40	0.321	<0.001
40–65	0.366	<0.001
65–75	0.393	<0.001
>75	0.289	<0.01

Spearman correlation coefficients (ρ) and *p*-values are shown for the overall cohort and each age stratum.

Table 1. Clinical and demographic characteristics of the obese cohort by age group

Variable	Age group (years)			
	18–40	40–65	65–75	>75
Individuals (n)	132	126	124	99
Female, n (%)	107 (81.1)	107 (84.9)	103 (83.1)	77 (77.8)
Diabetes mellitus, n (%)	7 (5.3)	41 (32.5)	41 (33.1)	35 (35.4)
Hypertension, n (%)	4 (3.0)	29 (23.0)	23 (18.5)	22 (22.2)
≥2 comorbidities, n (%)	4 (3.0)	27 (21.4)	22 (17.7)	14 (14.1)
Age (years)	30.0 (22.0–37.0)	51.0 (45.0–58.0)	68.0 (66.0–70.0)	78.0 (75.0–86.0)
BMI (kg/m^2)	35.5 (32.0–40.2)	35.6 (32.5–41.0)	34.7 (32.0–38.1)	34.6 (31.3–39.9)
Glucose (mg/dL)	87.5 (82.0–95.0)	96.5 (86.2–126.8)	99.0 (88.0–117.0)	103.0 (87.0–116.0)
Triglycerides (mg/dL)	113.5 (85.5–170.5)	134.5 (95.5–200.0)	134.0 (93.8–164.0)	118.0 (96.5–159.5)
LDL-C (mg/dL)	105.0 (90.0–126.0)	112.5 (95.0–135.2)	118.5 (100.0–145.0)	108.0 (91.5–138.5)
HDL-C (mg/dL)	44.5 (36.0–51.0)	48.0 (43.0–55.0)	47.0 (40.0–57.2)	44.0 (39.0–52.0)
Total cholesterol (mg/dL)	174.5 (154.2–201.0)	196.0 (171.2–228.8)	195.0 (169.0–226.5)	186.0 (159.5–220.0)
HbA1c (%)	5.5 (5.3–5.8)	6.0 (5.6–6.6)	6.0 (5.7–6.7)	6.1 (5.6–6.4)
Insulin (mIU/L)	15.0 (10.1–23.4)	11.9 (9.2–18.3)	10.4 (7.3–16.2)	10.2 (6.0–16.0)
HOMA-IR	3.4 (2.3–5.3)	3.3 (2.1–5.2)	2.7 (1.8–4.3)	2.6 (1.4–4.3)
METS-IR	44.2 (38.9–49.9)	45.2 (39.7–51.0)	42.5 (39.3–47.6)	43.1 (40.1–48.8)

Copyright© AE&M all rights reserved.

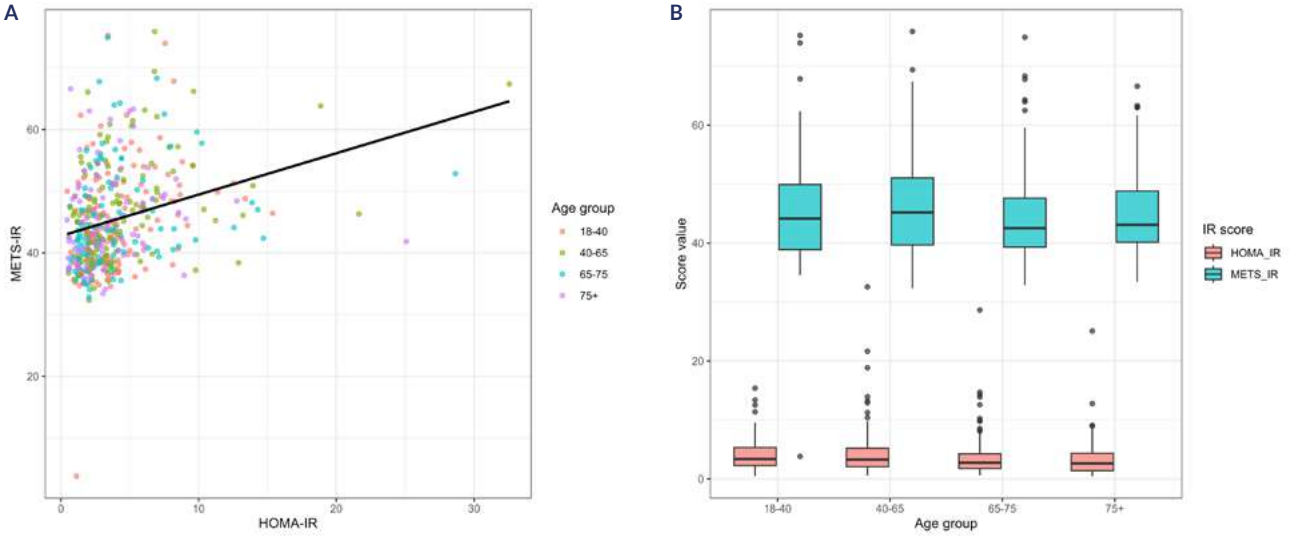


Figure 1. A) Scatter plot of METS-IR versus HOMA-IR by age group; each point represents one participant. **B)** Distributions of HOMA-IR and METS-IR across age groups; box plots depict the distributions of HOMA-IR (above) and METS-IR (below) by age group. Boxes represent the interquartile range, horizontal lines denote the median, and whiskers represent the approximate data range.

Association between HOMA-IR and METS-IR and comorbidity burden

METS-IR levels increased more consistently as the number of comorbidities increased, whereas no clear stepwise pattern was observed for HOMA-IR (**Table 3A**). In individuals without comorbidities, the median HOMA-IR was 3.0 (IQR: 2.01–4.55), while it was 2.52 (IQR: 1.57–5.02) in those with three comorbidities. Median METS-IR was 43.6 (IQR: 39.3–49.3) in participants without comorbidities and 44.5 (IQR: 41.2–50.7) in those with three comorbidities (**Table 3A**). Although absolute differences were limited, METS-IR showed a distinct and consistent upward trend as the number of comorbidities increased.

In ordinal logistic regression, a 1-SD increase in the HOMA-IR z-score did not significantly increase the likelihood of transitioning to a higher comorbidity category (OR = 1.12; 95% CI: 0.92–1.36; p = 0.256). Conversely, a 1-SD increase in the METS-IR z-score increased this likelihood approximately 1.8-fold (OR = 1.84; 95% CI: 1.26–2.69; p < 0.01). Box plots visually supported the more pronounced upward shift in METS-IR with increasing comorbidities (**Figures 2A** and **2B**).

Table 3A. Distribution of HOMA-IR and METS-IR across comorbidity categories

comorb_ord	n	HOMA-IR, median (IQR)	METS-IR, median (IQR)
0	335	3.0 (2.01–4.55)	43.6 (39.3–49.3)
1	79	2.96 (1.46–5.61)	45.0 (38.9–51.6)
2	52	3.13 (2.11–4.49)	43.1 (40.7–47.7)
3	15	2.52 (1.57–5.02)	44.5 (41.2–50.7)

Comorbidity categories are defined as the total number of documented chronic conditions (0–3). Values are presented as n and median (interquartile range).

Table 3B. Ordinal logistic regression for comorbidity burden

Predictor	OR	95% CI	*p*-value
HOMA-IR z-score	1.12	0.92–1.36	0.256
METS-IR z-score	1.84	1.26–2.69	<0.01

Ordinal logistic regression models estimate the odds of being in a higher comorbidity category per 1 standard deviation increase in HOMA-IR or METS-IR z-scores, adjusting for age, sex, and BMI.

Copyright© AE&M all rights reserved.

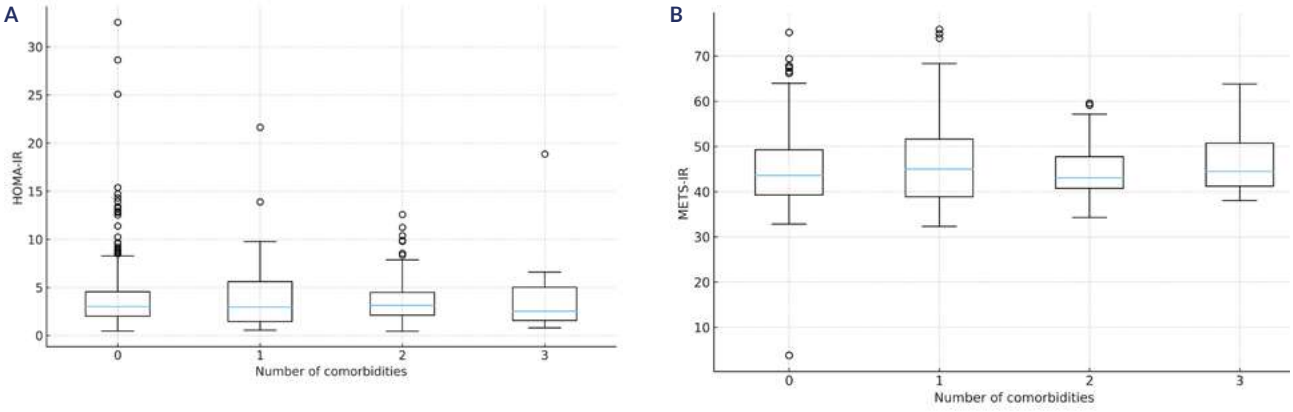


Figure 2. A) HOMA-IR by number of comorbidities; box plots showing HOMA-IR distributions across increasing comorbidity counts. A modest increase is observed with greater comorbidity burden, although overlapping between categories remained substantial. **B)** METS-IR by number of comorbidities; box plots showing the distributions of METS-IR across comorbidity categories. Unlike HOMA-IR, METS-IR showed a more monotonic trend across comorbidity categories, consistent with its association with overall cardiometabolic burden.

Diagnostic performance of HOMA-IR and METS-IR for T2DM and HT

In the obese cohort, HOMA-IR demonstrated limited discriminative ability for T2DM (AUC 0.500; 95% CI 0.439–0.562), and logistic regression revealed no significant association between a 1-SD increase and the odds of T2DM (OR 1.12; 95% CI 0.91–1.37; $p = 0.290$) (**Table 4**, **Figure 3A**). The AUC value of METS-IR was 0.537 (95% CI 0.478–0.595), and its discriminative performance was also limited. However, each 1-SD increase was significantly associated with the odds of T2DM (OR 2.51; 95% CI 1.60–3.93; $p < 0.001$) (**Table 4**, **Figure 3A**). For HT, the AUC of HOMA-IR was 0.471 (95% CI 0.396–0.546) and its OR was not significant (OR 1.03; 95% CI 0.80–1.31; $p = 0.814$); the AUC of METS-IR was 0.519 (95% CI 0.455–0.583), and while its discriminative ability remained limited, each 1-SD increase was associated with the odds of HT (OR 1.81; 95% CI 1.13–2.91; $p < 0.05$) (**Table 4**, **Figure 3B**). Overall, the AUC values near 0.5 indicated that both indices had limited discriminative capacity for T2DM and HT.

Change in HOMA-IR and METS-IR with age

A weak negative correlation between age and HOMA-IR emerged in the overall obese cohort (Spearman $p = -0.196$; $p < 0.001$; **Table 5**). In multivariable linear regression adjusted for age, sex, and BMI, each 1-year increase in age was associated with a mean 0.016-unit decrease in HOMA-IR (95% CI −0.030 to −0.001; $p = 0.045$) (**Table 5**). Curve plots of the age distribution supported this trend for HOMA-IR (**Figures 4A** and **4B**). The correlation between METS-IR and age was not statistically significant (Spearman $p = -0.020$; $p = 0.659$) (**Table 5**). In the adjusted linear regression model, the effect of age on METS-IR was also non-significant (95% CI −0.0102 to 0.0199; $p = 0.526$) (**Table 5**). In models including an age × T2DM interaction, these associations did not differ by T2DM status ($p = 0.149$ for HOMA-IR; $p = 0.745$ for METS-IR) (**Table 5**). Curve plots indicated no significant age-related trend for METS-IR (**Figures 4A** and **4B**).

Table 4. Discriminative performance of HOMA-IR and METS-IR for T2DM and HT

Outcome	Model	AUC	AUC 95% CI	OR per 1 SD	OR 95% CI	*p*-value
T2DM	HOMA-IR	0.500	0.439–0.562	1.12	0.91–1.37	0.290
	METS-IR	0.537	0.478–0.595	2.51	1.60–3.93	<0.001
HT	HOMA-IR	0.471	0.396–0.546	1.03	0.80–1.31	0.814
	METS-IR	0.519	0.455–0.583	1.81	1.13–2.91	<0.05

The area under curve (AUC) values and 95% confidence intervals (CI) are derived from ROC analyses using HOMA-IR and METS-IR as continuous predictors. Odds ratios (OR) are estimated per 1 standard deviation increase in the corresponding z-scores, adjusted for age, sex, and BMI.

Copyright© AE&M all rights reserved.

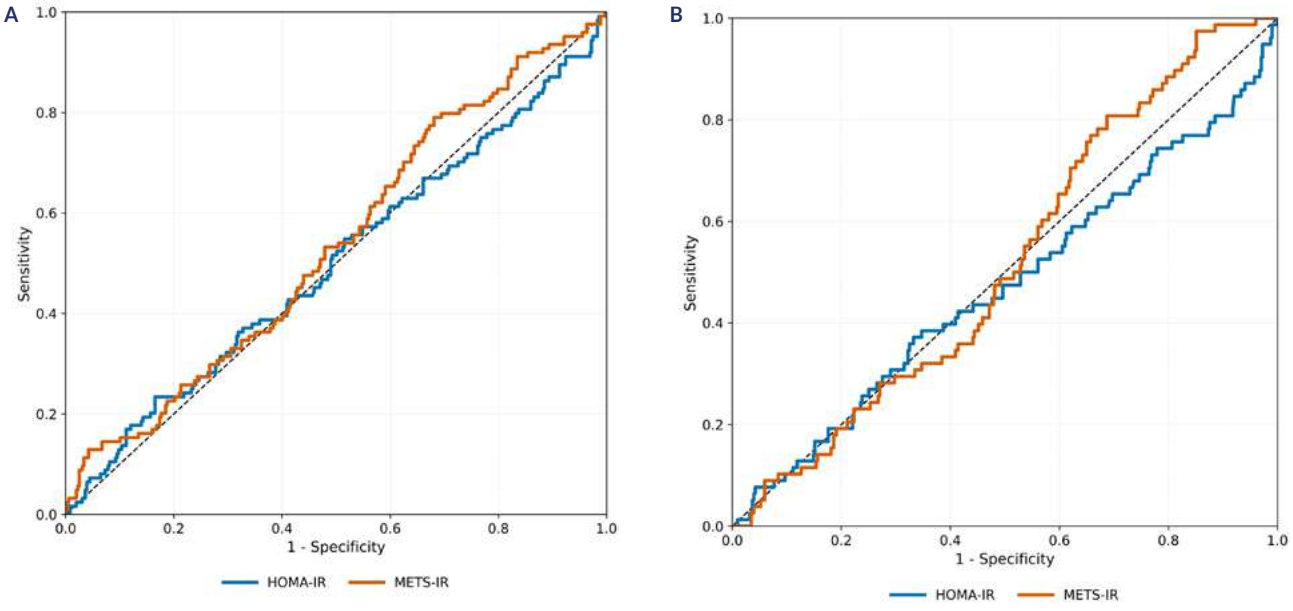


Figure 3. A) ROC curves of HOMA-IR and METS-IR for diabetes; ROC curves for diabetes, wherein HOMA-IR AUC: 0.500 (95% CI 0.439–0.562) and METS-IR AUC: 0.537 (95% CI 0.478–0.595). The diagonal line indicates no discrimination. **B)** ROC curves of HOMA-IR and METS-IR for hypertension. ROC curves for hypertension, wherein HOMA-IR AUC: 0.471 (95% CI: 0.396–0.546); METS-IR AUC: 0.519 (95% CI: 0.455–0.583). The diagonal line indicates no discrimination.

Table 5. Associations between age and insulin resistance indices

Score	Spearman rho	Spearman p	β_age (per year)	β 95% CI	*p* (linear regression)	Interaction *p* (age × DM status)
HOMA-IR	–0.196	<0.001	–0.016	–0.030––0.001	0.045	0.149
METS-IR	–0.020	0.659	0.0049	–0.010–0.019	0.526	0.745

Spearman correlations describe the monotonic relationship between age and each index. Linear regression estimates (β) reflect the average change in the index per 1-year increase in age, adjusted for sex and BMI. The interaction term tests whether the relationship between age and each index differs by diabetes status.

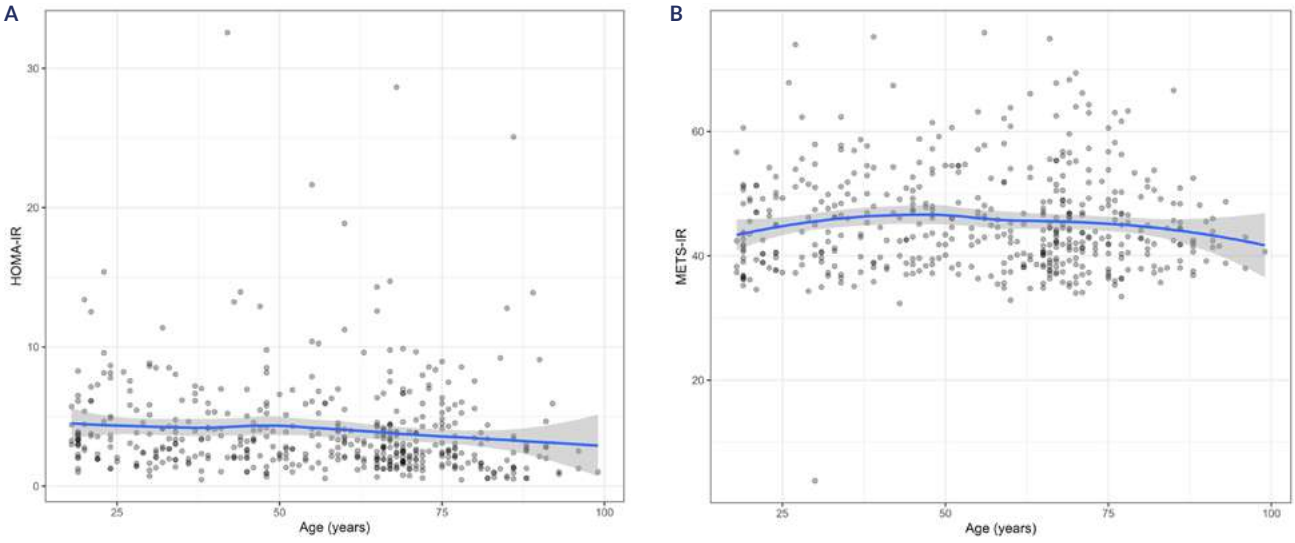


Figure 4. A) Relationship between age and HOMA-IR. Scatter plot showing individual HOMA-IR values across age groups. The LOESS smoothing curve is overlaid. **B)** Relationship between age and METS-IR; Scatter plot showing METS-IR values by age. The LOESS smoothing curve is overlaid.

Copyright© AEM All rights reserved.

DISCUSSION

The main finding of our study is that although METS-IR reflected comorbidity burden more strongly than HOMA-IR in obese adults, neither index demonstrated strong diagnostic utility for specific conditions in age-adjusted analyses. In addition, both indices provided only limited discriminative ability for T2DM and HT. Clinically, METS-IR serves as a non-insulin-based index reflecting cardiometabolic burden across the obesity spectrum.

Obesity induces IR through metabolic and hormonal alterations, and this resistance is central to the pathogenesis of metabolic syndrome (10). HOMA-IR and METS-IR are important indicators for evaluating IR, with METS-IR offering practical application and predictive power for cardiometabolic risk (11). Although BMI was relatively homogeneous across age groups, our findings showed that the prevalence of T2DM and HT increased markedly at older ages, which is consistent with large cohort studies suggesting that metabolically healthy obesity is rarely sustainable long-term (12–15). Our data support the observation that a significant proportion of obese individuals progress toward multiple cardiometabolic risk factors and organ damage, as evidenced by the age-related increase in clinical comorbidities.

Although HOMA-IR is frequently used to evaluate IR, its sensitivity can be influenced by age and sex. METS-IR has emerged as a promising alternative that may better reflect IR and predict cardiovascular disease risk in obese populations (6). In our population, although a statistically significant correlation was found between HOMA-IR and METS-IR in all age groups, this significance was not at levels that would be interpreted as a strong association. Nevertheless, the correlation coefficients not being high enough to completely overlap suggests that these two indices capture partially different dimensions of IR. Indeed, studies in different populations have shown that while METS-IR correlates moderately to highly with HOMA-IR, it often outperforms HOMA-IR in predicting long-term IR–related outcomes (16–18).

Hence, our study contributes by showing that, in a large cohort consisting of obese individuals and stratified by the age factor, this relationship remained relatively stable by age, albeit that the slope became clearly flatter in the most advanced age group. This suggests that while the HOMA-IR signal may weaken with age due to altered insulin secretion dynamics and body composition, METS-IR may provide more consistent information regarding metabolic stress via glucose and triglyceride levels. The concurrent rise in HOMA-IR and METS-IR with increasing comorbidities reflects the expected characteristics of increasing cardiometabolic burden together with IR in obese individuals. However, a 1-SD increase in the HOMA-IR z-score did not significantly increase the probability of a higher comorbidity count. In contrast, a 1-SD increase in the METS-IR z-score increased the likelihood of a higher comorbidity burden approximately 1.8-fold. The existing difference suggests that METS-IR behaves as a stronger risk marker in practice.

Recent studies have shown that METS-IR is associated with components of metabolic syndrome and target organ damage and, in some studies, has even been associated with subclinical atherosclerosis and clinical cardiovascular events (16,19–21). In fact, some researchers have concluded that the HOMA-IR score is a predictive factor for middle-aged and older populations (22). Others have reported that METS-IR predicts the development of HT, T2DM, and cardiovascular disease in populations with heterogeneous BMI distributions (16,23,24). Most of these studies were conducted in the general population or across mixed BMI groups. Our findings corroborate this literature within a cohort consisting only of obese individuals and using an easily measurable endpoint (e.g., number of comorbidities). The closer association between METS-IR and multiple comorbidities suggests that this index could be used in clinical practice as a dynamic risk score reflecting cumulative cardiometabolic burden and multimorbidity in obese patients.

The fact that the AUC of HOMA-IR and METS-IR for T2DM or HT were very close to 0.5 indicates that neither index is sufficient as a threshold-based diagnostic tool in obese individuals. These modest AUCs do not contradict the multivariable associations observed in our models, as association and discrimination quantify different statistical properties. In an obesity-only cohort, the restricted case-mix leads to overlapping

Copyright© AE&M all rights reserved.

score distributions between participants with and without T2DM or HT, limiting separability. Baseline cardiometabolic risk is uniformly high across the cohort, and a ceiling effect may further reduce discrimination. In addition, because outcomes were defined by cross-sectional diagnostic status, prior detection and treatment may have blurred intergroup differences. In contrast, some researchers who considered these outcomes to be clinically meaningful discrimination typically evaluated incident T2DM, HT, or cardiovascular events over long-term follow-up (9,18). Consequently, our results indicate that HOMA-IR and METS-IR cannot independently establish diagnostic thresholds for T2DM or HT in obese individuals. Instead, METS-IR is more appropriately interpreted as a chronic risk score reflecting the accumulation of comorbidities and cardiometabolic burden in obesity.

A study series consisting of adolescent obese individuals showed that the correlation of METS-IR with metabolic syndrome components and its strength in identifying IR persist across different ethnic and age groups (25–27). These findings suggest that METS-IR provides a signal of energy surplus that includes not only glycemic control but also impairments along the triglyceride and HDL cholesterol axes. In our study, the strong association between comorbidity count and METS-IR indicates that this risk signal translates into clinical disease burden in obese adults. Nonetheless, because our endpoint was the number of comorbidities and specific organ outcomes (e.g., chronic kidney disease or incident cardiovascular events) were not evaluated separately. Therefore, rather than directly comparing our diagnostic thresholds with previous studies, we emphasize that our findings provide a complementary perspective on cumulative risk.

Our study contributes to this discussion in two respects in that METS-IR shows a strong association with comorbidity burden in obese adults despite providing limited diagnostic performance for T2DM and HT. First, it demonstrates that even the best-performing indices may rapidly lose diagnostic discriminative ability in samples characterized by high baseline risk and phenotypic homogeneity. Second, it suggests that interpreting METS-IR within the family of non-insulin-based indices as a "general cardiometabolic burden score" may be a more realistic positioning than establishing a diagnosis of a single disease. Similarly, research in obese pediatric populations has shown that puberty-specific physiological IR necessitates age-specific HOMA-IR cut-off values (28). Although this study pertains to a pediatric population, the idea of the need for age-specific IR thresholds provides a relevant conceptual framework for evaluating HOMA-IR and METS-IR in obese adults. Our findings suggest a similar phenomenon emerges in older obese adults. We found that HOMA-IR decreased slightly with age, whereas METS-IR remained more stable and maintained its association with comorbidity burden. This suggests that using a single HOMA-IR or METS-IR cut-off value across all adult age groups is not clinically realistic in obese populations. Indeed, the literature indicates that age-adjusted thresholds or age-standardized scores yield more consistent results in this context (22,29,30).

Our findings may be interpreted as observational evidence supporting future studies aimed at determining age-specific IR thresholds, particularly given the context of sarcopenic obesity and changing body composition that may occur at older ages. Several key messages stand out regarding the clinical translation of our findings. First, even when HOMA-IR and METS-IR are elevated in obese individuals, using these scores in isolation to screen for T2DM or HT via fixed thresholds is not supported by our data. Second, the association between METS-IR and comorbidity burden suggests that integrating this score with BMI and routine biochemical parameters as a continuous risk indicator is clinically useful. Third, as age advances, caution is required particularly in interpreting HOMA-IR, and age-sensitive thresholds and long-term follow-up must be considered.

Despite this study's findings, several limitations should be addressed. First, the single-center, retrospective, cross-sectional design limits causal inference and increases the likelihood that unmeasured clinical factors may have influenced the observed associations. Second, because the cohort consisted exclusively of obese adults evaluated in an outpatient clinic, the findings should be generalized cautiously and should not be directly extrapolated to non-obese

Copyright© ACE&M all rights reserved.

populations, community-based screening cohorts, insulin-treated patients, or populations with substantially different demographic and metabolic profiles. Third, comorbidity burden was assessed using a count-based composite measure rather than organ-specific clinical outcomes, providing a practical but relatively coarse representation of disease burden. Fourth, the diagnostic analyses relied on cross-sectional disease status; prior diagnoses, treatments, and overlapping score distributions likely attenuated discrimination. Therefore, although our data support METS-IR as an adjunctive indicator of cardiometabolic burden in obese adults, they do not support its standalone use for threshold-based diagnosis. The external validity of these findings requires confirmation in prospective, multicenter cohorts with broader case-mix diversity. Despite these limitations, the study strengths include the concurrent evaluation of HOMA-IR and METS-IR within a single obese cohort spanning a broad adult age range, and the assessment of comorbidity burden using ordinal models that explicitly consider age interactions.

In conclusion, METS-IR demonstrated a stronger association with comorbidity burden than HOMA-IR in obese adults and remained more stable across age groups. METS-IR is a non-insulin-based continuous index derived from routinely available anthropometric and fasting laboratory measures. However, both METS-IR and HOMA-IR provided only limited discriminatory ability for T2DM and HT. Therefore, these indices should not be used as standalone diagnostic tools or isolated guides for treatment decision-making. Rather, their clinical role is more appropriate as adjunctive, continuous indicators of cardiometabolic burden when interpreted alongside age, phenotype, and other clinical and biochemical variables. Relying on these scores in isolation may be misleading in certain patient groups, as overlapping score distributions can reduce sensitivity and contribute to the under-recognition of clinically relevant disease. Given the single-center, retrospective, cross-sectional design and the restriction to obese outpatients, the broader applicability of these findings must be established in prospective, multicenter cohorts encompassing more diverse age groups and clinical profiles.

Authors' contributions: conceptualization: EST and MT; methodology: MT and EST; software: MT and MFU; validation: EST and MT; formal analysis: MT; research: EST and MFU; resources: EST and GA; data collection: MT and MFU; writing-original drafting: MT; writing-review and editing: EST, GA and HA; visualization: MT, GA and HA; supervision: EST, MFU and HA; project management: MT; funding: EST, GA. All authors have read and agree to the published version of the article.

Acknowledgments: when preparing this article, the authors utilized artificial intelligence to improve the writing fluency and grammatical structure of the text. The authors reviewed and edited the output and are fully responsible for the content of this publication.

Funding: this research has not received any external funding.

Ethical approval: this study was conducted in accordance with the principles of the Declaration of Helsinki (1964 and the 2013 revisions). The research protocol was approved by the Clinical Research Ethics Committee of Elazig Fethi Sekin City Hospital (date: 12/06/2025 and decision no: 2025/11-14).

Informed consent: since the data were based on retrospective chart review and anonymized, informed consent was not required.

Disclosure: no potential conflict of interest relevant to this article was reported.

Data availability: datasets related to this article will be available upon request to the corresponding author.

REFERENCES

1. Fahed G, Aoun L, Bou Zerdan M, Allam S, Bou Zerdan M, Bouferraa Y, Assi HI. Metabolic Syndrome: Updates on Pathophysiology and Management in 2021. Int J Mol Sci. 2022 Jan 12;23(2):786. doi: 10.3390/ijms23020786.
2. Horáková D, Štěpánek L, Štěpánek L, Pastucha D, Janoutová J, Janout V, et al. What are the real associations of homeostasis model assessment (HOMA) with body mass index and age? Endokrynol Pol. 2022;73(4):736-742. doi: 10.5603/EP.a2022.0031.
3. Muniyappa R, Lee S, Chen H, Quon MJ. Current approaches for assessing insulin sensitivity and resistance in vivo: advantages, limitations, and appropriate usage. Am J Physiol Endocrinol Metab. 2008 Jan;294(1):E15-26. doi: 10.1152/ajpendo.00645.2007.
4. Gayoso-Diz P, Otero-González A, Rodriguez-Alvarez MX, Gude F, García F, De Francisco A, et al. Insulin resistance (HOMA-IR) cut-off values and the metabolic syndrome in a general adult population: effect of gender and age: EPIRCE cross-sectional study. BMC Endocr Disord. 2013 Oct 16;13:47. doi: 10.1186/1472-6823-13-47.
5. Bello-Chavolla OY, Almeda-Valdes P, Gomez-Velasco D, Viveros-Ruiz T, Cruz-Bautista I, Romo-Romo A, et al. METS-IR, a novel score to evaluate insulin sensitivity, is predictive of visceral adiposity and incident type 2 diabetes. Eur J Endocrinol. 2018 May;178(5):533-544. doi: 10.1530/EJE-17-0883.
6. Qian T, Sheng X, Shen P, Fang Y, Deng Y, Zou G. Mets-IR as a predictor of cardiovascular events in the middle-aged and elderly population and mediator role of blood lipids. Front Endocrinol (Lausanne). 2023 Jul 17;14:1224967. doi: 10.3389/fendo.2023.1224967. PMID: 37534205; PMCID: PMC10393118.
7. Yang H, Gong R, Liu M, Deng Y, Zheng X, Hu T. HOMA-IR is positively correlated with biological age and advanced aging in the US adult population. Eur J Med Res. 2023 Oct 28;28(1):470. doi: 10.1186/s40001-023-01448-1.

Copyright© AE&M all rights reserved.

8. Duan M, Zhao X, Li S, Miao G, Bai L, Zhang Q, Yang W, Zhao X. Metabolic score for insulin resistance (METS-IR) predicts all-cause and cardiovascular mortality in the general population: evidence from NHANES 2001-2018. Cardiovasc Diabetol. 2024 Jul 10;23(1):243. doi: 10.1186/s12933-024-02334-8.
9. Matthews DR, Hosker JP, Rudenski AS, Naylor BA, Treacher DF, Turner RC. Homeostasis model assessment: insulin resistance and beta-cell function from fasting plasma glucose and insulin concentrations in man. Diabetologia. 1985 Jul;28(7):412-9. doi: 10.1007/BF00280883.
10. Blüher M. Metabolically Healthy Obesity. Endocr Rev. 2020 May 1;41(3):bnaa004. doi: 10.1210/endrev/bnaa004.
11. Han KY, Gu J, Wang Z, Liu J, Zou S, Yang CX, Liu D, Xu Y. Association Between METS-IR and Prehypertension or Hypertension Among Normoglycemia Subjects in Japan: A Retrospective Study. Front Endocrinol (Lausanne). 2022 Mar 18;13:851338. doi: 10.3389/fendo.2022.851338.
12. Yoon J, Jung D, Lee Y, Park B. The Metabolic Score for Insulin Resistance (METS-IR) as a Predictor of Incident Ischemic Heart Disease: A Longitudinal Study among Korean without Diabetes. J Pers Med. 2021 Jul 28;11(8):742. doi: 10.3390/jpm11080742.
13. Eckel N, Li Y, Kuxhaus O, Stefan N, Hu FB, Schulze MB. Transition from metabolic healthy to unhealthy phenotypes and association with cardiovascular disease risk across BMI categories in 90 257 women (the Nurses' Health Study): 30 year follow-up from a prospective cohort study. Lancet Diabetes Endocrinol. 2018 Sep;6(9):714-724. doi: 10.1016/S2213-8587(18)30137-2.
14. Bell JA, Hamer M, Sabia S, Singh-Manoux A, Batty GD, Kivimaki M. The natural course of healthy obesity over 20 years. J Am Coll Cardiol. 2015 Jan 6;65(1):101-102. doi: 10.1016/j.jacc.2014.09.077.
15. Goossens GH. The Metabolic Phenotype in Obesity: Fat Mass, Body Fat Distribution, and Adipose Tissue Function. Obes Facts. 2017;10(3):207-215. doi: 10.1159/000471488.
16. Liu XZ, Fan J, Pan SJ. METS-IR, a novel simple insulin resistance indexes, is associated with hypertension in normal-weight Chinese adults. J Clin Hypertens (Greenwich). 2019 Aug;21(8):1075-1081. doi: 10.1111/jch.13591.
17. Cai XT, Zhu Q, Liu SS, Wang MR, Wu T, Hong J, Hu JL, Li N. Associations Between the Metabolic Score for Insulin Resistance Index and the Risk of Type 2 Diabetes Mellitus Among Non-Obese Adults: Insights from a Population-Based Cohort Study. Int J Gen Med. 2021 Nov 6;14:7729-7740. doi: 10.2147/IJGM.S336990.
18. Peng H, Xiang J, Pan L, Zhao M, Chen B, Huang S, Yao Z, Liu J, Lv W. METS-IR/HOMA-IR and MAFLD in U.S. adults: dose-response correlation and the effect mediated by physical activity. BMC Endocr Disord. 2024 Aug 1;24(1):132. doi: 10.1186/s12902-024-01646-w.
19. Mena LJ, Felix VG, Melgarejo JD, Maestre GE. 24-Hour Blood Pressure Variability Assessed by Average Real Variability: A Systematic Review and Meta-Analysis. J Am Heart Assoc. 2017 Oct 19;6(10):e006895. doi: 10.1161/JAHA.117.006895.
20. Tamehri Zadeh SS, Cheraghloo N, Masrouri S, Esmaeili F, Azizi F, Hadaegh F. Association between metabolic score for insulin resistance and clinical outcomes: insights from the Tehran lipid and glucose study. Nutr Metab (Lond). 2024 Jun 12;21(1):34. doi: 10.1186/s12986-024-00808-w.
21. Wang Z, Li W, Li J, Liu N. The Nonlinear Correlation Between a Novel Metabolic Score for Insulin Resistance and Subclinical Myocardial Injury in the General Population. Front Endocrinol (Lausanne). 2022 May 24;13:889379. doi: 10.3389/fendo.2022.889379.
22. Cheng H, Jia Z, Li YT, Yu X, Wang JJ, Xie YJ, et al. Metabolic Score for Insulin Resistance and New-Onset Type 2 Diabetes in a Middle-Aged and Older Adult Population: Nationwide Prospective Cohort Study and Implications for Primary Care. JMIR Public Health Surveill. 2024 Jun 3;10:e49617. doi: 10.2196/49617.
23. Yabe D, Seino Y, Fukushima M, Seino S. β cell dysfunction versus insulin resistance in the pathogenesis of type 2 diabetes in East Asians. Curr Diab Rep. 2015 Jun;15(6):602. doi: 10.1007/s11892-015-0602-9.
24. Li Y, You A, Tomlinson B, Yue L, Zhao K, Fan H, Zheng L. Insulin resistance surrogates predict hypertension plus hyperuricemia. J Diabetes Investig. 2021 Nov;12(11):2046-2053. doi: 10.1111/jdi.13573.
25. Song K, Lee E, Lee HS, Lee H, Lee JW, Chae HW, Kwon YJ. Comparison of SPISE and METS-IR and Other Markers to Predict Insulin Resistance and Elevated Liver Transaminases in Children and Adolescents. Diabetes Metab J. 2025 Mar;49(2):264-274. doi: 10.4093/dmj.2024.0302.
26. Widjaja NA, Irawan R, Hanindita MH, Ugrasena I, Handajani R. METS-IR vs. HOMA-AD and Metabolic Syndrome in Obese Adolescents. J Med Invest. 2023;70(1.2):7-16. doi: 10.2152/jmi.70.7.
27. Yoon J, Heo SJ, Lee JH, Kwon YJ, Lee JE. Comparison of METS-IR and HOMA-IR for predicting new-onset CKD in middle-aged and older adults. Diabetol Metab Syndr. 2023 Nov 14;15(1):230. doi: 10.1186/s13098-023-01214-7.
28. Kurtoğlu S, Hatipoğlu N, Mazıcıoğlu M, Kendirici M, Keskin M, Kondolot M. Insulin resistance in obese children and adolescents: HOMA-IR cut-off levels in the prepubertal and pubertal periods. J Clin Res Pediatr Endocrinol. 2010;2(3):100-6. doi: 10.4274/jcrpe.v2i3.100.
29. Oguoma VM, Abu-Farha M, Coffee NT, Alsharrah S, Al-Refaei FH, Abubaker J, et al. Metabolically Healthy and Unhealthy Obese Phenotypes among Arabs and South Asians: Prevalence and Relationship with Cardiometabolic Indicators. Nutrients. 2022 Feb 22;14(5):915. doi: 10.3390/nu14050915.
30. Stein R, Koutny F, Riedel J, Dörr N, Meyer K, Colombo M, et al. Single Point Insulin Sensitivity Estimator (SPISE) As a Prognostic Marker for Emerging Dysglycemia in Children with Overweight or Obesity. Metabolites. 2023 Jan 7;13(1):100. doi: 10.3390/metabo13010100.

Copyright© AE&M all rights reserved.

Archives of Endocrinology and Metabolism
ISSN 2359-4292
OFFICIAL JOURNAL OF THE BRAZILIAN SOCIETY OF ENDOCRINOLOGY AND METABOLISM

original

Associations between peripheral blood whole-genome DNA methylation and obesity in young Chinese males

Meidan Nong[1]
https://orcid.org/0009-0002-4044-2930

Haiou Lu[1]
https://orcid.org/0009-0008-5009-2675

Maolin Zhao[1]
https://orcid.org/0009-0002-0716-5177

Lihong Xiao[1]
https://orcid.org/0009-0004-4973-9719

[1] General Medicine Department, Liuzhou People's Hospital, Liuzhou City, Guangxi Zhuang Autonomous Region, China

ABSTRACT

Objective: To explore the associations between peripheral blood whole-genome DNA methylation and obesity in young Chinese males. **Subjects and methods:** Four young Chinese males aged 18–25 years with obesity (body mass index [BMI] ≥ 30 kg/m²) from Liuzhou Peoples Hospital Health Management Center and 3 age-matched healthy controls with average weights were included. Methylation sequencing was conducted using whole-blood DNA extraction and an Illumina 850K methylation chip, followed by gene functional annotation, pathway enrichment analysis, and differential analysis using bioinformatics tools. **Results:** Methyl-Target technology was utilized for the methylation sequencing of 35 patients with obesity and 34 healthy controls, revealing 15 differential sites, two differential regions, and three differential genes. The differential regions included cg08667244 (site region 1stExon) and cg13928759 (site region TSS200, $p < 0.05$), with the differential genes being cg08667244 (corresponding to iodothyronine deiodinase 3, DIO3), cg13928759 (corresponding to leucine-rich glioma inactivated 1, LGI1), and cg18770216 (corresponding to integrin beta 5, ITGB5, $p < 0.05$). Further analysis revealed a negative correlation between cg13928759 methylation (*LGI1* gene) and body mass index ($R = -0.25$; $P = 0.04$). **Conclusion:** This study revealed 15 differential sites, two differential regions, and three differential genes between young individuals with obesity and healthy controls, among which cg13928759 methylation (LGI1 gene) was negatively correlated with body mass index. These findings suggest that DNA methylation may contribute to obesity development, with LGI1 methylation serving as a potential biomarker.

Keywords: Obesity; methylation; methyltarget technology; *LGI1* gene; body mass index

INTRODUCTION

Obesity among young males is a growing global concern, with a steady increase in cases occurring in recent years (1). World Health Organization (WHO) reports that more than 400 million people worldwide are battling obesity, and a significant number of them are young males. This condition involves more than carrying extra weight (2). It is linked to serious health issues, such as heart disease and diabetes, and significantly affects individuals' quality of life and health (3). However, our understanding of what causes obesity in young males, especially from an epigenetic perspective, remains limited (4). Epigenetics, particularly DNA methylation, plays a crucial role in controlling the expression of metabolism-related genes, including those involved in fat synthesis, energy use, and hormone levels, all of which are vital for managing weight and energy balance (5,6). Addressing obesity in young males requires a deeper understanding of how methylation affects gene expression and obesity (7). Exploring this relationship could unlock new ways to manage or even prevent obesity, not just in young males but potentially in wider populations (8). Simplifying complex scientific concepts and focusing on actionable insights can make discussions of obesity management more engaging and practical for a broader audience, thereby encouraging positive lifestyle changes and greater awareness of this global health challenge.

Received on Dec/10/2024
Accepted on Feb/13/2026

DOI: 10.20945/2359-4292-2026-0060

Correspondence to:
Lihong Xiao
8 Wenchang Road, Liuzhou City,
Guangxi Zhuang Autonomous Region, 545006, China
nongmeidan2009@126.com

Associated editor:
Marcio C. Mancini
https://orcid.org/0000-0003-1278-0406

This is an open-access article distributed under the terms of the Creative Commons Attribution License

Copyright© AE&M all rights reserved.

Currently, interventions for obesity mainly include dietary control, exercise, and drug therapy. However, these interventions have limitations in practical applications, such as limited long-term effectiveness and treatment tolerance; thus, further research and exploration are needed (9-11). This study aimed to address two fundamental questions: (1) What genome-wide DNA methylation signatures distinguish young males with obesity from lean young males in a Chinese population? (2) How do these epigenetic modifications correlate with clinical obesity indicators, such as body mass index (BMI)? The aim of this study was to identify differentially methylated regions (DMRs) in the promoter and gene body regions of metabolism-related genes using MethylTarget sequencing. We focused on CpG sites within the TSS200, 1stExon, and 5'UTR regions to explore their associations with BMI and obesity-related metabolic traits in young males. Additionally, this study extensively employed bioinformatics tools to analyze methylation data to identify core methylation genes and pathways related to obesity, thereby offering new insights and strategies for preventing and treating obesity in the future.

SUBJECTS AND MATERIALS

This cross-sectional study was approved by the Ethics Committee of Liuzhou People's Hospital (KY2021-019-01). Participants provided written informed consent to participate in this study.

Inclusion and exclusion criteria

The subjects in the obesity group included in this study were Chinese men aged 18–25 years who met the diagnostic criteria for simple obesity of the WHO (BMI ≥ 30 kg/m², excluding secondary factors such as endocrine disorders and genetic syndromes) and had no history of chronic metabolic diseases, such as diabetes, hypertension, or dyslipidemia. These subjects had not used any drugs that affect weight or metabolism in the past six months. Chinese men with an age difference of no more than 2 years and a BMI within the normal range (18.5–24.9 kg/m²) were included in the control group; a family history of obesity among their immediate family members was not required. The common exclusion criteria for the two groups included the presence of acute or chronic inflammatory diseases (such as autoimmune diseases or a recent history of infection); previous bariatric surgery or bariatric intervention; the use of drugs that affect DNA methylation, such as glucocorticoids or antipsychotic drugs; smoking more than 5 cigarettes per week or an alcohol intake > 140 grams; and participation in other clinical trials within the past 3 months.

Whole-blood genomic methylation sequencing method

DNA was extracted from whole-blood samples of each participant using commercial extraction kits (such as Qiagen or Omega Biotek), followed by quality and concentration testing to ensure the integrity and purity of the DNA. DNA libraries were prepared for methylation sequencing, and high-throughput sequencing of methylation sites was performed using Illumina 850K methylation chips to ensure coverage of methylation information across the entire genome. Methylation sequencing data were aligned, and methylation sites were identified using software such as Bismark or Bowtie, while low-quality sequences and polymerase chain reaction (PCR) duplicates were filtered out. Standardized beta values were subjected to singular value decomposition (SVD) to assess the correlation strength between each component and the factors in the data. These results reflected the existence of batch effects to some extent. If batch effects were found, batch effect correction was performed. The methylation result files for all samples were converted to bedGraph format files to visualize specific sites or regions of interest using Integrative Genomics Viewer (IGV) software (http://www.broadinstitute.org/igv/home).

Whole-genome methylation differential analysis

The Chip Analysis Methylation Pipeline (ChAMP) package was employed for differential methylation analysis using statistical tests such as the T test and Wilcoxon rank sum test. Multiple comparison corrections ensured the significance of the differential methylation sites.

Copyright© ACE&M all rights reserved.

Analysis of obesity-related methylation sites/regions

MethylTarget technology was used for targeted methylation site sequencing and to quantify methylation level differences. Correlation analysis revealed associations between differential methylation sites/regions and BMI.

Gene functional annotation and pathway enrichment analysis

The methylation data were processed for gene functional annotation using Bioconductor's methyl Kit and ChAMP packages. This processing included the localization of methylation sites on the genome and correlation analysis with gene function. Methylation site functions in the genome were evaluated on the basis of location information, such as whether the sites were located in promoter regions, gene bodies, 3'UTRs, or 5'UTRs. Further analysis was conducted to determine the enrichment of differential methylation sites in biological functions and pathways using tools such as Database for Annotation, Visualization and Integrated Discovery (DAVID) and Metascape, which included Gene Ontology (GO) and Kyoto Encyclopedia of Genes and Genomes (KEGG) pathway enrichment analysis. To determine the differential methylation sites related to obesity, the biological significance of the enriched pathways was analyzed, including whether they were involved in lipid metabolism, insulin secretion, and other obesity-related processes.

Data analysis

All statistical analyses were performed using R version 4.3.2 (R Foundation for Statistical Computing). Differential methylation analysis was conducted through a two-stage approach: 1) genome-wide screening using linear regression models adjusted for age and batch effects (limma package), and 2) targeted validation using paired T tests for confirmed CpG sites. The significance threshold was set at $p < 0.05$ for the initial discovery phase analyses, with false discovery rate (FDR) correction (Benjamini–Hochberg method) applied for multiple comparisons (an FDR < 0.15 was considered suggestive, and an FDR < 0.05 was deemed significant). Effect sizes were calculated using Cohen's d for differences in methylation beta values ($|d| > 0.5$ was considered a moderate effect). For correlation analyses between methylation levels and BMI, Pearson's correlation coefficients (for normally distributed data, Shapiro-Wilk test $p > 0.05$) or Spearman's rank correlation (for non-normally distributed data) were employed. Power analysis indicated 80% power to detect methylation differences with an effect size of $\Delta\beta = 0.2$ at $\alpha = 0.05$ (two-tailed) given our sample size (G*Power 3.1.9.7).

RESULTS

Analysis of sample size and basic characteristics of the population

Table 1 summarizes the baseline characteristics of the discovery cohort (4 patients with obesity vs. 3 controls). Compared with the control group, the obesity group had significantly greater BMI (40.1 ± 1.7 vs. 21.8 ± 1.4 kg/m², $p = 0.00$) and body weight (118.2 ± 14.0 vs. 64.6 ± 6.2 kg, $p = 0.01$), while no differences were observed in age (18.5 ± 1.0 vs. 18.3 ± 0.6 years, $p = 0.79$) or height (171.5 ± 11.4 vs. 172.3 ± 10.8 cm, $p = 0.93$). These findings were validated in the larger cohort (Table 2: 35 patients with obesity vs. 34 controls), where the obesity group again had elevated BMI (34.2 ± 2.1 vs. 20.5 ± 1.5 kg/m², $p < 0.001$) and weight (102.0 ± 11.2 vs. 58.3 ± 6.0 kg, $p < 0.001$), with comparable age (18.6 ± 0.7 vs. 18.4 ± 0.7 years, $p = 0.27$) and height (172.8 ± 7.3 vs. 168.4 ± 6.6 cm, $p = 0.01$). Both cohorts demonstrated robust anthropometric matching, minimizing confounding effects in subsequent methylation analyses. Data are presented as the mean ± SD; p values are derived from Student's T test ($p < 0.05$). Gene functional annotation and KEGG pathway enrichment analysis were conducted using R to select core methylation genes and sites related to obesity. Thirty-five young male patients with obesity and 34 age-matched healthy males with average weights were selected, and whole-blood DNA was extracted for targeted region methylation sequencing and methylation level detection. The two groups differed significantly in terms of the leading observational indicators, namely, BMI, weight, and height, while individuals with hypertension, diabetes, cardiovascular diseases, severe liver or kidney dysfunction, and chronic diseases were excluded. No significant differences were observed in the other data (Table 2).

Copyright© AE&M all rights reserved.

Table 1. Baseline characteristics of the discovery cohort (4 patients with obesity vs. 3 controls)

Age (years)		Height (cm)		Weight (kg)		BMI (kg/m²)		
Normal	Obesity	Normal	Obesity	Normal	Obesity	Normal	Obesity	
N (3)	N (4)	N (3)	N (4)	N (3)	N (4)	N (3)	N (4)	
18-25	18-25	172.33	171.50	64.57	118.15	21.76	40.11	Average
0.577	1.000	10.786	11.382	6.192	13.956	1.367	1.668	SD

Table 2. Baseline characteristics of the larger cohort (35 patients with obesity vs. 34 controls)

Age (years)		Height (cm)		Weight (kg)		BMI (kg/m²)		
Normal	Obesity	Normal	Obesity	Normal	Obesity	Normal	Obesity	
N (34)	N (35)	N (34)	N (35)	N (34)	N (35)	N (34)	N (35)	
18-25	18-25	168.38	172.76	58.27	102.02	20.53	34.20	Average
0.657	0.736	6.629	7.272	6.004	11.204	1.451	2.066	SD

Whole-genome methylation differential analysis

For the obesity group, comprising four cases, and the healthy group, comprising three cases, whole-blood DNA 850K methylation sequencing was performed, and 734,163 methylation sites were detected per sample. Using the ChAMP package in R, differential methylation analysis was conducted on the methylation sites between the obesity and healthy groups. The differential methylation results are displayed as a heatmap, which shows the expression patterns of the genes containing differentially methylated sites in the grouped samples (**Figure 1A**). The entire genome methylation sequence regions analyzed included the genome-wide region, promoter, intergenic region, gene body, 3'UTR, and 5'UTR (**Figure 1B**), with 23 differentially methylated regions identified. Differentially methylated sites or regions were mapped to the genome, and the differentially methylated genes were further analyzed (**Figure 1C**, **D**; $p < 0.05$).

Enrichment analysis of whole-genome methylation sites/region-associated genes

During the GO functional analysis, 309 biological processes (BPs), 99 cellular components (CCs), and 50 molecular functions (MFs) had corrected $P < 0.05$ among the differential methylation sites and regions. The top 10 functions of these sites are oligosaccharide binding, ligand-gated calcium channel activity, G-protein-coupled receptor binding, calcium release channel activity, phosphatidylinositol-4,5-bisphosphate binding, phosphatidylinositol bisphosphate binding, and protein binding, which play crucial roles in regulating obesity metabolism pathways. The focus of methylation binding regions is on regulating enzyme activity, carbon-nitrogen bond formation, protein serine/threonine/tyrosine kinase activity, intramolecular oxidoreductase activity, peptide antigen binding, epidermal growth factor receptor binding, fibroblast growth factor binding, cellular metabolic complex salvage, and cellular modified amino acid metabolism processes. These functions, along with pathway enrichment analyses, including cysteine and methionine metabolism, cortisol synthesis and secretion, parathyroid hormone synthesis and action, Rap1 signaling, aldosterone synthesis and secretion, and sphingolipid signaling pathways, among others, contributed to the enrichment of multiple lipid metabolism regulation and obesity-related signaling pathways. We identified thirty KEGG pathways and GenBank pathways associated with obesity on the basis of the enrichment results. Furthermore, we selected thirty-five obesity-related methylation sites and their associated genes (**Table 3**).

Copyright© AE&M all rights reserved.

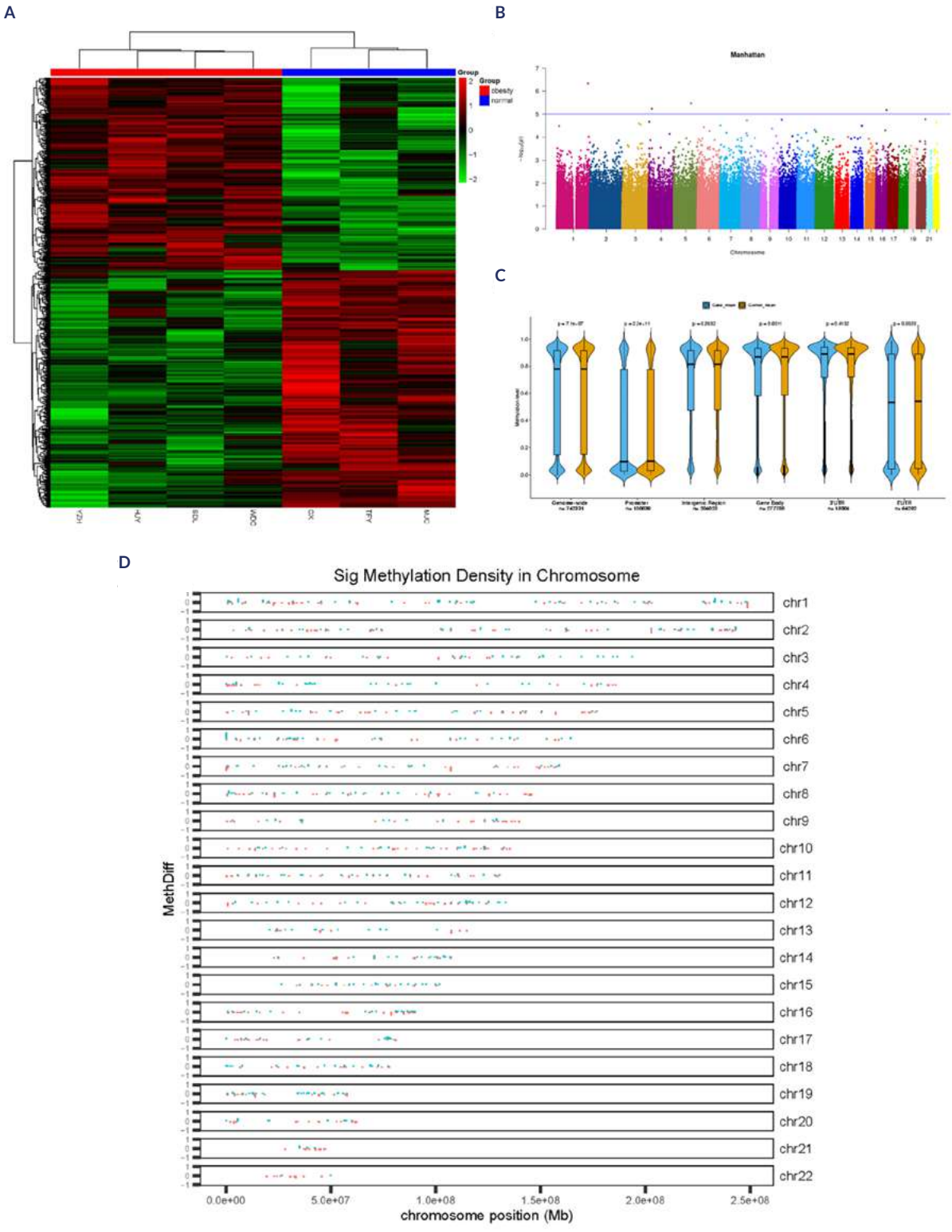


Figure 1. Genome-wide methylation profiling of obesity-associated CpG sites. (**A**) Hierarchical clustering of 7 samples (4 individuals with obesity: O1–O4; 3 controls: C1–C3) based on methylation levels at 23 differentially methylated CpG sites ($\Delta\beta > 0.2$, $p < 0.05$). Clustering was performed using the Pearson correlation distance with complete linkage. The heatmap colors represent beta values: hypomethylated (blue, $\beta < 0.3$), intermediately methylated (white, $0.3 \leq \beta \leq 0.7$), and hypermethylated (red, $\beta > 0.7$). Columns are annotated with group labels (obesity vs. control). (**B**) Distribution of methylation regions across genomic features (promoter, gene body, 3'UTR, 5'UTR, and intergenic regions). (**C**, **D**) IGV visualization of two significant differentially methylated regions (cg08667244 in DIO3 and cg13928759 in LGI1) mapped to their respective genomic loci.

Copyright© AE&M all rights reserved.

Table 3. GO and KEGG enrichment analysis of obesity-related methylation sites

CpG	CHR	Gene	Group	GO-BP	GO-MF	GO-CC	KEGG	FoldChange	P.Value
cg05872034	1	NPHP4	Body	GO:0098609,cell-cell adhesion	GO:0005515,protein binding	GO:0005813,centrosome		2.24	0.03
cg00371383	1	FMN2	Body	GO:0015031,protein transport	GO:0003779,actin binding	GO:0030659,cytoplasmic vesicle membrane	hsa04320 Dorso-ventral axis formation	1.23	0.00
cg21379113	1	AKT3	Body	GO:0006468,protein phosphorylation	GO:0004674,protein serine	GO:0016020,membrane	hsa05222 Small cell lung cancer	0.73	0.05
cg09858955	2	VRK2	5'UTR	GO:0006468,protein phosphorylation	GO:0004674,protein serine	GO:0005737,cytoplasm		1.30	0.00
cg11765003	2	NHEJ1	5'UTR	GO:0006310,DNA recombination	GO:0005515,protein binding	GO:0005634,nucleus	hsa03450 Non-homologous end-joining	1.27	0.01
cg16658156	2	HTR2B	5'UTR	GO:0006182,cGMP biosynthetic process	GO:0005096,GTPase activator activity	GO:0030054,cell junction	hsa04020 Calcium signaling pathway	1.28	0.04
cg05171197	2	HDAC4	Body	GO:0006954,inflammatory response	GO:0005515,protein binding	GO:0043234,protein complex	hsa04371 Apelin signaling pathway	1.16	0.00
cg25117092	3	MED12L	Body	GO:0006351,transcription, DNA-templated|	GO:0008013,beta-catenin binding	GO:0016592,mediator complex	hsa04919 Thyroid hormone signaling pathway	1.37	0.00
cg03199564	4	CYTL1	1stExon	GO:0007165,signal transduction	GO:0005102,receptor binding	GO:0005615,extracellular space		0.43	0.00
cg18770216	3	ITGB5	Body	GO:0007160,cell-matrix adhesion|	GO:0005515,protein binding	GO:0009986,cell surface	hsa04145 Phagosome	0.7	0.03
cg05688588	4	PI4K2B	Body	GO:0007032,endosome organization	GO:0005524,ATP binding	GO:0005768,endosome	hsa01100 Metabolic	2.15	0.002
cg20701305	4	STIM2	Body	cellular calcium ion homeostasis	|GO:0005515,protein binding	GO:0005783,endoplasmic reticulum	hsa04020 Calcium signaling pathway	1.62	#####
cg16006841	5	RGS14	Body	GO:0000278,mitotic cell cycle	GO:0005515,protein binding	GO:0030054,cell junction	hsa04015 Rap1 signaling pathway	1.63	0.04
cg22996185	6	SYNE1	Body	GO:0007030,Golgi organization	GO:0005515,protein binding	GO:0005794,Golgi apparatus		3.52	0.01
cg05977964	7	ADAP1	TSS200	GO:0007166,cell surface receptor signaling pathway	GO:0005515,protein binding	GO:0005737,cytoplasm		0.79	0.01
cg10020767	7	CREB5	Body	GO:0006366,transcription from RNA polymerase II promoter	GO:0005515,protein binding	GO:0005634,nucleus	hsa04152 AMPK signaling pathway	1.20	0.01
cg04790662	8	PAG1	5'UTR	GO:0007165,signal transduction	GO:0005515,protein binding	GO:0005886,plasma membrane		2.64	0.01
cg22137815	8	SDC2	Body	GO:0044267,cellular protein metabolic process	GO:0005515,protein binding	GO:0005788,endoplasmic reticulum lumen	hsa05418 Fluid shear stress and atherosclerosis	1.53	0.03

Copyright© AE&M all rights reserved.

CpG	CHR	Gene	Group	GO-BP	GO-MF	GO-CC	KEGG	FoldChange	P.Value
cg01284841	10	CDH23	Body	GO:0006816,calcium ion transport	GO:0005515,protein binding	GO:0005886,plasma membrane		1.25	2E-04
cg13928759	10	LGI1	TSS200	GO:0008283,cell proliferation	GO:0005515,protein binding	GO:0030054,cell junction		1.21	#####
cg11430259	10	FGFR2	5'UTR	GO:0043410,positive regulation of MAPK cascade	GO:0005515,protein binding	GO:0005794,Golgi apparatus	hsa04010 MAPK signaling pathway	1.45	0.04
cg17820828	11	KCNQ1	Body	GO:0071805,potassium ion transmembrane transport	GO:0005515,protein binding	GO:0005783,endoplasmic reticulum	hsa04974 Protein digestion and absorption	0.70	#####
cg18427217	11	SHANK2	3'UTR	GO:0060291,long-term synaptic potentiation	GO:0005515,protein binding	GO:0030054,cell junction	hsa04724 Glutamatergic synapse	1.19	0.002
cg01039401	12	TEAD4	5'UTR	GO:0006357,regulation of transcription from RNA polymerase II promoter	GO:0005515,protein binding	GO:0005634,nucleus	hsa04390 Hippo signaling pathway	0.82	#####
cg17640061	12	SYT1	Body	GO:0051260,protein homooligomerization	GO:0005515,protein binding	GO:0005794,Golgi apparatus	hsa04721 Synaptic vesicle cycle	2.42	0.02
cg15319704	13	KLF5	TSS1500	GO:0008284,positive regulation of cell proliferation	GO:0005515,protein binding	GO:0005794,Golgi apparatus		2.50	0.04
cg08667244	14	DIO3	1stExon	GO:0042404,thyroid hormone catabolic process	GO:0004800,thyroxine 5'-deiodinase activity	GO:0010008,endosome membrane	hsa04919 Thyroid hormone signaling pathway	0.81	#####
cg18266472	15	LINGO1	TSS200	GO:0007165,signal transduction	GO:0005515,protein binding	GO:0005578,proteinaceous extracellular matrix		2.82	0.003
cg03660162	16	WWOX	Body	GO:0072332,intrinsic apoptotic signaling pathway by p53 class mediator	GO:0046983,protein dimerization activity	GO:0005794,Golgi apparatus		0.58	#####
cg19944656	17	TIMP2	Body	GO:0045930,negative regulation of mitotic cell cycle	GO:0005515,protein binding	GO:0005578,proteinaceous extracellular matrix		3.29	0.002
cg03181524	19	RYR1	Body	GO:0051289,protein homotetramerization	GO:0005515,protein binding	GO:0005790,smooth endoplasmic reticulum	hsa04713 Circadian entrainment	1.53	0.02
cg12602339	20	DEFB126	TSS1500	GO:0042742,defense response to bacterium		GO:0005576,extracellular region		1.17	3E-04
cg17036908	20	CDH4	1stExon	GO:0007155,cell adhesion	GO:0005509,calcium ion binding	GO:0005886,plasma membrane	hsa04514 Cell adhesion molecules (CAMs)	1.26	2E-04
cg01531431	20	PPDPF	TSS1500	GO:0031017,exocrine pancreas development				0.84	#####
cg11287055	21	DSCR3	Body	GO:0006886,intracellular protein transport	GO:0006886,intracellular protein transport	GO:0005634,nucleus		2.30	0.006

Copyright© AE&M all rights reserved.

Analysis of differential methylation sites/ regions associated with obesity

Using MethylTarget technology, methylation sequencing and methylation level detection were performed for target methylation sites, methylation regions, and target genes. Fifteen differential methylation sites were identified between the obesity group (35 cases) and the healthy group (34 cases), along with two differential methylation regions (cg08667244 in the 1stExon region and cg13928759 in the TSS200 region; $p < 0.05$) and three differential methylation genes (cg08667244 corresponding to iodothyronine deiodinase 3 (DIO3), cg13928759 corresponding to leucine-rich glioma inactivated 1 (LGI1), and cg18770216 corresponding to integrin subunit Beta 5 (ITGB5); $p < 0.05$). Further analysis revealed a negative correlation between the methylation level of cg13928759 (LGI1 gene) and BMI, with R = -0.25 and P = 0.04 (**Supplementary Figure 1**, **Table 4**).

DISCUSSION

The occurrence of adolescent obesity involves a variety of complex mechanisms and factors. Genetic, lifestyle, environmental, and psychological factors may play essential roles in obesity (12-14). In addition, metabolic abnormalities, brain appetite regulation centers, and inflammatory responses are closely related to adolescent obesity (15). Some adolescent individuals with obesity may have metabolic abnormalities, such as insulin resistance and thyroid dysfunction, which can affect energy balance and fat metabolism, leading to obesity (16). Furthermore, the regulation of food intake by appetite control centers in the brain (such as the hypothalamus) is also associated with obesity (17). Abnormal signaling of some hormones (such as insulin and leptin) may affect satiety and appetite control, affecting weight regulation (18).

Additionally, studies have shown a close relationship between inflammation and obesity. In obesity, the levels of inflammatory factors increase in adipose tissue, which may lead to insulin resistance, increased adipocyte numbers, and obesity-related diseases (19). These factors interact, leading to an imbalance between energy intake and expenditure, resulting in excessive fat storage and obesity.

In this study, MethylTarget technology was used to conduct methylation sequencing analysis on adolescent patients with obesity, and differential methylation sites and genes associated with obesity were discovered. The differential methylation regions included cg08667244 (site region 1stExon) and cg13928759 (site region TSS200), and the corresponding

Table 4. Results of differential analysis of obesity-related methylation sites

Target	Position	Type	P-value (Ttest)	P-value (Utest)	P-value (Logistic)	FP Mean	FP Median
cg01531431_38_N	57	CG	0.043942892	0.043762878	0.05108085	0.404772099	0.393162393
cg03199564_9	125	CG	0.024366003	0.020188162	0.031946353	0.083718639	0.083509514
cg03199564_9	155	CG	0.015856406	0.021555529	0.021661689	0.037006892	0.034587996
cg05649108_34	29	CG	0.007584019	0.006146756	0.01204122	0.180212038	0.170242215
cg05649108_34	31	CG/cg02345961	0.022485902	0.032748724	0.028766069	0.12788573	0.125721616
cg05649108_34	86	CG	0.00444197	0.002957483	0.007497966	0.312951408	0.305280528
cg05649108_34	105	CG	0.036562359	0.028295131	0.042942078	0.224436596	0.215355805
cg05649108_34	159	CG	0.045160769	0.024057175	0.049919535	0.122291469	0.112239444
cg05649108_34	164	CG	0.023016181	0.023278119	0.027925446	0.109088574	0.099491238
cg13928759_23	102	CG/cg13928759	0.008878135	0.021555529	0.013841437	0.589745522	0.591511692
cg18266472_31	27	CG	0.053375892	0.022268526	0.058380429	0.012734543	0.012524085
cg18266472_31	46	CG	0.025650349	0.041384559	0.029540485	0.017254492	0.016991041
cg18266472_31	90	CG	0.028353871	0.012990731	0.035837213	0.019125757	0.018391889
cg18427217_26_N	59	CG	0.039450907	0.033537693	0.045690323	0.496114202	0.492574865
cg20701305_12_N	96	C.G./cg20701305	0.040809511	0.055205584	0.05153688	0.260917881	0.262063228

Copyright© AE&M all rights reserved.

differential genes included cg08667244 (corresponding gene DIO3), cg13928759 (corresponding gene LGI1), and cg18770216 (corresponding gene ITGB5). Further analysis revealed that the methylation level of cg13928759 (corresponding gene LGI1) was negatively correlated with BMI.

The brain and nervous system are essential for weight regulation, as they regulate appetite, metabolic rate, and fat distribution, which influence weight maintenance. The regulation of hunger and satiety, maintenance of energy balance, and coordination of food intake and expenditure are critical mechanisms through which the brain and nervous system regulate weight (20). Neural circuits include the hypothalamic-pituitary-adrenal (HPA) axis and the hypothalamic-pituitary-thyroid (HPT) axis, which may be regulated by endocrine factors and neurotransmitters, thereby affecting appetite, metabolism, and fat distribution and ultimately affecting the occurrence and development of obesity (21). LGI1 is a gene-encoding protein that is usually associated with neuronal activity and neurological diseases (22). Recent studies have suggested that LGI1 may also be associated with energy metabolism and weight control (23). Our research revealed a negative correlation between the methylation level of LGI1 and BMI, suggesting that LGI1 may play a role in the occurrence and development of obesity. Similarly, genes such as DIO3 and ITGB5 may also affect obesity through mechanisms such as the regulation of thyroid hormone metabolism, cell signaling, or inflammatory responses.

Previous studies have reported various associations between methylation and obesity-related factors. Compared with these studies, our findings on the differential methylation sites cg08667244, cg13928759, and cg18770216 and their corresponding genes DIO3, LGI1, and ITGB5 show both similarities and differences.

In terms of DIO3, several prior investigations have indeed demonstrated its link to energy metabolism, which aligns with our results. For instance, alterations in DIO3 methylation status influenced thyroid hormone-mediated energy expenditure in adipose tissue. Similar to these findings, our research also revealed that methylation of the DIO3 gene, specifically at the cg08667244 site, is associated with obesity, suggesting its potential role in disrupting energy balance. However, differences in the specific methylation sites identified were detected. While our study pinpoints cg08667244 as a key differential site, other studies may have focused on different regions of the DIO3 gene. Additionally, the regulatory mechanisms may vary. In our study, we hypothesized that methylation at cg08667244 could directly affect the binding of transcription factors to the DIO3 promoter region, thereby modulating gene expression and subsequent energy metabolism. In contrast, previous research might have proposed alternative regulatory pathways, such as post-translational modifications of the DIO3 protein.

With respect to LGI1, most prior research has focused predominantly on its role in neurological diseases. Our study offers a novel perspective by revealing its potential connection with obesity through the negative correlation between the methylation level of cg13928759 (LGI1 gene) and BMI. Although the exact mechanism remains unclear, the role of LGI1 in neuronal activity might indirectly influence appetite regulation or energy expenditure-related neural circuits, which are crucial for maintaining a healthy body weight. These findings expand the functional understanding of LGI1 beyond the neurological realm.

With respect to ITGB5, few studies have explored its relationship with obesity. Existing research on ITGB5 has focused mainly on its function in cell adhesion, migration, and tumor metastasis. For example, one study reported that ITGB5 is involved in the invasion and metastasis of cancer cells through the regulation of cell–extracellular matrix interactions. Our study is among the first to identify cg18770216 as a regulator of obesity. We propose that methylation in the ITGB5 gene may impact the inflammatory response and differentiation of adipocytes, which are key processes in obesity development. These findings provide new insights into the role of ITGB5 in the context of obesity-related pathophysiology.

Energy metabolism refers to the processes of energy synthesis, utilization, and storage in the body. In obesity, energy metabolism may be dysregulated, leading to an imbalance between energy intake and

Copyright© AE&M all rights reserved.

expenditure (24). Obesity is often accompanied by an imbalance in energy metabolism, such as excessive food intake and insufficient physical activity, which can lead to an energy surplus (25). In addition, the abnormal secretion or action of metabolic regulatory factors, such as insulin and thyroid hormones, may affect energy metabolism, thereby promoting the occurrence of obesity (26). This study revealed that the obesity-related differential gene cg08667244 (corresponding gene DIO3) has a potential influence on the obesity process. DIO3 encodes type 3 iodothyronine deiodinase, and the methylation status of the DIO3 gene is closely related to energy metabolism (27), suggesting that DIO3 may participate in obesity by affecting thyroid hormone levels and metabolic regulation.

Fat metabolism encompasses fat synthesis, breakdown, and storage processes. In cases of obesity, this metabolism can become imbalanced, leading to excessive fat accumulation and obesity development. Key characteristics of obesity include an increase in both the number and size of fat cells, possibly owing to imbalances in energy intake and release, resulting in heightened fat storage (28). Moreover, secretions from fat cells, such as inflammatory factors, may influence the body's metabolic state, impacting the onset and progression of obesity (29). The inflammatory response, particularly within adipose tissue (30), plays a crucial role in obesity, as adipose tissue is known for producing inflammatory factors that can provoke chronic low-grade inflammation (31). This inflammatory response can activate pathways such as the NF-κB pathway, promoting the release of inflammatory factors such as tumor necrosis factor α (TNF-α) and interleukin-6 (IL-6). These factors can influence insulin sensitivity, fat metabolism, and energy balance, ultimately contributing to obesity development (32). This study identified cg18770216 (associated with the ITGB5 gene) as a regulator of obesity. ITGB5 encodes the integrin β5 subunit, which is involved in cell communication and signal transduction. Methylation in the ITGB5 gene may impact the inflammatory response and adipocyte differentiation, affecting fat metabolism and deposition (33). However, further research is necessary to elucidate the specific role of ITGB5 in obesity, including its involvement in cell signaling pathways, expression and regulation in adipose tissue, and interactions with other molecules that regulate inflammation and fat metabolism.

Future studies could explore alternative interventions for obesity and metabolic diseases. For example, intense intermittent exercise combined with thyme extract, as suggested in a previous review, may improve metabolic parameters related to obesity. In their research, 8 weeks of intense intermittent exercise with thyme extract was shown to affect the expression of the apoptosis indicators Bax and p53 in liver tissue and insulin resistance in type 2 diabetic rats, which implies possible positive effects on obesity-related metabolic disorders. Additionally, physical activity has various effects on health-related outcomes, as summarized in another review. Although that review focused mainly on cancer prevention, recovery, and recurrence, physical activity plays a crucial role in obesity prevention and treatment. Further research on its specific role in obesity-related metabolic regulation is warranted. These alternative approaches could provide new perspectives and strategies for combating obesity and its associated metabolic diseases.

This study has several limitations that warrant consideration. First, our findings demonstrate associations between methylation changes and obesity, but the cross-sectional design precludes causal inferences. While we hypothesize that methylation may influence obesity pathogenesis, it is equally plausible that obesity-related metabolic changes drive epigenetic modifications or that unmeasured confounders mediate both processes. Second, the sample size for the genome-wide methylation analysis (4 patients with obesity vs. 3 controls) was small, potentially limiting the statistical power and generalizability. Although the targeted validation cohort included larger groups (35 patients with obesity vs. 34 controls), the homogeneity of the young male population from a single geographic region may restrict broader applicability. Third, methylation was measured in peripheral blood, which may not fully reflect epigenetic patterns in metabolically active tissues. Fourth, despite correction for multiple testing, the exploratory nature of genome-wide analyses increases the risk

Copyright© AE&M all rights reserved.

of false-positive findings. The functional validation of candidate genes in relevant tissues or cellular models is also lacking. Fifth, the modest effect size of the correlation between BMI and methylation suggests that additional biological or environmental factors may contribute to obesity pathogenesis. Beyond that, we focused on single CpG site methylation levels rather than mean DNA methylation (DNAm) levels across DMRs for correlation with BMI. Future studies integrating regional methylation changes may further elucidate the epigenetic landscape of obesity. Finally, the cross-sectional design precludes causal inferences. Future studies incorporating longitudinal designs, Mendelian randomization, and intervention-based approaches are essential to disentangle causality.

In conclusion, the onset of adolescent obesity involves multiple mechanisms and factors. Our study revealed differential methylation sites and genes associated with obesity, highlighting LGI1, DIO3, and ITGB5 as potential contributors to obesity development. Future investigations can elucidate the specific mechanisms of these genes and their interactions with other obesity-related factors, offering a more in-depth understanding and potential therapeutic targets for obesity prevention and treatment.

Funding: Liuzhou Science and Technology Plan Project (2021CBC0108).

Disclosure: no potential conflict of interest relevant to this article was reported.

Data availability: datasets related to this article will be available upon request to the corresponding author.

REFERENCES

1. Rafei A, Elliott MR, Jones RE, Riosmena F, Cunningham SA, Mehta NK. Obesity Incidence in U.S. Children and Young Adults: A Pooled Analysis. Am J Prev Med. 2022 Jul;63(1):51-59. doi: 10.1016/j.amepre.2021.12.021.
2. Onie S, Usman Y, Widyastuti R, Lusiana M, Angkasawati TJ, Musadad DA, et al. Indonesia's first suicide statistics profile: an analysis of suicide and attempt rates, underreporting, geographic distribution, gender, method, and rurality. Lancet Reg Health Southeast Asia. 2024 Feb 26;22:100368. doi: 10.1016/j.lansea.2024.100368.
3. Patel P, Selvaraju V, Babu JR, Geetha T. Association of the DNA Methylation of Obesity-Related Genes with the Dietary Nutrient Intake in Children. Nutrients. 2023 Jun 22;15(13):2840. doi: 10.3390/nu15132840.
4. Transgenerational inheritance of acquired epigenetic signatures at CpG islands in mice. Cell. 2023 Feb 16;186(4):715-731.e19. doi: 10.1016/j.cell.2022.12.047.
5. Epigenetic regulation in metabolic diseases: mechanisms and advances in clinical study. Signal Transduct Target Ther. 2023 Mar 2;8(1):98. doi: 10.1038/s41392-023-01333-7.
6. Owen L, Corfe B. The role of diet and nutrition on mental health and wellbeing. Proc Nutr Soc. 2017 Nov;76(4):425-426. doi: 10.1017/S0029665117001057.
7. Ling C, Rönn T. Epigenetics in Human Obesity and Type 2 Diabetes. Cell Metab. 2019 May 7;29(5):1028-1044. doi: 10.1016/j.cmet.2019.03.009.
8. Chu DT, Bui NL, Vu Thi H, Nguyen Thi YV. Role of DNA methylation in diabetes and obesity. Prog Mol Biol Transl Sci. 2023;197:153-170. doi: 10.1016/bs.pmbts.2023.01.008.
9. Muscogiuri G, El Ghoch M, Colao A, Hassapidou M, Yumuk V, Busetto L; Obesity Management Task Force (OMTF) of the European Association for the Study of Obesity (EASO). European Guidelines for Obesity Management in Adults with a Very Low-Calorie Ketogenic Diet: A Systematic Review and Meta-Analysis. Obes Facts. 2021;14(2):222-245. doi: 10.1159/000515381.
10. Sabatucci A, Berchet V, Bellia F, Maccarrone M, Dainese E, D'Addario C, et al. A new methodological approach for in vitro determination of the role of DNA methylation on transcription factor binding using AlphaScreen® analysis: Focus on CREB1 binding at hBDNF promoter IV. J Neurosci Methods. 2020 Jul 15;341:108720. doi: 10.1016/j.jneumeth.2020.108720.
11. Li Y. Modern epigenetics methods in biological research. Methods. 2021 Mar;187:104-113. doi: 10.1016/j.ymeth.2020.06.022.
12. Spina R, Ropars A, Bouazzi S, Dadi S, Lemiere P, Dupire F, et al. Screening of Anti-Inflammatory Activity and Metabolomics Analysis of Endophytic Fungal Extracts; Identification and Characterization of Perylenequinones and Terpenoids from the Interesting Active Alternaria Endophyte. Molecules. 2023 Sep 9;28(18):6531. doi: 10.3390/molecules28186531.
13. Pokala A, Quarles WR, Ortega-Anaya J, Jimenez-Flores R, Cao S, Zeng M, et al. Milk-Fat-Globule-Membrane-Enriched Dairy Milk Compared with a Soy-Lecithin-Enriched Beverage Did Not Adversely Affect Endotoxemia or Biomarkers of Gut Barrier Function and Cardiometabolic Risk in Adults with Metabolic Syndrome: A Randomized Controlled Crossover Trial. Nutrients. 2023 Jul 23;15(14):3259. doi: 10.3390/nu15143259.
14. Raza GS, Herzig KH, Leppäluoto J. Invited review: Milk fat globule membrane-A possible panacea for neurodevelopment, infections, cardiometabolic diseases, and frailty. J Dairy Sci. 2021 Jul;104(7):7345-7363. doi: 10.3168/jds.2020-19649.
15. Mynarek M, Pizer B, Dufour C, van Vuurden D, Garami M, Massimino M, et al. Evaluation of age-dependent treatment strategies for children and young adults with pineoblastoma: analysis of pooled European Society for Paediatric Oncology (SIOP-E) and US Head Start data. Neuro Oncol. 2017 Apr 1;19(4):576-585. doi: 10.1093/neuonc/now234.
16. Biswas A, Mallick S, Purkait S, Gandhi A, Sarkar C, Singh M, et al. Treatment outcome and patterns of failure in patients of pinealoblastoma: review of literature and clinical experience from a regional cancer centre in north India. Childs Nerv Syst. 2015 Aug;31(8):129,1-304. doi: 10.1007/s00381-015-2751-1.
17. Valsechi LC, da Costa MDS, Dastoli PA, Nicácio JM, Suzuki FS, Leite AL, et al. Prognostic factors of pediatric pineal region tumors at a single institution. Childs Nerv Syst. 2023 Sep;39(9):2329-2339. doi: 10.1007/s00381-023-05952-x.
18. Gagliardi F, De Domenico P, Garbin E, Snider S, Mortini P. Primary Gamma Knife Radiosurgery for pineal region tumors: A systematic review and pooled analysis of available literature with histological stratification. J Pineal Res. 2023 Dec;75(4):e12910. doi: 10.1111/jpi.12910.
19. Régnier M, Van Hul M, Knauf C, Cani PD. Gut microbiome, endocrine control of gut barrier function and metabolic diseases. J Endocrinol. 2021 Feb;248(2):R67-R82. doi: 10.1530/JOE-20-0473.
20. Qin Z, Xie L, Li W, Wang C, Li Y. New Insights into Mechanisms Traditional Chinese Medicine for Allergic Rhinitis by Regulating

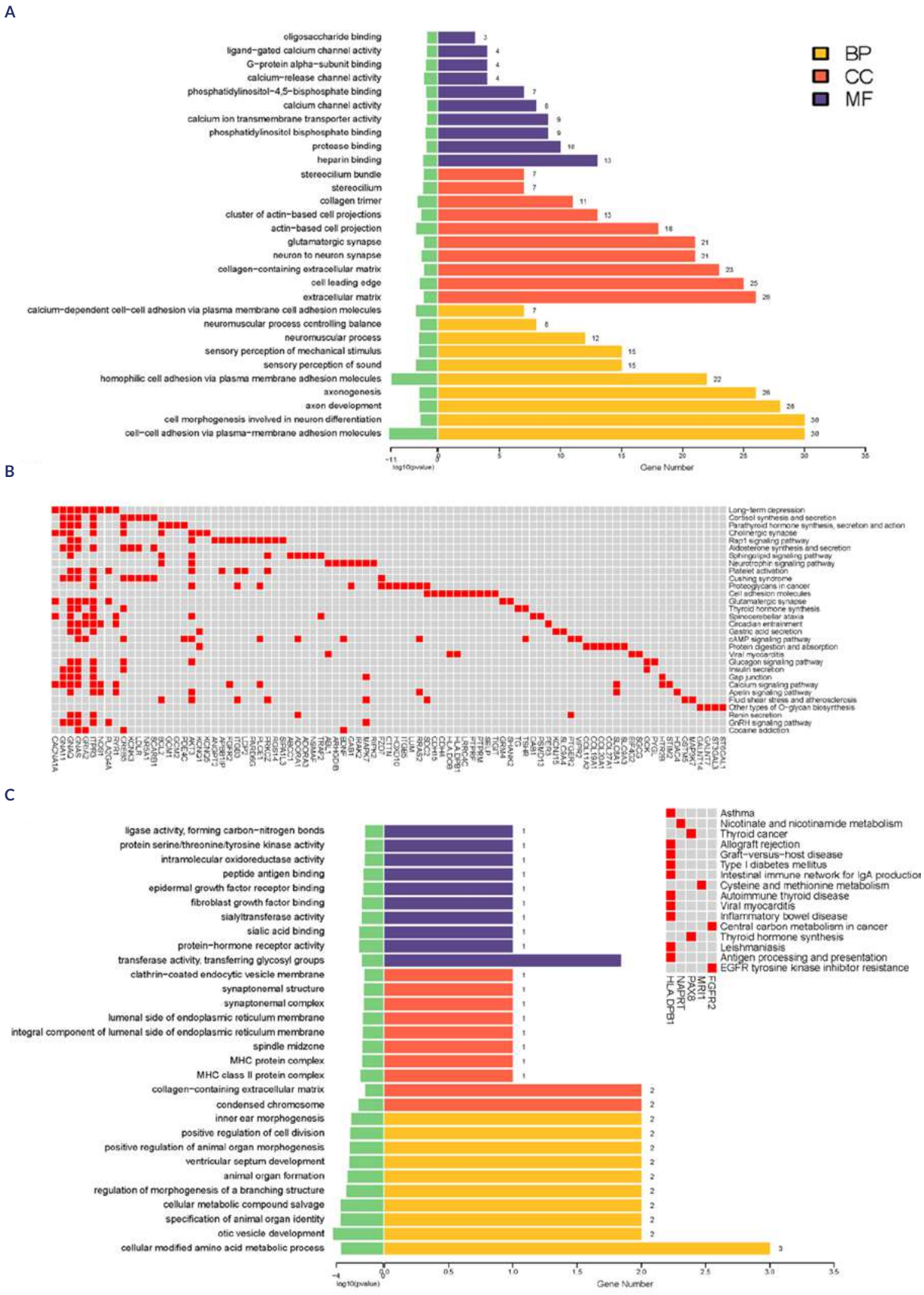
Copyright© AE&M all rights reserved.

Inflammatory and Oxidative Stress Pathways. J Asthma Allergy. 2024 Feb 19;17:97-112. doi: 10.2147/JAA.S444923.

21. Han SC, Kang JI, Choi YK, Boo HJ, Yoon WJ, Kang HK, et al. Intermittent Fasting Modulates Immune Response by Generating Tregs via TGF-β Dependent Mechanisms in Obese Mice with Allergic Contact Dermatitis. Biomol Ther (Seoul). 2024 Jan 1;32(1):136-145. doi: 10.4062/biomolther.2023.053.
22. Prasad JM, Young PA, Strickland DK. High Affinity Binding of the Receptor-associated Protein D1D2 Domains with the Low Density Lipoprotein Receptor-related Protein (LRP1) Involves Bivalent Complex Formation: CRITICAL ROLES OF LYSINES 60 AND 191. J Biol Chem. 2016 Aug 26;291(35):18430-9. doi: 10.1074/jbc.M116.744904.
23. Bao X, Liang Y, Chang H, Cai T, Feng B, Gordon K, et al. Targeting proprotein convertase subtilisin/kexin type 9 (PCSK9): from bench to bedside. Signal Transduct Target Ther. 2024 Jan 8;9(1):13. doi: 10.1038/s41392-023-01690-3.
24. Gruzdeva O, Borodkina D, Uchasova E, Dyleva Y, Barbarash O. Leptin resistance: underlying mechanisms and diagnosis. Diabetes Metab Syndr Obes. 2019 Jan 25;12:191-198. doi: 10.2147/DMSO.S182406.
25. Hidalgo-Lozada GM, Villarruel-López A, Nuño K, García-García A, Sánchez-Nuño YA, Ramos-García CO. Clinically Effective Molecules of Natural Origin for Obesity Prevention or Treatment. Int J Mol Sci. 2024 Feb 25;25(5):2671. doi: 10.3390/ijms25052671.
26. Yang K, Chen J, Zhang T, Yuan X, Ge A, Wang S, et al. Efficacy and safety of dietary polyphenol supplementation in the treatment of non-alcoholic fatty liver disease: A systematic review and meta-analysis. Front Immunol. 2022 Sep 9;13:949746. doi: 10.3389/fimmu.2022.949746.
27. Martinez ME, Pinz I, Preda M, Norton CR, Gridley T, Hernandez A. DIO3 protects against thyrotoxicosis-derived cranio-encephalic and cardiac congenital abnormalities. JCI Insight. 2022 Nov 8;7(21):e161214. doi: 10.1172/jci.insight.161214.
28. Kawai T, Autieri MV, Scalia R. Adipose tissue inflammation and metabolic dysfunction in obesity. Am J Physiol Cell Physiol. 2021 Mar 1;320(3):C375-C391. doi: 10.1152/ajpcell.00379.2020.
29. Li W, Hakkak R. Soy Protein Concentrate Diets Inversely Affect LPS-Binding Protein Expression in Colon and Liver, Reduce Liver Inflammation, and Increase Fecal LPS Excretion in Obese Zucker Rats. Nutrients. 2024 Mar 28;16(7):982. doi: 10.3390/nu16070982.
30. Xu GY, Xu S, Zhang YX, Yu ZY, Zou F, Ma XS, et al. Cell-Free Extracts from Human Fat Tissue with a Hyaluronan-Based Hydrogel Attenuate Inflammation in a Spinal Cord Injury Model through M2 Microglia/Microphage Polarization. Small. 2022 Apr;18(17):e2107838. doi: 10.1002/smll.202107838.
31. Urban H, Little CB. The role of fat and inflammation in the pathogenesis and management of osteoarthritis. Rheumatology (Oxford). 2018 May 1;57(suppl_4):iv10-iv21. doi: 10.1093/rheumatology/kex399.
32. Feng X, Du M, Li S, Zhang Y, Ding J, Wang J, et al. Hydroxysafflor yellow A regulates lymphangiogenesis and inflammation via the inhibition of PI3K on regulating AKT/mTOR and NF-κB pathway in macrophages to reduce atherosclerosis in ApoE-/- mice. Phytomedicine. 2023 Apr;112:154684. doi: 10.1016/j.phymed.2023.154684.
33. Datta R, Mukherjee D, Podolsky MJ, Yang CD, Alba DL, Singh S, et al. PTP1B mediates the inhibitory effect of MFGE8 on insulin signaling through the β5 integrin. J Biol Chem. 2024 Feb;300(2):105631. doi: 10.1016/j.jbc.2024.105631.

Copyright© AE&M all rights reserved.

SUPPLEMENTARY MATERIAL



Supplementary Figure 1. Genome-wide methylation site/region-related gene enrichment analysis. (**A**) GO functional enrichment analysis of differential methylation sites and regions; (**B**) KEGG signaling pathway enrichment analysis of differential methylation sites and regions; (**C**) GO and KEGG enrichment analysis of methylation binding regions.

Copyright© AE&M all rights reserved.

Archives of Endocrinology and Metabolism
ISSN 2359-4292
OFFICIAL JOURNAL OF THE BRAZILIAN SOCIETY OF ENDOCRINOLOGY AND METABOLISM

original

Factors associated with lifestyle practices for preventing cardiovascular disease in adults aware of metabolic syndrome

Jong Sun Ok[1]
https://orcid.org/0000-0002-1885-3015
Kyung-Jin Kim[2]
https://orcid.org/0000-0002-5796-3284
Kyung-Hee Kim[3]
https://orcid.org/0000-0003-0708-8685
Do Kyeong Song[4]
https://orcid.org/0000-0003-2101-6661
Kyung Jin Ahn[5]
https://orcid.org/0000-0002-6286-3157
Chan Seok Park[6]
https://orcid.org/0000-0002-3481-6206
Mi-Seung Shin[7]
https://orcid.org/0000-0002-0273-0109

[1] Department of Nursing, Konkuk University, Chungju, Korea
[2] Division of Cardiology, Department of Internal Medicine, Ewha Womans University College of Medicine, Seoul, Korea
[3] Division of Cardiology, Incheon Sejong Hospital, Incheon, Korea
[4] Department of Internal Medicine, Ewha Womans University School of Medicine, Seoul, Korea
[5] Department of Pediatrics, Gachon University Gil Medical Center, Incheon, Korea
[6] Division of Cardiology, Department of Internal Medicine, Bucheon St Mary's Hospital, The Catholic University of Korea, Seoul, Korea
[7] Division of Cardiology, Department of Internal Medicine, Gachon University Gil Medical Center, Incheon, Korea

ABSTRACT

Objective: The global increase in metabolic syndrome (MetS) highlights the need for effective lifestyle interventions to reduce cardiovascular disease (CVD) risk. This study aimed to identify factors associated with lifestyle behaviors for preventing CVD complications among adults aware of MetS. **Subjects and methods:** A cross-sectional online survey was conducted from January to February 2023 among 1,000 South Korean adults aged 20-69 years. After excluding 212 participants unaware of MetS, 788 respondents were included, of whom 710 engaged in at least three of nine recommended lifestyle behaviors: smoking cessation, alcohol abstinence, body weight monitoring, waist circumference measurement, blood pressure monitoring, regular hospital visits, adequate sleep, adherence to a low-salt diet, and regular physical activity. Participants were categorized into those with one or more MetS risk factors (META) and those without (Non-META). **Results:** participants with MetS risk factors were predominantly male and aged 50-69 years, while those without were more likely female and aged 20-39 years. Abdominal obesity was the most common risk factor, whereas waist circumference monitoring was the least practiced behavior. The META group showed higher rates of blood pressure monitoring and hospital visits, while the Non-META group reported more frequent smoking cessation and alcohol abstinence. **Conclusion:** Engagement in healthy lifestyle behaviors was positively associated with female sex, older age, and higher awareness of MetS-related complications. The limited practice of waist circumference monitoring underscores the need for targeted education and personalized preventive strategies to enhance CVD risk reduction among individual aware of MetS.

Keywords: Healthy lifestyle; metabolic syndrome; risk factor; adult; abdominal obesity

INTRODUCTION

Metabolic syndrome (MetS) has emerging as a major global public health concern, characterized by a cluster of interrelated metabolic abnormalities that substantially increase the risk of chronic diseases (1). Epidemiological evidence indicates that MetS affects approximately one-quarter to one-third of the global population, with prevalence rates continuing to rise across diverse regions (2). National data report prevalence estimates of 34.2% in the United States, 29.6% in Brazil, and 21% in South Korea, underscoring its widespread burden (3-5).

Clinically, MetS is defined by the presence of at least three of the following five criteria: abdominal obesity, elevated fasting blood glucose, elevated blood pressure, elevated triglycerides, and reduced

Received on Jul/22/2025
Accepted on Dec/2/2025
DOI: 10.20945/2359-4292-2026-0061

Correspondence to:
Mi-Seung Shin
Division of Cardiology, Department of Internal Medicine,
Gil Medical Center, Gachon University College of Medicine, 21
Namdong-daero 774 Beon-gil, Namdong-gu, Incheon
21565, Republic of Korea
msshin@gilhospital.com

Associated editor:
Marcio W. Lauria
https://orcid.org/0000-0001-7558-1231

This is an open-access article distributed under the terms of the Creative Commons Attribution License

Copyright© AE&M all rights reserved.

high-density lipoprotein (HDL) cholesterol level (1). This constellation of metabolic risk factors is strongly associated with an increased incidence of cardiovascular disease (CVD), type 2 diabetes mellitus, cognitive decline, and all-cause mortality (1). Moreover, the cumulative presence of multiple MetS components has been shown to exponentially elevate the risk of severe complications, including CVD events, diabetic complications, and stroke (6).

The etiology of MetS is multifactorial, arising from complex interactions among genetic predisposition and modifiable behaviors, psychosocial, and environmental factors such as diet, physical inactivity, stress, socioeconomic status (7). Among these, lifestyle behaviors represent key modifiable determinants for both the prevention and management of MetS (8). Current clinical guidelines, including the National Cholesterol Education Program Adult Treatment Panel (NCEP ATP) III, recommend lifestyle modification-comprising dietary regulation, increased physical activity, and weight control-as the first-line strategy for MetS management (9).

However, the interdependence among lifestyle behaviors present challenges in both assessment and intervention. Prior research has largely examined isolated behavioral or clinical components, limiting compressive understanding of how multiple lifestyle factors interact to influence MetS outcomes (8). A more integrated approach is therefore essential to elucidate behavioral patterns underlying lifestyle adherence and to develop effective, sustainable preventive strategies (8).

Awareness of MetS constitutes a critical precursor to behavioral change, serving as the foundation for adopting preventive health behaviors (10). Previous studies have demonstrated that individuals aware of MetS are more likely to engage in lifestyle modification aimed at mitigating associated risk factors (10). Enhanced awareness may further facilitate early detection and management of metabolic abnormalities, thereby reducing the risk of CVD—the more critical complication of MetS (1). Accordingly, the present study aimed to identify factors associated with lifestyle practices for the prevention of CVD among adults who are aware of MetS.

SUBJECTS AND METHODS

Study design and data collection

This study employed a cross-sectional design and was conducted from January to February 2023. With the exception of study design development, all survey administration procedures were implemented by MegaResearch, a professional research agency based in Seoul, South Korea. As of December 2022, the estimated adult population aged ≥20 years in South Korea was 37,121,412. To obtain a nationally representative sample of adults aged 20–69 years, a total of 1,000 participants were recruited using a stratified systematic sampling method based on sex (male/female), age group (20–29, 30–39, 40–49, 50–59, and 60–69 years), and geographical region (eight metropolitan and eight non-metropolitan areas).

Data were collected via structured, self-administered online questionnaires. Survey invitations containing a unique link to the web-based instrument were distributed to randomly selected panel members registered with the research agency. Participants completed the questionnaire independently, and responses were automatically recorded on a secure data server. To minimize item non-response, the survey system required participants to complete each question before proceeding to the next. All aspects of data collection were monitored in real time by the research agency to ensure data integrity, prevent duplicate entries, and maintain response accuracy (11).

Study population

The study population was derived from the nationally representative sample of South Korea adults through stratified sampling by sex, age, and region of residence to ensure demographic representativeness. Eligible participants were adults aged 20 to 69 years who provided informed consent and completed the online questionnaire after confirming full understanding of the study purpose and procedures. Exclusion criteria were as follows: (1) individuals younger than 20 or older than 69 years, (2) individuals without adequate internet access, (3) those who declined participation, (4) respondents who failed to complete the final survey item; and (5) participants from specific sex-age strata exceeding the predetermined sample quota (11).

Copyright© AE&M all rights reserved.

Participants who reported being unaware of MetS (n = 212) were excluded, resulting in a final analytical sample of 788 individuals with MetS awareness. Of these, 710 participants who reported engaging in at least three of the following nine lifestyle behaviors were included in the final analysis: smoking cessation, alcohol abstinence, body weight monitoring, waist circumference measurement, blood pressure monitoring, regular physical activity or adherence to a low-salt diet-recognized. Smoking cessation was considered essential lifestyle behavior for preventing CVD complications. Additionally, participants were required to engage in at least one of the two key lifestyle modifications—regular physical activity or adherence to a low-salt diet—recognized as critical for preventing MetS-related complications. In addition to these core behaviors, participants were required to practice at least one additional lifestyle behavior from the remaining items.

Participants were classified into two groups: those with one or more MetS risk factors (hypertension, hyperlipidemia, diabetes mellitus, or abdominal obesity) (META) and those without any risk factors (Non-META).

Questionnaire

Demographic variables included age, sex, educational attainment, monthly household income, occupation, marital status, presence of comorbidities, and family history of CVD. Comorbid conditions—specifically hypertension, diabetes mellitus, hyperlipidemia, and abdominal obesity—were evaluated as indicator of MetS risk factors.

MetS–related variables comprised the following: awareness of MetS (1 = "Very well aware", 2 = "Well aware", 3 = "Somewhat aware", 4 = "Unaware", 5 = "Completely unaware"); awareness of the association between MetS and CVD complications (1 = "Strongly agree", 2 = "Somewhat agree", 3 = "Slightly agree", 4 = "Do not agree", 5 = "Do not agree at all"); and frequency of waist circumference and body weight monitoring within the past three years (1 = "Frequently", 2 = "Occasionally", 3 = "Rarely", 4 = "Never"). The questionnaire also assessed engagement in lifestyle modification behaviors for MetS prevention and perceived barriers to implementing such behaviors.

Lifestyle practices for MetS prevention included blood pressure monitoring, regular hospital visits, adequate sleep, adherence to a low-salt diet, regular physical activity, vitamin supplementation, and dietary supplement intake. Participants who reported frequent monitoring of waist circumference and body weight during the previous three years were also classified as engaging in preventive lifestyle practices.

Smoking cessation and alcohol abstinence were assessed as additional lifestyle behaviors related to comorbidity management. Participants who reported abstinence from smoking or alcohol consumption were categorized as practicing these behaviors. Barriers to the adoption of MetS-related lifestyle practices were classified into seven categories: financial constraints, perception of already maintaining a healthy lifestyle, lack of time, excessive workload, insufficient knowledge of appropriate behaviors, disbelief in the effectiveness of lifestyle modification, and other unspecified factors.

Participants with one or more comorbidities (hypertension, diabetes mellitus, hyperlipidemia, or abdominal obesity) were categorized as the MetS risk factor group, whereas those without any of these conditions were classified as the non-risk factor group.

Given the established importance of smoking cessation in the prevention of non-communicable diseases and overall health promotion (12), this behavior was included as a core component of CVD–preventive lifestyle practices. Comprehensive lifestyle modification was operationally defined as engagement in at least three lifestyle behaviors (13), including one of either low-salt diet adherence or regular physical activity, in addition to at least one other behavior (excluding vitamin or supplement intake). The detailed questionnaire is provided in **Supplementary Material**.

Ethics

This study was reviewed and approved by the institutional Review Board (IRB) of the Gachon University Medical Center (IRB No. GFIRB2023-084). Given that the survey was conducted anonymously and did not involve the collection of personally identifiable information, the IRB waived the requirement for written informed consent. All participants provided implied consent by voluntarily completing the online questionnaire.

Copyright© AE&M all rights reserved.

Statistical analysis

Descriptive statistics were used to summarize the participants' demographic characteristics and MetS-related variables. Categorical variables were compared using the chi-square test, while continuous variables were assessed with the independent samples t-test. Multivariate logistic regression analysis was performed to identify factors independently associated with engagement in healthy lifestyle behaviors. All statistical tests were two-tailored, and a significance threshold of $p < 0.05$ was applied. Data analysis were conducted using R software version 4.2.0 for windows (The Comprehensive R Archive Network, Auckland, New Zealand).

RESULTS

General characteristics of participants and metabolic syndrome-related variables

The general characteristics of the study population and response to MetS-related questionnaire items are summarized in **Table 1**. The mean age of participants in MetS risk factor group (META) was significantly higher than that of the non-risk factor group (Non-META) (49.41 ± 12.60 years vs. 43.11 ± 13.02 years; $t = 6.27$, $p < 0.001$). Age distribution differed between groups: the META group had a higher proportion of individuals in their 50s and 60s, whereas the Non-META group had a higher proportion of participants in their 20s and 30s. Sex distribution also differed significantly, with male predominating in the META group (54.0%) and females in the non-META group (55.9%) ($x^2 = 39.20$, $p < 0.001$). Marital status showed a significant difference, with a higher proportion of married participants in the META group (72.2%) compared with the Non-META group (51.0%) ($x^2 = 40.90$, $p < 0.001$). Educational attainment did not differ significantly, with the majority holding a college degree or higher ($x^2 = 2.66$, $p = 0.264$). Similarly, monthly household income distribution was not significantly different between groups, with the largest proportion earning ≥ KRW 5.00 million ($x^2 = 7.66$, $p = 0.176$).

Occupational status differed significantly ($x^2 = 16.95$, $p = 0.031$). Office workers constituted the largest occupational category in both groups. The META group included a higher proportion of housewives and sales/service workers, whereas the Non-META group included a higher proportion of self-employed and technical workers

Regarding family history of CVD, a significantly greater proportion of participants in the META group reported a positive history compared with the Non-META group (30.0% vs. 10.1%; $x^2 = 34.80$, $p < 0.001$). Awareness of the relationship between MetS and CVD complications was also higher in the META group, with 44.7% reporting strong awareness versus 33.6% in the Non-META group ($x^2 = 9.84$, $p = 0.043$).

In terms of lifestyle practices, participants in the META group reported higher rates of blood pressure monitoring and regular hospital visits ($x^2 = 22.61$, $p < 0.001$; $x^2 = 31.42$, $p < 0.001$), whereas participants in the Non-META group reported higher rates of alcohol abstinence and smoking cessation ($x^2 = 17.69$, $p < 0.001$; $x^2 = 22.93$, $p < 0.001$) (**Figure 1**).

Although no statistically significant differences were observed between groups in perceived barriers to lifestyle modification, the most frequently reported barrier in both groups was insufficient knowledge regarding appropriate lifestyle practices ($x^2 = 5.12$, $p = 0.401$) (**Figure 2**).

Comparison of lifestyle practices and barriers according to types of metabolic syndrome risk factors

The MetS risk factors examined in this study included hypertension, hyperlipidemia, diabetes mellitus, and abdominal obesity. Lifestyle practices and perceived barriers to lifestyle modification stratified by these risk factors are summarized in **Table 2**. The prevalence of MetS risk factors among participants was 48.0% for hypertension, 50.3% for hyperlipidemia, 21.8% for diabetes, and 66.5% for abdominal obesity.

Among lifestyle practices, blood pressure monitoring was most frequently reported by participants with hypertension ($x^2 = 45.21$, $p < 0.001$), whereas regular hospital visits were most common among those with diabetes ($x^2 = 25.91$, $p < 0.001$). Additionally, consumption of health supplements, including vitamins and red ginseng, was highest among individuals with hyperlipidemia ($x^2 = 15.82$, $p = 0.001$) (**Figure 3**).

Copyright© AE&M all rights reserved.

Table 1. General characteristics of participants and Metabolic syndrome-related variables, n = 710

Variables		META N=463 n (%) or M±SD	Non-META N=247 n (%) or M±SD	x^2 or t	p
Age		49.41±12.60	43.11±13.02	6.27	**<0.001***
20s		46 (9.9)	56 (22.7)	39.20	**<0.001***
30s		61 (13.2)	51 (20.6)		
40s		94 (20.3)	52 (21.1)		
50s		132 (28.5)	50 (20.2)		
60s		130 (28.1)	38 (15.4)		
Sex	Male	250 (54.0)	109 (44.1)	5.88	**0.015***
	Female	213 (46.0)	138 (55.9)		
Marital status	Single	96 (20.7)	107 (43.3)	40.90	**<0.001***
	Married	339 (72.2)	126 (51.0)		
	Divorce/Bereave/Separate	28 (6.0)	14 (5.7)		
Education	≤Middle school	5 (1.0)	2 (0.8)	2.66	0.264
	High school	110 (23.8)	46 (18.6)		
	≥College	348 (75.2)	199 (80.6)		
Monthly household income (KRW)	≤100	15 (3.3)	7 (2.8)	7.66	0.176
	100-199	32 (6.9)	16 (6.5)		
	200-299	75 (16.2)	53 (21.4)		
	300-399	95 (20.5)	47 (19.0)		
	400-499	89 (19.2)	31 (12.6)		
	≥500	157 (33.9)	93 (37.7)		
Occupation	None	35 (7.5)	19 (7.7)	16.95	**0.031***
	Self-employment	32 (6.9)	25 (10.1)		
	Sales/Services	42 (9.1)	21 (8.5)		
	Technical	41 (8.9)	25 (10.1)		
	Office work	131 (28.3)	85 (34.4)		
	Administration/Management	39 (8.4)	8 (3.3)		
	Professional/Public official/Teacher	36 (7.8)	24 (9.7)		
	Housewife	79 (17.1)	25 (10.1)		
	Part time/Freelancer/College/Graduate student	28 (6.0)	15 (6.1)		
Family history of cardiovascular disease	Yes	139 (30.0)	25 (10.1)	34.80	**<0.001***
	No	324 (70.0)	222 (89.9)		
Awareness of the association between MetS and CVD complications	Strongly agree	207 (44.7)	83 (33.6)	9.84	**0.043***
	Somewhat agree	152 (32.8)	100 (40.5)		
	Slightly agree	75 (16.2)	45 (18.2)		
	Do not agree	2 (0.4)	0 (0.0)		
	Dd not agree at all	27 (5.9)	19 (7.7)		
Types of lifestyle practice (double check)	Waist circumference	38 (8.2)	22 (8.9)	0.031	0.859
	Body weight	192 (41.5)	103 (41.7)	0.000	1.000
	Blood pressure	135 (29.2)	32 (13.0)	22.61	**<0.001**
	Alcohol abstinence	306 (66.1)	201 (81.4)	17.69	**<0.001**
	Smoking cessation	325 (70.2)	214 (86.6)	22.93	**<0.001**
	Physical activity	254 (54.9)	152 (61.5)	2.67	0.102
	Adequate sleep	153 (33.1)	79 (32.0)	0.041	0.839
	Low salt diet	156 (33.7)	100 (40.5)	2.93	0.087
	Routine medical checkup	172 (37.2)	41 (16.6)	31.42	**<0.001**
	Taking health supplements (vitamins, red ginseng, etc.)	225 (48.6)	98 (39.7)	3.79	0.051

Copyright© AE&M all rights reserved.

Variables		META N=463 n (%) or M±SD	Non-META N=247 n (%) or M±SD	x^2 or t	p
barriers to practicing lifestyle	Maintaining a healthy lifestyle	67 (14.5)	42 (17.0)	5.12	0.401
	Economic burden	95 (20.5)	47 (19.0)		
	Lack of time	53 (11.5)	39 (15.8)		
	Too much to do	66 (14.3)	29 (11.7)		
	Not sure what to do	147 (31.8)	64 (25.9)		
	Lifestyle modification don't help	27 (5.8)	22 (8.9)		
	Others	8 (1.7)	4 (1.6)		

*p < 0.05, MetS: metabolic syndrome risk factor; CVD: cardiovascular disease; META: those with one or more MetS risk factors (hypertension, hyperlipidemia, diabetes mellitus, or abdominal obesity); Non-META: those without any risk factors

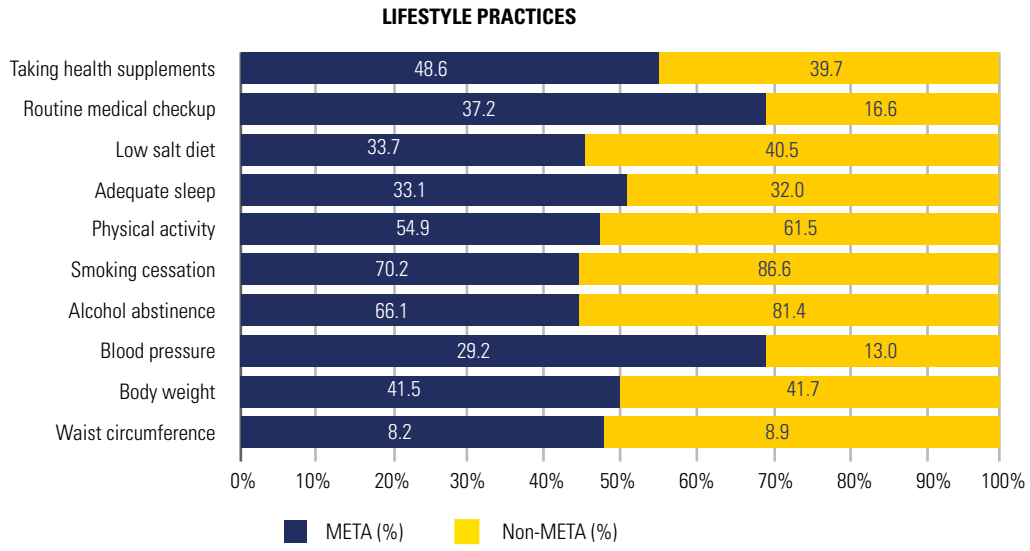


Figure 1. Comparisons of lifestyle practices between participants with and without metabolic syndrome risk factors. Participants with metabolic syndrome risk factors (META group) demonstrated significantly higher rates of blood pressure monitoring and regular hospital visits ($p < 0.001$), whereas those without metabolic syndrome risk factors (Non-META group) exhibited higher rates of alcohol abstinence and non-smoking ($p < 0.001$).

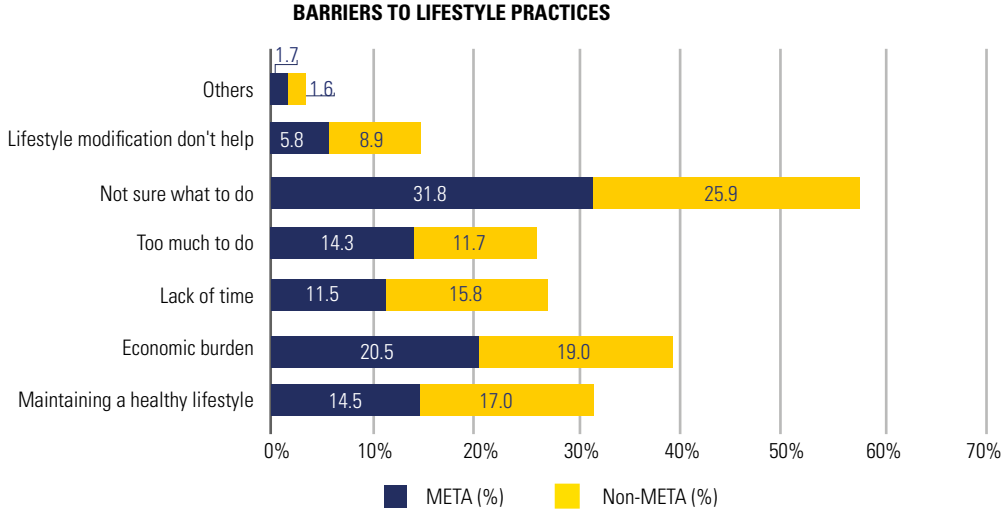


Figure 2. Comparisons of barriers to lifestyle practices between participants with and without metabolic syndrome risk factors. The most frequently reported barrier to lifestyle practice in both groups was a lack of knowledge regarding how to implement healthy lifestyle behaviors for the prevention of metabolic syndrome ($p = 0.401$).

Copyright© AE&M all rights reserved.

Table 2. Comparison of Lifestyle practices and barriers according to types of Metabolic syndrome risk factors, n = 710

Variables		MetS risk factors (double check)					
		HTN	Hyperlipidemia	DM	Abdomen obesity	x^2	p
		n (%)	n (%)	n (%)	n (%)		
		222 (48.0)	233 (50.3)	101 (21.8)	308 (66.5)		
Types of lifestyle practice (double check)	Waist circumference	22 (9.9)	23 (9.9)	13 (12.9)	25 (8.1)	2.63	0.452
	Body weight	94 (42.3)	113 (48.5)	47 (46.5)	127 (41.2)	1.97	0.578
	Blood pressure	96 (43.2)	82 (35.2)	40 (39.6)	84 (27.3)	45.21	**<0.001***
	Alcohol abstinence	142 (64.0)	152 (65.2)	65 (64.4)	187 (60.7)	1.13	0.769
	Smoking cessation	151 (68.0)	162 (69.5)	63 (62.4)	206 (66.9)	1.46	0.691
	Physical activity	120 (54.1)	141 (60.5)	57 (56.4)	170 (55.2)	1.49	0.685
	Adequate sleep	64 (28.8)	70 (30.0)	36 (35.6)	111 (36.0)	3.45	0.328
	Low salt diet	79 (35.6)	86 (36.9)	36 (35.6)	103 (33.4)	2.67	0.444
	Routine medical checkup	104 (46.9)	102 (43.8)	49 (48.5)	107 (34.7)	25.91	**<0.001***
	Taking health supplements (vitamins, red ginseng, etc.)	101 (45.5)	126 (54.1)	41 (40.6)	142 (46.1)	15.82	**0.001***
barriers to practicing lifestyle	Maintaining a healthy lifestyle	38 (17.1)	34 (14.6)	22 (21.8)	36 (11.7)	12.14	0.669
	Economic burden	42 (18.9)	56 (24.0)	22 (21.8)	71 (23.1)		
	Lack of time	24 (10.8)	24 (10.3)	16 (15.8)	38 (12.3)		
	Too much to do	32 (14.4)	26 (11.2)	13 (12.9)	48 (15.6)		
	Not sure what to do	68 (30.6)	77 (33.1)	21 (20.8)	90 (29.2)		
	Lifestyle modification don't help	15 (6.8)	10 (4.3)	6 (5.9)	18 (5.8)		
	Others	3 (1.4)	6 (2.6)	1 (1.0)	7 (2.3)		

*p < 0.05, MetS: metabolic syndrome.

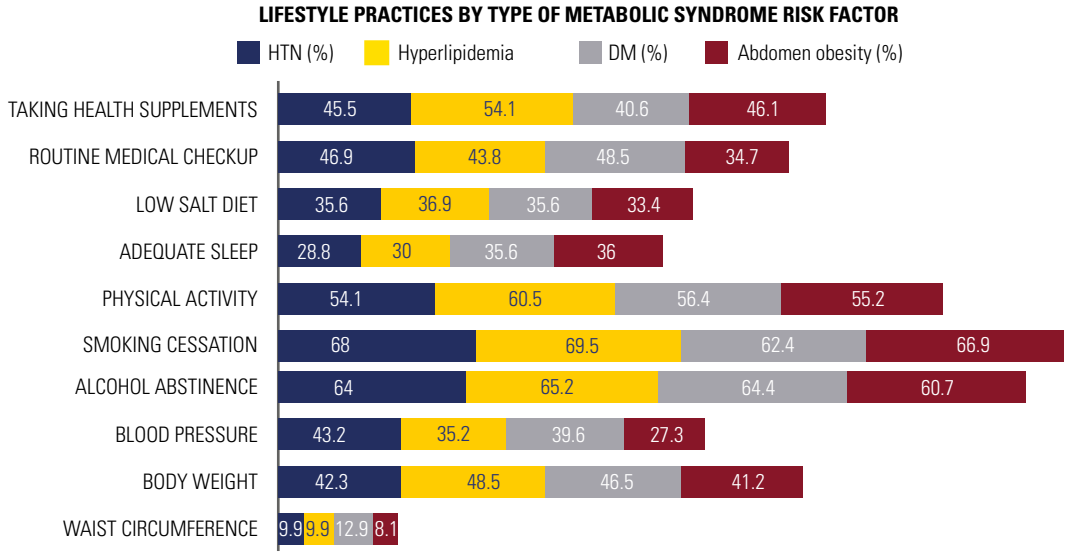


Figure 3. Comparison of lifestyle practices by type of metabolic syndrome risk factor. Four metabolic syndrome risk factors were examined: hypertension, hyperlipidemia, diabetes, and abdominal obesity. Among lifestyle practice items, the rate of blood pressure monitoring was the highest among participants with hypertension ($p < 0.001$), and regular hospital visits were the most frequent among those with diabetes ($p < 0.001$). Consumption of health supplements was highest among participants with hyperlipidemia ($p = 0.001$).

Although no statistically significant differences were observed in reported barriers to lifestyle modification across MetS risk factors ($x^2 = 12.14$, $p = 0.669$), the most frequently reported barrier among participants with hypertension, hyperlipidemia, and abdominal obesity was uncertainly regarding how to implement appropriate lifestyle changes. In contrast, financial burden was the predominant barrier among participants with diabetes (Figure 4).

Copyright© AE&M all rights reserved.

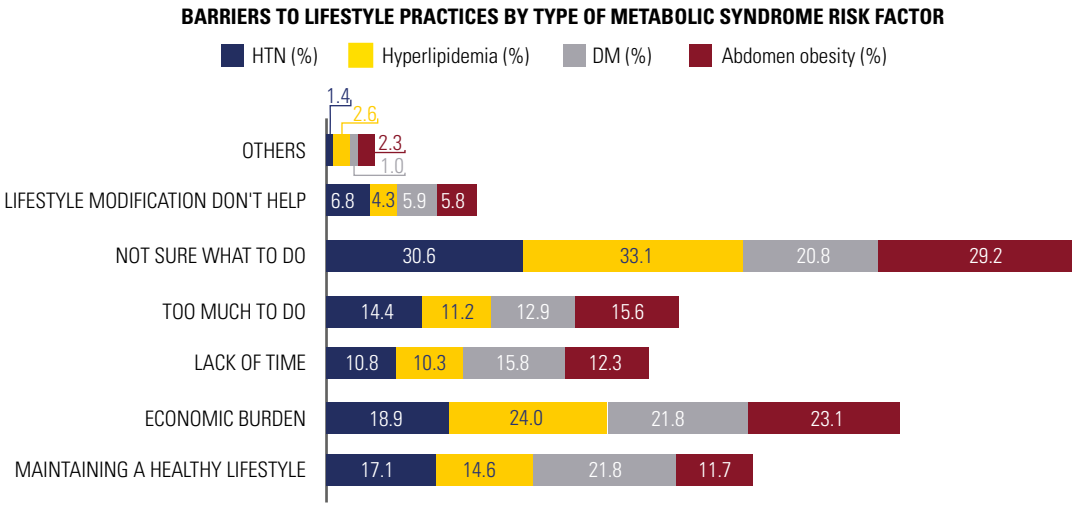


Figure 4. Comparison of barriers to lifestyle practices by type of metabolic syndrome risk factor. Four metabolic syndrome risk factors were examined: hypertension, hyperlipidemia, diabetes, and abdominal obesity. Among participants with diabetes, the primary barrier to adopting healthy lifestyle behaviors was financial burden, whereas for the other risk factor groups, the predominant barrier was a lack of knowledge regarding how to implement healthy lifestyle behaviors for the prevention of metabolic syndrome (p = 0.669).

Factors associated with lifestyle practices for the prevention of cardiovascular disease in adults aware of metabolic syndrome

Multivariate logistic regression analysis (Table 3) identified several significant predictors of engagement in heathy lifestyle practice. Female sex, older age, and greater awareness of complications associated with MetS were positively and independently associated with adherence to recommended lifestyle behaviors. These findings suggest that demographic factors and knowledge of MetS-related risks play a critical role in promoting preventive health behaviors among adults aware of their metabolic risk status.

DISCUSSION

This study investigated the prevalence of MetS risk factors, lifestyle practices, determinants of lifestyle adherence among a nationally representative sample of adults in South Korea. Among MetS risk factors, abdominal (central) obesity was the most prevalent in the META group. Central obesity, a core component of MetS, is influenced by hormonal factors such as gonadal steroids (14) and individuals of Asian descent are known to exhibit greater visceral adiposity compared to Caucasians at equivalent body mass indices (BMI) (15). The global increase in obesity has substantially contributed to the rising burden of MetS (1).

Despite the central role of abdominal obesity in MetS pathogenesis, waist circumference monitoring—a key metric for assessing central adiposity—was the least frequently practiced lifestyle behavior in both META and Non-META groups. Primary barriers identified was limited knowledge regarding appropriate lifestyle practices. Practical challenge, including privacy concerns, variability in seasonal clothing, and inconsistencies in clinical measurement techniques, may also hinder regular waist circumference monitoring. These findings highlight the need for targeted educational initiatives directed at both healthcare providers and the public, emphasizing waist circumference assessment alongside standard metrics such as blood pressure and body weight. Incorporating validated indices such as the A Body Shape Index (ABSI) or waist-to-height ratio, may enhance measurement reliability (16).

Participants without MetS risk factors demonstrated higher adherence to smoking cessation, alcohol abstinence, regular physical activity, and low-salt diet practices. These observations suggest that consistent engagement in healthy behaviors may delay the onset of MetS risk factors among individuals with awareness of the condition. Considering the trend of earlier MetS onset, particularly among individuals in their 30s and 40s (17), and increasing life expectancy,

Copyright© AE&M all rights reserved.

Table 3. Factors associated with Lifestyle practices for the prevention of Cardiovascular disease in adult aware of Metabolic syndrome, n = 710

Variables	Estimate	SE	Z	P	OR	CI
Age	0.028	0.009	3.161	**0.002***	**1.03**	1.01-1.05
Sex (Reference = Male)	0.383	0.187	2.045	**0.041***	**1.47**	1.02-2.12
Education (Reference = Middle school)	-0.255	0.202	-1.262	0.207	0.77	0.52-1.15
Monthly household income (Reference = ≤100)	0.076	0.066	1.166	0.244	1.08	0.95-1.23
Occupation_Housewife (Reference = None)	0.228	0.412	0.553	0.581	1.26	0.56-2.82
Occupation_ Part time/Freelancer/students (Reference = None)	-0.488	0.439	-1.112	0.266	0.61	0.26-1.45
Occupation_ Public official/Teacher/Professional (Reference = None)	-0.163	0.419	-0.388	0.698	0.85	0.37-1.93
Occupation_ Administration/Management (Reference = None)	-0.987	0.464	-2.218	0.033	0.37	0.15-0.92
Occupation_ Technical (Reference = None)	-1.551	0.425	-3.652	0.000	0.21	0.09-0.49
Occupation_ Sales/Services (Reference = None)	-0.917	0.412	-2.226	0.026	0.40	0.18-0.90
Occupation_ Office work (Reference = None)	-0.472	0.349	-1.355	0.175	0.62	0.31-1.23
Occupation_ Self-employment (Reference = None)	-0.662	0.416	-1.593	0.111	0.52	0.23-1.16
Family history of cardiovascular disease (Reference = No)	-0.662	0.208	-3.177	0.001	0.52	0.34-0.78
Marital status_Single (Reference = Divorce/Bereave/Separate)	0.458	0.411	1.115	0.265	1.58	0.71-3.54
Marital status_Married (Reference = Divorce/Bereave/Separate)	0.409	0.370	1.106	0.269	1.51	0.73-3.11
Awareness of MetS complications (Reference = Unknown)	0.255	0.094	2.709	**0.007***	**1.29**	1.07-1.55
Barriers to practicing lifestyle_ Economic burden (Reference = Maintaining a healthy lifestyle)	-0.221	0.287	-0.768	0.442	0.80	0.46-1.41
Barriers to practicing lifestyle_ Lack of time/Too much to do (Reference = Maintaining a healthy lifestyle)	0.036	0.269	0.134	0.893	1.04	0.61-1.76
Barriers to practicing lifestyle_Not sure what to do (Reference = Maintaining a healthy lifestyle)	-0.304	0.265	-1.148	0.251	0.74	0.44-1.24
Barriers to practicing lifestyle_Lifestyle modification don't help (Reference = Maintaining a healthy lifestyle)	0.184	0.386	0.477	0.633	1.20	0.56-2.56
Barriers to practicing lifestyle_Other (Reference = Maintaining a healthy lifestyle)	1.227	0.824	1.489	0.136	3.41	0.68-17.15
No. risk factors for metabolic syndrome	-0.340	0.080	-4.238	<.001	0.71	0.61-0.83
Null deviance: 983.99 Residual deviance: 868.12 AIC: 914.12						

*$p < 0.05$.

long-term and continuous education regarding MetS risk and complications is essential. Direct patient-provider interactions have been shown to enhance motivation for behavior change (18), and personalized intervention delivered by trained healthcare professionals may be particularly effective in promoting sustained lifestyle modification (19).

Among participants with MetS risk factors, regular hospital visits were the most commonly reported lifestyle practice, whereas lack of knowledge regarding appropriate lifestyle behaviors was the primary barrier. This suggests a predominant reliance on pharmacological management rather than comprehensive lifestyle modification. Effective prevention of CVD complications associated with MetS requires integrated interventions encompassing both dietary modifications and regular physical activity (13). Therefore, practical, targeted strategies are warranted to enhance adoption and maintenance of lifestyle changes.

Although low-to-moderate intensity exercise provided some health benefits (20), current guidelines, including the Physical Activity Guidelines for Americans, recommend moderate-to-vigorous physical activity (MVPA) for optimal cardiometabolic outcomes (21). Evidence indicates that increased MVPA is more strongly associated with reduced MetS prevalence in men compared to women (22). Structured programs modeled on cardiac rehabilitation may facilitate adherence by combining clinical oversight with individualized exercise plans, and the long-term sustainability of such interventions should be systematically evaluated.

While sodium restriction is commonly recommended, emerging evidence suggests that both excessive and insufficient sodium intake may contribute to metabolic dysfunction, including insulin resistance and obesity (23). Structured dietary interventions, such as the Dietary Approaches to Stop Hypertension

Copyright© AE&M all rights reserved.

(DASH) diet (24), Mediterranean diet, and Nordic diet (25), which emphasize nutrient balance rather than strict sodium reduction, may provide broader metabolic benefits. Additionally, accumulating evidence highlights the role of sleep quality in metabolic health (26), suggesting that sleep management should be integrated into comprehensive lifestyle programs, potentially through home-based or technology-assisted interventions to enhance, especially among younger populations.

This study identified female sex, older age, and greater awareness of MetS complications as significant predictors of engagement in healthy lifestyle behaviors. MetS prevalence increases with age in both sexes (27), with a pronounced rise in postmenopausal women (28). While some studies indicated that older women with lower healthy lifestyle adherence are at elevated risk of MetS, others evidence suggests that older adults may adopt protective health behaviors more consistently (27). Cohort studies have further demonstrated that lifestyle interventions may yield greater reduction in MetS risk among older men compared to younger adults or women, potentially reflecting pre-existing behavioral differences (29). These findings underscore the importance of tailoring interventions according to both age and sex.

Participants with higher awareness of the relationship between MetS and CVD complications were more likely to engage in preventive lifestyle behaviors. Furthermore, a family history of CVD was associated with a higher prevalence of MetS risk factors. These findings hightlight the need for tailored educational interventions that provide practical, real-world examples demonstrating that effective management of MetS can reduce CVD complications, lower healthcare costs, alleviate familial burden, and improved quality of life for patients and their families. Implementing a systematic management framework that includes assessments such as microalbuminuria testing and fundus examinations within national health screening programs may facilitate early detection of CVD complications associated with MetS. Consistent monitoring beginning in the third decade of life, with follow-up during routine health checkups, would promote sustained preventive management.

Despite the strengths of this study, including a large, nationally representative sample, several limitations should be acknowledged.

First, lifestyle practices were assessed via self-report, which may introduce reporting bias and limit the objectivity of behavioral measures. Second, adults age ≥70 years were excluded due to the online survey format, potentially limiting generalizability to older populations. Third, psychological variables such as stress, known to influence MetS risk and lifestyle adherence (30), were not assessed. Future research should incorporate stress and sleep quality, and other behavioral determinants to inform comprehensive lifestyle intervention programs. Finally, the observed variation in lifestyle adherence by age and sex emphasizes the necessity for personalized interventions. Developing and evaluating the effectiveness of tailored programs will be critical for reducing the burden of MetS and improving long-term health outcomes.

In conclusion, this study evaluated the prevalence of MetS risk factors and adherence to healthy lifestyle behaviors among South Korean adults. Among the assessed risk factors, abdominal (central) obesity was the most prevalent within the META group; however, awareness and routine monitoring—particularly waist circumference assessment—remained limited. Given its critical role in MetS pathogenesis and CVD risk, waist circumference measurement should be emphasized through targeted public education and systematic integration into routine clinical practice.

Female sex, older age, and greater awareness of MetS-related complications were significantly associated with higher adherence to healthy lifestyle behaviors. These findings underscore the importance of tailored, demographic-specific, and preventive interventions aimed at delaying or preventing the onset of MetS and its associated CVD complications. Implementation of such strategies has the potential to reduce healthcare costs, alleviate disease burden, and improved long-term health outcomes at both individual and population levels.

Author contributions: Jong Sun Ok, Prof, PhD: Formal analysis, methodology, validation, visualization, writing – original draft, writing – review & editing. Kyung-Jin Kim, PhD, MD: Validation, visualization, writing – review & editing. Kyung-Hee Kim, PhD, MD: Validation, visualization, writing – review & editing.

Copyright© AE&M all rights reserved.

Do Kyeong Song, PhD, MD: Validation, visualization, writing – review & editing. Kyung Jin Ahn, PhD, MD: Validation, visualization, writing – review & editing. Chan Seok Park, PhD, MD: Validation, visualization, writing – review & editing. Mi Seung Shin, PhD, MD: Conceptualization, data curation, funding acquisition, investigation, project administration, resources, software, supervision, validation, writing – original draft, writing – review & editing.

Statement of ethics: ethics approval was obtained from the Institutional Review Board of Gachon University Medical Center (IRB No. GFIRB2023-084).

Funding information: this research received no specific grant from any funding agency in the public, commercial, or not-for-profit sectors.

Disclosure: no potential conflict of interest relevant to this article was reported.

Data availability: datasets related to this article will be available upon request to the corresponding author.

REFERENCES

1. Saklayen MG. The Global Epidemic of the Metabolic Syndrome. Curr Hypertens Rep. 2018;20(2):12. doi: 10.1007/s11906-018-0812-z.
2. Mozumdar A, Liguori G. Persistent increase of prevalence of metabolic syndrome among US adults: NHANES III to NHANES 1999–2006. Diabetes care. 2011;34(1):216-219. doi: 10.2337/dc10-0879.
3. de Carvalho Vidigal F, Bressan J, Babio N, Salas-Salvado J. Prevalence of metabolic syndrome in Brazilian adults: a systematic review. BMC public health. 2013;13(1):1-10. doi: 10.1186/1471-2458-13-1198.
4. Korean National Health Insurance Service. Health screening statistical yearbook in 2021; 2021. Available from: https://sbsgm.saglik.gov.tr/Eklenti/45317/0/siy2021-ingilizcepdf.pdf. Accessed on Mar 20, 2024.
5. Moore JX, Chaudhary N, Akinyemiju T. Metabolic syndrome prevalence by race/ethnicity and sex in the United States, National Health and Nutrition Examination Survey, 1988–2012. Prev Chronic Dis. 2017;14(E24):1-16. doi: 10.5888/pcd14.160287.
6. Lorenzo C, Williams K, Hunt KJ, Haffner SM. The National Cholesterol Education Program–Adult Treatment Panel III, International Diabetes Federation, and World Health Organization definitions of the metabolic syndrome as predictors of incident cardiovascular disease and diabetes. Diabetes care. 2007;30(1):8-13. doi: 10.2337/dc06-1414.
7. Liu Y, Ozodiegwu ID, Yu Y, Hess R, Bie R. An association of health behaviors with depression and metabolic risks: data from 2007 to 2014 US National Health and Nutrition Examination Survey. J Affect Disord. 2017;217:190-196. doi: 10.1016/j.jad.2017.04.009.
8. Marcos-Delgado A, Hernández-Segura N, Fernández-Villa T, Molina AJ, Martin V. The effect of lifestyle intervention on health-related quality of life in adults with metabolic syndrome: a meta-analysis. Int J Environ Res Public Health. 2021;18(3):887. doi: 10.3390/ijerph18030887.
9. Grundy SM, Cleeman JI, Daniels SR, Donato KA, Eckel RH, Franklin BA, et al. Diagnosis and management of the metabolic syndrome: an American Heart Association/National Heart, Lung, and Blood Institute scientific statement. Circulation. 2005;112(17):2735-2752. doi: 10.1161/CIRCULATIONAHA.105.169404.
10. Moore SE, Harris C, Wimberly Y. Perception of Weight and Threat to Health. J Nati Med Asso. 2010;102(2):119-125. doi: 10.1016/s0027-9684(15)30499-5.
11. Kim HJ, Shin MS, Kim KH, Jung MH, Cho DH, Lee JH, et al. Metabolic Syndrome Awareness in the General Korean Population: Results from a Nationwide Survey. Korean J Intern Med. 2024;39(2):272-282. doi: 10.3904/kjim.2023.363.
12. Watanabe M, Yokotsuka M, Yamaoka K, Adachi M, Nemoto A, Tango T. Effects of a Lifestyle Modification Programme to Reduce the Number of Risk Factors for Metabolic Syndrome: A Randomised Controlled Trial. Public Health Nutr. 2017; 20(1):142-153. doi: 10.1017/S1368980016001920.
13. Park S, Lee J, Seok JW, Park CG, Jun J. Comprehensive Lifestyle Modification Interventions for Metabolic Syndrome: A Systematic Review and Meta-Analysis. J Nurs Scholarsh. 2024;56(2):249-259. doi: 10.1111/jnu.12946.
14. Lovejoy JC, Sainsbury A. Sex differences in obesity and the regulation of energy homeostasis. Obes Rev. 2009;10(2):154-167. doi: 10.1111/j.1467-789X.2008.00529.x.
15. Deurenberg P, Deurenberg-Yap M, Guricci S. Asians are different from Caucasians and from each other in their body mass index/body fat per cent relationship. Obes Rev. 2002;3(3):141-146. doi: 10.1046/j.1467-789x.2002.00065.x.
16. Krakauer NY, Krakauer JC. A new body shape index predicts mortality hazard independently of body mass index. PLoS One. 2012;7(7):e39504. doi: 10.1371/journal.pone.0039504.
17. Huh JH, Kang DR, Kim JY, Koh KK, and on behalf of the Taskforce Team of the Metabolic Syndrome Fact Sheet of the Korean Society of Cardiometabolic. Metabolic Syndrome Fact Sheet 2021: Executive Report. Cardiometab Syndr. J 2021;1(2):125-134. doi: 10.51789/cmsj.2021.1.e15.
18. Jeon HW, Kim JH. A study of factors influencing on health 1behavior compliance in metabolic syndrome risk group's. J Korean Academia-Industrial cooperation Society. 2022;23(1):236-246. doi: 10.5762/KAIS.2022.23.1.236.
19. Bassi N, Karagodin I, Wang S, Vassallo P, Priyanath A, Massaro E, et al. Lifestyle modification for metabolic syndrome: a systematic review. Am J Med. 2014;127(12):1242. e1-10. doi: 10.1016/j.amjmed.2014.06.035.
20. Morga P, Cieślik B, Sekułowicz M, Bujnowska-Fedak M, Drower I, Szczepanska-Gieracha J. Low-intensity exercise as a modifier of depressive symptoms and self-perceived stress level in women with metabolic syndrome. J Sports Sci Med. 2021;20(2):222-228. doi: 10.52082/jssm.2021.222.
21. Piercy KL, Troiano RP, Ballard RM, Carlson SA, Fulton JE, Galuska DA, et al. The physical activity guidelines for Americans. JAMA. 2018;320(19):2020-2028. doi: 10.1001/jama.2018.14854.
22. Li H, Lynn HS, Zipunnikov V. Sex and Age Differences in Association between Physical Activity and Metabolic Syndrome: Results from NHANES 2003-2006. Healthcare (Basel). 2023;11(8):1059. doi: 10.3390/healthcare11081059.
23. Wu Q, Burley G, Li LC, Lin S, Shi YC. The role of dietary salt in metabolism and energy balance: Insights beyond cardiovascular disease. Diabetes Obes Metab. 2023;25(5):1147-1161. doi: 10.1111/dom.14980.
24. Azadbakht L, Mirmiran P, Esmaillzadeh A, Azizi T, Azizi F. Beneficial effects of a Dietary Approaches to Stop Hypertension eating plan on features of the metabolic syndrome. Diabetes Care. 2005;28(12):2823-2831. doi: 10.2337/diacare.28.12.2823.
25. Dayi T, Ozgoren M. Effects of the Mediterranean diet on the components of metabolic syndrome. J Prev Med Hyg. 2022;63(2 Suppl 3):E56-E64. doi: 10.15167/2421-4248/jpmh2022.63.2S3.2747.
26. Chou FY, Chiu TF, Huang FW, Hsu TY, Liu CY, Lin CH, et al. The effect of exercise on the risk of metabolic syndrome associated with sleep insufficiency: a cross-sectional study. Front Cardiovasc Med. 2023;10:1192241. doi: 10.3389/fcvm.2023.1192241.
27. Vajdi M, Karimi A, Farhangi MA, Ardekani AM. The association between healthy lifestyle score and risk of metabolic syndrome in Iranian adults: a cross-sectional study. BMC Endocr Disord. 2023;23(1):16. doi: 10.1186/s12902-023-01270-0.
28. Patni R, Mahajan A. The Metabolic Syndrome and Menopause. J Midlife Health. 2018;9(3):111-112. doi: 10.4103/0976-7800.241951.
29. Garralda-Del-Villar M, Carlos-Chillerón S, Diaz-Gutierrez J, Ruiz-Canel M, Gea A, Martinez-Ginzalez MA, et al. Healthy Lifestyle and Incidence of Metabolic Syndrome in the SUN Cohort. Nutrients. 2018;11(1):65. doi: 10.3390/nu11010065.
30. Kuo WC, Bratzke LC, Oakley LD, Kuo F, Wang H, Brown RL. The association between psychological stress and metabolic syndrome: A systematic review and meta-analysis. Obes Rev. 2019;20(11):1651-1664. doi: 10.1111/obr.12915.

Copyright© AE&M all rights reserved.

SUPPLEMENTARY MATERIAL

1. Demographic characteristics

DQ1. Please answer your age
_____ years old

DQ2. Please answer your gender

① Male ② Female

DQ3. Please answer your highest level of education

① Middle school graduate or younger ② High school ③ College and university graduate or higher

DQ4. Please answer your household income (KRW)

① less than 1 million won ② less than 1 to 2 million won
③ less than 2 to 3 million won ④ less than 3 to 4 million won
⑤ less than 4 to 5 million won ⑥ 5 million won or more

DQ5. If you have suffered from or are suffering from any of the following conditions diagnosed by a doctor, please select the appropriate option

Hypertension (HTN)	Yes	No
Dyslipidemia (Hyperlipidemia)	Yes	No
DM	Yes	No
Drinking	Yes	No
Smoking	Yes	No
Abdomen obesity	Yes	No

DQ6. Please answer with your occupation

①	Self-employment (store, shops, restaurants, etc.)
②	Sales (office workers who work outside the office more than inside the office, salespeople, etc.)
③	Service/Customer service (clerks, bank tellers, etc.)
④	Technical/Operational (production workers, etc.)
⑤	General office work (office workers who work inside the office more than outside the office, office workers, etc.)
⑥	Administration/Management (manager, managing director, CEO, etc.)
⑦	Professional (professors, doctors, etc.)
⑧	Public official
⑨	Teacher
⑩	College/University student (including students on leave)
⑪	Graduate student (including students on leave)
⑫	Housewife (married woman without a job)
⑬	Part time/Freelancer
⑭	None
⑮	Others

DQ7. Does anyone in your family have CVD (cardiovascular disease)

① Yes ③ No

DQ8. Please answer whether you are married or not

① Single
② Married
③ Divorce/Bereaved
④ Others

2. Metabolic syndrome related questionnaire

1. Do you think you know(aware) about metabolic syndrome?

1) Know very well
2) Know it well
3) Know a little bit
4) Don't know
5) Don't know at all

2. Do you think that people with metabolic syndrome are more likely to develop diabetes or cardiovascular disease in the future?

1) Strongly agree
2) Somewhat agree
3) Slightly agree
4) Do not agree
5) Do not agree at all

3. Have you measured your waist circumference in the last three years?

1) Frequently
2) Occasionally
3) Rarely
4) Never

4. Have you measured your weight in the last three years?

1) Frequently
2) Occasionally
3) Rarely
4) Never

5. What lifestyle changes are you making to prevent metabolic syndrome (select all that apply)

1) Measure blood pressure
2) Routine medical checkup
3) Adequate sleep
4) Low salt diet
5) Physical activity
6) Taking vitamins
7) Taking health supplements (red ginseng, etc.)

6. What do you think are the barriers to implementing a healthy lifestyle to prevent metabolic syndrome

1) Economic burden (money or insurance)
2) Maintaining a healthy lifestyle
3) Lack of time
4) Too much to do
5) Not sure what to do
6) Lifestyle modification don't help (changing lifestyle will reduce my risk of developing the disease)
7) Others

Copyright© AE&M all rights reserved.

Archives of Endocrinology and Metabolism
ISSN 2359-4292
OFFICIAL JOURNAL OF THE BRAZILIAN SOCIETY OF ENDOCRINOLOGY AND METABOLISM

original

Relationships between glucose variability with white matter hyperintensity and cerebrovascular abnormalities

Cheng-Chieh Lin[1,2,3]
https://orcid.org/0000-0002-9625-6216

Chia-Ing Li[1,2]
https://orcid.org/0000-0002-7937-2928

Chiu-Shong Liu[1,2,3]
https://orcid.org/0000-0003-0274-2465

Chih-Hsueh Lin[1,3]
https://orcid.org/0000-0002-9159-6326

Shing-Yu Yang[4]
https://orcid.org/0009-0008-1873-5191

Tsai-Chung Li[4,5]
https://orcid.org/0000-0002-3346-7462

[1] School of Medicine, College of Medicine, China Medical University, Taichung, Taiwan
[2] Department of Medical Research, China Medical University Hospital, Taichung, Taiwan
[3] Department of Family Medicine, China Medical University Hospital, Taichung, Taiwan
[4] Department of Public Health, College of Public Health, China Medical University, Taichung, Taiwan
[5] Department of Audiology and Speech-Language Pathology, Asia University, Taichung, Taiwan

ABSTRACT

Objective: Epidemiological studies have revealed that glucose variability (GV) is a predictor of stroke, cognitive impairment, and dementia in patients with type 2 diabetes mellitus (T2DM). However, evidence on the associations of GV with white matter hyperintensity (WMH) and cerebrovascular abnormalities remains scarce. This study aimed to explore the relationships of GV with WMH and cerebrovascular abnormalities using epidemiological and Mendelian randomization (MR) approaches. The MR approach was used to assess the effects of genetic proxies for GV on MRI outcomes. **Subjects and methods:** This cross-sectional study was conducted at a medical center where patients with T2DM were recruited. The measures for fasting plasma glucose (FPG) and HbA1c variability included the standard deviation, coefficient of variation, average real variability (ARV), and variability independent of the mean (VIM). Brain magnetic resonance images were analyzed to assess WMHs and cerebrovascular abnormalities. For MR, instrumental variables were used to assess the causal relationships between glycemic variability and outcome based on two-stage regression analysis. **Results:** This study included 2,247 subjects, of whom 1,122 had WMH and 957 had cerebrovascular abnormalities. We found 80 independent single-nucleotide polymorphisms associated with GV but not with WMH or cerebrovascular abnormalities, which were subsequently used as genetic instruments. Genetically increased, unweighted FPG-VIM was linked with WMH (odds ratio 1.17 [95% CI 1.08, 1.27] per standard deviation). All genetically increased, unweighted and weighted GV measures were associated with cerebrovascular abnormalities, except FPG-ARV. **Conclusion:** Our study provided evidence that genetically predicted GV was associated with WMH and cerebrovascular abnormalities, supporting a potential causal link under MR assumptions.

Keywords: Type 2 diabetes; glycemic variability; white matter hyperintensity; cerebrovascular abnormalities

INTRODUCTION

A global pandemic of type 2 diabetes is currently underway, driven by factors such as rapid urbanization, an aging global population, and rising obesity rates associated with energy-dense diets and sedentary lifestyles. This public health crisis affects low-, middle-, and high-income countries. The global prevalence of type 2 diabetes increased markedly from 151 million in 2000 to 537 million by 2021, significantly exceeding the earlier 1998 projection of 300 million by 2021 (1,2). Type 2 diabetes is linked to a range of complications, including macrovascular conditions — such as coronary artery disease, stroke, and peripheral arterial disease — and microvascular complications. These outcomes, largely attributed to atherosclerotic processes, impose a considerable burden on health care systems worldwide (3-5). Cardiovascular diseases, including heart failure, coronary heart disease, cerebrovascular disease, and other cardiac conditions, remained the leading cause of mortality worldwide and accounted for more than 30% of all deaths in 2016 (6).

Received on Sep/23/2025
Accepted on Mar/20/2026
DOI: 10.20945/2359-4292-2026-0062

Correspondence to:
Tsai-Chung Li
China Medical University, No. 100, Sec. 1,
Jingmao Rd., Beitun Dist.,
Taichung City 406040,
Taiwan R.O.C.
tcli@mail.cmu.edu.tw

Associated editor:
Marcelo Mori
https://orcid.org/0000-0001-7112-5263

This is an open-access article distributed under the terms of the Creative Commons Attribution License

Copyright© AE&M all rights reserved.

A comprehensive meta-analysis of 102 prospective studies revealed that compared with nondiabetic individuals, individuals with diabetes face a 2- to 4-fold increased risk of ischemic stroke and coronary heart disease and a 1.5- to 3.6-fold increase in all-cause mortality. These risks are further exacerbated by poor glycemic control (7).

Glycemic control has long been considered a fundamental strategy for mitigating diabetic complications, with glycosylated hemoglobin (HbA1c) widely recognized as the "gold standard" biomarker for long-term glycemic regulation. However, randomized controlled trials have indicated that reduced blood glucose levels do not necessarily correspond to a decreased incidence of diabetic complications (8-10). One plausible explanation is that these studies did not adequately account for glucose variability—marked fluctuations in blood glucose levels over time—which may play a critical role in the development of diabetic complications. The concept of "glucose variability" or "glycemic variability" has garnered increasing attention from the research community. Mounting evidence suggests that visit-to-visit glucose fluctuations are significantly associated with diabetes-related complications and mortality. To date, experimental evidence confirming the harmful effects of glucose variability is lacking. Thus, further investigations using methodologies capable of establishing experimental causality are warranted to clarify the role of glucose variability in the pathogenesis of diabetes-related complications. Mendelian randomization (MR) provides an alternative methodological framework for inferring causal relationships and generating evidence analogous to experimental results.

Quantitative and noninvasive in nature, brain magnetic resonance imaging (MRI) has become increasingly accessible in clinical settings and is frequently utilized as a surrogate endpoint for identifying novel determinants of brain health (11). One commonly examined MRI parameter is white matter hyperintensity (WMH) volume, which represents lesions in the white matter of the brain. These lesions make the white matter appear hyperintense on fluid-attenuated inversion recovery (FLAIR) sequences. Brain MRI, particularly WMH assessment, is widely regarded as a marker of cerebral small vessel disease (12). Increased WMH volumes have been associated with increased risks of Alzheimer's disease, incident stroke, all-cause mortality, and cognitive decline (13). Advanced brain MRI techniques enable the visualization and quantification of structural and microvascular abnormalities, thereby facilitating the early detection of cerebrovascular disease even in asymptomatic individuals.

Previous studies that employed traditional epidemiologic or MR designs to examine the association of glucose level or variability with WMH and cerebrovascular abnormalities have been limited (14-16). One study explored the association between HbA1c levels and WMH in the general population (16). Research on glucose variability has focused primarily on individuals with type 1 diabetes (14), whereas another study investigated a small sample of older adults with type 2 diabetes who carried the APOE4 allele (15). One MR study investigated the association between HbA1c levels and WMH. Considering the limited number of studies and their small sample sizes, we aimed to assess the associations between visit-to-visit glucose variability and brain MRI measurements using observational epidemiologic and MR approaches. The MR approach was used to assess the effects of glucose variability (GV) on MRI outcomes.

SUBJECTS AND METHODS

Study subjects

A retrospective cohort study was conducted among individuals with type 2 diabetes who were enrolled in the Diabetes Care Management Program (DCMP) at China Medical University Hospital (CMUH). The inclusion criterion was individuals diagnosed with diabetes, identified by the International Classification of Diseases, Ninth Revision, Clinical Modification (ICD-9-CM) code 250. The exclusion criteria included individuals younger than 30 years, those with type 1 diabetes (ICD-9-CM codes 250.x1/x3), and those diagnosed with gestational diabetes (ICD-9-CM code 648.83). Participants were recruited between November 2001 and June 2022. The index date was defined as the date of the first available brain MRI measurement. Individuals lacking data on brain MRI, laboratory tests, or dietary records were excluded

Copyright© AE&M all rights reserved.

from the analysis (**Figure 1**). Measurements for other study variables were obtained from the date closest to the index date. This study was approved by the Ethical Review Board of the CMUH (CMUH112-REC1-007).

Data source

The data for this study were derived from the computerized databases of the Clinical Research Data Repository (CRDR) and the DCMP at CMUH in Taichung, Taiwan. Established in 2017, the CMUH-CRDR integrates data from multiple clinical sources with the goal of improving healthcare quality by consolidating trackable patient information generated during routine clinical practice. This repository includes comprehensive data, such as laboratory and physiological measurements, prescription records, hospitalizations, surgical procedures, and emergency department visits. It also contains whole-genome genotyping data generated using Affymetrix Axiom Genome-Wide TPM array chips (Affymetrix, Santa Clara, CA, USA). Moreover, the DCMP database contains information on individuals diagnosed with diabetes based on the diagnostic criteria set forth by the American Diabetes Association. Eligible patients were invited to enroll in the program by their physicians. Only healthcare professionals who have completed the required clinical education and training programs were authorized to recruit patients into the DCMP.

Measurements

Upon enrollment in the DCMP, patients underwent a series of assessments, such as anthropometric measurements and blood and urine tests. Information on dietary habits, lifestyle factors, and past or current medical conditions was collected by trained case nurses using a standardized computerized questionnaire. Detailed definitions of all study variables are provided in the sections below.

Key predictor variables

In this study, the primary predictor variable was glucose variability, which was using the following metrics: variability independent of the mean (VIM), average real variability (ARV), coefficient of variation (CV),

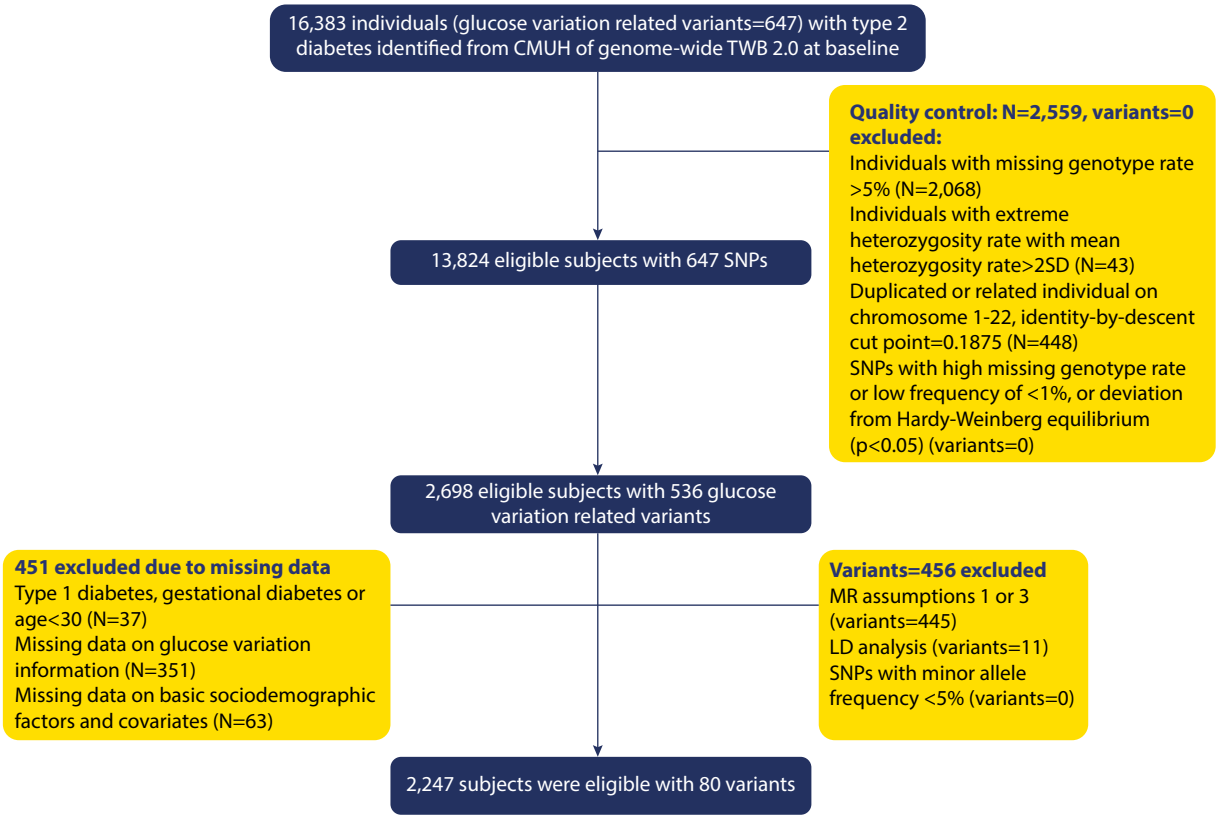


Figure 1. The study flowchart for study subject and SNP selection.

Copyright© AE&M all rights reserved.

standard deviation (SD), and slope of HbA1c and fasting plasma glucose (FPG). These indices were calculated on the basis of annual outpatient measurements over the 1-year period preceding the index date. As recommended in prior research, variability estimates were adjusted using a weighting factor equal to the reciprocal of √(n/(n − 1)) to account for differences in the number of glucose measurements per individual (17). Glucose variability metrics were derived only for participants with at least two recorded measurements of HbA1c and FPG.

Covariates

The demographic and family history variables included participants' sex; age at entry into the DCMP. Lifestyle variables, as recorded in the DCMP dataset, included physical activity, alcohol consumption, smoking, passive smoking, and habitual dietary intake.

The medication variables included the use of oral hypoglycemic agents and insulin. Oral agents were categorized into seven classes as follows: meglitinides, sulfonylureas, biguanides, insulin sensitizers, dipeptidyl peptidase-4 inhibitors, α-glucosidase inhibitors, and other compounds. Insulin types included insulin aspart, regular insulin, neutral protamine hagedorn, levemir, glucagon-like peptide-1 analogs, and lantus. The use of other medications, including antihypertensives (e.g., calcium channel blockers), nephropathy medications, and lipid-lowering agents (e.g., statins), was recorded electronically and classified as "yes" or "no", baseline comorbidities and diabetic complications were also classified dichotomously. Comorbidities included hyperlipidemia, hypertension, and obesity. Chronic complications included stroke, peripheral neuropathy, peripheral vascular disease, retinopathy, diabetic foot, nephropathy, and amputation. Acute complications included hyperglycemic hyperosmolar nonketotic coma (HHNK), severe hypoglycemia, and diabetic ketoacidosis.

Instrumental variables

Single-nucleotide polymorphism (SNP) genotyping in MR analysis

The SNP data used as instrumental variables were obtained from the iHi Genomics, CMUH-CRDR (18) and were based on DNA samples genotyped using the TPM array and analyzed with the Axiom Genome-Wide Array Plate System (Affymetrix, Santa Clara, CA, USA). Quality control included assessment of Hardy–Weinberg equilibrium using PLINK v2.0 (19), and genotype imputation was performed with IMPUTE2 software (20) using the 1000 Genomes Project as the reference panel. Genetic variants were selected under the guidance of previous studies employing candidate gene and genome-wide association study (GWAS) approaches for HbA1c (21-23) and FPG (24,25). A curated list of SNPs associated with HbA1c and FPG was constructed. For HbA1c, the variants in genes involved in glycemic pathways (e.g., *CDKAL1*, *DGKB*, *GCK*, *SLC30A8*, *MTAP*, and *KL*) and nonglycemic pathways (e.g., *SPATS2L*, *TRAM2-AS1*, *RPA2P2*, *KCNKS*, and *ARAP3*) were included. For FPG, SNPs from loci such as *HFE*, *MYB*, *ANK1*, *HK1*, and *PHB2* were considered. The MR literature was further searched for SNPs (16,26-32), especially those linked to the potential biological mechanisms of glucose variability. A total of 536 SNPs were found in the GWAS data from iHi Genomics. The SNPs not identified in the iHi genomics dataset, with minor allele frequencies < 5%, violating MR assumptions 1 and 3 (SNP = 445), and in high linkage disequilibrium (SNP = 11) were removed. Finally, 80 SNPs were included in the analysis. Approval was obtained from the Human Research Committee of CMUH (CMUH112-REC1-007), and this study was conducted in accordance with relevant regulations and guidelines.

Assessment of brain MRI scans

Brain MRI scans were performed using a 3.0 Tesla scanner (SIGNA HDxt), and imaging data were retrieved from the hospital's electronic medical records. Axial T2-weighted FLAIR sequences were used for the assessment of WMHs. WMHs were defined as those with subcortical or periventricular hyperintensities visible on FLAIR images and were assessed visually by a board-certified radiologist, who was blinded to the clinical information. WMH was operationalized as a binary variable, defined as "yes" if any WMH lesion was identified, and "no" otherwise. The inter- and intrarater reliability of cerebrovascular

Copyright© AE&M all rights reserved.

findings were evaluated on a sample of 60 MRI images, yielding kappa statistics exceeding 0.80 across all assessed conditions, indicating high agreement. Cerebrovascular abnormalities were also assessed by a radiologist. Cerebrovascular abnormalities included stenosis or occlusion of major intracranial or internal carotid arteries, aneurysms, lacunar or small infarctions, intracerebral hemorrhage, and lobar infarctions.

Statistical analysis

Descriptive statistics are reported as the means and standard deviations for continuous variables and as frequencies and proportions for categorical variables. Bivariate analyses were conducted using chi-square tests for categorical variables and two-sample *t*-tests for continuous variables. Multiple logistic regression was used to adjust for age, sex, lifestyle behaviors (smoking, alcohol consumption, physical activity, and BMI), diabetes-related variables (duration of diabetes and type of hypoglycemic drug use), comorbidities (stroke, hypertension, obesity, coronary artery disease, hyperlipidemia, peripheral neuropathy, neuropathy and nephropathy), drug-related variables (cardiovascular medications, hyperlipidemia medications, and hypertension medications) and biomarkers (HDL-C, TG, LDL-C, TC, eGFR, FPG, and HbA1c). All statistical analyses were performed using SAS version 9.4 (SAS Institute, Cary, NC) with two-tailed *p*-values and a significance threshold of 0.05.

MR analysis

Quality control excluded individuals with high genotyping missingness, extreme heterozygosity, or genetic relatedness. SNPs were removed for low minor allele frequency, high missingness, or Hardy–Weinberg disequilibrium (tested via chi-square in controls). MR assumptions were assessed as follows: For relevance (assumption 1), SNP associations with glucose variability were tested using ANOVA and linear regression (additive model); for exclusion restriction (assumption 3), chi-square tests ensured no association with brain MRI variables. Only SNPs meeting both criteria were used to construct weighted and unweighted genetic risk scores (GRSs).

Before the GRSs were constructed, linkage disequilibrium (LD) was assessed using pairwise r^2 in Haploview v4.2; for SNP pairs with $r^2 > 0.8$, one was retained on the basis of prior associations with glucose traits. The weighted GRS was calculated by summing the products of minor allele counts and their regression coefficients. GRS values were divided into quartiles to assess linearity, and analyzed as a continuous variable. Linear regression was used to test the association between GRSs and glucose variability (assumption 1), whereas multinomial logistic regression was used to assess the associations with covariates (assumption 2). Assumption 3 was tested via logistic regression with brain MRI variables.

MR analyses used two-stage instrumental variable regression with multivariable adjustment to estimate the causal effect of glucose variability on brain MRI outcomes. In stage one, glucose variability was predicted from the weighted GRS. In stage two, these predicted values were used in logistic regression with brain MRI measures. Models adjusted for first-stage residuals, covariates violating MR assumption 2, and the top 10 genetic principal components. Horizontal pleiotropy was assessed using MR–Egger regression, and between-instrument heterogeneity was evaluated using Cochran's Q statistics under the inverse-variance weighted framework. All tests were two-sided with $p < 0.05$.

RESULTS

Baseline characteristics of the study subjects

A total of 2,247 individuals with type 2 diabetes from the Taichung Diabetes Study were included, with a mean baseline age of 65.00 years (SD = 11.14). Among these participants, 1,122 (49.9%) had WMHs and 957 (42.6%) had cerebrovascular abnormalities. **Table 1** shows the characteristics of the study subjects grouped by WMH volume and cerebrovascular abnormalities. Individuals with WMH were significantly older and had a low proportion of men and smokers. They also had a long mean duration of diabetes, a high prevalence of cardiovascular and antihypertensive medication use, and low mean LDL-C level and eGFR. Moreover, significantly more individuals with cerebrovascular abnormalities were older and had a high

Copyright© AE&M all rights reserved.

Table 1. Comparisons of sociodemographic factors, lifestyle behaviors, diabetes-related variables, glucose variation and comorbidities according to WMH or cerebrovascular abnormality

Variables	WMH, N (%)		P value	Cerebrovascular abnormality, N (%)		P value
	No (N=1,125)	Yes (N=1,122)		No (N=1,290)	Yes (N=957)	
Sociodemographic factors						
Age, years, mean±SD	62.10±11.29	67.90±10.68	<0.001	64.07±11.50	66.24±11.06	<0.001
Gender			0.02			0.02
Men	634 (56.36)	576 (51.34)		666 (51.63)	544 (56.84)	
Women	491 (43.64)	546 (48.66)		624 (48.37)	413 (43.16)	
Education level (years)			<0.001			0.01
0	163 (42.23)	223 (57.77)		209 (54.15)	177 (45.85)	
1-6	250 (42.09)	344 (57.91)		323 (54.38)	271 (45.62)	
7-12	426 (54.62)	354 (45.38)		449 (57.56)	331 (42.44)	
≥12	286 (58.73)	201 (41.27)		309 (63.45)	178 (36.55)	
APOE4 (rs429358)			0.03			0.28
TT	902 (80.18)	939 (83.69)		1071 (83.02)	770 (80.46)	
CT	219 (19.47)	175 (15.60)		213 (16.51)	181 (18.91)	
CC	4 (0.36)	8 (0.71)		6 (0.47)	6 (0.63)	
Lifestyle behaviors						
Smoking			0.03			0.72
No	963 (85.6)	996 (88.77)		1128 (87.44)	831 (86.83)	
Yes	162 (14.4)	126 (11.23)		162 (12.56)	126 (13.17)	
Alcohol drinking			0.40			0.49
No	1068 (94.93)	1055 (94.03)		1223 (94.81)	900 (94.04)	
Yes	57 (5.07)	67 (5.97)		67 (5.19)	57 (5.96)	
Physical activity			0.43			0.95
No	600 (53.33)	618 (55.08)		698 (54.11)	520 (54.34)	
Yes	525 (46.67)	504 (44.92)		592 (45.89)	437 (45.66)	
BMI, kg/m^2, mean±SD	26.29±4.34	26.10±3.9	0.28	26.32±4.22	26.04±3.99	0.11
Diabetes-related variables						
Duration of diabetes, years, mean±SD	6.18±7.54	7.39±8.09	<0.001	6.38±7.48	7.33±8.28	0.005
Type of hypoglycemic drug use			0.59			0.02
No	62 (5.51)	48 (4.28)		73 (5.66)	37 (3.87)	
OAD	905 (80.44)	910 (81.11)		1049 (81.32)	766 (80.04)	
Inject insulin	16 (1.42)	16 (1.43)		21 (1.63)	11 (1.15)	
Both	142 (12.62)	148 (13.19)		147 (11.40)	143 (14.94)	
Comorbidity						
Stroke	75 (6.67)	87 (7.75)	0.36	41 (3.18)	121 (12.64)	<0.001
Hypertension	422 (37.51)	445 (39.66)	0.32	466 (36.12)	401 (41.9)	0.006
Obesity	248 (22.04)	243 (21.66)	0.86	289 (22.4)	202 (21.04)	0.49
Coronary artery disease	83 (7.38)	63 (5.61)	0.11	68 (5.27)	78 (8.15)	0.008
Hyperlipidemia	296 (26.31)	286 (25.49)	0.69	347 (26.9)	235 (24.56)	0.23
Peripheral neuropathy	75 (6.67)	83 (7.4)	0.55	92 (7.13)	66 (6.9)	0.89
Neuropathy	23 (2.04)	22 (1.96)	1.00	16 (1.24)	29 (3.03)	0.005
Nephropathy	54 (4.80)	73 (6.51)	0.10	66 (5.12)	61 (6.37)	0.24
Drug-related variables						
Cardiovascular medications	312 (27.73)	367 (32.71)	0.01	333 (25.81)	346 (36.15)	<0.001
Hyperlipidemia medications	213 (18.93)	237 (21.12)	0.21	268 (20.78)	182 (19.02)	0.33
Hypertension medications	391 (34.76)	445 (39.66)	0.02	435 (33.72)	401 (41.9)	<0.001
Biomarker						
HDL-C (mg/dL)	42.78±11.25	43.41±12.25	0.20	43.99±12.01	41.89±11.32	<0.001
TG (mg/dL)	160.88±152.24	153.10±125.42	0.19	152.25±127.1	163.39±154.53	0.07
LDL-C (mg/dL)	105.55±37.31	102.27±35.19	0.03	105.04±36.09	102.4±36.53	0.09
TC (mg/dL)	181.34±50.8	178.04±46.09	0.11	180.48±48.68	178.64±48.31	0.37
eGFR (ml/min/1.73 m^2)	78.69±26.26	70.33±26.53	<0.001	77.41±26.02	70.6±27.15	<0.001
FPG (mg/dL)	141.04±50.69	137.46±47.01	0.08	138.27±48.7	140.59±49.19	0.27
HbA1c (%)	7.78±1.71	7.67±1.58	0.11	7.55±1.56	7.95±1.73	<0.001

Differences in continue variables were tested using the Student's *t* test. Differences in categorical variables were tested using the chi-square test.

SBP: Systolic blood pressure; DBP: Diastolic blood pressure; FPG: Fasting plasma glucose; HbA1c: Hemoglobin A1c; TG: Triglyceride; TC: Total cholesterol; HDL-C: High-density lipoprotein-cholesterol; LDL-C: Low-density lipoprotein-cholesterol; eGFR: Estimated glomerular filtration rate.

"No" = absence and "Yes" = presence of WMH/cerebrovascular abnormality according to the MRI criteria in Methods.

Copyright© AE&M all rights reserved.

proportion of men and a greater prevalence of injection use, oral hypoglycemic drug use, hypertension, stroke, coronary artery disease, and neuropathy. They also had a long mean duration of diabetes, high HbA1c levels, a high prevalence of cardiovascular and hypertension medication use, and low mean HDL-C level and eGFR.

Associations between glucose variability and brain MRI variables determined using an epidemiologic approach

Table 2 presents the odds ratios (ORs) and confidence intervals (CIs) for the presence of WMH and cerebrovascular abnormalities associated with various glucose variability measures in the study subjects with type 2 diabetes as observed in an epidemiological study. After adjustment for age and sex or multivariate adjustment, no significant associations were found between any glucose variability measures and the presence of WMH (all p>0.05). With the exception of HbA1c-VIM, all glucose variability measures were significantly associated with the presence of cerebrovascular abnormalities after adjustment for age and sex. Following multivariate adjustment, only AC-CV, AC-SD, AC-VIM, and AC-ARV remained significantly associated with the presence of cerebrovascular abnormalities. The OR per 1 unit change for glucose variability ranged from 1.12 (95% CI: 1.02, 1.23) for AC-ARV to 1.28 (95% CI: 1.15, 1.41) for AC-CV.

Evaluation of MR assumptions 1 and 3 at the SNP level

Supplementary Table 1 shows the regression coefficients for glucose variability measures and ORs for the presence of WMH and cerebrovascular abnormalities of the significant SNPs meeting SNP-level MR assumptions 1 (all $p < 0.05$) and 3 (all $p > 0.05$) as determined using an additive model. For the SNPs exhibiting negative associations, i.e., those with regression coefficients less than 0 or an ORs less than 1, we reversed the codes to 2, 1, or 0 depending on the number of minor alleles to ensure that the direction of the regression coefficients or ORs consistently remained positive.

MR–Egger regression was performed to test horizontal pleiotropy. The absolute values of the intercepts for the brain MRI variables ranged from 0.0003 to 0.025 (Supplementary Table 2). The results of the Cochran's Q statistics suggest no apparent horizontal pleiotropy because all the intercepts were not significantly different from zero (all $p > 0.05$).

The LD of the SNPs satisfying MR assumptions 1 and 3 was examined. (Supplementary Figure 1). The retained SNPs included AC-CV (19), AC-SD (16), AC-VIM (19), and AC-ARV (20) for FPG variation measures and HbA1c-CV (18), HbA1c-SD (19), HbA1c-VIM (10), and HbA1c-ARV (13) for HbA1c variation measures. We derived weighted and unweighted GRSs using these glucose variability-associated SNPs. The numbers of

Table 2. The odds ratios of WMH or cerebrovascular abnormality for various glucose variation measures in patients with type 2 diabetes using observational epidemiologic approach

Glucose variation	WMH OR (95% CI) per standard deviation		Cerebrovascular abnormality OR (95% CI) per standard deviation	
	Age- and sex-adjusted model	Multivariate model	Age- and sex-adjusted model	Multivariate model
AC-CV	1.00 (0.91, 1.09)	0.96 (0.87, 1.06)	1.38 (1.27, 1.50)***	1.28 (1.15, 1.41)***
AC-SD	0.97 (0.89, 1.06)	0.92 (0.82, 1.02)	1.31 (1.20, 1.43)***	1.17 (1.05, 1.31)**
AC-VIM	1.03 (0.95, 1.13)	1.01 (0.92, 1.11)	1.32 (1.21, 1.45)***	1.27 (1.15, 1.39)***
AC-ARV	1.05 (0.96, 1.14)	1.04 (0.95, 1.14)	1.19 (1.09, 1.30)***	1.12 (1.02, 1.23)*
HbA1c-CV	1.02 (0.92, 1.12)	1.00 (0.89, 1.12)	1.17 (1.06, 1.29)**	1.02 (0.91, 1.15)
HbA1c -SD	1.01 (0.91, 1.11)	0.97 (0.85, 1.11)	1.20 (1.08, 1.32)***	1.00 (0.88, 1.15)
HbA1c-VIM	1.04 (0.95, 1.15)	1.03 (0.93, 1.14)	1.10 (1.00, 1.21)	1.06 (0.95, 1.17)
HbA1c-ARV	1.00 (0.90, 1.10)	0.96 (0.85, 1.08)	1.18 (1.07, 1.31)**	1.02 (0.9, 1.14)

Multivariate model adjusted for age, sex, lifestyle behaviors (smoking, alcohol drinking, physical activity, and BMI), diabetes-related variables (duration of diabetes and type of hypoglycemic drug use), comorbidity (stroke, hypertension, obesity, coronary artery disease, hyperlipidemia, peripheral neuropathy, neuropathy and nephropathy), drug-related variables (cardiovascular medications, hyperlipidemia medications, and hypertension medications) and biomarkers (HDL-C, TG, LDL-C, TC, eGFR, FPG, and HbA1c).
*: P<0.05; **: P<0.01; ***: P<0.001; OR: odds ratio; CI: confidence interval.

Copyright© AE&M all rights reserved.

SNPs at each stage of instrument selection for each GV metric, including the initial SNP set, exclusion based on association with MRI outcomes, weak association with GV, and LD pruning, are listed in **Supplementary Table 3**.

Evaluation of MR assumptions 1, 2, and 3 at the genetic risk score (GRS) level

We also investigated the GRS-level MR assumption 1, which examined the associations between weighted and unweighted GRSs and glucose variability measures (**Table 3**). Our findings indicate significant positive associations between weighted and unweighted GRSs and glucose variability measures with and without adjustment, thereby meeting assumption 1. As the weighted or unweighted GRS increases, the values of glucose variability measures correspondingly increase.

We then explored GRS-level MR assumption 2, which examined the relationship between unweighted and weighted GRSs and covariates. Linear regression analyses were conducted to examine the associations of glucose variability-related unweighted and weighted GRSs with various covariates including lifestyle behaviors, clinical and biochemical markers, sociodemographic factors, and comorbidities. The significant covariates associated with glucose variability measures are presented in **Supplementary Table 4**. These covariates failed to meet assumption 2 and thus were not considered for adjustment in the initial stage of modeling to derive the glucose variability-related scores using GRSs.

We also assessed GRS-level MR assumption 3, which investigated the association of unweighted and weighted GRSs with WMH and cerebrovascular abnormalities (**Figure 2**). The unweighted and weighted GRSs for glucose variability measures were not significantly associated with WMH or cerebrovascular abnormalities, regardless of whether age and sex were adjusted or multivariate adjustment was performed, thereby meeting assumption 3.

Table 3. Association of genetic risk scores with glucose variation in patients with type 2 diabetes (MR assumption 1)

Glucose variation	Age- and sex-adjusted model			Multivariate model		
	β (SE)	F-value	partial R squared	β (SE)	F-value	partial R squared
Unweighted						
$GRS_{AC\text{-}CV}$	2.91 (0.30)***	91.40***	0.039	2.35 (0.27)***	74.59***	0.033
$GRS_{AC\text{-}SD}$	5.95 (0.66)***	82.09***	0.041	4.06 (0.55)***	54.35***	0.024
$GRS_{AC\text{-}VIM}$	0.01 (0.001)***	87.22***	0.035	0.01 (0.001)***	82.79***	0.036
$GRS_{AC\text{-}ARV}$	3.56 (0.38)***	86.74***	0.037	3.09 (0.36)***	71.95***	0.031
$GRS_{HbA1c\text{-}CV}$	1.49 (0.16)***	90.08***	0.039	1.18 (0.14)***	76.48***	0.033
$GRS_{HbA1c\text{-}SD}$	0.19 (0.02)***	90.94***	0.037	0.12 (0.02)***	55.18***	0.024
$GRS_{HbA1c\text{-}VIM}$	0.02 (0.003)***	56.76***	0.038	0.02 (0.003)***	87.70***	0.038
$GRS_{HbA1c\text{-}ARV}$	1.97 (0.24)***	66.36***	0.032	1.33 (0.22)***	72.98***	0.032
Weighted						
$GRS_{AC\text{-}CV}$	2.98 (0.30)***	95.57***	0.051	2.38 (0.27)***	71.35***	0.041
$GRS_{AC\text{-}SD}$	6.09 (0.66)***	85.94***	0.054	4.1 (0.55)***	56.89***	0.033
$GRS_{AC\text{-}VIM}$	0.01 (0.001)***	91.22***	0.051	0.01 (0.001)***	52.46***	0.031
$GRS_{AC\text{-}ARV}$	3.59 (0.38)***	88.11***	0.054	3.11 (0.36)***	37.50***	0.022
$GRS_{HbA1c\text{-}CV}$	1.54 (0.16)***	95.71***	0.034	1.20 (0.14)***	74.00***	0.043
$GRS_{HbA1c\text{-}SD}$	0.19 (0.02)***	96.21***	0.038	0.12 (0.02)***	58.85***	0.034
$GRS_{HbA1c\text{-}VIM}$	0.02 (0.003)***	59.66***	0.039	0.02 (0.003)***	55.48***	0.032
$GRS_{HbA1c\text{-}ARV}$	2.01 (0.24)***	69.26***	0.020	1.35 (0.22)***	39.00***	0.023

Multivariate model adjusted for age, sex, lifestyle behaviors (smoking, alcohol drinking, physical activity, and BMI), diabetes-related variables (duration of diabetes and type of hypoglycemic drug use), comorbidity (stroke, hypertension, obesity, coronary artery disease, hyperlipidemia, peripheral neuropathy, neuropathy and nephropathy), drug-related variables (cardiovascular medications, hyperlipidemia medications, and hypertension medications) and biomarkers (HDL-C, TG, LDL-C, TC, eGFR, FPG, and HbA1c).
*: P<0.05; **: P<0.01; ***: P<0.001.

Copyright© AE&M all rights reserved.

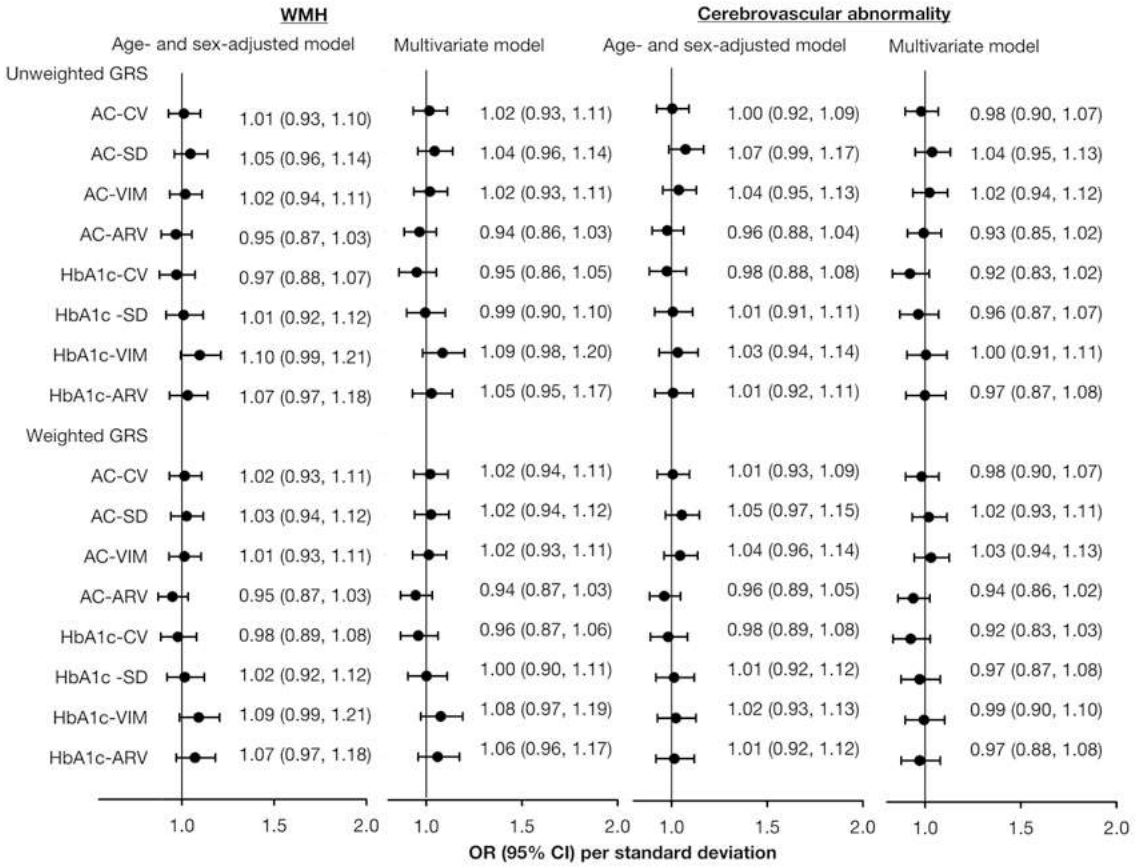


Figure 2. Association of genetic risk scores with WMH or cerebrovascular abnormality in patients with type 2 diabetes for genetic risk score level (MR assumption 3). Multivariate model adjusting for age, sex, lifestyle behaviors, diabetes-related variables, comorbidity, drug-related variables and biomarker.

Associations between glucose variability and brain MRI variables determined using an MR approach

Table 4 shows the ORs of the presence of WMH and cerebrovascular abnormalities associated with genetic-related glucose variability, derived from the unweighted and weighted GRSs with and without adjustment. The genetic-related glucose variability scores denoted a genetic predisposition to glucose variability and were obtained by regressing glucose variability measures on the unweighted and weighted GRSs. With respect to the presence of WMH per 1 SD increase in glucose variability scores with residual adjustment, the ORs were significant for AC-CV and AC-VIM in the unweighted GRS and for AC-VIM in the weighted GRS. After the multivariate adjustment, the ORs of the presence of WMH remained significant for AC-VIM in the unweighted GRS. In contrary, the ORs for AC-CV in the unweighted GRS and AC-VIM in the weighted GRS became insignificant after the multivariate adjustment. Among the glucose variability metrics in the unweighted GRS that were significantly associated with multivariate adjustment, only AC-VIM (OR per 1SD: 1.17, 95% CI: 1.08–1.27) was positively associated.

The ORs of the presence of cerebrovascular abnormalities per 1 SD increase in glucose variability scores with residual adjustment were significant for all the unweighted and weighted GRSs. After multivariate adjustment, all the significant ORs of the presence of cerebrovascular abnormalities remained significant for the unweighted and weighted GRSs, except for the AC-ARV unweighted GRS. Among the glucose variability metrics in the unweighted GRS that were significantly associated with multivariate adjustment, the OR per 1 unit change for glucose variability measures ranged from 1.14 (1.04, 1.25) for AC-SD to 1.37 (1.26, 1.50) for HbA1c-VIM.

Copyright© AE&M all rights reserved.

Table 4. The odds ratios of WMH or cerebrovascular abnormality for predictive glucose variation derived from unweighted and weighted GRS using MR approach

Glucose variation	WMH OR (95% CI) per standard deviation		Cerebrovascular abnormality OR (95% CI) per standard deviation	
	Model 1	Model 2	Model 1	Model 2
Unweighted				
GRS_{AC-CV}	1.09 (1.00, 1.18)*	1.05 (0.96, 1.14)	1.35 (1.24, 1.47)***	1.34 (1.23, 1.47)***
GRS_{AC-SD}	1.03 (0.95, 1.12)	1.06 (0.97, 1.16)	1.20 (1.10, 1.30)***	1.14 (1.04, 1.25)**
GRS_{AC-VIM}	1.16 (1.07, 1.27)***	1.17 (1.08, 1.27)***	1.34 (1.23, 1.46)***	1.33 (1.22, 1.45)***
GRS_{AC-ARV}	1.04 (0.96, 1.14)	1.00 (0.91, 1.09)	1.12 (1.03, 1.22)**	1.01 (0.92, 1.11)
$GRS_{HbA1c-CV}$	0.96 (0.89, 1.04)	0.96 (0.89, 1.05)	1.36 (1.25, 1.48)***	1.36 (1.25, 1.48)***
$GRS_{HbA1c-SD}$	1.01 (0.93, 1.09)	1.01 (0.93, 1.10)	1.36 (1.25, 1.48)***	1.36 (1.25, 1.48)***
$GRS_{HbA1c-VIM}$	1.02 (0.94, 1.11)	1.03 (0.95, 1.12)	1.37 (1.26, 1.49)***	1.37 (1.26, 1.50)***
$GRS_{HbA1c-ARV}$	0.98 (0.91, 1.07)	0.98 (0.91, 1.07)	1.34 (1.23, 1.46)***	1.34 (1.23, 1.46)***
Weighted				
GRS_{AC-CV}	1.08 (0.99, 1.17)	1.05 (0.96, 1.15)	1.21 (1.11, 1.31)***	1.14 (1.04, 1.25)**
GRS_{AC-SD}	1.03 (0.95, 1.12)	1.06 (0.97, 1.16)	1.21 (1.11, 1.32)***	1.16 (1.06, 1.27)**
GRS_{AC-VIM}	1.10 (1.02, 1.20)*	1.03 (0.94, 1.12)	1.28 (1.18, 1.40)***	1.23 (1.13, 1.35)***
GRS_{AC-ARV}	1.05 (0.97, 1.14)	1.02 (0.93, 1.11)	1.23 (1.13, 1.33)***	1.16 (1.06, 1.27)**
$GRS_{HbA1c-CV}$	0.96 (0.89, 1.05)	0.96 (0.89, 1.05)	1.36 (1.25, 1.48)***	1.37 (1.25, 1.49)***
$GRS_{HbA1c-SD}$	0.95 (0.87, 1.03)	0.95 (0.87, 1.04)	1.20 (1.10, 1.30)***	1.12 (1.02, 1.23)*
$GRS_{HbA1c-VIM}$	1.02 (0.94, 1.11)	1.03 (0.95, 1.12)	1.37 (1.25, 1.49)***	1.37 (1.26, 1.5)***
$GRS_{HbA1c-ARV}$	0.94 (0.86, 1.02)	0.95 (0.87, 1.04)	1.18 (1.08, 1.28)***	1.11 (1.02, 1.22)*

Model 1 adjusted for residuals.
Model 2 adjusting for residual, PCA and confounding variables.
*: P<0.05; **: P<0.01; ***: P<0.001; OR: odds ratio; CI: confidence interval.

DISCUSSION

In this study, the associations between glucose variability and brain MRI indicators were thoroughly assessed using MR and epidemiologic approaches. When applied the epidemiologic approach, we did not observe any significant associations between glucose variability and WMH. However, we found significant associations between all the FPG variability metrics and cerebrovascular abnormalities. With the MR approach, the absence of significant associations between the weighted or unweighted genetic risk scores and WMH or cerebrovascular abnormalities supports the validity of MR assumption 3, suggesting no evidence of direct genetic effects on the outcomes. In contrast, the two-stage MR analyses revealed a significant association between genetically predicted FPG variability, as measured by AC-VIM, and WMH, with a 17% increase in odds per 1 SD increase when the unweighted GRS was used. These findings reflect an indirect effect of genetic instruments on WMH mediated through glycemic variability rather than a direct instrument–outcome association. The association was not significant for AC-VIM in the weighted model after the multivariate adjustment, indicating the potential specificity of this metric in the unweighted genetic context. For cerebrovascular abnormalities, the glucose variability metrics in the unweighted and weighted GRS models showed consistent and significant associations after full adjustment, with the exception of the AC-ARV in the unweighted GRS group. Among the significant metrics in the unweighted GRS group, the strongest association was observed with HbA1c-VIM (OR per 1 unit increase: 1.37; 95% CI: 1.26–1.50), followed by AC-SD (OR: 1.14; 95% CI: 1.04–1.25), highlighting the clinical relevance of glycemic variability as an independent risk factor for cerebrovascular pathology.

These findings underscore the importance of glycemic variability — beyond average glucose levels—as a potential independent risk factor for cerebral small vessel disease and cerebrovascular abnormalities. The observed association between FPG variability

Copyright© AE&M all rights reserved.

(AC-VIM) and WMH, particularly in the context of unweighted genetic risk, suggests that fluctuations in fasting glucose levels may contribute to subclinical brain injury. Moreover, the consistent and significant associations between cerebrovascular abnormalities and multiple glucose variability metrics, especially the strong link with HbA1c-VIM, support the hypothesis that long-term glycemic instability may play a causal role in vascular brain damage. From a clinical perspective, these results highlight the need to monitor and manage chronic hyperglycemia and glycemic fluctuations, particularly in individuals at high genetic risk, as part of strategies to reduce the burden of cerebrovascular disease and cognitive decline.

Only a few epidemiological and MR studies have investigated the association between visit-to-visit glucose variability and brain MRI parameters (14-16). One epidemiological study examined individuals with type 1 diabetes (14), and another focused on APOE4 genotype carriers with type 2 diabetes (15). One MR study assessed the relationship between HbA1c levels — rather than HbA1c variability—and WMH (16). In a study of individuals with type 1 diabetes, no association between HbA1c variability and cerebral small vessel disease was found among 189 neurologically asymptomatic participants (14). In contrast, our work demonstrated a consistent association between glucose variability and cerebrovascular abnormalities. This discrepancy may be attributed to our large sample size and the use of a composite outcome measure that includes stenosis or occlusion of major intracranial or internal carotid arteries, aneurysms, lacunar or small infarctions, intracerebral hemorrhage, and lobar infarctions—features that may increase the prevalence and statistical power of a study. In the investigation of WMH, previous epidemiological and MR studies reported differing findings: the former identified associations (15), and the latter did not (16). In an investigation of individuals aged 65 years and older with type 2 diabetes and carrying the APOE4 genotype (n = 124), HbA1c variability was found to be significantly associated with high WMH burden in APOE4 carriers (15). Two-sample MR analysis revealed no significant association between genetic liability and type 2 diabetes or between HbA1c levels and WMH (16). Although a significant association between FPG-VIM and WMH was found in this work, most other glucose variability metrics were consistent with the MR findings. Substantial methodological differences were noted between the above studies and the current study. These epidemiological studies focused on older adults with type 2 diabetes who carry the APOE4 allele; despite having a relatively large sample size, our work focused on asymptomatic adults over the age of 30 years with type 2 diabetes. Thus, the prevalence of WMH in our study was relatively low, which may have resulted in limited statistical power. Further research is warranted to clarify these associations.

Several limitations of this study should be acknowledged. First, the glucose-related variables — FPG and HbA1c — were derived from routine clinical monitoring, resulting in variability in the number of measurements obtained across the participants. To mitigate this issue, we adjusted for the number of FPG and HbA1c measurements when calculating variability indices. Moreover, these glucose measurements were collected prior to the brain MRI assessments, and the duration between the two procedures may not have been sufficient to capture the full temporal relationship between glucose variability and brain MRI outcomes. Second, the study sample may not be representative of the broad type 2 diabetes population; the study subjects may have undergone brain MRI for specific clinical indications. In clinical settings, brain MRI is often performed in the presence of suspected or known cerebrovascular pathology. Hence, the participants included in this analysis may have had underlying cerebrovascular symptoms or risk factors, limiting the generalizability of the findings to individuals with type 2 diabetes who do not present with such concerns. Third, cerebrovascular abnormalities were analyzed as a composite binary variable encompassing heterogeneous lesion types, including large-vessel stenosis or occlusion, aneurysms, lacunar infarctions, intracerebral hemorrhage, and lobar infarctions. Owing to the structure of the Clinical Research Data Repository and the pre-specified data request at the time of application, lesion-specific information was not available for further stratified or severity-based analyses. The use of a composite endpoint may introduce heterogeneity, as

Copyright© AE&M all rights reserved.

these lesions differ in terms of their underlying pathophysiology and clinical significance. Such heterogeneity is more likely to bias associations toward the null, potentially diluting lesion-specific effects of glycemic variability rather than inflating them. Therefore, the observed associations should be interpreted as conservative estimates of the relationship between glycemic variability and overall cerebrovascular disease burden. Future studies with access to detailed neuroimaging phenotypes are warranted to disentangle lesion-specific associations and to evaluate whether glycemic variability differentially influences ischemic, hemorrhagic, and large-vessel cerebrovascular processes. Fourth, although WMH is a canonical marker of cerebral small-vessel disease, WMH was available only as a binary measure in the current dataset. Information on WMH volume or severity grade was not accessible because of the structure of the clinical imaging data repository. As a result, we were unable to examine dose–response relationships or formally assess effect modification by WMH burden in the association between glycemic variability and other cerebrovascular abnormalities. Future studies incorporating quantitative or graded WMH measures may provide further insights into whether the impact of glycemic variability differs across levels of small-vessel disease burden. Fifth, markers of neurodegenerative pathology, such as amyloid biomarkers or cognitive performance measures, were not available in this cohort. Although the APOE genotype was included in the genetic analyses, the lack of phenotypic neurodegenerative data limits our ability to distinguish between purely vascular pathology and mixed vascular–neurodegenerative processes underlying the observed MRI findings. Finally, causal inferences cannot be drawn because this cohort study was observational. The findings represent associations rather than definitive causal relationships. In addition, the association between glucose variability and WMH was not consistently observed across the epidemiological and MR approaches. For the MR analysis, this inconsistency may be attributed to the use of weak instrumental variables, which could limit the strength and reliability of the causal estimates.

In conclusion, this study thoroughly evaluated the associations between glucose variability and brain MRI outcomes using epidemiological and MR approaches. Epidemiological and MR analyses revealed no significant association between glucose variability and WMH. Meanwhile, FPG and HbA1c variability were significantly associated with cerebrovascular abnormalities across most metrics. These findings emphasize the importance of monitoring and managing glucose variability, beyond measuring average glucose levels, in persons with type 2 diabetes to potentially mitigate cerebrovascular risk.

Acknowledgements: we appreciate the iHi Research Platform/iHi Genomics from the Big Data Center of China Medical University Hospital for the data exploration, administrative, and statistical analytic support.

Funding: this study was supported primarily by the Ministry of Science and Technology, Taiwan (MOST 109-2314-B-039-031-MY2, MOST 110-2314-B-039-021-, and MOST 111-2314-B-039-018-), National Science and Technology Council, Taiwan (NSTC 112-2314-B-039-042-, NSTC 113-2314-B-039-042- and NSTC 114-2314-B-039-027-), and China Medical University Hospital, Taiwan (DMR-115-194).

Disclosure: no potential conflict of interest relevant to this article was reported.

Data availability: datasets related to this article will be available upon request to the corresponding author.

REFERENCES

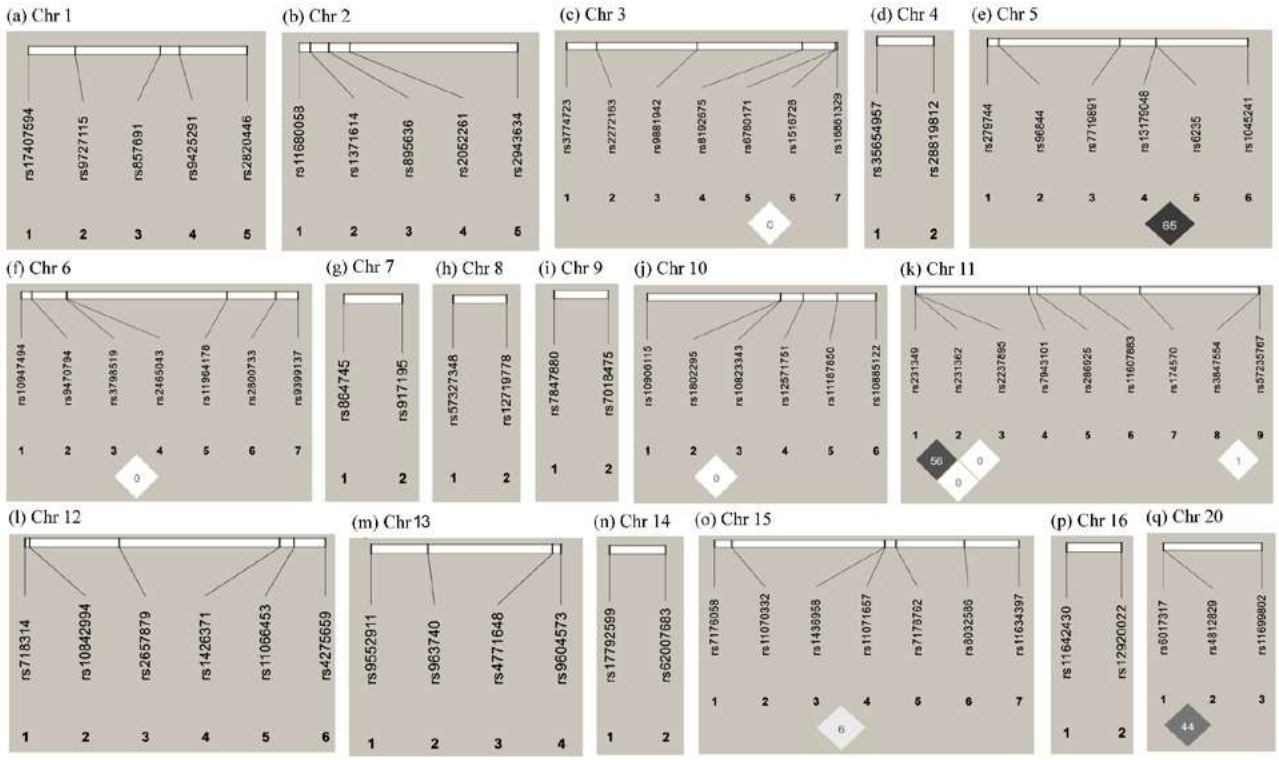
1. International Diabetes Federation (IDF). IDF Diabetes Atlas. 10th ed. Brussels: IDF; 2021. Available from: https://diabetesatlas.org/atlas/tenth-edition/.
2. King H, Aubert RE, Herman WH. Global burden of diabetes, 1995–2025: prevalence, numerical estimates, and projections. Diabetes Care. 1998;21(9):1414–31. doi: 10.2337/diacare.21.9.1414 .
3. Chatterjee S, Khunti K, Davies MJ. Type 2 diabetes. Lancet. 2017;389(10085):2239-51. doi: 10.1016/S0140-6736(17)30058-2.
4. Fowler MJ. Microvascular and Macrovascular Complications of Diabetes. Clinical Diabetes. 2011;29(3):116-22. doi: 10.2337/diaclin.29.3.116.
5. Lin X, Xu Y, Pan X, Xu J, Ding Y, Sun X, et al. Global, regional, and national burden and trend of diabetes in 195 countries and territories: an analysis from 1990 to 2025. Scientific reports. 2020;10(1):14790. doi: 10.1038/s41598-020-71908-9.
6. GBD 2016 Causes of Death Collaborators. Global, regional, and national age-sex specific mortality for 264 causes of death, 1980-2016: a systematic analysis for the Global Burden of Disease Study 2016. Lancet (London, England). 2017;390(10100):1151-210. doi: 10.1016/S0140-6736(17)32152-9.
7. Sarwar N, Gao P, Seshasai SR, Gobin R, Kaptoge S, Di Angelantonio E, et al. Diabetes mellitus, fasting blood glucose concentration, and risk of vascular disease: a collaborative meta-analysis of 102 prospective studies. Lancet (London, England). 2010;375(9733):2215-22. doi: 10.1016/S0140-6736(10)60484-9.
8. Duckworth W, Abraira C, Moritz T, Reda D, Emanuele N, Reaven PD, et al. Glucose control and vascular complications in veterans with type 2 diabetes. The New England journal of medicine. 2009;360(2):129-39. doi: 10.1056/NEJMoa0808431.

Copyright© AE&M all rights reserved.

9. Patel A, MacMahon S, Chalmers J, Neal B, Billot L, Woodward M, et al. Intensive blood glucose control and vascular outcomes in patients with type 2 diabetes. N Engl J Med. 2008;358(24):2560-72. doi: 10.1056/NEJMoa0802987.
10. Ismail-Beigi F, Craven T, Banerji MA, Basile J, Calles J, Cohen RM, et al. Effect of intensive treatment of hyperglycaemia on microvascular outcomes in type 2 diabetes: an analysis of the ACCORD randomised trial. Lancet (London, England). 2010;376(9739):419-30. doi: 10.1016/S0140-6736(10)60576-4.
11. Schmidt R, Scheltens P, Erkinjuntti T, Pantoni L, Markus HS, Wallin A, et al. White matter lesion progression: a surrogate endpoint for trials in cerebral small-vessel disease. Neurology. 2004;63(1):139-44. doi: 10.1212/01.WNL.0000134675.63950.9A.
12. Matsusue E, Sugihara S, Fujii S, Ohama E, Kinoshita T, Ogawa T. White matter changes in elderly people: MR-pathologic correlations. Magn Reson Med Sci. 2006;5(2):99-104. doi:10.2463/mrms.5.99.
13. Debette S, Markus HS. The clinical importance of white matter hyperintensities on brain magnetic resonance imaging: systematic review and meta-analysis. BMJ (Clinical research ed). 2010;341:c3666. doi: 10.1136/bmj.c3666.
14. Inkeri J, Adeshara K, Harjutsalo V, Forsblom C, Liebkind R, Tatlisumak T, et al. Glycemic control is not related to cerebral small vessel disease in neurologically asymptomatic individuals with type 1 diabetes. Acta diabetologica. 2022;59(4):481-90. doi: 10.1007/s00592-021-01821-2.
15. Livny A, Ravona-Springer R, Heymann A, Priess R, Kushnir T, Tsarfaty G, et al. Long-term Variability in Glycemic Control Is Associated With White Matter Hyperintensities in APOE4 Genotype Carriers With Type 2 Diabetes. Diabetes care. 2016;39(6):1056-9. doi: 10.2337/dc15-2686.
16. Garfield V, Farmaki AE, Fatemifar G, Eastwood SV, Mathur R, Rentsch CT, et al. Relationship Between Glycemia and Cognitive Function, Structural Brain Outcomes, and Dementia: A Mendelian Randomization Study in the UK Biobank. Diabetes. 2021;70(10):2313-21. doi: 10.2337/db20-0895.
17. Kilpatrick ES, Rigby AS, Atkin SL. A1C variability and the risk of microvascular complications in type 1 diabetes: data from the Diabetes Control and Complications Trial. Diabetes Care. 2008 Nov;31(11):2198-202. doi: 10.2337/dc08-0864.
18. Chiang HY, Liang LY, Lin CC, Chen YJ, Wu MY, Chen SH, et al. Electronic medical record-based deep data cleaning and phenotyping improve the diagnostic validity and mortality assessment of infective endocarditis: medical big data initiative of CMUH. Biomedicine (Taipei). 2021;11(3):59-67. doi: 10.37796/2211-8039.1267.
19. Purcell S, Neale B, Todd-Brown K, Thomas L, Ferreira MA, Bender D, et al. PLINK: a tool set for whole-genome association and population-based linkage analyses. Am J Hum Genet. 2007 Sep;81(3):559-75. doi: 10.1086/519795.
20. Howie BN, Donnelly P, Marchini J. A flexible and accurate genotype imputation method for the next generation of genome-wide association studies. PLoS Genet. 2009;5(6):e1000529. doi:10.1371/journal.pgen.1000529.
21. Chen P, Takeuchi F, Lee JY, Li H, Wu JY, Liang J, et al.; CHARGE Hematology Working Group; Gross MD, Assimes TL, Miki T, Shu XO, Qi L, Chen YT, Lin X, Aung T, Wong TY, Teo YY, Kim BJ, Kato N, Tai ES. Multiple nonglycemic genomic loci are newly associated with blood level of glycated hemoglobin in East Asians. Diabetes. 2014 Jul;63(7):2551-62. doi: 10.2337/db13-1815.
22. Soranzo N, Sanna S, Wheeler E, Gieger C, Radke D, Dupuis J, et al. Common variants at 10 genomic loci influence hemoglobin A□(C) levels via glycemic and nonglycemic pathways. Diabetes. 2010;59(12):3229-39. doi: 10.2337/db10-0502.
23. Wheeler E, Leong A, Liu CT, Hivert MF, Strawbridge RJ, Podmore C, et al. Impact of common genetic determinants of Hemoglobin A1c on type 2 diabetes risk and diagnosis in ancestrally diverse populations: A transethnic genome-wide meta-analysis. PLoS medicine. 2017;14(9):e1002383. doi: 10.1371/journal.pmed.1002383.
24. Hwang JY, Sim X, Wu Y, Liang J, Tabara Y, Hu C, et al. Genome-wide association meta-analysis identifies novel variants associated with fasting plasma glucose in East Asians. Diabetes. 2015;64(1):291-8. doi: 10.2337/db14-0563.
25. Ramos E, Chen G, Shriner D, Doumatey A, Gerry NP, Herbert A, et al. Replication of genome-wide association studies (GWAS) loci for fasting plasma glucose in African-Americans. Diabetologia. 2011;54(4):783-8. doi: 10.1007/s00125-010-2002-7.
26. Ai S, Wang X, Wang S, Zhao Y, Guo S, Li G, et al. Effects of glycemic traits on left ventricular structure and function: a mendelian randomization study. Cardiovascular diabetology. 2022;21(1):109. doi: 10.1186/s12933-022-01540-6.
27. Emanuelsson F, Marott S, Tybjærg-Hansen A, Nordestgaard BG, Benn M. Impact of Glucose Level on Micro- and Macrovascular Disease in the General Population: A Mendelian Randomization Study. Diabetes Care. 2020 Apr;43(4):894-902. doi: 10.2337/dc19-1850.
28. Gottsäter M, Hindy G, Orho-Melander M, Nilsson PM, Melander O. A genetic risk score for fasting plasma glucose is independently associated with arterial stiffness: a Mendelian randomization study. J Hypertens. 2018 Apr;36(4):809-814. doi: 10.1097/HJH.0000000000001646.
29. Leong A, Chen J, Wheeler E, Hivert MF, Liu CT, Merino J, et al. Mendelian Randomization Analysis of Hemoglobin A_{1c} as a Risk Factor for Coronary Artery Disease. Diabetes Care. 2019 Jul;42(7):1202-1208. doi: 10.2337/dc18-1712.
30. van Oort S, Beulens JWJ, van Ballegooijen AJ, Burgess S, Larsson SC. Cardiovascular risk factors and lifestyle behaviours in relation to longevity: a Mendelian randomization study. J Intern Med. 2021 Feb;289(2):232-243. doi: 10.1111/joim.13196.
31. Yang G, Au Yeung SL, Schooling CM. Sex differences in the association of fasting glucose with HbA1c, and their consequences for mortality: A Mendelian randomization study. EBioMedicine. 2022 Oct;84:104259. doi: 10.1016/j.ebiom.2022.104259.
32. Rasmussen-Torvik LJ, Li M, Kao WH, Couper D, Boerwinkle E, Bielinski SJ, et al. Association of a fasting glucose genetic risk score with subclinical atherosclerosis: The Atherosclerosis Risk in Communities (ARIC) study. Diabetes. 2011 Jan;60(1):331-5. doi: 10.2337/db10-0839.

Copyright© AE&M all rights reserved.

SUPPLEMENTARY MATERIALS



Supplementary figure 1. LD analysis of SNPs satisfying MR assumptions 1 and 3

Supplementary table 1. SNP-level characteristics and associations for GV metrics

SNP ID	Chromosome	Position	Effect allele	Other allele	EAF	Effect size on GV (β (SE)	P-value	OR with WMH	OR with cerebrovascular Abnormality
GRS_{AC-CV} (19 SNPs)									
rs857691	1	158626378	C	T	0.55	-0.88 (0.45)	0.049	0.99 (0.88, 1.11)	0.99 (0.88, 1.12)
rs1371614	2	27152874	C	T	0.83	-1.29 (0.58)	0.027	1.12 (0.96, 1.31)	0.93 (0.79, 1.09)
rs9881942	3	123082416	G	A	0.71	-1.29 (0.49)	0.008	1.02 (0.90, 1.16)	1.01 (0.88, 1.15)
rs28819812	4	157652753	A	C	0.25	1.15 (0.50)	0.023	0.91 (0.79, 1.04)	0.96 (0.84, 1.10)
rs96844	5	56196604	G	A	0.81	-1.15 (0.56)	0.040	0.94 (0.81, 1.09)	1.04 (0.90, 1.21)
rs13179048	5	95542726	C	A	0.65	-0.92 (0.46)	0.047	1.04 (0.92, 1.18)	1.01 (0.89, 1.15)
rs10947494	6	34263743	G	A	0.27	1.10 (0.49)	0.026	1.07 (0.94, 1.22)	0.94 (0.83, 1.08)
rs2800733	6	127416930	A	G	0.89	-1.48 (0.71)	0.037	1.20 (1.00, 1.45)	0.92 (0.76, 1.12)
rs7943101	11	32460873	T	C	0.07	1.84 (0.87)	0.034	1.16 (0.92, 1.47)	0.94 (0.74, 1.18)
rs286925	11	34642668	G	A	0.40	1.20 (0.45)	0.008	0.92 (0.81, 1.03)	0.91 (0.81, 1.03)
rs3847554	11	92668826	C	T	0.44	0.87 (0.43)	0.047	1.02 (0.90, 1.14)	0.91 (0.81, 1.02)
rs4275659	12	123447928	C	T	0.72	-0.98 (0.49)	0.045	0.89 (0.78, 1.02)	0.99 (0.87, 1.13)
rs963740	13	51096095	A	T	0.35	1.20 (0.46)	0.010	0.98 (0.87, 1.11)	1.04 (0.92, 1.18)
rs17792599	14	21770681	G	A	0.10	1.56 (0.76)	0.039	1.09 (0.89, 1.33)	1.01 (0.83, 1.24)
rs7176058	15	39464167	A	G	0.52	-0.97 (0.43)	0.025	1.1 (0.98, 1.24)	0.99 (0.89, 1.12)
rs11642430	16	30045789	C	G	0.56	-0.93 (0.43)	0.032	0.94 (0.84, 1.05)	0.90 (0.8,0 1.01)
rs12920022	16	89564055	T	A	0.87	-1.39 (0.65)	0.033	0.93 (0.78, 1.11)	1.06 (0.89, 1.27)
rs6017317	20	42946966	T	G	0.56	-1.03 (0.44)	0.020	0.91 (0.81, 1.02)	0.89 (0.79, 1.00)
rs112915006	22	50604696	G	A	0.10	1.88 (0.71)	0.008	1.17 (0.97, 1.41)	1.11 (0.92, 1.34)
GRS_{AC-SD} (16 SNPs)									
rs11680058	2	16574669	A	G	0.88	-3.10 (1.47)	0.035	0.96 (0.80, 1.15)	1.09 (0.91, 1.31)
rs9881942	3	123082416	G	A	0.71	-3.10 (1.05)	0.003	1.02 (0.90, 1.16)	1.01 (0.88, 1.15)
rs28819812	4	157652753	A	C	0.25	2.21 (1.09)	0.043	0.91 (0.79, 1.04)	0.96 (0.84, 1.10)
rs96844	5	56196604	G	A	0.81	-3.04 (1.20)	0.012	0.94 (0.81, 1.09)	1.04 (0.90, 1.21)
rs7719891	5	86577352	A	G	0.51	-2.35 (0.93)	0.012	1.02 (0.91, 1.15)	1.00 (0.89, 1.13)

Copyright© AE&M all rights reserved.

SNP ID	Chromosome	Position	Effect allele	Other allele	EAF	Effect size on GV (β (SE)	P-value	OR with WMH	OR with cerebrovascular Abnormality
rs9399137	6	135419018	C	T	0.23	2.37 (1.16)	0.042	1.09 (0.94, 1.26)	0.97 (0.84, 1.12)
rs7847880	9	20662703	C	T	0.76	-2.93 (1.11)	0.008	0.98 (0.85, 1.12)	0.93 (0.81, 1.07)
rs286925	11	34642668	G	A	0.40	2.34 (0.97)	0.015	0.92 (0.81, 1.03)	0.91 (0.81, 1.03)
rs11607883	11	45839709	A	G	0.24	2.49 (1.12)	0.026	0.97 (0.85, 1.12)	0.99 (0.86, 1.14)
rs963740	13	51096095	A	T	0.35	2.98 (1.00)	0.003	0.98 (0.87, 1.11)	1.04 (0.92, 1.18)
rs7176058	15	39464167	A	G	0.52	-2.25 (0.93)	0.016	1.10 (0.98, 1.24)	0.99 (0.89, 1.12)
rs11070332	15	41809205	G	A	0.84	-2.72 (1.31)	0.038	0.93 (0.79, 1.10)	0.90 (0.76, 1.06)
rs11634397	15	80432222	G	A	0.08	3.58 (1.72)	0.038	0.89 (0.72, 1.10)	1.09 (0.88, 1.35)
rs6017317	20	42946966	T	G	0.56	-3.00 (0.95)	0.002	0.91 (0.81, 1.02)	0.89 (0.79, 1.00)
rs4812829	20	42989267	G	A	0.55	-1.91 (0.96)	0.047	0.94 (0.84, 1.06)	0.91 (0.80, 1.02)
rs112915006	22	50604696	G	A	0.10	3.56 (1.52)	0.019	1.17 (0.97, 1.41)	1.11 (0.92, 1.34)
$GRS_{AC\text{-}VIM}$ (19 SNPs)									
rs857691	1	158626378	C	T	0.55	-0.004 (0.002)	0.026	0.99 (0.88, 1.11)	0.99 (0.88, 1.12)
rs2820446	1	219748818	G	C	0.23	0.004 (0.002)	0.049	0.96 (0.84, 1.10)	1.07 (0.93, 1.22)
rs2943634	2	227068080	A	C	0.08	0.007 (0.003)	0.016	0.88 (0.71, 1.10)	1.09 (0.87, 1.35)
rs13179048	5	95542726	C	A	0.65	-0.005 (0.002)	0.009	1.04 (0.92, 1.18)	1.01 (0.89, 1.15)
rs6235	5	95728898	C	G	0.67	-0.004 (0.002)	0.034	1.05 (0.93, 1.19)	1.00 (0.88, 1.14)
rs10947494	6	34263743	G	A	0.27	0.004 (0.002)	0.021	1.07 (0.94, 1.22)	0.94 (0.83, 1.08)
rs57327348	8	10808687	T	A	0.09	0.007 (0.003)	0.024	0.93 (0.75, 1.15)	1.01 (0.82, 1.25)
rs11187850	10	96068480	G	A	0.20	0.004 (0.002)	0.037	1.02 (0.88, 1.18)	1.12 (0.97, 1.30)
rs718314	12	26453283	G	A	0.72	-0.004 (0.002)	0.032	0.99 (0.87, 1.13)	0.99 (0.87, 1.13)
rs1426371	12	108629780	A	G	0.57	-0.004 (0.002)	0.022	1.03 (0.91, 1.16)	1.06 (0.94, 1.20)
rs4275659	12	123447928	C	T	0.72	-0.004 (0.002)	0.018	0.89 (0.78, 1.02)	0.99 (0.87, 1.13)
rs4771648	13	110431626	A	G	0.45	0.004 (0.002)	0.008	1.07 (0.95, 1.20)	1.02 (0.91, 1.15)
rs9604573	13	114542858	A	G	0.22	0.004 (0.002)	0.047	1.01 (0.88, 1.17)	1.02 (0.88, 1.18)
rs17792599	14	21770681	G	A	0.10	0.006 (0.003)	0.035	1.09 (0.89, 1.33)	1.01 (0.83, 1.24)
rs62007683	14	103894071	T	G	0.12	0.006 (0.003)	0.027	1.16 (0.97, 1.38)	1.05 (0.88, 1.26)
rs11642430	16	30045789	C	G	0.56	-0.005 (0.002)	0.004	0.94 (0.84, 1.05)	0.90 (0.80, 1.01)
rs34855406	17	40731411	C	G	0.24	0.005 (0.002)	0.013	0.91 (0.79, 1.04)	1.02 (0.89, 1.17)
rs11672660	19	46180184	T	C	0.20	0.004 (0.002)	0.043	1.07 (0.93, 1.24)	0.99 (0.86, 1.15)
rs112915006	22	50604696	G	A	0.10	0.006 (0.003)	0.037	1.17 (0.97, 1.41)	1.11 (0.92, 1.34)
$GRS_{AC\text{-}ARV}$ (20 SNPs)									
rs9425291	1	172312769	G	A	0.87	-1.63 (0.82)	0.046	0.99 (0.83, 1.17)	1.11 (0.93, 1.32)
rs2820446	1	219748818	G	C	0.23	1.32 (0.65)	0.042	0.96 (0.84, 1.10)	1.07 (0.93, 1.22)
rs1371614	2	27152874	C	T	0.83	-1.93 (0.73)	0.008	1.12 (0.96, 1.31)	0.93 (0.79, 1.09)
rs16861329	3	186666461	T	C	0.19	1.52 (0.72)	0.034	0.95 (0.82, 1.11)	0.97 (0.83, 1.13)
rs28819812	4	157652753	A	C	0.25	1.28 (0.63)	0.044	0.91 (0.79, 1.04)	0.96 (0.84, 1.10)
rs96844	5	56196604	G	A	0.81	-1.66 (0.70)	0.018	0.94 (0.81, 1.09)	1.04 (0.90, 1.21)
rs11964178	6	109562035	A	G	0.78	-1.48 (0.65)	0.024	1.13 (0.99, 1.30)	0.97 (0.84, 1.12)
rs7847880	9	20662703	C	T	0.76	-1.34 (0.65)	0.038	0.98 (0.85, 1.12)	0.93 (0.81, 1.07)
rs7018475	9	22137685	G	T	0.35	1.20 (0.58)	0.037	0.95 (0.85, 1.08)	0.92 (0.81, 1.04)
rs1802295	10	70931474	T	C	0.11	2.35 (0.88)	0.008	1.02 (0.84, 1.23)	1.10 (0.91, 1.32)
rs12571751	10	80942631	A	G	0.61	-1.12 (0.56)	0.045	0.97 (0.86, 1.09)	1.00 (0.88, 1.12)
rs231349	11	2672821	C	T	0.93	-2.19 (1.08)	0.042	1.06 (0.84, 1.33)	1.05 (0.83, 1.32)
rs231362	11	2691471	G	A	0.91	-2.45 (0.98)	0.013	0.98 (0.80, 1.21)	1.12 (0.91, 1.38)
rs3847554	11	92668826	C	T	0.44	1.29 (0.55)	0.018	1.02 (0.90, 1.14)	0.91 (0.81, 1.02)
rs1426371	12	108629780	A	G	0.57	-1.34 (0.56)	0.017	1.03 (0.91, 1.16)	1.06 (0.94, 1.20)
rs4275659	12	123447928	C	T	0.72	-1.31 (0.62)	0.034	0.89 (0.78, 1.02)	0.99 (0.87, 1.13)
rs7176058	15	39464167	A	G	0.52	-1.33 (0.54)	0.015	1.10 (0.98, 1.24)	0.99 (0.89, 1.12)
rs1436958	15	62338797	G	T	0.65	-1.15 (0.57)	0.045	1.03 (0.91, 1.16)	0.99 (0.88, 1.12)
rs11071657	15	62433962	A	G	0.65	-1.16 (0.58)	0.045	1.10 (0.97, 1.24)	1.12 (0.99, 1.27)
rs8032586	15	73081067	T	C	0.51	-1.15 (0.55)	0.035	0.93 (0.83, 1.05)	0.96 (0.86, 1.08)
$GRS_{HbA1c\text{-}CV}$ (18 SNPs)									
rs17407594	1	66170362	A	G	0.09	0.88 (0.41)	0.032	0.92 (0.72, 1.18)	0.95 (0.75, 1.22)
rs2052261	2	65355270	A	G	0.67	-0.50 (0.24)	0.039	1.07 (0.93, 1.23)	1.06 (0.92, 1.23)
rs3774723	3	63962339	G	A	0.61	-0.50 (0.23)	0.034	1.00 (0.87, 1.15)	1.10 (0.96, 1.27)
rs2272163	3	77671721	A	C	0.42	0.58 (0.23)	0.014	1.00 (0.87, 1.15)	0.97 (0.84, 1.12)
rs8192675	3	170724883	C	T	0.23	0.57 (0.27)	0.034	0.96 (0.82, 1.13)	0.93 (0.79, 1.10)
rs1516728	3	185829891	A	T	0.40	0.47 (0.24)	0.046	0.95 (0.82, 1.09)	1.00 (0.86, 1.15)
rs279744	5	53412620	A	C	0.26	0.59 (0.26)	0.023	1.03 (0.88, 1.20)	1.11 (0.95, 1.30)

Copyright© AE&M all rights reserved.

SNP ID	Chromosome	Position	Effect allele	Other allele	EAF	Effect size on GV (β (SE)	P-value	OR with WMH	OR with cerebrovascular Abnormality
rs1045241	5	118729286	T	C	0.15	0.63 (0.32)	0.048	0.94 (0.78, 1.13)	0.89 (0.73, 1.08)
rs864745	7	28180556	T	C	0.80	-0.63 (0.29)	0.031	1.10 (0.93, 1.31)	0.96 (0.81, 1.15)
rs12719778	8	145879883	C	T	0.35	0.73 (0.24)	0.003	1.03 (0.89, 1.19)	0.98 (0.85, 1.14)
rs10906115	10	12314997	A	G	0.62	-0.52 (0.23)	0.025	0.95 (0.83, 1.09)	1.03 (0.89, 1.18)
rs10885122	10	113042093	G	T	0.94	-1.12 (0.48)	0.019	1.18 (0.89, 1.56)	0.94 (0.70, 1.25)
rs10842994	12	27965150	T	C	0.19	0.57 (0.28)	0.043	1.05 (0.89, 1.24)	1.01 (0.85, 1.19)
rs2657879	12	56865338	G	A	0.09	0.96 (0.39)	0.016	1.11 (0.88, 1.40)	1.16 (0.92, 1.47)
rs9552911	13	23864657	A	G	0.25	0.68 (0.27)	0.010	1.09 (0.93, 1.28)	0.94 (0.80, 1.11)
rs7178762	15	63871292	C	T	0.92	-1.07 (0.43)	0.014	1.04 (0.80, 1.34)	1.13 (0.87, 1.47)
rs11642430	16	30045789	C	G	0.56	-0.50 (0.23)	0.030	0.97 (0.84, 1.10)	0.92 (0.80, 1.05)
rs11699802	20	48832135	T	C	0.54	-0.55 (0.23)	0.018	1.07 (0.94, 1.23)	0.96 (0.84, 1.10)
$GRS_{HbA1c-SD}$ (19 SNPs)									
rs2272163	3	77671721	A	C	0.42	0.06 (0.03)	0.036	1.00 (0.87, 1.15)	0.97 (0.84, 1.12)
rs6780171	3	185503456	A	T	0.26	0.07 (0.03)	0.039	0.97 (0.83, 1.13)	0.97 (0.83, 1.14)
rs35654957	4	1010077	C	T	0.27	0.07 (0.03)	0.023	1.08 (0.92, 1.25)	1.14 (0.98, 1.34)
rs1045241	5	118729286	T	C	0.15	0.08 (0.04)	0.042	0.94 (0.78, 1.13)	0.89 (0.73, 1.08)
rs9470794	6	38106844	C	T	0.35	0.06 (0.03)	0.031	0.93 (0.81, 1.07)	1.03 (0.89, 1.19)
rs2465043	6	51180765	G	A	0.39	0.06 (0.03)	0.026	1.02 (0.89, 1.17)	0.90 (0.79, 1.04)
rs864745	7	28180556	T	C	0.80	-0.08 (0.04)	0.028	1.10 (0.93, 1.31)	0.96 (0.81, 1.15)
rs12719778	8	145879883	C	T	0.35	0.10 (0.03)	0.002	1.03 (0.89, 1.19)	0.98 (0.85, 1.14)
rs10906115	10	12314997	A	G	0.62	-0.06 (0.03)	0.046	0.95 (0.83, 1.09)	1.03 (0.89, 1.18)
rs10823343	10	71091013	A	G	0.88	-0.09 (0.04)	0.036	0.88 (0.72, 1.09)	1.02 (0.82, 1.26)
rs10885122	10	113042093	G	T	0.94	-0.14 (0.06)	0.022	1.18 (0.89, 1.56)	0.94 (0.70, 1.25)
rs2237895	11	2857194	A	C	0.61	-0.06 (0.03)	0.045	0.95 (0.83, 1.10)	1.01 (0.88, 1.17)
rs174570	11	61597212	T	C	0.59	-0.06 (0.03)	0.038	1.09 (0.95, 1.25)	0.98 (0.85, 1.12)
rs10842994	12	27965150	T	C	0.19	0.07 (0.04)	0.049	1.05 (0.89, 1.24)	1.01 (0.85, 1.19)
rs2657879	12	56865338	G	A	0.09	0.14 (0.05)	0.005	1.11 (0.88, 1.40)	1.16 (0.92, 1.47)
rs9552911	13	23864657	A	G	0.25	0.07 (0.03)	0.028	1.09 (0.93, 1.28)	0.94 (0.80, 1.11)
rs7178762	15	63871292	C	T	0.92	-0.12 (0.05)	0.022	1.04 (0.80, 1.34)	1.13 (0.87, 1.47)
rs11642430	16	30045789	C	G	0.56	-0.06 (0.03)	0.031	0.97 (0.84, 1.10)	0.92 (0.80, 1.05)
rs11699802	20	48832135	T	C	0.54	-0.07 (0.03)	0.024	1.07 (0.94, 1.23)	0.96 (0.84, 1.10)
$GRS_{HbA1c-VIM}$ (10 SNPs)									
rs17407594	1	66170362	A	G	0.09	0.02 (0.007)	0.004	0.92 (0.72, 1.18)	0.95 (0.75, 1.22)
rs895636	2	45188353	C	T	0.58	-0.01 (0.004)	0.043	0.98 (0.85, 1.12)	0.94 (0.82, 1.08)
rs2272163	3	77671721	A	C	0.42	0.01 (0.004)	0.008	1.00 (0.87, 1.15)	0.97 (0.84, 1.12)
rs3798519	6	50788778	A	C	0.78	-0.01 (0.004)	0.035	0.90 (0.77, 1.06)	0.88 (0.75, 1.04)
rs917195	7	30728452	C	T	0.84	-0.01 (0.005)	0.014	0.92 (0.77, 1.11)	1.05 (0.87, 1.27)
rs12719778	8	145879883	C	T	0.35	0.01 (0.004)	0.009	1.03 (0.89, 1.19)	0.98 (0.85, 1.14)
rs10906115	10	12314997	A	G	0.62	-0.01 (0.004)	0.038	0.95 (0.83, 1.09)	1.03 (0.89, 1.18)
rs57235767	11	93013531	T	C	0.17	0.01 (0.005)	0.013	1.08 (0.91, 1.29)	1.08 (0.90, 1.29)
rs9552911	13	23864657	A	G	0.25	0.01 (0.004)	0.013	1.09 (0.93, 1.28)	0.94 (0.80, 1.11)
rs11642430	16	30045789	C	G	0.56	-0.01 (0.004)	0.023	0.97 (0.84, 1.10)	0.92 (0.80, 1.05)
$GRS_{HbA1c-ARV}$ (13 SNPs)									
rs9727115	1	99177253	A	G	0.36	0.88 (0.36)	0.015	1.04 (0.90, 1.19)	1.00 (0.87, 1.16)
rs6780171	3	185503456	A	T	0.26	0.93 (0.40)	0.020	0.97 (0.83, 1.13)	0.97 (0.83, 1.14)
rs2465043	6	51180765	G	A	0.39	0.78 (0.35)	0.027	1.02 (0.89, 1.17)	0.90 (0.79, 1.04)
rs864745	7	28180556	T	C	0.80	-0.93 (0.44)	0.037	1.10 (0.93, 1.31)	0.96 (0.81, 1.15)
rs12719778	8	145879883	C	T	0.35	1.04 (0.37)	0.005	1.03 (0.89, 1.19)	0.98 (0.85, 1.14)
rs7847880	9	20662703	C	T	0.76	-0.82 (0.41)	0.046	1.01 (0.86, 1.18)	0.88 (0.75, 1.03)
rs10823343	10	71091013	A	G	0.88	-1.19 (0.55)	0.029	0.88 (0.72, 1.09)	1.02 (0.82, 1.26)
rs2237895	11	2857194	A	C	0.61	-0.94 (0.36)	0.009	0.95 (0.83, 1.10)	1.01 (0.88, 1.17)
rs2657879	12	56865338	G	A	0.09	1.67 (0.60)	0.006	1.11 (0.88, 1.40)	1.16 (0.92, 1.47)
rs11066453	12	113365621	G	A	0.18	0.96 (0.45)	0.034	0.92 (0.77, 1.09)	0.96 (0.80, 1.15)
rs9552911	13	23864657	A	G	0.25	0.86 (0.41)	0.034	1.09 (0.93, 1.28)	0.94 (0.80, 1.11)
rs7178762	15	63871292	C	T	0.92	-1.40 (0.66)	0.035	1.04 (0.80, 1.34)	1.13 (0.87, 1.47)
rs11642430	16	30045789	C	G	0.56	-0.81 (0.35)	0.021	0.97 (0.84, 1.10)	0.92 (0.80, 1.05)

Copyright© AE&M all rights reserved.

Supplementary table 2. The Intercepts for the associations between glucose variation and WMH or cerebrovascular abnormality from MR-Egger regression

Glucose variation	MR-Egger regression			
	WMH		cerebrovascular abnormality	
	Estimate	p	Estimate	p
AC-CV	0.017	0.45	-0.025	0.10
AC-SD	-0.019	0.36	-0.011	0.55
AC-VIM	0.006	0.78	0.011	0.35
AC-ARV	-0.009	0.60	0.0003	0.98
HbA1c-CV	0.025	0.10	-0.001	0.95
HbA1c -SD	0.011	0.52	-0.009	0.64
HbA1c-VIM	-0.018	0.38	-0.018	0.41
HbA1c-ARV	-0.014	0.46	-0.015	0.49
			IVW heterogeneity test	
AC-CV	Cochran's Q test	p value	Cochran's Q test	p value
AC-SD	18.72	0.41	11.91	0.85
AC-VIM	13.15	0.59	10.60	0.78
AC-ARV	13.32	0.77	6.63	0.99
HbA1c-CV	12.94	0.84	11.77	0.90
HbA1c -SD	9.24	0.93	10.98	0.86
HbA1c-VIM	11.57	0.87	13.44	0.76
HbA1c-ARV	4.71	0.86	5.40	0.80

Supplementary table 3. The number of SNPs at each stage of instrument selection for each GV metric, including the initial SNP set, exclusion based on association with MRI outcomes, weak association with GV, and LD pruning

Item	Glucose variation							
	AC-CV	AC-SD	AC-VIM	AC-ARV	HbA1c-CV	HbA1c -SD	HbA1c-VIM	HbA1c-ARV
Initial SNP set	536	536	536	536	536	536	536	536
Associations with MRI outcomes (MR assumption 3)	502	502	502	502	502	502	502	502
Exclusions based on weak association with GV (MR assumption 1)	21	17	27	25	20	26	11	18
LD pruning	19	16	19	20	18	19	10	13

Supplementary table 4. List of confounding variables associated with genetic risk scores in patients with type 2 diabetes

Glucose variation	Confounding variables (p<0.05)
GRS_{AC-CV}	Duration of diabetes
GRS_{AC-SD}	HbA1c, stroke
GRS_{AC-VIM}	Coronary artery disease
GRS_{AC-ARV}	eGFR, AC, HbA1c
$GRS_{HbA1c-CV}$	Hypertension
$GRS_{HbA1c-SD}$	Coronary artery disease
$GRS_{HbA1c-VIM}$	BMI, AC
$GRS_{HbA1c-ARV}$	
$wGRS_{AC-CV}$	Duration of diabetes, HbA1c, obesity
$wGRS_{AC-SD}$	HbA1c
$wGRS_{AC-VIM}$	Age, eGFR
$wGRS_{AC-ARV}$	TG, eGFR, AC
$wGRS_{HbA1c-CV}$	BMI, hypertension
$wGRS_{HbA1c-SD}$	Duration of diabetes, coronary artery disease, hyperlipidemia medications, HbA1c
$wGRS_{HbA1c-VIM}$	BMI, hypertension, AC
$wGRS_{HbA1c-ARV}$	Coronary artery disease, HbA1c

Copyright© AE&M all rights reserved.

Archives of Endocrinology and Metabolism
ISSN 2359-4292
OFFICIAL JOURNAL OF THE BRAZILIAN SOCIETY OF ENDOCRINOLOGY AND METABOLISM

invited review

Reversible congenital hypogonadotropic hypogonadism: keys for clinical management

Chrysoula Archaki[1]
https://orcid.org/0009-0006-3253-894X

Maria Stamou[2*]
https://orcid.org/0000-0001-5992-2120

Andrew A. Dwyer[3*]
https://orcid.org/0000-0002-7023-6794

[1] Aristotle University of Thessaloniki, School of Medicine, Thessaloniki, Greece
[2] Massachusetts General Hospital, Reproductive Endocrine Unit and P50 Massachusetts General Hospital – Harvard Center for Reproductive Medicine, Boston, Massachusetts, USA
[3] Boston College William F. Connell School of Nursing and P50 Massachusetts General Hospital – Harvard Center for Reproductive Medicine, Chestnut Hill, Massachusetts, USA

*Contributed equally as co-senior authors.

ABSTRACT

Congenital hypogonadotropic hypogonadism (CHH) is characterized by absent/incomplete puberty and a treatable form of male infertility resulting from deficient gonadotropin-releasing hormone (GnRH) secretion/action. Traditionally, CHH has been considered a permanent, lifelong condition. However, evidence indicates a subset men undergo reversal and recover reproductive axis function. We conducted a structured literature search (Medline, PubMed) using keywords to retrieve articles on CHH reversal (1975-2025). We synthesize the literature to provide a high-level overview of CHH and the reversal phenomenon in males. Particular focus is given to clinical aspects of CHH and reversal using a case vignette to highlight keys to management. Approximately 10-15% of males with CHH undergo reversal with sustained normalized testosterone levels and spermatogenesis off treatment. A key sign of reversal is testicular growth while on testosterone replacement therapy. Those men with some degree of spontaneous puberty (i.e., larger testicular volume), detectable follicle stimulating hormone levels , and/or pathogenic variants in *GNRHR* are more likely to undergo reversal. In contrast, severe GnRH deficiency, pathogenic *ANOS1* and/or two or more combined pathogenic variants (oligogenicity) in CHH genes are less likely to recover reproductive axis function. Reversal is not lasting in all cases. The reversal phenomenon challenges the classical dogma that CHH is permanent and lifelong. Reversal cases highlight the plasticity of the neuroendocrine control of reproduction. Clinicians can tailor the approach to men with CHH using reversal predictors to guide supervise washout to identify reversal as well as long-term monitoring to assess potential relapse.

Keywords: Kallmann syndrome; male infertility; male reproduction; testosterone replacement

Clinical Vignette: A 19-year-old male presented for endocrine consultation and evaluation of delayed puberty. His history was unremarkable but for anosmia (noted at age 10 yrs.) and failure to spontaneously initiate puberty. At presentation, he was normal weight (BMI 23.1 kg/M^2) and his exam was notable for lack of virilization, Tanner II pubic hair, and small testes (5 mL bilaterally). Biochemical evaluation showed normal TSH, prolactin, and IGF1 levels – yet low serum gonadotropins (LH = 1.2 IU/L [ref: 1.6-8.0], FSH = 1.8 [ref: 1.5-9.3]) in the setting of frankly hypogonadal serum testosterone (T) (33 ng/dL [ref: 300-1,000]). The clinical and biochemical findings were consistent with Kallmann syndrome (i.e., congenital hypogonadotropic hypogonadism [CHH] with anosmia) and he initiated T enanthate injections. The dose was increased progressively, and he achieved normal serum T levels on a full adult dose (200 mg IM every two weeks). At his 6-month clinical follow-up visit, his testicular volume was noted to have increased to 9 mL bilaterally. He was instructed to stop treatment and serial monitoring demonstrated sustained, normal serum gonadotropin levels (LH: 5.5 IU/L, FSH: 3.6 IU/L) and eugonadal T (434 ng/dL) – consistent CHH reversal. Three months

Received on Jan/10/2026
Accepted on Mar/3/2026
DOI: 10.20945/2359-4292-2026-0063

Correspondence to:
Andrew A. Dwyer
Boston College, 140
Commonwealth Avenue
Maloney Hall 364
Chestnut Hill, MA 02465
andrew.dwyer@bc.edu

Associated editor:
Letícia F. Gontijo Silveira
https://orcid.org/0000-0002-0053-9167

This is an open-access article distributed under the terms of the Creative Commons Attribution License

Copyright© AE&M all rights reserved.

after discontinuing treatment, his testes had grown to 12 mL bilaterally and seminal fluid analysis revealed sperm in the ejaculate (0.4 X10^6/mL [ref: >15.0]).

INTRODUCTION

Puberty is one of the most striking periods of human life. In males, the most important physiological changes of puberty include accelerated linear growth, changes in body composition, development of secondary sex characteristics, and testicular enlargement. A range of hereditary and environmental factors influence the timing of pubertal onset (1). Delayed puberty in males is defined as lack of testicular development (testicular volume <4 mL) by the age of 14 years. In self-limited delayed puberty (SLDP), puberty begins later than peers yet occurs spontaneously and progresses to completion without needing intervention. In contrast, individuals with congenital hypogonadotropic hypogonadism (CHH) do not complete puberty on their own (2). Currently, there is no 'gold standard' test to differentiate SLDP from CHH, so it remains a diagnosis of exclusion, and CHH is often diagnosed late (3) – often contributing to psychosocial morbidity and diminished health-related quality of life (4,5). Clinically, CHH is characterized by absent or incomplete pubertal development and infertility. It is caused by isolated deficiency in secretion(or action) of gonadotropin releasing hormone (GnRH) – a key regulator of the hypothalamic-pituitary-gonadal (HPG) axis that governs reproduction (2). Biochemically, CHH is defined by low (or inappropriately normal) serum gonadotropin levels in the setting of low serum sex steroids and otherwise normal pituitary imaging and function (6). Notably, CHH is rare (1:48,000) and there is a 3:1 ratio of affected males to females (7). More than 60 genes have been identified to underlie CHH yet the known genes only account for about half of cases (8). Sex steroids are effective for inducing secondary sexual characteristics and fertility can be induced in about 75-80% of cases (9) using either gonadotropin therapy or pulsatile GnRH (10). Despite the notion that congenital disorders are lifelong, approximately 10%-15% of males with CHH experience a reversal and recover reproductive axis function with normalized serum testosterone and spermatogenesis (11,12). The reversal phenomenon highlights the plasticity of the hypothalamic neurons and the possible role of other neuronal populations in regulating the reproductive axis (12). Reversal has been observed in individuals harboring rare pathogenic variants in CHH genes suggesting the contribution of epigenetic factors in CHH reversal (13). This review provides an overview of the approach to managing the male patient with CHH with particular emphasis on the reversal phenomenon.

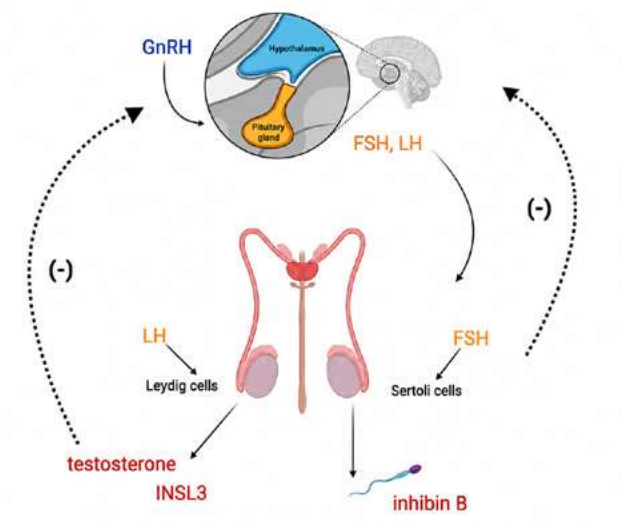
MATERIALS AND METHODS

We conducted a structured, systematic literature search using Medline and PubMed to identify relevant articles on CHH reversal published in English between 1975-2026. Keywords (i.e., Medical Subject Headings — MeSH terms) included "hypogonadism" or "Kallmann" and "reversal" or "recovery". Retrieved articles underwent title and abstract screening. Full-text review was used to exclude articles that did not include CHH cases, reports on adult-onset hypogonadism (i.e., complete spontaneous puberty), and functional hypogonadism (i.e., obesity or exercise-related). Peer-reviewed case reports, original research articles, and review articles documenting reversal of CHH were included for synthesis in this review.

Reproductive axis

Specialized GnRH-secreting neurons regulate the hypothalamic-pituitary-gonadal (HPG) axis and human reproduction. Around 14-weeks of gestation, GnRH neurons migrate from their initial location in the olfactory epithelium (embryonic olfactory placode) crossing the cribriform plate and past the developing olfactory bulb to the hypothalamus. There are only approximately 1,200–1,500 GnRH neurons (2) and the pulsatile secretion of GnRH triggers pituitary gonadotrophs to release luteinizing hormone (LH) and follicle-stimulating hormone (FSH). Gonadotropins (LH and FSH) stimulate the gonads to produce sex steroids and gametes. In males, LH acts on testicular Leydig cells stimulating testosterone (T) production while FSH acts on testicular Sertoli cells stimulating inhibin B secretion and spermatogenesis. Sex steroids and inhibin B regulate the HPG axis through negative feedback (**Figure 1**) (2).

Copyright© AE&M all rights reserved.



Created in BioRender. Archaki, C. (2025) https://BioRender.com/undefined

Figure 1. Schematic depicting the hypothalamic-pituitary-gonadal axis.

Pulsatile GnRH secretion stimulates the release of LH and FSH from pituitary gonadotrophs. In males, LH acts on testicular Leydig cells spurring testosterone (T) production while FSH supports spermatogenesis and stimulates testicular Sertoli cells to produce inhibin B. Both T and inhibin B exert negative feedback on the reproductive axis. GnRH: gonadotropin-releasing hormone; FSH: follicle-stimulating hormone; LH: luteinizing hormone; INSL3: insulin-like peptide 3.

There are three critical waves of HPG activation during development. The first activation occurs *in utero*. In males, maternal human chorionic gonadotropin (hCG) and fetal HPG axis activation stimulate Leydig cells to produce T and insulin-like peptide 3, resulting in normal penile development and the final phase of testicular descent, respectively. The second wave, or so-called minipuberty, occurs during the first 4–6 months of neonatal life. This brief window of HPG axis activation drives Sertoli and germ cell proliferation and is a key early-life determinant of future reproductive capacity (14). The third wave of HPG axis activation occurs at the onset of puberty, which is characterized by the development of secondary sexual characteristics and full reproductive capacity.

Presentation and diagnosis of CHH

The clinical presentation of CHH is heterogeneous ranging from isolated GnRH deficiency to syndromic forms with variable constellations of non-reproductive phenotypes (i.e., sensory, dental, muculoskeletal, neurologic) (**Table 1**) (2,15). Approximately half of cases exhibit non-reproductive phenotypes, the most common being lack of sense of smell (CHH + anosmia = Kallmann syndrome). Moreover, the degree of GnRH deficiency can be variable from absent minipuberty (e.g., cryptorchidism with/without micropenis) with complete absent of spontaneous puberty (i.e., testicular volume [TV] <4 mL) to partial spontaneous puberty (TV ≥4 mL) and the Pasqualini syndrome characterized by CHH with near-complete puberty development (TV: 8-10 mL) (16). Ultimately, CHH is a clinical diagnosis of exclusion yet the variable clinical presentation as well as lack of a 'gold standard' test to differentiate SLDP from CHH contribute to late diagnosis (i.e., at 18 yrs or later) (2,4).

Dynamic stimulation tests, such as GnRH stimulation and FSH-stimulated inhibin B, among others, have been proposed to differentiate CHH from SLDP, yet these tests lack sufficient specificity (17). Recent research has identified kisspeptin stimulation as a promising test for differentiating SLDP and CHH (18).

Table 1. CHH-associated phenotypes from the literature

Reproductive	Non-Reproductive (syndromic)		
	Sensory & Neurologic	**Skeletal & Dental**	**Developmental & Other**
• Cryptorchidism • Micropenis • Absent minipuberty • Absent puberty • Partial puberty • Reversal of CHH	• Anosmia/hyposmia • Hearing loss • Ear anomalies • Coloboma • Ano/micropthalmia • Synkinesia • Cerebellar ataxia	• Osteopenia/-porosis • Scoliosis • Syndactyly • Clinodactyly • camptodactyly • Split hand/foot • Joint hyperlaxity • Pectus excavatum • Eunuchoidal proportions • Missing/extra teeth	• Cleft lip/palate • Bifid uvula • Choanal atresia • Renal agenesis • Pituitary defects • Arrhinia • Ichthyosis • Achromic hair patches • Congenital heart defects • Developmental delay • Intellectual disability

Copyright© AE&M all rights reserved.

Kisspeptin is a neuropeptide "upstream" of the hypothalamus that triggers the release of GnRH and activates the HPG axis in the onset of puberty (2). While initial study results are promising, further work is needed to definitively prove effectiveness as a clinical diagnostic test.

Notably, several clinical 'red flags' (cryptorchidism, micropenis, anosmia) can help speed diagnosis leading to timely treatment (19). The vast majority of CHH cases are sporadic with only about 30% showing familial inheritance (2,8). The genetics of CHH is complex with autosomal dominant, autosomal recessive, X-linked, digenic (i.e., two rare variants), and oligogenic forms occurring in roughly 15% of cases (20). To date, more than 60 genes have been identified to underlie CHH, accounting for approximately half of cases (8). As such, panel testing can inform molecular diagnosis of CHH and speed diagnosis in some cases, yet it is not universally informative (21). It is worthwhile to note that late diagnosis ("diagnostic odyssey") is associated with psychosocial morbidity (e.g., anxiety, depression) (4), psychosexual sequelae (5) and diminished health-related quality of life (22). Evidence supports that earlier diagnosis enables timely initiation of treatment and helps alleviate some of the psychosocial impact and emotional distress of CHH (23).

Treatment of CHH

Unlike many rare diseases, effective treatments are available for CHH. Exogenous testosterone (T) treatment (i.e., transdermal gels or long-acting injectable esters) is effective for inducing secondary sexual characteristics (24). Treatment is initiated with low dose (e.g., 50 mg IM monthly) then progressively titrated to full adult dosage with trough T levels at the lower end of the normal reference range. However, a more rapid dose escalation is typically used for males who present with CHH well into adulthood (24). Adherence to treatment should be assessed at every visit (6) and men will typically need to remain on lifelong T treatment using either a transdermal preparation, an injectable T ester (e.g., enanthate, cypionate, undecanoate), or implantable T pellets. While T treatment induces virilization and can normalize sexual function, it will not induce testicular development or fertility. Importantly, increased TV on T treatment indicates activation of the HPG axis and may suggest reversal of CHH.

Unlike many forms of male infertility, CHH is treatable and approximately 75%– 80% of males with CHH can develop sperm in the ejaculate using either pulsatile GnRH (via microinfusion pump) or gonadotropin therapy (human chorionic gonadotropin [hCG], FSH) (9). Pulsatile GnRH is typically limited to specialized research centers while gonadotropins are much more widely used. There are several options for inducing fertility in males with CHH, including concurrent administration of hCG with FSH or sequential gonadotropin therapy (i.e., unopposed FSH followed by hCG + FSH) (10). Monotherapy with hCG alone is not the preferred approach given suboptimal outcomes (25). Many men with CHH are able to achieve fertility within a year (26). Research has identified history of cryptorchidism, complete absence of spontaneous pubertal development (TV <4 mL), and low serum inhibin B (<60 pg/mL) as negative predictors of outcome to fertility-inducing treatment (27,28). In such cases, sequential gonadotropin therapy, which aims to recreate the hormonal milieu of minipuberty, appears to provide the best chances for developing fertility (10,29). Although most men with CHH will not achieve WHO-defined normal sperm counts (>20x10^6/mL) (30), low sperm counts do not preclude fertility or conception (31). As previously noted, T treatment will not induce spermatogenesis, so fertility while on T should warrant evaluation of CHH reversal (12).

CHH reversal

Traditionally, CHH has been considered a congenital, permanent condition requiring lifelong treatment. A 1975 case report raised the first notion that CHH may be reversible (32). Subsequently, additional case reports over the next decades documented men with confirmed CHH who recovered their HPG axis function with normalized serum T levels (**Supplemental Table 1**). In 2007, the first prospective study of the CHH reversal phenomenon identified five reversal cases among a cohort of 50 CHH men, suggesting a reversal rate of 10% (13). Reversal cases are heterogeneous. Some men who undergo CHH reversal

Copyright© AE&M all rights reserved.

only have isolated GnRH deficiency while others exhibit a constellation of non-reproductive phenotypes (11,12). Some men exhibit signs of absent minipuberty and a complete absence of spontaneous pubertal puberty (TV < 4 mL) (33) while others exhibit the relatively mild GnRH deficiency with partial spontaneous puberty (i.e., Pasqualini syndrome) (16). While clinical presentation varies across reversal cases, all share a similar pattern – HPG axis activation (**Figure 2**) following a period of normalized serum sex steroid levels from either exogenous T, gonadotropins, or pulsatile GnRH therapy (11,12).

A 2024 study of 87 reversal cases across six international referral centers identified two distinct classes of reversals and several predictors (34). Men were more likely to undergo reversal if they exhibited milder GnRH deficiency (i.e., Pasqualini syndrome) with no micropenis, some degree of spontaneous testicular development (TV ≥8 mL), and detectable FSH (i.e., ~4.0 IU/L). Prior work conducting detailed neuroendocrine profiling (i.e., 12-hr LH pulsatility studies) found a LH threshold of 2.1 IU/L being a fairly reliable proxy for pulsatile LH secretion (15). That data

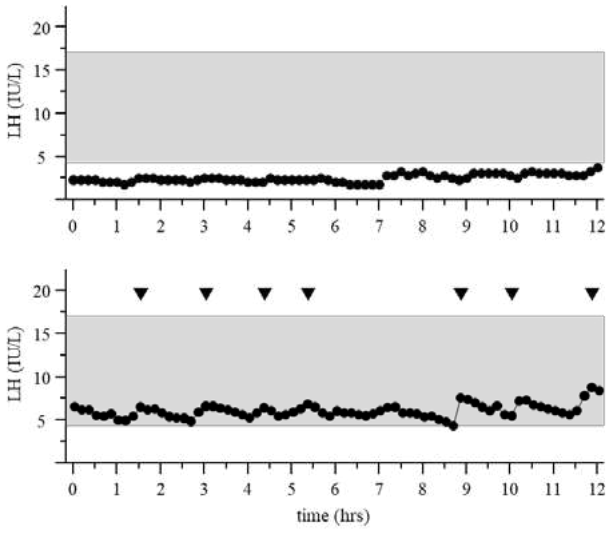


Figure 2. LH pulse study before and after reversal.

Panels depict serum LH levels during overnight (17:30-05:30) 12-hour frequent blood sampling studies (Q 10 min. x 12 hrs.). Upper panel: At diagnosis, the 19-year-old male exhibited apulsatile LH secretion and frankly hypogonadal testosterone (33 ng/dL). Testosterone therapy was initiated and continued for 18 months. The patient's testicular volume had increased from 4 mL to 6 mL on testosterone. Treatment was discontinued and he underwent a repeat frequent sampling study (lower panel) revealing LH pulses (inverted triangles) in the setting of normal serum testosterone levels (334 ng/dL). Gray shaded region depicts the mean LH ± 2 S.D.s of healthy volunteers (13).

was in line with the results of a 2015 Chinese study that identified 18 reversals (5.1%) in a cohort of 354 males with CHH study (35). Authors noted that larger testicular size and higher LH levels (both basal and tryptorelin-stimulated) were associated with reversal (35). However, the 2024 study of the largest reversal cohort (n=87) to date found no link between LH and reversal (34).

Genetics of reversal

It is notable that reversal cases have been documented in individuals harboring pathogenic rare variants in CHH genes (11,12) (**Supplemental Table 1**). To date, rare variants in more than 30 CHH genes have been found in cases with CHH reversal (**Table 2**). Genetic factors that can help us determine the likelihood of CHH reversal include: (i) variants in the autosomal recessive GnRH receptor gene (*GNRHR*). Recent data found that men who harbor pathogenic *GNRHR* variants are more likely to undergo reversal (34); (ii) variants in the X-linked gene, *ANOS1*. Among the largest reversal cohort studied to date (n=87), no pathogenic variants in *ANOS1* were detected. Notably, *ANOS1* variants cause a particularly severe form of GnRH deficiency (15,36) that is rather unresponsive to fertility-inducing treatment (10,15). Curiously, a 2007 case report described a reversal in a male harboring an *ANOS1* – then termed *KAL1* (37). Several factors raise questions about the validity of the *ANOS1* reversal case report. First, sequencing technology has advanced significantly and has since reduced the risk of pseudogene findings that were once more likely in *ANOS1* sequencing. Second, the patient's T level at diagnosis was 212 ng/dL – which is uncharacteristically higher than expected in light of the severe *ANOS1*-related GnRH deficiency. Third, no other cases of *ANOS1*-associated reversal have been documented (Supplemental Table 1). Thus, patients harboring *ANOS1* variants are unlikely to undergo reversal; (iii) The genetic load observed in patients screened. Men with pathogenic variants in more than one gene (i.e., oligogenicity) are less likely to undergo reversal (34).

Of note, when genetic testing is unavailable or cost-prohibitive, several key factors can increase our suspicion for an *ANOS1* variant, and thus, decrease the

Copyright© AE&M all rights reserved.

Table 2. CHH Genes identified in reversal grouped according to gene function

GnRH neuron migration	GnRH secretion	CHH & other overlapping syndromes
ANOS1 (XLR)	*AMH* (AR)	CHARGE syndrome
CCDC141 (AR)	*DMXL2* (AR)	• *CHD7* (AD)
DCC (AD)	*GNRH1* (AR)	
FEZF1 (AR)	*IGSF10* (AD)	Combined pituitary hormone deficiency
FGF8 (AD)	*KISS1* (AR)	• *SOX2* (AD)
FGFR1 (AD)	*KISS1R* (AR)	• *WDR11* (AD)
HS6ST1 (AD)	*LEPR* (AR)	
IL17RD (AR)	*TAC3* (AR)	Gordon Holmes Syndrome
NSMF (AR)	*TAC3R* (AR)	• *OTUD4* (AR)
PLXNA1 (AD)	**GnRH action**	• *PNPLA6* (AR)
PROK2 (AR)	*GNRHR* (AR)	• *RNF216* (AR)
PROKR2 (AR)		
SEMA3A (AD)		Pallister-Hall Syndrome
SEMA7A (AD)		• *GLI3* (AD)
		Waardenburg Syndrome (Type 2)
		• *SOX10* (AD)
		Warburg Micro Syndrome
		• *RAB3GAP1* (AR)
		• *RAB3GAP2* (AR)

AD: autosomal dominant; AR: autosomal recessive; XLR: X-linked recessive.

likelihood of CHH reversal (34). First, *ANOS1* invariably causes Kallmann syndrome, so complete anosmia is an essential hallmark of *ANOS1* variants. Individuals with *ANOS1* variants are more likely to exhibit mirror movements (i.e., synkinesia) and have renal agenesis (38). Further, as *ANOS1* follows an X-linked recessive inheritance. Thus, careful family history and pedigree analysis can provide critical clues. Last, CHH caused by *ANOS1* variants is typically a severe form of GnRH deficiency and is associated with cryptorchidism (with/without micropenis) and complete absence of spontaneous puberty (TV <4 mL) (15).

Proposed mechanisms of reversal

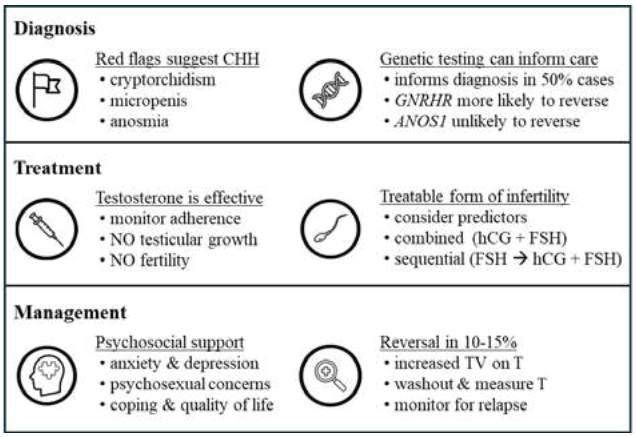
The mechanism(s) underlying CHH reversal remain unclear. The 2007 prospective study was the first reversal study to report with a pathogenic variant in a CHH gene (13). Authors hypothesized that genetic defects could affect GnRH neuron maturation, and androgens could upregulate genes involved in synchronized GnRH secretion. Additional support for the proposed mechanism came in a subsequent report of two men who were able to sustain HPG axis function (i.e., CHH reversal) reversal with intermittent exogenous androgen exposure (39). To date, a number of factors have been proposed, including epigenetic factors, non-coding regions of the genome, and other neuronal populations in the hypothalamus (astrocytes, tanycytes) that interact with GnRH neurons via KNDy neurons (kisspeptin, neurokinin B, and dynorphin) (40). Kisspeptin is a potent stimulator of GnRH secretion and it is well known that sex steroids exert feedback effects regulating the GnRH pulse pattern (41,42). Thus, CHH reversal appears to be related to the plasticity of the neuronal network involved in GnRH secretion.

Relapse of reversal

It is important to underscore that the recovery of HPG axis function may not be lasting, and some patients revert to a hypogonadal state. According to a large retrospective study of 308 patients with CHH, 39 men underwent reversal and 5/39 (13%) of them experienced a subsequent relapse to a hypogonadal state (43). Common characteristics among those who relapsed to a hypogonadal state included a significant stressor – either emotional, psychiatric, or metabolic. Such stressors can disrupt pubertal timing and development (44). Indeed, anxiety/depression and changes in energy balance can impair the reproductive axis

Copyright© AE&M all rights reserved.

with suppressed T levels and decreased LH pulse frequency/amplitude - akin to hypothalamic amenorrhea in females (45). Thus, ongoing surveillance and hormonal monitoring is warranted following reversal (2,6,11,12). If spermatogenesis is achieved during a window of CHH reversal, sperm banking should be offered to mitigate the loss of fertility in the event of relapse. The dynamic nature of the HPG axis is highlighted by individuals who undergo a 'second' reversal (i.e., T = 257 ng/dL) after relapse and recover reproductive function a second time (43).



Inset Box 1. Key points for diagnosis, treatment, and management of CHH

Return to case

Positive predictors for the patient's reversal include his partial puberty (with baseline TV of 5 mL bilaterally), detectable FSH and lack of severe GnRH deficiency during mini puberty (no cryptorchidism or micropenis). Following reversal, the patient returned to clinic every six months for ongoing surveillance. At the 18-month visit he complained of fatigue and decreased frequency and strength of his morning erections. Blood work showed hypogonadal T (205 ng/dL). Treatment options were discussed with the patient (i.e., T replacement vs. gonadotropin injections) and the patient opted to cryopreserve sperm, his current sperm count was now 1.7X10^6/mL, then initiate T replacement with ongoing monitoring.

CONCLUSION

In summary, CHH is clinically and genetically heterogenous and there are a number of key facets of comprehensive disease management (**Inset Box 1**). While CHH was traditionally considered lifelong, we know that approximately 10-15% of men undergo reversal, with recovery of HPG axis function following a period of normalized T levels (12). Increase in testicular size, in conjunction with the normalization of circulating levels of sex steroids while on T replacement is a reliable hallmark (11,12). Given the possibility of reversal, clinicians can consider key factors favoring reversal to target supervised treatment washouts every 1-2 years. Key signs that increase the likelihood of reversal include: history of partial puberty (TV >4 mL), detectable gonadotropins (FSH ~ 4 IU/L), and/or variant in *GNRHR*. On the other hand, signs suggestive of severe GnRH deficiency and absent minipuberty (i.e., cryptorchidism with/without micropenis) as well as pathogenic variants in *ANOS1* and/or variants in two or more CHH genes (i.e., oligogenicity) decrease the likelihood of reversal. Notably, reversal is not always permanent, so longitudinal monitoring is warranted. In conclusion, the reversal phenomenon challenges the dogma that congenital genetic conditions are lifelong and reversible CHH raises many questions regarding neuronal plasticity and epigenetic influences on the neuroendocrine control of reproduction.

Author contributions: C.A. contributed to the literature search, drafting the manuscript, and visualizations; M.S. contributed to conceptualizing the work, supervision, and critically reviewing/editing the manuscript; A.A.D. contributed to conceptualizing the work, literature search, visualizations, and critically reviewing/editing the manuscript, and acquiring funding. All authors reviewed and approved the manuscript for submission.

Funding: National Institutes of Health Eunice Kennedy Shriver National Institute of Child Health and Human Development (1P50HD104224-01).

Disclosure: no potential conflict of interest relevant to this article was reported.

Data availability: datasets related to this article will be available upon request to the corresponding author.

REFERENCES

1. Sisk CL, Foster DL. The neural basis of puberty and adolescence. Nat Neurosci. 2004;7(10):1040–7. doi: 10.1038/nn1326.
2. Boehm U, Bouloux PM, Dattani MT, de Roux N, Dodé C, Dunkel L, et al. Expert consensus document: European Consensus Statement on congenital hypogonadotropic hypogonadism--pathogenesis, diagnosis and treatment. Nat Rev Endocrinol. 2015 Sep;11(9):547-64. doi: 10.1038/nrendo.2015.112.
3. Harrington J, Palmert MR. Distinguishing Self-limited Delayed Puberty From Permanent Hypogonadotropic Hypogonadism: How and Why?

Copyright© AE&M all rights reserved.

J Clin Endocrinol Metab. 2021 Nov 19;106(12):e5264-e5266. doi: 10.1210/clinem/dgab498.

4. Dwyer AA, Smith N, Quinton R. Psychological Aspects of Congenital Hypogonadotropic Hypogonadism. Front Endocrinol (Lausanne). 2019;10:353. doi: 10.3389/fendo.2019.00353.
5. Dwyer AA. Psychosexual effects resulting from delayed, incomplete, or absent puberty. Curr Opin Endocr Metab Res. 2020;14:15-21. doi: 10.1016/j.coemr.2020.04.003.
6. Young J, Xu C, Papadakis GE, Acierno JS, Maione L, Hietamaki J, et al. Clinical Management of Congenital Hypogonadotropic Hypogonadism. Endocr Rev. 2019;40(2):669-710. doi: 10.1210/er.2018-00116.
7. Laitinen EM, Vaaralahti K, Tommiska J, Eklund E, Tervaniemi M, Valanne L, et al. Incidence, phenotypic features and molecular genetics of Kallmann syndrome in Finland. Orphanet J Rare Dis. 2011;6:41. doi: 10.1186/1750-1172-6-41.
8. Silveira LFG, Seraphim CE, Latronico AC. Genetic Basis and Heterogeneity of Congenital Hypogonadotropic Hypogonadism. Semin Reprod Med. 2025 Dec;43(4):282-295. doi: 10.1055/a-2806-2848.
9. Rastrelli G, Corona G, Mannucci E, Maggi M. Factors affecting spermatogenesis upon gonadotropin-replacement therapy: a meta-analytic study. Andrology. 2014 Nov;2(6):794-808. doi: 10.1111/andr.262.
10. Dwyer AA, McDonald IR, Quinton R. Current landscape of fertility induction in males with congenital hypogonadotropic hypogonadism. Ann N Y Acad Sci. 2024 Oct;1540(1):133-146. doi: 10.1111/nyas.15214.
11. Dwyer AA, Raivio T, Pitteloud N. MANAGEMENT OF ENDOCRINE DISEASE: Reversible hypogonadotropic hypogonadism. Eur J Endocrinol. 2016 Jun;174(6):R267-74. doi: 10.1530/EJE-15-1033.
12. Dwyer AA, Stamou M. Reversal of Congenital Hypogonadotropic Hypogonadism. J Clin Endocrinol Metab. 2026 Jan 21;111(2):e352-e361. doi: 10.1210/clinem/dgaf610.
13. Raivio T, Falardeau J, Dwyer A, Quinton R, Hayes FJ, Hughes VA, et al. Reversal of idiopathic hypogonadotropic hypogonadism. N Engl J Med. 2007 Aug 30;357(9):863-73. doi: 10.1056/NEJMoa066494.
14. Rohayem J, Alexander EC, Heger S, Nordenström A, Howard SR. Mini-Puberty, Physiological and Disordered: Consequences, and Potential for Therapeutic Replacement. Endocr Rev. 2024 Jul 12;45(4):460-492. doi: 10.1210/endrev/bnae003.
15. Dwyer AA, Stamou MI, Anghel E, Hornstein S, Chen D, Salnikov KB, et al. Reproductive Phenotypes and Genotypes in Men With IHH. J Clin Endocrinol Metab. 2023 Mar 10;108(4):897-908. doi: 10.1210/clinem/dgac615.
16. Dwyer AA, Stamou M, McDonald IR, Anghel E, Cox KH, Salnikov KB, et al. Reversible hypogonadotropic hypogonadism in men with the fertile eunuch/Pasqualini syndrome: A single-center natural history study. Front Endocrinol (Lausanne). 2022 Nov 2;13:1054447. doi: 10.3389/fendo.2022.1054447.
17. Mosbah H, Bouvattier C, Maione L, Trabado S, De Filippo G, Cartes A, et al. GnRH stimulation testing and serum inhibin B in males: insufficient specificity for discriminating between congenital hypogonadotropic hypogonadism from constitutional delay of growth and puberty. Hum Reprod. 2020 Oct 1;35(10):2312-2322. doi: 10.1093/humrep/deaa185.
18. Chan YM, Lippincott MF, Sales Barroso P, Alleyn C, Brodsky J, Granados H, et al. Using Kisspeptin to Predict Pubertal Outcomes for Youth With Pubertal Delay. J Clin Endocrinol Metab. 2020 Aug 1;105(8):e2717-25. doi: 10.1210/clinem/dgaa162.
19. Swee DS, Quinton R. Congenital Hypogonadotrophic Hypogonadism: Minipuberty and the Case for Neonatal Diagnosis. Front Endocrinol (Lausanne). 2019 Feb 21;10:97. doi: 10.3389/fendo.2019.
20. Cassatella D, Howard SR, Acierno JS, Xu C, Papadakis GE, Santoni FA, et al. Congenital hypogonadotropic hypogonadism and constitutional delay of growth and puberty have distinct genetic architectures. Eur J Endocrinol. 2018 Apr;178(4):377-388. doi: 10.1530/EJE-17-0568.
21. Al Sayed Y, Howard SR. Panel testing for the molecular genetic diagnosis of congenital hypogonadotropic hypogonadism - a clinical perspective. Eur J Hum Genet. 2023 Apr;31(4):387-394. doi: 10.1038/s41431-022-01261-0.
22. Varimo T, Hero M, Laitinen EM, Sintonen H, Raivio T. Health-related quality of life in male patients with congenital hypogonadotropic hypogonadism. Clin Endocrinol (Oxf). 2015 Jul;83(1):141-3. doi: 10.1111/cen.12701.
23. Dwyer AA, Zeng Z, Lee CS. Validating online approaches for rare disease research using latent class mixture modeling. Orphanet J Rare Dis. 2021 May 10;16(1):209. doi: 10.1186/s13023-021-01827-z.
24. Federici S, Goggi G, Quinton R, Giovanelli L, Persani L, Cangiano B, et al. New and Consolidated Therapeutic Options for Pubertal Induction in Hypogonadism: In-depth Review of the Literature. Endocr Rev. 2022 Sep 26;43(5):824-851. doi: 10.1210/endrev/bnab043.
25. Muir CA, Zhang T, Jayadev V, Conway AJ, Handelsman DJ. Efficacy of Gonadotropin Treatment for Induction of Spermatogenesis in Men With Pathologic Gonadotropin Deficiency: A Meta-Analysis. Clin Endocrinol (Oxf). 2025 Feb;102(2):167-177. doi: 10.1111/cen.15151.
26. Gialouris JV, Conway AJ, Idan A, Savkovic S, Hermosilla R, Muir CA, et al. Efficacy of Gonadotropin Therapy to Induce Spermatogenesis and Fertility in Men with Pathologic Gonadotropin Deficiency. J Clin Endocrinol Metab. 2026 Apr 22;111(5):1450-1458. doi: 10.1210/clinem/dgaf588.
27. Cangiano B, Goggi G, Federici S, Bresesti C, Cotellessa L, Guizzardi F, et al. Predictors of reproductive and non-reproductive outcomes of gonadotropin mediated pubertal induction in male patients with congenital hypogonadotropic hypogonadism (CHH). J Endocrinol Invest. 2021 Nov;44(11):2445-2454. doi: 10.1007/s40618-021-01556-x.
28. Pitteloud N, Hayes FJ, Dwyer A, Boepple PA, Lee H, Crowley WF Jr. Predictors of outcome of long-term GnRH therapy in men with idiopathic hypogonadotropic hypogonadism. J Clin Endocrinol Metab. 2002 Sep;87(9):4128-36. doi: 10.1210/jc.2002-020518.
29. Dwyer AA, Sykiotis GP, Hayes FJ, Boepple PA, Lee H, Loughlin KR, et al. Trial of recombinant follicle-stimulating hormone pretreatment for GnRH-induced fertility in patients with congenital hypogonadotropic hypogonadism. J Clin Endocrinol Metab. 2013 Nov;98(11):E1790-5. doi: 10.1210/jc.2013-2518.
30. Björndahl L, Kirkman Brown J; other Editorial Board Members of the WHO Laboratory Manual for the Examination and Processing of Human Semen. The sixth edition of the WHO Laboratory Manual for the Examination and Processing of Human Semen: ensuring quality and standardization in basic examination of human ejaculates. Fertil Steril. 2022 Feb;117(2):246-251. doi: 10.1016/j.fertnstert.2021.12.012.
31. Burris AS, Clark RV, Vantman DJ, Sherins RJ. A low sperm concentration does not preclude fertility in men with isolated hypogonadotropic hypogonadism after gonadotropin therapy. Fertil Steril. 1988 Aug;50(2):343-7. doi: 10.1016/s0015-0282(16)60084-5.
32. Resvani I, DiGeorge AM, Reitano J, Snyder P. J. Delayed puberty and anosmia: coincidence or Kallmann variant? [abstract]. Pediatric Research. 1975;9:294.
33. Gianetti E, Tusset C, Noel SD, Au MG, Dwyer AA, Hughes VA, et al. TAC3/TACR3 mutations reveal preferential activation of gonadotropin-releasing hormone release by neurokinin B in neonatal life followed by reversal in adulthood. J Clin Endocrinol Metab. 2010;95(6):2857-2867.
34. Dwyer AA, McDonald IR, Cangiano B, Giovanelli L, Maione L, Silveira LFG, et al. Classes and predictors of reversal in male patients with congenital hypogonadotropic hypogonadism: a cross-sectional study of six international referral centres. Lancet Diabetes Endocrinol. 2024;12(4):257-66. doi: 10.1016/S2213-8587(24)00028-7.
35. Mao JF, Xu HL, Duan J, Chen RR, Li L, Li B, et al. Reversal of idiopathic hypogonadotropic hypogonadism: a cohort study in Chinese patients. Asian J Androl. 2015 May-Jun;17(3):497-502. doi: 10.4103/1008-682X.145072.

Copyright© AE&M all rights reserved.

36. Sykiotis GP, Hoang XH, Avbelj M, Hayes FJ, Thambundit A, Dwyer A, et al. Congenital idiopathic hypogonadotropic hypogonadism: evidence of defects in the hypothalamus, pituitary, and testes. J Clin Endocrinol Metab. 2010 Jun;95(6):3019-27. doi: 10.1210/jc.2009-2582.
37. Ribeiro RS, Vieira TC, Abucham J. Reversible Kallmann syndrome: report of the first case with a KAL1 mutation and literature review. Eur J Endocrinol. 2007 Mar;156(3):285-90. doi: 10.1530/eje.1.02342.
38. Costa-Barbosa FA, Balasubramanian R, Keefe KW, Shaw ND, Al-Tassan N, Plummer L, et al. Prioritizing genetic testing in patients with Kallmann syndrome using clinical phenotypes. J Clin Endocrinol Metab. 2013 May;98(5):E943-53. doi: 10.1210/jc.2012-4116.
39. Santhakumar A, Balasubramanian R, Miller M, Quinton R. Reversal of isolated hypogonadotropic hypogonadism: long-term integrity of hypothalamo-pituitary-testicular axis in two men is dependent on intermittent androgen exposure. Clin Endocrinol (Oxf). 2014;81(3):473-6. doi: 10.1111/cen.12347.
40. Prevot V, Sharif A. The polygamous GnRH neuron: Astrocytic and tanycytic communication with a neuroendocrine neuronal population. J Neuroendocrinol. 2022;34(5):e13104. doi: 10.1111/jne.13104.
41. Prashar V, Arora T, Singh R, Sharma A, Parkash J. Hypothalamic Kisspeptin Neurons: Integral Elements of the GnRH System. Reprod Sci. 2023;30(3):802-22. doi: 10.1007/s43032-022-01027-5.
42. Koysombat K, Tsoutsouki J, Patel AH, Comninos AN, Dhillo WS, Abbara A. Kisspeptin and neurokinin B: roles in reproductive health. Physiol Rev. 2025;105(2):707-64. doi: 10.1152/physrev.00015.2024.
43. Sidhoum VF, Chan YM, Lippincott MF, Balasubramanian R, Quinton R, Plummer L, et al. Reversal and relapse of hypogonadotropic hypogonadism: resilience and fragility of the reproductive neuroendocrine system. J Clin Endocrinol Metab. 2014 Mar;99(3):861-70. doi: 10.1210/jc.2013-2809.
44. Esquivel-Zuniga R, Rogol AD. Functional hypogonadism in adolescence: an overlooked cause of secondary hypogonadism. Endocr Connect. 2023 Sep 27;12(11):e230190. doi: 10.1530/EC-23-0190.
45. Dwyer AA, Chavan NR, Lewkowitz-Shpuntoff H, Plummer L, Hayes FJ, Seminara SB, et al. Functional Hypogonadotropic Hypogonadism in Men: Underlying Neuroendocrine Mechanisms and Natural History. J Clin Endocrinol Metab. 2019;104(8):3403-14. doi: 10.1210/jc.2018-02697.

Copyright© AE&M all rights reserved.

SUPPLEMENTARY MATERIAL

Supplemental Table 1. Reports of CHH reversal (1975-2025)

Year (ref.)	Article type (# cases)	Notes (genes reported)
1975 (1)	case report (n=1)	first case report, anosmic (KS), TRT only, increased TV, spermatogenesis
1980 (2)	case series (n=2)	both anosmic with Pasqualini syndrome, conceived with proven paternity
1983 (3)	case report (n=1)	anosmic (KS), TRT only (21 mos.), conceived with proven paternity
1986 (4)	case report (n=1)	anosmic (KS), TRT only, increased TV, normal T sustained off treatment s/p 7 yrs.
1989 (5)	cohort (n=4)	LH pulses in 4/10 CHH off long-term pulsatile GnRH therapy
1994 (6)	case report (n=1)	anosmic (KS), hCG then TRT, spermatogenesis & normal T sustained off treatment, conception
1995 (7)	case report (n=1)	anosmic with Pasqualini syndrome, TRT only, increased TV & spermatogenesis, conceived
1996 (8)	cohort (n=1)	anosmic (KS), TRT only, LH pulses, normal T sustained off treatment
1999 (9)	case series (n=5)	all anosmic (KS), increased TV on TRT, spermatogenesis documented in 4/5
2007 (10)	cohort (n=15)	prospective study, 5/50 with normalized T off long-term treatment (*GNRHR, FGFR1*)
2007 (11)	case report (n=1)	all anosmic (KS), increased TV on TRT, spermatogenesis, conceived (*ANOS1*)
2008 (12)	case report (n=1)	anosmic (KS), sustained normalized T & spermatogenesis off treatment (*PROKR2*)
2010 (13)	cohort (n=6)	reversals reported as part of a gene discovery project; reversal = LH pulsatility, increased TV and T, or spermatogenesis (*TAC3, TACR3*)
2011 (14)	cohort (n=1)	reversals reported as part of a gene discovery project; anosmic (KS), normal T sustained off treatment for several years (*HS6ST1*)
2012 (15)	cohort (n=6)	cohort of reversal cases (anosmic: n=2, normosmic: n=4) increased TV, normalized T & spermatogenesis off treatment (*CHD7, FGFR1, GNRHR*)
2013 (16)	case report (n=1)	hCG then TRT, spermatogenesis & normal T sustained off treatment (*GNRHR*)
2013 (17)	case series (n=6)	TRT only, increased TV, normal T sustained off treatment
2013 (18)	cohort (n=2)	reversals reported as part of a FGF synexpression group gene discovery project (*IL17RD, SPRY4*)
2014 (19)	cohort (n=18)	cohort of reversal cases (anosmic: n=5, normosmic: n=13) mix of hCG & TRT treatment, increased TV, normal T sustained off treatment
2014 (20)	cohort (n=44)	cohort of reversal cases, reversal & relapse, first report o (*FGFR1, GNRHR, PROKR2, TACR3, TAC3,HS6ST1, NELF*)
2014 (21)	case series (n=2)	both anosmic (KS), TRT only, increased TV, required intermittent T "booster' to trigger reversal after relapse
2014 (22)	cohort (n=1)	reversals reported as part of a gene discovery project; normal T sustained off treatment (*GNRHR*)
2016 (23)	case report (n=1)	anosmic (KS), TRT only, increased TV, normal T & spermatogenesis sustained off treatment (*SOX10*)
2017 (24)	case report (n=1)	Pasqualini syndrome, TRT only, increased TV, normal T sustained off treatment
2017 (25)	case report (n=1)	anosmic (KS), TRT only, increased TV, normal T sustained off treatment (*PROK2*)
2019 (26)	cohort (n=6)	reversals reported as part of a gene discovery project (anosmic: n=3, normosmic: n=3) increased TV, normal T sustained off treatment, one relapse (*GNRHR, IGSF10*)
2020 (27)	cohort (n=1)	reversals reported as part of a gene discovery project; normosmic female (*CCDC141*)
2022 (28)	cohort (n=13)	reversal cases recorded in a large cohort of patients (anosmic: n=6, normosmic: n=7) increased TV, spermatogenesis and/or fertility, normal T sustained off treatment (*CHD7, IL17RD, PROKR2*)
2022 (29)	case report (n=1)	increased TV, normal T sustained off treatment (*GNRHR*)
2022 (30)	case report (n=1)	increased TV, spermatogenesis, normal T off treatment, multiple relapses
2022 (31)	cohort (n=16)	reversal cases recorded in a cohort of patients with Pasqualini syndrome (n=38); increased TV, spermatogenesis and/or fertility, normal T off treatment (*FGFR1, GNRHR*)
2024 (32)	cohort (n=87)	cohort of reversal cases (n=87), multicenter study, predictors of reversal (34 genes reported)
2025 (33)	case report (n=2)	single consanguineous family, TRT only, increased TV, normal T sustained off treatment (*KISS1*)

GnRH: gonadotropin-releasing hormone; hCG: human chorionic gonadotropin; KS: Kallmann syndrome; T: testosterone; TRT: testosterone replacement therapy; TV: testicular volume.

Copyright© AE&M all rights reserved.

Archives of Endocrinology and Metabolism
ISSN 2359-4292
OFFICIAL JOURNAL OF THE BRAZILIAN SOCIETY OF ENDOCRINOLOGY AND METABOLISM

case report

Catheterization of the petrosal sinus: possible advantage of desmopressin stimulation in Cushing disease

Heraldo Mendes Garmes[1]
https://orcid.org/0000-0001-6117-8548

Sara Calazans de Siqueira[1]
https://orcid.org/0009-0004-1400-5459

Karla Borges Daniel[1]
https://orcid.org/0000-0002-4247-5819

Marilia Bortolotto Felippe Trentin[1]
https://orcid.org/0000-0001-8067-4838

Mariana Tazima Fujiwara[1]
https://orcid.org/0009-0008-7986-0869

Caroline Schinoll[1]
https://orcid.org/0009-0001-7603-5491

Mateus Dal Fabbro[2]
https://orcid.org/0000-0002-8645-0103

Fabio Rogerio[3]
https://orcid.org/0000-0001-5712-7617

Leonardo Deus-Silva[4]
https://orcid.org/0000-0003-3775-401X

Fabiano Reis[5]
https://orcid.org/0000-0003-2256-4379

[1] Serviço de Endocrinologia, Departamento de Medicina Clínica, Faculdade de Ciências Médicas, Universidade Estadual de Campinas (Unicamp), Campinas, SP, Brasil
[2] Departamento de Neurocirurgia, Faculdade de Ciências Médicas, Universidade Estadual de Campinas (Unicamp), Campinas, SP, Brasil
[3] Departamento de Patologia, Faculdade de Ciências Médicas, Universidade Estadual de Campinas (Unicamp), Campinas, SP, Brasil
[4] Setor de Neurorradiologia Intervencionista; Departamento de Radiologia, Faculdade de Ciências Médicas, Universidade Estadual de Campinas (Unicamp), Campinas, SP, Brasil
[5] Departamento de Radiologia e Oncologia, Faculdade de Ciências Médicas, Universidade Estadual de Campinas (Unicamp), Campinas, SP, Brasil

ABSTRACT

The diagnosis of Cushing syndrome can be challenging, particularly when bilateral inferior petrosal sinus sampling (BIPSS) is required to differentiate ectopic tumors from pituitary adrenocorticotropic hormone (ACTH)-releasing tumors. When corticotropin-releasing hormone (CRH) is used as a stimulus, a state of hypercortisolism is required to suppress CRH receptors in pituitary corticotrophs, preventing the release of ACTH by normal pituitary tissue. By contrast, desmopressin acts through vasopressin receptors that are preferentially expressed in ACTH-secreting pituitary tumors, suggesting potentially different physiological behaviors during stimulation. We present the case of a 26-year-old woman with ACTH-dependent Cushing's syndrome who underwent desmopressin-stimulated BIPSS. Hormone levels on the day of catheterization indicated eucortisolism; however, ACTH levels in the petrosal sinus confirmed the diagnosis of Cushing disease. Following transsphenoidal surgery, immunohistochemical analysis confirmed a corticotroph adenoma with positive Tpit and ACTH staining. We hypothesize that desmopressin stimulation during BIPSS may provide diagnostic information even in the absence of biochemical confirmation of hypercortisolism at the time of the procedure, because vasopressin receptors are expressed in pituitary corticotroph adenomas rather than in normal corticotroph cells. Further studies are needed to evaluate and confirm this hypothesis.

Keywords: Cyclic hypercortisolism; desmopressin; petrosal sinus; Cushing's syndrome

INTRODUCTION

In patients with a confirmed diagnosis of ACTH-dependent Cushing syndrome, intravenous desmopressin testing is not a reliable method for differentiating pituitary tumors from ectopic ACTH-producing tumors, as a subset of ectopic tumors express aberrant amounts of vasopressin receptors and respond to desmopressin stimulation, resulting in increased ACTH levels in the peripheral circulation (1).

Bilateral inferior petrosal sinus sampling (BIPSS) with CRH stimulation is the gold standard test used for this differential diagnosis, but CRH is currently unavailable. Furthermore, in patients with cyclical Cushing syndrome, catheterization of the inferior petrosal sinus should be performed during hypercortisolemic phases to prevent normal corticotroph cells from responding to CRH stimulation (2). Desmopressin has been successfully used in BIPSS and is currently considered equally accurate as CRH because ACTH-producing pituitary tumors overexpress vasopressin receptors (3,4).

Scheduling BIPSS with CRH stimulation during hypercortisolemic phases can be challenging. This case

Received on Aug/25/2025
Accepted on Feb/12/2026
DOI: 10.20945/2359-4292-2026-0064

Correspondence to:
Heraldo Mendes Garmes
Rua Maruba, 330
13098-340 – Campinas, SP, Brasil
heraldmg@unicamp.br

Associated editor:
Leandro Kasuki
https://orcid.org/0000-0003-1339-3192

This is an open-access article distributed under the terms of the Creative Commons Attribution License

Copyright© AE&M all rights reserved.

illustrates the use of desmopressin as an alternative to CRH in BIPSS and highlights the discussion of its physiological basis, given that normal pituitary tissue does not express vasopressin V2 receptors.

CASE REPORT

A 26-year-old previously healthy woman was referred to our neuroendocrinology specialized center 6 months after the beginning of the investigation for weight gain, violaceous striae on the abdomen, fatigue, acne, myalgia, lower limb edema, moon facies, hair loss, and hirsutism. Initial laboratory investigations revealed intermittent ACTH-dependent hypercortisolism, followed by a period of normal urinary free cortisol (UFC) levels (**Table 1**).

Pituitary magnetic resonance imaging (MRI) revealed an irregular nodule located on the lateral aspect of the adenohypophysis, projecting into the left cavernous sinus and in contact with the internal carotid artery, measuring 0.9 × 0.9 × 0.6 cm (**Figure 1**).

The patient underwent BIPSS with desmopressin (10 µg), and correct catheterization was verified by angiography and contrast infusion.

At the time of the procedure, eucortisolism was confirmed by a basal serum cortisol concentration of 6.31 µg/dL and a 24-hour UFC level of 51 µg/24 h collected the day before (reference range: 36–137 µg/24 h). Based on the current evidence, if CRH had been used as the stimulus, the procedure would have been postponed because of normal cortisolemia.

In the BIPSS test performed at our institution, peripheral blood sampling is extended to 30 minutes after desmopressin infusion to assess the peripheral ACTH response, as in an acute desmopressin test. The procedure involves administering desmopressin through a vein in one forearm while blood is collected from the contralateral arm to differentiate ACTH-dependent

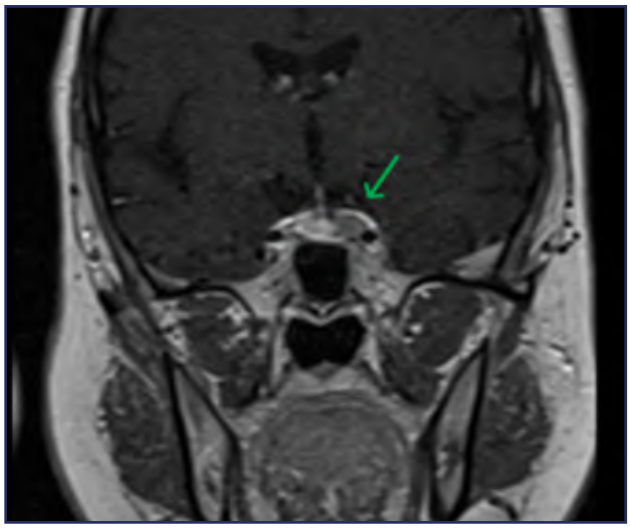


Figure 1. Magnetic resonance imaging of the sella turcica: Coronal T1-weighted image shows a left pituitary microadenoma.

Cushing syndrome from nontumoral endogenous hypercortisolism (pseudo-Cushing syndrome).

The peripheral serum cortisol concentration after the desmopressin stimulus ranged from 6.42 mcg/dL at baseline to 19.11 mcg/dL, an increase of 198%, while the basal ACTH concentration ranged from 83.14 pg/mL to 149.40 pg/ml, an increase of 79%. These results from peripheral samples favored the diagnosis of ACTH-dependent Cushing syndrome rather than nontumorous hypercortisolism. Still, they did not exclude the possibility of an ectopic ACTH-producing tumor that may express vasopressin receptors. In the inferior petrosal sinus samples, the high central-to-peripheral ACTH gradient confirmed the presence of vasopressin receptors in a pituitary ACTH-secreting tumor, confirming the diagnosis of cyclic CD (**Table 2**).

The patient underwent transsphenoidal resection of the microadenoma. Immunohistochemical analysis confirmed a corticotroph tumor with 80%–90% ACTH positivity and 80% Tpit positivity in neoplastic cells. She experienced clinical and biochemical remission after surgery.

Table 1. Results showing ACTH-dependent intermittent hypercortisolism

Exams 2023	April	May	June	October	November BIPSS
Cortisol	35.7		47.0	6.3	6.31
ACTH	198.0		156.0		
1 mg-DST	28.16	20.3			
UFC 24h				19 (13-85)	51 (36-137)

ACTH: adrenocorticotropic hormone in pg/mL; 1 mg-DST: 1 mg-dexamethasone suppression test; UFC: urinary free cortisol in ug/dL.

Copyright© AE&M all rights reserved.

Table 2. Results of samples collected from the inferior petrosal sinuses and peripheral veins

BIPSS	Basal	1 minute	3 minutes	5 minutes	10 minutes	30 minutes
ACTH IPS L	756.2	1155.0	> 1500.0	1454.0	> 1500.0	
ACTH IPS R	316.0	387.0	368.0	1095.0	> 1500.0	
ACTH P	83.1	58.8	73.0	77.5	121.7	149.4
PRL IPS L	86.1					
PRL IPS R	61.0					
PRL P	13.9					
Cortisol P	6.4				8.9	19.1
IPS L/P	9.1	19.6	20.5	18.7	0.9	
IPS R/P	3.1	6.6	5.0	14.1	12.3	

ACTH: adrenocorticotropic hormone in pg/mL; IPS: inferior petrosal sinus; L: left; R: right; P: peripheral; PRL: prolactin in ng/mL.

The most recent postoperative follow-up tests revealed a 24-hour UFC of 23 µg/24 h (reference range: 13–85), a late-night salivary cortisol concentration of 1.5 nmol/L (23:00 h; reference value < 7.6), and a serum cortisol concentration of 0.7 µg/dL after dexamethasone suppression (reference value < 1,8).

DISCUSSION

This case illustrates that, in ACTH-dependent Cushing syndrome, BIPSS with desmopressin stimulation may help differentiate a pituitary from an ectopic ACTH source, even during the eucortisolemic phases of cyclic Cushing syndrome.

First, it is worth noting that, because our patient presented with a normal urinary free cortisol level on the day of the BIPSS, the possibility of spontaneous remission of CD could be considered. A recent systematic review of the literature evaluating cases of spontaneous remission in Cushing disease revealed that tumor apoplexy is considered the most likely etiology for this rare phenomenon (5); however, our patient did not present clinical signs or radiological evidence of pituitary apoplexy. Furthermore, the greatly elevated ACTH levels in the petrosal sinuses before and after desmopressin stimulation indicate the presence of an ACTH-producing pituitary tumor, which was found intraoperatively and confirmed histopathologically with immunohistochemistry demonstrating ACTH positivity in 80%–90% and T-Pit positivity in 80% of the neoplastic cells, making spontaneous remission an unlikely explanation for this patient.

A recent meta-analysis confirmed that performing BIPSS using desmopressin as a stimulus for ACTH secretion yields results comparable to those obtained with CRH stimulation for determining the etiology of ACTH-dependent Cushing syndrome (3).

Regarding the literature on cyclic Cushing syndrome, cases of misdiagnosis due to BIPSS with CRH stimulation performed during periods without hypercortisolemia are common (6-8), sometimes falsely suggesting EAS in patients with cyclic CD (7) or CD in patients with EAS (6,7). Notably, these cases were later confirmed histologically. Albani and cols. (6) reported the case of a patient with cyclic EAS who, after undergoing an initial BIPSS during the eucortisolemic phase, underwent unnecessary pituitary surgery. The true EAS diagnosis was confirmed only after a second BIPSS was performed during the active phase of the tumor.

According to a recent review by Nowak and cols., the positive and negative predictive values of BIPSS with CRH decrease from 100% to 42% and from 100% to 73%, respectively, when performed outside hypercortisolemic phases (9). Therefore, BIPSS with CRH stimulation should be performed only during an active disease period. Additionally, notably, a sustained period of hypercortisolism is necessary to suppress normal corticotroph function, which requires serial cortisol assessments before BIPSS with CRH stimulation is performed in patients with cyclic ACTH-dependent CS. This requirement for hypercortisolism represents a major challenge, significantly delaying diagnosis and treatment (10).

Furthermore, some authors have reported that the prevalence of cyclic Cushing syndrome is substantial, ranging from 14% to 19% of patients with CD,

Copyright© AE&M all rights reserved.

suggesting that this condition is not as rare as previously believed (10-13).

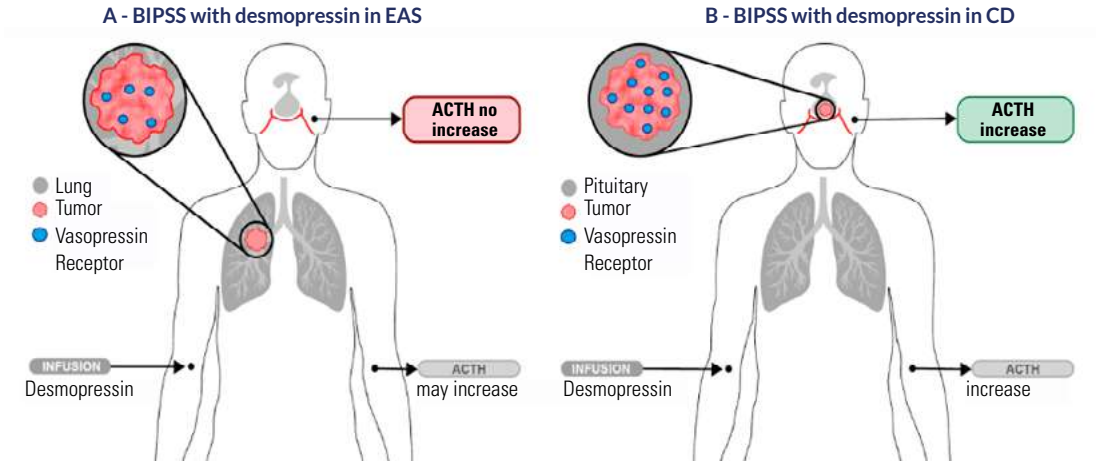
Desmopressin is a vasopressin analog that is relatively selective for V2 renal receptors but has a weak affinity for V3 pituitary receptors in healthy individuals (14). However, due to the overexpression of vasopressin receptors in corticotroph adenomas and some ectopic ACTH-secreting tumors, desmopressin induces a rapid increase in ACTH release in affected patients. By contrast, studies have shown that this increase is absent in normal individuals or those with non-neoplastic hypercortisolism (15,16).

With respect to the need for hypercortisolism when performing BIPSS to investigate the source of ACTH in ACTH-dependent Cushing syndrome, two distinct pathophysiological scenarios can be considered: When corticotropin-releasing hormone (CRH) is used as the stimulus, the ACTH response depends on the expression of CRH receptors, which are present in both pituitary corticotroph adenomas and normal pituitary corticotroph cells. In this setting, sustained hypercortisolism is required to suppress normal corticotroph responsiveness; in its absence, CRH-induced ACTH secretion from normal corticotrophs may occur, potentially leading to false-positive results and a misdiagnosis of Cushing disease (17). By contrast, when desmopressin is used as the stimulus, the ACTH response is primarily determined by the expression of vasopressin receptors, which are characteristically overexpressed in ACTH-secreting pituitary adenomas but minimally or not expressed in normal corticotroph cells. Based on this physiological distinction, the lack of suppression of CRH receptors in normal corticotrophs by hypercortisolism is less relevant for desmopressin-stimulated BIPSS, potentially allowing discrimination between pituitary and ectopic ACTH secretion even during periods of normocortisolism.

Supporting this concept, studies using desmopressin stimulation on peripheral blood samples have differentiated patients with CD from those with pseudo-Cushing states, demonstrating that ACTH-producing pituitary tumors respond to desmopressin, whereas the normal pituitary gland does not (16).

Based on this observation, we question whether desmopressin-stimulated BIPSS could have diagnostic utility even when performed during the eucortisolemic phase. In this context, an increased central-to-peripheral ACTH gradient would support a pituitary source of ACTH secretion, which is consistent with the presence of a corticotroph adenoma expressing vasopressin receptors. Conversely, in ectopic ACTH-producing tumors, desmopressin stimulation would not be expected to generate a significant central-to-peripheral ACTH gradient (**Figure 2**).

Hypercortisolism remains the standard prerequisite for BIPSS, and our findings should be interpreted as an exploratory observation that provides a basis for further evaluation by the scientific community. Thus, further studies including patients with cyclic Cushing disease during periods of eucortisolism are needed to



EAS: ectopic ACTH syndrome; CD: Cushing's disease; BIPSS: bilateral inferior petrosal sinus sampling.

Figure 2. Results of ACTH measurement after desmopressin infusion in patients with EAS (**A**) or CD (**B**). Because pituitary tumors are known to express vasopressin receptors, increased ACTH in the petrosal sinus occurs only in patients with CD, regardless of cortisolemia.

Copyright© AE&M all rights reserved.

determine whether these results can be reproduced and whether all these patients will respond to vasopressin stimulation in the BIPSS.

CONCLUSION

Our case report suggests that BIPSS with desmopressin stimulation might be used for the etiological diagnosis of ACTH-dependent cyclic Cushing syndrome, even during the normocortisolemic phase. This strategy may facilitate earlier diagnosis and treatment, mitigating the challenges posed by the requirement for hypercortisolism in conventional BIPSS with CRH stimulation. However, further studies are needed to confirm these findings and clarify their clinical applicability.

Acknowledgments: we would like to thank the audiovisual department of the Faculty of Medical Sciences of the State University of Campinas for their support in drawing Figure 2.

Funding: no funding was received for this study or publication of this article.

Compliance with ethical standards: this study was performed in line with the principles of the Declaration of Helsinki. Approval was granted by the Ethics Committee of State University of Campinas (CAAE 83886024.4.0000.5404) and the patient wrote and signed an informed consent form.

Author contributions: HMG, SCS, KBD, MBFT, MTF and CS were responsible for data collection. All the authors contributed to the technical procedures in monitoring this case. The first draft of the manuscript was written by HMG and SCS. All authors commented on previous versions of the manuscript, read and approved the final submitted version.

Disclosure: no potential conflict of interest relevant to this article was reported.

Data availability: the original contributions presented in the study are included in the article. Further inquiries can be directed to the corresponding author.

REFERENCES

1. Tsagarakis S, Tsigos C, Vasiliou V, Tsiotra P, Kaskarelis J, Sotiropoulou C, et al. The desmopressin and combined CRH-desmopressin tests in the differential diagnosis of ACTH-dependent Cushing's syndrome: constraints imposed by the expression of V2 vasopressin receptors in tumors with ectopic ACTH secretion. J Clin Endocrinol Metab. 2002 Apr;87(4):1646-53. doi: 10.1210/jcem.87.4.8358.
2. Ferriere A, Nunes ML, Tabarin A. Approach to the Patient With Cyclical Cushing Syndrome. J Clin Endocrinol Metab. 2025 Jun 17;110(7):e2338-e2346. doi: 10.1210/clinem/dgae864.
3. Valizadeh M, Ahmadi AR, Ebadinejad A, Rahmani F, Abiri B. Diagnostic accuracy of bilateral inferior petrosal sinus sampling using desmopressin or corticotropic- releasing hormone in ACTH-dependent Cushing's syndrome: A systematic review and meta-analysis. Rev Endocr Metab Disord. 2022 Oct;23(5):881-892. doi: 10.1007/s11154-022-09723-y.
4. de Almeida TS, Rodrigues TDC, Costenaro F, Scaffaro LA, Farenzena M, Gastaldo F, et al. Enhancing Cushing's disease diagnosis: exploring the impact of desmopressin on ACTH gradient during BIPSS. Front Endocrinol (Lausanne). 2023 Aug 3;14:1224001. doi: 10.3389/fendo.2023.1224001.
5. Popa Ilie IR, Herdean AM, Herdean AI, Georgescu CE. Spontaneous remission of Cushing's disease: A systematic review. Ann Endocrinol (Paris). 2021 Dec;82(6):613-621. doi: 10.1016/j.ando.2021.10.002.
6. Albani A, Berr CM, Beuschlein F, Treitl M, Hallfeldt K, Honegger J, et al. A pitfall of bilateral inferior petrosal sinus sampling in cyclic Cushing's syndrome. BMC Endocr Disord. 2019 Oct 22;19(1):105. doi: 10.1186/s12902-019-0433-9.
7. Yamamoto Y, Davis DH, Nippoldt TB, Young WF, Huston J, Parisi JE. False-positive inferior petrosal sinus sampling in the diagnosis of Cushing's disease. Report of two cases. J Neurosurg. 1995;83(6):1087-1091. doi: 10.3171/jns.1995.83.6.1087.
8. Bonert V, Bose N, Carmichael JD. Cyclic Cushing's disease with misleading inferior petrosal sinus sampling results during a trough phase. Neurosurg Focus. 2015;38(2):E7. doi: 10.3171/2014.12.FOCUS14780.
9. Nowak E, Vogel F, Albani A, Braun L, Rubinstein G, Zopp S, Ritzel K, Beuschlein F, Theodoropoulou M, Reincke M. Diagnostic challenges in cyclic Cushing's syndrome: a systematic review. Lancet Diabetes Endocrinol. 2023 Aug;11(8):593-606. doi: 10.1016/S2213-8587(23)00150-X.
10. Jahandideh D, Swearingen B, Nachtigall LB, Klibanski A, Biller BMK, Tritos NA. Characterization of cyclic Cushing's disease using late night salivary cortisol testing. Clin Endocrinol (Oxf). 2018;89(3):336-345. doi: 10.1111/cen.13758.
11. Alexandraki KI, Kaltsas GA, Isidori AM, Akker SA, Drake WM, Chew SL, et al. The prevalence and characteristic features of cyclicity and variability in Cushing's disease. Eur J Endocrinol. 2009 Jun;160(6):1011-8. doi: 10.1530/EJE-09-0046.
12. Streeten DH, Anderson GH Jr, Dalakos T, Joachimpillai AD. Intermittent hypercortisolism: a disorder strikingly prevalent after hypophysial surgical procedures. Endocr Pract. 1997 May-Jun;3(3):123-9. doi: 10.4158/EP.3.3.123.
13. McCance DR, Gordon DS, Fannin TF, Hadden DR, Kennedy L, Sheridan B, et al. Assessment of endocrine function after transsphenoidal surgery for Cushing's disease. Clin Endocrinol (Oxf). 1993 Jan;38(1):79-86. doi: 10.1111/j.1365-2265.1993.tb00976.x.
14. Castinetti F, Lacroix A. Is Desmopressin Useful in the Evaluation of Cushing Syndrome? J Clin Endocrinol Metab. 2022 Nov 23;107(11):e4295-e4301. doi: 10.1210/clinem/dgac533.
15. Yang J, Yang Y, Wang Y, Zhang S, Cheng H, Wang S, et al. Role of Vasopressin Receptor 2 and 3 in ACTH-Secreting Tumors and their Potential Therapeutic Implications. Exp Clin Endocrinol Diabetes. 2020 Apr;128(4):263-269. doi: 10.1055/a-0808-4227.
16. Vassiliadi DA, Tsagarakis S. DIAGNOSIS OF ENDOCRINE DISEASE: The role of the desmopressin test in the diagnosis and follow-up of Cushing's syndrome. Eur J Endocrinol. 2018 May;178(5):R201-R214. doi: 10.1530/EJE-18-0007.
17. Perlman JE, Johnston PC, Hui F, Mulligan G, Weil RJ, Recinos PF, et al. Pitfalls in Performing and Interpreting Inferior Petrosal Sinus Sampling: Personal Experience and Literature Review. J Clin Endocrinol Metab. 2021 Apr 23;106(5):e1953-e1967. doi: 10.1210/clinem/dgab012.

Copyright© AE&M all rights reserved.

Archives of Endocrinology and Metabolism
ISSN 2359-4292
OFFICIAL JOURNAL OF THE BRAZILIAN SOCIETY OF ENDOCRINOLOGY AND METABOLISM

case report

Pheochromocytoma and multicentric giant cell tumor of bone

João Vicente Silveira[1]
https://orcid.org/0000-0002-4426-0512

Madson Q. Almeida[2]
https://orcid.org/0000-0002-2957-6148

Olavo Pires de Camargo[3]
https://orcid.org/0000-0002-1128-7292

Julio Cesar Carvalho Nardelli[3]
https://orcid.org/0000-0002-6034-6332

Andre Ferrari de Franca Camargo[3]
https://orcid.org/0000-0003-0317-3807

Henrique Barbosa Ribeiro[1]
https://orcid.org/0000-0003-1273-1823

Luiz Aparecido Bortolotto[1]
https://orcid.org/0000-0002-4865-6442

Heno Ferreira Lopes[1]
https://orcid.org/0000-0002-9591-3093

Fernanda M. Consolim-Colombo[1,4]
https://orcid.org/0000-0003-3220-019X

[1] Instituto do Coração do Hospital das Clínicas da Faculdade de Medicina da Universidade de São Paulo, São Paulo, SP, Brasil
[2] Unidade de Suprarrenal, Endocrinologia do Desenvolvimento, Laboratório de Hormônios e Genética Molecular – LIM42, Divisão de Endocrinologia e Metabologia, Hospital das Clínicas, Faculdade de Medicina da Universidade de São Paulo, São Paulo, SP, Brasil
[3] Instituto de Ortopedia e Traumatologia do Hospital das Clínicas da Faculdade de Medicina da Universidade de São Paulo, São Paulo, SP, Brasil
[4] Universidade Nove de Julho, São Paulo, SP, Brasil

ABSTRACT

Pheochromocytomas and paragangliomas (PPGLs) are rare catecholamine-secreting tumors that can affect systemic physiology, including bone metabolism. Although they are typically associated with genetic syndromes such as MEN2 and von Hippel-Lindau disease, PPGLs are not commonly linked to primary bone tumors. However, recent findings suggest a novel cancer syndrome involving both PPGLs and giant cell tumor of bone (GCTB) through H3F3A mutations. We report a rare case of a 53-year-old woman with multicentric GCTB, initially diagnosed at age 24, who subsequently developed bilateral pheochromocytomas. Following multiple recurrences of skeletal tumors and eventual leg amputation, imaging and biochemical evaluation revealed bilateral adrenal tumors with markedly elevated catecholamine levels. Genetic analysis identified mosaicism for a pathogenic H3F3A (G35W) variant in both adrenal and bone tumors. Surgical resection of both adrenal glands normalized catecholamine levels and resolved hypertension. The patient has remained tumor-free and normotensive for five years following adrenalectomy. This case supports the existence of a shared pathogenic mechanism linking PPGLs and GCTBs, likely mediated by postzygotic H3F3A mutations. Recognition of this association is crucial for early diagnosis, genetic counseling, and management of similar cases.

Keywords: Pheochromocytoma; paragangliomas; giant cell bone tumors; hypertension; genetic

INTRODUCTION

Pheochromocytomas and paragangliomas (PPGLs) are rare tumors arising from neural crest cells and are characterized by catecholamine secretion. These tumors frequently exhibit genetic mutations affecting various biological pathways, notably influencing bone metabolism via catecholamine excess, which increases bone resorption and leads to secondary osteoporosis. Although PPGLs are commonly associated with genetic syndromes such as Multiple Endocrine Neoplasia type 2 (MEN2) and von Hippel-Lindau disease (1), pheochromocytomas are not typically linked with primary bone tumors. However, a prior publication identified a novel cancer syndrome connecting PPGLs with giant cell tumors of bone (GCT) through specific genetic mutations (2). Additionally, case reports in the literature have described occurrences of PPGLs coexisting with giant cell bone tumors. These discoveries highlight the need for further investigation into possible shared origins of these tumors, emphasizing the importance of understanding genetic risk in affected individuals.

Received on Sep/30/2025
Accepted on Feb/25/2026
DOI: 10.20945/2359-4292-2026-0065

Correspondence to:
Heno Ferreira Lopes
Departamento de Cardiopneumologia,
Instituto do Coração, Hospital das Clínicas,
Faculdade de Medicina da Universidade de São Paulo
Avenida Dr. Eneas de C. Aguiar, 44,
05403-900 – São Paulo, SP, Brasil
hipheno@incor.usp.br

Associated editor:
Miguel Madeira
https://orcid.org/0000-0001-6752-2880

This is an open-access article distributed under the terms of the Creative Commons Attribution License

Copyright© AE&M all rights reserved.

CASE PRESENTATION

We present the case of a 53-year-old woman who was initially diagnosed with a giant cell tumor of bone in the right tibia in 1995 at the age of 24. During follow-up, the tumor spread to various segments of her skeleton. In 2008, she began attending the outpatient clinic of the Orthopedic Unit at the Clinical Hospital, with a diagnosis of multicentric giant cell tumor of bone, as confirmed by a 2015 scintigraphy examination and biopsy fragments, which revealed a giant cell tumor of bone with areas of necrosis and a fibrocystic pattern. Due to multiple recurrences of the tumor in the right tibia, she underwent several resections, ultimately leading to a leg amputation in 2018, at the age of 47. Additionally, during a chest and lung tomography performed in the same period, two nodular images in the region of the adrenal glands were detected, measuring approximately 5.9 cm on the left and 4.5 cm on the right. These findings were considered indeterminate in this non-contrast study and were not further investigated at that time.

In 2019, on day 1, the patient began reporting episodes of headache, palpitations, and sweating, which had begun six months prior. She was diagnosed with hypertension at another clinic and was treated with losartan 50 mg twice daily, which reduced but did not normalize her blood pressure (140/90 mmHg). Her headache episodes became more frequent and were associated with thoracic discomfort.

On day 2, the patient presented to the emergency room with a hypertensive emergency (BP 240/120 mmHg), complicated by acute pulmonary edema and myocardial injury, following the sudden onset of severe dyspnea and chest pain during physiotherapy. After stabilization on day 3, cardiac catheterization confirmed a type II myocardial infarction, excluding coronary and renal artery obstruction. However, findings of atypical adrenal vasculature prompted bilateral adrenal angiography, which revealed large masses in both adrenal glands (**Figures 1A–1B**). Subsequently, a CT scan of the abdomen was performed, revealing masses in the adrenal regions (40 Hounsfield units), measuring 10 cm in the left adrenal gland and 8 cm in the right adrenal gland. Both masses were compressing the kidneys. In this context, the possibility of pheochromocytoma was appropriately considered (**Figure 1C**). The suspicion of pheochromocytoma prompted confirmatory laboratory and specific imaging tests. The results of the confirmatory laboratory tests are presented in **Table 1**. Positron emission tomography/magnetic resonance imaging (PET/MRI) with somatostatin analog (68Ga-DOTATATE) demonstrated globular lesions in the adrenal glands with heterogeneous radiopharmaceutical uptake, well-defined margins, and regular contours. The left adrenal lesion exhibited a markedly higher concentration of radiopharmaceutical, measuring 8.0 × 6.2 × 5.5 cm (AP × CC × LL) and displaced the tail of the pancreas anteriorly. The right adrenal lesion showed a moderate concentration of radiopharmaceutical and measured 5.4 × 5.2 × 4.3 cm (AP × CC × LL), maintaining extensive contact with the inferior vena cava. Additionally,

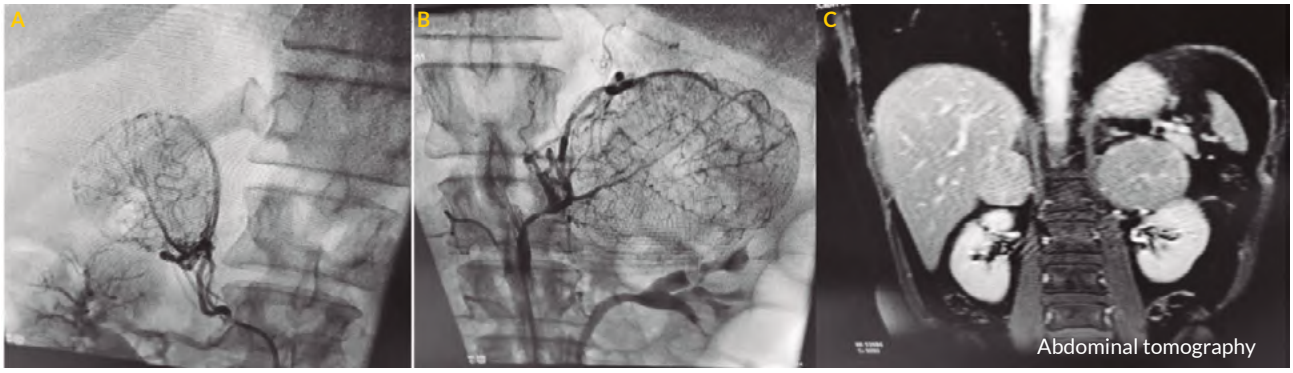


Figure 1. Adrenal artery catheterization (A and B) and abdominal CT scan (C). A and **B**) Injection of contrast into the adrenal arteries highlighting intense vascularization in the regions of the right and left adrenal glands, indicating the presence of bilateral tumor mass; **C**) Abdominal CT scan evidencing large tumor masses in both adrenal glands.

Copyright© AE&M all rights reserved.

Table 1. Plasma and urine catecholamine, plasma and urine metanephrine measurements pre-adrenalectomy

Variables	Values	Reference values
Plasma norepinephrine (pg/mL)	**15,809**	70-750 pg/mL
Plasma epinephrine (pg/mL)	Undetectable	0–110 pg/mL
Plasma dopamine (pg/mL)	Undetectable	Undetectable
Plasma metanephrine (nmol/L)	**4.1**	< 0.5 nmol/L
Urine norepinephrine (µg/24 h)	**1,292**	14–80 µg/24 h
Urine epinephrine (µg/24 h)	**68**	0.5–20 µg/24 h
Urine dopamine (µg/24 h)	**1,536**	65–400 µg/24 h
Urine metanephrine (µg/24 h)	**2.5**	0.05–1.2 µg/24 h

a focal area of discrete anomalous radiopharmaceutical accumulation was observed in the intramedullary region of the left distal radius (**Figure 2**).

Additional laboratory evaluation showed normal adrenal hormone levels (cortisol and aldosterone). Laboratory tests revealed prediabetes, severe hypercholesterolemia (LDL-C 270 mg/dL), markedly elevated TSH (9.29 µUI/mL [0.55–4.78 µUI/mL] and low FT4 0.86 ng/dL [0.93–1.7 ng/dL]) suggesting hypothyroidism—normal renal function and electrolytes, unremarkable complete blood count except mild leukocytosis, and borderline-high triglycerides. Calcium metabolism markers were within normal limits: PTH 33 pg/mL (10–65), vitamin D 21 ng/mL (>20), ionized calcium 4.92 mg/dL (4.49–5.29), and phosphorus 4.2 mg/dL (2.7–4.5).

Evaluation for hypertensive target organ damage showed on echocardiogram: aortic sinus 43 mm, left atrium 36 mm, left ventricular diastolic diameter 39 mm, systolic diameter 23 mm, interventricular septum thickness 18 mm, left ventricular wall thickness 10 mm, LV mass index 109 g/m^2, and ejection fraction 73% (Teicholz method), with normal valves and pericardium. After this comprehensive evaluation, bilateral pheochromocytomas were confirmed. Blood pressure was controlled with prazosin and metoprolol; bilateral adrenalectomy was recommended.

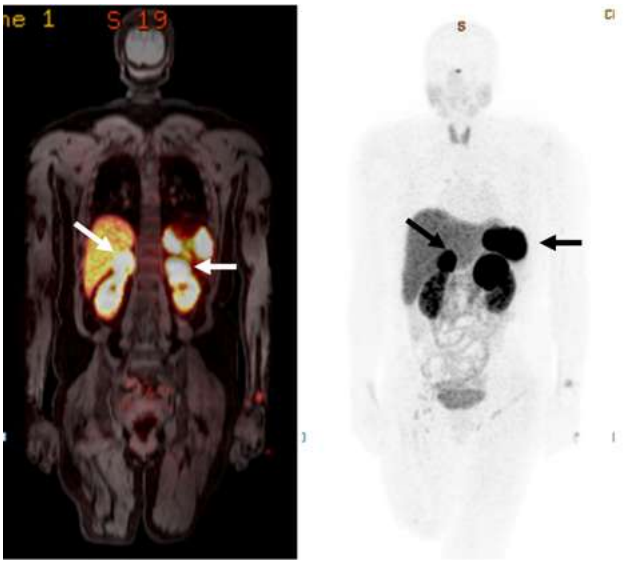


Figure 2. PET/MRI with somatostatin analog (68Ga-DOTATATE). Whole-body PET/MRI scan with Somatostatin analog (68Ga-DOTATATE) demonstrating heterogeneous radiopharmaceutical uptake at the left adrenal region (measuring 8.0 × 6.2 × 5.5 cm; AP × CC × LL), at the right adrenal region (measuring es 5.4 × 5.2 × 4.3 cm; AP × CC × LL), and in the intramedullary region of the left distal radius (indicated by the arrows).

Surgical procedure and patient evolution

The patient first underwent left adrenalectomy, followed by right adrenalectomy seven days later. For the left pheochromocytoma, histology identified two adverse features(vascular and capsular invasion) each contributing 1 point, for a total pheochromocytoma of the adrenal scaled score (PASS) of 2. All other PASS criteria were absent, including large nests/diffuse growth (>10%) central or confluent necrosis, high cellularity, cellular monotony, spindle cell component, >3 mitotic figures per 10 high-power fields, atypical mitoses, adipose tissue invasion, marked nuclear pleomorphism, and nuclear hyperchromasia. Surgical margins were clear. For the right adrenal pheochromocytoma, PASS evaluation showed large nests/diffuse architecture (>10%) and high cellularity, each scoring 2 points, for a total PASS of 4/20. All other criteria were absent, including central or confluent necrosis, cellular monotony, spindle cell component, increased mitotic activity (>3/10 HPF), atypical mitoses, adipose tissue

Copyright© AE&M all rights reserved.

invasion, vascular invasion, capsular invasion, marked nuclear pleomorphism, and nuclear hyperchromasia.

Pathological exams confirmed the presence of the bilateral pheochromocytoma, with positivity Tumor cells were positive for Chromogranin, Synaptophysin, and S100 (in sustentacular cells in the left adrenal and focal areas in the right adrenal). Ki-67 proliferation index was 3–5% in the left and 1–2% in the right adrenal. Mosaicism for the pathogenic *H3F3A* c.103G>T/p.G35W variant was observed with bilateral pheochromocytomas and recurrent bone giant cell tumors. Both pheochromocytomas harbored this *H3F3A* variant, which was also found in a low allele frequency (<10%) in germline DNA. Germline DNA was analyzed using a targeted next-generation sequencing panel for pheochromocytoma susceptibility genes, and the results were negative for RET.

The patient's variant (p.G35W) corresponds to the canonical *H3F3A* hotspot mutation historically referred to as p.G34W. There is no difference between the mutations themselves; the discrepancy arises solely from nomenclature. The updated HGVS guidelines recommend numbering based on the full-length reference sequence, including the initiator methionine, which shifts the amino acid position by +1. Under this updated system, the traditional p.G34W is now designated as p.G35W.

Four days after left adrenal removal, 24-hour urine catecholamines, plasma metanephrine, and 24-hour urine metanephrine were measured. Three days after right adrenal removal, a 24-hour urine sample was collected for catecholamine and metanephrine measurements (**Table 2**).

During surgery, part of the normal left adrenal parenchyma was preserved. For this reason, the patient does not require fludrocortisone replacement. Over the course of follow-up, she has maintained normal sodium and potassium levels, as well as renin at 26 μIU/mL (4.4–46.1 μIU/mL), with normal blood pressure and no orthostatic hypotension. The patient is receiving hydrocortisone supplementation and is taking atorvastatin 40 mg daily for cholesterol control. The most recent LDL-cholesterol value, measured in November 2024, was 104 mg/dL. Following adrenal resection, the white blood cell count decreased to 6,290 mm^3. Plasma metanephrine and normetanephrine levels have remained stable and within normal limits during five years of follow-up (**Table 2**). The patient has not experienced recurrence of the giant cell tumor.

Plasma metanephrines during five years of follow-up were as follows: metanephrine <0.2 nmol/L in 2022, 0.2 nmol/L in 2023, <0.2 nmol/L in 2024; normetanephrine 0.5 nmol/L in 2022, 0.6 nmol/L in 2023, and 0.5 nmol/L in 2024. Post-adrenalectomy, the patient became normotensive off medication, and follow-up echocardiography showed regression of left ventricular hypertrophy.

DISCUSSION

Pheochromocytomas and paragangliomas are rare catecholamine-secreting tumors of neural crest origin, arising from sympathetic lineage cells in the adrenal

Table 2. 24-Hour urine catecholamines and plasma and urine metanephrine measurements after left and right adrenalectomy, respectively

Variables	Values	Reference values
Catecholamines and metanephrine levels after removal of left adrenal gland		
Plasma metanephrine (nmol/L)	**0.8**	< 0.5 nmol/L
Urine norepinephrine (μg/24 h)	**279**	14–80 μg/24 h
Urine epinephrine (μg/24 h)	Undetectable	0.5–20 μg/24 h
Urine dopamine (μg/24 h)	**651**	65–400 μg/24 h
Urine metanephrine (μg/24 h)	**6.3**	0.05–1.2 μg/24 h
Catecholamines and metanephrine levels after removal of right adrenal gland		
Urine norepinephrine (μg/24 h)	18	14–80 μg/24 h
Urine epinephrine (μg/24 h)	Undetectable	0.5–20 μg/24 h
Urine dopamine (μg/24 h)	232	65–400 μg/24 h
Urine metanephrine (μg/24 h)	0.27	0.05–1.2 μg/24 h

Copyright© AE&M all rights reserved.

medulla and paraganglia, respectively. Notably, over 40% of pheochromocytomas are caused by dominant driver mutations in various susceptibility genes, affecting multiple biological pathways (3).

Pheochromocytomas significantly influence bone metabolism via catecholamine excess, which drives bone resorption and secondary osteoporosis, as shown in numerous studies (4–7). This is primarily attributed to sympathetic overstimulation, which disrupts bone microarchitecture, resulting in increased bone fragility, particularly in trabecular bone (6–9). Disabling bone pain has been reported in malignant pheochromocytoma (10). Pheochromocytomas are commonly associated with genetic syndromes, including MEN2, von Hippel-Lindau disease, and neurofibromatosis type 1 (1,11); however, these do not generally include primary bone tumors within their clinical spectrum. Therefore, the correlation between pheochromocytomas and primary bone tumors is not well established in the medical literature.

Recent studies investigating the molecular biology of PPGLs have identified a novel cancer syndrome linking PPGLs and GCT (3), attributed to a postzygotic G34W mutation in the histone 3.3 gene, H3F3A. These findings suggest that chromatin architecture changes in a substantial subset of PPGLs may be mediated by diverse mechanisms—including direct mutations of chromatin modifiers. In the context of histone 3.3 mutations, this misregulation manifests within a distinct clinical and developmental framework. The unique postzygotic H3.3 mutation pattern seen in our cases, previously unreported in other H3.3-mutant tumors, warrants further investigation into possible common progenitors for sympathetic lineage and bone tumors. This finding has important implications for assessing mutation transmission risk in affected individuals.

CONCLUSION

This case provides compelling evidence for PPGL–GCTB syndrome caused by mosaic H3F3A mutations. Our findings underscore the importance of considering genetic testing in patients presenting with concurrent rare tumors, as this is essential for accurate diagnosis, genetic counseling, and long-term management.

Acknowledgments: the authors would like to thank the patient for her cooperation in performing all the requested tests during the follow-up period and for allowing us to publish this clinical case, which can greatly contribute to the medical literature and benefit a large number of patients.

Funding: the authors did not receive any financial support for this work.

Disclosure: no potential conflict of interest relevant to this article was reported.

Data availability: datasets related to this article will be available upon request to the corresponding author.

REFERENCES

1. Neumann HP, Berger DP, Sigmund G, Blum U, Schmidt D, Parmer RJ, et al. Pheochromocytomas, multiple endocrine neoplasia type 2, and von Hippel-Lindau disease. N Engl J Med. 1993 Nov 18;329(21):1531-8. doi: 10.1056/NEJM199311183292103.
2. Iwata S, Yonemoto T, Ishii T, Araki A, Hagiwara Y, Tatezaki SI. Multicentric Giant Cell Tumor of Bone and Paraganglioma: A Case Report. JBJS Case Connect. 2013 Jan-Mar;3(1):e23. doi: 10.2106/JBJS.CC.L.00155.
3. Dahia PL. Pheochromocytoma and paraganglioma pathogenesis: learning from genetic heterogeneity. Nat Rev Cancer. 2014 Feb;14(2):108-19. doi: 10.1038/nrc3648.
4. Yokomoto-Umakoshi M, Umakoshi H, Sakamoto R, Fukumoto T, Ogata M, Nakano Y, et al.; Q-AND-A study group. Role of deteriorated bone quality in the development of osteoporosis in pheochromocytoma and paraganglioma. Bone. 2021 Jan;142:115607. doi: 10.1016/j.bone.2020.115607.
5. Dutta D, Nagendra L, Chandran M, Sharma M, Bhattacharya S, Mukhopadhyay S. Impact of Pheochromocytoma or Paraganglioma on Bone Metabolism: A Systemic Review and Meta-analysis. J Clin Densitom. 2024 Jul-Sep;27(3):101501. doi: 10.1016/j.jocd.2024.101501.
6. Kim BJ, Kwak MK, Kim JS, Lee SH, Koh JM. Higher sympathetic activity as a risk factor for skeletal deterioration in pheochromocytoma. Bone. 2018 Nov;116:1-7. doi: 10.1016/j.bone.2018.06.023.
7. Qi W, Cui L, Jiajue R, Pang Q, Chi Y, Liu W, et al. Deteriorated bone microarchitecture caused by sympathetic overstimulation in pheochromocytoma and paraganglioma. J Endocrinol Invest. 2024 Apr;47(4):843-856. doi: 10.1007/s40618-023-02198-x.
8. Kim BJ, Kwak MK, Ahn SH, Kim H, Lee SH, Song KH, et al. Lower Bone Mass and Higher Bone Resorption in Pheochromocytoma: Importance of Sympathetic Activity on Human Bone. J Clin Endocrinol Metab. 2017 Aug 1;102(8):2711-2718. doi: 10.1210/jc.2017-00169.
9. Ayala-Ramirez M, Palmer JL, Hofmann MC, de la Cruz M, Moon BS, Waguespack SG, et al. Bone metastases and skeletal-related events in patients with malignant pheochromocytoma and sympathetic paraganglioma. J Clin Endocrinol Metab. 2013 Apr;98(4):1492-7. doi: 10.1210/jc.2012-4231.
10. Tan M, Camargo CA, Mojtahed A, Mihm F. Malignant pheochromocytoma presenting as incapacitating bony pain. Pain Pract. 2012 Apr;12(4):286-9. doi: 10.1111/j.1533-2500.2011.00499.x.
11. Lopes HF, Silva HB, Bortolloto LA, Frimm CC, Bellotti GM, Pileggi F, et al. [Pheochromocytoma. Its diagnostic and therapeutic characteristics]. Arq Bras Cardiol 1992;59(5):395-400. PMID: 1340739.

Copyright© AE&M all rights reserved.

Archives of Endocrinology and Metabolism
ISSN 2359-4292
OFFICIAL JOURNAL OF THE BRAZILIAN SOCIETY OF ENDOCRINOLOGY AND METABOLISM

letter to the editor

Comment on: Evaluation of three inflammation-associated blood indices for predicting malignancy in thyroid nodules

Yusuf Öztürk[1]
https://orcid.org/0000-0001-7526-6063

[1] Sakarya University Training and Research Hospital, Department of Endocrinology and Metabolism, Sakarya, Turkey

Dear Editor,

We read with great interest the article by Çatak and cols. entitled "Evaluation of three inflammation-associated blood indices for predicting malignancy in thyroid nodules" (1). The authors should be commended for their comparative evaluation of systemic inflammatory indices, including the systemic immune-inflammation index (SII), systemic inflammation response index (SIRI), and pan-immune-inflammation value (PIV).

However, we believe that the prognostic assessment presented in the study is methodologically limited. The associations between inflammatory indices and tumor-related features in the malignant cohort were evaluated solely using Pearson or Spearman correlation analyses. While these methods are useful for identifying simple associations, they do not account for potential confounding variables and are insufficient to establish independent prognostic value. In particular, binary clinical outcomes such as lymph node metastasis or advanced stage require regression-based modeling.

Furthermore, the absence of receiver operating characteristic (ROC) analyses and multivariate regression models for prognostic endpoints is noteworthy. Therefore, the lack of significant prognostic findings may reflect methodological limitations rather than a true absence of association.

Received on Apr/10/2026
Accepted on Apr/13/2026

DOI: 10.20945/2359-4292-2026-0069

Correspondence to:
Yusuf Öztürk
yusuf_ozturk40@hotmail.com

Editor in chief:
César Boguszewski
https://orcid.org/0000-0001-7285-7941

This is an open-access article distributed under the terms of the Creative Commons Attribution License

In contrast, in our study including 376 patients with differentiated thyroid carcinoma, PIV demonstrated significant discriminative ability for distant metastasis and ATA high-risk category, and emerged as an independent risk factor in multivariate analyses (2). These findings suggest that PIV may reflect tumor aggressiveness within malignant cohorts rather than serving as a diagnostic discriminator.

Additionally, we found that absolute monocyte count (AMC) was significantly associated with TNM stage, ATA high-risk category, and distant metastasis (2). This observation provides an important perspective on the authors' suggestion that the monocyte component of PIV may introduce heterogeneity. On the contrary, given the well-established role of monocyte-derived tumor-associated macrophages in tumor progression and metastasis, the monocyte component may represent a key biological driver of the prognostic signal captured by PIV.

In conclusion, we believe that the clinical utility of inflammatory indices depends on the appropriate definition of their intended context. While these markers may have limited value in distinguishing benign from malignant nodules, they may be more useful in identifying aggressive disease and high-risk patients within malignant populations. Accordingly, prognostic evaluations should be performed using appropriate statistical methodologies and clinically relevant endpoints.

Funding: this research did not receive any specific grant from funding agencies in the public, commercial, or not-for-profit sectors.

Disclosure: no potential conflict of interest relevant to this article was reported.

Data availability: datasets related to this article will be available upon request to the corresponding author.

Copyright© AE&M all rights reserved.

REFERENCES

1. Çatak M, Koca B, Çetin Z, Başer ÖÖ. Evaluation of three inflammation-associated blood indices for predicting malignancy in thyroid nodules. Arch Endocrinol Metab. 2026 Apr 1;70(2):e260014. doi: 10.20945/2359-4292-2026-0014.
2. Öztürk Y, Kocabaş M, Karaköse M, Kulaksizoğlu M, Karakurt F. Prognostic significance of the pan-immune-inflammation value (PIV) in patients with differentiated thyroid carcinoma. Arch Endocrinol Metab. 2025 Apr 11;68:e240217. doi: 10.20945/2359-4292-2024-0217.

Copyright© AE&M all rights reserved.

Archives of Endocrinology and Metabolism
ISSN 2359-4292
OFFICIAL JOURNAL OF THE BRAZILIAN SOCIETY OF ENDOCRINOLOGY AND METABOLISM

letter to the editor

Response to the letter to the editor: Evaluation of three inflammation-associated blood indices for predicting malignancy in thyroid nodules

Merve Çatak[1]
https://orcid.org/0000-0003-2654-3911

Bülent Koca[2]
https://orcid.org/0000-0001-7614-122X

Zeynep Çetin[3]
https://orcid.org/0000-0001-7824-4644

Özden Özdemir BAŞER[4]
https://orcid.org/0000-0001-8368-3182

[1] Tokat Gaziosmanpasa University, Faculty of Medicine, Department of Endocrinology and Metabolism, Tokat, Türkiye
[2] Tokat Gaziosmanpasa University, Faculty of Medicine, Department of General Surgery, Tokat, Türkiye
[3] Amasya Sabuncuoğlu Şerefeddin Training and Research Hospital, Amasya Şerefettin Sabuncuoğlu, Faculty of Medicine, Department of Endocrinology and Metabolism, Amasya, Türkiye
[4] Dokuz Eylul University, Faculty of Medicine, Department of Endocrinology and Metabolism, Izmir, Türkiye

Dear Editor,

We would like to thank Öztürk for their interest in our study and for their thoughtful comments regarding the prognostic implications of inflammation-associated indices (1).

As correctly pointed out, regression-based models and receiver operating characteristic analyses are valuable tools for evaluating independent prognostic performance. However, we would like to clarify that the primary aim of our study was to investigate the diagnostic utility of systemic inflammatory indices in differentiating benign from malignant thyroid nodules, rather than their prognostic significance within malignant cases (2).

In our cohort, exploratory analyses performed within the malignant group did not reveal significant associations between the evaluated indices and tumor-related features. In accordance with standard statistical methodology, further multivariate analyses were not performed in the absence of significant findings in univariate analyses. Therefore, our findings should be interpreted as indicating that no significant prognostic association was identified in our dataset, rather than definitively excluding a possible prognostic role for these indices.

We also acknowledge that the relatively limited number of patients with advanced disease characteristics, particularly distant metastasis, may have reduced the statistical power to detect subtle prognostic associations. In this regard, previously published studies demonstrating the prognostic value of PIV in larger cohorts provide important contributions to the literature (3).

In conclusion, while our findings mainly support the potential diagnostic value of systemic inflammatory indices, further large-scale prospective studies focusing specifically on prognostic outcomes are needed to better clarify their potential clinical utility in thyroid malignancies.

Disclosure: no potential conflict of interest relevant to this article was reported.

Data availability: datasets related to this article will be available upon request to the corresponding author.

REFERENCES

1. Öztürk Y. Comment on: Evaluation of three inflammation-associated blood indices for predicting malignancy in thyroid nodules Arch Endocrinol Metab. 2026;70(4). doi: 10.20945/2359-4292-2026-0069.

Received on May/16/2026
Accepted on May/18/2026

DOI: 10.20945/2359-4292-2026-0070

Correspondence to:
Merve Çatak
Tokat Gazıosmanpasa University,
Faculty of Medicine,
Department of Endocrinology and Metabolism
Gaziosmanpaşa Üniversite Hastanesi,
Kaleardi, 60030, Merkez Tokat, Turkey
merve.catak@gop.edu.tr

Associated editor:
Madson Queiroz de Almeida
https://orcid.org/0000-0002-2957-6148

This is an open-access article distributed under the terms of the Creative Commons Attribution License

Copyright© AE&M all rights reserved.

2. Çatak M, Koca B, Çetin Z, Başer ÖÖ. Evaluation of three inflammation-associated blood indices for predicting malignancy in thyroid nodules. Arch Endocrinol Metab. 2026 Apr 1;70(2):e260014. doi: 10.20945/2359-4292-2026-0014.

3. Öztürk Y, Kocabaş M, Karaköse M, Kulaksizoğlu M, Karakurt F. Prognostic significance of the pan-immune-inflammation value (PIV) in patients with differentiated thyroid carcinoma. Arch Endocrinol Metab. 2025 Apr 11;68:e240217. doi: 10.20945/2359-4292-2024-0217.

Copyright© ACE&M all rights reserved.